A Step Forward to Unravel Open Histamine H_2 Receptor Questions: Synthesis and Biological Evaluation of Novel H_2R Ligands Including Radio- and Fluorescence-Labeled Pharmacological Tools

Dissertation

Zur Erlangung des Doktorgrades der Naturwissenschaften

(Dr. rer. nat.)

an der Fakultät für Chemie und Pharmazie

der Universität Regensburg

vorgelegt von

Katharina Tropmann

aus Jagotino (Russland)

2021

The experimental work was carried out between June 2017 and February 2021 at the University of Regensburg, Institute of Pharmacy under the supervision of PD Dr. Andrea Strasser.

Date of submission: 04.03.2021

Date of colloquium: 31.05.2021

Board of examiners:

Prof. Dr. Achim Göpferich	(Chair)
PD Dr. Andrea Strasser	(1st Referee)
Prof. Dr. Joachim Wegener	(2nd Referee)
Prof. Dr. Frank-Michael Matysik	(Examiner)

Universität Regensburg

To my family

&

Daniel

Table of Contents

1 Introduction 1

1.1 General Information on G Protein Coupled Receptors, the Histamine Receptor Family, and the Histamine H_2 Receptor 1

1.2 The Histamine H_2 Receptor in the Brain 2

1.3 The Signaling Pathways of the Histamine H_2 Receptor 3

1.4 Biased Signaling of the Histamine H_2 Receptor 3

1.5 Histamine H_2 Receptor Agonists 5

1.6 In Silico Studies of Histamine H_2 Receptor Ligands 7

1.7 Histamine H_2 Receptor Antagonists 10

1.8 References 12

2 Discovery of a G Protein Biased Radioligand for the Histamine H_2 Receptor with Reversible Binding Properties 20

2.1 Introduction 21

2.2 Results and Discussion 24

2.2.1 Chemistry 24

2.2.2 H_2R Affinity and Receptor Subtype Selectivity 25

2.2.3 Functional Studies at the Human and Guinea Pig H_2R 28

2.2.4 Synthesis of the Radiolabeled Ligand [^{3}H]**2.23** 32

2.2.5 Saturation Binding Experiments Using [^{3}H]**2.23** 33

2.2.6 Kinetic Binding Experiments Using [^{3}H]**2.23** 36

2.2.7 Competition Binding Experiments Using [^{3}H]**2.23** 38

2.2.8 Red Blood Cell Partitioning of [^{3}H]**2.10** and [^{3}H]**2.23** 42

2.3 Summary and Conclusion 43

2.4 Experimental Section 43

2.4.1 General Experimental Section 43

2.4.2 Compound Characterization 44

2.4.3 Synthesis and Analytical Data 45

2.4.4 Control of the Chemical Stability of the “Cold” Radioligand **2.23** by HPLC 52

2.4.5 Functional Assays 52

2.4.6 Radioligand Binding Experiments 53

2.4.7 Red Blood Cell Partitioning of [^{3}H]**2.10** and [^{3}H]**2.23** 55

2.4.8 Statistical Analysis 56

2.5 References 56

Appendix 1 Discovery of a G Protein Biased Radioligand for the Histamine H_2 Receptor with Reversible Binding Properties 61

App1.1 Generation of the HEK293T-CRE-Luc-gpH_2R and the HEK293T NlucN-mGs/gpH_2R-NlucC Cell Lines 61
App1.1.1 Molecular Cloning 61
App1.1.2 Generation of Stable Cell Lines 61
App1.1.3 Cell Culture 62
App1.1.4 [^{3}H]**2.23** Saturation Binding Using gpH_2R Expressing Cells 62
App1.2 Mini-G Protein Recruitment Assay Using HEK293T Cells Co-Expressing the NlucN-mGs and gpH_2R-NlucC Fusion Proteins 63
App1.3 Red Blood Cell Partitioning of [^{3}H]**2.10** and [^{3}H]**2.23** 65
App1.4 Bias Analysis for Compounds **2.20-2.25** 66
App1.5 References 70
3 Synthesis and Pharmacological Characterization of Fluorescent Histamine H_2 Receptor Carbamoylguanidine-Type Agonist 71
3.1 Introduction 72
3.2 Results and Discussion 74
3.2.1 Design 74
3.2.2 Chemistry 75
3.2.3 H_2R Affinity and Receptor Subtype Preference 77
3.2.4 Functional Studies at the Human H_2R 81
3.2.5 Association and Dissociation Kinetics of **3.32**, **3.34** and **3.35** at the hH_2R Expressed in HEK293T-qs5-HA Cells Studied by Flow Cytometry 85
3.2.6 Investigation of Unlabeled H_2R Standard Ligands in Competition Binding Experiments Using Flow Cytometry 88
3.2.7 Cellular Localization of **3.32**, **3.34**-**3.35** and **3.39**-**3.40** at Human H_2R Expressing Cells Determined by Confocal Microscopy 89
3.3 Summary and Conclusion 92
3.4 Experimental Section 92
3.4.1 General Experimental Section 92
3.4.2 Synthesis and Analytical Data 93
3.4.3 Cell Culture 103
3.4.4 Generation of the HEK293T-SP-FLAG-hH_2R K33 Cell Line 103
3.4.5 Radioligand Binding Experiments Using Sf9 Membranes 104
3.4.6 Radioligand Binding Experiments Using HEK293T-hH_2R-qs5-HA Cells 104
3.4.7 Flow Cytometric Binding Assays Using Whole HEK293T-hH_2R-qs5-HA Cells 106
3.4.8 Functional Assays 108
3.4.9 Confocal Microscopy 108
3.5 References 109

Appendix 2 Synthesis and Pharmacological Characterization of Fluorescent Histamine H_2 Receptor Carbamoylguanidine-Type Agonists 114

App2.1 Experimental Details for **3.23-3.27** 114

App2.2 ^{1}H- and/or ^{13}C-NMR Spectra of **3.26** and **3.28-3.40** 116

App2.3 RP-HPLC Chromatograms of **3.26** and **3.28-3.40** 125

App2.4 Absorption and Emission Spectra 132

App2.5 Saturation Binding Experiments of **3.28-3.31**, **3.36-3.37** and **3.40** at HEK293T-hH_2R-qs5 Cells Studied by Flow Cytometry 135

App2.6 Confocal Microscopy 137

App2.7 Bias Analysis 144

App2.8 References 145

4 Synthesis and Pharmacological Characterization of 2-Arylbenzimidazole Derivatives as Histamine H_2 Receptor Ligands 146

4.1 Introduction 147

4.2 Results and Discussion 149

4.2.1 Chemistry 149

4.2.2 Covalent Binding Experiments 162

4.2.3 Pharmacological Studies 165

4.3 Summary and Conclusion 175

4.4 Experimental Section 175

4.4.1 General Experimental Section 175

4.4.2 General Procedures 176

4.4.3 Preparation of 2-(1-Trityl-1*H*-imidazol-4-yl)ethan-1-amine (**4.4**) 178

4.4.4 Preparation of the Amine Building Blocks **4.17-4.19** 179

4.4.5 Preparation of the Amine Building Block **4.26** 185

4.4.6 Preparation of the Building Blocks **4.32** and **4.35** 187

4.4.7 Preparation of the Cbz- or Phthalimide-Protected Amines **4.42-4.43**, **4.46** and **4.49** 190

4.4.8 Preparation of the Amine Building Blocks **4.66-4.72** 195

4.4.9 Preparation of the Mixed Squaramate Building Blocks **4.75** and **4.76** as well as the Amine Building Block **4.78** 205

4.4.10 Preparation of the 2-Arylbenzimidazoles **4.82-4.97**, **4.104-4.110, 4.112** and **4.114-4.116**, the Squareamide **4.117** as well as Carbamoylguanidine **4.120** 207

4.4.11 Radioligand Binding Experiments 232

4.4.12 Functional Assays 233

4.5 References 233

Appendix 3 Synthesis and Pharmacological Characterization of 2-Arylbenzimidazole Derivatives as Histamine H_2 Receptor Ligands 239

App3.1 ^{1}H- and/or ^{13}C-NMR Spectra of **4.82-4.97**, **4.104-4.110**, **4.112**, **4.114-1.117** and **4.120** 239

App3.2 RP-HPLC Chromatograms of **4.82-4.97**, **4.104-4.110**, **4.112**, **4.114-1.117** and **4.120** 273

App3.3 Assay Curves of Selected Ligands **4.85**, **4.86** (PB513), **4.88**, **4.108**, **4.110** and **4.114** (Radioligand Binding-, Mini-G Recruitment-, [^{35}S]GTPγS Binding- and β-Arrestin2 Recruitment Assays) 288

App3.4 References 290

5 Abolishing Dopamine D_{2long}/D_3 Receptor Affinity of Subtype-Selective Carbamoylguanidine-Type Histamine H_2R Agonists 291

5.1 Introduction 292

5.2 Results and Discussion 295

5.2.1 Chemistry 295

5.2.2 Chemical Stability of Carbamoylguanidines 297

5.2.3 H_2R Affinity and Receptor Subtype Selectivity 299

5.2.4 D_{2long}R and D_3R Affinities of N^G-Carbamoylated Guanidines 304

5.2.5 Functional Studies at the Human H_2R 306

5.2.6 Functional Studies at the Guinea Pig H_2R 309

5.2.7 Functional Studies at the Human $D_{2long/3}$ Receptors 310

5.2.8 Molecular Docking Studies 312

5.3 Summary and Conclusion 317

5.4 Experimental Section 317

5.4.1 General Experimental Section 317

5.4.2 Compound Characterization 319

5.4.3 Synthesis and Analytical Data 319

5.4.4 Control of the Chemical Stability of **5.30-5.35**, **5.37**, **5.41** and **5.57** 341

5.4.5 Cell Culture 342

5.4.6 Radioligand Binding Experiments 342

5.4.7 Functional Assays 343

5.4.8 Docking 343

5.4.9 Data Processing 344

5.5 References 344

Appendix 4 Abolishing Dopamine D_{2long}/D_3 Receptor Affinity of Subtype-Selective Carbamoylguanidine-Type Histamine H_2R Agonists 351

App4.1 Experimental Details for the Amines **5.8-5.17** and the Guanidinylating Reagents **5.18-5.29** 351

App4.1.1 Synthesis of the Amine **5.9** 351

App4.1.2 Synthesis of the Amine **5.11** 353
App4.1.3 Synthesis of the Amine **5.14** 359
App4.1.4 Synthesis of the Amine **5.15** 361
App4.1.5 Synthesis of the Amine **5.16** 363
App4.1.6 Synthesis of the Amine **5.17** 366
App4.2 Experimental Details for the Acylhydrazides **5.108** and **5.109** 370
App4.3 Determination of the pK_a Value 375
App4.4 Bias Analysis 376
App4.5 References 381
6 Summary 384
7 Zusammenfassung 387
8 List of Abbreviations and Acronyms 390
9 List of Posters and Publications 396
10 Danksagungen 397

1 Introduction

1.1 General Information on G Protein Coupled Receptors, the Histamine Receptor Family, and the Histamine H_2 Receptor

G protein coupled receptors (GPCRs) constitute one of the most important class of bioactive complexes in humans, consisting of seven hydrophobic transmembrane (TM) domains with three extracellular and three intracellular loops.[1-2] The extracellular and the transmembrane domains are important for ligand binding (e.g. biogenic amines, peptides, hormones, or lipids).[3] The intracellular domains are involved in signaling and feedback mechanisms.[3]

Their versatile role in cell signal transduction makes these proteins valuable pharmacological targets for the pharmaceutical industry (~35% of Food and Drug Administration- and European Medicines Agency-approved drugs) and in academic research.[1-2] A well-studied GPCR subclass is the histamine receptor family (H_1R, H_2R, H_3R, and H_4R), which belongs to the rhodopsin-like family (class A) and interacts with histamine (**1.1**) as the endogenous ligand.[4-7] The H_1R is expressed on the surface of a wide variety of cell types, including epithelial, vascular endothelial, smooth vascular, neuronal, glial, and immune cells.[8-9] H_1R is therapeutically best known for its role in allergic and anaphylactic responses as well as nausea and vomiting due motion sickness.[9-10] The H_2R is located on neuronal, epithelial, endothelial, immune, smooth muscle, and gastric parietal cells and is involved in the regulation of gastric acid secretion, heart rate and contraction force, and blood pressure.[9, 11] The H_3R is mostly expressed in the brain (e.g. basal ganglia, hippocampus, cortex, and striatal area) and linked to various neurophysiological processes, including cognition, sleep-wake cycle, weight regulation, and energy homeostasis.[9, 12] To a lesser extent, the H_3R is also expressed in the periphery, like e.g., the bronchial and cardiovascular system and gastrointestinal tract.[9, 13] Finally, the H_4R is found to be predominantly expressed in bone marrow and hematopoietic cells (e.g. eosinophils, mast cells, basophils, neutrophils, dendritic cells, monocytes, and T cells).[9, 14-15]

Although the H_2R is a well-studied receptor, its function in the central nervous system (CNS) is still elusive. To gain a better understanding, selective ligands which may cross the blood brain barrier as well as studies in laboratory animals are necessary. A major challenge is that the different H_2R species isoforms interact in a similar way with their endogenous ligand histamine (**1.1**) and synthetic antagonists, but quite differently with most synthetic agonists.[16-17] One reason for this might be the difference in H_2R species sequence identities within the several isoforms: canine (c, 359 amino acids (aa))[18], human (h, 359 aa)[19], rat (r, 358 aa)[20], guinea pig (gp, 359 aa)[21], mouse (m, 358 aa)[22], chicken (369 aa)[23], and zebra fish (410 aa)[24].

The amino acid sequence alignments of human H_2R and its orthologs revealed moderate (<60% for zebra fish and chicken) to high (>80% for canine, guinea pig, rat, and mouse) overall sequence identity.[9] The highest conservation exists within the seven α-helical transmembrane domains (sequence identity of more than 90%), whereas the N-terminal domain together with the extracellular end of TM1 and the C-terminal domain are the least conserved regions. Since the canine, guinea pig, rat, and mouse H_2Rs possess a high sequence overlap with the human H_2R, these animals (especially the rodents) should be well suited for studying the function of H_2R in the brain.

1.2 The Histamine H_2 Receptor in the Brain

The H_2R is widely expressed in the brain and the spinal cord, which was visualized in rats, guinea pigs, dogs, and humans by mapping with radioligands (e.g. [^{125}I]iodaminopotentidine ([^{125}I]**1.27**)) as well as with Northern hybridization (quantification of messenger ribonucleic acid in tissues).[5, 25-27] It was found that the H_2Rs are located primarily on the bodies of neuronal cells.[28] The highest density of H_2Rs is concentrated in the basal ganglia, especially in the caudate-putamen and nucleus accumbens as well as in parts of the limbic system, e.g. hippocampus, amygdala, and cerebral cortex.[5, 25] The lowest amounts are found in the cerebellum and the hypothalamus.[5, 25]

Stimulation of the H_2R has mostly excitatory effects or potentiates excitation.[29] H_2Rs in the brain couple to Gs proteins, which stimulate the adenylyl cyclase (AC).[30-33] The downstream elements of AC stimulation (3`,5`-cyclic AMP (cAMP), protein kinase A (PKA) and cAMP response element binding protein (CREB)) are key regulators of neuronal physiology and plasticity through interaction with e.g. SK-[34-35] , HCN2-[36-37], and Kv3.2-ion-channels[38]. Moreover, Selbach et al. published, that histamine (**1.1**) induced excitation in rat hippocampal subfield Cornu Ammonis 1 pyramidal cells could be prevented by the H_2R antagonist cimetidine (**1.20**) and mimicked by the H_2R agonist impromidine (**1.7**). In addition, positive effects of the H_2-antagonist famotidine (**1.23**) against schizophrenia and an improvement in L-DOPA-induced dyskinesia are reported in the literature.[39-47] Furthermore, it was observed that H_2R knockout mice exhibit selective cognitive deficits, an impairment in hippocampal long-term potentiation[48], abnormalities in pain perception[49-50] as well as unusual gastric and immune functions[39, 51-53].

Since most H_2R ligands hardly pass the blood-brain barrier and possess a lack of receptor selectivity (for more details see Chapter 1.5: Histamine H_2 Receptor Agonists), the behavioral testing of H_2R functions in vivo remains a great challenge. Therefore, the development of

centrally active H_2R ligands as pharmacological tools will be necessary to study the role of this receptor in the brain.

1.3 The Signaling Pathways of the Histamine H_2 Receptor

The H_2R predominantly couples to the Gs the proteins[54] leading to an activation of the AC and production of cAMP in various cell types, e.g. CNS-derived cells, gastric mucosa, cardia myocytes, fat cells, vascular smooth cells, basophils and neutrophils.[55-56] Increased cAMP concentrations activate PKA, which is the downstream effector kinase of this pathway, phosphorylating a wide variety of proteins, e.g. CREB, in the above mentioned cells.[56]

In addition, the H_2R also couples to Gq/11 proteins, resulting in inositol triphosphate (IP3) formation and an increase of the cytosolic Ca^{2+} concentration in some, but not all, H_2R expressing cells.[54, 57-62] On the other hand, also interactions with Gi and G12 proteins in human embryonic kidney (HEK) 293 cells were previously reported, using a sensitive bioluminescence resonance energy transfer (BRET) technique[54] and the constitutive activity of the H_2R was observed in some other recombinant test systems.[17, 63-64]

Continuous or repeated stimuli of the H_2R lead to receptor phosphorylation (specifically serine/threonine residues in the third intracellular loop and C-terminal tail (T308 and T315 in cH_2R[65]) by G protein-coupled kinases (GRK) 2 and 3.[65-67] In turn, GRK-mediated phosphorylation facilitates the binding of the third intracellular loop and the C-terminal tail of the receptor to β-arrestin1 and 2, which leads to physical uncoupling of the receptor from the G protein.[65, 68-69] Another event that occurs after H_2R stimulation is receptor internalization, in which the receptor is translocated from the plasma membrane to endosomes. Previous studies have demonstrated that the H_2R is internalized via a dynamin- and clathrin-dependent mechanism (most likely via clathrin-coated pits).[68, 70] Moreover, for U937 or Chinese hamster ovary (CHO) cells expressing both H_1- and H_2-receptors, GRK2-dependent cross-desensitization between both receptors and subsequent co-internalization by forming heterodimers was demonstrated.[71] However, the exact mechanism by which H_2R is internalized could not be elucidated until today.

1.4 Biased Signaling of the Histamine H_2 Receptor

In the classical ternary complex model for receptor activity (two-state model), agonist activation of the receptor requires three principal components to initiate signaling: ligand, receptor, and signaling protein (e.g. G protein or β-arrestin).[72] Ligand binding to the receptor influences the equilibrium between the two receptor states: agonists shift the equilibrium

towards the active conformation, while inverse agonists favor the inactive conformation and neutral antagonists bind to both without a clear preference. This model distinguishes between an active receptor state, which can bind to and activate transducers, and an inactive receptor state, which is incapable of signaling. Thus, different agonists induce the same downstream response(s), but the strength of the response varies depending on the specific ligand.

Progress in molecular biology provided recombinant test systems allowing the independent observation of multiple ligand induced receptor behaviors, including activation of different G proteins (Gs, Gi/o, Gq/11, and G12/13[73]), arrestins (arrestin1-4[74]) or other effects like receptor phosphorylation (GRK 1-7[75]) and internalization.[69, 76] This refined methodology revealed discrepancies of the reported function of certain ligands when different cellular effectors were independently analyzed.[69] Some of the earlier observations, e.g. receptor internalization by ligands described as antagonists, differential activation of ACs or phospholipase C (PLC) through ligands acting on the same receptor, or the G protein independent activation of arrestins, are incompatible with the existence of a single active state of a receptor.[77] According to the current understanding, receptors rather exist in ensembles of multiple conformations that interact with various downstream effectors.[78-79] In this "multistate model" the functional selectivity of a ligand is explained by its ability to stabilize distinct conformations of the receptor leading to an activation of only a subset of cellular signaling proteins.[78, 80-81] Such molecules, which preferably induce one specific receptor signaling pathway over others, are referred to as "biased" ligands.

In the long history of research on the H_2R, several biased ligands were identified, e.g. some of which modulate the receptor internalization pathways in different ways. On the one hand, amthamine (**1.4**) mainly induces recycling of receptors to the cell surface, whereas famotidine (**1.23**) stimulation results in receptor downregulation.[9, 82] In addition to these observations, several monomeric and dimeric H_2R ligands were recently investigated for biased agonism regarding G protein activation ([^{35}S]GTPγS assay) and β-arrestin recruitment (split luciferase-based assay).[69] While all antagonists were unbiased, the investigated acyl- and carbamoyl-guanidine-based agonists revealed varying degrees of G protein bias.[69] Further investigation of such biased ligands might lead to an application as molecular tools to generate a deeper understanding of a specific receptor, or contribute to the development of more selective drugs with an improved safety profile.

1.5 Histamine H_2 Receptor Agonists

The known H_2R agonists can be divided into a total of four chemical classes: the amine- (**1.1-1.5**), the guanidine- (**1.6-1.10**), the acylguanidine- (**1.11-1.14**), and the carbamoylguanidine- (**1.15-1.18**) type agonists (cf. Figure 1.1). The first developed H_2R agonists were of the amine-type and were very similar in size and structure to the endogenous ligand histamine (**1.1**), e.g. 4-methylhistamine (**1.2**) and dimaprit[83] (**1.3**). Incorporation of the isothiourea partial structure of **1.3** into a heterocycle led to amthamine (**1.4**).[84] Further replacement of the sulfur atom in **1.4** by selenium (cf. amselamine (**1.5**)) was found to result in similar activity.[85] Replacement of the free amine by a guanidine group resulted in Smith, Kline & French (SK&F) 91486 (**1.6**),[86] which is the first member of the second class of H_2R agonists and served for more than three decades as prototypic pharmacophore for the development of high affinity guanidine-type H_2R agonists, e.g. impromidine (**1.7**) or arpromidine (**1.8**).[87-88] Until today, **1.7** is the only agonist, which was effective in clinical studies for the treatment of catecholamine-refractory myocardial insufficiency.[89] However, its unfavorable side effect profile, such as massive gastric acid production and arrhythmias, prevented **1.7** from being approved as a drug.[89] Another problem of guanidine-type H_2R ligands is their high basicity ($pK_a \sim 13$) which leads to nearly quantitative protonation at physiological pH and has a negative effect on their bioavailability and CNS permeability.[90-92] To solve this problem, a carbonyl function adjacent to the guanidine moiety was introduced, which lowered the basicity by 4-5 orders of magnitude ($pK_a \sim 8$[92-93], e.g. UR-AK24[92] (**1.11**)). Such N^G-acylated guanidines (third class of H_2R agonists) can be absorbed from the gastrointestinal tract and are capable of penetrating the blood brain barrier.[92] However, this class of molecules turned out to undergo hydrolytic cleavage in aqueous solution.[94-95] Finally, replacement of the acylguanidine moiety by a carbamoylguanidine group ($pK_a \sim 8$) resulted in chemically stable H_2R ligands (fourth class).[94-95] The linkage of two pharmacophores with an alkyl spacer resulted in dimeric ligands (guanidine- (e.g. SK&F 93082[96] (**1.9**)), acylguanidine- (e.g. UR-AK480[97] (**1.12**)), and carbamoylguanidine-type (e.g. UR-NK60[94] (**1.15**))) with increased potency at the H_2R compared with their monomeric counterparts.[94, 97-98] This high potency might result from an interaction of the ligand with a second binding site at the same receptor because the simultaneous occupation of two orthosteric binding sites in a H_2R dimer is unlikely due to the short spacer length (necessary spacer length is about 20 CH_2 groups).[99]

After the discovery of the histamine H_3 and H_4 receptors, it was found that almost all H_2R agonists showed high affinities for the new receptors with amthamine being the only exception.[100] To generate subtype selective ligands, the imidazole ring of the guanidines and

N^G-acylated or N^G-carbamoylated analogues was bioisosterically replaced by the 2-amino-4-methylthiazole group (UR-Po448[98] (**1.10**), UR-AK477[101] (**1.13**), UR-AK381[97] (**1.14**), UR-NK22[94] (**1.16**), UR-MB-69[95] (**1.17**) and UR-KAT523[95] (**1.18**)).[101]

However, the 2-aminothiazole motif is also a part of some dopamine receptor agonists, e.g. pramipexole (**1.19**, for structure see Figure 1.1) which is used as a drug for treatment of Parkinson`s disease.[102-103] Radioligand binding studies of selected H_2R agonists with a 2-aminothiazolyl ring (e.g. **1.17**[95] and **1.18**[95]) revealed a considerable affinity for dopamine receptors of the D_2-like family (D_2, D_3, and D_4 receptors), especially D_3 receptors.[95, 104] To avoid experimental bias during the elucidation of the activity of the H_2R in the brain, it is necessary to modify the structure of N^G-carbamoylated agonists in such way that these ligands bind selectively to the H_2R.

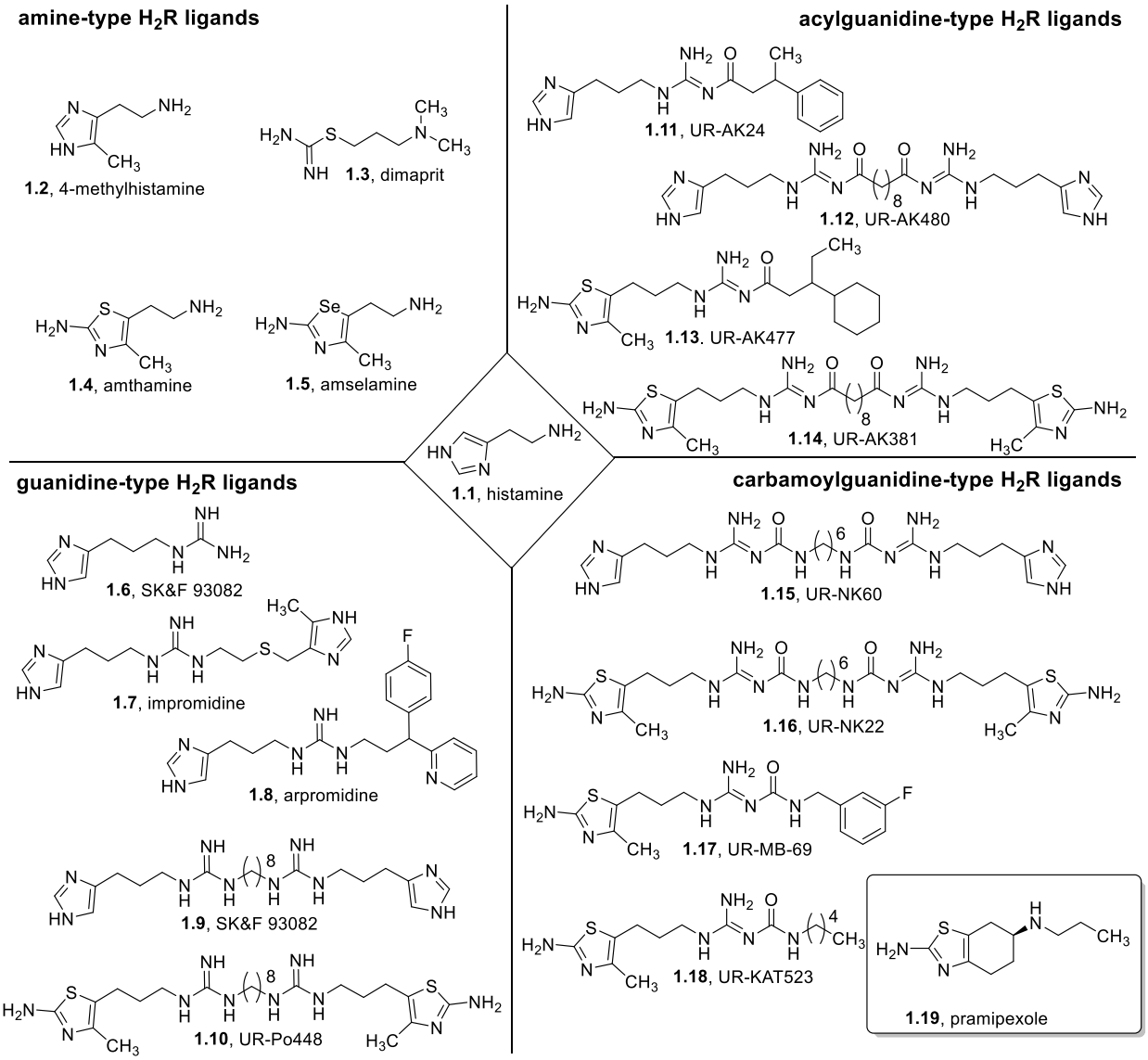

Figure 1.1. Chemical structures of selected H_2R agonists (**1.1-1.18**) and the D_2-like ($D_{2/3/4}$) receptor agonist pramipexole (**1.19**).

1.6 In Silico Studies of Histamine H_2 Receptor Ligands

Several docking experiments on the H_2R with different ligands and objectives were carried out and reported in the literature, some of these studies were supported by mutagenesis studies. The results of these studies are summarized in the following four paragraphs.

The first studies examined how the endogenous ligand, histamine (**1.1**), binds to the H_2R and which amino acids of the H_2R are crucial for the interaction with **1.1**. On the basis of mutagenesis data and molecular modelling using a H_2R model based on the H_1R X-ray structure[105], **1.1** is thought to bind in the orthosteric binding pocket with a different orientation, compared to the $H_{1,3,4}$ receptors (cf. Figure 1.2).[5, 106] In the proposed model, **1.1** binds in the binding pocket in a such way, that N^{τ} and N^{π} form hydrogen bonds with $D^{5.42}$ and $T^{5.46}$, respectively, and the protonated aliphatic amino group forms a salt bridge with $D^{3.32}$ (confirmed by mutagenesis studies) (cf. Figure 1.2).[106-107] A possible interaction with $Y^{5.38}$ instead of $T^{5.46}$ was also proposed (cf. Figure 1.3),[16, 92, 101, 108-111] but this hypothesis was later weakened by mutagenesis studies, as the potencies of imidazole-containing ligands (e.g. **1.1**) tested on the hH_2R-$Y^{5.38}F$ mutant in [^{35}S]GTPγS binding assay were unaffected in contrast to the hH_2R-$T^{5.46}A$ mutant.[111-112] Moreover, it was reported that the increased distance between the negatively charged $D^{5.42}$ and N^{τ} might lead to a reduced affinity for the H_2R compared with the H_3R and H_4R (hH_2R-$G_{s\alpha S}$: 6.58, hH_3R: 7.59 and hH_4R: 7.60).[98, 113]

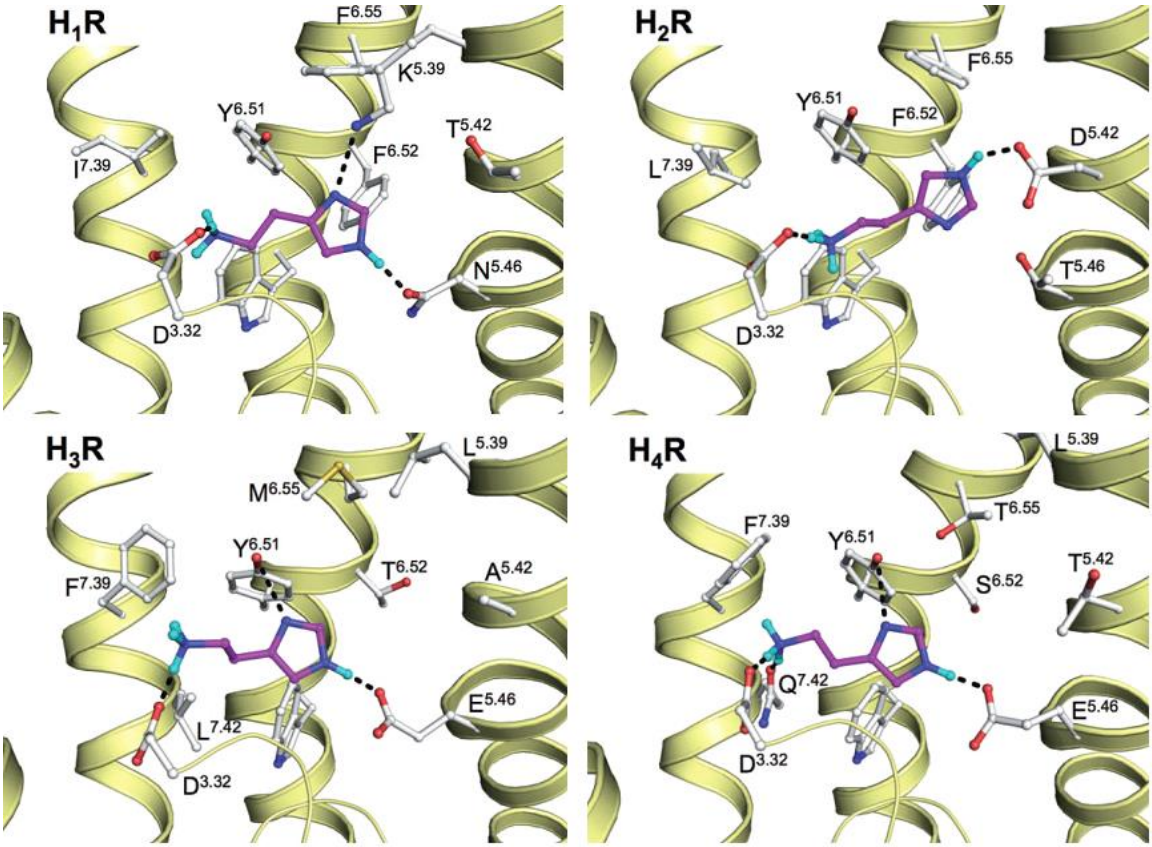

Figure 1.2. Proposed binding modes of histamine (**1.1**) in the four histamine receptors as based on mutagenesis data and docking studies on the H_1 receptor X-ray structure (protein data base (PDB) ID 3RZE[105]) and on homology models of the H_2, H_3, and H_4 receptors based on the H_1 receptor X-ray structure. Residues are numbered as found in the human sequences and with the corresponding Ballesteros-Weinstein[114] numbering. Reprinted with permission from ASPET, Pharmacol. Rev.[5]

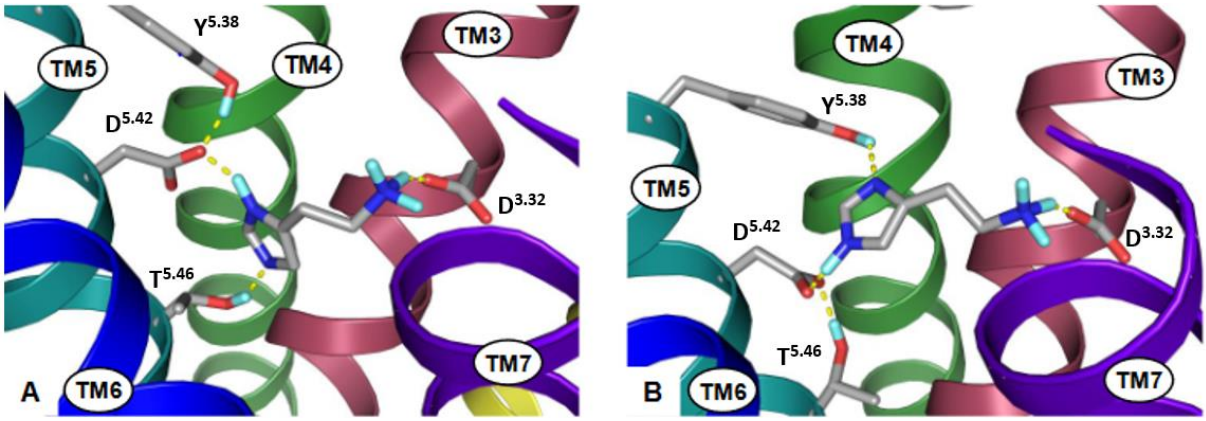

Figure 1.3. Docking modes of histamine (**1.1**) in the orthosteric binding pocket of the hH_2R homology model based on the crystal structure of the nanobody-stabilized active state of the β_2-adrenoceptor (PDB ID 3P0G)[115]. **A**: Histamine in the N^{π}H tautomeric form forming H-bonds with $D^{5.42}$ and $Y^{5.38}$. **B**: Histamine in the N^{τ}H tautomeric form forming the H-bonds with $D^{5.42}$ and $T^{5.46}$. Images taken from Ph.D. thesis of Dr. T. Holzammer.[111]

Another set of in silico studies investigated the binding mode of the 2-amino-4-methylthiazole partial structure at the H_2R and its influence on the subtype selectivity. Docking studies supported that the 2-amino-4-methylthiazole partial structure interacts with the H_2R like a bioisoster for the imidazole partial structure.[101] However, mutagenesis studies suggested a different binding mode for these heterocycles. In contrast to imidazole-type H_2R ligands (e.g. histamine) the mutation of hH_2R-$T^{5.46}A$ did not affect the potencies/efficacies of thiazole-type ligands (e.g. amthamine, but also dimaprit).[112] On the other hand, the hH_2R- $Y^{5.38}F$ mutation had also no significant effect on either heterocycle.[111-112] Moreover, docking studies on receptor models of $hH_{1\text{-}4}R$ ($hH_{2\text{-}4}R$: homology models based on the inactive state H_1R crystal structure: 3RZE) demonstrated that the different steric effects of the amino acids which enclose the orthosteric binding pocket, might be responsible for the subtype selectivity of the 2-amino-4-methylthiazole containing ligands.[98] While in the hH_2R less voluminous residues are located in the positions 3.33, extracellular loop (ECL) 2.54 and ECL2.55 ($V^{3.33}$, $V^{ECL2.54}$-$Q^{ECL2.55}$), the hH_1R, hH_3R and hH_4R possess more voluminous residues in these positions (hH_1R: $Y^{3.33}$, $F^{ECL2.54}$-$Y^{ECL2.55}$, hH_3R: $Y^{3.33}$, $F^{ECL2.54}$-$F193^{ECL2.55}$, and hH_4R $Y^{3.33}$, $F^{ECL2.54}$-$F^{ECL2.55}$).[98] Finally, also the absence or altered location of important acidic amino acids in TM5 (in case of hH_1R, hH_3R and hH_4R compared with the hH_2R) might further contribute to the hH_2R subtype selectivity of 2-amino-4-methylthiazole-containing compounds.[98]

Another docking study examined why the guanidine-type ligands impromidine (**1.7**) and arpromidine (**1.8**) possess a higher potency at the H_2R, if compared with the endogenous ligand histamine (**1.1**) and the guanidine analog SK&F 91486 (**1.6**). Furthermore, the authors investigated, why **1.7** and **1.8** are more potent and efficacious at the gpH_2R than at the hH_2R. The results of their docking studies stated that the imidazolylpropylguanidine moiety binds like histamine to the gpH_2R, maintaining the key interactions with $D^{3.32}$ (D98), $D^{5.42}$ (D186) and $T^{5.46}$ (T190) (cf. Figure 1.4).[110] In addition, the imidazolylpropyl side chain fits into a pocket consisting of $V^{ECL2.54}$ (V176), $Y^{6.51}$ (Y250), $F^{6.52}$ (F251) and $F^{6.55}$ (F254).[110] Since **1.6** is only a weakly active partial H_2R agonist, the phenyl(pyridyl)propyl substituent of **1.8** appears to increase the affinity to the receptor by an interaction with another aromatic pocket consisting of $Y^{2.64}$ (Y78), $Y^{3.28}$ (Y94), $W^{7.40}$ (W275) and $Y^{7.43}$(Y278) (cf. Figure 1.4b).[110] Moreover, the combination of $D^{7.36}$ (D271) and $Y^{1.31}$ (Y17), which are only present in the gpH_2R, might stabilize the active, impromidine-bound conformation by hydrogen bond formation with the $N^{\tau}H$ of the imidazole ring.[16, 110] The modelling results presented in Figure 1.4a support that this interaction is the reason for the preference of **1.7** for the gpH_2R over the hH_2R. On the other hand, the pyridyl moiety of **1.8** might bind with an ion-dipole interaction to $D^{7.36}$ (D271) (cf.

Figure 1.4b), indicating that a positive charge around the pyridyl region increases the potency at the gpH_2R.[110] Side-directed mutagenesis studies (hH_2R-$A^{7.36}$D-$G_{s\alpha S}$ and hH_2R-$C^{1.31}$Y-$G_{s\alpha S}$ (double) mutant(s)) and analysis of chimeric h/gpH_2Rs confirmed the computer modeling results, proving that the combination of $D^{7.36}$ (D271) and $Y^{1.31}$ (Y17) accounts for the species selective action of guanidine-based ligands.[16, 110, 116]

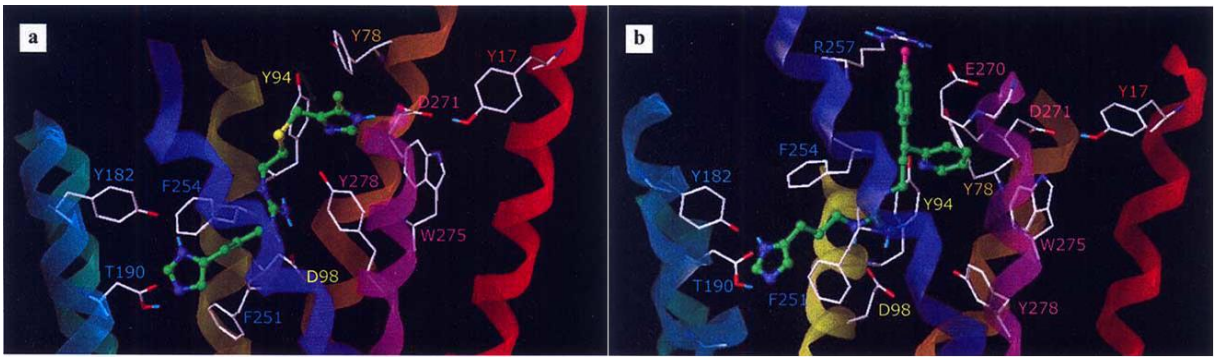

Figure 1.4. Putative binding of (a) impromidine (**1.7**) and (b) arpromidine (**1.8**), respectively, to the gpH_2R. The TM regions are presented as ribbons in spectral colors: TM1-red, TM2-orange, TM3-yellow, TM4-green blue, TM5-cyan, TM6-violet. Reprinted with permission from Bentham Science Publisher Ltd.[110]

Finally, also the binding mode of the acylguanidine motif at the H_2R was examined in an in silico study because in many cases a lower potency of acylguanidine-type ligands compared with their corresponding guanidine counterparts was observed.[92] Surprisingly, the docking studies indicated that the acylguanidine moiety binds to the H_2R exactly like the guanidine group.[92] As a consequence, the authors postulated that the carbonyl group of the acylguanidine must be the reason for the reduced potency due to the restricted overall flexibility of the molecule.[92]

1.7 Histamine H_2 Receptor Antagonists

In contrast to the H_2R agonists, the H_2R antagonists (**1.20**-**1.23** and **1.25**) revolutionized the drug market in the therapy of gastric ulcers (cf. Figure 1.5). With the approval of cimetidine (**1.20**) in 1976 (discovered by SK&F (now GlaxoSmithKline (GSK)), one of the first blockbusters of the pharma industry was created.[117] However, cimetidine's greatest drawback is the potent inhibition of certain cytochrome P450 enzymes.[118] The follow-up drugs (ranitidine (**1.21**), nizatidine (**1.22**), famotidine (**1.23**), and roxatidine (**1.25**)) possess less than 10% of the negative effects on cytochrome P450 metabolism as **1.20** and could be applied in much lower dosage due to their superior affinity.[118-119] The safety of the newer H_2R antagonists even led to

the availability of some of these compounds as over-the-counter drugs.[118] Nowadays, proton pump inhibitors like omeprazole have replaced the H_2R antagonists as first line therapy due to their improved therapeutic profile.[118]

In addition, several antagonists (**1.24** and **1.26**-**1.31**) for other/special applications were synthesized (cf. Figure 1.5), e.g. the slightly brain penetrating zolantidine[120] (**1.26**), the radioligands [^{125}I]iodoaminopotentidine[25] ([^{125}I]**1.27**), [^{3}H]tiotidine[121] ([^{3}H]**1.24**) and [^{3}H]UR-DE257[122] ([^{3}H]**1.29**) and some fluorescence ligands[123-127] (e.g. UR-KAT478 (**1.30**)) structurally derived from Bristol-Myers Squibb (BMY)-25368[128] (**1.28**). However, some antagonists containing the piperidinomethylphenoxyalkylamine-motif (e.g. **1.27**[25], **1.29**[122], **1.30**[127] and lavoltidine (**1.31**)) showed insurmountable, specifically non-competitive, binding in functional and kinetic studies. Unfortunately, blocking of the H_2R with such long-binding H_2R antagonists, was found to be associated with the emergence of gastric cancer in rodents.[129-131] Therefore, these molecules did not find any clinical applications.

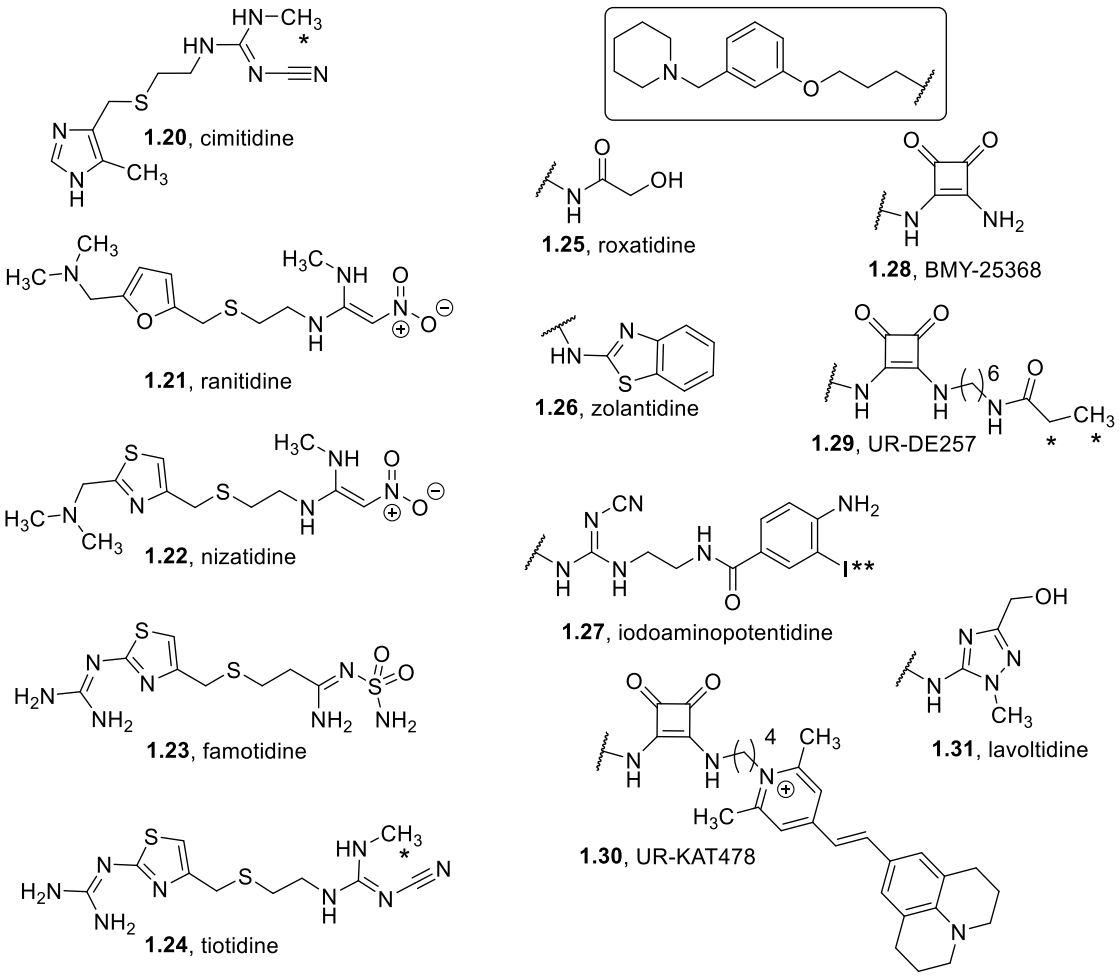

Figure 1.5. Chemical structures of selected H_2R antagonists. *[^{3}H]-labeled position(s). **[^{125}I]-labeled position.

1.8 References

1. Kobilka, B. K., G protein coupled receptor structure and activation. *Biochim. Biophys. Acta - Biomembranes* **2007,** *1768*, 794-807.
2. Rosenbaum, D. M.; Rasmussen, S. G. F.; Kobilka, B. K., The structure and function of G-protein-coupled receptors. *Nature* **2009,** *459*, 356-363.
3. Luttrell, L. M., Reviews in molecular biology and biotechnology: transmembrane signaling by G protein-coupled receptors. *Mol. Biotechnol.* **2008,** *39*, 239-264.
4. Hill, S. J.; Ganellin, C. R.; Timmerman, H.; Schwartz, J. C.; Shankley, N. P.; Young, J. M.; Schunack, W.; Levi, R.; Haas, H. L., International union of pharmacology. XIII. Classification of histamine receptors. *Pharmacol. Rev.* **1997,** *49*, 253-278.
5. Panula, P.; Chazot, P. L.; Cowart, M.; Gutzmer, R.; Leurs, R.; Liu, W. L.; Stark, H.; Thurmond, R. L.; Haas, H. L., International union of basic and clinical pharmacology. XCVIII. Histamine receptors. *Pharmacol. Rev.* **2015,** *67*, 601-655.
6. Hough, L. B., Genomics meets histamine receptors: new subtypes, new receptors. *Mol. Pharmacol.* **2001,** *59*, 415-419.
7. Foord, S. M.; Bonner, T. I.; Neubig, R. R.; Rosser, E. M.; Pin, J. P.; Davenport, A. P.; Spedding, M.; Harmar, A. J., International union of pharmacology. XLVI. G protein-coupled receptor list. *Pharmacol. Rev.* **2005,** *57*, 279-288.
8. Traiffort, E.; Leurs, R.; Arrang, J. M.; Tardivel-Lacombe, J.; Diaz, J.; Schwartz, J. C.; Ruat, M., Guinea pig histamine H_1 receptor. I. Gene cloning, characterization, and tissue expression revealed by in situ hybridization. *J. Neurochem.* **1994,** *62*, 507-518.
9. Mocking, A. M.; Bosma, R.; Rahman, S. N.; Verweij, E. W. E.; McNaught-Flores, D. A.; Vischer, H. F., (2016) Molecular Aspects of Histamine Receptors. In: Blandina, P., Passani, M. (eds) Histamine Receptors. The Receptors, vol 28. Humana Press, Cham.
10. Simons, F. E.; Simons, K. J., Histamine and H_1-antihistamines: celebrating a century of progress. *J. Allergy Clin. Immunol.* **2011,** *128*, 1139-1150.
11. Yellin, T. O.; Sperow, J. W.; Buck, S. H., Antagonism of tolazoline by histamine H_2-receptor blockers. *Nature* **1975,** *253*, 561-563.
12. Lovenberg, T. W.; Roland, B. L.; Wilson, S. J.; Jiang, X.; Pyati, J.; Huvar, A.; Jackson, M. R.; Erlander, M. G., Cloning and functional expression of the human histamine H_3 receptor. *Mol. Pharmacol.* **1999,** *55*, 1101-1107.
13. Malinowska, B.; Godlewski, G.; Schlicker, E., Histamine H_3 receptors--general characterization and their function in the cardiovascular system. *J. Physiol. Pharmacol.* **1998,** *492*, 191-211.
14. Nakamura, T.; Itadani, H.; Hidaka, Y.; Ohta, M.; Tanaka, K., Molecular cloning and characterization of a new human histamine receptor, hH_4R. *Biochem. Biophys. Res. Commun.* **2000,** *279*, 615-620.
15. Cogé, F.; Guénin, S.-P.; Rique, H.; Boutin, J. A.; Galizzi, J.-P., Structure and expression of the human histamine H_4-receptor gene. *Biochem. Biophys. Res. Commun.* **2001,** *284*, 301-309.
16. Kelley, M. T.; Bürckstürmmer, T.; Wenzel-Seifert, K.; Dove, S.; Buschauer, A.; Seifert, R., Distinct interaction of human and guinea pig histamine H_2-receptor with guanidine-type agonists. *Mol. Pharmacol.* **2001,** *60*, 1210-1225.
17. Preuss, H.; Ghorai, P.; Kraus, A.; Dove, S.; Buschauer, A.; Seifert, R., Constitutive activity and ligand selectivity of human, guinea pig, rat, and canine histamine H_2 receptors. *J. Pharmacol. Exp. Ther.* **2007,** *321*, 983-995.
18. Gantz, I.; Schäffer, M.; DelValle, J.; Logsdon, C.; Campbell, V.; Uhler, M.; Yamada, T., Molecular cloning of a gene encoding the histamine H_2 receptor. *Proc. Natl. Acad. Sci. USA* **1991,** *88*, 429-433.

19. Gantz, I.; Munzert, G.; Tashiro, T.; Schäffer, M.; Wang, L.; DelValle, J.; Yamada, T., Molecular cloning of the human histamine H_2 receptor. *Biochem. Biophys. Res. Co.* **1991,** *178*, 1386-1392.
20. Ruat, M.; Traiffort, E.; Arrang, J.-M.; Leurs, R.; Schwartz, J.-C., Cloning and tissue expression of a rat histamine H_2-receptor gene. *Biochem. Biophys. Res. Co.* **1991,** *179*, 1470-1478.
21. Traiffort, E.; Vizuete, M. L.; Tardivellacombe, J.; Souil, E.; Schwartz, J. C.; Ruat, M., The guinea pig histamine H_2 receptor: gene cloning, tissue expression and chromosomal localization of its human counterpart. *Biochem. Biophys. Res. Co.* **1995,** *211*, 570-577.
22. Kobayashi, T.; Inoue, I.; Jenkins, N. A.; Gilbert, D. J.; Copeland, N. G.; Watanabe, T., Cloning, RNA expression, and chromosomal location of a mouse histamine H_2 receptor gene. *Genomics* **1996,** *37*, 390-394.
23. UniProtKB, Gastric receptor I (HRH2), gallus gallus (chicken) [Online], Dec 02, 2020, accesion number A0A3Q2TUM1. https://www.uniprot.org/uniprot/A0A3Q2TUM1 (accessed Dec 20, 2020).
24. Peitsaro, N.; Sundvik, M.; Anichtchik, O. V.; Kaslin, J.; Panula, P., Identification of zebrafish histamine H_1, H_2 and H_3 receptors and effects of histaminergic ligands on behavior. *Biochem. Pharmacol.* **2007,** *73*, 1205-1214.
25. Traiffort, E.; Pollard, H.; Moreau, J.; Ruat, M.; Schwartz, J. C.; Martinez-Mir, M. I.; Palacios, J. M., Pharmacological characterization and autoradiographic localization of histamine H_2 receptors in human brain identified with [^{125}I]iodoaminopotentidine. *J. Neurochem.* **1992,** *59*, 290-299.
26. Vizuete, M. L.; Traiffort, E.; Bouthenet, M. L.; Ruat, M.; Souil, E.; Tardivel-Lacombe, J.; Schwartz, J. C., Detailed mapping of the histamine H_2 receptor and its gene transcripts in guinea-pig brain. *Neuroscience* **1997,** *80*, 321-343.
27. Honrubia, M. A.; Vilaró, M. T.; Palacios, J. M.; Mengod, G., Distribution of the histamine H_2 receptor in monkey brain and its mRNA localization in monkey and human brain. *Synapse* **2000,** *38*, 343-354.
28. Haas, H. L.; Sergeeva, O. A.; Selbach, O., Histamine in the nervous system. *Physiol. Rev.* **2008,** *88*, 1183-1241.
29. Haas, H.; Panula, P., The role of histamine and the tuberomamillary nucleus in the nervous system. *Nat. Rev. Neurosci.* **2003,** *4*, 121-130.
30. Daly, J. W., The nature of receptors regulating the formation of cyclic AMP in brain tissue. *Life Sci.* **1976,** *18*, 1349-1358.
31. Kanof, P. D.; Greengard, P., Pharmacological properties of histamine-sensitive adenylate cyclase from mammalian brain. *J. Pharmacol. Exp. Ther.* **1979,** *209*, 87-96.
32. Baudry, M.; Martres, M. P.; Schwartz, J. C., H_1 and H_2 receptors in the histamine-induced accumulation of cyclic AMP in guinea pig brain slices. *Nature* **1975,** *253*, 362-364.
33. Garbarg, M.; Schwartz, J. C., Synergism between histamine H_1- and H_2-receptors in the cAMP response in guinea pig brain slices: effects of phorbol esters and calcium. *Mol. Pharmacol.* **1988,** *33*, 38-43.
34. Haas, H. L.; Konnerth, A., Histamine and noradrenaline decrease calcium-activated potassium conductance in hippocampal pyramidal cells. *Nature* **1983,** *302*, 432-434.
35. Pedarzani, P.; Storm, J. F., Pka mediates the effects of monoamine transmitters on the K^+ current underlying the slow spike frequency adaptation in hippocampal neurons. *Neuron* **1993,** *11*, 1023-1035.
36. Pedarzani, P.; Storm, J. F., Protein kinase A-independent modulation of ion channels in the brain by cyclic AMP. *Proc. Natl. Acad. Sci. U. S. A.* **1995,** *92*, 11716-11720.
37. McCormick, D.; Williamson, A., Modulation of neuronal firing mode in cat and guinea pig LGNd by histamine: possible cellular mechanisms of histaminergic control of arousal. *J. Neurosci.* **1991,** *11*, 3188-3199.

38. Atzori, M.; Lau, D.; Tansey, E. P.; Chow, A.; Ozaita, A.; Rudy, B.; McBain, C. J., H_2 histamine receptor-phosphorylation of Kv3.2 modulates interneuron fast spiking. *Nat. Neurosci.* **2000,** *3*, 791-798.
39. Schneider, E. H.; Neumann, D.; Seifert, R., Modulation of behavior by the histaminergic system: lessons from H_1R-and H_2R-deficient mice. *Neurosci. Biobeh. Rev.* **2014,** *42*, 252-266.
40. Deutsch, S. I.; Rosse, R. B.; Schwartz, B. L., Histamine H_2 receptor antagonists in schizophrenia. *CNS Drugs* **1997,** *8*, 276-284.
41. Farzin, D.; Hosseini, S. H.; Shafaat, A., A randomized double blind clinical trial in famotidine adjuvant therapy in schizophrenia. *Iran. J. Med. Sci.* **2005,** *30*, 59-62.
42. Johnston, T. H.; van der Meij, A.; Brotchie, J. M.; Fox, S. H., Effect of histamine H_2 receptor antagonism on levodopa–induced dyskinesia in the MPTP-macaque model of Parkinson's disease. *Mov. Disord.* **2010,** *25*, 1379-1390.
43. Meskanen, K.; Ekelund, H.; Laitinen, J.; Neuvonen, P. J.; Haukka, J.; Panula, P.; Ekelund, J., A randomized clinical trial of histamine 2 receptor antagonism in treatment-resistant schizophrenia. *J. Clin. Psychopharmacol.* **2013,** *33*, 472-478.
44. Shi, H.; Yang, X.; Zhao, H.; Zhang, S.; Zu, J.; Zhang, W.; Shen, X.; Cui, G.; Hua, F.; Yan, C., Ranitidine reduced levodopa-induced dyskinesia by remodeling neurochemical changes in hemiparkinsonian model of rats. *Neuropsychiatr. Dis. Treat.* **2015,** *11*, 1331-1337.
45. Ahmed, M. R.; Jayakumar, M.; Ahmed, M. S.; Zamaleeva, A. I.; Tao, J.; Li, E. H.; Job, J. K.; Pittenger, C.; Ohtsu, H.; Rajadas, J., Pharmacological antagonism of histamine H_2R ameliorated L-DOPA-induced dyskinesia via normalization of GRK3 and by suppressing FosB and ERK in PD. *Neurobiol Aging* **2019,** *81*, 177-189.
46. Oyewumi, L. K.; Vollick, D.; Merskey, H.; Plumb, C., Famotidine as an adjunct treatment of resistant schizophrenia. *J. Psychiatry Neurosci.* **1994,** *19*, 145-150.
47. White, J. M.; Rumbold, G. R., Behavioural effects of histamine and its antagonists: a review. *Psychopharmacology* **1988,** *95*, 1-14.
48. Dai, H.; Kaneko, K.; Kato, H.; Fujii, S.; Jing, Y.; Xu, A.; Sakurai, E.; Kato, M.; Okamura, N.; Kuramasu, A.; Yanai, K., Selective cognitive dysfunction in mice lacking histamine H_1 and H_2 receptors. *Neurosci. Res.* **2007,** *57*, 306-313.
49. Mobarakeh, J. I.; Takahashi, K.; Sakurada, S.; Nishino, S.; Watanabe, H.; Kato, M.; Naghdi, N.; Yanai, K., Enhanced antinociception by intracerebroventricularly administered orexin A in histamine H_1 or H_2 receptor gene knockout mice. *Pain* **2005,** *118*, 254-262.
50. Mobarakeh, J. I.; Takahashi, K.; Sakurada, S.; Kuramasu, A.; Yanai, K., Enhanced antinociceptive effects of morphine in histamine H_2 receptor gene knockout mice. *Neuropharmacology* **2006,** *51*, 612-622.
51. Jutel, M.; Watanabe, T.; Klunker, S.; Akdis, M.; Thomet, O. A. R.; Malolepszy, J.; Zak-Nejmark, T.; Koga, R.; Kobayashi, T.; Blaser, K.; Akdis, C. A., Histamine regulates T-cell and antibody responses by differential expression of H_1 and H_2 receptors. *Nature* **2001,** *413*, 420-425.
52. Teuscher, C.; Poynter, M. E.; Offner, H.; Zamora, A.; Watanabe, T.; Fillmore, P. D.; Zachary, J. F.; Blankenhorn, E. P., Attenuation of Th1 effector cell responses and susceptibility to experimental allergic encephalomyelitis in histamine H_2 receptor knockout mice is due to dysregulation of cytokine production by antigen-presenting cells. *Am. J. Pathol.* **2004,** *164*, 883-892.
53. Kobayashi, T.; Tonai, S.; Ishihara, Y.; Koga, R.; Okabe, S.; Watanabe, T., Abnormal functional and morphological regulation of the gastric mucosa in histamine H_2 receptor-deficient mice. *J. Clin. Invest.* **2000,** *105*, 1741-1749.
54. Okashah, N.; Wan, Q.; Ghosh, S.; Sandhu, M.; Inoue, A.; Vaidehi, N.; Lambert, N. A., Variable G protein determinants of GPCR coupling selectivity. *Proc. Natl. Acad. Sci. U. S. A.* **2019,** *116*, 12054-12059.

55. Del Valle, J.; Gantz, I., Novel insights into histamine H_2 receptor biology. *Am. J. Physiol.* **1997,** *273*, 987-996.
56. Hegyesi, H.; Darvas, Z.; Thurmond, R. L.; Falus, A., (2005) Histamine Receptors and Signaling. In: Damjanovich S. (eds) Biophysical Aspects of Transmembrane Signaling. Springer Series in Biophysics, vol 8. Springer, Berlin, Heidelberg.
57. Kühn, B.; Schmid, A.; Harteneck, C.; Gudermann, T.; Schultz, G., G proteins of the G_q family couple the H_2 histamine receptor to phospholipase C. *Mol. Endocrinol.* **1996,** *10*, 1697-1707.
58. Houston, C.; Wenzel-Seifert, K.; Bürckstümmer, T.; Seifert, R., The human histamine H_2-receptor couples more efficiently to Sf9 insect cell G_s-proteins than to insect cell G_q-proteins: limitations of Sf9 cells for the analysis of receptor/G_q-protein coupling. *J. Neurochem.* **2002,** *80*, 678-696.
59. Seifert, R.; Höer, A.; Schwaner, I.; Buschauer, A., Histamine increases cytosolic Ca^{2+} in HL-60 promyelocytes predominantly via H_2 receptors with an unique agonist/antagonist profile and induces functional differentiation. *Mol. Pharmacol.* **1992,** *42*, 235-241.
60. Wellner-Kienitz, M.-C.; Bender, K.; Meyer, T.; Pott, L., Coupling to G_s and $G_{q/11}$ of histamine H_2 receptors heterologously expressed in adult rat atrial myocytes. *BBA-Mol. Cell Res.* **2003,** *1642*, 67-77.
61. Hill, S. J., Distribution, properties, and functional characteristics of three classes of histamine receptor. *Pharmacol. Rev.* **1990,** *42*, 45-83.
62. Leopoldt, D.; Harteneck, C.; Nürnberg, B., G proteins endogenously expressed in Sf9 cells: interactions with mammalian histamine receptors. *Naunyn-Schmiedeberg's Arch. Pharmacol.* **1997,** *356*, 216-224.
63. Plank, N. Dimeric Histamine H_2 Receptor Agonists as Molecular Tools and Genetically Engineered HEK293T Cells as an Assay Platform to Unravel Signaling Pathways of hH_1R and hH_2R. Ph. D. Thesis. University of Regensburg, 2015.
64. Höring, C.; Seibel, U.; Tropmann, K.; Grätz, L.; Mönnich, D.; Pitzl, S.; Bernhardt, G.; Pockes, S.; Strasser, A., A dynamic, split-luciferase-based mini-G protein sensor to functionally characterize ligands at all four histamine receptor subtypes. *Int. J. Mol. Sci.* **2020,** *21, 8440*.
65. Fukushima, Y.; Asano, T.; Takata, K.; Funaki, M.; Ogihara, T.; Anai, M.; Tsukuda, K.; Saitoh, T.; Katagiri, H.; Aiharai, M.; Matsuhashi, N.; Oka, Y.; Yazaki, Y.; Sugano, K., Role of the C terminus in histamine H_2 receptor signaling, desensitization, and agonist-induced internalization. *J. Biol. Chem.* **1997,** *272*, 19464-19470.
66. Fernandez, N.; Gottardo, F. L.; Alonso, M. N.; Monczor, F.; Shayo, C.; Davio, C., Roles of phosphorylation-dependent and -independent mechanisms in the regulation of histamine H_2 receptor by G protein-coupled receptor kinase 2. **2011,** *286*, 28697-28706.
67. Rodriguez-Pena, M. S.; Timmerman, H.; Leurs, R., Modulation of histamine H_2 receptor signalling by G-protein-coupled receptor kinase 2 and 3. *Br. J. Pharmacol.* **2000,** *131*, 1707-1715.
68. Fernandez, N.; Monczor, F.; Baldi, A.; Davio, C.; Shayo, C., Histamine H_2 receptor trafficking: role of arrestin, dynamin, and clathrin in histamine H_2 receptor internalization. *Mol. Pharmacol.* **2008,** *74*, 1109-1118.
69. Felixberger, J. Luciferase Complementation for the Determination of Arrestin Recruitment: Investigation of Histamine and NPY receptors. Ph.D. Thesis. University of Regensburg, 2014.
70. Xu, A.-J.; Kuramasu, A.; Maeda, K.; Kinoshita, K.; Takayanagi, S.; Fukushima, Y.; Watanabe, T.; Yanagisawa, T.; Sukegawa, J.; Yanai, K., Agonist-induced internalization of histamine H_2 receptor and activiation of extracellular signal-regulated kinases are dynamin-dependent. *J. Neurochem.* **2008,** *107*, 208-217.
71. Alonso, N.; Fernandez, N.; Notcovich, C.; Monczor, F.; Simaan, M.; Baldi, A.; Gutkind, J. S.; Davio, C.; Shayo, C., Cross-desensitization and cointernalization of H_1 and H_2 histamine

receptors reveal new insights into histamine signal integration. *Mol. Pharmacol.* **2013,** *83*, 1087-1098.
72. Kenakin, T.; Morgan, P.; Lutz, M.; Weiss, J., (2020) The Evolution of Drug-Receptor Models: The Cubic Ternary Complex Model for G Protein-Coupled Receptors. In: Kenakin T., Angus J. A. (eds) The Pharmacology of Functional, Biochemical, and Recombinant Receptor Systems. Handbook of Experimental Pharmacology, vol 148. Springer, Berlin, Heidelberg.
73. Wettschureck, N.; Offermanns, S., Mammalian G proteins and their cell type specific functions. *Physiol. Rev.* **2005,** *85*, 1159-1204.
74. Gurevich, E. V.; Gurevich, V. V., Arrestins: ubiquitous regulators of cellular signaling pathways. *Genome Biol.* **2006,** *7*, 236-236.
75. Watari, K.; Nakaya, M.; Kurose, H., Multiple functions of G protein-coupled receptor kinases. *J. Mol. Signal.* **2014,** *9*, 1.
76. Kenakin, T., Functional selectivity and biased receptor signaling. *J. Pharmacol. Exp. Ther.* **2011,** *336*, 296-302.
77. Spengler, D.; Waeber, C.; Pantaloni, C.; Holsboer, F.; Bockaert, J.; Seeburg, P. H.; Journot, L., Differential signal transduction by five splice variants of the PACAP receptor. *Nature* **1993,** *365*, 170-175.
78. Liu, J. J.; Horst, R.; Katritch, V.; Stevens, R. C.; Wüthrich, K., Biased signaling pathways in β_2-adrenergic receptor characterized by ^{19}F-NMR. *Science* **2012,** *335*, 1106-1110.
79. Liang, Y.-L.; Khoshouei, M.; Glukhova, A.; Furness, S. G. B.; Zhao, P.; Clydesdale, L.; Koole, C.; Truong, T. T.; Thal, D. M.; Lei, S.; Radjainia, M.; Danev, R.; Baumeister, W.; Wang, M.-W.; Miller, L. J.; Christopoulos, A.; Sexton, P. M.; Wootten, D., Phase-plate cryo-EM structure of a biased agonist-bound human GLP-1 receptor–Gs complex. *Nature* **2018,** *555*, 121-125.
80. Kahsai, A. W.; Xiao, K.; Rajagopal, S.; Ahn, S.; Shukla, A. K.; Sun, J.; Oas, T. G.; Lefkowitz, R. J., Multiple ligand-specific conformations of the β_2-adrenergic receptor. *Nat. Chem. Biol.* **2011,** *7*, 692-700.
81. Nygaard, R.; Zou, Y.; Dror, R. O.; Mildorf, T. J.; Arlow, D. H.; Manglik, A.; Pan, A. C.; Liu, C. W.; Fung, J. J.; Bokoch, M. P.; Thian, F. S.; Kobilka, T. S.; Shaw, D. E.; Mueller, L.; Prosser, R. S.; Kobilka, B. K., The dynamic process of β_2-adrenergic receptor activation. *Cell* **2013,** *152*, 532-542.
82. Lemos Legnazzi, B.; Shayo, C.; Monczor, F.; Martin, M. E.; Fernandez, N.; Brodsky, A.; Baldi, A.; Davio, C., Rapid desensitization and slow recovery of the cyclic AMP response mediated by histamine H2 receptors in the U937 cell line. *Biochem. Pharmacol.* **2000,** *60*, 159-166.
83. Durant, G. J.; Ganellin, C. R.; Parsons, M. E., Dimaprit, (*S*-[3-(*N*,*N*-dimethylamino)propyl]isothiourea). A highly specific histamine H_2-receptor agonist. Part 2. Structure-activity considerations. *Agents Actions* **1977,** *7*, 39-43.
84. Eriks, J. C.; van der Goot, H.; Sterk, G. J.; Timmerman, H., Histamine H_2-receptor agonists. Synthesis, in vitro pharmacology, and qualitative structure-activity relationships of substituted 4- and 5-(2-aminoethyl)thiazoles. *J. Med. Chem.* **1992,** *35*, 3239-3246.
85. van der Goot, H.; Eriks, J. C.; Leurs, R.; Timmerman, H., Amselamine, a new selective histamine H_2-receptor agonist. *Bioorg. Med. Chem. Lett.* **1994,** *4*, 1913-1916.
86. Parsons, M. E.; Blakemore, R. C.; Durant, G. J.; Ganellin, C. R.; Rasmussen, A. C., Proceedings: 3-(4(5)-imidazolyl) propylguanidine (SK&F 91486) - a partial agonist at histamine H_2-receptors. *Agents Actions* **1975,** *5*, 464.
87. Durant, G. J.; Duncan, W. A. M.; Ganellin, C. R.; Parsons, M. E.; Blakemore, R. C.; Rasmussen, A. C., Impromidine (SK&F 92676) is a very potent and specific agonist for histamine H_2 receptors. *Nature* **1978,** *276*, 403-405.

88. Buschauer, A., Synthesis and in vitro pharmacology of arpromidine and related phenyl(pyridylalkyl)guanidines, a potential new class of positive inotropic drugs. *J. Med. Chem.* **1989,** *32*, 1963-1970.
89. Baumann, G.; Permanetter, B.; Wirtzfeld, A., Possible value of H_2-receptor agonists for treatment of catecholamine-insensitive congestive heart failure. *Pharmacol. Ther.* **1984,** *24*, 165-177.
90. Lipinski, C. A.; Lombardo, F.; Dominy, B. W.; Feeney, P. J., Experimental and computational approaches to estimate solubility and permeability in drug discovery and development settings. *Adv. Drug Deliv. Rev.* **1997,** *23*, 3-25.
91. Manallack, D. T., The pK_a distribution of drugs: application to drug discovery. *Perspect. Medicin. Chem.* **2007,** *1*, 25-38.
92. Ghorai, P.; Kraus, A.; Keller, M.; Götte, C.; Igel, P.; Schneider, E.; Schnell, D.; Bernhardt, G.; Dove, S.; Zabel, M.; Elz, S.; Seifert, R.; Buschauer, A., Acylguanidines as bioisosteres of guanidines: N^G-acylated imidazolylpropylguanidines, a new class of histamine H_2 receptor agonists. *J. Med. Chem.* **2008,** *51*, 7193-7204.
93. Keller, M.; Pop, N.; Hutzler, C.; Beck-Sickinger, A. G.; Bernhardt, G.; Buschauer, A., Guanidine−acylguanidine bioisosteric approach in the design of radioligands: synthesis of a tritium-labeled N^G-propionylargininamide ([^{3}H]-UR-MK114) as a highly potent and selective neuropeptide Y Y_1 receptor antagonist. *J. Med. Chem.* **2008,** *51*, 8168-8172.
94. Kagermeier, N.; Werner, K.; Keller, M.; Baumeister, P.; Bernhardt, G.; Seifert, R.; Buschauer, A., Dimeric carbamoylguanidine-type histamine H_2 receptor ligands: a new class of potent and selective agonists. *Bioorg. Med. Chem.* **2015,** *23*, 3957-3969.
95. Biselli, S.; Bresinsky, M.; Tropmann, K.; Forster, L.; Honisch, C.; Buschauer, A.; Bernhardt, G.; Pockes, S., Pharmacological characterization of a new series of carbamoylguanidines reveals potent agonism at the H_2R and D_3R. *Eur. J. Med. Chem.* **2021,** *214*, 113190.
96. Sterk, G. J.; Kramer, K.; van der Goot, H.; Timmerman, H., Studies on histaminergic compounds, Part VII.1 Histamine H_2-binding on guinea-pig cerebral cortex compared to histamine (ANT)agonism. *J. Recept. Res.* **1989,** *9*, 417-427.
97. Birnkammer, T.; Spickenreither, A.; Brunskole, I.; Lopuch, M.; Kagermeier, N.; Bernhardt, G.; Dove, S.; Seifert, R.; Elz, S.; Buschauer, A., The bivalent ligand approach leads to highly potent and selective acylguanidine-type histamine H_2 receptor agonists. *J. Med. Chem.* **2012,** *55*, 1147-1160.
98. Pockes, S.; Wifling, D.; Keller, M.; Buschauer, A.; Elz, S., Highly potent, stable, and selective dimeric hetarylpropylguanidine-type histamine H_2 receptor agonists. *ACS Omega* **2018,** *3*, 2865-2882.
99. Portoghese, P. S., Bivalent ligands and the message-address concept in the design of selective opioid receptor antagonists. *Trends Pharmacol. Sci.* **1989,** *10*, 230-235.
100. Lim, H. D.; van Rijn, R. M.; Ling, P., Evaluation of histamine H_1-, H_2- and H_3-receptor ligands at the human histamine H_4 receptor: identification of 4-methylhistamine as the first potent and selective H_4 receptor agonist. *J. Pharmacol. Exp. Ther.* **2005,** *314*, 1310-1321.
101. Kraus, A.; Ghorai, P.; Birnkammer, T.; Schnell, D.; Elz, S.; Seifert, R.; Dove, S.; Bernhardt, G.; Buschauer, A., N^G-Acylated aminothiazolylpropylguanidines as potent and selective histamine H_2 receptor agonists. *ChemMedChem* **2009,** *4*, 232-240.
102. Mierau, J., Pramipexole: a dopamine-receptor agonist for treatment of Parkinson's disease. *Clin. Neuropharmacol.* **1995,** *18*, 195-206.
103. Bennett, J. P., Jr.; Piercey, M. F., Pramipexole-a new dopamine agonist for the treatment of Parkinson's disease. *J. Neurol. Sci.* **1999,** *163*, 25-31.
104. Biselli, S. Synthesis and Pharmacological Characterization of Subtype-Selective Ligands, Including Radio- and Fluorescence Labeled Ligands, for the Histamine H_2 Receptor. Ph.D. Thesis. University of Regensburg, 2020.

105. Shimamura, T.; Shiroishi, M.; Weyand, S.; Tsujimoto, H.; Winter, G.; Katritch, V.; Abagyan, R.; Cherezov, V.; Liu, W.; Han, G. W.; Kobayashi, T.; Stevens, R. C.; Iwata, S., Structure of the human histamine H_1 receptor complex with doxepin. *Nature* **2011,** *475*, 65-70.
106. Kooistra, A. J.; Kuhne, S.; de Esch, I. J. P.; Leurs, R.; de Graaf, C., A structural chemogenomics analysis of aminergic GPCRs: lessons for histamine receptor ligand design. *Br. J. Pharmacol.* **2013,** *170*, 101-126.
107. Gantz, I.; DelValle, J.; Wang, L. D.; Tashiro, T.; Munzert, G.; Guo, Y. J.; Konda, Y.; Yamada, T., Molecular basis for the interaction of histamine with the histamine H_2 receptor. *J. Biol. Chem.* **1992,** *267*, 20840-20843.
108. Nederkoorn, P. H. J.; van Gelder, E. M.; Donné-Op den Kelder, G. M.; Timmerman, H., The agonistic binding site at the histamine H_2 receptor. II. Theoretical investigations of histamine binding to receptor models of the seven α-helical transmembrane domain. *J. Comput. Aided Mol. Des.* **1996,** *10*, 479-489.
109. Sun, X.; Li, Y.; Li, W.; Xu, Z.; Tang, Y., Computational investigation of interactions between human H_2 receptor and its agonists. *J. Mol. Graph. Model.* **2011,** *29*, 693-701.
110. Dove, S.; Elz, S.; Seifert, R.; Buschauer, A., Structure-activity relationships of histamine H_2 receptor ligands. *Mini-Re. Med. Chem.* **2004,** *4*, 941-954.
111. Holzammer, T. Homology Modeling, Molecular Dynamics Simulations and Site-directed Mutagenesis of Histamine H_2 Receptors. Ph.D. Thesis. University of Regensburg, 2013.
112. Kagermeier, N.; Holzhammer, T.; Bernhardt, G.; Dove, S.; Buschauer, A., Thr190 in the human histamine H_2 receptor (hH_2R) contributes to binding of imidazole type ligands. 6th Summer School Medicinal Chemistry, September 26-28, 2012, University of Regensburg. **2012**.
113. Shin, N.; Coates, E.; Murgolo, N. J.; Morse, K. L.; Bayne, M.; Strader, C. D.; Monsma, F. J., Jr., Molecular modeling and site-specific mutagenesis of the histamine-binding site of the histamine H_4 receptor. *Mol. Pharmacol.* **2002,** *62*, 38-47.
114. Ballesteros, J. A.; Weinstein, H., [19] Integrated Methods for the Construction of Three-Dimensional Models and Computational Probing of Structure-Function Relations in G Protein-Coupled Receptors. In *Methods in Neurosciences*, Sealfon, S. C., Ed. Academic Press: 1995; Vol. 25, pp 366-428.
115. Rasmussen, S. G. F.; DeVree, B. T.; Zou, Y.; Kruse, A. C.; Chung, K. Y.; Kobilka, T. S.; Thian, F. S.; Chae, P. S.; Pardon, E.; Calinski, D.; Mathiesen, J. M.; Shah, S. T. A.; Lyons, J. A.; Caffrey, M.; Gellman, S. H.; Steyaert, J.; Skiniotis, G.; Weis, W. I.; Sunahara, R. K.; Kobilka, B. K., Crystal structure of the β_2 adrenergic receptor–Gs protein complex. *Nature* **2011,** *477*, 549-555.
116. Preuss, H.; Ghorai, P.; Kraus, A.; Dove, S.; Buschauer, A.; Seifert, R., Mutations of Cys-17 and Ala-271 in the human histamine H_2 receptor determine the species selectivity of guanidinetype agonists and increase constitutive activity. *J. Pharmacol. Exp. Ther.* **2007,** *321*, 975-982.
117. Ganellin, R., 1980 Award in medicinal chemistry. Medicinal chemistry and dynamic structure-activity analysis in the discovery of drugs acting at histamine H_2 receptors. *J. Med. Chem.* **1981,** *24*, 913-920.
118. Stark, H., Histamine receptors. *Biotrend Reviews* **2007,** *1*, 1-8.
119. Barry, M.; Feely, J., Enzyme induction and inhibition. *Pharmacol. Ther.* **1990,** *48*, 71-94.
120. Calcutt, C. R.; Ganellin, C. R.; Griffiths, R.; Leigh, B. K.; Maguire, J. P.; Mitchell, R. C.; Mylek, M. E.; Parsons, M. E.; Smith, I. R.; Young, R. C., Zolantidine (SK&F 95282) is a potent selective brain-penetrating histamine H_2-receptor antagonist. *Br. J. Pharmacol.* **1988,** *93*, 69-78.

121. Gajtkowski, G. A.; Norris, D. B.; Rising, T. J.; Wood, T. P., Specific binding of ^{3}H-tiotidine to histamine H_2 receptors in guinea pig cerebral cortex. *Nature* **1983,** *304*, 65-67.
122. Baumeister, P.; Erdmann, D.; Biselli, S.; Kagermeier, N.; Elz, S.; Bernhardt, G.; Buschauer, A., [^{3}H]UR-DE257: development of a tritium-labeled squaramide-type selective histamine H_2 receptor antagonist. *ChemMedChem* **2015,** *10*, 83-93.
123. Malan, S. F.; Marle, A. v.; Menge, W. M.; Zuliana, V.; Hoffman, M.; Timmerman, H.; Leurs, R., Fluorescent ligands for the histamine H_2 receptor: synthesis and preliminary characterization. *Bioorg. Med. Chem.* **2004,** *12*, 6495-6503.
124. Li, L.; Kracht, J.; Peng, S.; Bernhardt, G.; Elz, S.; Buschauer, A., Synthesis and pharmacological activity of fluorescent histamine H_2 receptor antagonists related to potentidine. *Bioorg. Med. Chem. Lett.* **2003,** *13*, 1717-1720.
125. Xie, S.-X.; Petrache, G.; Scheiner, E.; Ye, Q.-Z.; Bernhardt, G.; Seifert, R.; Buschauer, A., Synthesis and pharmacological characterization of novel fluorescent histamine H_2-receptor ligands derived from aminopotentidine. *Bioorg. Med. Chem. Lett.* **2006,** *16*, 3886-3890.
126. Biselli, S.; Alencastre, I.; Tropmann, K.; Erdmann, D.; Chen, M.; Littmann, T.; Maia, A. F.; Gomez-Lazaro, M.; Tanaka, M.; Ozawa, T.; Keller, M.; Lamghari, M.; Buschauer, A.; Bernhardt, G., Fluorescent H_2 receptor squaramide-type antagonists: synthesis, characterization and applications. *ACS Med. Chem. Lett.* **2020,** *11*, 1521-1528.
127. Grätz, L.; Tropmann, K.; Bresinsky, M.; Müller, C.; Bernhardt, G.; Pockes, S., NanoBRET binding assay for histamine H_2 receptor ligands using live recombinant HEK293T cells. *Sci. Rep.* **2020,** *10, e13288*.
128. Cavanagh, R. L.; Buyniski, J. P., Effect of BMY-25368, a potent and long-acting histamine H_2-receptor antagonist, on gastric secretion and aspirin-induced gastric lesions in the dog. *Aliment. Pharmacol. Ther.* **1989,** *3*, 299-313.
129. Brittain, R. T.; Jack, D.; Reeves, J. J.; Stables, R., Pharmacological basis for the induction of gastric carcinoid tumours in the rat by loxtidine, an insurmountable histamine H_2-receptor blocking drug. *Br. J. Pharmacol.* **1985,** *85*, 843-847.
130. Washington, N., *(1991) Antacids and Anti Reflux Agents*. Boca Raton: CRC Press.
131. Poynter, D.; Pick, C. R.; Harcourt, R. A.; Selway, S. A.; Ainge, G.; Harman, I. W.; Spurling, N. W.; Fluck, P. A.; Cook, J. L., Association of long lasting unsurmountable histamine H_2 blockade and gastric carcinoid tumours in the rat. *Gut* **1985,** *26*, 1284-1295.

2 Discovery of a G Protein Biased Radioligand for the Histamine H_2 Receptor with Reversible Binding Properties

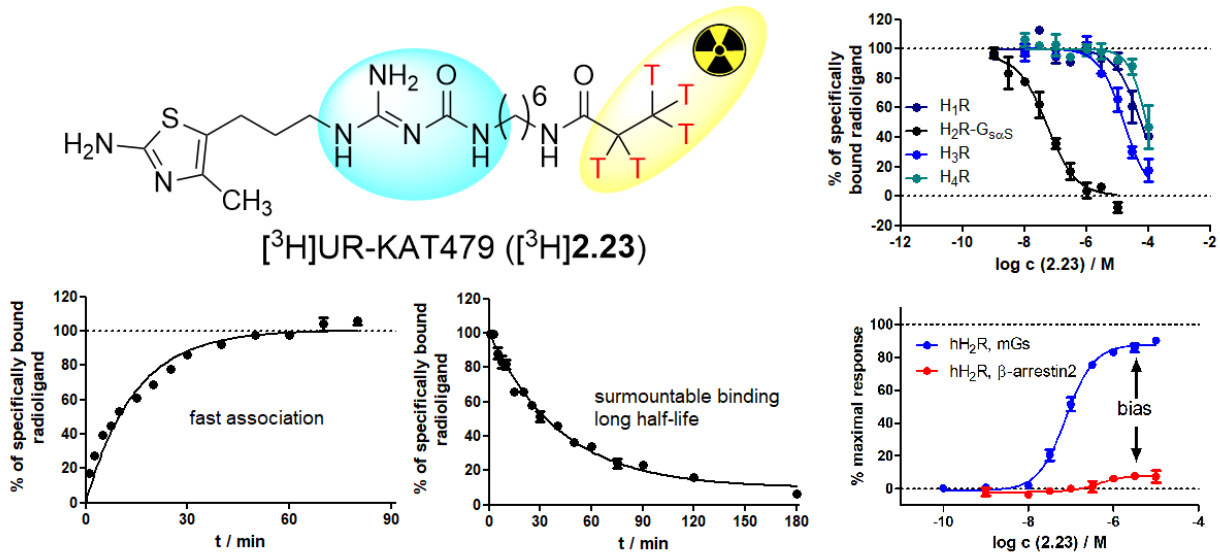

Currently employed histamine H_2 receptor (H_2R) radioligands possess several drawbacks, e.g. high non-specific, insurmountable binding, or short half-life. We report the synthesis and the chemical- and pharmacological characterization of the highly stable carbamoylguanidine-type radioligand [^{3}H]UR-KAT479 ([^{3}H]**2.23**), a subtype selective histamine H_2 receptor G protein biased agonist. [^{3}H]**2.23** was characterized in saturation, kinetic and competition binding assays at human, guinea pig and mouse H_2 receptors (co-)expressed in HEK293(T) cells. [^{3}H]**2.23** reversibly bound to the respective H_2Rs with moderate to high affinity (human/guinea pig/mouse: K_d 24/28/94 nM). In order to investigate the applicability of carbamoylguanidine-type ligands in animal studies elucidating the role of the H_2R in the brain, we performed a preliminary partitioning experiment in whole human/mouse blood, which indicated a low binding of [^{3}H]**2.23** to red blood cells. These properties turn [^{3}H]**2.23** into a powerful tool for the determination of binding affinities and demonstrate the promising pharmacokinetic profile of carbamoylguanidine-type ligands.

This chapter has been published in:

K. Tropmann, C. Höring, N. Plank, and S. Pockes, *J. Med. Chem.* **2020**, *63*, 13090-13102

Author contributions:

K.T. conceived the project with input from S.P.; K.T. performed the synthesis and the analytical characterization of the chemical compounds; K.T. and S.P. performed the radiosynthesis and analytical characterization of the radioligand; K.T. performed and analyzed the radioligand binding (saturation, competition, kinetic)-, β-arrestin2 recruitment-, mini-G recruitment-, and RBC proportioning experiments with supervision from S.P.; C.H. cloned the pcDNA3.1(+) gpH_2R-NlucC vector, generated the HEK293T NlucN-mGs/gpH_2R-NlucC cell line and established the mini-G protein recruitment assay for gpH_2R; N.P. cloned the pcDNA3.1 gpH_2R vector and generated the HEK293T-CRE-Luc-gpH_2R cell line; K.T. and S.P. wrote the manuscript with input from all co-authors.

2.1 Introduction

The human histamine H_2 receptor (H_2R) has been subject of many research studies due to its interesting and versatile physiological properties.[1-2] It belongs to class A G protein-coupled receptors (GPCRs) and is expressed throughout the whole human body, including brain, uterus, airways, gastric parietal cells and the cardiac tissues.[1-4] The stimulation of the H_2R has positive inotropic and chronotropic effects in atrial and ventricular tissues[5], but its most prominent effect is the stimulation of gastric acid secretion.[2, 6] Therefore, many H_2R antagonists were developed by academia and the pharmaceutical industry to treat the gastroesophageal reflux disease and gastroduodenal ulcers.[1, 7] On the other hand, H_2R agonists did not find broad application as drug molecules, but are used as molecular tools for pharmacological investigations and might contribute to a better understanding of the until today widely unknown role of the H_2R in the CNS.

Within the last decades many radioactively labeled agonists (**2.1**-**2.3**) and antagonists (**2.4**-**2.5**, **2.7**-**2.10**) for the H_2R were developed (Figure 2.1A).[8-21] However, most of these ligands possess significant drawbacks which hamper their ability to study the H_2R accurately: e.g. Wood et al. found that [^{3}H]cimetidine (**2.4**) binds to an imidazole recognition site rather than to the H_2R ligand binding domain.[11] Furthermore, the H_2R affinities and potencies of histamine (**2.1**) and ranitidine (**2.5**) are low, limiting their application potential as molecular tools.[20, 22] Although [^{3}H]tiotidine (**2.7**) is often employed as a radioligand in biological assays, it is reported that it has a very high non-specific binding and addresses only a subpopulation of the H_2R.[19-20] Moreover, [^{125}I]iodoaminopotentidine (**2.9**) turned out to be a potent radioligand, which was used for autoradiography of the H_2R in primates (human/non-human (brain)) and rodents (brain/heart), as well as for saturation, competition and kinetic binding studies.[22-24] The downside of **2.9** is, however, that the preparation and usage of [^{125}I]-labeled molecules requires higher safety precautions compared to tritiated compounds and that the ligands can only be used for 4-5 weeks after preparation, due to their short half-life.[25] To deal with these drawbacks, our group recently published the high affinity, potent and tritium labeled H_2R antagonist [^{3}H]UR-DE257[25] (**2.10**), which is structurally related to the squaramide BMY-25368[26] (**2.11**, Figure 2.1A), as an alternative to [^{125}I]iodoaminopotentidine.[25] **2.10** proved to be very useful for the determination of pK_i values, but turned out to be an insurmountable antagonist in functional and kinetic assays.[25]

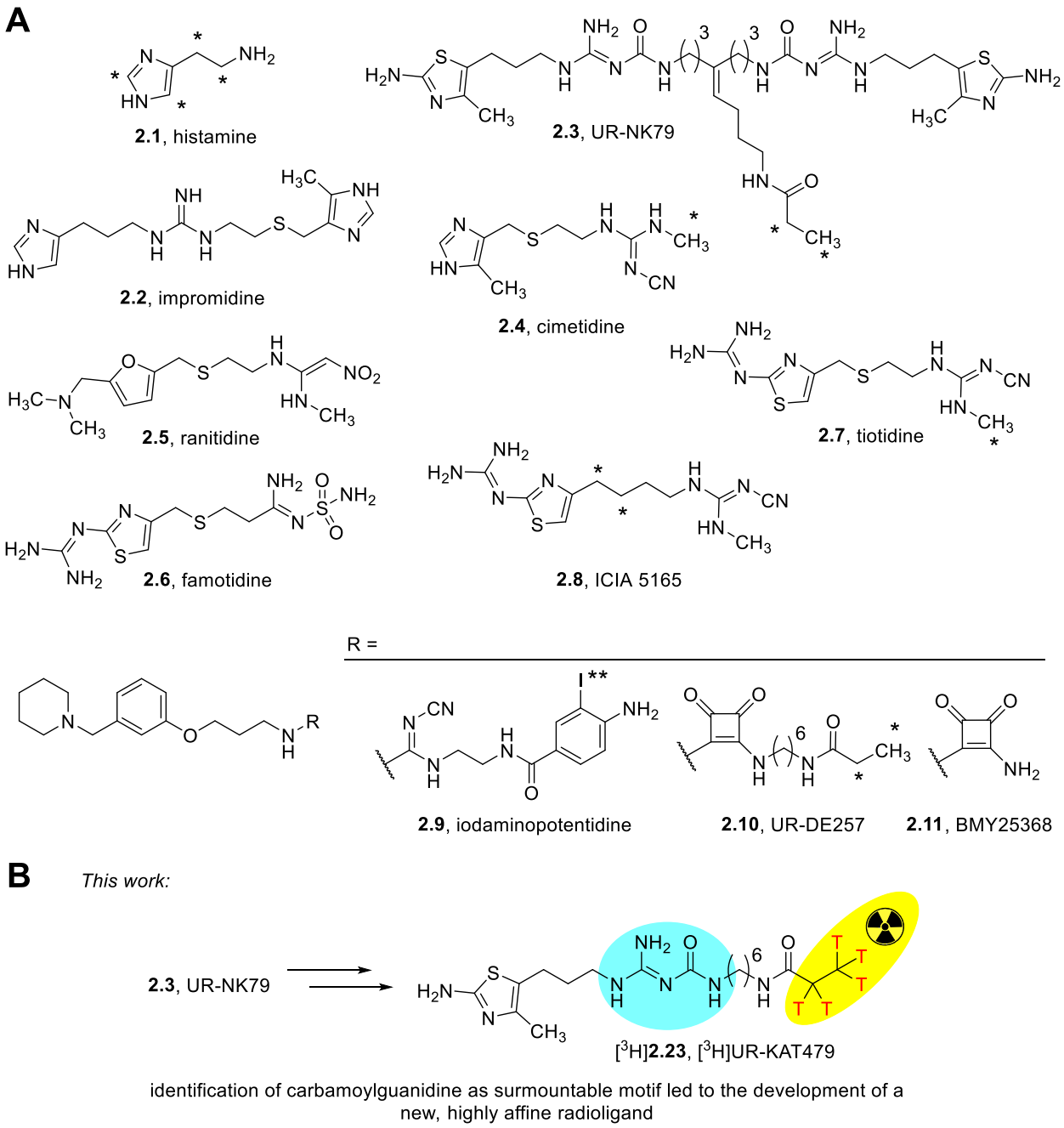

Figure 2.1. A: Structures of the endogenous ligand histamine (**2.1**), impromidine (**2.2**), the dimeric agonist UR-NK79[9] (**2.3**) and selected standard H_2R antagonists (**2.4**-**2.11**). **B**: Our approach for the synthesis of a new, high affinity, and surmountable radioligand as molecular tool for the exploration of the H_2R functions. *[^{3}H]-labeled position(s). For impromidine and ranitidine the exact location of the tritium label was not indicated in the literature. **[^{125}I]-labeled position. Famotidine and BMY-25368 have not been synthesized in radiolabeled form.

These findings motivated us to develop a new, high affinity but surmountable H_2R radioligand. Despite the high non-specific binding of [^{3}H]**2.3**, we considered carbamoylguanidine-containing amines as promising precursors for further optimization (Figure 2.1B), as some observations indicated an improved kinetic behaviour.[9] This study presents the synthesis and pharmacological characterization (saturation-, kinetic- and competition experiments) of [^{3}H]UR-KAT479 ([^{3}H]**2.23**) at human (h), guinea pig (gp) and mouse (m) H_2Rs (co)expressed in HEK293(T) cells. Although the rat is more commonly used to study species differences, we chose to investigate the guinea pig because of its historic significance for the development and evaluation of antihistamines in general and for H_2R ligands in particular.[3, 8, 11, 15, 18-20, 22, 25] We believe that [^{3}H]**2.23** could act as model substance for other carbamoylguanidine-type H_2R agonists and could be used to explore the pharmacokinetic properties of this compound class in more detail. The obtained in vitro results (especially on the mouse H_2R) should build the basis for future in vivo experiments to clarify the widely unknown role of the H_2R in the CNS.

2.2 Results and Discussion

2.2.1 Chemistry

The synthesis of the radioligand candidates was straight forward (Scheme 2.1). In the first step, the mono-Boc protected diamines **2.14**-**2.16** were treated with triphosgene to give the corresponding isocyanates, which were allowed to react with mono-Boc-protected *S*-methylisothiourea **2.13** to give the guanidinylating reagents **2.17**-**2.19**. The corresponding Boc-protected intermediates were prepared by treating the amine building block **2.12**[27] with **2.17**-**2.19** in presence of $HgCl_2$ and base. Addition of TFA gave the amine precursors **2.20**-**2.22**, which were finally propionylated with *N*-succinimidyl propionate giving the amides **2.23**-**2.25**.

Scheme 2.1. Synthesis of the Carbamoylguanidine Containing Amines 2.20-2.22 and the Resulting Propionylated Amides 2.23-2.25[a]

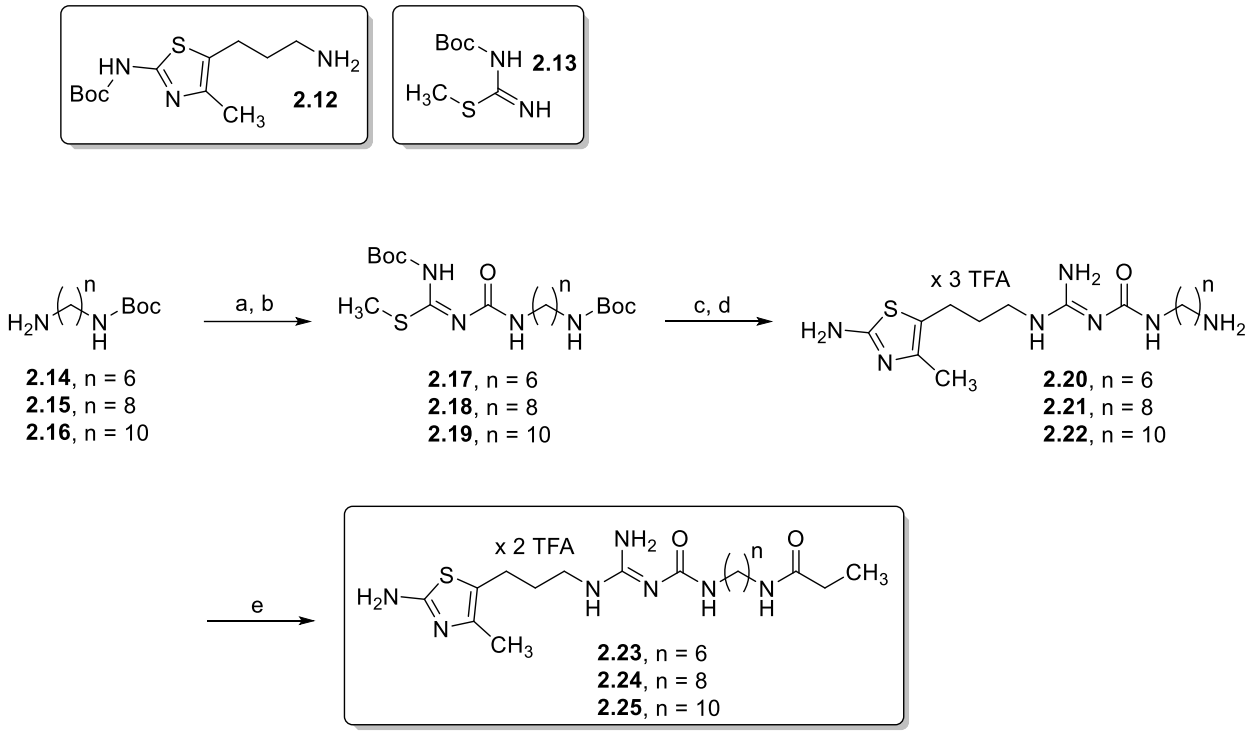

[a]Reagents and conditions: (a) triphosgene, DIPEA, CH_2Cl_2, 0 °C, 30 min; (b) **2.13**, rt, 2.5 h, **2.17**: 38%, **2.18**: 17%, **2.19**: 15% over two steps; (c) **2.12**, NEt_3, $HgCl_2$, CH_2Cl_2, rt, 4-16 h; (d) 30% TFA, CH_2Cl_2, rt, 7-18 h, **2.20**: 48%, **2.21**: 36%, **2.22**: 25% over two steps; (e) *N*-succinimidyl propionate, NEt_3, DMF, rt, 2 h, **2.23**: 47-78%, **2.24**: 75%, **2.25**: 42%.

2.2.2 H_2R Affinity and Receptor Subtype Selectivity

To investigate the affinities of the compounds **2.20**-**2.25** at the four hHR subtypes, competition binding studies were performed using the radioligands [^{3}H]mepyramine (hH_1R), [^{3}H]**2.10**[25] (hH_2R-$G_{s\square S}$), [^{3}H]N^{α}-methylhistamine or [^{3}H]UR-PI294[28] (hH_3R) and [^{3}H]**2.1** (hH_4R) and membranes of Sf9 insect cells expressing the respective hHR (Table 2.1). Among the studied amides, **2.23**, containing a hexyl spacer, exhibited the highest affinity at the hH_2R-$G_{s\alpha S}$ fusion protein, and the highest selectivity over the other three hHR subtypes (K_i ($H_{1,3,4}R$)/K_i (H_2R) >380, Table 2.1). Following these promising results, we further determined the pK_i value of **2.23** towards the hH_2R, expressed in HEK293T cells. The reason for this is that the affinity of H_2R

agonists on HEK293T cells may be lower than the affinity to the hH_2R-$G_{s\alpha S}$ fusion protein expressed in Sf9 membranes, which was recently reported.[29] Fortunately, the pK_i value of **2.23** using HEK293T cells (pK_i = 7.78, Table 2.1) agreed with the pK_i value determined using Sf9 membranes (pK_i = 7.59, Table 2.1). Since the pK_i value at the gpH_2R-$G_{s\alpha S}$ (pK_i = 7.94, Table 2.1) also matched the value at the hH_2R-$G_{s\alpha S}$, we chose amide **2.23** for the preparation of the corresponding radioligand [^{3}H]**2.23** (Figure 2.5A).

Table 2.1. Binding Data of the Compounds 2.20-2.25 on Human Histamine Receptor Subtypes[a]

	pK_i								H_2R selectivity K_i ($H_{1,3,4}R$)/K_i (H_2R)		
compd.	hH_1R[b]	N	hH_2R-$G_{s\alpha S}$[c]	N	hH_3R[d,e]	N	hH_4R[f]	N	H_1	H_3	H_4
His	5.62 ± 0.03[30]	3	6.58 ± 0.04[31]	48	7.59 ± 0.01[31]	42	7.60 ± 0.01[31]	45	9	0.1	0.1
2.20	5.03 ± 0.10	3	6.88 ± 0.10	5	<5[d,e]	3	<5	3	71	>76	>76
2.21	6.71 ± 0.04	3	7.66 ± 0.17	3	5.06 ± 0.10[e]	3	<5	3	9	398	>457
2.22	6.80 ± 0.04	3	7.85 ± 0.17	3	5.82 ± 0.07[e]	3	5.36 ± 0.17	3	11	107	309
2.23	<5	3	7.59 ± 0.12	3	4.91 ± 0.17[e]	3	<5	4	>389	479	>389
	HEK293T:		7.78 ± 0.11[g]	3							
	gpH_2R-$G_{s\alpha S}$:		7.94 ± 0.12[h]	3							
2.24	5.26 ± 0.09	3	7.40 ± 0.02	3	<5[e]	3	<5	3	138	>251	>251
2.25	5.17 ± 0.05	3	7.12 ± 0.09	3	5.12 ± 0.11[e]	3	5.23 ± 0.01	3	89	100	78

[a]Competition binding assay at membranes of Sf9 cells expressing the hH_1R + RGS4, the hH_2R-$G_{s\alpha S}$, the hH_3R + $G_{\alpha i2}$ + $G_{\beta 1\gamma 2}$ or the hH_4R + $G_{\alpha i2}$ + $G_{\beta 1\gamma 2}$. Data shown are mean values ± SEM of N independent experiments, each performed in triplicate. Data were analyzed by nonlinear regression and were best fitted to sigmoidal concentration-response curves. The displacement curves are presented in Figure 2.2 & 2.3. [b]Displacement of 5 nM [^{3}H]mepyramine (K_d = 4.5 nM[9]). [c]Displacement of 20 nM [^{3}H]**2.10**[25] (K_d = 12.1 nM[29]). [d]Displacement of 8.6 nM [^{3}H]N^{α}-methylhistamine (K_d = 3 nM[31]). [e]Displacement of 2 nM [^{3}H]UR-PI294[28] (K_d = 3 nM). [f]Displacement of 30 nM [^{3}H]**2.1** (K_d = 47.5 nM[32]). [g]pK_i value obtained in competition binding with [^{3}H]**2.10**[25] (c = 25 nM, K_d = 40 nM) using HEK293T-hH_2R-qs5-HA cells[33]. [h]pK_i value obtained in competition binding with [^{3}H]**2.10**[25] (c = 30 nM, K_d = 37 nM[25]) using membranes of Sf9 cells expressing the gpH_2R-$G_{s\alpha S}$.

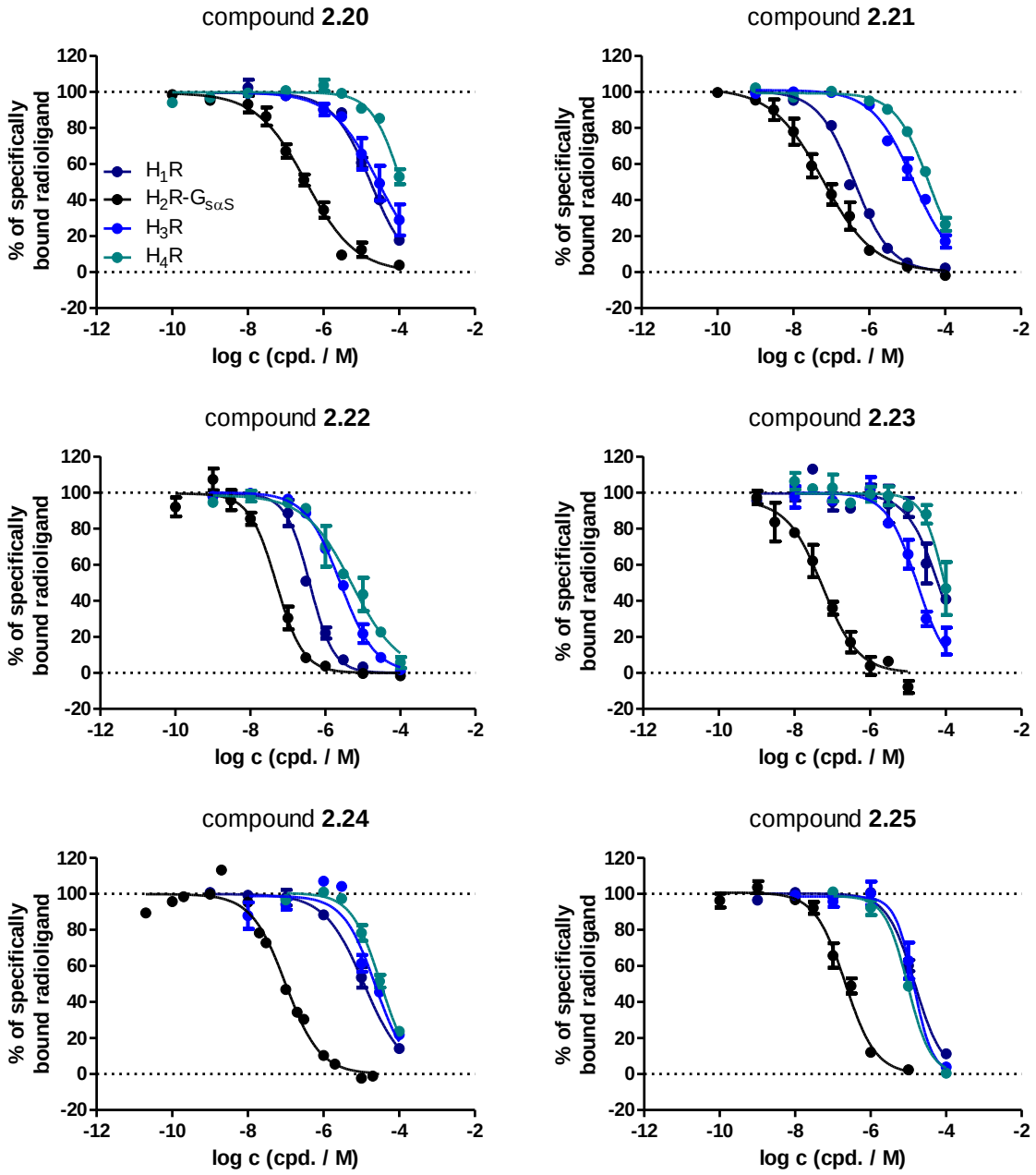

Figure 2.2. Displacement curves obtained from competition binding experiments with [^{3}H]mepyramine[9] (hH_1R, c = 5 nM, K_d = 4.5 nM[9]), [^{3}H]**2.10**[25, 29] (hH_2R, c = 20 nM, K_d = 12.1 nM[25]), [^{3}H]UR-PI294[28] (hH_3R, c = 2 nM, K_d = 3 nM) or [^{3}H]**2.1**[32] (hH_4R, c = 30 nM, K_d = 47.5 nM[32]) and **2.20**-**2.25** at membranes of Sf9 cells expressing the hH_1R + RGS4, the hH_2R-$G_{s\alpha S}$, the hH_3R + $G_{\alpha i2}$ + $G_{\beta 1\gamma 2}$ or the hH_4R + $G_{\alpha i2}$ + $G_{\beta 1\gamma 2}$ or at intact HEK293T-hH_2R-qs5-HA cells[33]. Data represent mean values ± SEM from at least three independent experiments (performed in triplicate).

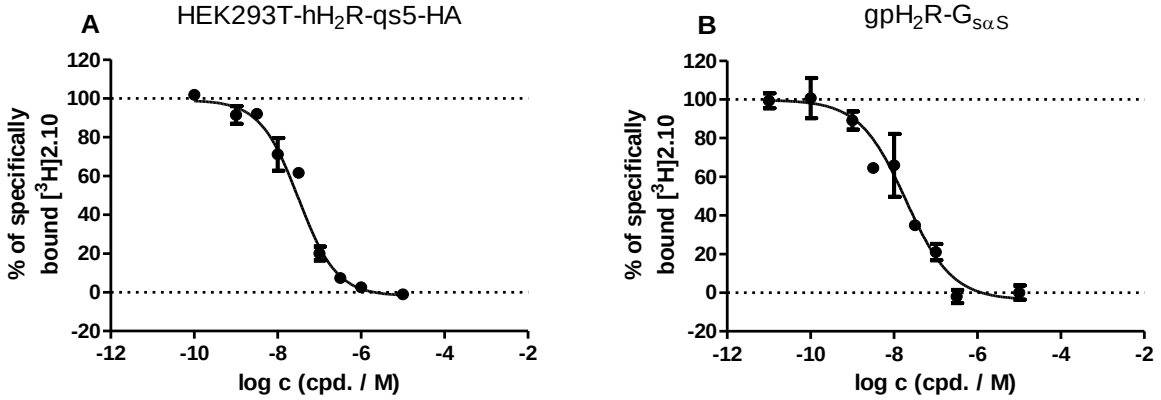

Figure 2.3. A. Displacement curves obtained from competition binding with [^{3}H]**2.10**[25] (c = 25 nM, K_d = 40 nM) and **2.23** using HEK293T-hH_2R-qs5-HA cells[33]. **B.** Displacement curves obtained from competition binding with [^{3}H]**2.10**[25] (c = 30 nM, K_d = 37 nM[25]) and **2.23** using membranes of Sf9 cells expressing the gpH_2R-$G_{s\alpha S}$ fusion protein. Data represent mean values ± SEM from three independent experiments (performed in triplicate).

2.2.3 Functional Studies at the Human and Guinea Pig H_2R

The target compounds **2.20**-**2.25** were investigated for H_2R agonism in both β-arrestin2 and mini-G protein recruitment assays using genetically engineered HEK293T cells. The results are presented in Table 2.2. The responses in both assays were normalized to the maximum effect induced by 100 µM histamine (E_{max} = 1.00) and buffer control (E_{max} = 0). Thus, histamine is defined as a full, unbiased agonist in either readout. Histamine exhibits a significantly lower potency in the β-arrestin2 recruitment assay compared to the mini-G protein recruitment assay (pEC_{50} (β-arrestin2) = 5.42; pEC_{50} (mGs) = 6.94; Table 2.2). Similarly, the potencies of the investigated N^G-carbamoylated guanidines were lower in the β-arrestin2 recruitment assay. A possible explanation for this trend could be the employed mGs protein, since mG proteins have been reported to stabilize the active states of GPCRs, which favours agonist binding.[34-37]

All tested ligands were strong partial agonists in the mini-G protein recruitment assay (E_{max} = 0.83 - 0.88, Table 2.2) and only weak partial agonists in the β-arrestin2 recruitment assay (E_{max} = 0.07 - 0.28, Table 2.2). This discrepancy results in a significant G protein bias of the propionylated amides **2.23**-**2.25** (for detailed bias analysis see Appendix 1, App1.4 Bias Analysis

for Compounds **2.20**-**2.25**). A key advantage of such agonistic G protein biased ligands is that they are unlikely to be internalized due to their low β-arrestin2 recruitment and therefore can also be applied to cells without taking any measures against internalization (e.g. hypotonic buffer).[38]

The obtained pEC_{50} values were in good agreement with the pK_i values from the radioligand competition binding assays, especially in the case of the mini-G protein recruitment assay (Table 2.2). In the mini-G protein recruitment assay at the gpH_2R, **2.20**-**2.25** were strong partial agonists with slightly increased potencies. Moreover, **2.23** was investigated for agonist-induced chronotropic response at the guinea-pig right atrium as a more complex, but well established model for the characterization of H_2R ligands under more physiological conditions.[1] **2.23** acted as a strong partial agonist (E_{max} = 0.90) in this assay with a pEC_{50} value of 7.47 (Table 2.2), which is similar to the result observed in the mini-G protein recruitment assay.

Table 2.2. Potencies and Efficacies of the Tested Carbamoylated Guanidines in the β-Arrestin2 and Mini-G Protein Recruitment Assay at the Human or Guinea Pig H_2R[a]

	human H_2R						guinea pig H_2R		
	β-arrestin2 recruitment[b]			mGs recruitment[c]			mGs recruitment[d]		
compd.	pEC_{50}[e]	E_{max}[f]	N	pEC_{50}[e]	E_{max}[f]	N	pEC_{50}[e]	E_{max}[f]	N
His	5.42 ± 0.02[39]	1.00[39]	3	6.94 ± 0.06[37]	1.00[37]	9	6.60 ± 0.07	1.00	3
2.20	6.55 ± 0.22	0.28 ± 0.01	3	7.53 ± 0.03	0.83 ± 0.02	3	7.89 ± 0.05	0.87 ± 0.01	3
2.21	6.87 ± 0.12	0.23 ± 0.01	4	7.84 ± 0.04	0.84 ± 0.03	3	7.94 ± 0.08	0.85 ± 0.01	3
2.22	6.91 ± 0.10	0.15 ± 0.01	4	7.83 ± 0.12	0.85 ± 0.02	3	8.04 ± 0.08	0.83 ± 0.01	3
2.23	6.53 ± 0.08	0.07 ± 0.02	4	7.61 ± 0.04	0.88 ± 0.01	3	7.74 ± 0.04	0.83 ± 0.01	3
							7.47 ± 0.07[g]	0.90 ± 0.10[g]	3
2.24	7.06 ± 0.05	0.10 ± 0.02	4	7.89 ± 0.05	0.87 ± 0.02	3	7.94 ± 0.03	0.87 ± 0.09	3
2.25	6.80 ± 0.09	0.12 ± 0.01	3	7.66 ± 0.03	0.88 ± 0.01	3	7.72 ± 0.07	0.89 ± 0.01	3

[a]Data represent mean values ± SEM from N independent experiments, each performed in triplicate. Data were analyzed by nonlinear regression and were best fitted to sigmoidal concentration-response curves (for curves see Figure 2.4). [b]β-arrestin2 recruitment assays were performed with a HEK293T-ARRB2-H_2R[39] cell line as described by Grätz et al.[29] [c]Mini-G protein recruitment assays were performed with a HEK293T NlucN-mGs/hH_2R-NlucC cell line as described by Höring et al.[37] [d]Mini-G protein recruitment assays were performed with a HEK293T NlucN-mGs/gpH_2R-NlucC cell line as described in the Appendix 1, App1.2 Mini-G Protein Recruitment Assay at HEK293T Cells Expressing NlucN-mGs/gpH_2R-NlucC. [e]pEC_{50} = -logEC_{50}. [f]The response in both assays was normalized to the maximal effect induced by 100 µM histamine (E_{max} = 1.00) and buffer control (E_{max} = 0.00). [g]pEC_{50} and E_{max} values determined at the guinea pig right atrium. Experiments on the isolated, spontaneously beating guinea pig right atrium were performed as described by Pockes et al.[31]

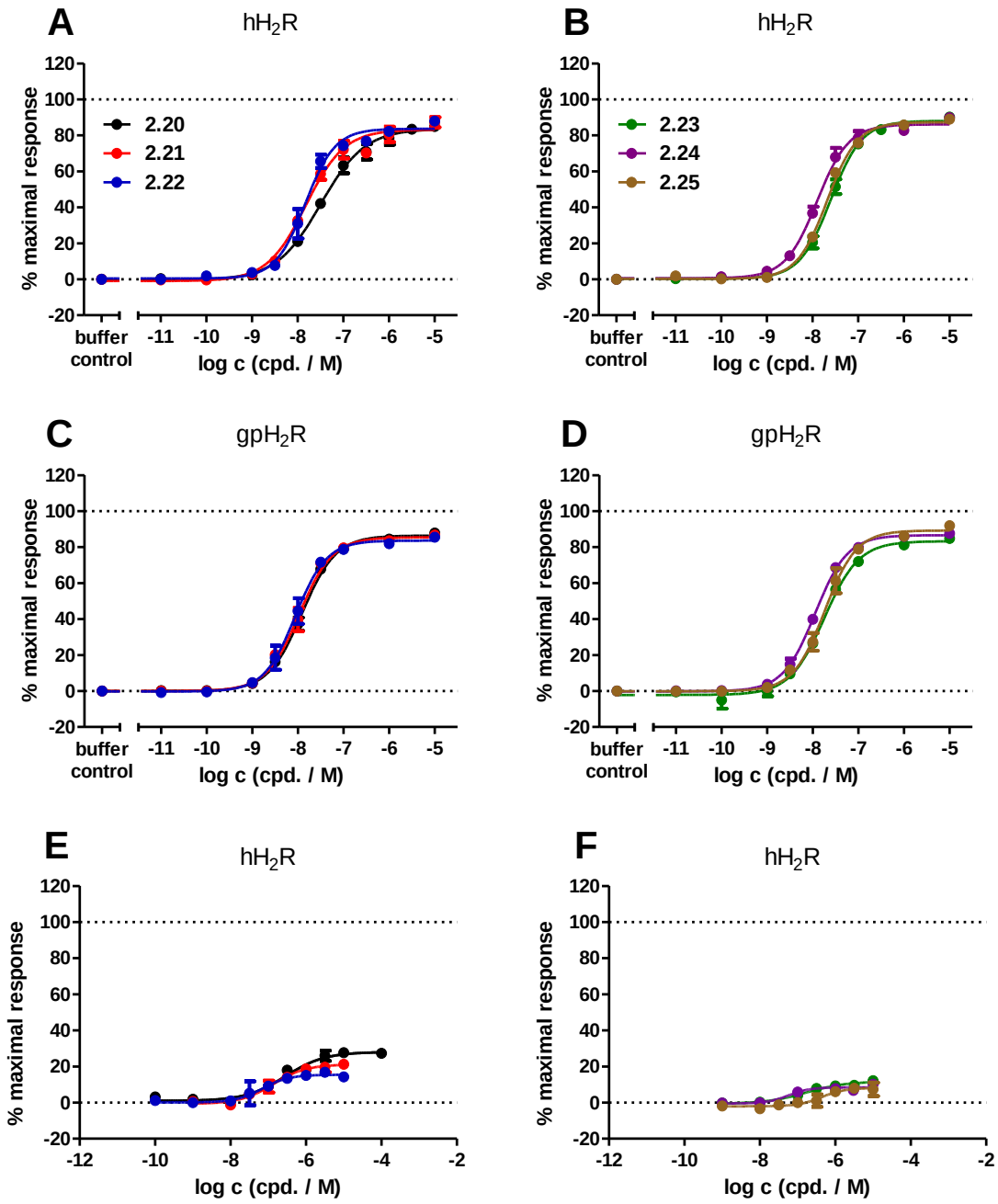

Figure 2.4. Investigation of H_2R agonism of **2.20**-**2.25** in the mini-G protein recruitment assay using HEK293T NlucN-mGs/hH_2R-NlucC cells (**A**: **2.20**-**2.22** and **B**: **2.23**-**2.25**) or HEK293T NlucN-mGs/gpH_2R-NlucC cells (**C**: **2.20**-**2.22** and **D**: **2.23**-**2.25**) and in the β-arrestin2 recruitment assay using HEK293T-ARRB2-H_2R cells[39] (**E**: **2.20**-**2.22** and **F**: **2.23**-**2.25**).. The response in both assays was normalized to the maximal effect induced by 100 µM histamine (maximal response: 100%) and buffer control (maximal response: 0%). Data represent mean values ± SEM from at least three independent experiments (performed in triplicate).

2.2.4 Synthesis of the Radiolabeled Ligand [^{3}H]2.23

Based on the results obtained in the assays, **2.23** was selected for the synthesis of the corresponding tritiated ligand. A 9-fold excess of the precursor **2.20** was treated with commercially available succinimidyl [^{3}H]propionate in the presence of triethylamine at room temperature (Figure 2.5A). [^{3}H]**2.23** was isolated by RP-HPLC in high (radio)chemical purity (≥98%, Figure 2.5B). After storage of [^{3}H]**2.23** in EtOH/H_2O (70:30) at -20 °C for 9 months, approx. 3% were decomposed (Figure 2.5C), showing that [^{3}H]**2.23** has a high chemical stability. Moreover, the chemical stability of the "cold" form **2.23** in binding buffer[9] (pH 7.4) at 23 °C was investigated for 2 weeks. Under these conditions, compound **2.23** proved to be stable. For details see the chemical stability section in the Experimental Section and for chromatograms see Figure 2.6.

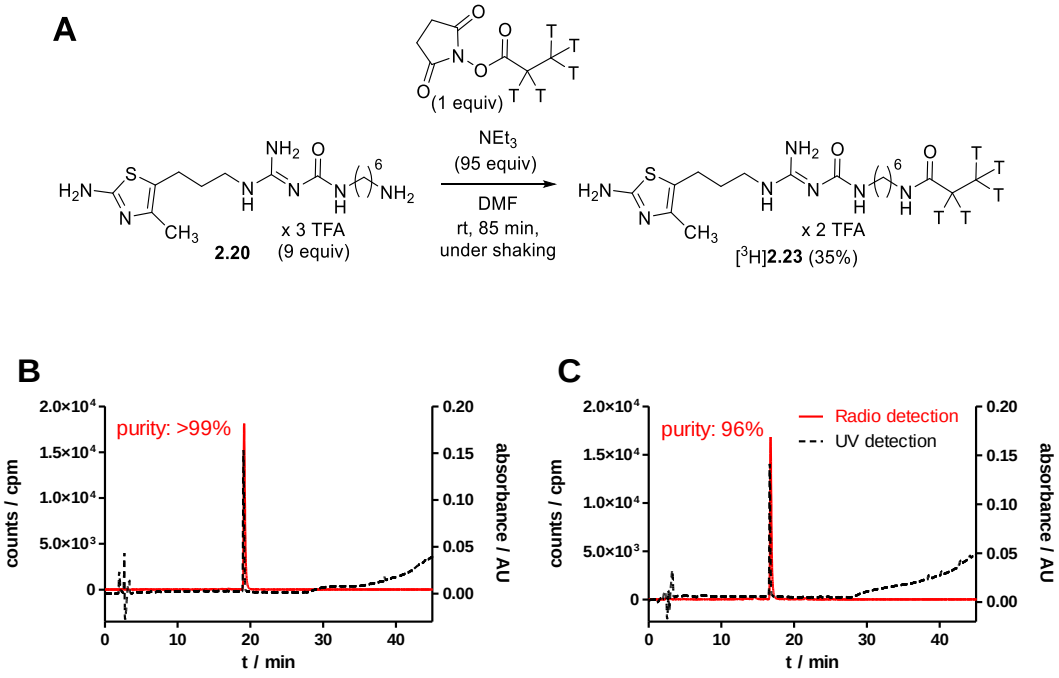

Figure 2.5. Synthesis, analytical characterization, and long-term stability of [^{3}H]**2.23**. **A**: Synthesis of [^{3}H]**2.23** by propionylation of the precursor **2.20**. Radiochemical yield 35%. **B**: Chromatograms of [^{3}H]**2.23**, spiked with the "cold" form of **2.23**, recorded 36 days after synthesis. **C**: Long-term stability test after 9 months of storage at -20 °C in EtOH/H_2O (70:30) using radiometric and UV detection (for details see Experimental Section). The same stock solution of **2.23** was used for spiking in both HPLC runs and the identity of **2.23** was verified at both time points by means of LC-HRMS. The minor differences in t_R result from serial detection of the UV and radiometric signals.

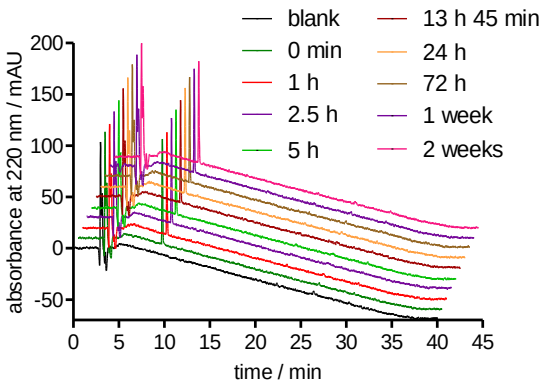

Figure 2.6. Chromatograms of **2.23** after different periods of incubation in binding buffer (pH 7.4) at rt.

2.2.5 Saturation Binding Experiments Using [^{3}H]2.23

The radioligand [^{3}H]**2.23** was characterized by saturation binding experiments using HEK293T-hH_2R-qs5-HA cells[33], HEK293T-CRE-Luc-gpH_2R cells or HEK293-mH_2R cells in suspension. All cells stably expressed the respective H_2R. Representative saturation binding curves and the corresponding Scatchard plots are depicted in Figure 2.7. The specific binding of [^{3}H]**2.23** was best fitted by nonlinear regression to a one-site binding model and the non-specific binding by linear regression. [^{3}H]**2.23** bound to all H_2R orthologs in a saturable manner revealing comparable K_d values at the h/gpH_2R (K_d (hH_2R) = 23.6 nM; K_d (gpH_2R) = 27.8 nM, Table 2.4) with the exception of the mH_2R (K_d = 94.3 nM, Table 2.4). The determined K_d values were similar to the K_i values obtained for unlabeled compound **2.23** in competition binding assays with [^{3}H]**2.10** (hH_2R: 16.6 nM (HEK293T), 25.7 nM (Sf9); gpH_2R: 11.5 nM (Sf9), Table 2.1). In general, the non-specific binding determined in the presence of **2.6** (1 mM, Figure 2.1A) was low (3 - 14% at c = K_d, cf. Figure 2.7).

Since the H_2R has historically been studied in dogs (Heidenhain pouch), we wanted to elucidate the affinity of the new radioligand [^{3}H]**2.23** at the canine H_2R (cH_2R).[40-41] We investigated it on cH_2R-$G_{s\alpha S}$ Sf9 insect cell membrane preparations.[20, 42] The obtained K_d value is in good agreement with the K_d values at the hH_2R-$G_{s\alpha S}$ and gpH_2R-$G_{s\alpha S}$, which were also recorded on Sf9 membrane preparations for a better comparison (cf. Figure 2.8 and Table 2.3).

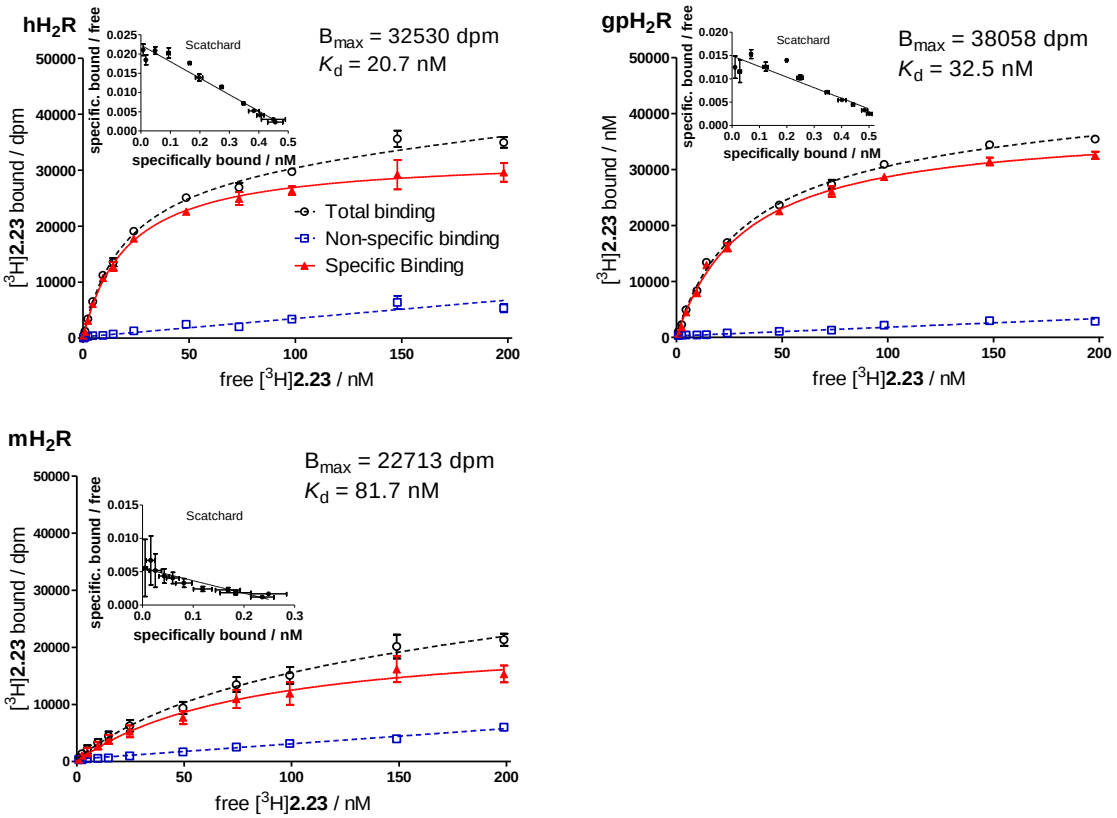

Figure 2.7. Representative data from saturation binding experiments at the hH_2R, co-expressed in HEK293T-qs5-HA cells[33], the gpH_2R, co-expressed in HEK293T-CRE-Luc cells and the mH_2R, expressed in HEK293 cells. Total binding (dashed black curve), specific binding (red curve), and non-specific binding (dashed blue line, determined in the presence of **2.6** (1 mM)) of [^{3}H]**2.23** are depicted. Inserts: Scatchard transformations of shown specific binding curves. The experiments were performed in triplicate. Error bars of specific binding and Scatchard plots were calculated according to the Gaussian law of error propagation. Error bars of total and non-specific binding represent SEMs.

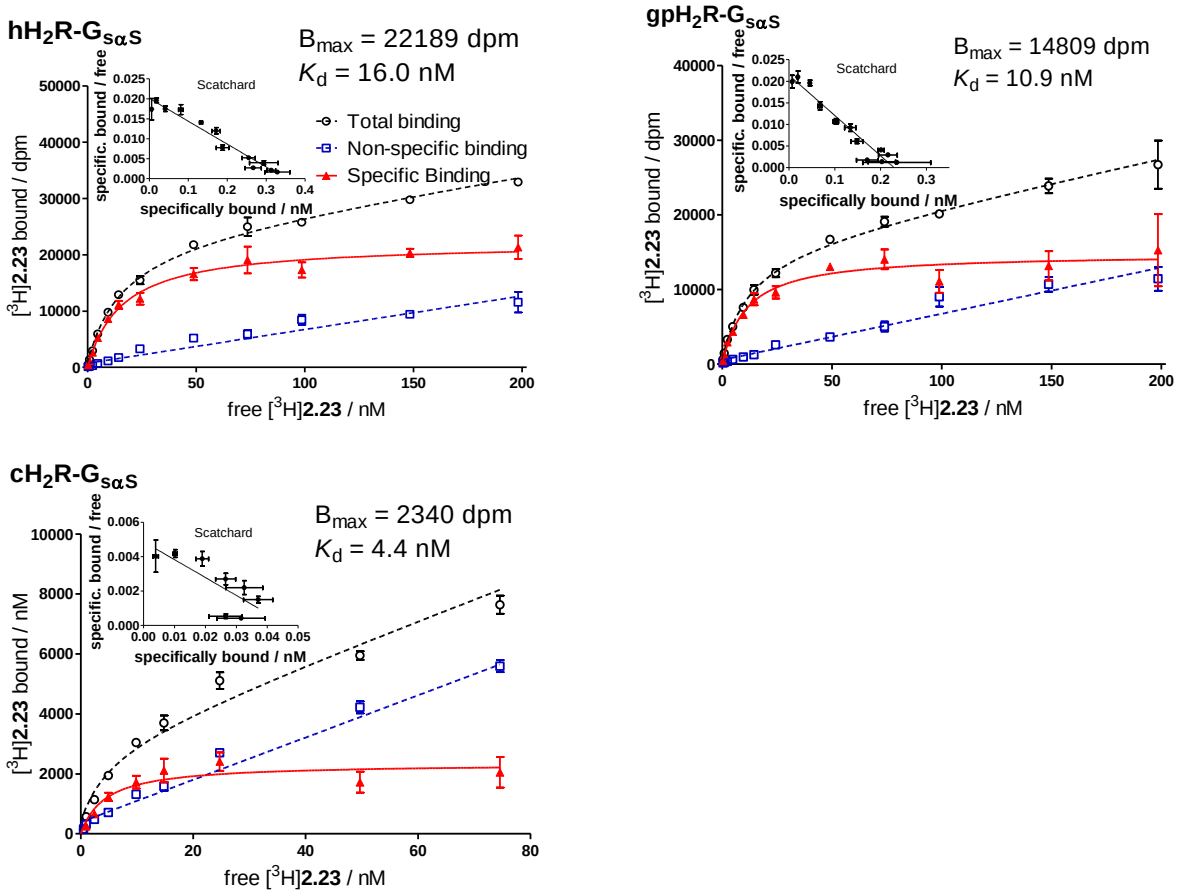

Figure 2.8. Representative data from saturation binding experiments at the hH_2R-$G_{s\alpha S}$, gpH_2R-$G_{s\alpha S}$ or cH_2R-$G_{s\alpha S}$ fusion proteins, expressed in membrane preparations of Sf9 insect cells. Total binding (dashed black curve), specific binding (red curve), and nonspecific binding (dashed blue line, determined in the presence of famotidine (1 mM)) of [^{3}H]**2.23** are depicted. Inserts: Scatchard transformations of shown specific binding curves. The experiments were performed in triplicate. Error bars of specific binding and in the Scatchard plots were calculated according to the Gaussian law of error propagation. Error bars of total and nonspecific binding represent SEMs.

Table 2.3. K_d Values of [^{3}H]2.23 on Membrane Preparations of Sf9 Cells Expressing the hH$_2$R-G$_{s\alpha S}$, gpH$_2$R-G$_{s\alpha S}$ or cH$_2$R-G$_{s\alpha S}$ Fusion Proteins[a]

H$_2$R-G$_{s\alpha S}$	K_d [nM]	N
h	14.6 ± 1.7	3
gp	13.2 ± 1.4	3
c	4.6 ± 0.2	3

[a]Data are mean values ± SEM of three independent experiments, each performed in triplicate.

2.2.6 Kinetic Binding Experiments Using [^{3}H]2.23

To further characterize [^{3}H]**2.23**, kinetic binding experiments were performed using HEK293T-hH$_2$R-qs5-HA cells[33], HEK293T-CRE-Luc-gpH$_2$R cells or HEK293-mH$_2$R cells in suspension. The association and dissociation curves of [^{3}H]**2.23** are depicted in Figure 2.9. The association of the radioligand to the ortholog H$_2$Rs was complete after 60 min and could be described by a monophasic fit with k_{on} values ranging from 0.00011 to 0.00164 min^{-1} x nM^{-1} (cf. Figure 2.9 & Table 2.4). k_{obs} (approx. 0.06 min^{-1} (h/gp/m) (Table 2.4)) was calculated from the linearization of the association curve. The dissociation of [^{3}H]**2.23** (h/gpH$_2$R: c = 25 nM, mH$_2$R: c = 50 nM, 120 min preincubation) in the presence of **2.6** (1500-fold excess) was performed using HEK293(T) cells. The obtained data suggested a reversible binding and the equilibrium dissociation constants, calculated from kinetics ($K_d = k_{off}/k_{on}$, 24.7 nM (h), 12.8 nM (gp), 551.5 nM (m), Table 2.4), were consistent with the K_d values obtained from saturation binding experiments (23.6 nM (h), 27.8 nM (gp), 94.3 nM (m); cf. Table 2.4).

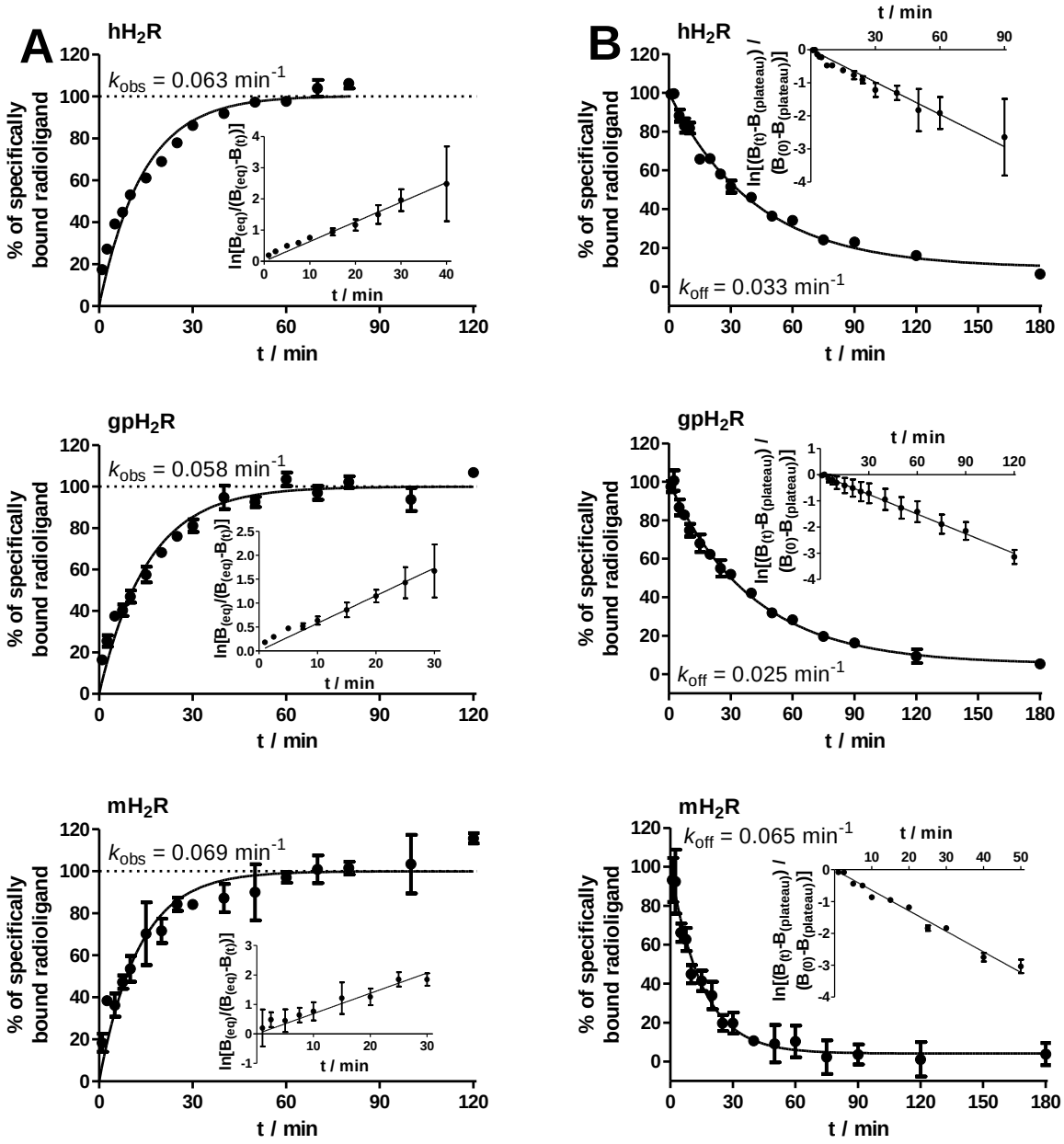

Figure 2.9. Comparison of the kinetic binding experiments with [^{3}H]**2.23** using HEK293T-hH_2R-qs5-HA cells[33], HEK293T-CRE-Luc-gpH_2R cells or HEK293-mH_2R cells. A: Representative associations of [^{3}H]**2.23** (c (h/gpH_2R) = 25 nM; c (mH_2R) = 50 nM) as a function of time. Inserts: Transformation of the depicted association kinetics using $\ln[B_{(eq)}/B_{(eq)}\text{-}B_{(t)}]$ versus time (k_{obs}, observed association rate constant). B: Representative dissociations of [^{3}H]**2.23** (preincubation: 120 min, c (h/gpH_2R) = 25 nM; c (mH_2R) = 50 nM) in the presence of 2.6 (1500-fold excess) as a function of time, showing a complete monophasic exponential decline [plateau: 15% (hH_2R), 4% (gpH_2R), 3% (mH_2R)]. Inserts: transformation of the depicted dissociation kinetics using $\ln[B_{(t)}\text{-}B_{(plateau)}/(B_{(0)}\text{-}B_{(plateau)}]$ versus time (k_{off}, dissociation rate constant). Each experiment was performed in triplicate. Error bars represent propagated errors according to the Gaussian law of error propagation.

Table 2.4. Comparison of Kinetic and Thermodynamic Binding Constants of [^{3}H]2.23 at the Human (h), Guinea Pig (gp), and Mouse (m) H_2Rs

H_2R	K_d (sat)[a] [nM]	N	K_d (kin)[b] [nM]	k_{obs} [min^{-1}][c]	k_{on} [min^{-1} x nM^{-1}][d]	k_{off} [min^{-1}],[e] $t_{1/2}$ [min][e]
h	23.6 ± 3.0	3	24.7 ± 8.4	0.064 ± 0.006	0.00129 ± 0.00028	0.032 ± 0.004, 25 ± 3
gp	27.8 ± 2.4	3	12.8 ± 3.1	0.062 ± 0.003	0.00164 ± 0.00024	0.021 ± 0.002, 33 ± 3
m	94.3 ± 12.8	4	551.5 ± 104.4	0.066 ± 0.002	0.00011 ± 0.00001	0.061 ± 0.006, 11 ± 1

[a]Equilibrium dissociation constant determined by saturation binding using HEK293T-hH_2R-qs5-HA cells[33], HEK293T-CRE-Luc-gpH_2R cells or HEK293-mH_2R cells; mean values ± SEM from N independent experiments each performed in triplicate. [b]Kinetically derived dissociation constant ± propagated error (K_d (kin) = k_{off}/k_{on}). [c]Observed association rate constant represents mean values ± SEM from three independent experiments each performed in triplicate using HEK293T-hH_2R-qs5-HA cells[33], HEK293T-CRE-Luc-gpH_2R cells or HEK293-mH_2R cells. [d]Association rate constant ± propagated error (k_{on} = (k_{obs}-k_{off})/[RL]). [e]Dissociation rate constant and derived half-life represent mean values ± SEM from three independent experiments each performed in triplicate using HEK293T-hH_2R-qs5-HA cells[33], HEK293T-CRE-Luc-gpH_2R cells or HEK293-mH_2R cells.

2.2.7 Competition Binding Experiments Using [^{3}H]2.23

Finally, we performed competition binding experiments with [^{3}H]**2.23** and several standard ligands for the H_2R (**2.1**, **2.5**-**2.7**, Figure 2.1A) using HEK293T-hH_2R-qs5-HA cells[33], HEK293T-CRE-Luc-gpH_2R cells or HEK293-mH_2R cells in suspension (Table 2.5). [^{3}H]**2.23** was completely displaced by endogenous agonist histamine (**2.1**) and **2.23** (the cold form of the radioligand), as well as by the standard H_2R antagonists/inverse agonists ranitidine, famotidine and tiotidine (**2.5**-**2.7**) (cf. Figure 2.10). All competition curves were monophasic and best fitted by a one-site competition model.

The K_d values determined from saturation binding were used for the calculation of K_i values by means of the Cheng-Prusoff equation.[43] Table 2.5 shows the data of the radioligand [^{3}H]**2.23** (colored columns) compared to binding or functional data from different laboratories and different expression systems. Data from Leurs' lab (CHO-hH_2R homogenates[24]) and from our lab (NanoBRET-based binding assay, HEK293T-Nluc-hH_2R cells[29]) are in good agreement with the pK_i values determined using [^{3}H]**2.23**, while data from Sf9 insect cell membranes expressing the hH_2R-$G_{s\alpha S}$ fusion protein[25] show larger deviations. We observed that histamine possess

higher affinity at Sf9 membranes (cf. Table 2.5; **2.1**), whereas antagonists/inverse agonists show lower affinities (cf. Table 2.5; **2.5-2.7**). Possible explanations for this trend might be the direct fusion of the receptor to the $G_{s\alpha S}$ protein and the allosteric effect of sodium on the binding of agonists to several GPCRs, which was previously discussed.[29] The pK_i values determined for the gpH_2R agreed very well with the pK_i values for hH_2R. Moreover, the data were in the ranges defined by pK_i values determined using [^{3}H]**2.10** and the gpH_2R-$G_{s\alpha S}$ fusion protein expressed in Sf9 membranes, [^{3}H]**2.9** at striatal membranes or pK_b and pEC_{50} values reported for experiments on the isolated, spontaneously beating guinea pig right atrium. Lower affinities could be measured for the mH_2R, while the order of affinities remained the same. Unfortunately, there are no pK_i values described in the literature for the gpH_2R expressed in cells and none at all for the mH_2R. Therefore, a comparison with literature data was not possible, but a first set of pK_i values was provided for these systems. Noteworthily, the pK_i values obtained at the mH_2R are one order of magnitude lower than at the hH_2R and gpH_2R, indicating a species dependent difference in binding affinities (see also Figure 2.10). Although a lot of research has been done focusing on the relevant amino acids in the orthosteric binding pocket of different H_2R orthologs[20, 44-46], there was no convincing evidence to explain such differences. Therefore, this phenomenon could be subject of further research studies to elucidate its origin.

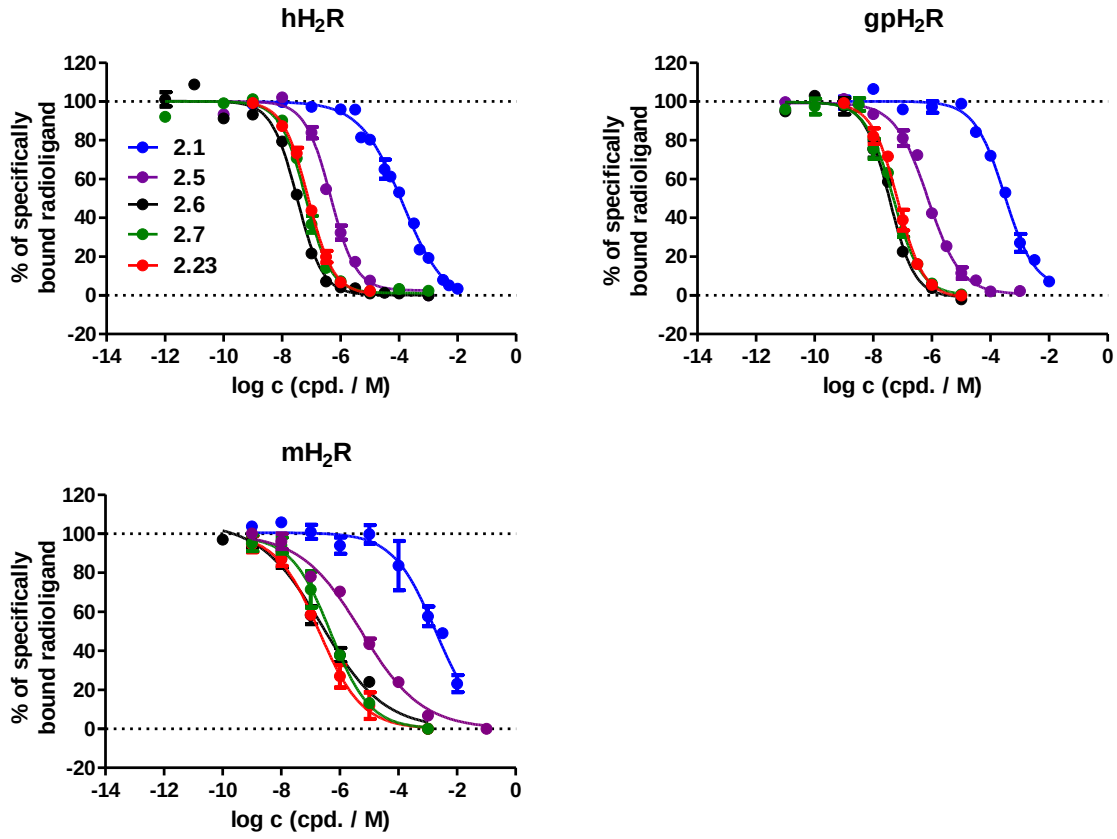

Figure 2.10. Radioligand displacement curves from competition binding experiments performed with [^{3}H]**2.23** (25 nM, hH_2R; 26.5 nM gpH_2R; 50 nM, mH_2R) at the hH_2R, co-expressed in HEK293T-qs5-HA cells[33], gpH_2R, co-expressed in HEK293T-CRE-Luc cells or mH_2R, expressed in HEK293 cells. Data represent mean values ± SEM of three independent experiments each performed in triplicate.

Table 2.5. Comparison of the Determined Binding Data (p*K*i) of Unlabeled hH_2R Ligands (2.1, 2.5-2.7 and 2.23), Using [^{3}H]2.23 as Radioligand at the H_2R Orthologs, with Reference Data

	hH_2R					**gpH_2R**				**mH_2R**	
	[a1]HEK cells [^{3}H]**2.23**		[c5]Sf9 membranes [^{3}H]**2.10**	[c4]CHO membranes [^{3}H]**2.9**	[d]NanoBRET HEK cells UR-KAT478[29]	[a2]HEK cells [^{3}H]**2.23**		[c2]Sf9 membranes [^{3}H]**2.10**	[c6]striatal membranes [^{3}H]**2.9**	[e]right atrium	[a3]HEK cells [^{3}H]**2.23**	
compd.	p*K*i[b]	N	p*K*i	p*K*i	p*K*i	p*K*i[b]	N	p*K*i	p*K*i	pEC_{50}/(p*K*b)/{E_{max}}	p*K*i[b]	N
2.1	4.18 ± 0.04	3	6.27[25]	4.10[24], 5.69[24]	4.96[29]	3.83 ± 0.06	3	6.82[25]	4.55[3]	6.14[22] {1.00} 6.16[31] {1.00}	3.10 ± 0.17	3
2.23	7.42 ± 0.04	3	7.59 ± 0.12	n.d.	n.d.	7.45 ± 0.07	3	7.83 ± 0.14	n.d.	7.47 ± 0.07 {0.90 ± 0.10}	6.89 ± 0.06	3
2.5	6.65 ± 0.07	3	5.76[25]	7.07[24]	7.19[29]	6.45 ± 0.01	3	n.d.	7.30[3]	(7.20)[22]	5.47 ± 0.12	3
2.6	7.78 ± 0.04	3	6.87[25]	7.80[24]	7.94[29]	7.79 ± 0.07	3	6.30[25]	8.25[3]	(7.80)[22]	6.71 ± 0.06	3
2.7	7.51 ± 0.06	3	6.57[25]	7.77[24]	n.d.	7.66 ± 0.08	3	7.30[25]	8.30[3]	(7.82)[22]	6.59 ± 0.12	3

[a]Data from competition binding experiments (p*K*i) with [^{3}H]**2.23** ([1]25 nM, hH_2R; [2]26.5 nM, gpH_2R; [3]50 nM, mH_2R) for H_2R ligands at the [1]hH_2R, co-expressed in HEK293T-qs5-HA cells[33], [2]gpH_2R, co-expressed in HEK293T-CRE-Luc cells or [3]mH_2R, expressed in HEK293 cells. [b]The p*K*i values represent mean values ± SEM from three independent experiments each performed in triplicate. [c]Data from competition binding experiments (p*K*i) with [4,6][^{3}H]**2.9** or [5][^{3}H]**2.10**, [4]performed at membranes of CHO cells stably expressing the hH_2R[24], [5]membranes of Sf9 insect cells expressing the h or gp H_2R-$G_{s\alpha s}$[25], [6]striatal membranes from male Hartley guinea pigs[22]. [d]NanoBRET experiments were performed with HEK293T cells stably expressing NLuc-hH_2R.[29] [e]pEC_{50}/p*K*b and E_{max} values determined using the guinea pig right atrium.[22]

2.2.8 Red Blood Cell Partitioning of [^{3}H]2.10 and [^{3}H]2.23

To investigate the unknown role of the H_2R in the CNS, we envisage the application of carbamoylguanidine-type ligands in laboratory mice in future. For this purpose, the ligand has to be applied intravenously (i.v.) or perorally (p.o.). In a preliminary study the aim was to compare the distribution of [^{3}H]**2.10** and [^{3}H]**2.23** in whole human and mouse blood (Figure 2.11, for details see the Experimental Section and Table App1.2 in the Appendix 1). [^{3}H]**2.23** showed a similar binding to human and mouse plasma, whereas the binding of [^{3}H]**2.10** was lower in mouse plasma. On the other hand, [^{3}H]**2.10** accumulated to a significantly higher degree in human or mouse red blood cells (RBCs) than [^{3}H]**2.23**, which might lead to undesired pharmacokinetic properties of [^{3}H]**2.10**.[47-49] Due to the low binding of [^{3}H]**2.23** to RBCs we believe that the carbamoylguanidine H_2R ligand subclass is suitable for further investigations to clarify the role of the H_2R in murine brain after i.v. or p.o. application.

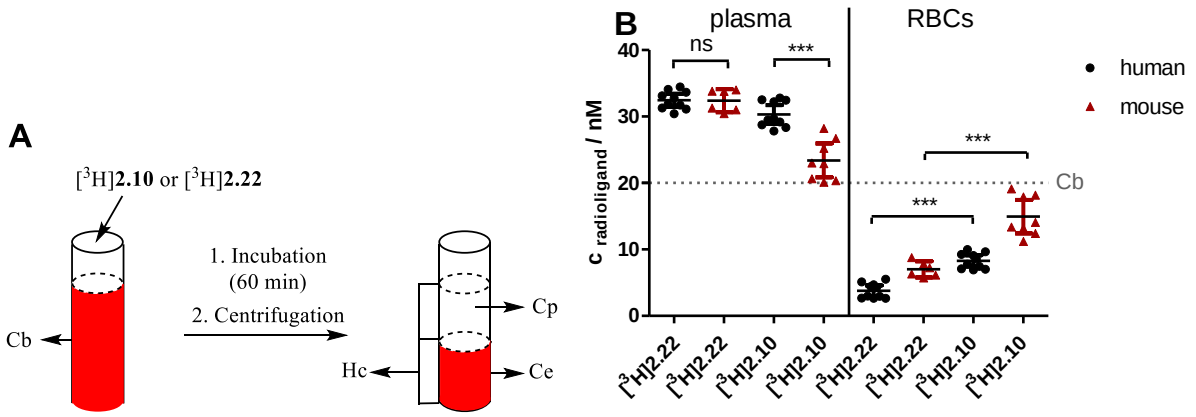

Figure 2.11. A: Determination of extent of red blood cell (RBCs) partitioning of [^{3}H]**2.10** and [^{3}H]**2.23** in whole blood. Cb, drug concentration in whole blood; Cp, drug concentration in plasma; Ce, drug concentration in red blood cells; Hc, haematocrit (packed red blood cell volume). Calculated by assuming a Hc of 0.41 and plasma 0.55 (human and mouse). **B**: Dot plot of binding of [^{3}H]**2.10** and [^{3}H]**2.23** to human and mouse plasma and red blood cells. Dot plots represent mean values ± CI 95%. Black dots are used for human and red triangles for mouse plasma/red blood cells subsets. Mann-Whitney test: *** <0.001 between [^{3}H]**2.10** and [^{3}H]**2.23** subsets in human vs. mouse RBCs, ns: not significant.

2.3 Summary and Conclusion

In summary, we synthesized and characterized a novel, potent, selective, and G protein biased H_2R radioligand by derivatizing amino-functionalized precursors, structurally related to amthamine. UR-KAT479 (**2.23**) proved to be a high affinity hH_2R agonist with >380-fold selectivity over the other three hHRs. Subsequent tritiation with commercially available *N*-succinimidyl [2,3-^{3}H]propionate yielded [^{3}H]**2.23** with a specific activity of 149 Ci/mmol in a radiochemical yield of 35% and a high (radio)chemical purity (≥98%). Binding of [^{3}H]**2.23** to HEK293(T) cells (co)expressing human, guinea pig or mouse H_2R was saturable and highly specific showing only low non-specific binding (3 - 14% at c = K_d). [^{3}H]**2.23** possessed high affinities to human and guinea pig H_2Rs (K_d = 24/28 nM, h/gp) and a moderate affinity to mouse H_2R (K_d = 94 nM). The saturation binding curves were best described by a one-site model and the Scatchard plots were linear, suggesting that [^{3}H]**2.23** binds to a single binding site. Kinetic experiments showed a rapid association of [^{3}H]**2.23** to (60 min) and a complete dissociation from the receptor (60-180 min). The resulting dissociation constants were in good agreement with the K_d values obtained in saturation binding assays for all three orthologs. The determined binding constants of standard H_2R ligands were consistent with data reported in the literature. Moreover, we are the first group to report pK_i values for histamine, as well as standard antagonists/inverse agonists at the gpH_2R and mH_2R expressed in cells. In contrast to the other commonly employed radioligands (e.g. [^{3}H]**2.10**), a significant advantage of [^{3}H]**2.23** is its surmountability at the H_2R enabling the determination of K_i values in a true equilibrium according to the Cheng-Prusoff equation. Since all acquired data recommend [^{3}H]**2.23** as a suitable radioligand for the characterization of H_2R ligands in different species, a further application of carbamoylguanidine-type ligands to study the role of the H_2R in the CNS is planned.

2.4 Experimental Section

2.4.1 General Experimental Section

Unless otherwise stated, chemicals and solvents were from commercial suppliers and were used as received. All the solvents were of analytical grade or were distilled prior to use. For column chromatography silica gel 60 (0.04-0.063 mm, Merck, Darmstadt, Germany) was used. Flash-chromatography was performed on an Intelli Flash-310 flash chromatography workstation

from Varian Deutschland GmbH (Darmstadt, Germany) with SuperFlash columns (Si35) from Agilent Technologies (Waldbronn, Germany). Reactions were monitored by thin layer chromatography (TLC) on Merck silica gel 60 F254 aluminium sheets, and spots were visualized with UV light at 254 nm or ninhydrin staining. NMR spectra were recorded on a Bruker Avance 300 (^{1}H: 300 MHz, ^{13}C: 75.5 MHz) and a Bruker Avance 600 (^{1}H: 600 MHz, ^{13}C: 150.9 MHz) (Bruker, Karlsruhe, Germany) with deuterated solvents from Deutero (Kastellaun, Germany). HRMS was performed on an Agilent 6540 UHD Accurate-Mass Q-TOF LC/MS system (Agilent Technologies, Santa Clara, CA, USA) using an ESI source. Preparative HPLC was performed with a system from Knauer (Berlin, Germany) consisting of two K-1800 pumps, a K-2001 detector and the column was a Phenomenex Kinetex (250 x 21 mm, 5 µm) (Phenomenex, Aschaffenburg, Germany). As mobile phase mixtures of MeCN and 0.1% aqueous TFA were used. The UV detection was carried out at 220 nm. Prior to lyophilization (ScanVac CoolSafe 4-15L freeze dryer from Labogene (LMS, Brigachtal, Germany), equipped with a RZ 6 rotary vane vacuum pump (Vacuubrand, Wertheim, Germany)), MeCN was removed under reduced pressure. Analytical HPLC experiments were performed on a 1100 HPLC system from Agilent Technologies equipped with Instant Pilot controller, a G1312A Bin Pump, a G1329A ALS autosampler, a G1379A vacuum degasser, a G1316A column compartment and a G1315B DAD detector. The column was a Phenomenex Kinetex XB-C18 column (250 x 4.6 mm, 5 µm) (Phenomenex, Aschaffenburg, Germany), tempered at 30 °C. As mobile phase, mixtures of MeCN/aqueous TFA were used. Gradient mode: MeCN/TFA (0.05 %) (v/v) 0 min: 10:90, 30 min: 90:10, 33 min: 95:5, 40 min: 95:5; flow rate: 0.8 mL/min, t_0 = 3.21 min; capacity factor $k = (t_R\text{-}t_0)/t_0$. Absorbance was detected at 220 nm. Compound purities were calculated as the percentage peak area of the analyzed compound by UV detection at 220 nm.

2.4.2 Compound Characterization

Target compounds (**2.20**-**2.25**) were characterized by ^{1}H-NMR, ^{13}C-NMR, and 2D NMR (COSY, HSQC, HMBC) spectroscopy, HRMS, and RP-HPLC analysis. The purities of the H_2R ligands used for pharmacological investigation were >95%. The corresponding ^{1}H- and ^{13}C-NMR spectra and RP-HPLC chromatograms are shown in the Supporting Information of the published manuscript. The Supporting Information is available free of charge at https://pubs.acs.org/doi/10.1021/acs.jmedchem.0c01494.

2.4.3 Synthesis and Analytical Data

The amine building block 5-(3-aminopropyl)-4-methylthiazol-2-amine (**2.12**) was synthesized as previously reported.[27] The mono-Boc protected *S*-methylisothiourea **2.13**, a well-established guanidinylation reagent[50], was prepared as previously described.[27] The mono-Boc protected diamines **2.14**-**2.16** were synthesized from the unprotected diamines as published elsewhere.[51-53]

General Procedure for the Synthesis of the Guanidinylating Reagents (2.17-2.19). The guanidinylating reagents **2.17**-**2.19** were prepared using the procedure of Kagermeier et al.[9] Triphosgene (0.5 equiv) was dissolved in dry CH_2Cl_2 (1 mL) in an argon flushed round bottom flask and cooled to 0 °C (ice-bath). DIPEA (5.6 equiv) and mono-Boc protected diamine (**2.14**, **2.15** or **2.16**, 1 equiv) were dissolved in dry CH_2Cl_2 (2 mL) and added dropwise to the triphosgene solution over a period of 30 min. After addition of **2.13** (4 equiv), the ice-bath was removed, and the reaction mixture was stirred at room temperature for 2.5 h. The solvent was removed in vacuo and the residue was purified by flash chromatography (eluent PE/EtOAc or CH_2Cl_2 or CH_2Cl_2/MeOH).

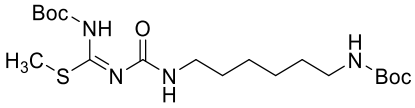

***N*-*tert*-Butoxycarbonyl-*N*'-[*N*-(6-*tert*-butoxycarbonylaminohexyl)aminocarbonyl]-*S*-methylisothiourea (2.17).** The title compound was prepared from **2.14** (0.50 g, 2.31 mmol, 1 equiv), DIPEA (2.2 mL, 12.9 mmol, 5.6 equiv), triphosgene (0.34 g, 1.16 mmol, 0.5 equiv) and **2.13** (1.76 g, 9.24 mmol, 4 equiv) according to the general procedure yielding the product as white solid (380 mg, 38%). ^{1}H-NMR (300 MHz, $CDCl_3$) δ 12.30 (s, 1H), 5.58 (t, J = 6.0 Hz, 1H), 4.51 (s, 1H), 3.21 (q, J = 6.77 Hz, 2H), 3.10 (q, J = 6.77 Hz, 2H), 2.30 (s, 3H), 1.40-1.56 (m, 22H), 1.39-1.29 (m, 4H). ^{13}C-NMR (101 MHz, $CDCl_3$) δ 167.23, 161.93, 155.98, 151.12, 82.51, 77.20, 40.38, 39.95, 29.99, 29.61, 28.40, 28.12, 28.01, 26.49, 26.35, 14.24. R_f = 0.70 (CH_2Cl_2/EtOAc 15:1, ninhydrin). HRMS: calcd. for $C_{19}H_{37}N_4O_5S^+$: 433.2479; found: 433.2510. MF: $C_{19}H_{36}N_4O_5S$. MW: 432.58.

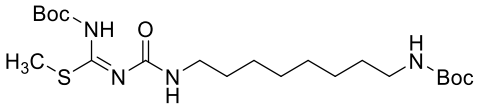

***N*-*tert*-Butoxycarbonyl-*N*'-[*N*-(8-*tert*-butoxycarbonylaminooctyl)aminocarbonyl]-*S*-methylisothiourea (2.18).** The title compound was prepared from **2.15** (0.21 g, 0.86 mmol, 1 equiv), DIPEA (0.82 mL, 4.8 mmol, 5.6 equiv), triphosgene (0.13 g, 0.42 mmol, 0.5 equiv) and **2.13** (0.16 g, 0.86 mmol, 1 equiv) according to the general procedure (eluent PE/EtOH; 0-20 min: 100:0-90:10, 40 min: 90:10) yielding the product as a colorless oil (70 mg, 17%). ^{1}H-NMR (300 MHz, $CDCl_3$): δ 12.30 (s, 1H), 5.58 (t, *J* = 6.0 Hz, 1H), 4.53 (s, 1H), 3.24-3.12 (m, 2H), 3.07 (q, *J* = 6.7 Hz, 2H), 2.27 (s, 3H), 1.36-1.55 (m, 22H), 1.34-1.21 (m, 8H). ^{13}C-NMR (75 MHz, $CDCl_3$) δ 167.08, 161.84, 155.88, 151.06, 82.44, 78.93, 40.50, 40.06, 29.94, 29.58, 29.12, 29.08, 28.35, 28.12, 27.95, 26.78, 26.62, 14.19. R_f = 0.71 (CH_2Cl_2/MeOH 97.5:2.5). HRMS: calcd. for $C_{21}H_{41}N_4O_5S^+$: 461.2792; found: 461.2830. MF: $C_{21}H_{40}N_4O_5S$. MW: 460.63.

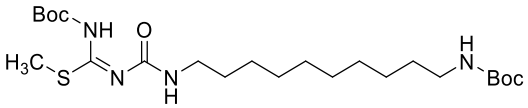

***N*-*tert*-Butoxycarbonyl-*N*'-[*N*-(10-*tert*-butoxycarbonylaminodecyl)aminocarbonyl]-*S*-methylisothiourea (2.19).** The title compound was prepared from **2.16** (0.27 g, 0.99 mmol, 1 equiv), DIPEA (0.95 mL, 5.6 mmol, 5.6 equiv), triphosgene (0.148 g, 0.49 mmol, 0.5 equiv) and **2.13** (0.189 g, 0.99 mmol, 1 equiv) according to the general procedure (eluent CH_2Cl_2, isokratic) yielding the product as a colorless oil (74 mg, 15%). R_f = 0.74 (PE/EtOAc 5:1) or 0.89 (CH_2Cl_2/MeOH 97.5:2.5). ^{1}H-NMR (300 MHz, $CDCl_3$) δ 12.29 (s, 1H), 5.59 (t, *J* = 6.3 Hz, 1H), 4.54 (s, 1H), 3.18 (q, *J* = 6.7 Hz, 2H), 3.05 (q, *J* = 6.8 Hz, 2H), 2.27 (s, 3H), 1.56-1.35 (m, 22H), 1.33-1.14 (s, 12H). ^{13}C-NMR (75 MHz, $CDCl_3$) δ 167.01, 161.82, 151.03, 134.88, 82.41, 80.11, 40.52, 40.07, 29.94, 29.58, 29.34, 29.32, 29.16, 29.13, 28.33, 28.12, 27.92, 26.82, 26.66, 14.16. HRMS: calcd. for $C_{23}H_{45}N_4O_5S^+$: 489.3105; found: 489.3111. MF: $C_{23}H_{44}N_4O_5S$. MW: 488.69.

General Procedure for the Synthesis of the Carbamoylguanidine-Type Precursors 2.20-2.22. In this general procedure mercuric chloride ($HgCl_2$) is used as reagent, which is very toxic and potentially cancerogenic. It should only be used in a well-ventilated fume hood after reading the safety precautions and wearing proper lab safety equipment (gloves, safety googles and lab

coat). Future synthetic work should consider replacements for mercuric chloride. The guanidinylating reagents **2.17**-**2.19** (1 equiv) and 5-(3-aminopropyl)-4-methylthiazol-2-amine (**2.12**, 2.1 equiv) were dissolved in CH_2Cl_2 (3 mL). NEt_3 (2.5 equiv) and $HgCl_2$ (4 equiv) were added and the mixture was stirred for 4-16 h. The reaction mixture was diluted with CH_2Cl_2 (10 mL). The precipitate was removed by filtration through Celite 545 and washed with CH_2Cl_2 (20 mL) and EtOAc (20 mL). The solvent was removed in vacuo and the crude product was purified by column chromatography on silica gel (eluent PE (A), EtOAc (B); gradient: 0-20 min: A/B 100:0-50:50) and dried in vacuo. Subsequently, deprotection was performed by stirring with 30% TFA in CH_2Cl_2 for 7-18 h. The obtained carbamoylguanidine-type precursors were purified by preparative HPLC.

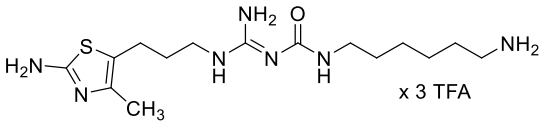

1-(Amino{[3-(2-amino-4-methylthiazol-5-yl)propyl]amino}methylene)-3-(6-aminohexyl)urea trihydrotrifluoroacetate (2.20). The title compound was prepared from **2.17** (50 mg, 0.116 mmol, 1 equiv), **2.12** (66 mg, 0.24 mmol, 2.1 equiv), NEt_3 (80 µL, 0.58 mmol, 5 equiv) and $HgCl_2$ (126 mg, 0.46 mmol, 4 equiv) according to the general procedure, yielding the product as a white fluffy hygroscopic solid (38.49 mg, 48%). HPLC: 96%, (t_R = 6.51 min, k = 1.03). ^{1}H-NMR (300 MHz, MeOD) δ 3.37-3.32 (m, 2H), 3.21 (t, J = 7.0 Hz, 2H), 2.92 (t, J = 7.6 Hz, 2H), 2.72 (t, J = 7.6 Hz, 2H), 2.18 (s, 3H), 1.89 (quint, J = 7.2 Hz, 2H), 1.73-1.49 (m, 4H), 1.49-1.33 (m, 4H). 1H-NMR (600 MHz, DMSO-d_6) δ 10.52 (br s, 1H), 9.11-8.35 (m, 5H), 7.97-7.40 (m, 4H), 3.24 (q, J = 6.6 Hz, 2H), 3.09 (q, J = 6.6 Hz, 2H), 2.82-2.72 (m, 2H), 2.59 (t, J = 7.5 Hz, 2H), 2.07 (s, 3H), 1.72 (quint, J = 7.3 Hz, 2H), 1.51 (quint, J = 7.4 Hz, 2H), 1.43 (quint, J = 7.2 Hz, 2H), 1.34-1.20 (m, 4H). ^{13}C-NMR (151 MHz, DMSO-d_6) δ 167.44, 158.17 (q, J = 32.41 Hz, TFA), 153.81, 153.70, 133.06, 116.84 (q, J = 306.6 Hz, TFA), 116.26, 40.05, 39.09, 38.74, 28.95, 28.75, 26.91, 25.73, 25.45, 22.03, 11.78. HRMS: calcd. for $C_{15}H_{30}N_7OS^+$: 356.2227; found: 356.2228. MF: $C_{15}H_{29}N_7OS$ x $C_6H_3F_9O_6$. MW: (355.51 + 342.07).

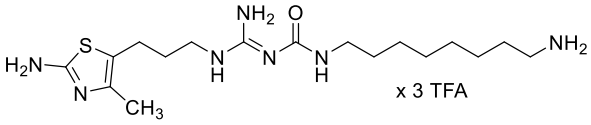

1-(Amino{[3-(2-amino-4-methylthiazol-5-yl)propyl]amino}methylene)-3-(8-aminooctyl)urea trihydrotrifluoroacetate (2.21). The title compound was prepared from **2.18** (70 mg, 0.15 mmol, 1 equiv), **2.12** (87 mg, 0.32 mmol, 2.1 equiv), NEt_3 (105 µL, 0.76 mmol, 5 equiv) and $HgCl_2$ (165 mg, 0.61 mmol, 4 equiv) according to the general procedure, yielding the product as a white fluffy hygroscopic solid (40.22 mg, 36%). HPLC: 100%, (t_R = 7.17 min, k = 1.23). ^{1}H-NMR (300 MHz, MeOD) δ 3.37-3.31 (m, 2H), 3.19 (t, J = 7.0 Hz, 2H), 2.90 (t, J = 7.6 Hz, 2H), 2.71 (t, J = 7.5 Hz, 2H), 2.18 (s, 3H), 1.89 (quint, J = 7.1 Hz, 2H), 1.73-1.46 (m, 4H), 1.45-1.30 (m, 8H). ^{1}H-NMR (600 MHz, DMSO-d_6) δ 10.49 (br s, 1H), 9.23-8.21 (m, 5H), 8.05-7.22 (m, 4H), 3.24 (q, J = 6.6 Hz, 2H), 3.08 (q, J = 6.6 Hz, 2H), 2.84-2.69 (m, 2H), 2.59 (t, J = 7.5 Hz, 2H), 2.07 (d, J = 2.0 Hz, 3H), 1.72 (quint, J = 7.3 Hz, 2H), 1.56-1.47 (m, 2H), 1.46-1.37 (m, 2H), 1.29-1.25 (m, 8H). ^{13}C-NMR (151 MHz, DMSO-d_6) δ 167.54, 158.75 (q, J = 32.0 Hz, TFA), 153.82, 153.68, 132.45, 116.75 (q, J = 299.3 Hz, TFA), 116.27, 40.06, 39.19, 38.80, 28.90 (2C), 28.45, 26.96, 26.10 (2C), 25.73, 22.02, 11.70. HRMS: calcd. for $C_{17}H_{34}N_7OS^+$: 384.2540; found: 384.2545. MF: $C_{17}H_{33}N_7OS$ x $C_6H_3F_9O_6$. MW: (383.56 + 342.07).

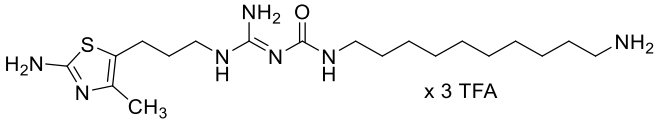

1-(Amino{[3-(2-amino-4-methylthiazol-5-yl)propyl]amino}methylene)-3-(8-aminooctyl)urea trihydrotrifluoroacetate (2.22). The title compound was prepared from **2.19** (74 mg, 0.152 mmol, 1 equiv), **2.12** (87 mg, 0.32 mmol, 2.1 equiv), NEt_3 (105 µL, 0.76 mmol, 5 equiv) and $HgCl_2$ (165 mg, 0.61 mmol, 4 equiv) according to the general procedure, yielding the product as a white fluffy hygroscopic solid (28.0 mg, 25%). HPLC: 99%, (t_R = 9.05 min, k = 1.82). ^{1}H-NMR (300 MHz, MeOD) δ 3.37-3.32 (m, 2H), 3.19 (t, J = 7.0 Hz, 2H), 2.96-2.84 (m, 2H), 2.72 (t, J = 7.5 Hz, 2H), 2.18 (s, 3H), 1.98-1.82 (m, 2H), 1.73-1.46 (m, 4H), 1.43-1.28 (m, 12H). ^{1}H-NMR (600 MHz, DMSO-d_6) δ 10.57 (br s, 1H), 9.26-8.34 (m, 4H), 7.96-7.37 (m, 4H), 3.24 (q, J = 6.6 Hz, 2H), 3.08 (q, J = 6.6 Hz, 2H), 2.82-2.70 (m, 2H), 2.59 (t, J = 7.5 Hz, 2H), 2.07 (s, 3H), 1.72 (quint, J = 7.3 Hz, 2H), 1.51 (quint, J = 7.4 Hz, 2H), 1.46-1.38 (m, 2H),

1.32-1.19 (m, 12H). ^{13}C-NMR (151 MHz, DMSO-d_6) δ 167.70, 158.94 (q, J = 31.8 Hz, TFA), 153.85, 153.70, 132.39, 116.85 (q, J = 296.6 Hz, TFA), 116.27, 40.06, 39.20, 38.81, 28.92 (2C), 28.86, 28.78, 28.66, 28.50, 26.98, 26.21, 25.77, 22.00, 11.56. HRMS: calcd. for $C_{19}H_{38}N_7OS^+$: 412.2853; found: 412.2860. MF: $C_{19}H_{37}N_7OS$ x $C_6H_3F_9O_6$. MW: (411.61 + 342.07).

General Procedure for the Synthesis of the Propionic Amides 2.23-2.25. The reactions were carried out in a 1.5-mL micro tube (Sarstedt, Nümbrecht, Germany). The respective amine precursor (1 equiv) was dissolved in DMF (50 µL) and NEt_3 (7.5 equiv) was added. The *N*-succinimidyl propionate (1.01-1.2 equiv) was dissolved in DMF (30 µL) and added to the mixture. The reaction was stirred for 2 h at rt and was stopped by adding 10% aqueous TFA (10 µL).

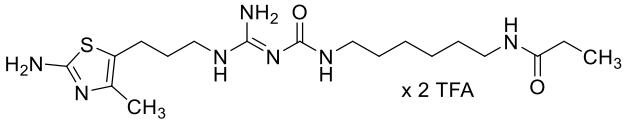

***N*-{6-(Amino{[3-(2-amino-4-methylthiazol-5-yl)propyl]amino}methylene)ureido-1-hexyl}propionic amide dihydrotrifluoroacetate (2.23).** The title compound was prepared from **2.20** (22.1 mg, 44 µmol, 1 equiv), succinimidyl propionate (9.1 mg, 53 µmol, 1.2 equiv) and NEt_3 (46 µL, 0.33 mmol, 7.5 equiv) according to the general procedure, yielding the product as a white fluffy hygroscopic solid (13.2 mg, 47%). The same reaction was also performed in a 4.32 mg scale. The yield was 3.1 mg (78%). Both batches were unified and used to analytically and pharmacologically characterize the "cold" radioligand. HPLC: 99%, (t_R = 9.21, k = 1.87). ^{1}H-NMR (300 MHz, MeOD) δ 3.33 (t, J = 6.9 Hz, 2H), 3.20 (t, J = 7.0 Hz, 2H), 3.16 (t, J = 7.1 Hz, 2H), 2.72 (t, J = 7.5 Hz, 2H), 2.22-2.15 (m, 5H), 1.90 (quint, J = 7.1 Hz, 2H), 1.58-1.46 (m, 4H), 1.36 (quint, J = 3.5 Hz, 4H), 1.12 (t, J = 7.6 Hz, 3H). ^{1}H-NMR (600 MHz, DMSO-d_6): δ 9.86 (br s, 1H), 8.93 (br s, 1H), 8.44 (br s, 2H), 7.80-7.61 (m, 1H), 7.54-7.37 (m, 1H), 3.22 (q, J = 6.7 Hz, 2H), 3.07 (q, J = 6.6 Hz, 2H), 3.02-2.96 (m, 2H), 2.57 (t, J = 7.5 Hz, 2H), 2.08-1.97 (m, 5H), 1.71 (quint, J = 7.3 Hz, 2H), 1.46-1.32 (m, 4H), 1.29-1.20 (m, 5H), 0.96 (t, J = 7.6 Hz, 3H). ^{13}C-NMR (151 MHz, MeOD) δ 177.16, 170.45, 163.52 (q, J = 35.7 Hz, TFA), 156.14, 155.60, 132.96, 118.55, 118.23 (q, J = 293.9 Hz, TFA), 41.55, 40.80, 40.36, 30.49, 30.44, 30.38, 30.03, 27.65, 27.55, 23.74, 11.63, 10.76. HRMS: calcd. for $C_{18}H_{34}N_7O_2S^+$: 412.2489; found: 412.2491. MF: $C_{18}H_{33}N_7O_2S$ x $C_4H_2F_6O_4$. MW: (411.57 + 228.05).

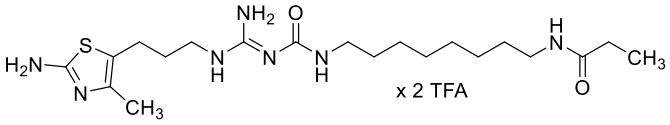

***N*-{8-(Amino{[3-(2-amino-4-methylthiazol-5-yl)propyl]amino}methylene)ureido-1-octyl}propionic amide dihydrotrifluoroacetate (2.24).** The title compound was prepared from **2.21** (12.72 mg, 17.5 µmol, 1 equiv), succinimidyl propionate (3.7 mg, 21.0 µmol, 1.2 equiv) and NEt_3 (18 µL, 131 µmol, 7.5 equiv) according to the general procedure, yielding the product as a white fluffy hygroscopic solid (8.78 mg, 75%). HPLC: 97%, (t_R = 11.26 min, k = 2.51). ^{1}H-NMR (300 MHz, MeOD) δ 3.37-3.31 (m, 2H), 3.19 (t, J = 7.0 Hz, 2H), 2.91 (t, J = 7.6 Hz, 2H), 2.72 (t, J = 7.5 Hz, 2H), 2.18 (s, 3H), 1.90 (quint, J = 7.1 Hz, 2H), 1.74-1.47 (m, 4H), 1.45-1.31 (m, 8H). ^{1}H-NMR (600 MHz, DMSO-d_6) δ 10.28 (br s, 1H), 9.02 (br s, , 3H), 8.50 (br s, 2H), 7.69 (t, J = 5.6 Hz, 1H), 7.48 (br s, 1H), 3.24 (q, J = 6.6 Hz, 2H), 3.08 (q, J = 6.6 Hz, 2H), 3.03-2.97 (m, 2H), 2.59 (t, J = 7.6 Hz, 2H), 2.08 (s, 3H), 2.04 (q, J = 7.6 Hz, 2H), 1.73 (quint, J = 7.3 Hz, 2H), 1.43 (t, J = 6.9 Hz, 2H), 1.36 (t, J = 6.9 Hz, 2H), 1.29-1.20 (m, 9H), 0.97 (t, J = 7.6 Hz, 3H). ^{13}C-NMR (151 MHz, DMSO-d_6) δ 172.60, 167.76, 158.88 (q, J = 32.4 Hz, TFA), 153.78, 153.63, 131.91, 116.87 (q, J = 297.4 Hz, TFA), 116.30, 40.06, 39.24, 38.36, 29.14, 28.90, 28.83, 28.65, 28.60, 28.50, 26.33, 26.14, 21.98, 11.47, 10.03. HRMS: calcd. for $C_{20}H_{38}N_7O_2S^+$: 440.2802; found: 440.2804. MF: $C_{20}H_{37}N_7O_2S$ x $C_4H_2F_6O_4$. MW: (439.62 + 228.05).

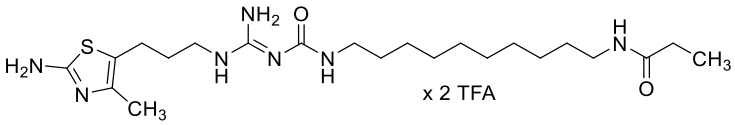

***N*-{10-(Amino{[3-(2-amino-4-methylthiazol-5-yl)propyl]amino}methylene)ureido-1-decyl}propionic amide dihydrotrifluoroacetate (2.25).** The title compound was prepared from **2.22** (13.23 mg, 17.6 µmol, 1 equiv), succinimidyl propionate (3.0 mg, 17.7 µmol, 1.01 equiv) and NEt_3 (17.5 µL, 132 µmol, 7.5 equiv) according to the general procedure, yielding the product as a white fluffy hygroscopic solid (5.12 mg, 42%). HPLC: 100%, (t_R = 13.53 min, k = 3.21). ^{1}H-NMR (400 MHz, MeOD) δ 3.38-3.32 (m, 2H), 3.23-3.10 (m, 4H), 2.72 (t, J = 7.6 Hz, 2H), 2.25-2.11 (m, 5H), 1.90 (quint, J = 7.2 Hz, 2H), 1.60-1.40 (m, 4H), 1.39-1.24 (m, 12H), 1.12 (t, J = 7.6 Hz, 3H). ^{1}H-NMR (600 MHz, DMSO-d_6) δ 10.22 (br s, 1H), 9.16-8.33 (m, 4H), 7.82-7.39 (m, 2H), 3.24 (q, J = 6.6 Hz, 2H), 3.08 (q, J = 6.6 Hz, 2H), 3.03-2.95 (m, 2H), 2.59 (t, J = 7.5 Hz, 2H), 2.07 (s, 3H), 2.03 (q, J = 7.6 Hz, 2H), 1.72 (quint, J = 7.3 Hz, 2H),

1.48-1.40 (m, 2H), 1.36 (quint, *J* = 6.9 Hz, 2H), 1.30-1.19 (m, 12H), 0.97 (t, *J* = 7.6 Hz, 3H). ^{13}C-NMR (151 MHz, DMSO-d_6) δ 172.58, 167.49, 158.60 (q, *J* = 31.3 Hz, TFA), 153.76, 153.60, 132.89, 116.98 (q, *J* = 298.7 Hz, TFA), 116.29, 40.06, 39.29, 38.37, 29.16, 28.90 (2C), 28.71, 28.63, 28.50, 26.38, 26.18, 22.03, 11.73, 10.03. HRMS: calcd. for $C_{22}H_{42}N_7O_2S^+$: 468.3115; found: 468.3124. MF: $C_{22}H_{41}N_7O_2S$ x $C_4H_2F_6O_4$. MW: (467.30 + 228.05).

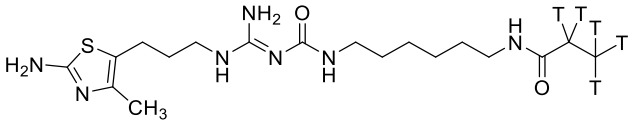

***N*-{6-(Amino{[3-(2-amino-4-methylthiazol-5-yl)propyl]amino}methylene)ureido-1-hexyl}2,3-ditritiopropionic amide dihydrotrifluoroacetate ([^{3}H]2.23).** Succinimidyl [2,3-^{3}H]propionate was from Novandi Chemistry AB (Södertälje, Sweden), provided in heptane/ethyl acetate 3:2 (specific radioactivity >100 Ci/mmol (2.7 TBq/mmol), radioactive concentration = 2 mCi/mL (74 MBq/mL). The reaction was carried out in a 1.5 mL micro tube (Sarstedt). The hexane/ethyl acetate mixture was removed in a vacuum concentrator for about 45 min. The precursor **2.20** (192 nmol, 134 µg) was dissolved in a mixture of DMF (40 µL) and TEA (2.1 µmol, 0.3 µL). This mixture was added to succinimidyl [2,3-^{3}H]propionate (22 nmol, 2.2 mCi). The mixture was stirred for 1.5 h with a vortexer at rt. 10 µL of 2% aqueous TFA and 350 µL Millipore water + 5% MeCN + 0.05% TFA were added. The product was isolated with a Waters HPLC system (column: Phenomenex Luna C18 (150 x 4.6 mm, 3 µm)). Eluent: mixtures of 0.04% TFA in MeCN (A) and 0.04% aqueous TFA (B), gradient 0-14 min: A/B 10:90 to 21:79, 25 min: 21:79, 27 min: 96:5, 35 min: 95:5 (flow: 0.8 mL/min). The eluates were collected in a 1.5 mL vessel. The combined fractions were concentrated in a vacuum concentrator to a volume of 300 µL and 700 µL EtOH were added. This solution was transferred in a glass storage vial. The Eppendorf vial was rinsed two times with 100 µL EtOH/H_2O 70:30 (v/v) and the wash solution was added to the 1000 µL radioligand solution to a total volume of 1200 µL.

Quantification: The concentration of the radioligand was determined by a 4-point calibration with **2.23**. The solutions for the calibration were prepared freshly prior to injection. All the solutions were prepared separately in mobile phase from a 20 µM solution of **2.23**. Eluent: mixtures of 0.04% TFA in MeCN (A) and 0.04% aqueous TFA (B), gradient: 0-14 min: A/B 10:90 to 21:79, 25 min: 21:79, 27 min: 96:5, 35 min: 95:5 (flow: 0.8 mL/min, column:

Phenomenex Luna C18 (150 x 4.6 mm, 3 µm)). The molarity of the [^{3}H]**2.23**-solution was calculated from the peak areas of the standards.

Determination of the specific activity: 12 aliquots of the diluted radioligand in mobile phase were counted in 10 mL H_2O and 10 mL Quicksave A (Zinsser Analytic GmbH, Eschborn, Germany) (measurement time = 9.799 min) using a Quantulus 1220 liquid scintillation counter (Perkin Elmer, Rodgau, Germany). The calculated specific activity was 146.3 Ci/mmol (5.41 TBq/mmol). This corresponds to a concentration of 6.45 µM. The radioligand was obtained in a yield of 35% (7.74 nmol) with a radiochemical purity of >99%. The identity of the radioligand was confirmed by HPLC analysis of the labelled and the corresponding unlabelled compound (**2.23**, [^{3}H]**2.23**) under the same conditions, resulting in identical retention times. The radioligand [^{3}H]**2.23** was stored at -20°C.

2.4.4 Control of the Chemical Stability of the "Cold" Radioligand 2.23 by HPLC

The chemical stability of the "cold" radioligand **2.23** was investigated at physiological pH (7.4) in binding buffer (12.5 mM $MgCl_2$, 1 mM EDTA and 75 mM Tris/HCl, pH 7.4)[1] at 23 °C for a period of 2 weeks. Incubation was started by addition of 25 µL of a 1 mM solution of the compound in EtOH/Millipore H_2O 1:4 (v/v), which were freshly prepared from a 5 mM stock solution in EtOH, to 475 µL of binding buffer to give a final concentration of 50 µM. The sample was shaken for up to 2 weeks at 700 rpm. After different time periods, a 70 µL aliquot was taken and diluted with 70 µL of a mixture of MeCN, Millipore H_2O and 10% aqueous TFA (60:90:1). Prior to HPLC analysis the samples were stored at -20 °C. 50 µL of the resulting solution were analyzed by HPLC as described in the general experimental section of the chapter 2. The absorption was detected at 220 nm. The blank HPLC run was performed under identical conditions without any ligand.

2.4.5 Functional Assays

Functional studies in the β-arrestin2 or mini-G protein recruitment assays at HEK293T-ARRB2-H_2R cells[29, 39], HEK293T NlucN-mGs/hH_2R-NlucC cells[37], HEK293T NlucN-mGs/gpH_2R-NlucC cells and using the isolated spontaneously beating guinea pig right atrium[31] were performed as previously described or as described in the Appendix 1, App1.2 Mini-G Protein Recruitment Assay at HEK293T Cells Expressing NlucN-mGs/gpH_2R-NlucC.

2.4.6 Radioligand Binding Experiments

Binding data on recombinant histamine receptor subtypes and guinea pig ortholog expressed in Sf9 cells (hH_1R + RGS4[54]; hH_2R-$G_{s\alpha S}$[20]; gpH_2R-$G_{s\alpha S}$[20]; hH_3R + $G_{\alpha i2}$ + $G_{\beta 1\gamma 2}$[55], hH_4R + $G_{\alpha i2}$ + $G_{\beta 1\gamma 2}$[56]) or HEK293T-hH_2R-qs5-HA cells[33] were assessed using the following radioligands: [^{3}H]mepyramine (hH_1R, Hartmann Analytics, Braunschweig, Germany or Novandi Chemistry AB), [^{3}H]**2.10**[25] (hH_2R), [^{3}H]N^{α}-methylhistamine (Hartmann Analytics) or [^{3}H]UR-PI294[28] (hH_3R), [^{3}H]**2.1** (hH_4R, Hartmann Analytics) according to recently published protocols.[9, 25] Modifications were made as follows: the washing steps were performed with PBS (pH 7.4) and not with binding buffer. Saturation binding, binding kinetics and competition binding studies with [^{3}H]**2.23** were performed by analogy with the previously reported protocols[25, 28, 32, 57-59] using PBS (pH 7.4) as washing buffer and using a MicroBeta2 1450 scintillation counter (PerkinElmer, Rodgau, Germany) in the 96-well plate format.

For competition binding, saturation binding and kinetic binding experiments with [^{3}H]**2.23**, the radioligand solution [6.45 µM in EtOH/H_2O 70/30 (v/v)] was mixed with a solution of **2.23** [6.45 µM in EtOH/H_2O 70/30 (v/v), ratio: 1:5 to 1:10 (v/v), depending on the experiment] because of economic reasons. Cells were maintained in 75 cm² flasks (Sarstedt) in a humidified atmosphere (95% air, 5% CO_2) at 37 °C. Dulbecco`s Modified Eagle Medium (DMEM, Sigma-Aldrich, Taufkirchen, Germany), containing 4.5 g/L glucose, 3.7 g/L $NaHCO_3$, 110 mg/L sodium pyruvate and supplemented with 0.584 g/L L-glutamine (Sigma-Aldrich) and 10% fetal calf serum (FCS, Biochrom, Berlin, Germany) was used as culture medium. Additionally, 100 µg/mL hygromycin B (A. G. Scientific, Inc., San Diego, CA) and 400 µg/mL G418 (Biochrom) were added to the culture medium of HEK293T-hH_2R-qs5-HA cells.[33] The culture medium of HEK293T-CRE-Luc-gpH_2R cells (for generation of this cell line see Appendix 1, App1.1 Generation of the HEK293T-CRE-Luc-gpH2R and the HEK293T NlucN-mGs/gpH2R-NlucC Cell Lines) was supplemented with 250 µg/mL hygromycin B and 600 µg/mL G418 and the culture medium of HEK293-mH_2R cells was supplemented with 200 µg/mL hygromycin B. On the day of the experiment, the cells were detached with trypsin (0.05% trypsin, 0.02% EDTA in PBS w/o Ca^{2+} and w/o Mg^{2+}, Biochrom). After subsequent centrifugation (500 x *g*, 5 min), the pellet was resuspended in Leibovitz's L-15 (Life Technologies Corporation, Grand Island, NY, USA) supplemented with 1% FCS and HEPES (10 mM, Serva, Heidelberg, Germany) and the density of the suspension was adjusted to 1.0 x 10^6 cells/mL.

For saturation binding experiments, 10 µL of a solution of **2.6** (10 mM) or 10 µL of Leibovitz's L-15 containing 10 mM HEPES were pipetted per cavity of a 96-well plate (ratiolab, Dreieich, Germany) either for the determination of non-specific or total binding and 80 µL of the cell suspension were added per well. Samples were completed by addition of 10 µL of the respective [^{3}H]**2.23** solution (10-fold concentrated feed-solutions compared to final concentration). The plates were shaken at 300 rpm for 120 min. Cell-bound radioactivity was transferred to a glass fibre filter GF/C (Whatman, Maidstone, UK) pre-treated with polyethylenimine (0.3% (v/v), Sigma-Aldrich) by a 96-well Brandel harvester (Brandel Inc., Unterföhring, Germany). After four washing steps with PBS (pH 7.4, 4 °C), filter pieces were stamped and transferred into untapped 96-well flexible sample plates (Perkin Elmer). Each well was supplemented with 200 µL of scintillation cocktail (Rotiscint Eco plus, Roth, Karlsruhe, Germany) and incubated in the dark for 12 h. Radioactivity was measured with a MicroBeta2 1450 scintillation counter. Specific binding data (dpm) were plotted against the free radioligand concentration (nM) and analyzed by non-linear regression (one site - specific binding equation) to obtain K_d and B_{max} values (GraphPad Prism 5). Non-specific binding data were fitted by linear regression (GraphPad Prism 5).

Saturation binding experiments on membrane preparations of Sf9 insect cells, expressing the h, gp or c H_2R-$G_{s\alpha S}$[20, 42] were performed in analogy to the above described protocol for HEK293(T) cells with minor modifications: Leibovitz's L-15 was replaced by binding buffer[9] (which is typically used as buffer for Sf9 membranes) and instead of the HEK293(T) cell suspension Sf9 membrane preparations were used. The Sf9 membrane preparations were thawed and sedimented by centrifugation at 13000 x *g* and 4 °C for 10 min. The membranes were resuspended in cold (4 °C) binding buffer so that the final concentration was 2-6 µg of protein per 1 µL binding buffer[9]. 10 µL of this membrane suspension and 70 µL binding buffer were used per well. The total volume in a well was 100 µL. Data analysis was performed as described in the protocol for HEK293(T) cells.

For competition binding experiments, cells were incubated with the unlabelled ligands of interest in presence of either 25 nM (hH_2R, gpH_2R) or 50 nM (mH_2R) of [^{3}H]**2.23** according to the conditions for the saturation binding experiments. Total binding was plotted versus logarithmic concentration of the competitor and normalized (100% = bound radioligand (dpm) in the absence of a competitor, 0% non-specifically bound radioligand (dpm) in the presence of **2.6**

(1 mM, h, gp, m H_2R)). Applying a log(inhibitor) vs. response - variable slope equation (GraphPad Prism 5), pIC_{50} values were obtained. The corresponding IC_{50} values were converted to K_i values by applying the Cheng-Prusoff equation followed by the calculation of pK_i.[43]

For kinetic experiments, the cells were prepared as described for binding assays. In association experiments, wells contained [^{3}H]**2.23** at a concentration of 25 nM (h/gp) or 50 nM (m) and the respective h, gp or m H_2R (co)expressing HEK293(T) cells at a concentration of 0.8 x 10^6 cells/mL in Leibovitz's L-15 supplemented with 1% FCS and 10 mM HEPES. The final volume per well was 100 µL. Non-specific binding was determined for each time point in the presence of **2.6** (7.5 µM (h/gp); 15 µM (m)). The plates were shaken at 300 rpm. The incubation was stopped after different time points (0-120 min) by transfer of the cells to a glass fibre filter using the harvester. In case of dissociation experiments, the cells were pre-incubated with [^{3}H]**2.23** (25 nM (h/gp) or 50 nM (m)) for 120 min. The final volume per well during the preincubation was 100 µL. The dissociation was started by addition of Leibovitz's L-15 medium (100 µL) containing **2.6** ((75 µM (h/gp); 150 µM (m)) after different periods of time (between 1 and 180 min; starting with the longest incubation time) followed by the transfer of the cells to a glass fibre filter using the harvester. The plates were shaken at 300 rpm. To determine non-specific binding, **2.6** (7.5 µM (h/gp); 15 µM (m)) was added during the preincubation step.

The specific binding data (dpm) from association experiments were fitted by a one-phase equation (one-phase association, GraphPad Prism 5) to a maximum to obtain k_{obs} (observed association rate constant) and B_{eq} (maximum specifically bound radioligand), which was used to calculate the specifically bound radioligand B_t in %, that is plotted over time. Data from dissociation experiments B_t in % were plotted over time and were analyzed by a three-parameter equation (one phase decay, GraphPad Prism 5).

2.4.7 Red Blood Cell Partitioning of [^{3}H]2.10 and [^{3}H]2.23

The extent of RBC partitioning of [^{3}H]**2.10** and [^{3}H]**2.23** was determined in vitro. The experiment with mouse blood was performed according to the *German Animal Welfare Act* (article 15) as well as to the *European Guidelines* (2010/63/EU). If vertebrates are euthanized without any pretreatment (e.g. to collect organs or tissues or blood) there is no approval from the governmental authorities needed, which is true in our case. Therefore, [^{3}H]**2.10** or [^{3}H]**2.23** was added to human (h, 1 mL aliquots/1.5 mL micro tubes (Sarstedt) or mouse (m, stem name: β B1

CTGF line 6 (CD1), 0.5 mL aliquots/1.5 mL micro tubes) heparinized (h: Li-Heparin S-Monovette, 4.9 mL, Sarstedt; m: Liquemin) freshly drawn blood (t <30 min) so that the final concentration was 20 nM. In the case of mouse blood, the volume of the aliquots was reduced to 0.5 mL in order to keep the number of required animals as low as possible. Immediately after the addition of the radioligand, the micro tubes were shaken vigorously for few seconds and were then carefully shaken using a RED ROCKER shaker (Hoefer Scientific Instruments, San Francisco, CA) for 60 min at rt. After 60 min, the plasma and RBCs were separated by centrifugation (500 x *g*, 10 min, 4 °C). The plasma was transferred with a pipette to 1.5 mL micro tubes. The border area between plasma and RBCs was rejected. Defined volume or plasma or RBCs (h: 100 µL; m: 25 µL; 2 times per sample) was lysed with four times the volume of lysis puffer (h: 400 µL; m: 100 µL) for 60 min while shaking. The lysis buffer consisted of urea (8 M, Roth), acetic acid (3 M, Merck) and Triton-X 100 (1%, Sigma-Aldrich) in water. 5 µL of the lysed plasma or RBCs were transferred to 3 mL Rotiscint®eco plus in scintillation counting mini-vials (6 mL, HD-PE, Sarstedt) and the radioactivity of the samples was determined using a Beckman LS 6500 liquid scintillations counter (Beckmann Coulter, München, Germany). The concentrations of the radioligand in plasma and RBCs were calculated using the specific activity of each radioligand ([^{3}H]**2.10**: 55.7 Ci/mmol; [^{3}H]**2.23**: 146.3 Ci/mmol) and a hematocrit value (packed red blood cell volume) of 0.41 and a plasma value of 0.55 for human as well as for mouse. The calculated concentrations of [^{3}H]**2.10** and [^{3}H]**2.23** in human or mouse plasma or RBCs are shown in Table App1.2 in the Appendix 1.

2.4.8 Statistical Analysis

Results are reported as scatter plot representing mean values ± 95% CI. Statistic differences were analyzed using a Mann-Whitney test. All reported p values are two-sided, and p values lower than 0.05 were considered to indicate statistical significance. All calculations were performed using the GraphPad Prism 5 software.

2.5 References

1. Hill, S. J.; Ganellin, C. R.; Timmerman, H.; Schwartz, J. C.; Shankley, N. P.; Young, J. M.; Schunack, W.; Levi, R.; Haas, H. L., International union of pharmacology. XIII. Classification of histamine receptors. *Pharmacol. Rev.* **1997,** *49,* 253-278.

2. Panula, P.; Chazot, P. L.; Cowart, M.; Gutzmer, R.; Leurs, R.; Liu, W. L. S.; Stark, H.; Thurmond, R. L.; Haas, H. L., International union of basic and clinical pharmacology. XCVIII. Histamine receptors. *Pharmacol. Rev.* **2015,** *67*, 601-655.
3. Traiffort, E.; Pollard, H.; Moreau, J.; Ruat, M.; Schwartz, J. C.; Martinez-Mir, M. I.; Palacios, J. M., Pharmacological characterization and autoradiographic localization of histamine H_2 receptors in human brain identified with [^{125}I]iodoaminopotentidine. *J. Neurochem.* **1992,** *59*, 290-299.
4. Dove, S.; Elz, S.; Seifert, R.; Buschauer, A., Structure-activity relationships of histamine H_2 receptor ligands. *Mini-Re. Med. Chem.* **2004,** *4*, 941-954.
5. Levi, R. C.; Allotti, G., Histamine modulates calcium current in guinea pig ventricular myocytes. *J. Pharmacol. Exp. Ther.* **1988,** *246* (1), 377-383.
6. Black, J. W.; Duncan, W. A. M.; Durant, C. J.; Genellin, C. R.; M., P. E., Definition and antagonism of histamine H_2-receptors. *Nature* **1972,** *236*, 385-390.
7. Yanagisawa, I.; Hirata, Y.; Ishii, A., Studies on histamine H_2 receptor antagonists. 2. Synthesis and pharmacological activities of *N*-sulfamoyl and *N*-sulfonyl amidine derivatives. *J. Med. Chem.* **1987,** *30*, 1787-1793.
8. Sinkins, W. G.; Kandel, M.; Kandel, S. I.; Schunack, W.; Wells, J. W., G protein-linked receptors labeled by [^{3}H]histamine in guinea pig cerebral cortex. I. Pharmacological characterization [corrected]. *Mol. Pharmacol.* **1993,** *43*, 569-582.
9. Kagermeier, N.; Werner, K.; Keller, M.; Baumeister, P.; Bernhardt, G.; Seifert, R.; Buschauer, A., Dimeric carbamoylguanidine-type histamine H_2 receptor ligands: a new class of potent and selective agonists. *Bioorg. Med. Chem.* **2015,** *23*, 3957-3969.
10. Warrander, S. E.; Norris, D. B.; Rising, T. J.; Wood, T. P., ^{3}H-cimetidine and the H_2-receptor. *Life Sci.* **1983,** *33*, 1119-1126.
11. Rising, T. J.; Norris, D. B.; Warrander, S. E.; Wood, T. P., High affinity ^{3}H-cimetidine binding in guinea-pig tissues. *Life Sci.* **1980,** *27*, 199-206.
12. Kendall, D. A.; Ferkany, J. W.; Enna, S. J., Properties of ^{3}H-cimetidine binding in rat brain membrane fractions. *Life Sci.* **1980,** *26*, 1293-1302.
13. Smith, I. R.; Cleverley, M. T.; Ganellin, C. R.; Metters, K. M., Binding of [^{3}H]cimetidine to rat brain tissue. *Agents Actions* **1980,** *10*, 422-426.
14. Bristow, D. R.; Hare, J. R.; Hearn, J. R.; Martin, L. E., Radioligand binding studies using [^{3}H]-cimetidine and [^{3}H]-ranitidine. *Br. J. Pharmacol.* **1980,** *72*, 547-548.
15. Tanaka, A.; Nishihara, S.; Misawa, T.; Ibayashi, H., Effects of H_2-receptor antagonists on ^{3}H-cimetidine binding and histamine-stimulation of cellular cAMP in isolated guinea pig gastric glands. *Jpn. J. Pharmacol.* **1987,** *45*, 97-105.
16. Devoto, P.; Marchisio, A. M.; Carboni, E.; Spano, P. F., Detection of ^{3}H-cimetidine specific binding in rat anterior pituitary. *Eur. J. Pharmacol.* **1980,** *63*, 91-93.
17. Kandel, S. I.; Steinberg, G. H.; Wells, J. W.; Kandel, M.; Gornall, A. G., Separate binding sites for histaminic drugs in rat cerebral cortex. *Biochem. Pharmacol.* **1980,** *29*, 2269-2272.
18. Nielsen, S. T., Binding of [^{3}H]ICIA 5165, an H_2-receptor antagonist to guinea pig gastric mucosa. *Agents Actions* **1986,** *18*, 524-531.
19. Gajtkowski, G. A.; Norris, D. B.; Rising, T. J.; Wood, T. P., Specific binding of ^{3}H-tiotidine to histamine H_2 receptors in guinea pig cerebral cortex. *Nature* **1983,** *304*, 65-67.

20. Kelley, M. T.; Bürckstürmmer, T.; Wenzel-Seifert, K.; Dove, S.; Buschauer, A.; Seifert, R., Distinct interaction of human and guinea pig histamine H_2-receptor with guanidine-type agonists. *Mol. Pharmacol.* **2001,** *60*, 1210-1225.
21. Schwartz, J. C.; Arrang, J. M.; Garbarg, M.; Pollard, H.; Ruat, M., Histaminergic transmission in the mammalian brain. *Physiol. Rev.* **1991,** *71*, 1-51.
22. Ruat, M.; Traiffort, E.; Bouthenet, M. L.; Schwartz, J. C.; Hirschfeld, J.; Buschauer, A.; Schunack, W., Reversible and irreversible labeling and autoradiographic localization of the cerebral histamine H_2 receptor using [^{125}I]iodinated probes. *Proc. Natl. Acad. Sci. USA* **1990,** *87*, 1658-1662.
23. Martinez-Mir, M. I.; Pollard, H.; Moreau, J.; Arrang, J. M.; Ruat, M.; Traiffort, E.; Schwartz, J. C.; Palacios, J. M., Three histamine receptors (H_1, H_2 and H_3) visualized in the brain of human and non-human primates. *Brain Res.* **1990,** *526*, 322-327.
24. Leurs, R.; Smit, M. J.; Menge, W. M.; Timmerman, H., Pharmacological characterization of the human histamine H_2 receptor stably expressed in chinese hamster ovary cells. *Br. J. Pharmacol.* **1994,** *112*, 847-854.
25. Baumeister, P.; Erdmann, D.; Biselli, S.; Kagermeier, N.; Elz, S.; Bernhardt, G.; Buschauer, A., [^{3}H]UR-DE257: development of a tritium-labeled squaramide-type selective histamine H_2 receptor antagonist. *ChemMedChem* **2015,** *10*, 83-93.
26. Cavanagh, R. L.; Buyniski, J. P., Effect of BMY-25368, a potent and long-acting histamine H_2-receptor antagonist, on gastric secretion and aspirin-induced gastric lesions in the dog. *Aliment. Pharmacol. Ther.* **1989,** *3*, 299-313.
27. Kraus, A.; Ghorai, P.; Birnkammer, T.; Schnell, D.; Elz, S.; Seifert, R.; Dove, S.; Bernhardt, G.; Buschauer, A., N^G-Acylated aminothiazolylpropylguanidines as potent and selective histamine H_2 receptor agonists. *ChemMedChem* **2009,** *4*, 232-240.
28. Igel, P.; Schnell, D.; Bernhardt, G.; Seifert, R.; Buschauer, A., Tritium-labeled N^1-[3-(1H-imidazol-4-yl)propyl]-N^2-propionylguanidine ([^{3}H]UR-PI294), a high-affinity histamine H_3 and H_4 receptor radioligand. *ChemMedChem* **2009,** *4*, 225-231.
29. Grätz, L.; Tropmann, K.; Bresinsky, M.; Müller, C.; Bernhardt, G.; Pockes, S., NanoBRET binding assay for histamine H_2 receptor ligands using live recombinant HEK293T cells. *Sci. Rep.* **2020,** *10, e13288*.
30. Pertz, H. H.; Görnemann, T.; Schurad, B.; Seifert, R.; Straßer, A., Striking differences of action of lisuride stereoisomers at histamine H_1 receptors. *N.-S. Arch. Pharmacol.* **2006,** *374*, 215-222.
31. Pockes, S.; Wifling, D.; Keller, M.; Buschauer, A.; Elz, S., Highly potent, stable, and selective dimeric hetarylpropylguanidine-type histamine H_2 receptor agonists. *ACS Omega* **2018,** *3*, 2865-2882.
32. Bartole, E.; Littmann, T.; Tanaka, M.; Ozawa, T.; Buschauer, A.; Bernhardt, G., [^{3}H]UR-DEBa176: a 2,4-diaminopyrimidine-type radioligand enabling binding studies at the human, mouse, and rat histamine H_4 receptors. *J. Med. Chem.* **2019,** *62*, 8338-8356.
33. Mosandl, J. Radiochemical and Luminescence-Based Binding and Functional Assays for Human Histamine Receptors Using Genetically Engineered Cells. Ph.D. Thesis. University of Regensburg, 2009.
34. Carpenter, B.; Tate, C. G., Engineering a minimal G protein to facilitate crystallisation of G protein-coupled receptors in their active conformation. *Protein Eng. Des. Sel.* **2016,** *29*, 583-594.

35. Nehmé, R.; Carpenter, B.; Singhal, A.; Strege, A.; Edwards, P. C.; White, C. F.; Du, H.; Grisshammer, R.; Tate, C. G., Mini-G proteins: novel tools for studying GPCRs in their active conformation. *PLOS ONE* **2017,** *12*, e0175642.
36. Wan, Q.; Okashah, N.; Inoue, A.; Nehmé, R.; Carpenter, B.; Tate, C. G.; Lambert, N. A., Mini G protein probes for active G protein–coupled receptors (GPCRs) in live cells. *J. Biol. Chem.* **2018,** *293*, 7466-7473.
37. Höring, C.; Seibel, U.; Tropmann, K.; Grätz, L.; Mönnich, D.; Pitzl, S.; Bernhardt, G.; Pockes, S.; Strasser, A., A dynamic, split-luciferase-based mini-G protein sensor to functionally characterize ligands at all four histamine receptor subtypes. *Int. J. Mol. Sci.* **2020,** *21, 8440*.
38. Fernandez, N.; Monczor, F.; Baldi, A.; Davio, C.; Shayo, C., Histamine H_2 receptor trafficking: role of arrestin, dynamin, and clathrin in histamine H_2 receptor internalization. *Mol. Pharmacol.* **2008,** *74*, 1109-1118.
39. Felixberger, J. Luciferase Complementation for the Determination of Arrestin Recruitment: Investigation of Histamine and NPY receptors. Ph.D. Thesis. University of Regensburg, 2014.
40. Daly, M. J.; Humphray, J. M.; Bunce, K. T.; Stables, R., The effect of ranitidine on gastric acid secretory response curves to histamine, pentagastrin or bethanechol in the dog with a heidenhain pouch. *Agents Actions* **1981,** *11*, 160-164.
41. Durant, G. J.; Duncan, W. A. M.; Ganellin, C. R.; Parsons, M. E.; Blakemore, R. C.; Rasmussen, A. C., Impromidine (SK&F 92676) is a very potent and specific agonist for histamine H_2 receptors. *Nature* **1978,** *276*, 403-405.
42. Preuss, H.; Ghorai, P.; Kraus, A.; Dove, S.; Buschauer, A.; Seifert, R., Constitutive activity and ligand selectivity of human, guinea pig, rat, and canine histamine H_2 receptors. *J. Pharmacol. Exp. Ther.* **2007,** *321*, 983-995.
43. Cheng, Y. C.; Prusoff, W. H., Relationship between the inhibition constant (K_i) and the concentration of inhibitor which causes 50 percent inhibition (I_{50}) of an enzymatic reaction. *Biochem. Pharmacol.* **1973,** *22*, 3099-3108.
44. Preuss, H.; Ghorai, P.; Kraus, A.; Dove, S.; Buschauer, A.; Seifert, R., Point mutations in the second extracellular loop of the histamine H_2 receptor do not affect the species-selective activity of guanidine-type agonists. *N.-S. Arch. Pharmacol.* **2007,** *376*, 253-264.
45. Sun, X.; Li, Y.; Li, W.; Xu, Z.; Tang, Y., Computational investigation of interactions between human H_2 receptor and its agonists. *J. Mol. Graph. Model.* **2011,** *29*, 693-701.
46. Zhang, J.; Qi, T.; Wei, J., Homology modeling and antagonist binding site study of the human histamine H_2 receptor. *Med. Chem.* **2012,** *8*, 1084-1092.
47. Hinderling, P. H., Kinetics of partitioning and binding of digoxin and its analogues in the subcompartments of blood. *J. Pharm. Sci.* **1982,** *73*, 1043-1053.
48. Hinderling, P. H., Red blood cells: A neglected compartment in pharmacokinetics and pharmacodynamics. *Pharmacol. Rev.* **2000,** *49*, 279-473.
49. Kalamaridis, D.; DiLoreto, K., Drug Partition in Red Blood Cells. In *Optimization in Drug Discovery: In Vitro Methods, Methods in Pharmacology and Toxicology*, Springer, Ed. New York, 2014; pp 39-47.
50. Gers, T.; Kunce, D.; Markowski, P.; Izdebski, J., Reagents for efficient conversion of amines to protected guanidines. *Synthesis* **2004,** *1*, 37-42.
51. Cinelli, M. A.; Cordero, B.; Dexheimer, T. S.; Pommier, Y.; Cushman, M., Synthesis and biological evaluation of 14-(aminoalkyl-aminomethyl)aromathecins as topoisomerase I

inhibitors: investigating the hypothesis of shared structure–activity relationships. *Bioorg. Med. Chem.* **2009,** *17*, 7145-7155.
52. Morrell, A.; Placzek, M. S.; Steffen, J. D.; Antony, S.; Agama, K.; Pommier, Y.; Cushman, M., Investigation of the lactam side chain length necessary for optimal indenoisoquinoline topoisomerase I inhibition and cytotoxicity in human cancer cell cultures. *J. Med. Chem.* **2007,** *50*, 2040-2048.
53. Pockes, S.; Wifling, D.; Buschauer, A.; Elz, S., Structure-activity relationship of hetarylpropylguanidines aiming at the development of selective histamine receptor ligands. *ChemistryOpen* **2019,** *8*, 285-297.
54. Houston, C.; Wenzel-Seifert, K.; Bürckstümmer, T.; Seifert, R., The human histamine H_2-receptor couples more efficiently to Sf9 insect cell G_s-proteins than to insect cell G_q-proteins: limitations of Sf9 cells for the analysis of receptor/G_q-protein coupling. *J. Neurochem.* **2002,** *80*, 678-696.
55. Schnell, D.; Strasser, A.; Seifert, R., Comparison of the pharmacological properties of human and rat histamine H_3-receptors. *Biochem. Pharmacol.* **2010,** *80*, 1437-1449.
56. Schneider, E. H.; Schnell, D.; Papa, D.; Seifert, R., High constitutive activity and a G-protein-independent high-affinity state of the human histamine H_4-receptor. *Biochemistry* **2009,** *48*, 1424-1438.
57. Igel, P.; Geyer, R.; Strasser, A.; Dove, S.; Seifert, R.; Buschauer, A., Synthesis and structure-activity relationships of cyanoguanidine-type and structurally related histamine H_4 receptor agonists. *J. Med. Chem.* **2009,** *52*, 6297-6313.
58. Geyer, R.; Kaske, M.; Baumeister, P.; Buschauer, A., Synthesis and functional characterization of imbutamine analogs as histamine H_3 and H_4 receptor ligands. *Arch. Pharm.* **2014,** *347*, 77-88.
59. Pegoli, A.; X., S.; Wifling, D.; Hübner, H.; Bernhardt, G.; Gmeiner, P.; Keller, M., Radiolabeled dibenzodiazepinone-type antagonists give evidence of dualsteric binding at the M_2 muscarinic acetylcholine receptor. *J. Med. Chem.* **2017,** *60*, 3314-3334.

Appendix 1 Discovery of a G Protein Biased Radioligand for the Histamine H_2 Receptor with Reversible Binding Properties

App1.1 Generation of the HEK293T-CRE-Luc-gpH_2R and the HEK293T NlucN-mGs/gpH_2R-NlucC Cell Lines

App1.1.1 Molecular Cloning

In order to generate the pcDNA3.1(+) gpH_2R vector, the cDNA encoding the gpH_2R was isolated from the pVL 1392-SF-gpH_2R-$G_{s\alpha S}$[1] by PCR, whereby a stop codon was added (forward primer: 5`-ataaagcttATGGCGTTCAATGGCA-3`; reverse primer: 5`-atatctagattaCCTGTTTGTGGCTCCCT-3`). Afterwards, the construct was subcloned into a pcDNA3.1(+) vector backbone using *Hin*dIII and *Xb*aI.

For construction of the pcDNA3.1(+) gpH_2R-NlucC vector, the receptor gene was amplified by PCR without a stop codon (forward primer: 5'-gatcaagcttgctagcgccaccATGGCGTTCAATGGCACG-3'; reverse primer: 5'-gatctctagactcgagccCCTGTTTGTGGCTCCCTG-3') and subcloned into the pcDNA3.1(+) H_1R-NlucC vector replacing the H_1R gene by digest with *Hin*dIII and *Xb*aI as described previously.[2] Both constructs encoding the gpH_2R were verified by sequencing (Eurofins Genomics LLC, Ebersberg, Germany).

App1.1.2 Generation of Stable Cell Lines

In order to generate HEK293T cells stably co-expressing the CRE-Luc and the gpH_2R, the parental cell line HEK293T-CRE-Luc[3] was seeded into a 6-well dish at a density of 0.5 x 10^6 cells/mL one day prior to the transfection. The day of the transfection, the pcDNA3.1(+) gpH_2R plasmid was digested for 2 h at 37 °C with *Pv*uI (New England Biolabs, Frankfurt am Main, Germany) and purified using a PCR purification KIT (Quiagen, Leipzig, Germany). Thereafter, 2 µg of the linearized cDNA were transfected using the FuGENE HD transfection reagent (Roche Diagnostics GmbH, Mannheim, Germany) according to the manufacturer's instructions.

Stable expression of the gpH_2R-NlucC was achieved using HEK293T cells which already stably expressed NlucN-mGs[2] and which were seeded into a 6-well dish (0.3 x 10^6 cells/mL) the day prior to the transfection. 2 µg of the pcDNA3.1(+) gpH_2R-NlucC vector were

transfected using the transfection reagent XtremeGENE HP according to the manufacturer's protocol (Merck KGaA, Darmstadt, Germany).

App1.1.3 Cell Culture

HEK293T-CRE-Luc-gpH_2R cells were cultured in DMEM supplemented with 10% FCS, 250 µg/mL hygromycin B and 600 µg/mL G418 and HEK293T NlucN-mGs/gpH_2R-NlucC cells were cultured in DMEM containing 10% FCS, 1 µg/mL puromycin (InvivoGen, Toulouse, France) and 600 µg/mL G418. The cells were incubated at 37°C in a water-saturated atmosphere containing 5% CO_2. Periodically, the cells were tested for mycoplasma contamination using the Venor GeM Mycoplasma Detection Kit (Minerva Biolabs, Berlin, Germany) and were negative.

App1.1.4 [^{3}H]2.23 Saturation Binding Using gpH_2R Expressing Cells

[^{3}H]**2.23** bound in a specific, saturable manner to both the HEK293T-CRE-Luc-gpH_2R (for more details see Figure 2.7 and Table 2.4 in the chapter 2) & HEK293T NlucN-mGs/gpH_2R-NlucC cells (K_d = 29 ± 3 nM, N = 3, representative curve is shown in Figure App1.1). Non-specific binding was determined in the presence of 1 mM famotidine. The determined B_{max} values allowed the calculation of the number of specific binding sites per cell, revealing a comparably high receptor expression level for both cell lines, 0.89 ± 0.01 millions receptors/cell (N = 3) for the HEK293T-CRE-Luc-gpH_2R and 0.39 ± 0.01 millions receptors/cell (N = 3) for the HEK293T NlucN-mGs/gpH_2R-NlucC cells, respectively.

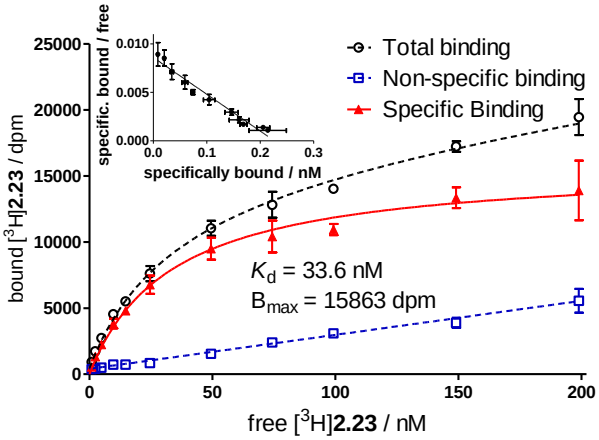

Figure App1.1. Representative data from saturation binding experiments at the gpH_2R, co-expressed in HEK293T NlucN-mGs cells. Total binding (dashed black curve), specific binding (red curve), and nonspecific binding (dashed blue line, determined in the presence of famotidine (1 mM)) of [^{3}H]**2.23** are depicted. Inserts: Scatchard transformations of shown specific binding curves. The experiments were performed in triplicate. Error bars of specific binding and in the Scatchard plots were calculated according to the Gaussian law of error propagation. Error bars of total and nonspecific binding represent SEMs.

App1.2 Mini-G Protein Recruitment Assay Using HEK293T Cells Co-Expressing the NlucN-mGs and gpH_2R-NlucC Fusion Proteins

The assay was performed and evaluated as recently published for the hH_2R by Höring et al.[2] The results of standard H_2R agonists and antagonists/inverse agonists are summarized in Table App1.1 and the curves are shown in Figure App1.2. The curves of **2.20**-**2.25** are shown in Figure 2.4 in the chapter 2.

Table App1.1. pEC_{50}, E_{max} and pK_b Values of Standard H_2R Agonists and Antagonists/Inverse Agonists Analyzed in Mini-G Protein Recruitment Assay using HEK293T Cells Expressing NlucN-mGs and gpH_2R-NlucC[a]

compd.	pEC_{50}[b]/(pK_b)[c]	E_{max}[d]	N
histamine, **2.1**	6.65 ± 0.07	1.00	5
amthamine	7.60 ± 0.06	1.01 ± 0.01	4
dimaprit	6.50 ± 0.04	0.94 ± 0.01	4
4-methylhistamine	6.21 ± 0.05	0.93 ± 0.02	4
cimetidine, **2.4**	6.06 ± 0.02	-0.07 ± 0.01	3
	(6.18 ± 0.06)		3
ranitidine, **2.5**	6.32 ± 0.09	-0.07 ± 0.01	3
	(6.46 ± 0.04)		3
famotidine, **2.6**	7.04 ± 0.07	-0.07 ± 0.01	3
	(7.91 ± 0.05)		3

[a]Data represent mean values ± SEM from N independent experiments, each performed in triplicate. Data were analyzed by nonlinear regression and were best fitted to sigmoidal concentration-response curves (GraphPad Prism 5, log(agonist or antagonist) vs. response–variable slope). [b]pEC_{50} = -logEC_{50}. [c]pK_b = -logK_b. K_b values were calculated according to the Cheng-Prusoff equation.[4] The K_b values of antagonists and inverse agonists were determined in the antagonist mode versus 1 µM histamine. [d]The response was normalized to the effect induced by 100 µM histamine (E_{max} = 1.00) and buffer control (E_{max} = 0.00).

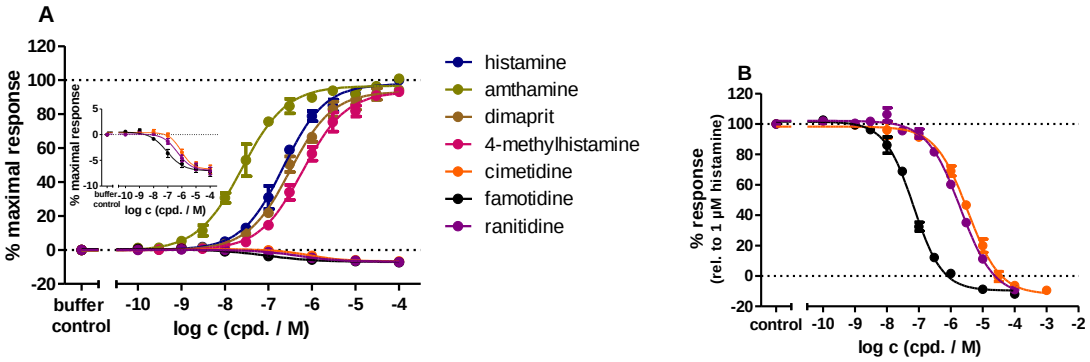

Figure App1.2. Characterization of standard ligands at the gpH_2R using the developed mini-G protein recruitment assay. Live HEK293T cells, stably expressing the NlucN-mGs and gpH_2R-NlucC, were analyzed regarding their response to standard agonists and antagonists/inverse agonists in the agonist mode (**A**; inset: increase of the range y = 5 to -10% maximal response) and antagonist mode (**B**; only in case of antagonists/inverse agonists). **A**: The response was normalized to the maximal effect induced by 100 µM histamine (maximal response: 100%) and buffer control (maximal response: 0%). **B**: The response was normalized to the effect induced by 1 µM histamine (response: 100%) and buffer control (response: 0%). pEC_{50}, E_{max}, and pK_b values are listed in Table App1.1 and were in good accordance with data described in literature. Data are presented as means ± SEM from at least three independent experiments, each performed in triplicate.

App1.3 Red Blood Cell Partioning of [^{3}H]2.10 and [^{3}H]2.23

Table App1.2. Calculated Concentrations of [^{3}H]2.10 and [^{3}H]2.23 in Human (h) or Mouse (m) Plasma or Red Blood Cells (RBCs)

	plasma c[^{3}H]**2.10**	N	**plasma** c[^{3}H]**2.23**	N	**RBCs** c[^{3}H]**2.10**	N	**RBCs** c[^{3}H]**2.23**	N	c[^{3}H]**2.10** found (plasma + RBCs)	c[^{3}H]**2.23** found (plasma + RBCs)
h	30.3 ± 0.6	10	32.5 ± 0.4	10	3.8 ± 0.3	10	8.3 ± 0.4	10	20.1 ± 1.2	19.6 ± 2.0
m	23.4 ± 1.0	8	32.4 ± 0.6	6	15.0 ± 1.0	6	7.0 ± 0.4	6	20.7 ± 1.7	19.0 ± 2.1

App1.4 Bias Analysis for Compounds 2.20-2.25

A bias analysis for **2.20**-**2.25** was performed as described by van der Westhuizen et al.[5] based on the operational model using the endogenous ligand histamine as a reference agonist. This model was chosen because several publications recommend the use of this model to overcome a systemic bias between two readouts systems as described in the chapter 2 regarding the lower potencies of all tested compounds in the β-arrestin2 recruitment assay compared to the mini-G protein recruitment assay.[6-8] Table App1.3 shows the absolute ($\log(\tau/K_A)$) and the normalized ($\Delta\log(\tau/K_A)$) transduction coefficients as well as the relative effectiveness for both assays and the $\Delta\Delta\log(\tau/K_A)$ ratios and bias factors of the ligands between the G-protein and arrestin pathways. The determined $\Delta\Delta\log(\tau/K_A)$ ratios allowed for the quantification of the functional selectivity which can be observed in the functional data of the carbamoylguanidine-type ligands (Figure App1.4). Based on these analyses, **2.23** showed a significant preference for the G-protein mediated pathway ($\Delta\Delta\log(\tau/K_A) >0$). Although until today no flawless model for bias quantification has been developed, the presented results can be considered as decent evidence for functionally selective signaling profiles of the investigated carbamoylguanidines.

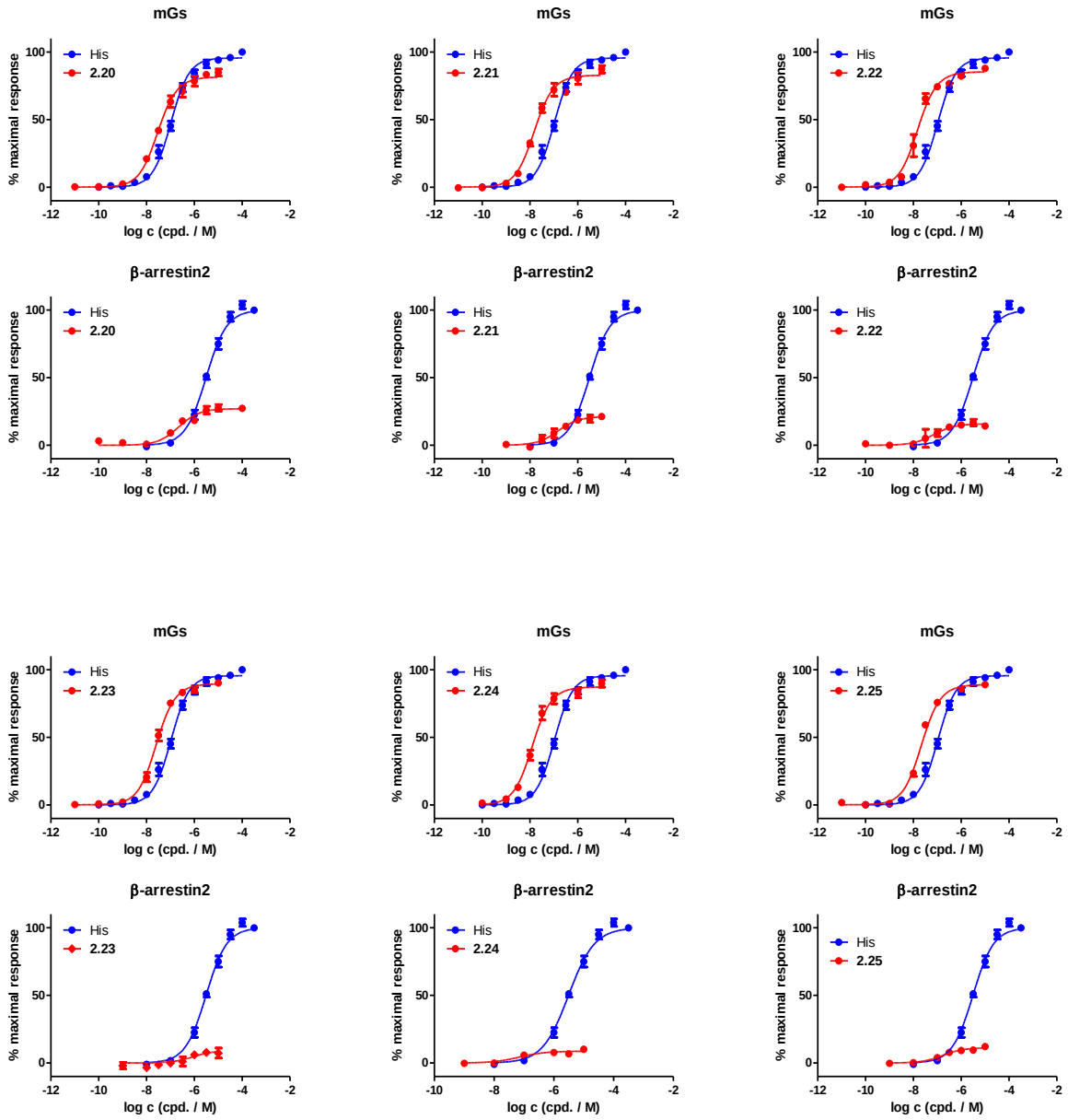

Figure App1.3. Concentration-response curves of **2.20**-**2.25** in comparison with the endogenous ligand histamine fitted with the operational model of agonism as described by van der Westhuizen.[5]

Table App1.3. Calculated Δlog(τ/K_A) Ratios, ΔΔlog(τ/K_A) Ratios and Bias Factors for the Endogenous Ligand Histamine and 2.20-2.25

compd.	β-arrestin2			mGs			mGs-β-arrestin2	
	log (τ/K_A)[a]	Δlog (τ/K_A)[b]	relative effecti-veness	log (τ/K_A)[a]	Δlog (τ/K_A)[b]	relative effecti-veness	ΔΔlog (τ/K_A)[c]	bias factor
His	5.52 ± 0.04	0.00 ± 0.06	1.00	6.95 ± 0.05	0.00 ± 0.07	1.00	0.00 ± 0.09	1.00
2.20	5.80 ± 0.10	0.51 ± 0.11	3.21	7.45 ± 0.03	0.50 ± 0.06	3.19	0.00 ± 0.12	0.99
2.21	6.20 ± 0.16	0.68 ± 0.16	4.82	7.74 ± 0.03	0.80 ± 0.06	6.26	0.11 ± 0.17	1.30
2.22	6.35 ± 0.23	0.83 ± 0.24	6.75	7.74 ± 0.13	0.79 ± 0.14	6.20	-0.04 ± 0.27	0.92
2.23	5.13 ± 0.27	-0.39 ± 0.28	0.41	7.54 ± 0.04	0.59 ± 0.07	3.89	0.98 ± 0.28	9.56
2.24	6.11 ± 0.04	0.59 ± 0.06	3.93	7.81 ± 0.06	0.87 ± 0.08	7.36	0.27 ± 0.10	1.87
2.25	5.82 ± 0.17	0.30 ± 0.17	2.00	7.58 ± 0.04	0.63 ± 0.07	4.30	0.33 ± 0.18	2.15

[a]Data were analyzed by non-linear regression using the operational model equation described by van der Westhuizen et al.[5] in GraphPad Prism 5 to determine the log(τ/K_A) ratios. [b]ΔLog(τ/K_A) ratios were calculated from the log(τ/K_A) ratios, considering histamine as the reference ligand as described by van der Westhuizen.[5] [c]Subtraction of the Δlog(τ/K_A) ratios of the β-arrestin2- from the Δlog(τ/K_A) ratios of mini-G protein recruitment assay yielded the ΔΔlog(τ/K_A) ratios for the tested compounds. The standard errors were calculated according to the Gaussian law of error propagation. Data are the mean ± standard error of 3-9 independent experiments performed in triplicates.

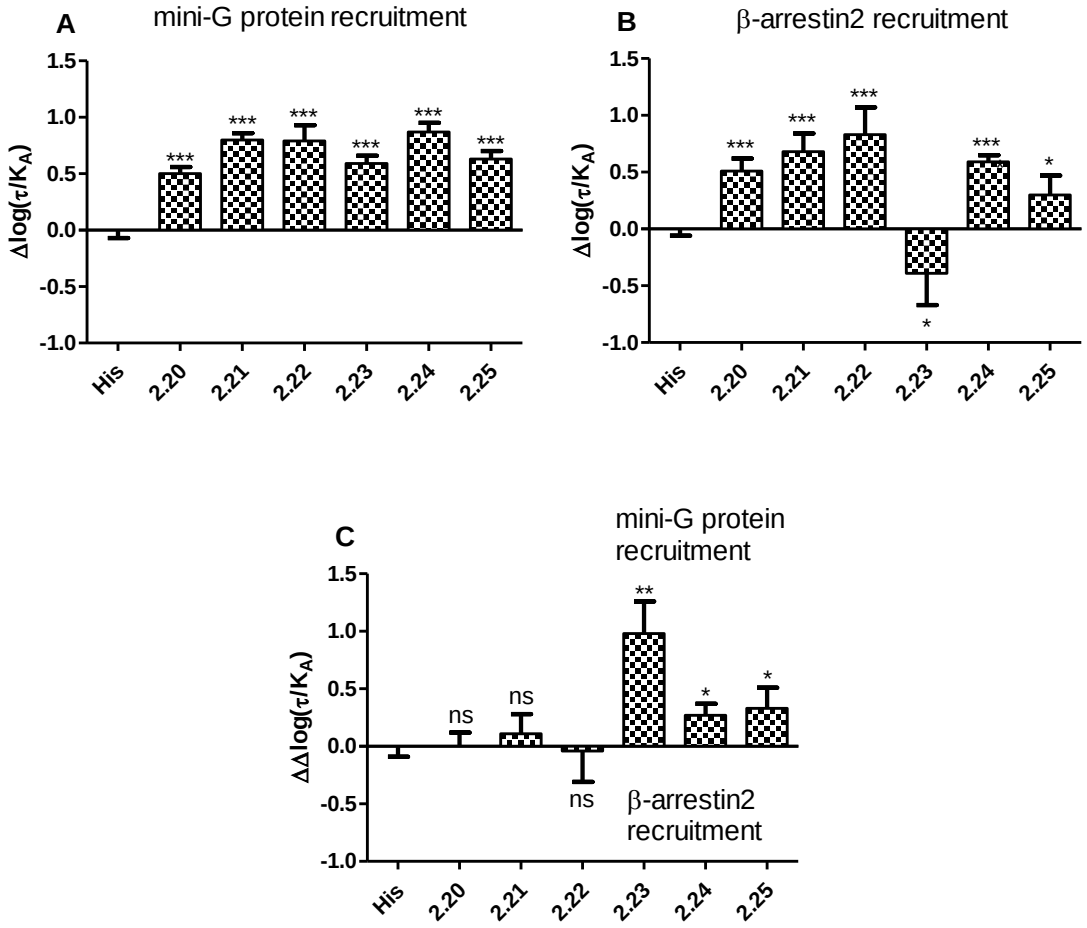

Figure App1.4. Quantification of the functional bias of the tested H_2R agonists **2.20**-**2.25** between the mini-G protein- and the β-arrestin2 recruitment assays. The $\Delta\log(\tau/K_A)$ ratios for the G-protein pathway (**A**, mGs recruitment) and arrestin pathway (**B**, β-arrestin2 recruitment) were calculated as described by Westhuizen et al., using histamine as reference agonist.[5] Subtraction of the $\Delta\log(\tau/K_A)$ ratios of the β-arrestin2- from the $\Delta\log(\tau/K_A)$ ratios of the mini-G protein recruitment assay yielded the $\Delta\Delta\log(\tau/K_A)$ ratios for the tested compounds (**C**). A $\Delta\Delta\log(\tau/K_A)$ ratio = 0 indicate an equal activation of the G-protein- and arrestin pathways, while a $\Delta\Delta\log(\tau/K_A)$ ratio ≠ 0 indicate a preference for one signal pathway over the other. Data represent mean ± standard error of 3-9 independent experiments performed in triplicates. Data were analyzed in a pairwise manner using a two-tailed unpaired student's t-test (***p <0.001, **p <0.01, *p <0.05) to determine the significance of the $\Delta\log(\tau/K_A)$ and $\Delta\Delta\log(\tau/K_A)$ ratios.

App1.5 References

1. Kelley, M. T.; Bürckstürmmer, T.; Wenzel-Seifert, K.; Dove, S.; Buschauer, A.; Seifert, R., Distinct interaction of human and guinea pig histamine H_2-receptor with guanidine-type agonists. *Mol. Pharmacol.* **2001,** *60*, 1210-1225.
2. Höring, C.; Seibel, U.; Tropmann, K.; Grätz, L.; Mönnich, D.; Pitzl, S.; Bernhardt, G.; Pockes, S.; Strasser, A., A dynamic, split-luciferase-based mini-G protein sensor to functionally characterize ligands at all four histamine receptor subtypes. *Int. J. Mol. Sci.* **2020,** *21, 8440*.
3. Nordemann, U.; Wifling, D.; Schnell, D.; Bernhardt, G.; Stark, H.; Seifert, R.; Buschauer, A., Luciferase reporter gene assay on human, murine and rat histamine H_4 receptor orthologs: correlations and discrepancies between distal and proximal readouts. *PLOS ONE* **2013,** *8, e73961*.
4. Cheng, Y. C.; Prusoff, W. H., Relationship between the inhibition constant (K_i) and the concentration of inhibitor which causes 50 percent inhibition (I_{50}) of an enzymatic reaction. *Biochem. Pharmacol.* **1973,** *22*, 3099-3108.
5. van der Westhuizen, E. T.; Breton, B.; Christopoulos, A.; Bouvier, M., Quantification of ligand bias for clinically relevant β_2-adrenergic receptor ligands: implications for drug taxonomy. *Mol. Pharmacol.* **2014,** *85*, 492-509.
6. Black, J. W.; Leff, P., Operational models of pharmacological agonism. *Proc. R. Soc. London, Ser. B* **1983,** *220*, 141-162.
7. Kenakin, T.; Watson, C.; Muniz-Medina, V.; Christopoulos, A.; Novick, S., A simple method for quantifying functional selectivity and agonist bias. *ACS Chem. Neurosci.* **2012,** *3*, 193-203.
8. Rajagopal, S.; Ahn, S.; Rominger, D. H.; Gowen-MacDonald, W.; Lam, C. M.; Dewire, S. M.; Violin, J. D.; Lefkowitz, R. J., Quantifying ligand bias at seven-transmembrane receptors. *Mol. Pharmacol.* **2011,** *80*, 367-377.

3 Synthesis and Pharmacological Characterization of Fluorescent Histamine H_2 Receptor Carbamoylguanidine-Type Agonists

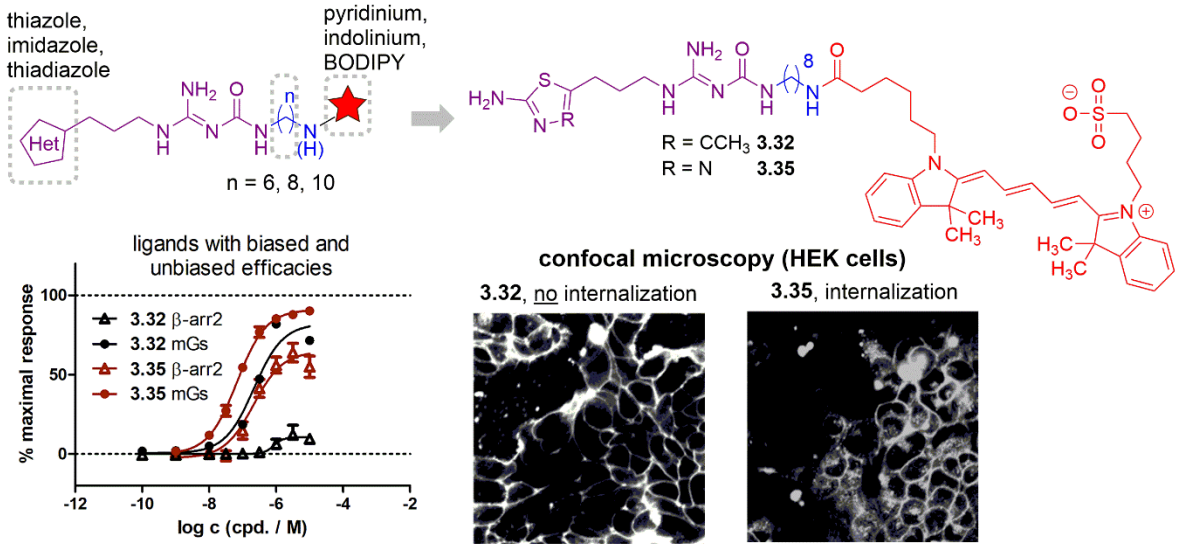

So far, only little is known about the internalization process of the histamine H_2 receptor (H_2R). One promising approach to study such dynamic processes is the use of agonistic fluorescent ligands. Therefore, a series of carbamoylguanidine-type H_2R agonists containing various fluorophores, heterocycles, and linkers (**3.31**-**3.40**) was synthesized. The ligands were pharmacologically characterized in several binding and functional assays. These studies revealed a significantly biased efficacy (E_{max}) for some of the compounds, e.g. **3.32**: whereas **3.32** acted as strong partial (E_{max}: 0.77, mini-Gs recruitment) or full agonist (E_{max}: 1.04, [^{35}S]GTPγS binding) with respect to G protein activation, it was only a weak partial agonist regarding β-arrestin1/2 recruitment (E_{max}: 0.09-0.12) and failed to promote H_2R internalization (confocal microscopy). On the other hand, H_2R internalization was observed for compounds that exhibited moderate agonistic activity in the β-arrestin1/2 pathways ($E_{max} \geq 0.22$). The direct comparison of such differentially biased ligands gave valuable insights into the internalization process of the H_2R and supports that activation of β-arrestin plays a crucial role in this process.

Ulla Seibel cloned the pIRESneo3-SP-FLAG-hH_2R vector and generated the HEK293T-SP-FLAG-hH_2R K33 cell line. Lukas Grätz synthesized the Py-5 label. The confocal microscopy experiments were performed with the help and instructions of Dr. Timo Littmann.

3.1 Introduction

The histamine H_2 receptor (H_2R) is a member of class A G protein-coupled receptors (GPCR) and is important for the regulation of gastric acid secretion, cell differentiation and proliferation, immune reactions, and central nervous system functions.[1-2] The H_2R can induce signal transduction in multiple ways, e.g. via heterotrimeric G proteins, G protein receptor kinases (GRK) and β-arrestins (β-arr).[2-6] Furthermore, it was also reported that different agonists can activate different downstream signaling cascades.[3, 7]

In detail, agonistic stimulation of the H_2R results in activation of both adenylate cyclase and phospholipase C via Gs and Gq proteins, respectively.[4, 8-15] In addition, it was recently published that the H_2R can also interact to a lesser extent with Gi and G12 proteins in HEK293 cells.[11] Excessive continuous or repeated stimulation of the H_2R by an agonist leads to receptor desensitization. In turn, GRK2 and GRK3 mediated phosphorylation of the receptor facilitates the interaction with β-arrestin1 and β-arrestin2 which leads to uncoupling of the receptor from its G protein.[16-18] The desensitization of the H_2R has been previously investigated in the human gastric cell line HGT-1[19-20], in clonal cytolytic T lymphocytes[21] and in the human monocytic cell line U937[22], in which the H_2R rapidly desensitizes in response to histamine (**3.1**, Figure 3.1) stimulation. Another event that occurs after H_2R stimulation is internalization, in which the receptor is translocated from the plasma membrane into intracellular endosomes. Previous findings showed that the H_2R undergoes rapid agonist-induced internalization (visualized by immunofluorescence).[23-24] Agonist-induced GPCR internalization is a very complex process and can occur through several distinct pathways including (1) clathrin-coated pit pathway, (2) caveolae-pathway, and (3) dynamin-independent pathway.[25-26] However, little is known about the exact mechanism by which the H_2R is internalized, although previous studies suggest the involvement of β-arrestin2.[27] One way to study such processes in detail is by use of fluorescent ligands.

Fluorescent GPCR ligands gained increased popularity to study various aspects of receptor pharmacology.[28-32] These ligands allow the direct visualization of dynamic processes such as internalization, trafficking and characteristics of diffusion in the plasma membrane of cells.[33] Many different antagonistic (**3.2**-**3.18**, Figure 3.1)[34-39] and agonistic (**3.19**-**3.21**, Figure 3.2A)[40] fluorescent ligands for the H_2R have been reported. However, only the agonistic fluorescent ligands can be used to clarify the mechanisms, underlying the H_2R internalization, since only agonists can trigger this process. But although the fluorescent agonist-based probes developed by Kagermeier et al.[40] (**3.19**-**3.21**) possess high affinity, their high level of non-specific (non-sp.) binding and receptor-independent diffusion through the cell membrane, limited their applications in studies with live cells.

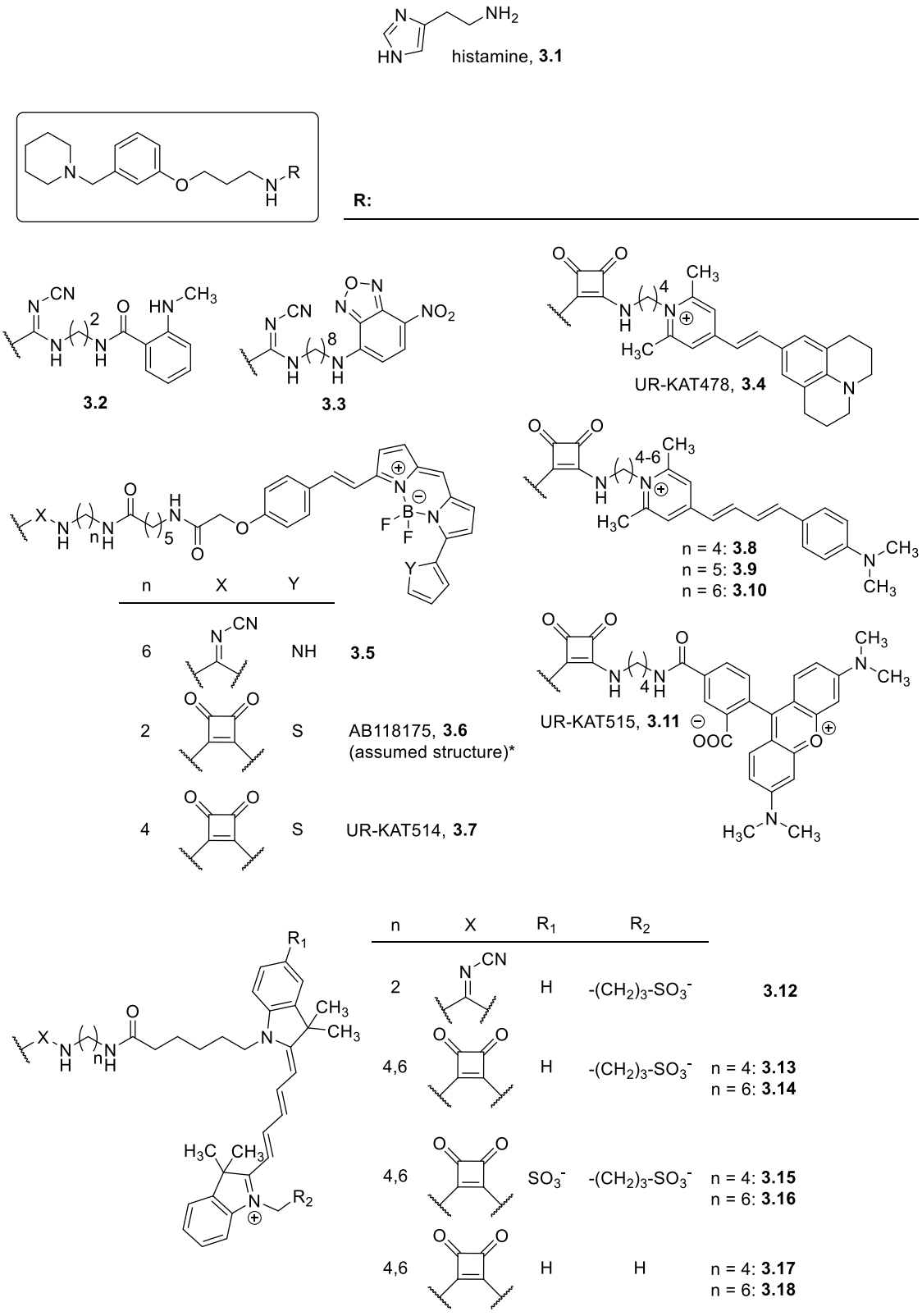

Figure 3.1. Chemical structures of histamine (**3.1**) and reported fluorescent H_2R antagonists **3.2**-**3.18**[34-38]. *The exact chemical structure of AB118175 (**3.6**) is not published and was derived from the formula ($C_{48}H_{56}BF_2N_9O_4S$) and the reported presence of the aminopotentidine and BODIPY 630/650 motifs.[39]

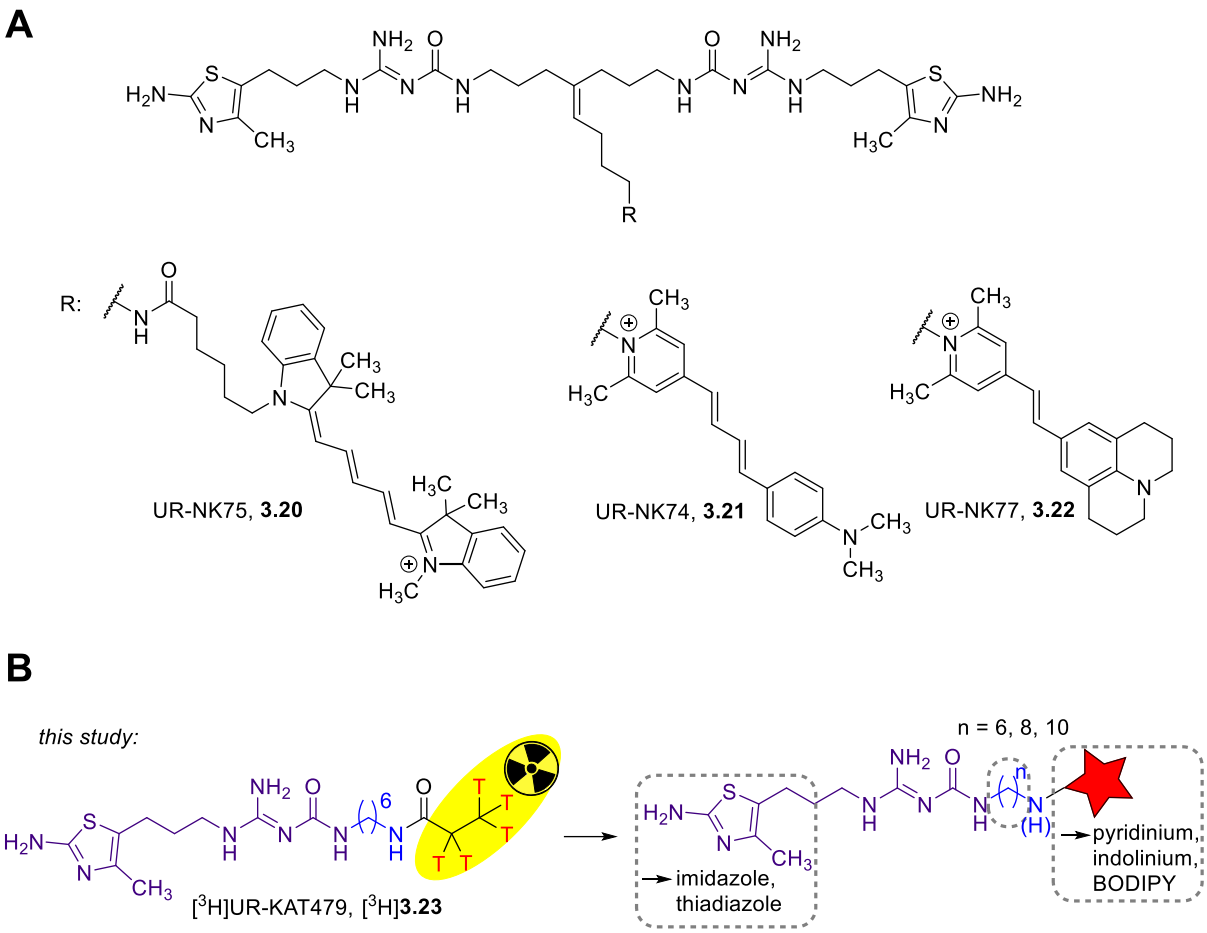

Figure 3.2. (**A**) Chemical structures of literature known fluorescent H_2R agonists **3.19-3.21**[40]. (**B**) Our approach for the synthesis of novel fluorescent agonists for the H_2R.

Consequently, there is still a need to develop novel, agonistic fluorescent ligands with reduced non-specific interactions.

In this study, we describe the design, synthesis, and pharmacological evaluation (radioligand competition binding- and different functional-assays; flow cytometry and confocal microscopy) of several fluorescent carbamoylguanidine-type H_2R agonists containing various fluorophores, heterocycles, and linker lengths.

3.2 Results and Discussion

3.2.1 Design

Recently, the G protein efficacy (E_{max}) biased carbamoylguanidine-type radioligand [^{3}H]UR-KAT479 ([^{3}H]**3.23**) (mini-G: E_{max} = 0.88 ± 0.01; β-arr2: E_{max} = 0.07 ± 0.02) was described (for structure see Figure 3.2B).[7] Due to its beneficial properties (e.g. low non-specific binding and

reversible binding to the receptor), the structurally similar carbamoylguanidine containing amine **3.23**[7] (cf. Scheme 3.1) was considered as a promising starting point for the development of novel fluorescent agonists. As the linker length can affect the pharmacological properties,[41] two additional precursor analogues with different chain lengths were also evaluated (**3.24**-**3.25**[7], cf. Scheme 3.1). Moreover, also the heterocycle was altered (**3.26**-**3.27**, cf. Scheme 3.1) since it is reported that different heterocycles may lead to varying degrees of G protein efficacy bias (thiazole[3, 7, 42], imidazole[3], thiadiazole[43]). Finally, the amine precursors were labeled with three different types of electrically charged or net-uncharged, red-emitting fluorophores: Py-5[44-45] (positive), differently charged indolinium dyes [S0223 (positive), S0436 (net-uncharged) and S0386 (negative)) and BODIPY 630/650 X (net-uncharged)].[46-47]

3.2.2 Chemistry

The amine precursors **3.23**-**3.27**[7, 43] and the Py-5 label[44-45] were prepared according to known synthetic routes (for more details see Appendix 2, App2.1 Experimental Details for **3.23**-**3.27**). The fluorophores S0436, S0387, S0223 and BODIPY 630/650 X were purchased as succinimidyl (NHS) esters and coupled with the precursors **3.23**-**3.27** in the presence of triethyl amine (NEt_3) to give **3.31**-**3.40** (Scheme 3.1). Reaction of **3.23**-**3.25** with Py-5 gave the positively charged pyridinium salts **3.28**-**3.30** (Scheme 3.1). Purification by preparative RP-HPLC afforded **3.28**-**3.40** with high purities [≥95% (220 nm)]. Fluorescence ligands containing the imidazole (compd. **3.37**) or thiadiazole (compd. **38**) moiety were synthesized only with the octyl linker, as this linker led to the highest H_2R affinities within the thiazole series regardless of which fluorophore was used (Py-5: **3.28**-**3.30**, S0346: **3.31**-**3.33**, S0387: **3.36**-**3.38**, for details see Table 3.1). Analytical characterizations (^{1}H-NMR, HPLC purity, excitation spectra and emission spectra) of the fluorescent ligands **3.28**-**3.40** are provided in the Appendix 3.

Scheme 3.1. Synthesis of the Carbamoylguanidine-Type Fluorescent Ligands 3.28-3.40.[a]

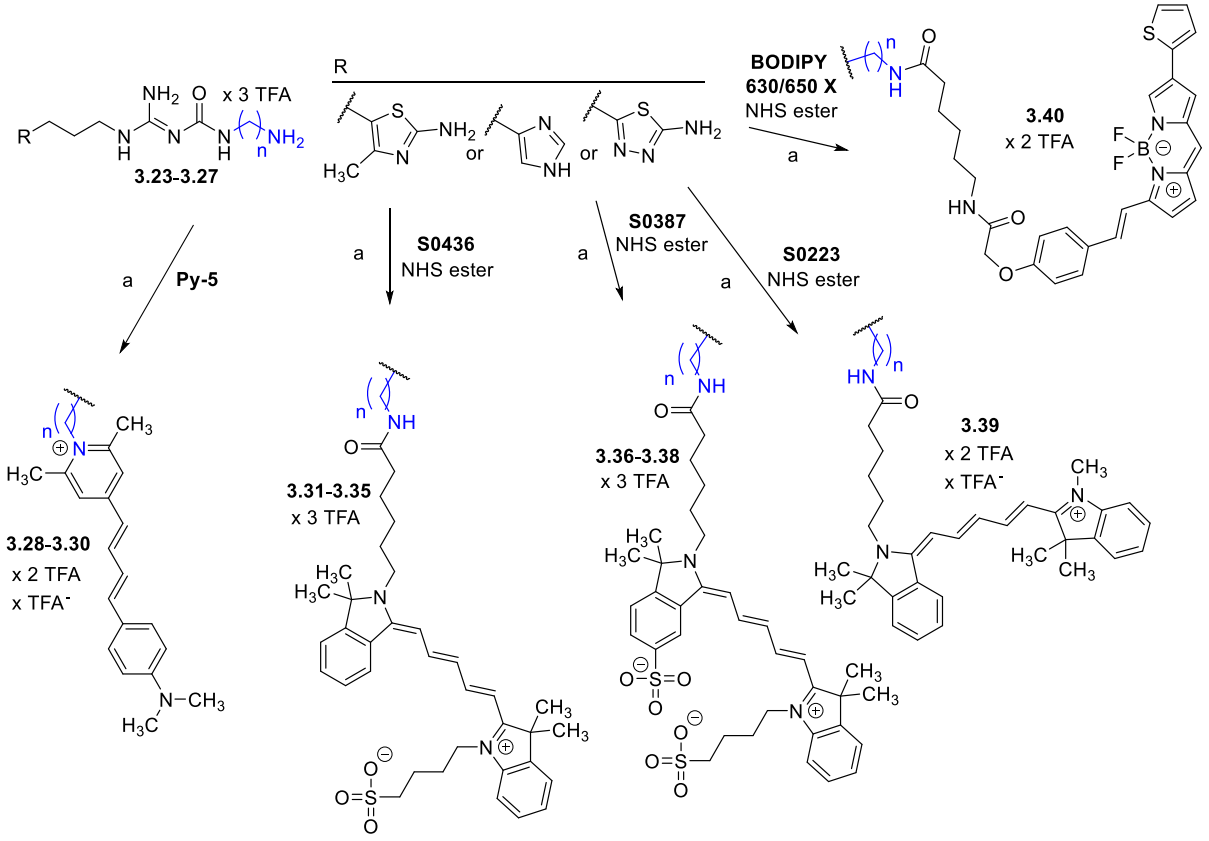

compd.	R	dye
3.23 (n = 6), **3.24** (n = 8), **3.25** (n = 10)	thiazole	-
3.26 (n = 8)	imidazole	-
3.27 (n = 8)	thiadiazole	-
3.28 (n = 6), **3.29** (n = 8), **3.30** (n = 10)	thiazole	Py-5
3.31 (n = 6), **3.32** (n = 8), **3.33** (n = 10)	thiazole	S0436
3.34 (n = 8)	imidazole	S0436
3.35 (n = 8)	thiadiazole	S0436
3.36 (n = 6), **3.37** (n = 8), **3.38** (n = 10)	thiazole	S0387
3.39 (n = 6)	thiazole	S0223
3.40 (n = 8)	thiazole	BODIPY 630/650 X

[a]Reagents and conditions: (a) Py-5, S0436-, S0387-, S0223- or BODIPY 630/650 X-NHS ester, NEt_3, DMF, 2 h, dark, rt, 18-89%.

3.2.3 H_2R Affinity and Receptor Subtype Preference

The amine precursor **3.26** (pK_i values of the precursors **3.23**-**25**[7] and **3.27**[41] were reported elsewhere) and the fluorescent ligands **3.28**-**3.40** were investigated in competition binding experiments on membrane preparations of Sf9 insect cells expressing the human (h) H_2R-$G_{s\alpha S}$ fusion protein (Table 3.1). In general, the incorporation of the fluorophore into the precursors resulted in a reduced hH_2R affinity compared to the unlabeled precursors (**3.23**-**3.27**; pK_i 6.88-7.85), with exception of **3.39** (cf. Table 3.1). The introduction of Py-5 (**3.28**-**3.30**, pK_i 6.64-7.20), S0223 (**3.39**, pK_i 7.66) or BODIPY 630/650 X (**3.40**, pK_i 7.52) was better tolerated than the introduction of S0436 (**3.31**-**3.35**, pK_i 6.25-7.18) or S0387 (**3.36**-**3.38**, pK_i <6-6.74) (cf. Table 3.1). Fluorescent ligands, containing an octyl linker (**3.29**, **3.32** and **3.37**), exhibited higher affinity compared to those containing a hexyl (**3.28**, **3.31** and **3.36**) or decyl linker (**3.30**, **3.33** and **3.38**) (cf. Table 3.1). To confirm the determined pK_i values, the fluorescent ligands **3.28**-**3.37** and **3.39**-**3.40** (not **3.38** because of the very low pK_i <6) were investigated in flow cytometric saturation binding studies using whole HEK293T-qs5-HA cells co-expressing the hH_2R. None of the Py-5-labeled ligands (**28**-**30**) bound in a saturable manner (see Figure App2.33A-C in the Appendix 2). The S0223- (**3.39**), BODIPY 630/650 X- (**3.40**) and S0387- (**3.36**-**3.37**) labeled ligands showed high non-specific binding (see Figure S3.3E and Figure App2.34A-C in the Appendix 2). Only the S0436-labeled ligands **3.32**-**3.35** bound in saturable manner with concomitantly low non-specific binding (7-20% at a concentration abound the K_d value; see Figure S3.3A-D). The pK_d values determined for these compounds (**32**-**35**) were in agreement with the pK_i values from radioligand competition binding experiments (cf. Table 3.1).

To investigate the subtype selectivity, selected compounds were screened for affinity at the other three human histamine receptors (h$H_{1,3,4}$Rs, Table 3.1). Thiazole- (**3.31**-**3.33** and **3.39**-**3.40**) or thiadiazole- (**3.35**) containing compounds showed a preference for the H_2R. The affinity at the h$H_{1,3,4}$Rs was between a half and two orders of magnitude lower than at the hH_2R. In contrast, the imidazole containing ligand **3.34** had even higher affinity for human H_3 receptor than for the H_2R (cf. Table 3.1 and Figure 3.4C). Similar results were reported in the literature[40, 43, 48-51], where thiazoles or thiadiazoles showed higher H_2 receptor selectivity compared to structurally identical imidazoles. In addition, a decrease in H_2R selectivity could be observed for the precursors **3.23**-**3.25** and the S0436-labeled fluorescent ligands **3.31**-**3.33** by extending the linker from hexyl to decyl (cf. Table 3.1).

Table 3.1. pK_d Values of 3.28-3.40 Determined by Saturation Binding (hH_2R) and Binding Data (pK_i) of 3.1 and 3.23-3.40 to Human Histamine Receptors (H_1R, H_2R, H_3R and H_4R) Determined in Radioligand Binding Studies

	pK_d flow cytom.		pK_i radioligand competition								H_2R selectivity K_i ($H_{1,3,4}$R)/K_i(H_2R)		
Cmpd.	**hH_2R**[a]	N	**hH_2R-G$_{s\alpha S}$**[b]	N	**hH_1R**[c]	N	**hH_3R**[d,e]	N	**hH_4R**[f]	N	H_1	H_3	H_4
3.1	-	-	6.58 ± 0.04[50]	3	5.62 ± 0.03[52]	48	7.59 ± 0.01[b,c50]	42	7.60 ± 0.01[50]	45	9	0.1	0.1
3.23	-	-	6.88 ± 0.10[7]	5	5.03 ± 0.10[7]	3	<5[c 7]	3	<5[7]	3	71	>76	>76
3.24	-	-	7.66 ± 0.17[7]	3	6.71 ± 0.04[7]	3	5.06 ± 0.10[c7]	3	<5[7]	3	9	398	>457
3.25	-	-	7.85 ± 0.17[7]	3	6.80 ± 0.04[7]	3	5.82 ± 0.07[c7]	3	5.36 ± 0.17[7]	3	11	107	309
3.26	-	-	7.58 ± 0.05[43]	3	6.96 ± 0.08[43]	3	7.51 ± 0.13[c43]	2	6.20 ± 0.16[43]	2	4	1	41
3.27	-	-	7.48 ± 0.14	3	6.28 ± 0.09	3	<5[c]	2	<5	3	16	302	302
3.28	n.m.	2	6.64 ± 0.05	3	n.d.	-	n.d.	-	n.d.	-	-	-	-
3.29	n.m.	2	7.20 ± 0.11	3	n.d.	-	n.d.	-	n.d.	-	-	-	-
3.30	n.m.	2	6.95 ± 0.16	3	n.d.	-	n.d.		n.d.	-	-	-	-
3.31	6.00 ± 0.07	6	6.39 ± 0.12	4	<5	2	<5[b]	4	<5	2	>25	>25	>25
3.32	7.15 ± 0.05	5	6.60 ± 0.04	3	5.51 ± 0.10	3	5.67 ± 0.19[b,c]	2	5.65 ± 0.10*	2	12	9	9
3.33	6.64 ± 0.08	6	6.25 ± 0.06	3	5.41 ± 0.13*	2	5.54 ± 0.09[c]*	2	5.44 ± 0.12*	2	7	5	6
3.34	7.25 ± 0.02	4	7.02 ± 0.05	3	6.29 ± 0.09*	2	7.77 ± 0.09[c]	2	6.87 ± 0.06	3	5	0.2	1
3.35	6.95 ± 0.09	3	7.18 ± 0.10	3	5.20 ± 0.01*	2	5.33 ± 0.04[c]	3	5.64 ± 0.03*	2	95	71	35
3.36	<6	2	6.58 ± 0.04	3	n.d.	-	n.d.	-	n.d.	-	-	-	-
3.37	<6	3	6.74 ± 0.17*	2	n.d.	-	n.d.	-	n.d.	-	-	-	-
3.38	n.d.	-	<6	2	n.d.	-	n.d.	-	n.d.	-	-	-	-
3.39	7.48 ± 0.06	3	7.66 ± 0.18	3	6.79 ± 0.08*	2	6.92 ± 0.07[c]*	2	6.13 ± 0.08*	2	10	7	46
3.40	7.09 ± 0.10	3	7.52 ± 0.03	3	6.02 ± 0.14	3	5.97 ± 0.16[c]*	2	5.96 ± 0.13	3	32	35	36

[a]Determined by flow cytometric saturation binding at HEK293T-hH_2R-qs5-HA cells. [b-f]Determined by radioligand competition binding with [b][^{3}H]UR-DE257[53] (K_d = 11.2 nM[38], c = 20 nM), [c][^{3}H]mepyramine (K_d = 4.5 nM[40], c = 5 nM), [d][^{3}H]N^{α}-methylhistamine (K_d = 8.6 nM[50], c = 3 nM), [e][^{3}H]UR-PI294[54] (K_d = 3.0 nM[7], c = 2 nM) or [f][^{3}H]histamine (K_d = 47.5 nM[55], c = 30 nM) at membrane preparations of Sf9 insect cells expressing the [b]hH_2R-G$_{s\alpha S}$ fusion protein, [c]co-expressing the hH_1R + RGS4, [d,e]co-expressing the hH_3R + G$_{\alpha i2}$ + G$_{\beta 1\gamma 2}$ or [f]co-expressing the hH_4R + G$_{\alpha i2}$ + G$_{\beta 1\gamma 2}$. Presented are mean values ± SEM (N ≥3) or SE (N = 2, indicated with *) from N independent experiments (each performed in duplicate (*a*) or triplicate (*b*, *c*, *d*, *e*, *f*)). n.d.: not determined. n.m.: not measurable: the one site - specific binding fit failed due to non-saturable binding of **3.31**-**3.33**. For the calculation of the selectivity ratios, the pK_i values were converted to the corresponding K_i by applying the equation $K_i = 10^{-pK_i}$.

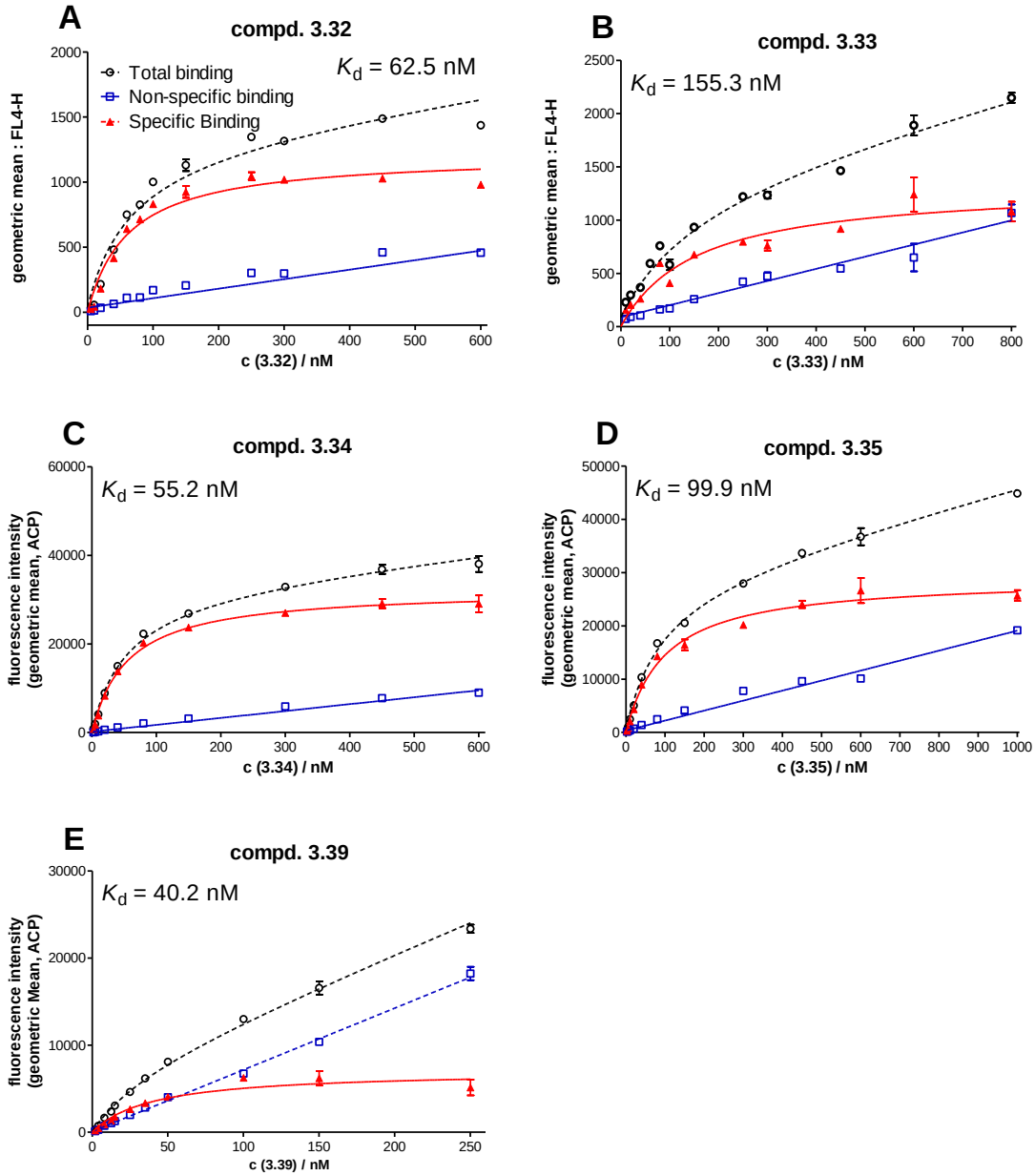

Figure 3.3. Representative flow cytometric saturation binding experiments performed with the fluorescent ligands **3.32** (**A**), **3.33** (**B**), **3.34** (**C**), **3.35** (**D**) and **3.39** (**E**) at intact HEK293T-hH_2R-qs5-HA cells. Non-specific binding was determined in the presence of famotidine (300-fold excess adjusted to the respective concentration of the fluorescent ligand). Cells were incubated with the fluorescent ligands at room temperature (rt) in the dark for 90 min. Error bars of specific binding represent propagated errors calculated according to the Gaussian law of error propagation. Error bars of total and non-specific binding represent the SEM. Experiments were performed in duplicate. For representative flow cytometric saturation binding experiments of **3.28-3.31**, **3.36-3.37** and **3.40** see Appendix 2, Figures App2.33 and App2.34.

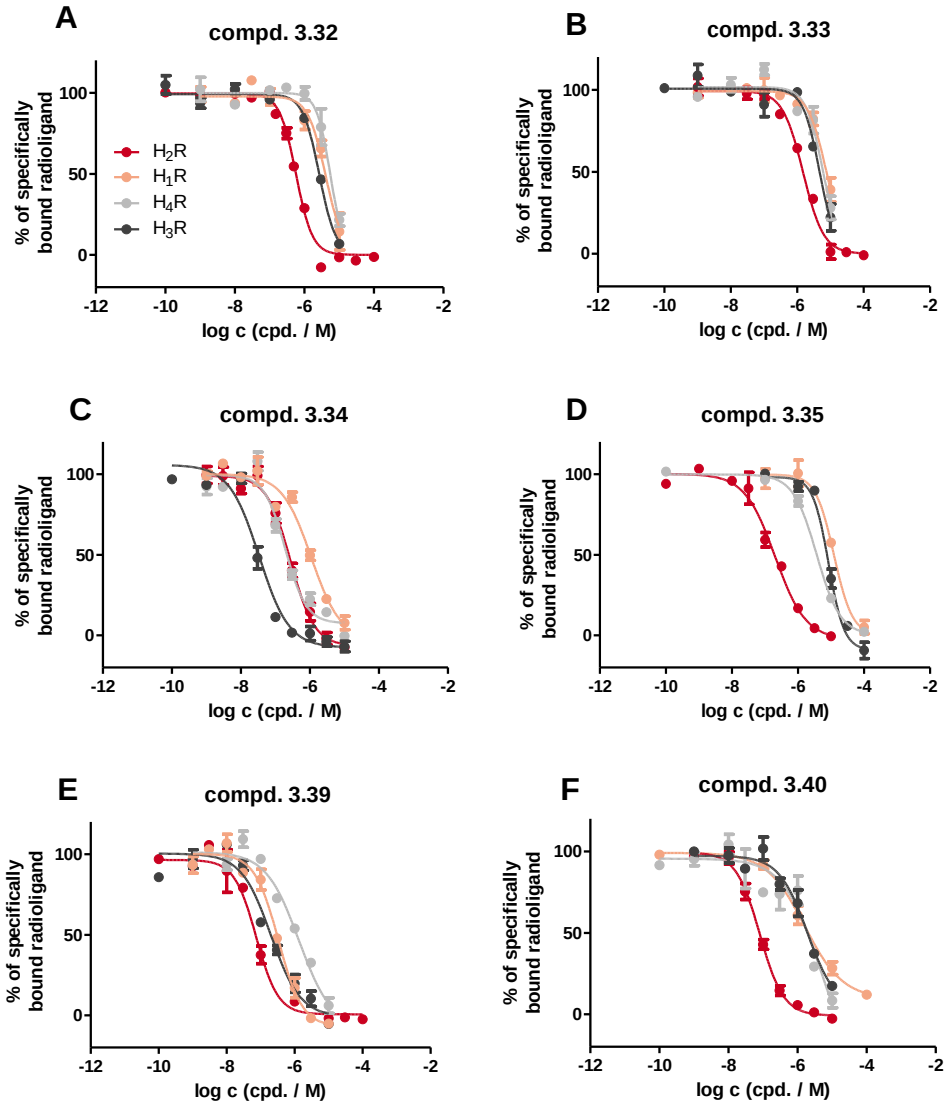

Figure 3.4. Displacement curves obtained from competition binding experiments with [^{3}H]mepyramine (hH$_1$R, K_d = 4.5 nM[40], c = 5 nM), [^{3}H]UR-DE257[53] (hH$_2$R, K_d = 11.2 nM[38], c = 20 nM), [^{3}H]UR-PI294[54] (hH$_3$R, K_d = 3 nM[7], c = 2 nM) or [^{3}H]histamine (hH$_4$R, K_d =47.5 nM[55], c = 30 nM) and **3.32** (**A**), **3.33** (**B**), **3.34** (**C**), **3.35** (**D**), **3.39** (**E**) or **3.40** (**F**) at membranes of Sf9 cells (co-)expressing the hH$_1$R + RGS4, the hH$_2$R-G$_{s\alpha S}$ fusion protein, the hH$_3$R + G$_{\alpha i2}$ + G$_{\beta 1\gamma 2}$ or the hH$_4$R + G$_{\alpha i2}$ + G$_{\beta 1\gamma 2}$. Data represent mean values ± SEM from at least two independent experiments (each performed in triplicate).

3.2.4 Functional Studies at the Human H_2R

To test the functional differences regarding Gs versus β-arrestin activation, the compounds **3.23**-**3.40** were investigated in different assay systems (cf. Table 3.2). G protein activation was investigated in the [^{35}S]GTPγS binding assay using membrane preparations of Sf9 insect cells expressing the hH_2R-$G_{s\alpha S}$ fusion protein.[40, 50, 56] In case of compound **3.35** the mini-G protein recruitment assay using the HEK293T NlucN-mGs/hH_2R-NlucC cells stably expressing the NlucN-mGs and hH_2R-NlucC fusion constructs[57] was used, because the [^{35}S]GTPγS reagent was no longer commercially available in sufficient purity and at an affordable price.[58] Therefore, selected compounds **3.26**, **3.32**, **3.34** and **3.39** were additionally analyzed in the mini-G protein recruitment assay for comparison. β-Arrestin2 recruitment was determined in the luciferase complementation assay using the HEK293T-ARRB2-hH_2R cells stably expressing hH_2R-ElucC and the β-arrestin2-ElucN fusion constructs.[3, 37-38] Selected compounds **3.32**, **3.34**, **3.35** and **3.39** were also investigated in the analogous β-arrestin1 recruitment assay to rule out potential preference for one of the two β-arrestin isoforms (results are shown in the footnote of Table 3.2).

Labeled and unlabeled compounds **3.23**-**3.39** acted as moderate partial to full agonists in [^{35}S]GTPγS binding and/or mini-G protein recruitment assays (E_{max} = 0.47-1.04) with pEC_{50} values in the range of 5.62 to 8.12 and were weak to strong partial agonists in β-arrestin1/2 recruitment assays (E_{max} = 0.06-0.87) with pEC_{50} values in the range of 5.41 to 7.02 (Table 3.2). In general, the potencies were in good agreement with the respective binding affinities (pK_i values, cf. Table 3.2). Among the fluorescence ligands, the difference in activating the G protein and β-arrestin pathways was most pronounced for the aminothiazole containing, S0436-labeled compounds **3.32** and **3.33**, which were strong partial to full agonists in the G protein pathway (**3.32**: GTPγS: E_{max} = 1.04; mGs: E_{max} = 0.77; **3.33**: GTPγS: E_{max} = 0.93), while showing very weak partial agonistic activity in arrestin recruitment assays (**3.32**: β-arr1: E_{max} = 0.09; β-arr2: E_{max} = 0.12; **3.33**: β-arr2: E_{max} = 0.09) (cf. Table 3.2 and Figures 3.5A & B). In addition, the BODIPY 630/650 X-labeled compound **3.40** showed an "extreme bias"[59]. It acted as a strong partial agonist in the [^{35}S]GTPγS binding assay (E_{max} = 0.70), but as an antagonist in the β-arrestin2 recruitment assay (E_{max} = 0.01) (cf. Table 3.2 and Figure 3.5F). In contrast, three compounds (**3.34**-**3.35** and **3.39**) acted as moderate partial agonists in the β-arrestin2 recruitment assay. The imidazole containing, S0436-labeled compound **3.34** was a partial agonist in the G protein pathway (GTPγS: E_{max} = 0.66; mGs: E_{max} = 0.83) and showed the third highest efficacy regarding β-arrestin activation (**3.34**: β-arr1: E_{max} = 0.25; β-arr2:

E_{max} = 0.22) (Table 3.2). The S0223-labeled aminothiazole **3.39** also displayed a high G protein efficacy (GTPγS: E_{max} = 0.93; mGs: E_{max} = 0.81) and the second highest efficacy of all carbamoylguanidines regarding β-arrestin2 activation (E_{max} = 0.44) (Table 3.2). Finally, also the thiadiazole containing ligand **3.35** acted as a strong partial agonist in the G protein pathway (mGs: E_{max} = 0.90) and showed the highest efficacy in the β-arrestin2 recruitment assay among the tested compounds (E_{max} = 0.61, Table 3.2). In the β-arrestin1 assay **3.35** and **3.39** showed similarly high efficacies (**3.35**: E_{max} = 0.55; **3.39**: E_{max} = 0.57) (cf. Table 3.2). These results are in agreement with the literature, where imidazoles and thiadiazoles were reported to possess no or only a low G protein bias.[3, 43]

In order to statistically examine these observed efficacy differences, a bias analysis[60] for selected ligands **3.32**-**3.35** and **3.39** using the data obtained from [^{35}S]GTPγS binding, mini-G protein recruitment and β-arrestin2 recruitment assays was carried out. As expected, the greatest efficacy bias factors (eBF's) were calculated for **3.32** ([^{35}S]GTPγS: eBF = 8.35; mGs: eBF = 6.35) and **3.33** ([^{35}S]GTPγS: eBF = 10.16), which were proved to be significant by using one-way ANOVA and Dunnett`s post-tests (for more details see App2.7 Bias Analysis in the Appendix 2). In contrast, for **3.34**-**3.35** and **3.39** only low / not significant eBF's were observed.

Table 3.2. Functional Data of Compounds 3.1 and 3.23-3.40 Determined at the hH_2R in the [^{35}S]GTPγS Binding[a] or Mini-G Protein[b] Recruitment and β-Arrestin1/2 Recruitment[c] Assays

	[^{35}S]GTPγS binding[a]			β-arrestin2 recruitment[c]		
compd.	pEC_{50}	E_{max}	N	pEC_{50}	E_{max}	N
3.1	5.85 ± 0.06[40]	1.00[40]	-	5.42 ± 0.02[3]	1.00[3]	3
	6.94 ± 0.06[57,b]	1.00[57,b]	9			
3.23	7.19 ± 0.12	0.87 ± 0.07	4	6.55 ± 0.22[7]	0.28 ± 0.01[7]	3
	7.53 ± 0.03[7,b]	0.83 ± 0.02[7,b]	3			
3.24	7.58 ± 0.15	0.78 ± 0.05	4	6.87 ± 0.12[7]	0.23 ± 0.01[7]	4
	7.84 ± 0.04[7,b]	0.84 ± 0.03[7,b]	3			
3.25	7.75 ± 0.13	0.85 ± 0.04	4	6.91 ± 0.10[7]	0.15 ± 0.01[7]	4
	7.83 ± 0.12[7,b]	0.85 ± 0.02[7,b]	3			
3.26	6.88 ± 0.06	0.86 ± 0.07	3	6.70 ± 0.14[43]	0.87 ± 0.04[43]	5
	8.13 ± 0.05[43,b]	0.93 ± 0.01[43,b]	3			
3.27	7.47 ± 0.10	0.94 ± 0.04	4	7.02 ± 0.12	0.51 ± 0.06	5
	8.12 ± 0.02[b]	0.90 ± 0.02[b]	3			
3.28	6.92 ± 0.33*	0.78 ± 0.09*	2	5.60 ± 0.05	0.27 ± 0.09	3
3.29	7.16 ± 0.20	0.47 ± 0.05	3	5.86 ± 0.12	0.16 ± 0.05	3
3.30	7.05 ± 0.14	0.49 ± 0.10	3	5.91 ± 0.20	0.07 ± 0.02	3
3.31	6.25 ± 0.17	0.94 ± 0.07	4	5.41 ± 0.13	0.41 ± 0.04	3
3.32†	6.47 ± 0.09	1.04 ± 0.04	6	5.96 ± 0.11	0.12 ± 0.04	3
	6.89 ± 0.02[b]	0.77 ± 0.01[b]	3			
3.33	6.17 ± 0.14	0.93 ± 0.05	5	5.84 ± 0.27	0.09 ± 0.02	3
3.34†	6.92 ± 0.10	0.66 ± 0.02	4	6.47 ± 0.05	0.22 ± 0.02	3
	6.94 ± 0.03[b]	0.83 ± 0.01[b]	3			
3.35†	7.19 ± 0.06[b]	0.90 ± 0.01[b]	4	6.59 ± 0.08	0.61 ± 0.03	5
3.36	6.69 ± 0.08	0.72 ± 0.09	3	6.17 ± 0.13	0.36 ± 0.06	3
3.37	5.89 ± 0.16	0.74 ± 0.07	4	6.12 ± 0.24	0.06 ± 0.02	3
3.38	5.62 ± 0.18	0.77 ± 0.08	3	5.69 ± 0.06	0.10 ± 0.02	3
3.39†	6.73 ± 0.07	1.01 ± 0.06	4	6.30 ± 0.14	0.44 ± 0.07	5
	6.72 ± 0.10[b]	0.81 ± 0.02[b]	3			
3.40	7.14 ± 0.15	0.70 ± 0.07	4	(7.61 ± 0.19)‡	0.01 ± 0.02[l]	5

[a][^{35}S]GTPγS binding assay on membranes of Sf9 cells expressing the hH_2R-$G_{s\alpha S}$ fusion protein.[40, 50, 56] [b]Mini-G protein recruitment assay on HEK293T NlucN-mGs/hH_2R-NlucC cells.[57] [c]β-Arrestin2 recruitment assay on HEK293T-ARRB2-hH_2R cells.[3, 37-38] Data shown are geometric mean values ± SEM (N ≥3) or SE (N = 2, indicated with *) of N independent experiments each performed in triplicate. pEC_{50}: negative logarithm of the agonistic potency (EC_{50}). E_{max}: efficacy. The E_{max} value of **3.1** was set to 1.00 and the E_{max} of buffer control was set to 0.00 and values of the other compounds were referenced to these values. ‡The pK_b value of **3.40** was determined in the antagonist mode versus **3.1** (c = 8 µM); $pK_b = -\log K_b$. The K_b value was calculated from the corresponding IC_{50} values (obtained by the GraphPad Prims 5 software) by using the Cheng-Prusoff equation[61]. [l]E_{max} at c = 10 µM. n.d.: not determined. †Selected compounds were also investigated in the β-arrestin1 recruitment assay on HEK293T-ARRB1-hH_2R cells: **3.1**: pEC_{50} = 5.26 ± 0.03[3], E_{max} = 1.00[3], N = 5; **3.32**: pEC_{50} = 6.21 ± 0.06, E_{max} = 0.09 ± 0.01, N = 3; **3.34**: pEC_{50} = 6.37 ± 0.05, E_{max} = 0.25 ± 0.01, N = 3; **3.35**: pEC_{50} = 6.47 ± 0.05, E_{max} = 0.55 ± 0.04, N = 3; **3.39**: pEC_{50} = 6.29 ± 0.15, E_{max} = 0.57 ± 0.06, N = 3. The obtained results were in good agreement with the results from the β-arrestin2 recruitment assay.

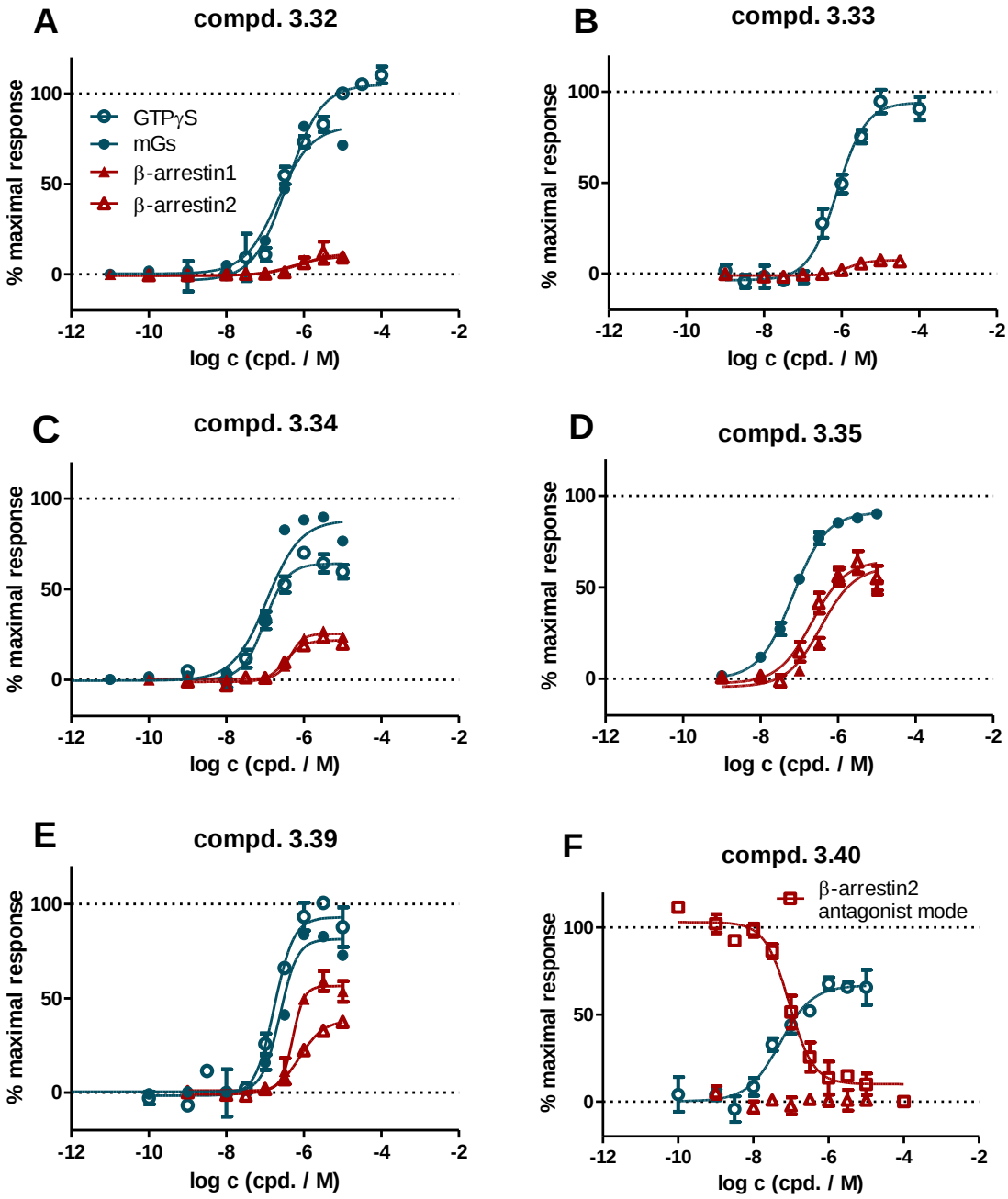

Figure 3.5. Concentration-response curves of S0436-labeled ligands **3.32**-**3.35** (**A**-**D**), S0223-labeled ligand **3.39** (**E**) and BODIPY 630/650 X-labeled ligand **3.40** (**F**) investigated in the [^{35}S]GTPγS binding assay (○ empty circles), mini-G protein recruitment assay (● filled circles), β-arrestin1 recruitment assay (▲ filled triangles, agonist mode), or β-arrestin2 recruitment assay (△ empty triangles, agonist mode; □ empty squares, antagonist mode). The responses in all four assays were normalized to the maximal effects induced by histamine (**3.1**) (100% value) and buffer control (0% value). Data are mean values ± SEM of 3-6 independent experiments, each performed in triplicate. Data were analyzed by nonlinear regression and best fitted to sigmoidal concentration-response curves.

3.2.5 Association and Dissociation Kinetics of 3.32, 3.34 and 3.35 at the hH_2R Expressed in HEK293T-qs5-HA Cells Studied by Flow Cytometry

Besides investigating their affinities, potencies, and efficacies, it is also of importance to elucidate the binding kinetics of new potential molecular tools, providing information on how much time is needed until an equilibrium between receptors and ligands has been established. This is especially important when performing competition binding experiments. Therefore, we performed kinetic experiments with S0436-labeled ligands **3.32** (thiazole, c = 120 nM), **3.34** (imidazole, c = 60 nM) and **3.35** (thiadiazole, c = 100 nM), which showed the most promising properties (e.g. low non-specific binding and high K_d) using flow cytometry. Association of **3.32** and **3.34** was complete after 60 min, while **3.35** showed a faster association, which was already complete after 20 min. Dissociation in the presence of 300-fold excess of famotidine was monophasic with k_{off} values between 0.017-0.063 min^{-1}, with **3.32** showing the slowest dissociation from the receptor. After 180 min, the residual specific binding was approximately 10-20%. For all experiments, the kinetically derived dissociation constants were calculated [using two methods: non-linear regression (Table 3.3A) and linear transformation (Table 3.3B)] which were in good agreement with the pK_d values determined by saturation binding.

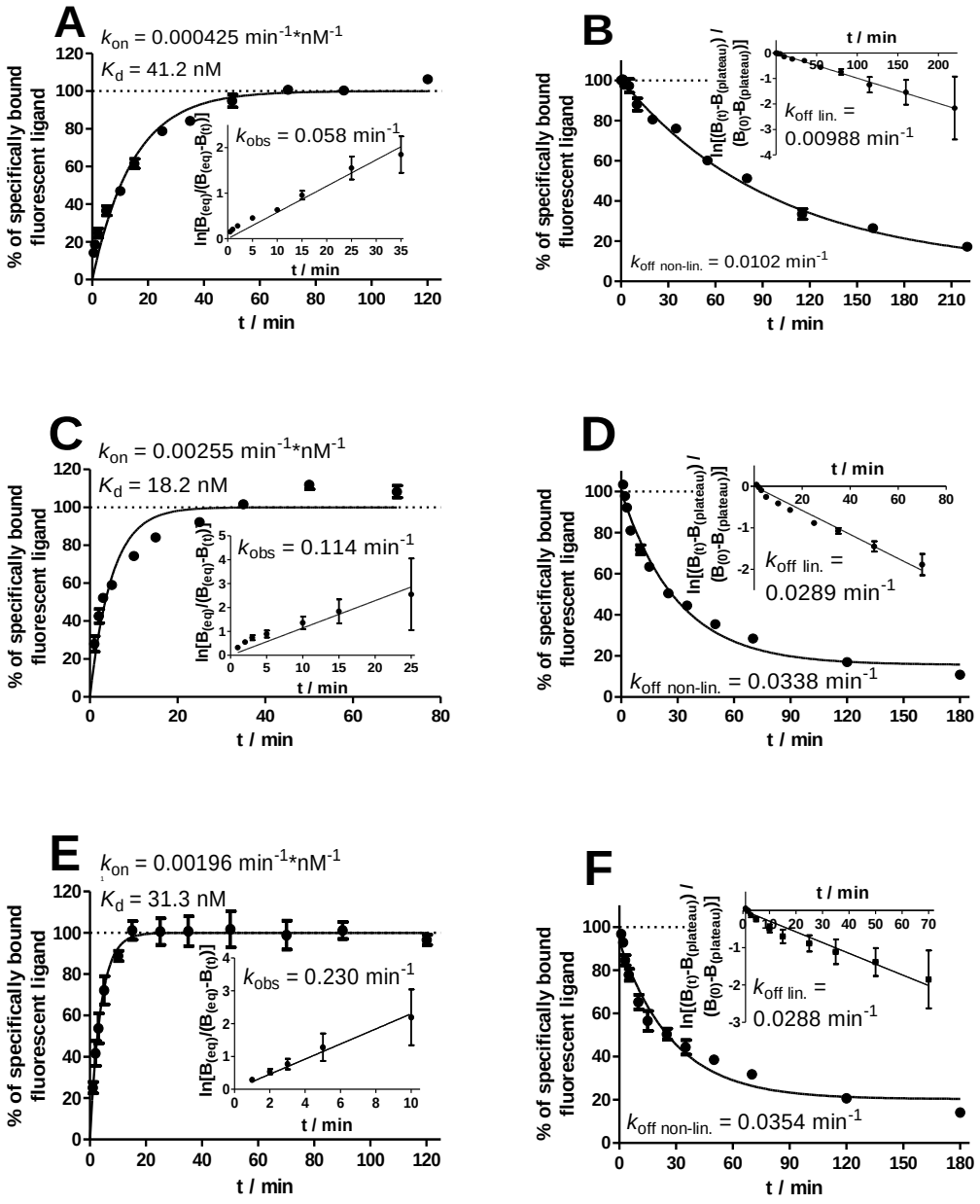

Figure S3.6. Specific binding kinetics of **3.32** (**A**, **B**), **3.34** (**C**, **D**), **3.35** (**E**, **F**) determined at live HEK293T-hH_2R-qs5-HA cells by flow cytometry. Association was induced by the addition of **3.32**, **3.34** or **3.35** [final concentration: 120 nM (**3.32**), 60 nM (**3.34**) or 100 nM (**3.35**)]. Dissociation was initiated after 90 min preincubation by the addition of famotidine (300-fold excess). **A**, **C** and **E**: Inserts: Transformation of the depicted association kinetics using $\ln[B_{(eq)}/(B_{(eq)}-B_{(t)})]$ versus time. **B**, **E** and **F**: Inserts: Transformation of the depicted kinetics using $\ln[(B_{(t)}-B_{(plateau)})/(B_{(0)}-B_{(plateau)})]$ versus time. The results shown are representatives of at least three experiments, each performed in duplicate. Data are presented as means ± errors. Errors were calculated according to the Gaussian law of error propagation.

Table 3.3. hH_2R Binding Characteristics of 3.32, 3.34 and 3.35 Determined by Flow Cytometry Using Suspended HEK293T-hH_2R-qs5-HA Cells at Room Temperature [(A) Non-Linear Regression and (B) Linear Transformation]

A compd.	k_{off}[a] [min^{-1}]	N	k_{on}[b] [min^{-1} * nM^{-1}]	N	k_{off} / k_{on}[c] K_d (kin.) [nM]	pK_d (kin.)[d]	pK_d (sat.)
3.32	0.0175 ± 0.0030	5	0.00045 ± 0.000023	3	34, 43, 41	7.41 ± 0.02	7.15 ± 0.05
3.34	0.0461 ± 0.0084	3	0.0029 ± 0.00058	3	18, 32, 15	7.69 ± 0.06	7.25 ± 0.02
3.35	0.0634 ± 0.0142	3	0.0022 ± 0.00044	5	31, 119, 26, 27, 18	7.47 ± 0.13	6.95 ± 0.09

[a]Dissociation rate constant derived from nonlinear regression (GraphPad Prism 5, equation: dissociation – one phase exponential decay). [b]Association rate constant derived from nonlinear regression (GraphPad Prism 5, equation: association kinetics – one conc. of hot); calculated from k_{obs}, k_{off} and the fluorescent ligand concentration. [c]Kinetically determined dissociation constant (K_d (kin.) = k_{off} / k_{on}). [d]Negative decadic logarithm of the kinetically determined dissociation constant (pK_d (kin.) = -log(K_d (kin.))). Data represent means ± SEM from N independent experiments (each performed in duplicate).

B compd.	k_{off}[a] [min^{-1}]	N	k_{obs}[b] [min^{-1}]	N	k_{on}[c]	k_{off} / k_{on}[d] K_d (kin.) [nM]	pK_d (kin.)[d]
3.32	0.0159 ± 0.0019	5	0.00607 ± 0.00123	3	0.0003737 ± 0.0000189	43 ± 6	7.37
3.34	0.0357 ± 0.0051	3	0.1528 ± 0.0328	3	0.0019522 ± 0.0005532	18 ± 6	7.74
3.35	0.0458 ± 0.0084	3	0.1671 ± 0.0207	5	0.0012132 ± 0.0002234	38 ± 10	7.42

[a]Dissociation rate constant derived from linearization ln[(B_t-$B_{plateau}$)/(B_0-$B_{plateau}$)] versus time (GraphPad Prism 5, linear regression; k_{off} = slope^{-1}). [b]Observed association rate constant derived from linearization ln[B_{eq}/(B_{eq}-B_t)] versus time (GraphPad Prism 5, linear regression; k_{obs} = slope). [c]Association rate constant calculated from k_{obs}, k_{off} and the fluorescent ligand concentration [k_{on} = (k_{obs}/ - k_{off}) / c (fluorescent ligand)]. [d]Kinetically determined dissociation constant (K_d (kin.) = k_{off}/k_{on}). [d]Negative decadic logarithm of the kinetically determined dissociation constant (pK_d (kin.) = -log(K_d (kin.)). [a,b]Data represent means ± SEM from N independent experiments (each performed in duplicate). [c,d]Data represent result ± propagated error.

3.2.6 Investigation of Unlabeled H_2R Standard Ligands in Competition Binding Experiments Using Flow Cytometry

To show the versatility of possible uses of the presented fluorescent agonists (**3.32**, **3.34** or **3.35**), equilibrium competition binding experiments with different reported H_2R agonists [**3.1** and amthamine (amt)] and antagonists/inverse agonists [famotidine (fam), ranitidine (rani), tiotidine (tio) and BMY 25368], using a fixed concentration of **3.32** (c = 60 nM), **3.34** (c = 60 nM) or **3.35** (c = 100 nM) and various concentrations of the respective ligands were performed. The results are summarized in Table 3.4. The fluorescence ligands **3.32**, **3.34** and **3.35** were completely displaceable by the employed standard H_2R ligands. The calculated pK_i values were comparable - independent from the fluorescent ligand (**3.32**, **3.34** or **3.35**) used. Moreover, the pK_i values were in good agreement with radioligand binding data at the same cell line using [^{3}H]UR-DE257[53] as radioligand and with radioligand binding data published in the literature. (Table 3.4).[7, 38, 53, 62] Therefore, our new agonistic fluorescence ligands **3.32**, **3.34** or **3.35** can be used as well as the published antagonistic fluorescence ligands or radioligands to determine the pK_i values of unlabeled ligands.[37-38]

Table 3.4. Comparison of the Determined Binding Data (pK_i) of Unlabeled H_2R Standard Ligands, Using 3.32, 3.34 or 3.35 as Fluorescent Ligands or [^{3}H]UR-DE257[53] as Radioligand at Live HEK293T-hH_2R-qs5-HA Cells, to Reference Data[a]

compd.	**3.32** pK_i[c]	N	**3.34** pK_i[c]	N	**3.35** pK_i[c]	N	[^{3}H]UR-DE257[b] pK_i	N	Reference[d]
fam	7.29 ± 0.04	3	7.37 ± 0.04	3	7.28 ± 0.02	3	7.67 ± 0.01	3	6.87-7.94[1-3]
rani	6.93 ± 0.06	3	7.18 ± 0.13	3	6.81 ± 0.14	3	6.66 ± 0.06	3	5.76-7.19[1-3]
tio	7.38 ± 0.01	2	7.55 ± 0.08	3	7.44 ± 0.10	3	7.69 ± 0.02	3	6.57-7.77[1-2]
BMY 25368	7.17 ± 0.06	3	n.d.	-	n.d.	-	n.d.	-	7.72[1]; pK_b: 7.36[e]
amt	4.75 ± 0.12	3	n.d.	-	n.d.	-	n.d.	-	4.70-6.82[1-2, 4]
3.1	3.89 ± 0.19	4	4.29 ± 0.12	3	3.89 ± 0.09	4	3.90 ± 0.05	3	4.00-6.27[1-2, 4]

[a]Determined by competition binding with **3.32** (c = 60 nM, K_d = 71 nM), **3.34** (c = 60 nM, K_d = 56 nM), or **3.35** (c = 100 nM, K_d = 112 nM) at live HEK293T-hH_2R-qs5-HA[63] cells. [b]Determined by competition binding with [^{3}H]UR-DE257[53] (c = 25 nM, K_d = 40 nM) at live HEK293T-hH_2R-qs5-HA[63] cells. Data were analyzed by nonlinear regression and were best fitted to four-parameter sigmoidal concentration-response curves. [c]The pK_i values represent mean values ± SEM from N independent experiments each performed in duplicated or triplicate. [d]Data from competition binding experiments (pK_i) with [1][^{125}I]iodaminopotentidine[62], [2,4][^{3}H]UR-DE257[53, 64] or [3]UR-KAT478[38], performed on [1]membrane preparations of CHO cells, expressing the hH_2R[62], [2]membrane preparations of Sf9 insect cells, expressing the hH_2R-$G_{s\alpha S}$ fusion protein[53], [3]HEK293T cells, stably expressing the NLuc-hH_2R (NanoBRET binding experiments)[38], [4]HEK293T CRE-Luc cells, stably expressing the hH_2R[64]. [e]Data from steady-state [^{32}P]GTPase assay, performed on membrane preparations of Sf9 insect cells, expressing the hH_2R-$G_{s\alpha S}$ fusion protein.[64]

3.2.7 Cellular Localization of 3.32, 3.34-3.35 and 3.39-3.40 at Human H_2R Expressing Cells Determined by Confocal Microscopy

The S0436-labeled ligands **3.32-3.35** turned out as the most promising compounds [high affinity (Table 3.1) and low non-specific binding (Figure 3.3A-D)] for the investigation of the β-arrestin-mediated internalization by confocal microscopy. However, **3.33** was excluded from the studies in favor of **3.32** because the octyl linker containing compound **3.32** was structurally more similar to **3.34** and **3.35**. In addition, also the S0223-labeled ligand **3.39** and the BODIPY 630/650 X-labeled ligand **3.40** were employed in the confocal microscopy experiments, despite their high level of non-specific binding observed in the flow cytometric saturation binding

experiments (cf. Figure 3.3E and Figure 2.34C in the Appendix 2). The reason for this is that **3.39** had the second highest efficacy in the β-arrestin2 recruitment assay and **3.40** showed an "extreme bias" (cf. Table 3.2 and Figure 3.5F). For this series of experiments, we used live HEK293T-hH_2R-qs5-HA[63] and/or HEK293T-SP-FLAG-hH_2R K33 cells. Non-specific binding was determined in the presence of the non-fluorescent H_2R antagonist famotidine (300-fold excess). Fluorescence ligand **3.32**, which showed very weak partial agonistic activity in β-arrestin recruitment assays (β-arr1: E_{max} = 0.09, β-arr2: E_{max} = 0.12) also failed to promote receptor internalization (fluorescence is mainly localized at the cell membrane, cf. Figure 3.7), despite the fact that it was able to activate the Gs protein-mediated signaling ([^{35}S]GTPγS assay and mini-Gs protein recruitment assay, Table 3.2). However, hH_2R internalization could be observed (fluorescence is localized at the cell membrane and inside the cell, cf. Figure 3.7) if the fluorescence ligands **3.34** (imidazole, S0436), **3.35** (thiadiazole, S0436) or **3.39** (thiazole, S0223), which displayed higher efficacy regarding β-arrestin recruitment (**3.34**: β-arr1: E_{max} = 0.25, β-arr2: E_{max} = 0.22; **3.35**: β-arr1: E_{max} = 0.55, β-arr2: E_{max} = 0.61; **3.39**: β-arr1: E_{max} = 0.57, β-arr2: E_{max} = 0.44) were applied (cf. Table 3.2). Surprisingly, a significant intracellular fluorescence could be observed in the case of the "extremely biased" ligand **3.40**, which was identified as an antagonist in the β-arrestin2 recruitment assay. However, this internalization presumably occurred in a receptor-independent manner since it could be also observed in the presence of the H_2R selective competitor famotidine (selected frames from confocal microscopy experiments with **3.40** are shown in the Figure App2.40, see Appendix 2). We concluded that H_2R specific internalization is only observed if the respective ligand is able to at least moderately recruit β-arrestin ($E_{max} \geq 0.22$). Therefore, the binding of **3.32** was examined in HEK293T-SP-FLAG-hH_2R K33 cells as well, which should prove that the lack of internalization is not due to the chimeric Gqs protein expressed in the HEK293T-hH_2R-qs5-HA cells.[63] Also in this case, we could not observe any internalization within 120 min (cf. Figure 3.7, **3.32***). Our results are in agreement with the observations published by Fernandez et al.[5] who proposed the involvement of β-arrestin2 in the internalization of the H_2R.[5]

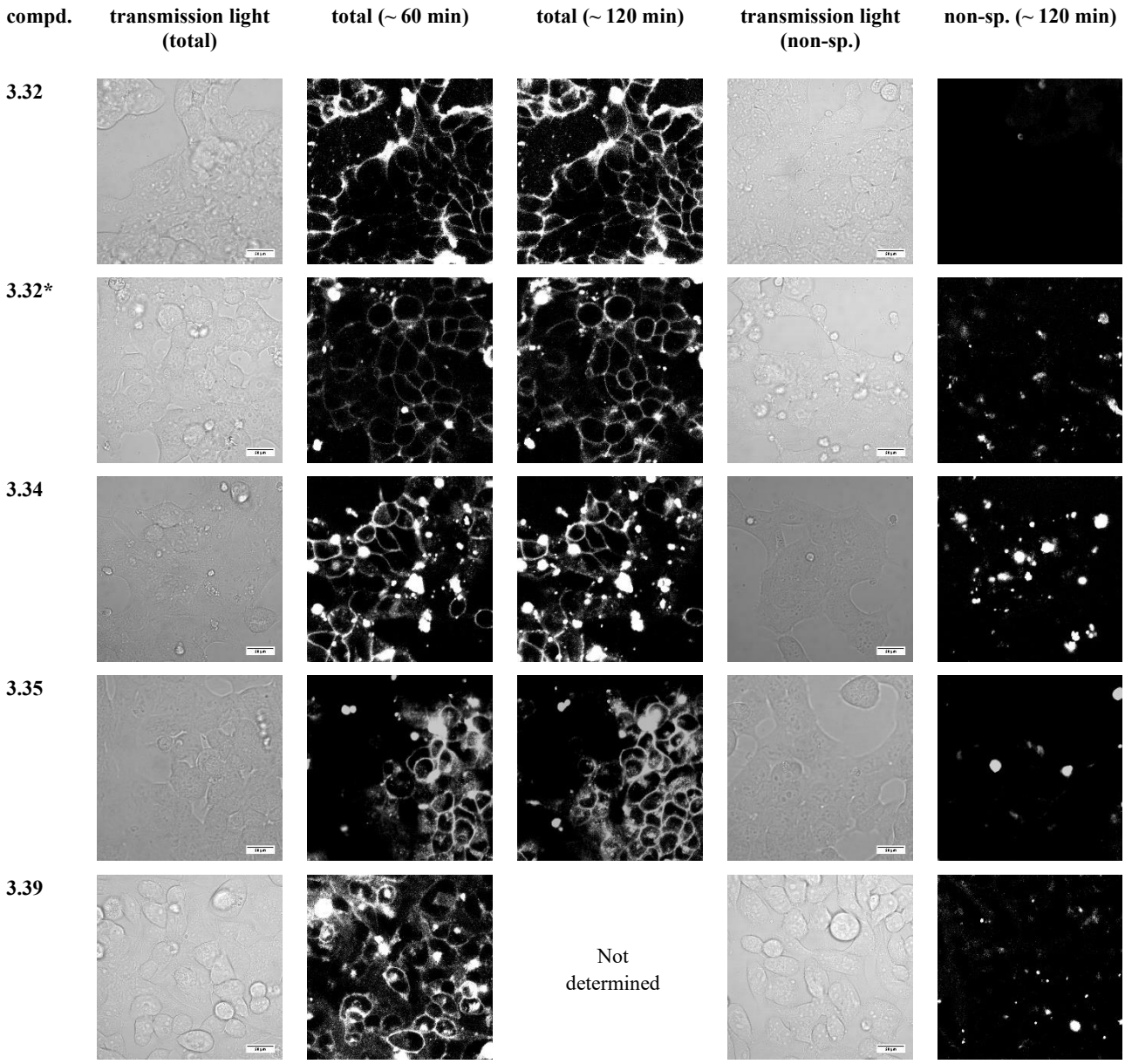

Figure 3.7. Selected frames from confocal microscopy experiments with **3.32** (180 nM), **3.34** (200 nM), **3.35** (300 nM) and **3.39** (100 nM) ($c \approx 2.5 \times K_i$, determined using Sf9 cell membranes expressing the hH_2R-$G_{s\alpha S}$) at HEK293T-hH_2R-qs5-HA cells or *HEK293T-SP-FLAG-hH_2R K33 cells. Cells were incubated with the respective fluorescent agonist at room temperature. Non-specific binding was determined in the presence of famotidine (300-fold excess). In case of **3.32**: after 120 min the fluorescence is mainly localized at the cell membrane suggesting that no receptor internalization had occurred. In case of **3.34**-**3.35** and **3.39**: after 60 or 120 min the fluorescence is localized at the cell membrane and inside the cell suggesting that receptor internalization had occurred. All images were acquired with a Zeiss Axiovert 200 M microscope, equipped with an LSM laser scanner. Settings: Plan-Apochromat 63x/1.4 Oil objective; scale bar [transmitted light (total/non-sp.)]: 20 µm. For more time-resolved frames see in the Appendix 2 (Figures App2.35-App2.39).

3.3 Summary and Conclusion

In summary, we synthesized several novel histamine H_2 receptor ligands containing different heterocycles, linker lengths, and fluorophores (indolinium, pyridinium, BODIPY). The compounds exhibited weak to high H_2 receptor affinity with pK_i values ranging from <6 to 7.7. The octyl linker led to the highest affinity within a series of the same fluorophore (only investigated for the thiazoles). Interestingly, only fluorescent ligands containing an electroneutral fluorophore (S0436), such as **3.32**-**3.35**, bound in a saturable manner with low non-specific binding in the range of the respective K_d value. By contrast, compounds containing fluorophores with a net charge (Py-5, S0223 or S0387) or BODIPY 630/650 X, showed high non-specific binding. Investigation of the ligands in a [^{35}S]GTPγS binding assay using membranes of Sf9 insect cells or in a split luciferase mini-G protein recruitment assay (HEK293T cells) and in a split luciferase β-arrestin1/2 recruitment assays (HEK293T cells) revealed a difference in activating the G protein and β-arrestin pathways. Some of the molecules (e.g. **3.32**) showed a significant biased efficacy: whereas the fluorescent H_2R ligands acted as strong partial or full agonists with respect to G protein activation, most of them were only weak to moderate partial agonists regarding β-arrestin recruitment. This was consistent with the results from investigations at HEK293T-hH_2R-qs5-HA or HEK293T-SP-FLAG-hH_2R K33 cells by confocal microscopy, since no H_2R specific endocytosis was observed for **3.32** (β-arr1: E_{max} = 0.09, β-arr2: E_{max} = 0.12). However, three ligands (**3.34**, **3.35** and **3.39**) showed partial agonism (E_{max} ≥0.22) in the β-arrestin recruitment assay and induced internalization of the H_2 receptor which was confirmed by confocal microscopy. These results visually support that β-arrestin plays a critical role for H_2 receptor internalization.

The development of these fluorescent probes will help to understand the cellular regulation of the H_2R (e.g. trafficking) and enables studies on the co-localization of the receptor-ligand complex with various proteins involved in the internalization process throughout further studies.

3.4 Experimental Section

3.4.1 General Experimental Section

Unless otherwise stated, chemicals and solvents were from commercial suppliers and were used as received. All solvents were of analytical grade or were distilled prior to use. Reactions were monitored by thin layer chromatography (TLC) on silica gel 60 F254 aluminium sheets (Merck, Darmstadt, Germany), and spots were visualized with UV light at 254 nm and/or

ninhydrin stain. Flash-chromatography was performed on an Intelli Flash-310 flash chromatography workstation from Varian Deutschland GmbH (Darmstadt, Germany) with SuperFlash columns (Si50) from Agilent Technologies. NMR spectra were recorded on a Bruker Avance 600 (^{1}H: 600 MHz, ^{13}C: 151 MHz) (Bruker, Karlsruhe, Germany) with deuterated solvents from Deutero (Kastellaun, Germany). All chemical shifts are reported in δ-scale as parts per million (ppm, multiplicity, coupling constant (*J*), number of protons) relative to the solvent residual peaks as the internal standard.[65-66] The spectra were analyzed by first order and coupling constants are given in Hertz (Hz). Abbreviations for the multiplicities of the signals are s (singlet), d (doublet), t (triplet), q (quartet), quint (quintet), m (multiplet), dd (double of doublets), br s (broad singlet). HRMS was performed on an Agilent 6540 UHD Accurate-Mass Q-TOF LC/MS system (Agilent Technologies, Santa Clara, CA, USA) using an ESI source. Preparative HPLC was performed with a system from Knauer (Berlin, Germany) consisting of two K-1800 pumps, a K-2001 detector and the column was a Phenomenex Kinetex (250 x 21 mm, 5 µm) (Phenomenex, Aschaffenburg, Germany). As mobile phase mixtures of MeCN and 0.1% aqueous TFA were used. The UV detection was carried out at 220 nm. Lyophilisation was carried out using a ScanVac CoolSafe 4-15L freeze dryer from Labogene (LMS, Brigachtal, Germany), equipped with a RZ 6 rotary vane vacuum pump (Vacuubrand, Wertheim, Germany). Analytical HPLC experiments were performed on a 1100 HPLC system from Agilent Technologies equipped with Instant Pilot controller, a G1312A binary pump, a G1329A ALS autosampler, a G1379A vacuum degasser, a G1316A column compartment and a G1315B DAD detector. The column was a Phenomenex Kinetex XB-C18 column (250 x 4.6 mm, 5 µm) (Phenomenex, Aschaffenburg, Germany), tempered at 30 °C. As mobile phase, mixtures of MeCN/aqueous TFA were used. The following linear gradient was applied: MeCN/TFA (0.05 %) (v/v) 0 min: 10:90, 30 min: 90:10, 33 min: 95:5, 40 min: 95:5; flow rate: 0.8 mL/min, t_0 = 3.21 min. The injection volume was 50 µL. Absorbance was detected at 220 nm. Compound concentration was between 50-200 µM.

3.4.2 Synthesis and Analytical Data

General Procedure for the Synthesis of Fluorescent Ligands 3.28-3.40. The reactions were carried out in a 1.5 mL micro tube (eppendorf, Hamburg, Germany). The amine precursor (**3.23-3.27**, 1.1-2 equiv) was dissolved in 30 µL DMF and NEt_3 (6-15 equiv) was added. The fluorescence dye (Py-5[44], S0436-, S0387-, S0223- or BODIPY 630/650 X-NHS ester, 1 equiv) was dissolved in 20 µL DMF and this solution was added to the mixture, the cup was rinsed

two times with DMF (20 µL and 10 µL). The rinsing solution was also added to the reaction mixture. After stirring for 2 h at rt, the reaction was stopped by addition of 10% aqueous TFA (20 µL). The crude product was purified by preparative HPLC.

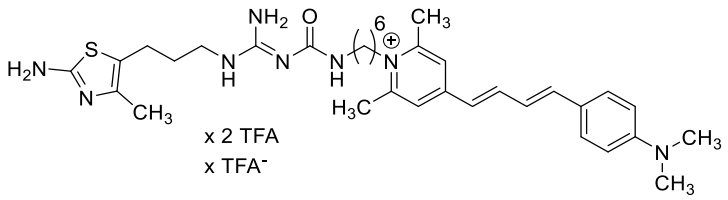

1-(6-(3-((*Z*)-Amino((3-(2-amino-4-methylthiazol-5-yl)propyl)amino)methylene)ureido)hexyl)-4-((1*E*,3*E*)-4-(4-(dimethylamino)phenyl)buta-1,3-dien-1-yl)-2,6-dimethylpyridin-1-ium trifluoroacetate dihydrotrifluoroacetate (3.28). The title compound was prepared from **3.23** (2.4 mg, 3.44 µmol, 1.6 equiv), Py-5 (0.79 mg, 2.15 µmol, 1 equiv) and NEt_3 (1.79 µL, 12.9 µmol, 6 equiv) according to the general procedure yielding **3.28** as a red solid (1.67 mg, 81%). RP-HPLC: 97% (t_R = 13.1 min, k = 3.08). ^{1}H-NMR (600 MHz, DMSO-d_6) δ 9.77 (br s, 1H), 8.90 (br s, 1H), 8.44 (br s, 2H), 7.84 (s, 2H), 7.69 (dd, J = 15.3, 10.4 Hz, 1H), 7.50 (br s, 1H), 7.49-7.43 (m, 2H), 7.04-6.91 (m, 2H), 6.75-6.70 (m, 2H), 6.58 (d, J = 15.3 Hz, 1H), 4.32-4.27 (m, 2H), 3.22 (q, J = 6.7 Hz, 2H), 3.10 (q, J = 6.7 Hz, 2H), 2.97 (s, 6H), 2.75 (s, 6H), 2.55 (t, J = 7.5 Hz, 2H), 2.02 (s, 3H), 1.79-1.67 (m, 4H), 1.51-1.39 (m, 4H), 1.38-1.31 (m, 2H), 1 H signal is missing. HRMS: calcd. for $C_{34}H_{50}N_8OS^{2+}$: 309.1909; found: 309.1922. MF: $C_{34}H_{49}N_8OS^+$ x $C_6H_2F_9O_6^-$. MW: (617.88 + 341.06).

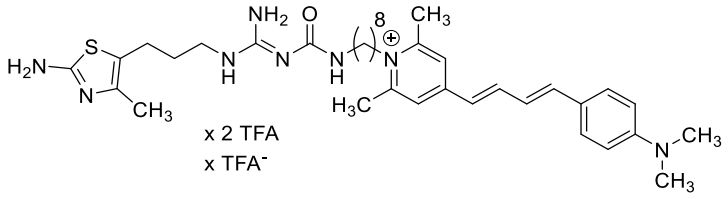

1-(8-(3-((*Z*)-Amino((3-(2-amino-4-methylthiazol-5-yl)propyl)amino)methylene)ureido)octyl)-4-((1*E*,3*E*)-4-(4-(dimethylamino)phenyl)buta-1,3-dien-1-yl)-2,6-dimethylpyridin-1-ium trifluoroacetate dihydrotrifluoroacetate (3.29). The title compound was prepared from **3.24** (7.72 mg, 10.64 µmol, 1 equiv), Py-5 (3.91 mg, 10.65 µmol, 1 equiv) and NEt_3 (11.06 µL, 79.79 µmol, 7.5 equiv) according to the general procedure yielding **3.29** as a red solid (3.60 mg, 34%). RP-HPLC: 99% (t_R = 13.3 min, k = 3.14). ^{1}H-NMR (600 MHz, DMSO-d_6) δ 9.89 (br s, 1H), 8.93 (br s, 1H), 8.46 (br s, 2H),

7.85 (s, 2H), 7.70 (dd, *J* = 15.3, 10.4 Hz, 1H), 7.54-7.43 (m, 3H), 7.01-6.93 (m, 2H), 6.73 (d, *J* = 9.8 Hz, 2H), 6.59 (d, *J* = 15.7 Hz, 1H), 4.30 (t, *J* = 8.0 Hz, 2H), 3.23 (q, *J* = 6.9 Hz, 2H, overlapped with water signal), 3.09 (q, *J* = 6.1 Hz, 2H), 2.97 (s, 6H), 2.75 (s, 6H), 2.58 (t, *J* = 7.5 Hz, 2H, overlapped with DMSO signal), 2.07 (s, 3H), 1.81-1.65 (m, 4H), 1.51-1.20 (m, 10H), 1 H signal is missing. HRMS: calcd. for $C_{36}H_{54}N_8OS^{2+}$: 323.2065; found: 323.2072. MF: $C_{36}H_{53}N_8OS^{+}$ x $C_6H_2F_9O_6^{-}$. MW: (645.93 + 341.06).

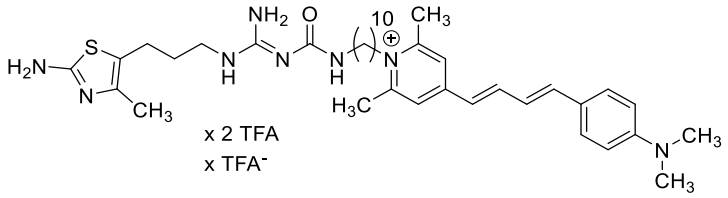

1-(10-(3-((*Z*)-Amino((3-(2-amino-4-methylthiazol-5-yl)propyl)amino)methylene)ureido)decyl)-4-((1*E*,3*E*)-4-(4-(dimethylamino)phenyl)buta-1,3-dien-1-yl)-2,6-dimethylpyridin-1-ium trifluoroacetate dihydrotrifluoroacetate (3.30). The title compound was prepared from **3.25** (2.64 mg, 3.50 µmol, 1 equiv), Py-5 (1.29 mg, 3.51 µmol, 1 equiv) and NEt_3 (3.6 µL, 25.97 µmol, 7.4 equiv) according to the general procedure yielding **3.30** as a red solid (1.87 mg, 53%). RP-HPLC: 98% (t_R = 14.6 min, *k* = 3.55). ^{1}H-NMR (600 MHz, DMSO-d_6) δ 9.53 (br s, 1H), 8.88 (br s, 1H), 8.42 (br s, 2H), 7.84 (s, 2H), 7.69 (dd, *J* = 15.8, 9.6 Hz, 1H), 7.42 (d, *J* = 9.6 Hz, 3H), 7.04-6.91 (m, 2H), 6.72 (d, *J* = 8.7 Hz, 2H), 2.58 (d, *J* = 14.7 Hz, 1H), 4.29 (t, *J* = 8.9 Hz, 2H), 3.24-3.19 (m, 2H, overlapped with water signal), 3.11-3.04 (m, 2H), 2.97 (s, 6H), 2.75 (s, 6H), 2.57-2.53 (m, 2H, overlapped with DMSO signal), 2.01 (s, 3H), 1.77-1.66 (m, 4H), 1.48-1.37 (4H), 1.35-1.22 (m, 10H), 1 H signal is missing. HRMS: calcd. for $C_{38}H_{57}N_8OS^{+}$: 673.4371; found: 673.4370. MF: $C_{38}H_{57}N_8OS^{+}$ x $C_6H_2F_9O_6^{-}$. MW: (673.99 + 341.06).

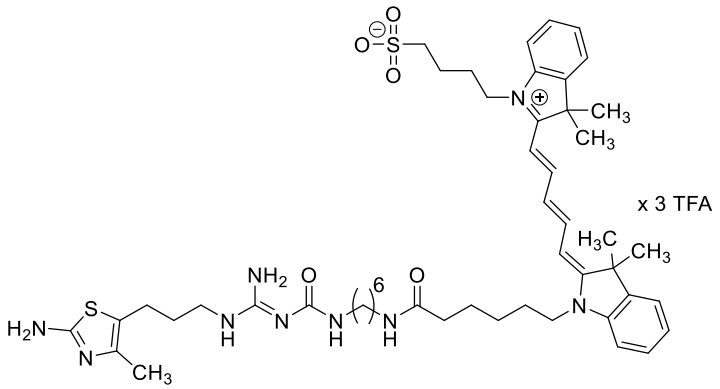

2-((1*E*,3*E*)-5-((*E*)-1-(1-(2-Amino-4-methylthiazol-5-yl)-5-imino-7,16-dioxo-4,6,8,15-tetraazahenicosan-21-yl)-3,3-dimethylindolin-2-ylidene)penta-1,3-dien-1-yl)-3,3-dimethyl-1-(4-sulfobutyl)-3*H*-indol-1-ium trihydrotrifluoroacetate (3.31). The title compound was prepared from **3.23** (2.4 mg, 3.44 µmol, 1.73 equiv), S0436 NHS ester (1.4 mg, 1.99 µmol, 1 equiv) and NEt_3 (2.6 µL, 18.8 µmol, 9.4 equiv) according to the general procedure yielding **3.31** as a blue solid (0.63 mg, 25%). RP-HPLC: 98% (t_R = 17.0 min, k = 4.30). ^{1}H-NMR (600 MHz, DMSO-d_6) δ 10.02 (s, 1H), 8.80 (s, 1H), 8.39 (s, 2H), 8.32 (t, J = 13.1 Hz, 2H), 7.73 (t, J = 5.7 Hz, 1H), 7.63-7.58 (m, 2H), 7.43-7.35 (m, 4H), 7.28 (s, 1H), 7.26-7.21 (m, 2H), 6.57 (t, J = 12.4 Hz, 1H), 6.34 (d, J = 13.8 Hz, 1H), 6.26 (d, J = 13.8 Hz, 1H), 5.39 (s, 1H), 4.13-4.01 (m, 4H), 3.20 (q, J = 6.7 Hz, 2H, overlapped with water signal), 3.07 (q, J = 6.5 Hz, 2H), 2.99 (q, J = 6.6 Hz, 2H), 2.71-2.63 (m, 2H), 2.55 (t, J = 7.5 Hz, 2H), 2.10-1.97 (m, 5H), 1.83-1.74 (m, 4H), 1.72-1.68 (m, 2H), 1.67-1.66 (m, 12H), 1.54 (q, J = 7.3 Hz, 2H), 1.43-1.30 (m, 6H), 1.26-1.20 (m, 6H). HRMS: calcd. for $C_{50}H_{72}N_9O_5S_2^+$: 942.5092; found: 942.5099. MF: $C_{50}H_{71}N_9O_5S_2$ x $C_6H_3F_9O_6$. MW: (943.30 + 342.07).

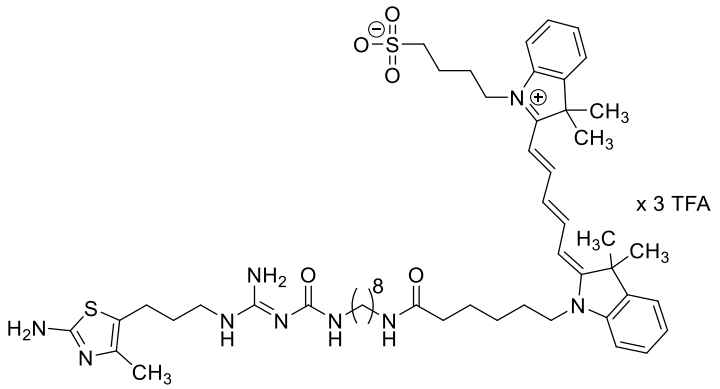

4-(2-((1*E*,3*E*)-5-((*E*)-1-(1-(2-Amino-4-methylthiazol-5-yl)-5-imino-7,18-dioxo-4,6,8,17-tetraazatricosan-23-yl)-3,3-dimethylindolin-2-ylidene)penta-1,3-dien-1-yl)-3,3-dimethyl-

3*H*-indol-1-ium-1-yl)butane-1-sulfonate trihydrotrifluoroacetate (3.32). The title compound was prepared from **3.24** (2.3 mg, 3.17 µmol, 2 equiv), S0436 NHS ester (1.11 mg, 1.58 µmol, 1 equiv) and NEt_3 (2.42 µL, 17.46 µmol, 11 equiv) according to the general procedure yielding **3.32** as a blue solid (0.67 mg, 33%). RP-HPLC: 97% (t_R = 17.6 min, k = 4.48). ^{1}H-NMR (600 MHz, DMSO-d_6) δ 10.00 (br s, 1H), 8.82 (br s, 1H), 8.39 (br s, 2H), 8.32 (t, J = 13.2 Hz, 2H), 7.71 (t, J = 5.4 Hz, 1H), 7.60 (d, J = 7.6 Hz, 2H), 7.42-7.36 (m, 4H), 7.30 (br s, 1H), 7.25-7.21 (m, 2H), 6.57 (t, J = 12.5 Hz, 1H), 6.33 (d, J = 13.9 Hz, 1H), 6.27 (d, J = 13.6 Hz, 1H), 4.13-4.03 (m, 4H), 3.22 (q, J = 6.5 Hz, 2H, overlapped with water signal), 3.06 (q, J = 6.1 Hz, 2H), 2.98 (q, J = 6.1 Hz, 2H), 2.65 (t, J = 6.8 Hz, 2H), 2.57 (t, J = 7.6 Hz, 2H), 2.08-2.00 (m, 5H), 1.81-1.73 (m, 4H), 1.72-1.69 (m, 2H), 1.68-1.66 (m, 12H), 1.53 (quint, J = 7.2 Hz, 2H), 1.43-1.29 (m, 6H), 1.27-1.17 (m, 10H), 1 H signal is missing. HRMS: calcd. for $C_{52}H_{76}N_9O_5S_2^+$: 970.5405; found: 970.5392; calcd. for $C_{52}H_{77}N_9O_5S_2^{2+}$: 485.7739; found: 485.7748. MF: $C_{52}H_{75}N_9O_5S_2$ x $C_6H_3F_9O_6$. MW: (970.35 + 342.07).

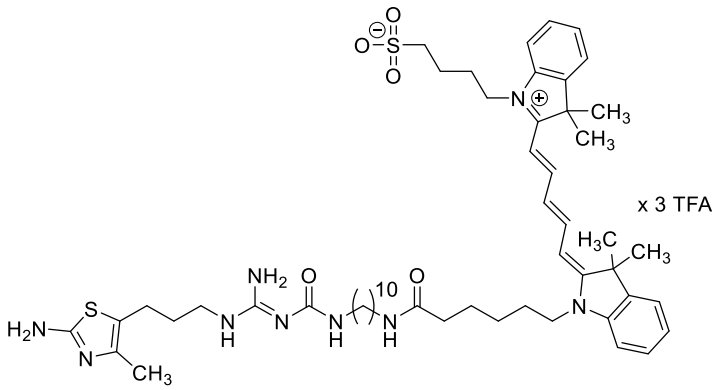

4-(2-((1*E*,3*E*)-5-((*E*)-1-(1-(2-Amino-4-methylthiazol-5-yl)-5-imino-7,20-dioxo-4,6,8,19-tetraazapentacosan-25-yl)-3,3-dimethylindolin-2-ylidene)penta-1,3-dien-1-yl)-3,3-dimethyl-3*H*-indol-1-ium-1-yl)butane-1-sulfonate trihydrotrifluoroacetate (3.33). The title compound was prepared from **3.25** (2.21 mg, 2.93 µmol, 2 equiv), S0436 NHS ester (1.03 mg, 1.47 µmol, 1 equiv) and NEt_3 (2.23 µL, 16.09 µmol, 11 equiv) according to the general procedure yielding **3.33** as a blue solid (1.00 mg, 51%). RP-HPLC: 99% (t_R = 18.7 min, k = 4.83). ^{1}H-NMR (600 MHz, DMSO-d_6) δ 9.93 (br s, 1H), 8.84 (br s, 1H), 8.40 (br s, 2H), 8.32 (t, J = 13.0 Hz, 2H), 7.71 (t, J = 5.5 Hz, 1H), 7.62-7.58 (m, 2H), 7.41-7.35 (m, 4H), 7.31 (br s, 1H), 7.26-7.21 (m, 2H), 6.57 (t, J = 12.4 Hz, 1H), 6.33 (d, J = 14.1 Hz, 1H), 6.27 (d, J = 13.8 Hz, 1H), 4.12-4.04 (m, 4H), 3.22 (q, J = 6.1 Hz, 2H, overlapped with water signal), 3.05 (q, J = 6.1 Hz, 2H), 2.97 (q, J = 6.1 Hz, 2H), 2.64 (t, J = 6.8 Hz, 2H), 2.58 (t, J = 7.4 Hz,

2H), 2.06 (s, 3H), 2.03 (t, *J* = 7.4 Hz, 2H), 1.82-1.74 (m, 4H), 1.72-1.69 (m, 2H), 1.68-1.63 (m, 12H), 1.53 (quint, *J* = 7.5 Hz, 2H), 1.41-1.29 (m, 6H), 1.26-1.15 (m, 14H), 1 H signal is missing. HRMS: calcd. for $C_{54}H_{80}N_9O_5S^+$: 998.5718; found: 998.5714; calcd. for $C_{54}H_{81}N_9O_5S^{2+}$: 499.7896; found: 499.7909. MF: $C_{54}H_{79}N_9O_5S_2$ x $C_6H_3F_9O_6$. MW: (998.40+ 342.07).

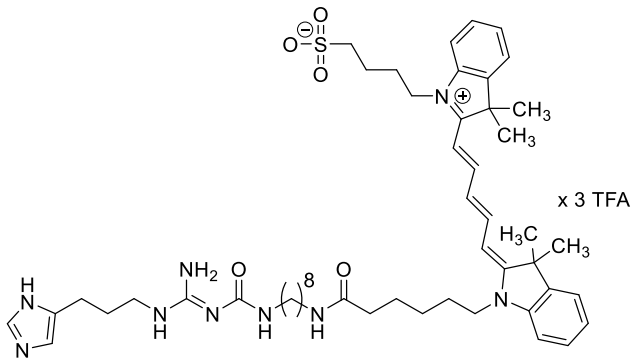

4-(2-((1*E*,3*E*)-5-((*E*)-1-(1-(1*H*-Imidazol-5-yl)-5-imino-7,18-dioxo-4,6,8,17-tetraazatricosan-23-yl)-3,3-dimethylindolin-2-ylidene)penta-1,3-dien-1-yl)-3,3-dimethyl-3*H*-indol-1-ium-1-yl)butane-1-sulfonate trihydrotrifluoroacetate (3.34). The title compound was prepared from **3.26** (8.87 mg, 13.05 µmol, 2.35 equiv), S0436 NHS ester (3.9 mg, 5.56 µmol, 1 equiv) and NEt_3 (8.47 µL, 61.10 µmol, 11 equiv) according to the general procedure yielding **3.34** as a blue solid (1.28 mg, 18%). RP-HPLC: 98% (t_R = 17.6 min, *k* = 4.48). ^{1}H-NMR (600 MHz, DMSO-d_6) δ 10.03 (br s, 1H), 8.97-8.86 (m, 2H), 8.43-8.27 (m, 4H), 7.72 (t, *J* = 5.1 Hz, 1H), 7.63-7.58 (m, 2H), 7.45-7.29 (m, 6H), 7.26-7.21 (m, 2H), 6.57 (t, *J* = 12.6 Hz, 1H), 6.33 (d, *J* = 13.4 Hz, 1H), 6.27 (d, *J* = 14.2 Hz, 1H), 4.12-4.02 (m, 4H), 3.27 (quint, *J* = 6.6 Hz, 2H, overlapped with water signal), 3.06 (q, *J* = 5.1 Hz, 2H), 2.98 (q, *J* = 5.9 Hz, 2H), 2.69-2.63 (m, 4H), 2.03 (t, *J* = 7.5 Hz, 2H), 1.84 (quint, *J* = 7.5 Hz, 2H), 1.81-1.72 (m, 4H), 1.67 (s, 12H), 1.53 (quint, *J* = 7.5 Hz, 2H), 1.43-1.29 (m, 6H), 1.26-1.17 (m, 10H). HRMS: calcd. for $C_{51}H_{75}N_9O_5S^{2+}$: 462.7800; found: 462.7826. MF: $C_{51}H_{73}N_9O_5S$ x $C_6H_3F_9O_6$. MW: (924.26 + 342.07).

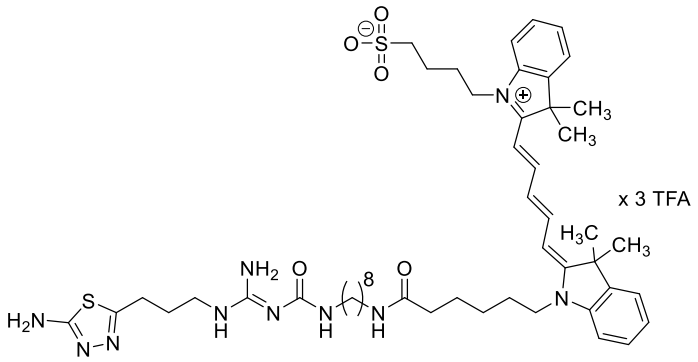

4-(2-((1*E*,3*E*)-5-((*E*)-1-(1-(5-Amino-1,3,4-thiadiazol-2-yl)-5-imino-7,18-dioxo-4,6,8,17-tetraazatricosan-23-yl)-3,3-dimethylindolin-2-ylidene)penta-1,3-dien-1-yl)-3,3-dimethyl-3*H*-indol-1-ium-1-yl)butane-1-sulfonate trihydrotrifluoroacetate (3.35). The title compound was prepared from **3.27** (4.4 mg, 6.17 µmol, 1.1 equiv), S0436 NHS ester (3.9 mg, 5.56 µmol, 1 equiv) and NEt_3 (8.5 µL, 61.3 µmol, 11 equiv) according to the general procedure yielding **3.35** as a blue solid (1.92 mg, 26%). RP-HPLC: 97% (t_R = 18.6 min, k = 4.79). ^{1}H-NMR (600 MHz, DMSO-d_6) δ 9.92 (br s, 1H), 8.85 (br s, 1H), 8.41 (br s, 2H), 8.32 (t, J = 13.1 Hz, 2H), 7.71 (t, J = 5.6 Hz, 1H), 7.60 (d, J = 7.4 Hz, 2H), 7.45-7.34 (m, 4H), 7.31 (br s, 1H, is incorrectly integrated as 0.01 by the software), 7.26-7.20 (m, 2H), 7.19-7.05 (m, 2H), 6.57 (t, J = 12.4 Hz, 1H), 6.34 (d, J = 13.8 Hz, 1H), 6.27 (d, J = 13.7 Hz, 1H), 4.14-4.03 (m, 4H), 3.27 (q, J = 6.7 Hz, 2H), 3.06 (q, J = 6.5 Hz, 2H), 2.98 (q, J = 6.6 Hz, 2H), 2.83 (t, J = 7.6 Hz, 2H), 2.63 (t, J = 6.8 Hz, 2H), 2.03 (t, J = 7.2 Hz, 2H), 1.87 (quint, J = 7.3 Hz, 2H), 1.82-1.72 (m, 4H), 1.67 (d, J = 1.7 Hz, 12H), 1.53 (quint, J = 7.4 Hz, 2H), 1.43-1.30 (m, 6H), 1.28-1.15 (m, 10H). HRMS: calcd. for $C_{50}H_{74}N_{10}O_5S_2^{2+}$: 479.2637; found: 479.2652. MF: $C_{50}H_{72}N_{10}O_5S_2$ x $C_6H_3F_9O_6$. MW: (957.31 + 342.07).

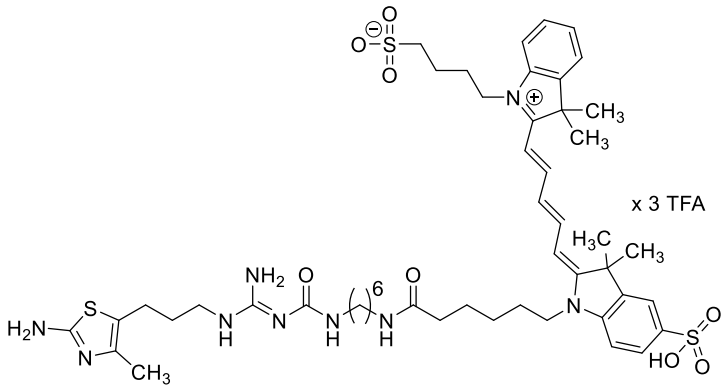

4-(2-((1*E*,3*E*)-5-((*E*)-1-((*Z*)-5-Amino-1-(2-amino-4-methylthiazol-5-yl)-7,16-dioxo-4,6,8,15-tetraazahenicos-5-en-21-yl)-3,3-dimethyl-5-sulfoindolin-2-ylidene)penta-1,3-

dien-1-yl)-3,3-dimethyl-3*H*-indol-1-ium-1-yl)butane-1-sulfonate trihydrotrifluoroacetate (3.36). The title compound was prepared from **3.23** (2.3 mg, 3.30 µmol, 2 equiv), S0387 NHS ester (1.3 mg, 1.62 µmol, 1 equiv) and NEt_3 (2.5 µL, 18.04 µmol, 11 equiv) according to the general procedure yielding **3.36** as a blue solid (0.6 mg, 27%). RP-HPLC: 95% (t_R = 13.1 min, k = 3.08). ^{1}H-NMR (600 MHz, DMSO-d$_6$) δ 10.03 (br s, 1H), 8.97-8.86 (m, 1H), 8.43-8.27 (m, 4H), 7.81 (d, J = 1.6 Hz, 1H), 7.72 (t, J = 5.1 Hz, 1H), 7.63-7.58 (m, 2H), 7.45-7.37 (m, 2H), 7.33-7.23 (m, 3H), 6.57 (t, J = 12.6 Hz, 1H), 6.38 (d, J = 13.4 Hz, 1H), 6.24 (d, J = 14.2 Hz, 1H), 4.12-4.02 (m, 4H), 3.20 (q, J = 6.6 Hz, 2H, overlapped with water signal), 3.06 (q, J = 5.1 Hz, 2H), 2.98 (q, J = 5.9 Hz, 2H), 2.63 (t, J = 6.9 Hz, 2H), 2.55 (t, J = 7.2 Hz, 2H), 2.05-1.98 (m, 5H), 1.81-1.72 (m, 6H), 1.68 (s, 6H), 1.67 (s, 6H), 1.53 (quint, J = 7.5 Hz, 2H), 1.43-1.37 (m, 2H), 1.32-1.28 (m, 4H), 1.29-1.17 (m, 6H), 2 H signals are missing. HRMS: calcd. for $C_{50}H_{72}N_9O_8S_3^+$: 1022.4660; found: 1022.4671; calcd. for $C_{50}H_{73}N_9O_8S_3^{2+}$: 511.7367; found: 511.7376. MF: $C_{50}H_{71}N_9O_8S_3$ x $C_6H_3F_9O_6$. MW: (1022.35 + 342.07).

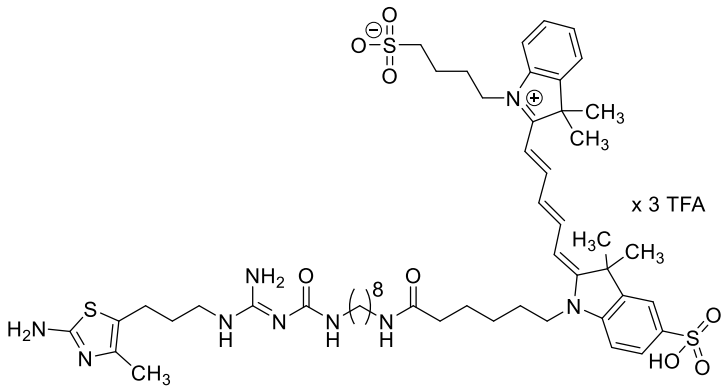

4-(2-((1*E*,3*E*)-5-((*E*)-1-((Z)-5-Amino-1-(2-amino-4-methylthiazol-5-yl)-7,18-dioxo-4,6,8,17-tetraazatricos-5-en-23-yl)-3,3-dimethyl-5-sulfoindolin-2-ylidene)penta-1,3-dien-1-yl)-3,3-dimethyl-3*H*-indol-1-ium-1-yl)butane-1-sulfonate trihydrotrifluoroacetate (3.37). The title compound was prepared from **3.24** (7.48 mg, 10.31 µmol, 1.2 equiv), S0387 NHS ester (6.91 mg, 8.60 µmol, 1 equiv) and NEt_3 (13.11 µL, 94.58 µmol, 11 equiv) according to the general procedure yielding **3.37** as a blue solid (3.00 mg, 25%). RP-HPLC: 99% (t_R = 14.6 min, k = 3.55). ^{1}H-NMR (600 MHz, DMSO-d$_6$) δ 9.99 (br s, 1H), 8.83 (br s, 1H), 8.52-8.25 (m, 4H), 7.82 (d, J = 1.5 Hz, 1H), 7.72 (t, J = 5.6 Hz, 1H), 7.67-7.58 (m, 2H), 7.47-7.37 (m, 2H), 7.36-7.21 (m, 3H), 6.59 (t, J = 12.3 Hz, 1H), 6.39 (d, J = 13.9 Hz, 1H), 6.26 (d, J = 13.9 Hz, 1H), 4.12 (t, J = 7.3 Hz, 2H), 4.06 (t, J = 6.5 Hz, 2H), 3.23 (q, J = 6.0 Hz, 2H, overlapped with water signal), 3.07 (q, J = 5.9 Hz, 2H), 2.99 (q, J = 6.2 Hz, 2H), 2.62 (t,

J = 6.9 Hz, 2H, overlapped with DMSO signal), 2.58 (t, *J* = 6.9 Hz, 2H), 2.08-2.00 (m, 5H), 1.85-1.62 (m, 18H), 1.54 (quint, *J* = 7.2 Hz, 2H), 1.43-1.16 (m, 16H), 2 H signals are missing. HRMS: calcd. for $C_{52}H_{76}N_9O_8S_3^+$: 1050.4973; found: 1050.4978; calcd. for $C_{52}H_{77}N_9O_8S_3^{2+}$: 525.7523; found: 525.7532. MF: $C_{52}H_{75}N_9O_8S_3$ x $C_6H_3F_9O_6$. MW: (1050.41 + 342.07).

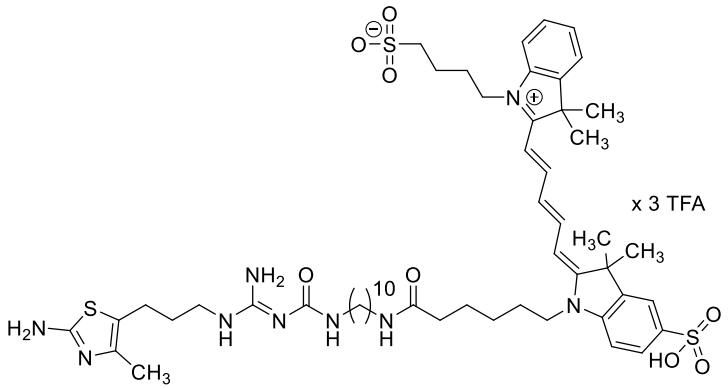

4-(2-((1*E*,3*E*)-5-((*E*)-1-((*Z*)-5-Amino-1-(2-amino-4-methylthiazol-5-yl)-7,20-dioxo-4,6,8,19-tetraazapentacos-5-en-25-yl)-3,3-dimethyl-5-sulfoindolin-2-ylidene)penta-1,3-dien-1-yl)-3,3-dimethyl-3*H*-indol-1-ium-1-yl)butane-1-sulfonate trihydrotrifluoroacetate (3.38). The title compound was prepared from **3.25** (2.70 mg, 3.58 µmol, 1.5 equiv), S0387 NHS ester (1.91 mg, 2.38 µmol, 1 equiv) and NEt_3 (3.61 µL, 26.04 µmol, 11 equiv) according to the general procedure yielding **3.38** as a blue solid (1.74 mg, 51%). RP-HPLC: 92% (t_R = 15.6 min, *k* = 3.86). ^{1}H-NMR (600 MHz, DMSO-d_6) 9.89 (br s, 1H), 8.84 (br s, 1H), 8.48-8.27 (m, 4H), 7.82 (d, *J* = 1.3 Hz, 1H), 7.72 (t, *J* = 6.0 Hz, 1H), 7.67-7.59 (m, 2H), 7.47-7.36 (m, 2H), 7.36-7.22 (m, 3H), 6.58 (t, *J* = 12.5 Hz, 1H), 6.38 (d, *J* = 13.8 Hz, 1H), 6.27 (d, *J* = 14.2 Hz, 1H), 4.12 (t, *J* = 7.2 Hz, 2H), 4.06 (t, *J* = 7.3 Hz, 2H), 3.23 (q, *J* = 6.5 Hz, 2H, overlapped with water signal), 3.06 (q, *J* = 5.7 Hz, 2H), 2.98 (q, *J* = 6.0 Hz, 2H), 2.66-2.60 (m, 2H), 2.59-2.55 (t, *J* = 7.2 Hz, 2H), 2.10-1.99 (m, 5H), 1.84-1.62 (m, 18H), 1.54 (quint, *J* = 7.2 Hz, 2H), 1.44-1.29 (m, 6H), 1.28-1.16 (m, 14H), 2 H signals are missing. HRMS: calcd. for $C_{54}H_{80}N_9O_8S_3^+$: 1078.5286, found: 1078.5281, calcd. for $C_{54}H_{81}N_9O_8S_3^{2+}$: 539.7680, found: 539.7684. MF: $C_{54}H_{79}N_9O_8S_3$ x $C_6H_3F_9O_6$. MW: (1078.46 + 342.07).

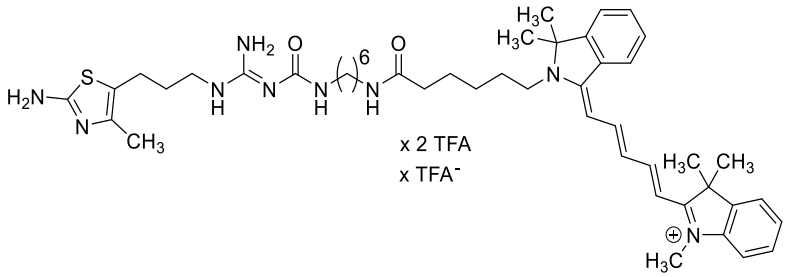

2-((1*E*,3*E*)-5-((*E*)-2-(1-(2-Amino-4-methylthiazol-5-yl)-5-imino-7,16-dioxo-4,6,8,15-tetraazahenicosan-21-yl)-3,3-dimethylisoindolin-1-ylidene)penta-1,3-dien-1-yl)-1,3,3-trimethyl-3*H*-indol-1-ium trifluoroacetate dihydrotrifluoroacetate (3.39). The title compound was prepared from **3.23** (2.32 mg, 3.33 µmol, 1.8 equiv), S0223 NHS ester (1.2 mg, 1.82 µmol, 1 equiv) and NEt_3 (3.6 µL, 25.97 µmol, 14 equiv) according to the general procedure yielding **3.39** as a blue solid (1.12 mg, 53%). RP-HPLC: 98% (t_R = 17.5 min, k = 4.45). ^{1}H-NMR (600 MHz, DMSO-d_6) δ 9.95 (br s, 1H), 8.93 (br s, 1H), 8.45 (br s, 2H), 8.32 (t, J = 12.3 Hz, 2H), 7.70 (t, J = 5.7 Hz, 1H), 7.60 (d, J = 6.9 Hz, 2H), 7.46 (br s, 1H), 7.42-7.34 (m, 4H), 7.27-7.21 (m, 2H), 6.55 (t, J = 12.3 Hz, 1H), 6.27 (q, J = 13.6 Hz, 2H), 4.07 (t, J = 6.6 Hz, 2H), 3.59 (s, 3H, overlapped with water signal), 3.21 (q, J = 6.9 Hz, 2H, overlapped with water signal), 3.06 (q, J = 6.9 Hz, 2H), 2.97 (q, J = 6.9 Hz, 2H), 2.56 (t, J = 8.2 Hz, 2H, overlapped with DMSO signal), 2.07-2.00 (m, 5H), 1.73-1.68 (m, 2H), 1.67-1.66 (m, 12H), 1.52 (quint, J = 6.9 Hz, 2H), 1.43-1.37 (m, 2H), 1.36-1.29 (m, 4H), 1.28-1.17 (m, 6H), 1 H signal is missing. HRMS: calcd. for $C_{47}H_{67}N_9O_2S^{2+}$: 410.7564; found: 410.7567. MF: $C_{47}H_{66}N_9O_2S^+$ x $C_6H_2F_9O_6^-$. MW: (821.17 + 341.06).

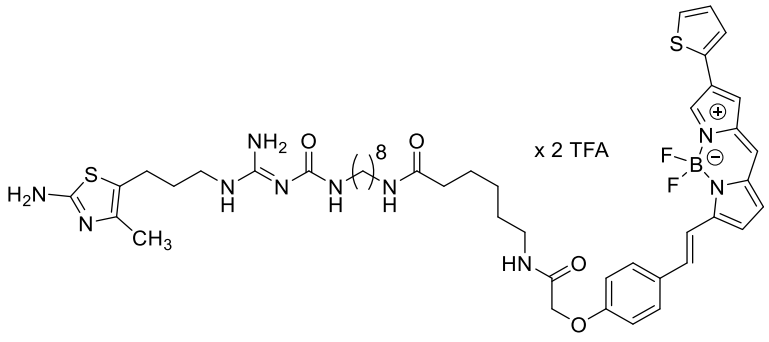

***N*-(8-(3-((*E*)-Amino((3-(2-amino-4-methylthiazol-5-yl)propyl)amino)methylene)ureido)octyl)-6-(2-(4-((*E*)-2-(5,5-difluoro-8-(thiophen-2-yl)-5*H*-5l4,6l4-dipyrrolo[1,2-c:2',1'-f][1,3,2]diazaborinin-3-yl)vinyl)phenoxy)acetamido)hexanamide dihydrotrifluoroacetate (3.40).** The title

compound was prepared from **3.24** (3.8 mg, 5.24 µmol, 1.7 equiv), BODIPY 630/650-X NHS ester (2.1 mg, 3.17 µmol, 1 equiv) and NEt_3 (4.7 µL, 33.91 µmol, 11 equiv) according to the general procedure yielding **3.40** as a blue solid (3.27 mg, 89%). RP-HPLC: 96% (t_R = 20.2 min, k = 5.29). ^{1}H-NMR (600 MHz, DMSO-d_6) δ 9.88-9.72 (m, 1H), 8.92 (br s, 1H), 8.43 (br s, 2H), 8.11 (t, J = 6.0 Hz, 1H), 8.03 (dd, J = 3.8, 0.9 Hz, 1H), 7.82 (dd, J = 5.1, 0.9 Hz, 1H), 7.73 (d, J = 16.4 Hz, 1H), 7.69 (t, J = 5.6 Hz, 1H), 7.62-7.58 (m, 3H), 7.44 (t, J = 5.4 Hz, 1H), 7.41-7.36 (m, 2H), 7.30-7.25 (m, 3H), 7.06 (d, J = 8.9 Hz, 2H), 6.94 (d, J = 4.0 Hz, 1H), 4.52 (s, 2H), 3.21 (q, J = 6.3 Hz, 2H), 3.11 (q, J = 6.3 Hz, 2H), 3.06 (q, J = 6.0 Hz, 2H), 2.99 (q, J = 6.0 Hz, 2H), 2.56 (t, J = 7.6 Hz, 2H), 2.07-1.99 (m, 5H), 1.70 (quint, J = 7.2 Hz, 2H), 1.50-1.38 (m, 6H), 1.34 (quint, J = 6.6 Hz, 2H), 1.25-1.18 (m, 10H), 2 H signals are missing. HRMS: calcd. for $C_{46}H_{61}BF_2N_{10}O_4S_2^+$: 929.4302; found: 929.4302. MF: $C_{46}H_{60}BF_2N_{10}O_4S_2$ x $C_4H_2F_6O_4$. MW: (929.98 + 228.05).

3.4.3 Cell Culture

Cells were cultured in 25 or 75 cm^2 flasks (Sarstedt, Nümbrecht, Germany) in a humidified atmosphere (95% air, 5% CO2) at 37 °C. HEK293T-ARRB1-hH_2R[3] cells, HEK293T-ARRB2-hH_2R[3] cells, HEK293T NlucN-mGs/hH_2R-NlucC[57] cells and HEK293T-hH_2R-qs5-HA[63] cells were cultured as described previously. HEK293T-SP-FLAG-hH_2R clone (K) 33 cells were cultured in Dulbecco's modified Eagle's medium (DMEM, Sigma-Aldrich, Taufkirchen, Germany) containing 4.5 g/L glucose, 3.7 g/L $NaHCO_3$, and 110 mg/L sodium pyruvate and supplemented with 0.584 g/L L-glutamine (Sigma-Aldrich), 10% fetal calf serum (FCS, Biochrom, Berlin, Germany) and 600 µg/mL G418 (Biochrom). The used cell lines were regularly monitored for mycoplasma infection using the Venor GeM Mycoplasma Detection Kit (Minerva Biolabs, Berlin, Germany).

3.4.4 Generation of the HEK293T-SP-FLAG-hH_2R K33 Cell Line

Molecular cloning of the hH_2R receptor as well as the generation of the stable cell line were performed according to the procedure described for the HEK293T-SP-FLAG3-hH_3R K16 cell line.[45] Briefly, the pIRESneo3-SP-FLAG-hH_2R construct was generated using the pIRESneo3-SP-FLAG-hH_4R[45] vector as template. The hH_4R sequence was replaced by the hH_2R sequence using the PCR Protocol for Phusion Hot Start Flex DNA Polymerase (New England Biolabs GmbH, Frankfurt/Main, Germany) and the NEBuilder HiFi DNA Assembly Reaction Protocol (New England Biolabs GmbH, Frankfurt/Main, Germany). The quality of the vector was

controlled by sequencing (Eurofins Genomics GmbH, Ebersberg, Germany). Subsequently, HEK293T cells were transfected with the pIRESneo3-SP-FLAG-hH_2R vector, and individual clones were selected as previously described for the HEK293T-SP-FLAG-hH_4R K3 cell line[45]. Based on the highest receptor expression (determining using radioligand saturation binding experiments, data not shown), the HEK293T-SP-FLAG-hH_2R K33 cell line was selected for further experiments.

3.4.5 Radioligand Binding Experiments Using Sf9 Membranes

Competition binding experiments were performed using membrane preparations of Sf9 insect cells expressing the hH_1R + RGS4[10], hH_2R-$G_{s\alpha S}$ fusion protein[56], hH_3R + $G_{\alpha i2}$ + $G_{\beta 1\gamma 2}$[67] or the hH_4R + $G_{\alpha i2}$ + $G_{\beta 1\gamma 2}$[68]. General procedures for the generation of recombinant baculoviruses, culture of Sf9 cells and membrane preparations have been described elsewhere.[69] The competition binding experiments were performed as previously described in detail[40, 50] with one minor modification: PBS (8 g NaCl, 0.2 g KCl, 1.0 g Na_2HPO_4 x 2 H_2O, 0.15 g NaH_2PO_4 x H_2O, 0.1 g KH_2PO_4 in 1 L Millipore H_2O; pH 7.4; 4 °C) was used as washing buffer while harvesting instead of the previously used binding buffer[40, 50]. [^{3}H]mepyramine (specific activity: 20.0 or 87 Ci/mmol) was from Hartmann analytics (Braunschweig, Germany) or Novandi Chemistry AB (Södertälje, Sweden), [^{3}H]histamine (specific activity: 25.0 Ci/mmol) and [^{3}H]N^{α}-methylhistamine (specific activity: 85.3 Ci/mmol) were from Hartmann analytics (Braunschweig, Germany). [^{3}H]UR-DE257[53] (specific activity: 63.0 Ci/mmol) and [^{3}H]UR-PI294[54] (specific activity: 41.8 Ci/mmol) were synthesized and characterized in our laboratories. In case of fluorescent ligands, 96-well Primaria plates (CORNING, NY, USA) were used because of the strong adsorption of the fluorescent ligands to the surface of the typically employed PP plates during the incubation period.

3.4.6 Radioligand Binding Experiments Using HEK293T-hH_2R-qs5-HA Cells

For the assay, approx. 2 x 10^6 cells were seeded into two 75 cm^2 culture flasks (Sarstedt, Nümbrecht, Germany) and grown to approx. 80% confluency (3-4 days) before the radioligand binding assays. The cells were detached by trypsin treatment (0.05% trypsin, 0.02% EDTA in PBS w/o Ca^{2+} and w/o Mg^{2+}, Biochrom, Berlin, Germany) and centrifuged for 5 min at 500 x *g*. The pellet was resuspended in Leibovitz`s L-15 medium (Life Technologies Corporation, Grand Island, NY, USA) containing 1% FCS and 10 mM HEPES (Serva, Heidelberg, Germany). The cells were counted in a hemocytometer and finally adjusted to a density of

1 x 10^6 cells/mL. For saturation binding experiments, 10 µL of a famotidine (Alfa Aesar) solution (10 mM in Leibovitz`s L-15 medium containinng 10 mM HEPES) or 10 µL of a Leibovitz`s L-15 medium were pipeted per cavity of a 96-well plate (PP microplates 96 well, Greiner Bio-One, Frickenhausen, Germany) either for the determination of non-specific or total binding, respectively. 10 µL of the respective [^{3}H]UR-DE257[53] solution (10-fold concentrated feed-solutions compared to final concentration in Leibovitz`s L-15 medium containinng 10 mM HEPES). Samples were completed by addition of 80 µL of the cell suspension per well. Samples were shaken at 400 rpm for 60 min prior harvesting. Cell-bound radioactivity was transferred to a glass fibre filter GF/C pretreated with PEI (0.3 % (v/v), PEI was from Sigma) by the 96-well harvester (Brandel Inc., Unterföhring, Germany). The filter was washed four times with PBS (4 °C). Filter discs with the cell-bound radioactivity were transferred into a second 96-well plate (96-well flexible PET microplate, Perkin Elmer, Rodgau, Germany). 200 µL of scintilator liquid (Rotiszint eco plus, Roth, Karlsruh, Germany) per well were added and the samples were shaken at 400 rpm for 6-10 h prior to measurement using MicroBeta21450 PlateCounter (Perkin Elmer, Rodgau, Germany). Data were transferred to GraphPad Prism 5. Specific binding was determined by substraction of non-specific binding from the respective values of total binding. Specific binding data (dpm) were plotted against the free radioligand concentration (nM) and analyzed by a two-parameter equation describing hyperbolic binding to obtain K_d and B_{max} values. The free radioligand concentration is the difference between the amount of specifically bound [^{3}H]UR-DE257[53] (nM) and total radioligand concentration. Non-specific binding was fitted by a linear regression.

In competition binding experiments, the concentration of [^{3}H]UR-DE257[53] was 25 nM, while increasing concentrations of unlabeled ligands (famotidine (fam), ranitidine (rani, Alfa Aesar), tiotidine (tio) or histamine (his, TCI)) were applied. The plates were shaken at 400 rpm for 60 min. For the analysis of the data, total binding (dpm) was plotted versus log (concentration competitor) and normalized [100% = bound radioligand (dpm) in the absence of a competitior, 0% = non-specific bound radioligand (dpm) in the presence of 1 mM famotidine]. Applying a four-parameter logistic equation (GraphPad Prism 5), IC_{50} values were obtained for each individual experiment. The IC_{50} values were converted to K_i values by applying the Cheng-Prusoff equation.[61] The K_i values were converted to the respective negative logarithms (pK_i values) folowed by the calculation of the mean pK_i.

3.4.7 Flow Cytometric Binding Assays Using Whole HEK293T-hH_2R-qs5-HA Cells

The flow cytometric measurements were performed with FACSCalibur cytometer or with FACSCanto II flow cytometer (Becton Dickinson, Heidelberg, Germany), both equipped with an argon laser (488 nm) and a red diode laser (FACSCalibur: 635 nm and FACSCanto II: 633 nm) (settings: FACSCalibur: FSC: E-1, SSC: 290 V, FL-3: 800 V and FL-4:480 V; FACSCanto II: FCS: A, log, 0 V; SSC: A, log, 252 V; ACP: A,H,W, log, 350 V) according to general protocols with minor modifications.[37-38, 63, 70] All samples were prepared in duplicates and recorded either in channel FL-3 (FACSCalibur, pyridinium dye (Py-5), excitation: 488 nm, emission filter: >679 nm), in FL-4 (FACSCalibur, cyanine dyes (S0436, S0387 and S0223), excitation: 635 nm, emission filter: 661 ± 18 nm) or in APC (FACSCanto II, cyanine dyes or BODIPY 630/650 X, excitation: 633 nm). Data acquisition was complete after 20,000 (FACSCalibur) or 10,000 (FACSCanto II) gated events.

On the day of the experiment, HEK293T-hH_2R-qs5-HA[63]cells (~ 80% confluence) were trypsinized (0.05% trypsin, 0.02% EDTA in PBS w/o Ca^{2+} and w/o Mg^{2+}, Biochrom) and detached with Leibovitz`s L-15 medium (Life Technologies Corporation) containing 1% FCS. After centrifugation (500 x *g*, 5 min), the cell pellet was resuspended in Leibovitz`s L-15 medium containing 1% FCS and the concentration was adjusted to 1 x 10^6 cells/mL.

Saturation binding:[37-38, 63] The solutions of the dilution series of the tested fluorescent ligands (**3.28-3.37** and **3.39-3.40**) and famotidine (non-specific binding) were prepared in DMSO/H_2O (1:1, v/v). The incubation was performed in 96-well Primaria plates (CORNING). 200 µL of the cell suspension (1 x 10^6 cells/mL) were either added to 2 µL of DMSO/H_2O (1:1, v/v, total binding) or to 2 µL of famotidine (300-fold excess to the fluorescent ligand adjusted to the respective concentration of the fluorescent ligand, non-specific binding). Incubation was started by addition of 2 µL of fluorescent ligand solution of interest in different concentrations (100-fold concentrated) starting with the highest concentration of total binding. The 96-well plates were incubated under shaking at rt in the dark for 90 min. The samples were transferred to 5 mL polystyrol FACS tubes (Sarstedt) and immediately measured. For the analysis of data obtained with FACSCalibur the software FlowJo V10 (FlowJo, LLC, Ashland, USA) was used. The data from FACS CANTO II were analyzed with the Software FACS Diva (Becton Dickenson). The geometric means of the signal areas detected in the APC channel (FACSCanto II) and the geometric means of the signal heights detected in channels FL-3 or FL-4 (FACSCalibur) were determined for a subpopulation of the gated H_2R-expressing cells. Specific binding data from flow cytometric saturation binding experiments, obtained by subtracting unspecific binding

data from total binding data, were plotted against the fluorescent ligand concentration, and analyzed by a non-linear regression (one site-specific binding equation; GraphPad Prism 5, GraphPad Software, San Diego, CA) in order to obtain K_d values. K_d values of individual experiments were transformed to pK_d values.

Competition binding:[37, 63] The dilution series of the respective unlabeled competitors (ranitidine, famotidine, tiotidine, BMY 25368 (self-synthesized), amthamine (Axon Medchem, Groningen, Netherlands) or histamine) were prepared in DMSO/H_2O (1:1, v/v). The incubation was performed in 96-well Primaria plates (CORNING). To 200 µL of the cell suspension (1 x 10^6 cells/mL), 2 µL of competitor (100-fold concentrated) and 2 µL of fluorescent ligand (concentration in the assay: 60 nM (**3.32** or **3.34**) or 100 nM (**3.35**) were added. The 96-well plates were incubated under shaking for 90 min at rt in the dark. The samples were transferred to 5 mL polystyrol FACS tubes and immediately measured. Total binding data were plotted against the logarithmic concentration of the competitor and normalized [100% = bound fluorescent ligand in the absence of a competitor and 0% = non-specifically bound fluorescent ligand in the presence of famotidine (c = 1 mM). Applying a log(inhibitor) vs. response-variable slope equation (GraphPad Prism 5), pIC_{50} values were obtained. The corresponding IC_{50} values were converted to K_i values by applying the Cheng-Prusoff equation,[61] followed by calculation of the pK_i.

Kinetic studies:[37] For the kinetic experiments the HEK293T-hH_2R-qs5-HA cell suspension was prepared as described for the binding assays. 5-mL microtubes (eppendorf) containing **3.32** (120 nM), **3.34** (60 nM) or **3.35** (100 nM) and the cell suspension at a concentration 1 x 10^6 cells/mL in Leibovitz`s L15 medium supplemented with 1% FCS were employed. The mixtures were shaken at 500 rpm (Multi Reax Vortexer, Heidolph Instruments, Schwabach, Germany) at rt. Association experiments were started by the addition of the respective fluorescence ligand (**3.32**, **3.34** or **3.35**) to the cell-containing tube. At each time point 200 µL aliquots were withdrawn from the tube and measured. Non-specific binding was determined for each time point in the presence of famotidine (**3.32**: 36 µM, **3.34**: 18 µM or **3.35**: 30 µM). For the dissociation experiments, the tubes containing **3.32** (120 nM), **3.34** (60 nM) or **3.35** (100 nM) and the cell suspension at a concentration 1 x 10^6 cells/mL in Leibovitz`s L15 medium supplemented with 1% FCS were incubated for 90 min, centrifuged (500 x *g*, 5 min) and the supernatant, containing excess fluorescent ligand was removed. Leibovitz`s L-15 medium containing 1% FCS and famotidine (**3.32**: 36 µM, **3.34**: 18 µM, or **3.35**: 30 µM, same volume as removed) was added to the cell pellet, before the cells were resuspended. The

incubation at rt was stopped after different periods of time (0-220 min) by measuring the samples.

The kinetic experiments were analyzed using two methods: non-linear regression and linear transformation (for details see 3.2.5 Association and Dissociation Kinetics of **3.32**, **3.34** and **3.35** at the hH_2R Expressed in HEK293T-qs5-HA Cells Studied by Flow Cytometry in the chapter 3).

3.4.8 Functional Assays

The [^{35}S]GTPγS assay was performed on Sf9 membranes expressing the hH_2R-$G_{s\alpha S}$ fusion protein as previously described[40, 50, 56] with one minor modification: PBS (8 g NaCl, 0.2 g KCl, 1.0 g Na_2HPO_4 x 2 H_2O, 0.15 g NaH_2PO_4 x H_2O, 0.1 g KH_2PO_4 in 1 L Millipore H_2O; pH 7.4; 4 °C) was used as washing buffer while harvesting instead of the previously used binding buffer. In case of fluorescent ligands 96-well Primaria plates (CORNING) were used, because of the strong adsorption of the fluorescent ligands to the typically used PP plates during the incubation period. The [^{35}S]GTPγS binding assay was evaluated as described in detail by Biselli et al.[37]

Functional studies in the mini-G protein or β-arrestin2 recruitment assays using HEK293T NlucN-mGs/hH_2R-NlucC[57]-, HEK293T-ARRB2-H_2R[3, 38]-, HEK293T-ARRB1-H_2R[3] cells were performed as previously described.

3.4.9 Confocal Microscopy

Two or three days prior to microscopy, HEK293T-hH_2R-qs5-HA[63] or HEK293T-SP-FLAG-hH_2R K33 cells (~ 80% confluence) were trypsinized (0.05% trypsin, 0.02% EDTA in PBS w/o Ca^{2+} and w/o Mg^{2+}, Biochrom) and detached with Leibovitz`s L-15 medium (Life Technologies Corporation) containing 10% FCS. After centrifugation (500 x *g*, 5 min), the cell pellet was resuspended in Leibovitz`s L-15 medium containing 10% FCS and the concentration was adjusted to 0.3 x 10^6 cells/mL. Appr. 6 x 10^4 HEK293T-hH_2R-qs5-HA or HEK293T-SP-FLAG-hH_2R K33 cells (corresponds to 200 µL cell suspension) were seeded per cavity of sterile µ-Slide 8 well plates (ibidi, Munich, Germany). The µ-Slide 8 well plates were previously coated with poly-L-lysin (Sigma-Aldrich, Munich, Germany) according to the manufacturer`s instructions. The cells were cultured at 37 °C in a water saturated atmosphere w/o $CO_2$. On the day of the investigation, the medium was carefully removed and replaced by 120 µL fresh Leibovitz`s L-15 medium supplemented with 1% FCS and 10 mM HEPES (Serva)

per well. Until the measurements were performed, the cells were incubated at 37 °C in water saturated atmosphere w/o CO_2. Subsequently, the sample for the total binding was prepared by addition of 40 µL of Leibovitz`s L-15 medium + 1% FCS + 10 mM HEPES and 40 µL of fluorescence ligand solution (5-fold concentrated). Dilutions of the ligands were prepared from the 5 mM stock solution in DMSO in Leibovitz`s L-15 medium + 1% FCS + 10 mM HEPES. The sample of the non-specific binding was prepared in a different cavity by addition of 40 µL of famotidin solution (300-fold higher concentration compared to fluorescence ligand, 5-fold concentrated) and 40 µL of fluorescence ligand solution (5-fold concentrated). The samples were analyzed in the dark at room temperature with a Carl Zeiss Axiovert 200 M microscope, using a LSM S10 laser scanner combined with the Plan-Apochromat 63x/1.4 Oil (Carl Zeiss Microscopy GmbH, Oberkochen, Germany). The settings (exitation wavelenght, laser transmittance, filter and pinhole) used for the detection of **3.32**, **3.34**, **3.35** and **3.39** are shown in Figures App2.35-App2.40 in the Appendix 2. Data from confocal microscopy were processed with the Carl Zeiss Zen 2.1 and the ImageJ 1.52i [71] software.

3.5 References

1. Hill, S. J.; Ganellin, C. R.; Timmerman, H.; Schwartz, J. C.; Shankley, N. P.; Young, J. M.; Schunack, W.; Levi, R.; Haas, H. L., International union of pharmacology. XIII. Classification of histamine receptors. *Pharmacol. Rev.* **1997,** *49*, 253-278.
2. Panula, P.; Chazot, P. L.; Cowart, M.; Gutzmer, R.; Leurs, R.; Liu, W. L.; Stark, H.; Thurmond, R. L.; Haas, H. L., International union of basic and clinical pharmacology. XCVIII. Histamine receptors. *Pharmacol. Rev.* **2015,** *67*, 601-655.
3. Felixberger, J. Luciferase Complementation for the Determination of Arrestin Recruitment: Investigation of Histamine and NPY receptors. Ph.D. Thesis. University of Regensburg, 2014.
4. Del Valle, J.; Gantz, I., Novel insights into histamine H_2 receptor biology. *Am. J. Physiol.* **1997,** *273*, 987-996.
5. Fernandez, N.; Monczor, F.; Baldi, A.; Davio, C.; Shayo, C., Histamine H_2 receptor trafficking: role of arrestin, dynamin, and clathrin in histamine H_2 receptor internalization. *Mol. Pharmacol.* **2008,** *74*, 1109-1118.
6. Plank, N. Dimeric Histamine H_2 Receptor Agonists as Molecular Tools and Genetically Engineered HEK293T Cells as an Assay Platform to Unravel Signaling Pathways of hH_1R and hH_2R. Ph. D. Thesis. University of Regensburg, 2015.
7. Tropmann, K.; Höring, C.; Plank, N.; Pockes, S., Discovery of a G protein biased radioligand for the histamine H_2 receptor with reversible binding properties. *J. Med. Chem.* **2020,** *63*, 13090-13102.
8. Hegyesi, H.; Darvas, Z.; Thurmond, R. L.; Falus, A., (2005) Histamine Receptors and Signaling. In: Damjanovich S. (eds) Biophysical Aspects of Transmembrane Signaling. Springer Series in Biophysics, vol 8. Springer, Berlin, Heidelberg.
9. Kühn, B.; Schmid, A.; Harteneck, C.; Gudermann, T.; Schultz, G., G proteins of the G_q family couple the H_2 histamine receptor to phospholipase C. *Mol. Endocrinol.* **1996,** *10*, 1697-1707.

10. Houston, C.; Wenzel-Seifert, K.; Bürckstümmer, T.; Seifert, R., The human histamine H_2-receptor couples more efficiently to Sf9 insect cell G_s-proteins than to insect cell G_q-proteins: limitations of Sf9 cells for the analysis of receptor/G_q-protein coupling. *J. Neurochem.* **2002,** *80*, 678-696.
11. Okashah, N.; Wan, Q.; Ghosh, S.; Sandhu, M.; Inoue, A.; Vaidehi, N.; Lambert, N. A., Variable G protein determinants of GPCR coupling selectivity. *Proc. Natl. Acad. Sci. U. S. A.* **2019,** *116*, 12054-12059.
12. Seifert, R.; Höer, A.; Schwaner, I.; Buschauer, A., Histamine increases cytosolic Ca^{2+} in HL-60 promyelocytes predominantly via H_2 receptors with an unique agonist/antagonist profile and induces functional differentiation. *Mol. Pharmacol.* **1992,** *42*, 235-241.
13. Wellner-Kienitz, M.-C.; Bender, K.; Meyer, T.; Pott, L., Coupling to G_s and $G_{q/11}$ of histamine H_2 receptors heterologously expressed in adult rat atrial myocytes. *BBA-Mol. Cell Res.* **2003,** *1642*, 67-77.
14. Hill, S. J., Distribution, properties, and functional characteristics of three classes of histamine receptor. *Pharmacol. Rev.* **1990,** *42*, 45-83.
15. Leopoldt, D.; Harteneck, C.; Nürnberg, B., G proteins endogenously expressed in Sf9 cells: interactions with mammalian histamine receptors. *Naunyn-Schmiedeberg's Arch. Pharmacol.* **1997,** *356*, 216-224.
16. Rodriguez-Pena, M. S.; Timmerman, H.; Leurs, R., Modulation of histamine H_2 receptor signalling by G-protein-coupled receptor kinase 2 and 3. *Br. J. Pharmacol.* **2000,** *131*, 1707-1715.
17. Fukushima, Y.; Asano, T.; Takata, K.; Funaki, M.; Ogihara, T.; Anai, M.; Tsukuda, K.; Saitoh, T.; Katagiri, H.; Aiharai, M.; Matsuhashi, N.; Oka, Y.; Yazaki, Y.; Sugano, K., Role of the C terminus in histamine H_2 receptor signaling, desensitization, and agonist-induced internalization. *J. Biol. Chem.* **1997,** *272*, 19464-19470.
18. Shayo, C.; Fernandez, N.; Legnazzi, B. L.; Monczor, F.; Mladovan, A.; Baldi, A.; Davio, C., Histamine H_2 receptor desensitization: involvement of a select array of G protein-coupled receptor kinases. *Mol. Pharmacol.* **2001,** *60*, 1049-1056.
19. Prost, A.; Emami, S.; Gespach, C., Desensitization by histamine of H_2 receptor-mediated adenylate cyclase activation in the human gastric cancer cell line HGT-1. *FEBS Lett.* **1984,** *177*, 227-230.
20. Emami, S.; Gespach, C., Desensitization by histamine of H_2 receptor activity in HGT-1 human cancerous gastric cells. *Agents Actions* **1986,** *18*, 129-133.
21. Schreurs, J.; Dailey, M. O.; Schulman, H., Pharmacological characterization of histamine H_2 receptors on clonal cytolytic T lymphocytes: Evidence for histamine-induced desensitization. *Biochem. Pharmacol.* **1984,** *33*, 3375-3382.
22. Smit, M. J.; Leurs, R.; Shukrula, S. R.; Bast, A.; Timmerman, H., Rapid desensitization of the histamine H_2 receptor on the human monocytic cell line U937. *Eur. J. Pharmacol.* **1994,** *288*, 17-25.
23. Fukushima, Y.; Oka, Y.; Katagiri, H.; Saitoh, T.; Asano, T.; Ishihara, H.; Matsuhashi, N.; Kodama, T.; Yazaki, Y.; Sugano, K., Desensitization of canine histamine H_2 receptor expressed in Chinese hamster ovary cells. *Biochem. Biophys. Res. Commun.* **1993,** *190*, 1149-1155.
24. Smit, M. J.; Timmerman, H.; Alewijnse, A. E.; Punin, M.; van den Nieuwenhof, I.; Blauw, J.; van Minnen, J.; Leurs, R., Visualization of agonist-induced internalization of histamine H_2 receptors. *Biochem. Biophys. Res. Commun.* **1995,** *214*, 1138-1145.
25. Claing, A.; Perry, S. J.; Achiriloaie, M.; Walker, J. K.; Albanesi, J. P.; Lefkowitz, R. J.; Premont, R. T., Multiple endocytic pathways of G protein-coupled receptors delineated by GIT1 sensitivity. *Proc. Natl. Acad. Sci. U. S. A.* **2000,** *97*, 1119-1124.

26. Xu, A.-J.; Kuramasu, A.; Maeda, K.; Kinoshita, K.; Takayanagi, S.; Fukushima, Y.; Watanabe, T.; Yanagisawa, T.; Sukegawa, J.; Yanai, K., Agonist-induced internalization of histamine H_2 receptor and activiation of extracellular signal-regulated kinases are dynamin-dependent. *J. Neurochem.* **2008,** *107*, 208-217.
27. Claing, A.; Perry, S. J.; Achiriloaie, M.; Walker, J. K.; Albanesi, J. P.; Lefkowitz, R. J.; Premont, R. T., Multiple endocytic pathways of G protein-coupled receptors delineated by GIT1 sensitivity. *Proc. Natl. Acad. Sci. U.S.A.* **2000,** *97*, 1119-1124.
28. Daly, C. J.; McGrath, J. C., Fluorescent ligands, antibodies, and proteins for the study of receptors. *Pharmacol. Ther.* **2003,** *100*, 101-118.
29. Ciruela, F.; Jacobson, K. A.; Fernandez-Duenas, V., Portraying G protein-coupled receptors with fluorescent ligands *ASC Chem. Biol.* **2014,** *9*, 1918-1928.
30. Stoddart, L. A.; Kilpatrick, L. E.; Briddon, S. J.; Hill, S. J., Probing the pharmacology of G protein-coupled receptors with fluorescent ligands. *Neuropharmacology* **2015,** *98*, 48-57.
31. Sridharan, R.; Zuber, J.; Connelly, S. M.; Mathew, E.; Dumont, M. E., Fluorescent approaches for understanding interactions of ligands with G protein coupled receptors. *Biochim. Biophys. Acta Biomembr.* **2014,** *1838*, 15-33.
32. Soave, M.; Briddon, S. J.; Hill, S. J.; Stoddart, L. A., Fluorescent ligands: bringing light to emerging GPCR paradigms. *Br. J. Pharmacol.* **2020,** *177*, 978-991.
33. Stoddart, L. A.; Vernall, A. J.; Briddon, S. J.; Kellam, B.; Hill, S. J., Direct visualisation of internalization of the adenosine A_3 receptor and localization with arrestin3 using a fluorescent agonist. *Neuropharmacology* **2015,** *98*, 68-77.
34. Erdmann, D. Histamine H_2 and H_3 - Receptor Antagonists Synthesis and Characterization of Radiolabelled and Fluorescent Pharmacological Tools. Ph. D. Thesis. University of Regensburg, 2010.
35. Xie, S.-X.; Petrache, G.; Scheiner, E.; Ye, Q.-Z.; Bernhardt, G.; Seifert, R.; Buschauer, A., Synthesis and pharmacological characterization of novel fluorescent histamine H_2-receptor ligands derived from aminopotentidine. *Bioorg. Med. Chem. Lett.* **2006,** *16*, 3886-3890.
36. Li, L.; Kracht, J.; Peng, S.; Bernhardt, G.; Elz, S.; Buschauer, A., Synthesis and pharmacological activity of fluorescent histamine H_2 receptor antagonists related to potentidine. *Bioorg. Med. Chem. Lett.* **2003,** *13*, 1717-1720.
37. Biselli, S.; Alencastre, I.; Tropmann, K.; Erdmann, D.; Chen, M.; Littmann, T.; Maia, A. F.; Gomez-Lazaro, M.; Tanaka, M.; Ozawa, T.; Keller, M.; Lamghari, M.; Buschauer, A.; Bernhardt, G., Fluorescent H_2 receptor squaramide-type antagonists: synthesis, characterization and applications. *ACS Med. Chem. Lett.* **2020,** *11*, 1521-1528.
38. Grätz, L.; Tropmann, K.; Bresinsky, M.; Müller, C.; Bernhardt, G.; Pockes, S., NanoBRET binding assay for histamine H_2 receptor ligands using live recombinant HEK293T cells. *Sci. Rep.* **2020,** *10, e13288*.
39. Hill, S. J.; Kellam, B.; Briddon, S. J. Fluorescence-based high content screening of compounds for functional response or pharmacological properties. WO 2006/032926, Mar 30, 2006; *Chem. Abstr.* **2006**, *144*, 343538, 2006.
40. Kagermeier, N.; Werner, K.; Keller, M.; Baumeister, P.; Bernhardt, G.; Seifert, R.; Buschauer, A., Dimeric carbamoylguanidine-type histamine H_2 receptor ligands: a new class of potent and selective agonists. *Bioorg. Med. Chem.* **2015,** *23*, 3957-3969.
41. Baker, J. G.; Middleton, R.; Adams, L.; May, L. T.; Briddon, S. J.; Kellam, B.; Hill, S. J., Influence of fluorophore and linker composition on the pharmacology of fluorescent adenosine A1 receptor ligands. *Br. J. Pharmacol.* **2010,** *159*, 772-786.
42. Biselli, S. Synthesis and Pharmacological Characterization of Subtype-Selective Ligands, Including Radio- and Fluorescence Labeled Ligands, for the Histamine H_2 Receptor. Ph.D. Thesis. University of Regensburg, 2020.

43. Tropmann, K.; Forster, L.; Bresinsky, M.; Buschauer, A.; Wittmann, H.-J.; Pockes, S; Strasser, A., Abolishing dopamine D_{2long}/D_3 receptor affinity of subtype-selective carbamoylguanidine-type histamine H_2 receptor agonists. *J. Med. Chem., submitted for publication* **2020**.
44. Höfelschweiger, B. K. The Pyrylium Dyes: A New Class of Biolabels. Synthesis, Spectroscopy, and Application as Labels and in General Protein Assay. Ph.D. Thesis. University Regensburg, 2005.
45. Bartole, E.; Grätz, L.; Littmann, T.; Wifling, D.; Seibel, U.; Buschauer, A.; Bernhardt, G., UR-DEBa242: A Py-5-Labeled Fluorescent Multipurpose Probe for Investigations on the Histamine H_3 and H_4 Receptors. *J. Med. Chem.* **2020,** *63*, 5297-5311.
46. Nienhaus, G. U.; Nienhaus, K., (2017) Fluorescence Labeling. In: Kubitscheck, U. (eds) Fluorescence microscopy: from principles to biological applications, 2nd Edition; Wiley-VCH: Weinheim, Germany.
47. Keller, M.; Mahuroof, S. A.; Hong Yee, V.; Carpenter, J.; Schindler, L.; Littmann, T.; Pegoli, A.; Hübner, H.; Bernhardt, G.; Gmeiner, P.; Holliday, N. D., Fluorescence labeling of neurotensin(8–13) via arginine residues gives molecular tools with high receptor affinity. *ACS Med. Chem. Lett.* **2020,** *11*, 16-22.
48. Kraus, A.; Ghorai, P.; Birnkammer, T.; Schnell, D.; Elz, S.; Seifert, R.; Dove, S.; Bernhardt, G.; Buschauer, A., N^G-Acylated aminothiazolylpropylguanidines as potent and selective histamine H_2 receptor agonists. *ChemMedChem* **2009,** *4*, 232-240.
49. Birnkammer, T.; Spickenreither, A.; Brunskole, I.; Lopuch, M.; Kagermeier, N.; Bernhardt, G.; Dove, S.; Seifert, R.; Elz, S.; Buschauer, A., The bivalent ligand approach leads to highly potent and selective acylguanidine-type histamine H_2 receptor agonists. *J. Med. Chem.* **2012,** *55*, 1147-1160.
50. Pockes, S.; Wifling, D.; Keller, M.; Buschauer, A.; Elz, S., Highly potent, stable, and selective dimeric hetarylpropylguanidine-type histamine H_2 receptor agonists. *ACS Omega* **2018,** *3*, 2865-2882.
51. Biselli, S.; Bresinsky, M.; Tropmann, K.; Forster, L.; Honisch, C.; Buschauer, A.; Bernhardt, G.; Pockes, S., Pharmacological characterization of a new series of carbamoylguanidines reveals potent agonism at the H_2R and D_3R. *Eur. J. Med. Chem.* **2021,** *214*, 113190.
52. Pertz, H. H.; Görnemann, T.; Schurad, B.; Seifert, R.; Straßer, A., Striking differences of action of lisuride stereoisomers at histamine H_1 receptors. *N.-S. Arch. Pharmacol.* **2006,** *374*, 215-222.
53. Baumeister, P.; Erdmann, D.; Biselli, S.; Kagermeier, N.; Elz, S.; Bernhardt, G.; Buschauer, A., [^{3}H]UR-DE257: development of a tritium-labeled squaramide-type selective histamine H_2 receptor antagonist. *ChemMedChem* **2015,** *10*, 83-93.
54. Igel, P.; Schnell, D.; Bernhardt, G.; Seifert, R.; Buschauer, A., Tritium-labeled N^1-[3-(1H-imidazol-4-yl)propyl]-N^2-propionylguanidine ([^{3}H]UR-PI294), a high-affinity histamine H_3 and H_4 receptor radioligand. *ChemMedChem* **2009,** *4*, 225-231.
55. Bartole, E.; Littmann, T.; Tanaka, M.; Ozawa, T.; Buschauer, A.; Bernhardt, G., [^{3}H]UR-DEBa176: a 2,4-diaminopyrimidine-type radioligand enabling binding studies at the human, mouse, and rat histamine H_4 receptors. *J. Med. Chem.* **2019,** *62*, 8338-8356.
56. Kelley, M. T.; Bürckstürmmer, T.; Wenzel-Seifert, K.; Dove, S.; Buschauer, A.; Seifert, R., Distinct interaction of human and guinea pig histamine H_2-receptor with guanidine-type agonists. *Mol. Pharmacol.* **2001,** *60*, 1210-1225.
57. Höring, C.; Seibel, U.; Tropmann, K.; Grätz, L.; Mönnich, D.; Pitzl, S.; Bernhardt, G.; Pockes, S.; Strasser, A., A dynamic, split-luciferase-based mini-G protein sensor to functionally characterize ligands at all four histamine receptor subtypes. *Int. J. Mol. Sci.* **2020,** *21, 8440*.

58. In the [^{35}S]GTPγS binding assay GTPγS labelled with ^{35}S is used. The half-life of this sulfur isotope is 87.37 d, so that the reagent can only be used for a limited time. Therefore, several batches have to be ordered in the course of a project. At the beginning of the project, our supplier still delivered the reagent in good quality, so we were able to perform this assay without any problems. However, the batches ordered towards the end of the project were of inadequate quality (was self-tested in our radiology lab with inadequate purity results). Since we did not find an alternative supplier with sufficient reagent quality, we could not perform this assay anymore. Thus, not all compounds could be characterized in the [^{35}S]GTPγS assay. All data given in the manuscript are comparable and have been performed with [^{35}S]GTPγS batches of high quality.
59. Rankovic, Z.; Brust, T. F.; Bohn, L. M., Biased agonism: An emerging paradigm in GPCR drug discovery. *Bioorg. Med. Chem. Lett.* **2016,** *26*, 241-250.
60. Thomsen, A. R. B.; Hvidtfeldt, M.; Bräuner-Osborne, H., Biased agonism of the calcium-sensing receptor. This model is only valid for ligands which are agonists in both pathways. The model can not be applied to ligands which are e.g. agonists in G protein and antagonists in arrestin pathway. *Cell Calcium* **2012,** *51*, 107-116.
61. Yung-Chi, C.; Prusoff, W. H., Relationship between the inhibition constant (K_i) and the concentration of inhibitor which causes 50 per cent inhibition (I_{50}) of an enzymatic reaction. *Biochem. Pharmacol.* **1973,** *22*, 3099-3108.
62. Leurs, R.; Smit, M. J.; Menge, W. M.; Timmerman, H., Pharmacological characterization of the human histamine H_2 receptor stably expressed in chinese hamster ovary cells. *Br. J. Pharmacol.* **1994,** *112*, 847-854.
63. Mosandl, J. Radiochemical and Luminescence-Based Binding and Functional Assays for Human Histamine Receptors Using Genetically Engineered Cells. Ph.D. Thesis. University of Regensburg, 2009.
64. Baumeister, P. Molecular Tools for G-Protein Coupled Receptors: Synthesis, Pharmacological Characterization and [^{3}H]-Labeling of Subtype-selective Ligands for Histamine H_4 and NPY Y_2 Receptors. Ph. D. Thesis. University of Regensburg, 2014.
65. Fulmer, G. R.; Miller, A. J. M.; Sherden, N. H.; Gottlieb, H. E.; Nudelman, A.; Stoltz, B. M.; Bercaw, J. E.; Goldberg, K. I., NMR chemical shifts of trace impurities: common laboratory solvents, organics, and gases in deuterated solvents relevant to the organometallic chemist. *Organometallics* **2010,** *29*, 2176-2179.
66. Gottlieb, H. E.; Kotlyar, V.; Nudelman, A., NMR chemical shifts of common laboratory solvents as trace impurities. *J. Org. Chem.* **1997,** *62*, 7512-7515.
67. Schnell, D.; Strasser, A.; Seifert, R., Comparison of the pharmacological properties of human and rat histamine H_3-receptors. *Biochem. Pharmacol.* **2010,** *80*, 1437-1449.
68. Schneider, E. H.; Schnell, D.; Papa, D.; Seifert, R., High constitutive activity and a G-protein-independent high-affinity state of the human histamine H_4-receptor. *Biochemistry* **2009,** *48*, 1424-1438.
69. Pop, N.; Igel, P.; Brennauer, A.; Cabrele, C.; Bernhardt, G.; Seifert, R.; Buschauer, A., Functional reconstitution of human neuropeptide Y (NPY) Y_2 and Y_4 receptors in Sf9 insect cells. *J. Recept. Signal Transduct.* **2011,** *31*, 271-285.
70. Schneider, E.; Mayer, M.; Ziemek, R.; Li, L.; Hutzler, C.; Bernhardt, G.; Buschauer, A., A simple and powerful flow cytometric method for the simultaneous determination of multiple parameters at G protein-coupled receptor subtypes. *ChemBioChem* **2006,** *7*, 1400-1409.
71. Rueden, C. T.; Schindelin, J.; Hiner, M. C.; DeZonia, B. E.; Walter, A. E.; Arena, E. T.; Eliceiri, K. W., ImageJ2: ImageJ for the next generation of scientific image data. *BMC Bioinform.* **2017,** *18*, 529.

Appendix 2 Synthesis and Pharmacological Characterization of Fluorescent Histamine H_2 Receptor Carbamoylguanidine-Type Agonists

App2.1 Experimental Details for 3.23-3.27

The precursors **3.23**-**3.25**[1] and **3.27**[2], the amine **3.41**[3], the guanidinylating reagent **3.42**[1] as well as the tetrafluoroborate salt of Py-5[4-5] were synthesized as reported elsewhere (structures are shown in Figure App2.1).

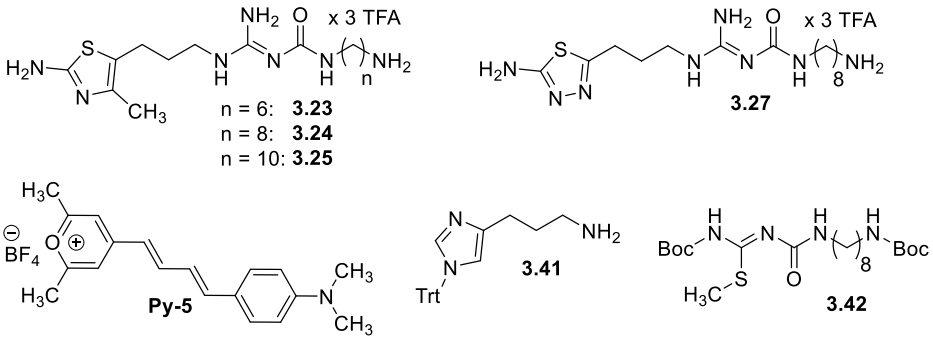

Figure App2.1. Chemical structures of the amine precursors **3.23**-**3.25** and **3.27**, the amine **3.41**, the guanidinylating reagent **3.42** as well as the tetrafluoroborate salt of Py-5.

Synthesis of the Amine Precursor 3.26

The precursor **3.26** was prepared in analogy to the described procedure for **3.23**-**3.25**[1] and **3.27**[2] by treating **3.41**[3] with the guanidinylating reagent **3.42**[1] in the presence of mercuric chloride ($HgCl_2$) and triethylamine (NEt_3). Treating the protected carbamoylguanidine-type intermediate **3.43** with trifluoracetic acid (TFA) gave compound **3.26** (Scheme App2.1), which was purified by preparative HPLC.

Scheme App2.1. Synthesis of the Precursor 3.26[a]

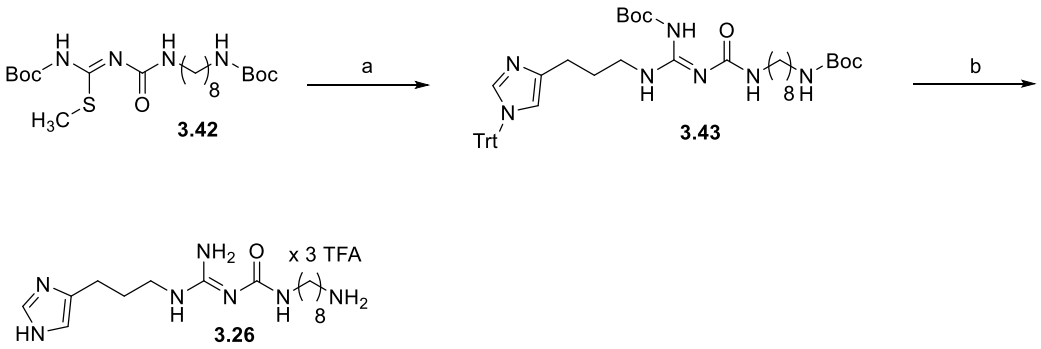

[a]Reagents and conditions: (a) **3.41**, $HgCl_2$, NEt_3, CH_2Cl_2, 16 h, room temperature (rt); (b) 40% TFA, CH_2Cl_2, 16 h, rt, 20% over 2 steps.

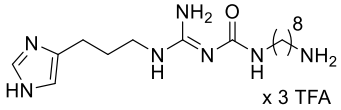

1-(Amino{[3-(1*H*-imidazol-4-yl)propyl]amino}dmethylene)-3-(8-aminooctyl)urea trihydrotrifluoroacetate (3.26). The guanidinylating reagent **3.42** (70 mg, 0.15 mmol, 1 equiv) and the amine **3.41** (84 mg, 0.23 mmol, 1.5 equiv) were dissolved in CH_2Cl_2 (3 mL). NEt_3 (105 µL, 0.76 mmol, 2.5 equiv) and $HgCl_2$ (165 mg, 0.608 mmol, 4 equiv) were added to the mixture and stirring was continued for 16 h. The reaction mixture was diluted with CH_2Cl_2 (10 mL). The precipitate was removed by filtration through Celite 545 and washed with CH_2Cl_2 (20 mL) and EtOAc (20 mL). The solvent was removed under reduced pressure and the crude product was purified by flash chromatography on silica gel (eluent PE (A), EtOAc (B); gradient: 0-20 min: A/B 100:0-50:50) and dried under reduced pressure. Subsequently, deprotection was performed by stirring with 40% TFA in CH_2Cl_2 for 16 h. The obtained carbamoylguanidine-type precursor **3.42** was purified by preparative HPLC yielding a white, foamlike and hydroscopic solid (20.67 mg, 20%). RP-HPLC: 99% (t_R = 7.3 min, k = 1.27). ^{1}H-NMR (300 MHz, MeOD) δ 8.79 (d, J = 1.4 Hz, 1H), 7.36 (d, J = 1.2 Hz, 1H), 3.36 (t, J = 6.9 Hz, 2H), 3.19 (t, J = 7.0 Hz, 2H), 2.95-2.76 (m, 4H), 2.10-1.93 (m, 2H), 1.77-1.43 (m, 4H), 1.42-1.30 (m, 8H). ^{1}H-NMR (600 MHz, DMSO-d_6) δ 14.45 (br s, 2H), 10.68 (br s, 1H), 9.09 (br s, 1H), 8.94 (d, J = 1.4 Hz, 1H), 8.55 (br s, 2H), 7.80 (br s, 3H), 7.53 (br s, 1H), 7.46-7.33 (m, 1H), 3.29 (q, J = 6.6 Hz, 2H), 3.09 (q, J = 6.6 Hz, 2H), 2.81-2.72 (m, 2H), 2.68 (t, J = 7.6 Hz, 2H), 1.86 (quint, J = 7.3 Hz, 2H), 1.51 (quint, J = 7.4 Hz, 2H), 1.42 (q, J = 6.8 Hz, 2H), 1.32-1.23 (m, 8H). ^{13}C-NMR (151 MHz, DMSO-d_6) δ 158.81 (q, J = 31.7 Hz, TFA), 153.91, 153.75, 133.92, 132.49, 116.96 (q, J = 299.1 Hz, TFA), 115.71, 39.92, 39.14, 38.79, 28.90, 28.46,

28.44, 26.97, 26.76, 26.10, 25.73, 21.13. HRMS: calcd. for $C_{16}H_{32}N_7O^+$: 338.2663; found: 338.2662. MF: $C_{16}H_{31}N_7O$ x $C_6H_3F_9O_6$. MW: (337.47 + 342.07).

App2.2 ^{1}H- and/or ^{13}C-NMR Spectra of 3.26 and 3.28-3.40

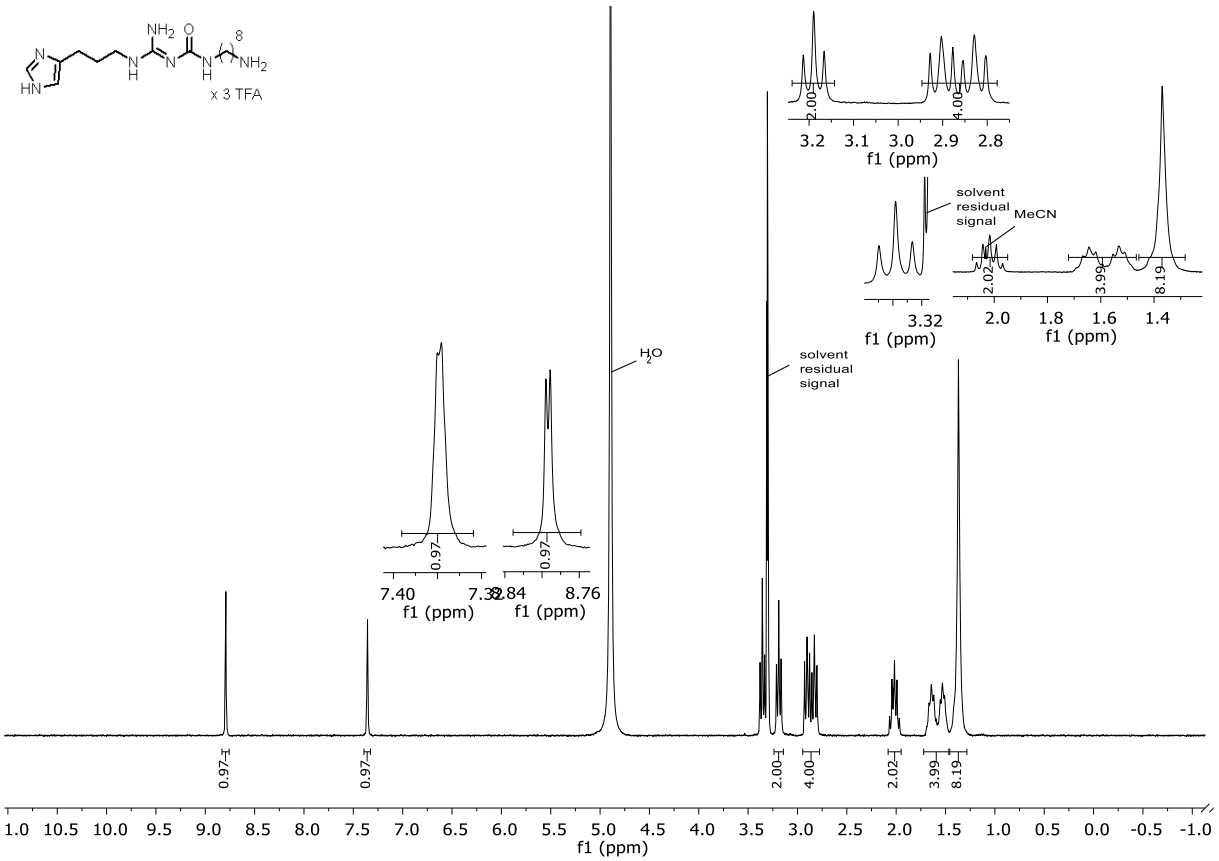

Figure App2.2. ^{1}H-NMR spectrum (400 MHz, MeOD) of compound **3.26**.

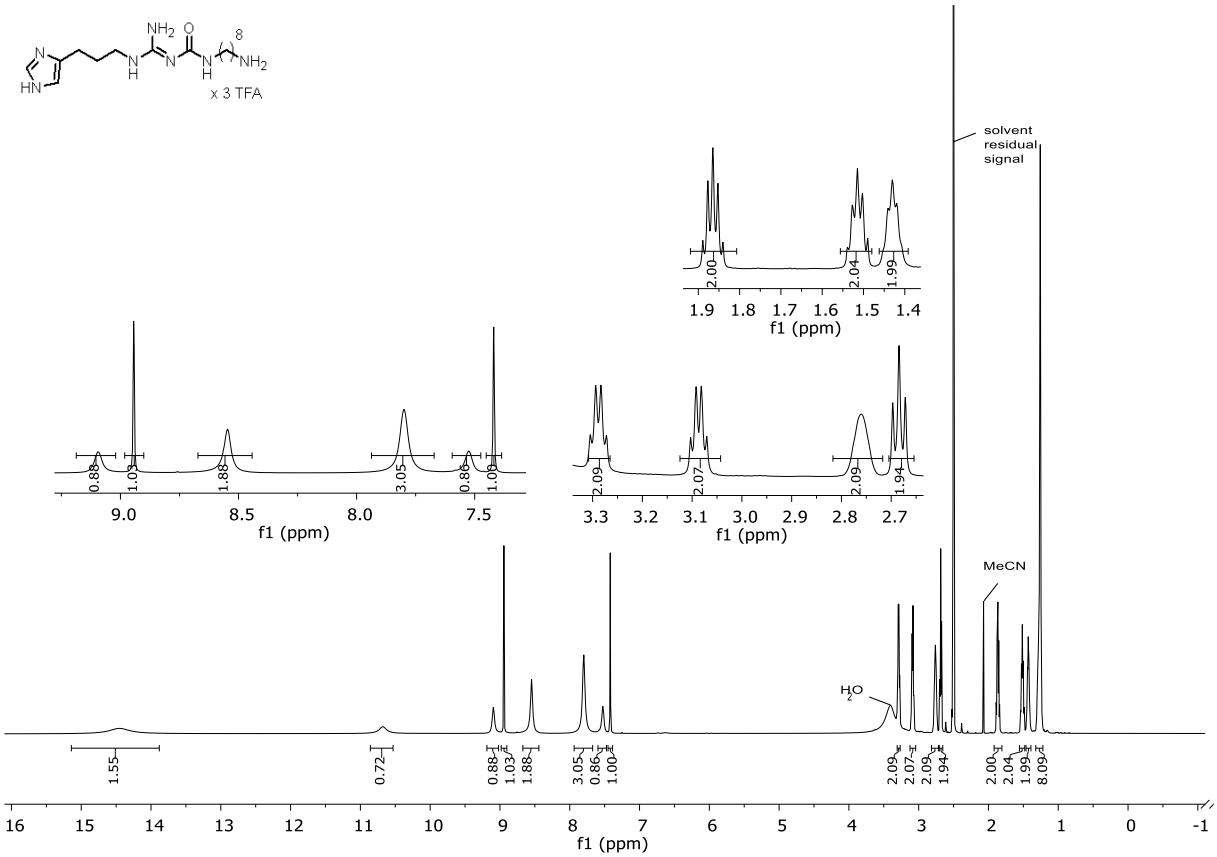

Figure App2.3. ^{1}H-NMR spectrum (600 MHz, DMSO-d_6) of compound **3.26**.

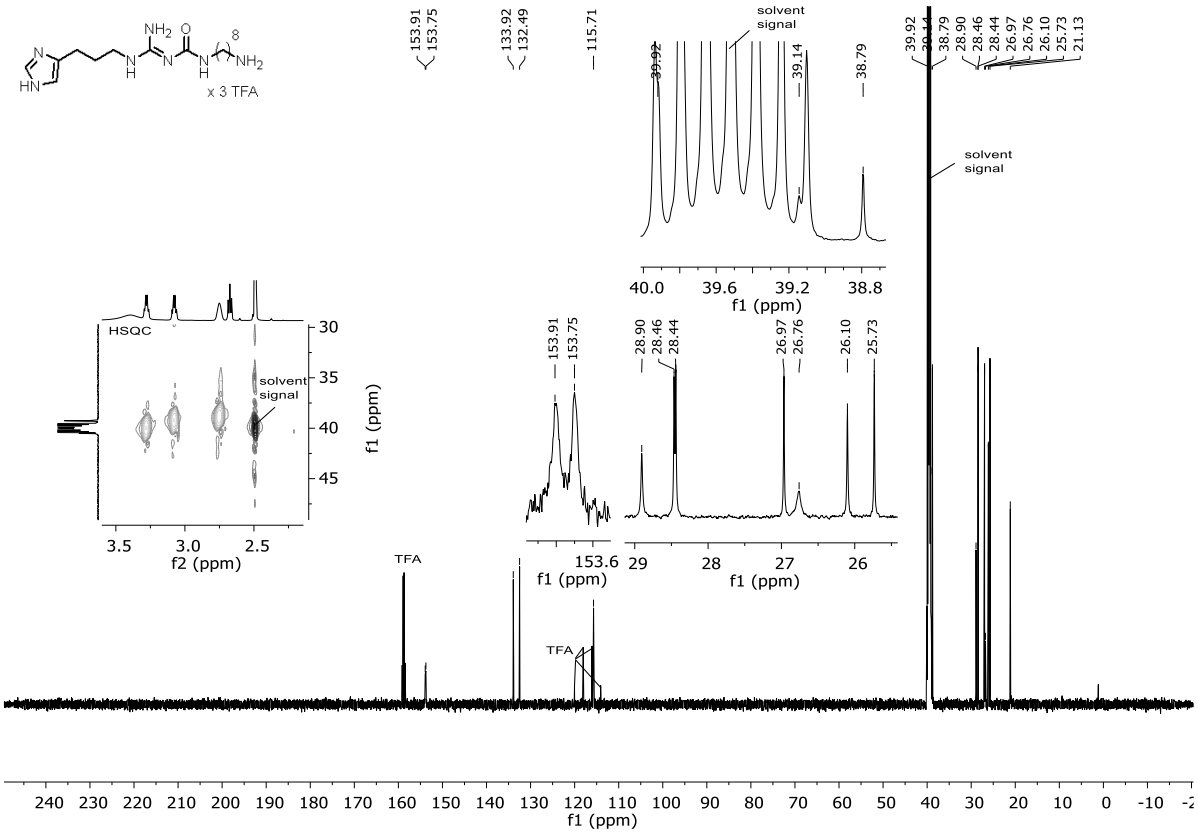

Figure App2.4. ^{13}C-NMR spectrum (600 MHz, DMSO-d_6) of compound **3.26**.

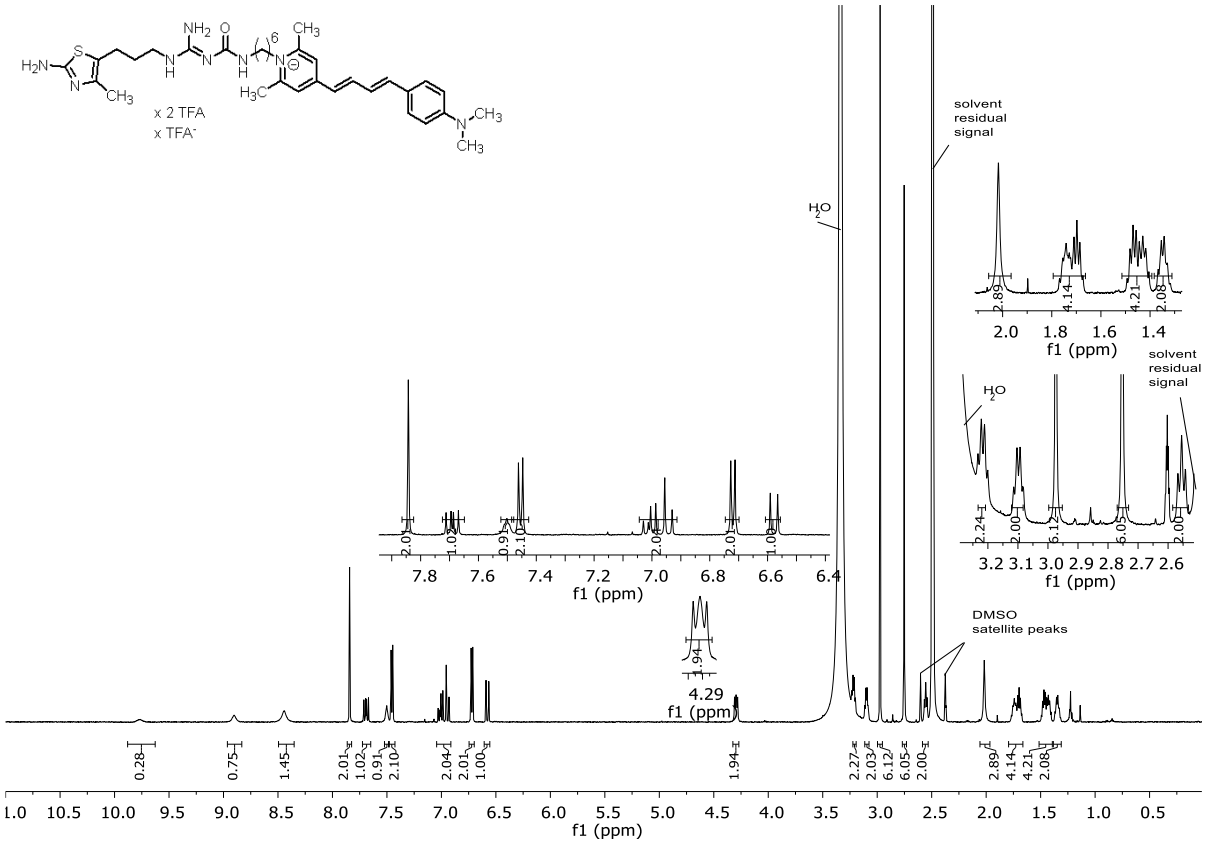

Figure App2.5. ^{1}H-NMR spectrum (600 MHz, DMSO-d_6) of compound **3.28**.

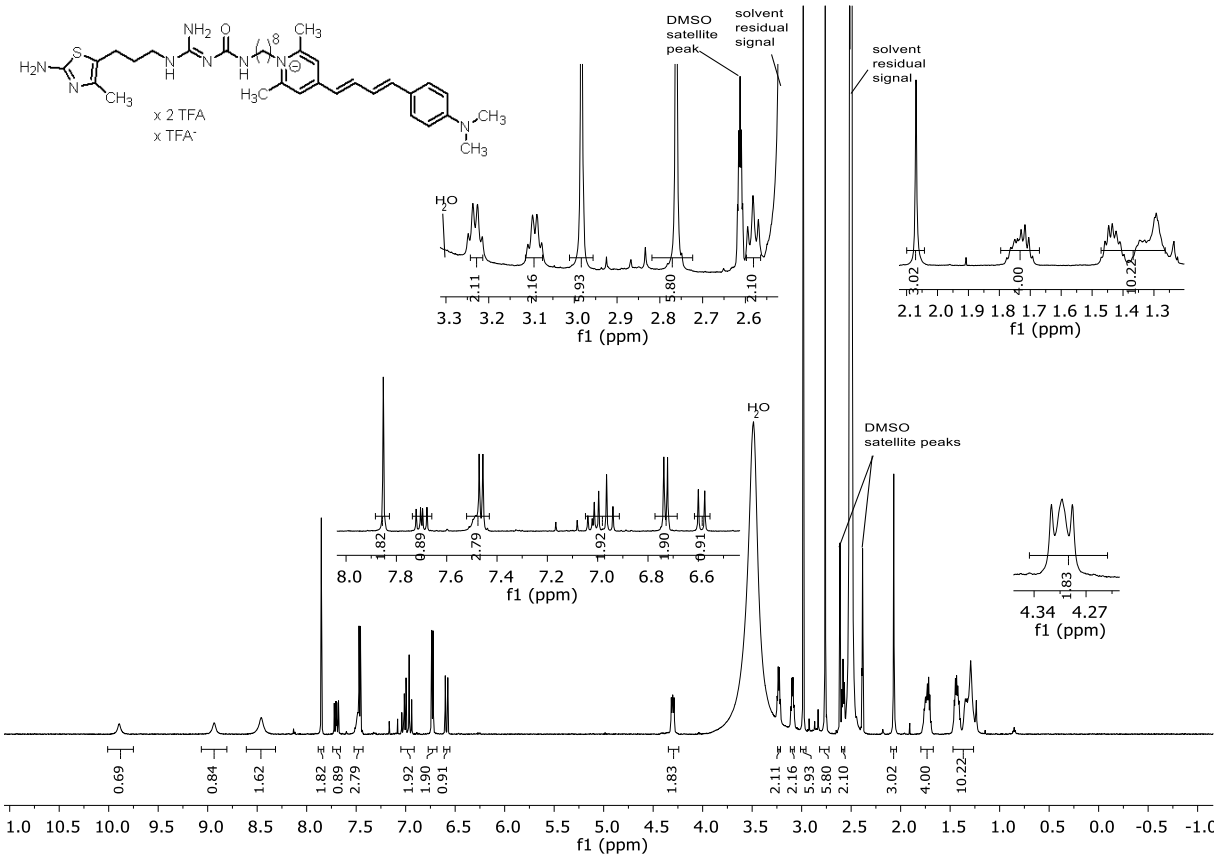

Figure App2.6. ^{1}H-NMR spectrum (600 MHz, DMSO-d_6) of compound **3.29**.

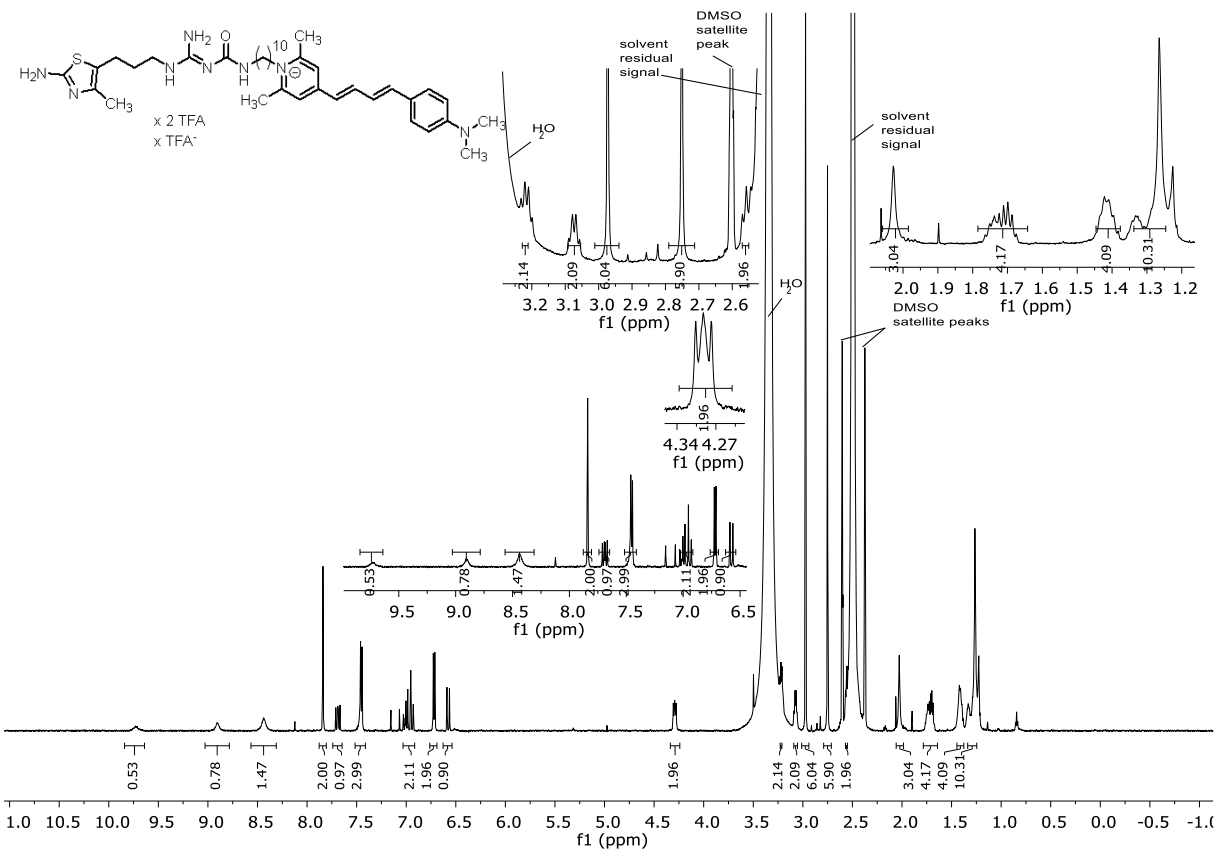

Figure App2.7. ^{1}H-NMR spectrum (600 MHz, DMSO-d_6) of compound **3.30**.

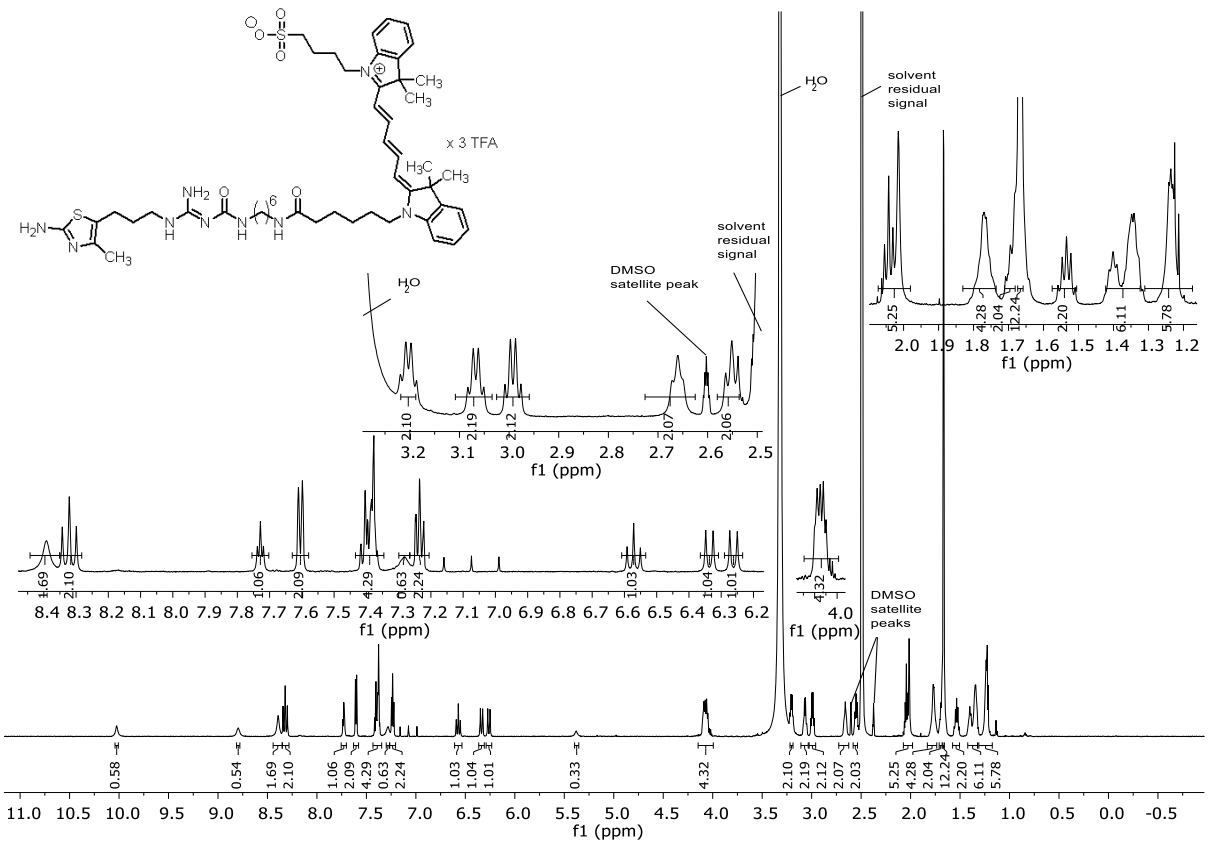

Figure App2.8. ^{1}H-NMR spectrum (600 MHz, DMSO-d_6) of compound **3.31**.

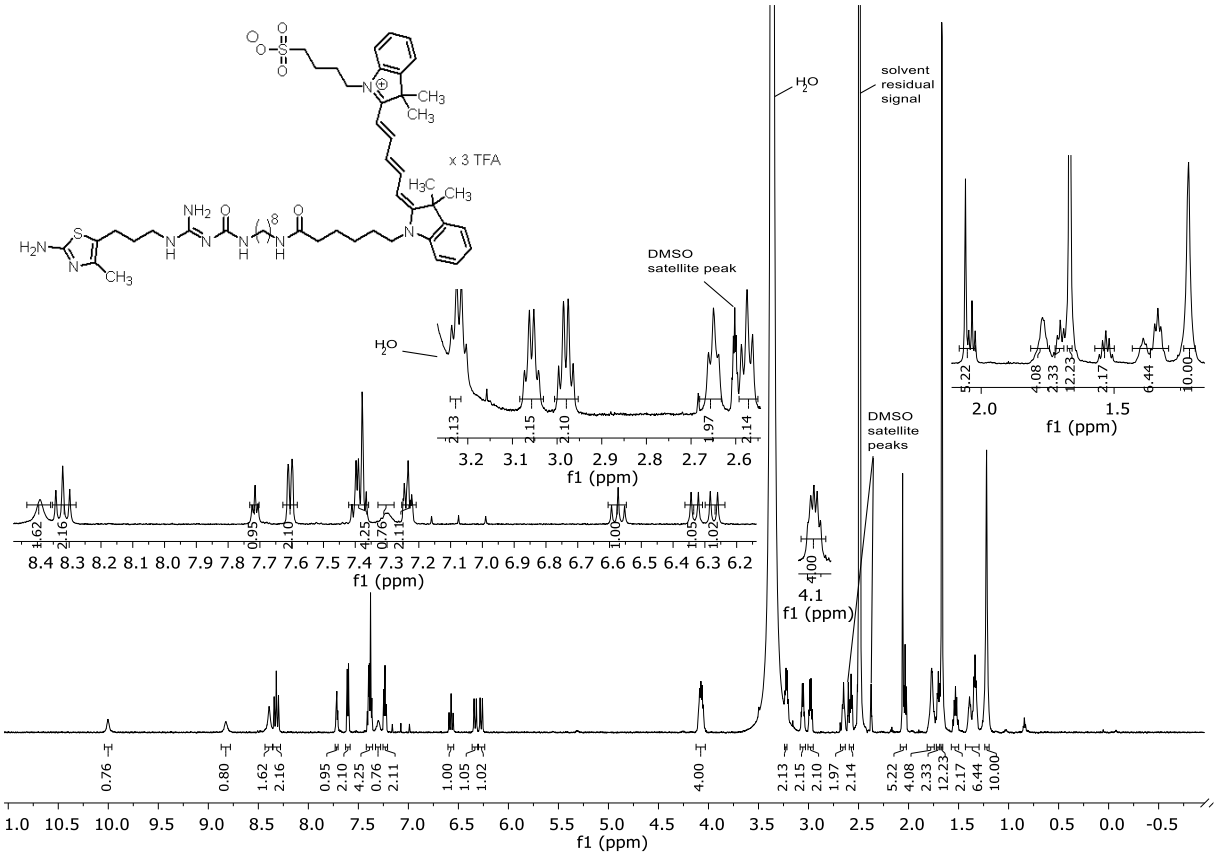

Figure App2.9. ^{1}H-NMR spectrum (600 MHz, DMSO-d_6) of compound **3.32**.

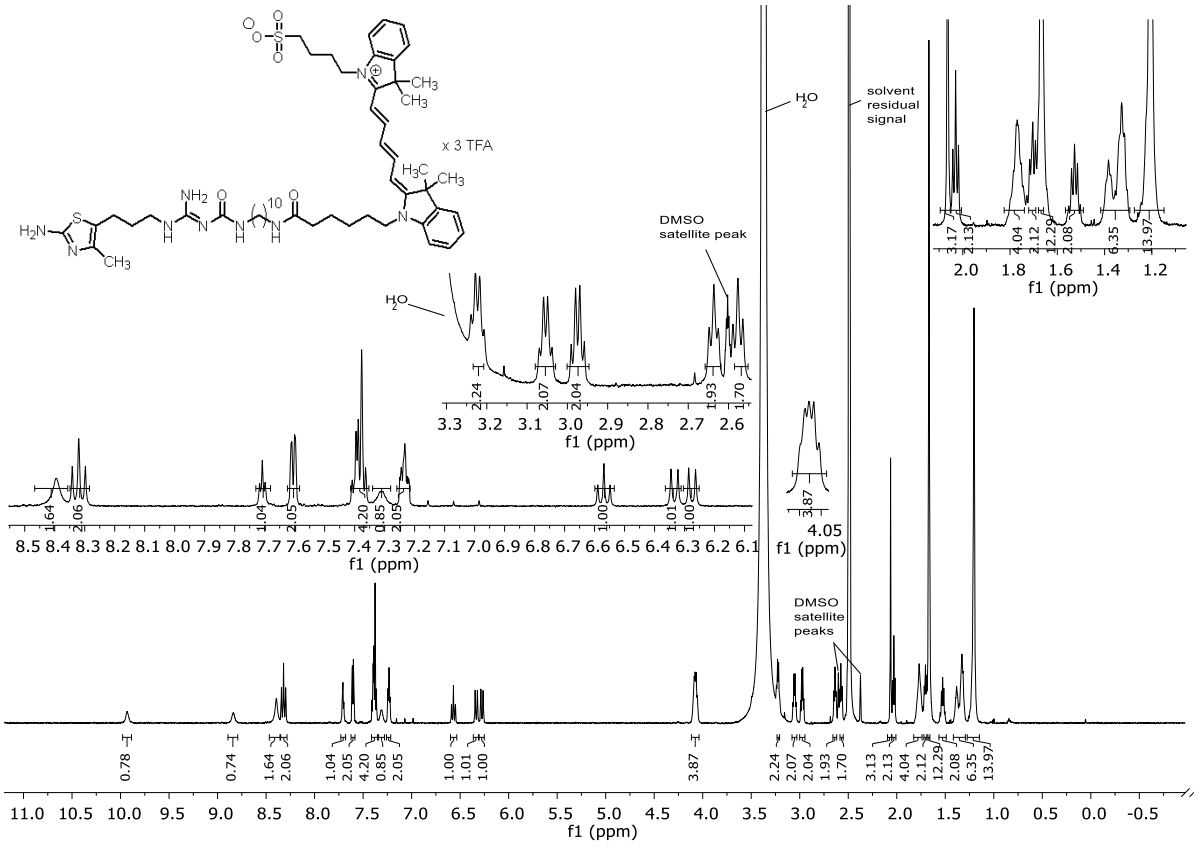

Figure App2.10. ^{1}H-NMR spectrum (600 MHz, DMSO-d_6) of compound **3.33**.

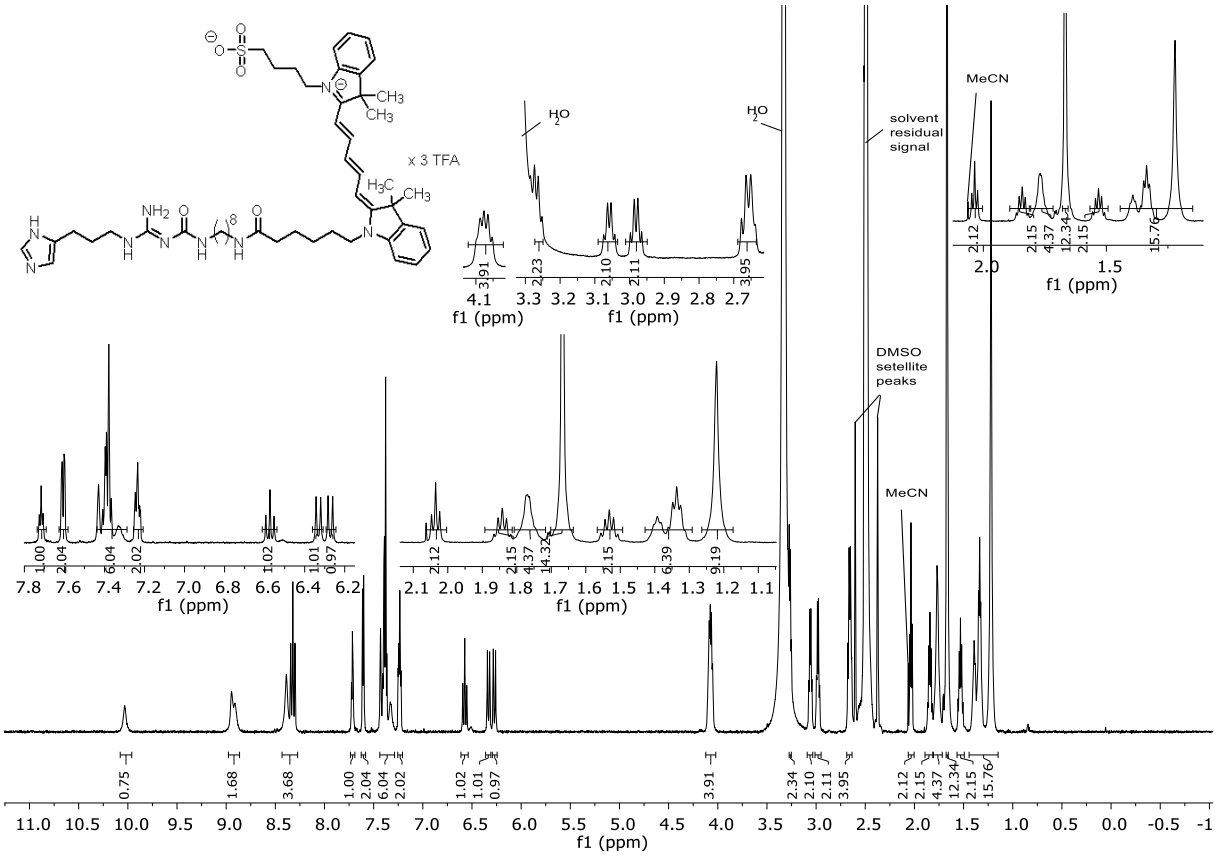

Figure App2.11. ^{1}H-NMR spectrum (600 MHz, DMSO-d_6) of compound **3.34**.

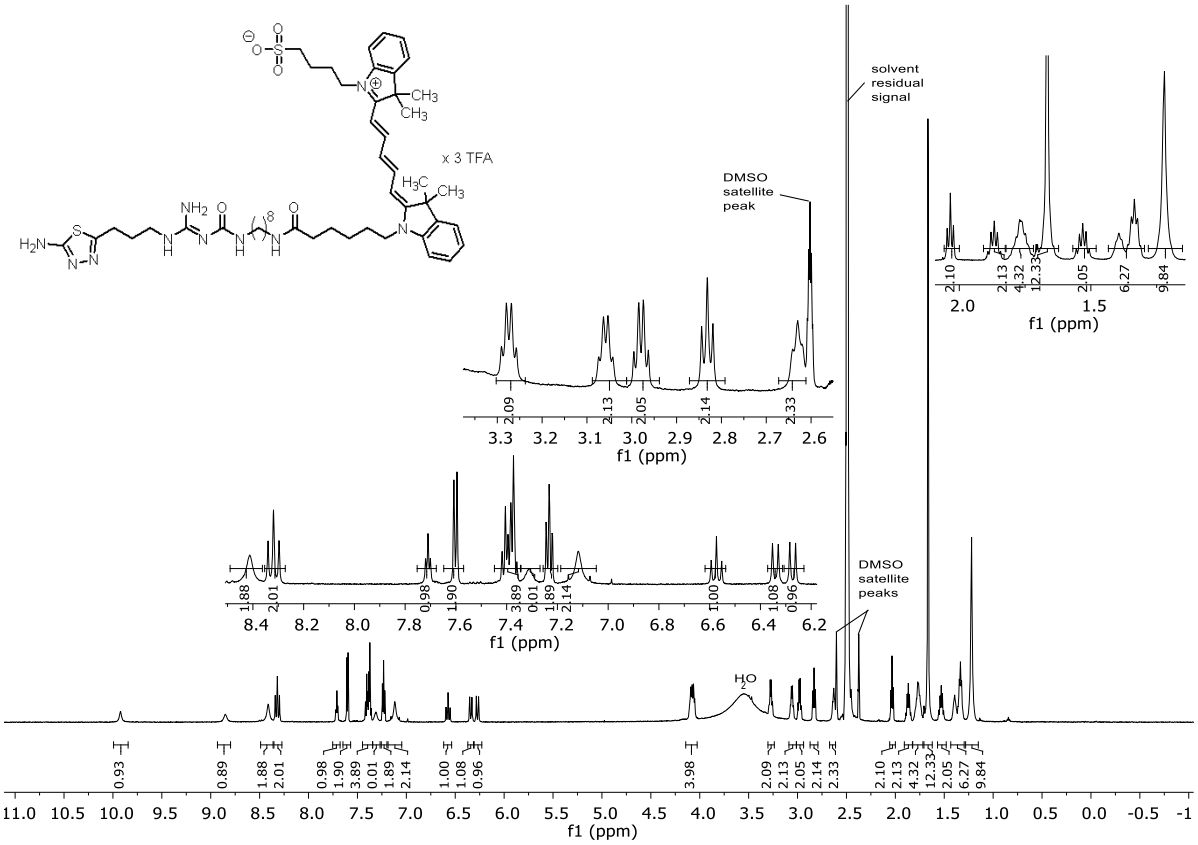

Figure App2.12. ^{1}H-NMR spectrum (600 MHz, DMSO-d_6) of compound **3.35**.

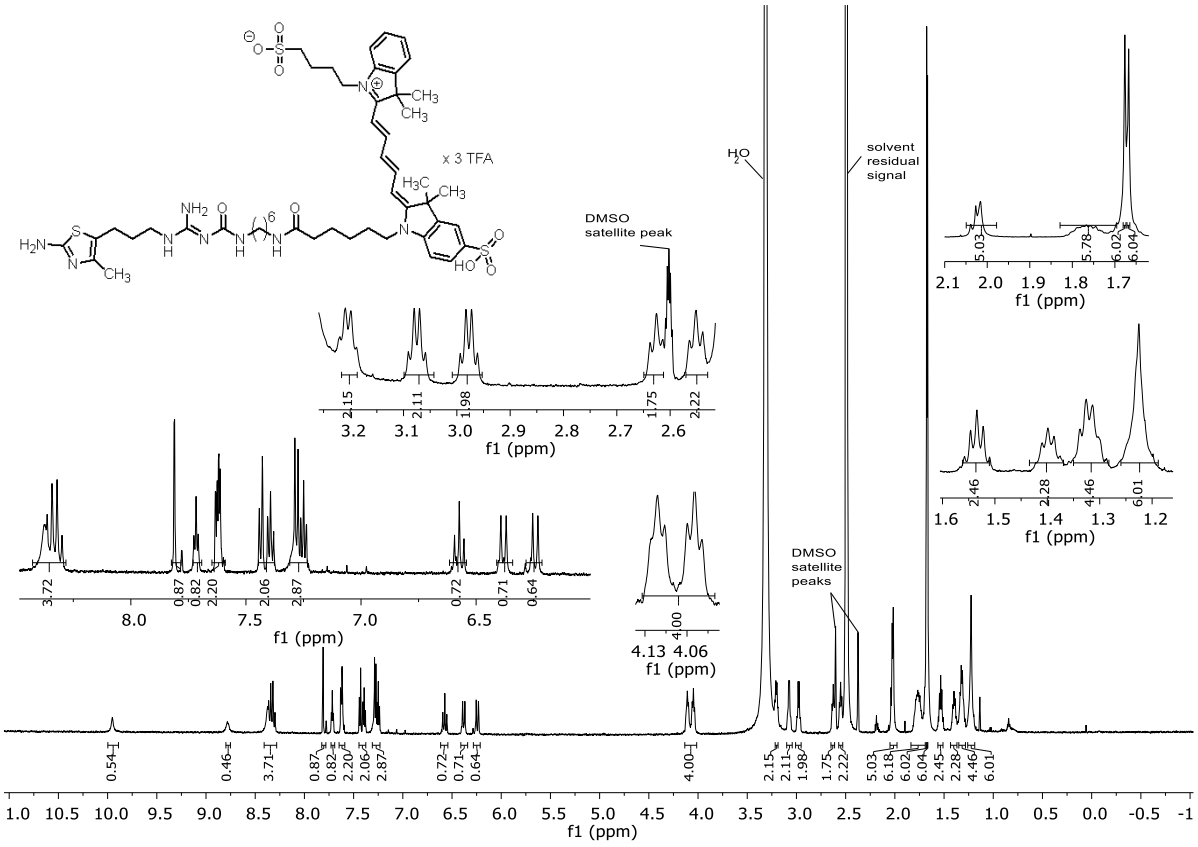

Figure App2.13. ^{1}H-NMR spectrum (600 MHz, DMSO-d_6) of compound **3.36**.

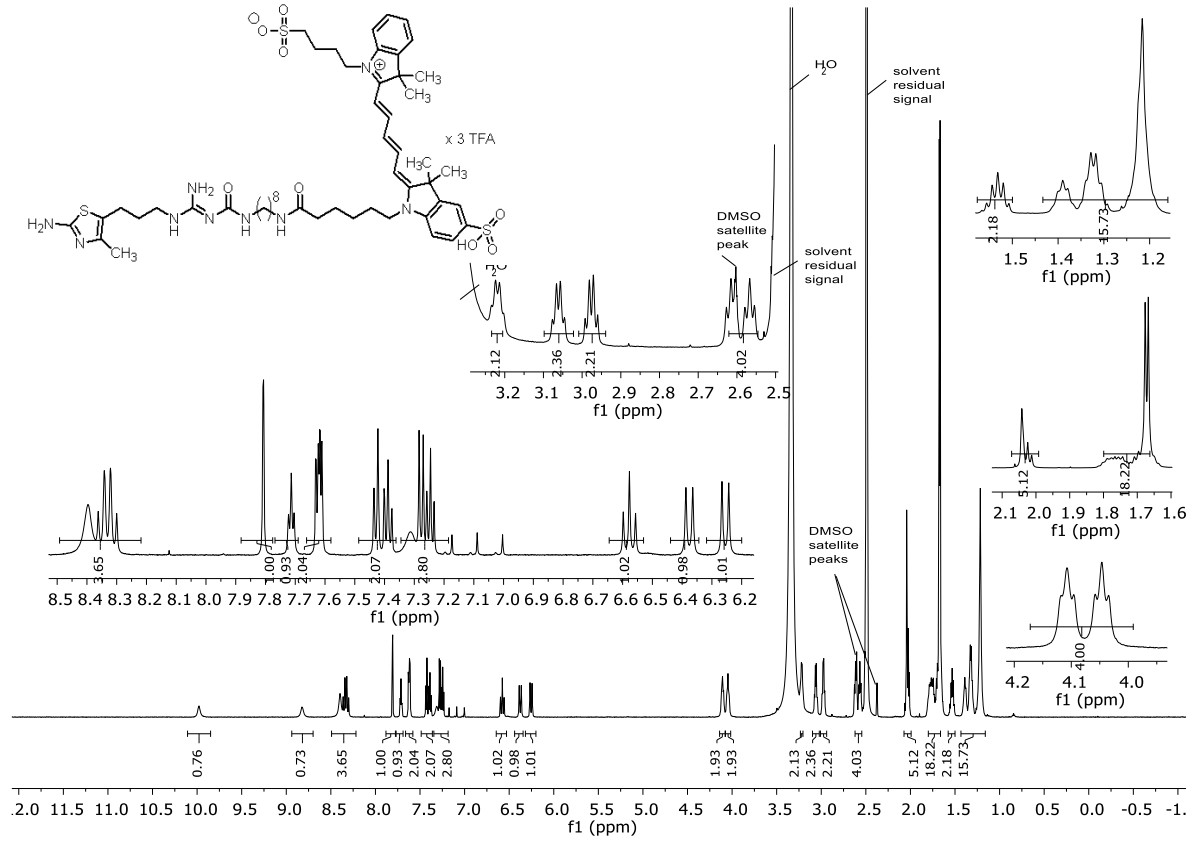

Figure App2.14. ^{1}H-NMR spectrum (600 MHz, DMSO-d_6) of compound **3.37**.

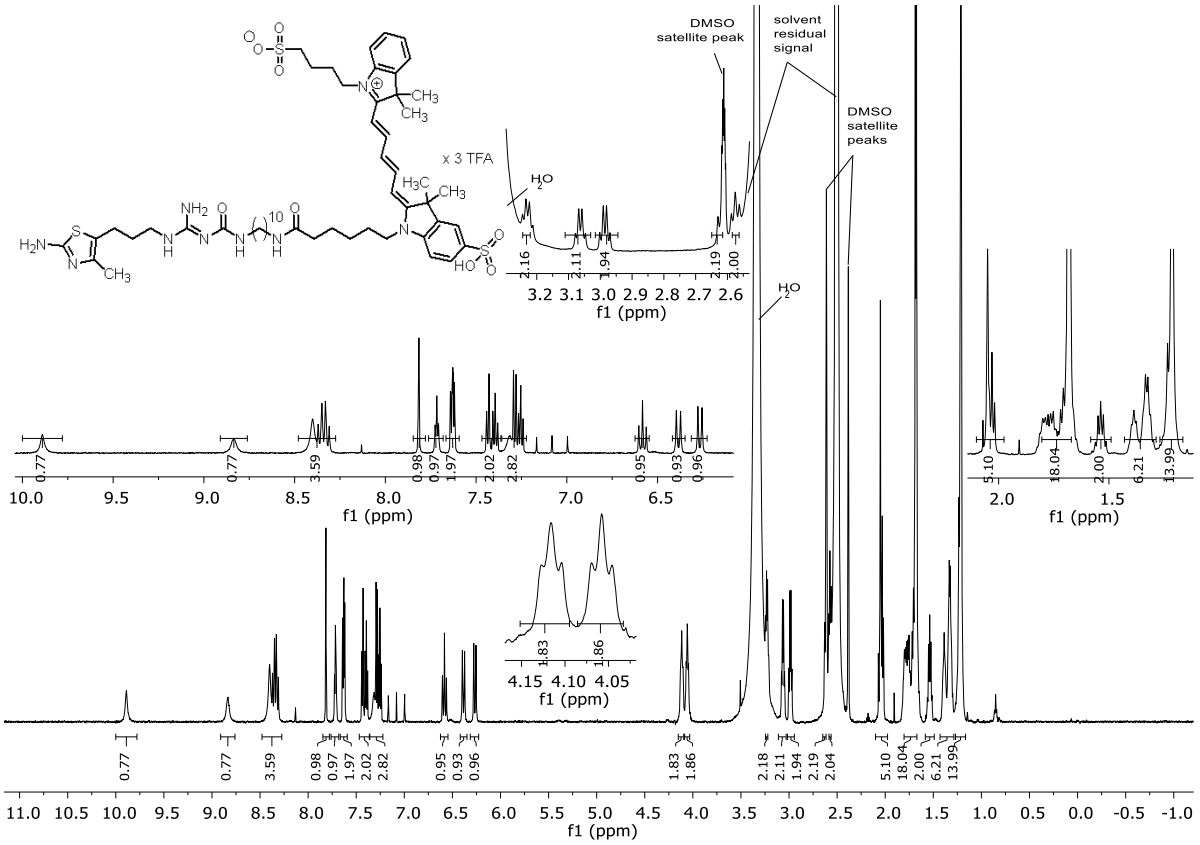

Figure App2.15. ^{1}H-NMR spectrum (600 MHz, DMSO-d_6) of compound **3.38**.

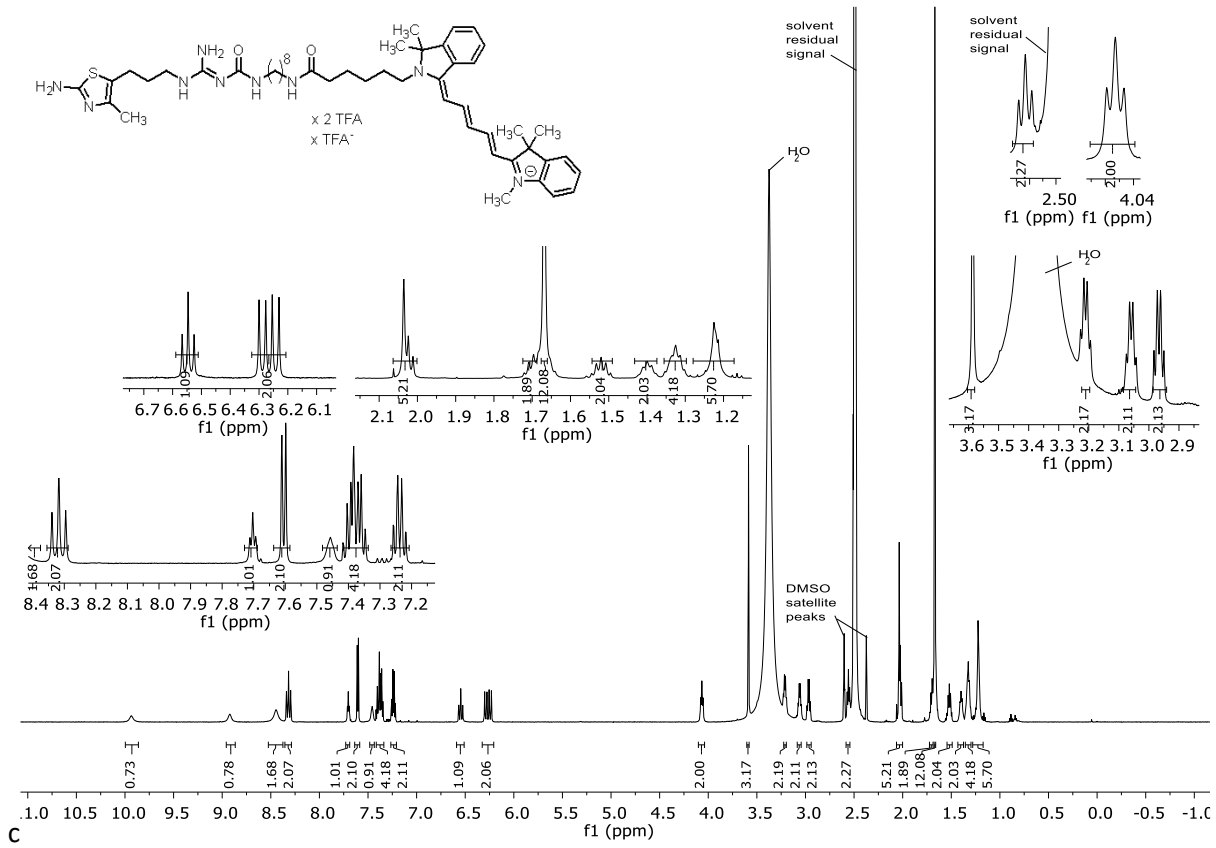

Figure App2.16. ^{1}H-NMR spectrum (600 MHz, DMSO-d_6) of compound **3.39**.

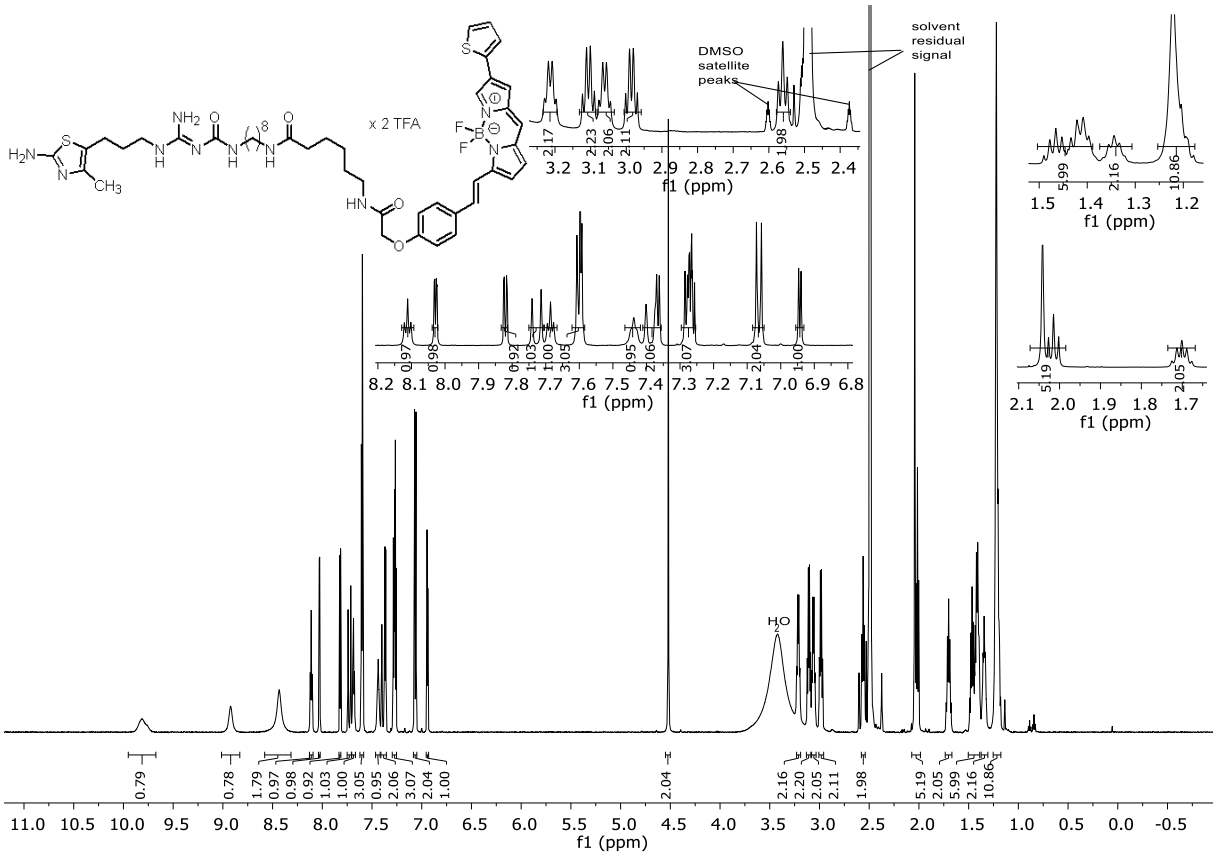

Figure App2.17. ^{1}H-NMR spectrum (600 MHz, DMSO-d_6) of compound **3.40**.

App2.3 RP-HPLC Chromatograms of 3.26 and 3.28-3.40

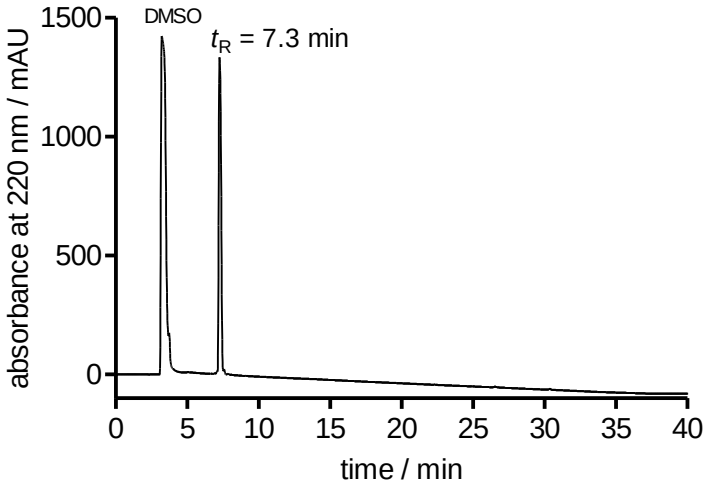

Figure App2.18. RP-HPLC analysis (purity control) of **3.26**.

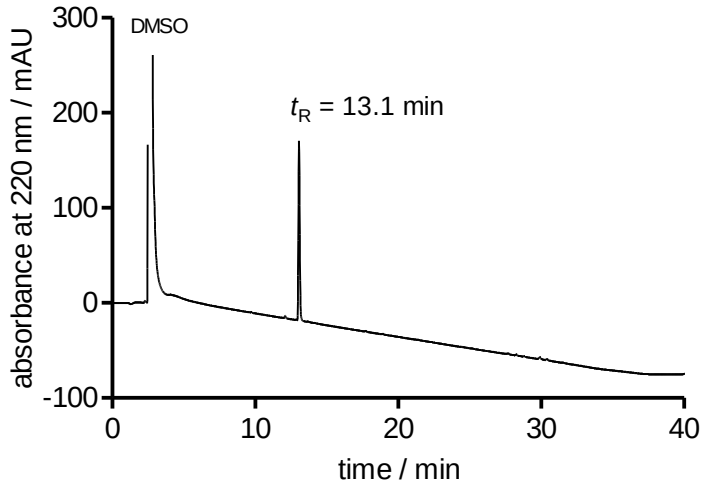

Figure App2.19. RP-HPLC analysis (purity control) of **3.28**.

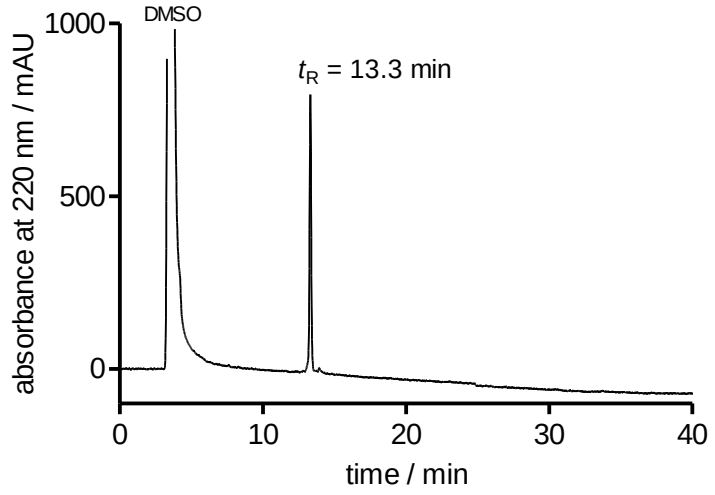

Figure App2.20. RP-HPLC analysis (purity control) of **3.29**.

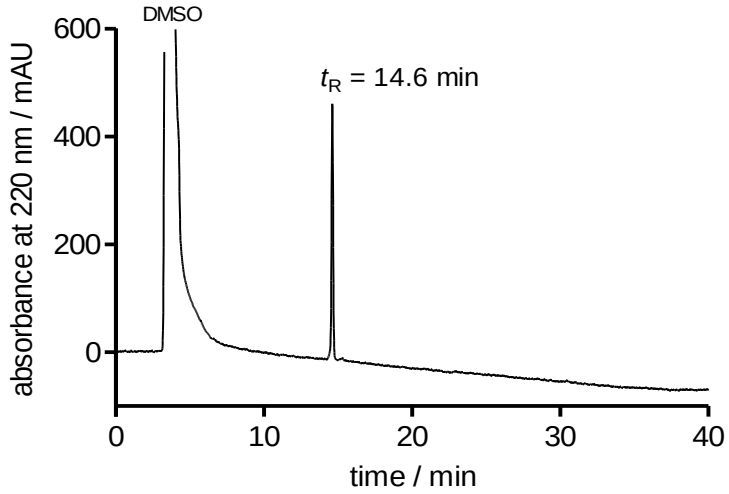

Figure App2.21. RP-HPLC analysis (purity control) of **3.30**.

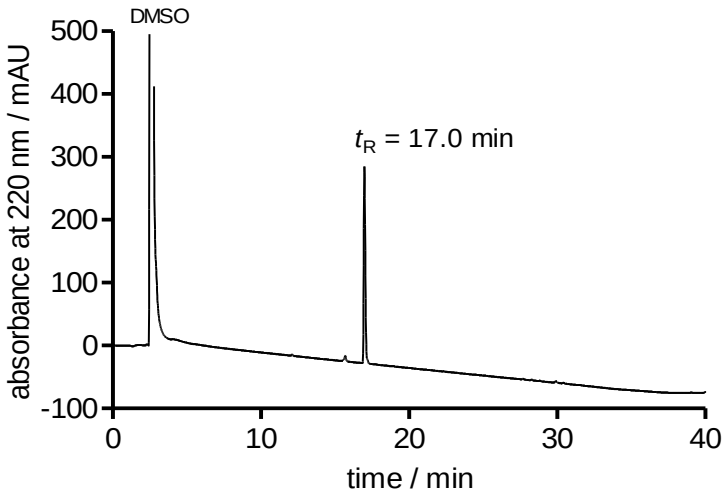

Figure App2.22. RP-HPLC analysis (purity control) of **3.31**.

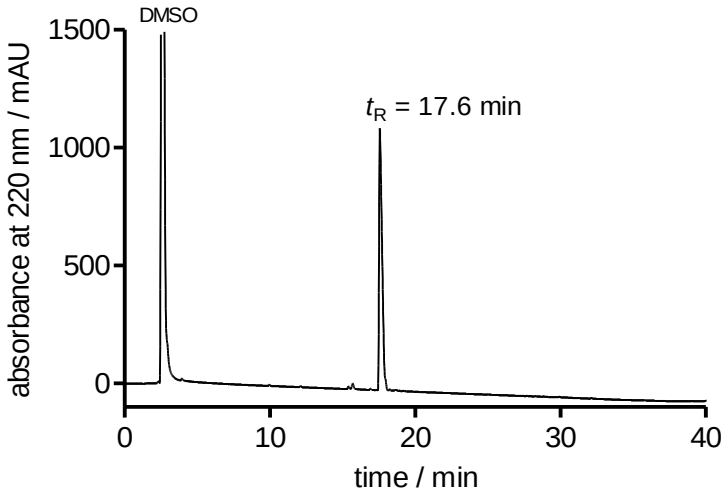

Figure App2.23. RP-HPLC analysis (purity control) of **3.32**.

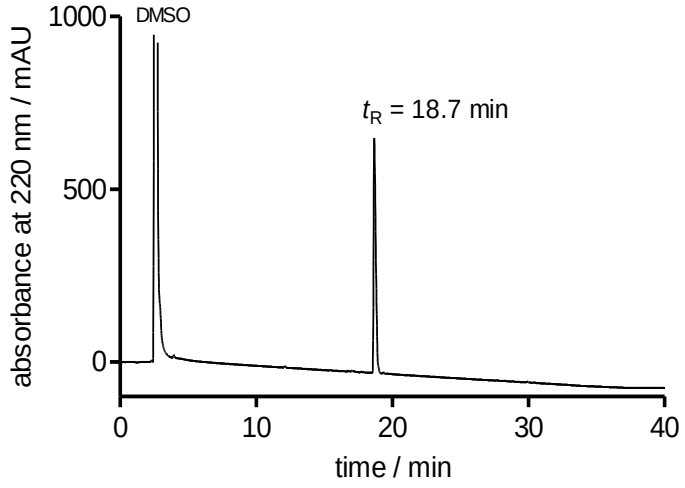

Figure App2.24. RP-HPLC analysis (purity control) of **3.33**.

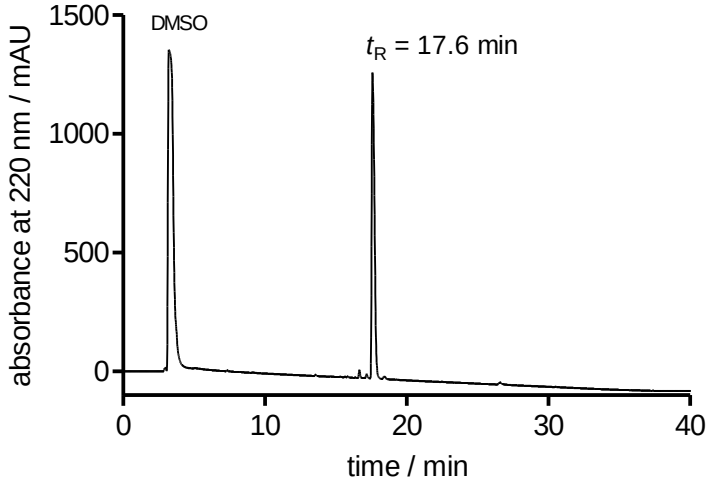

Figure App2.25. RP-HPLC analysis (purity control) of **3.34**.

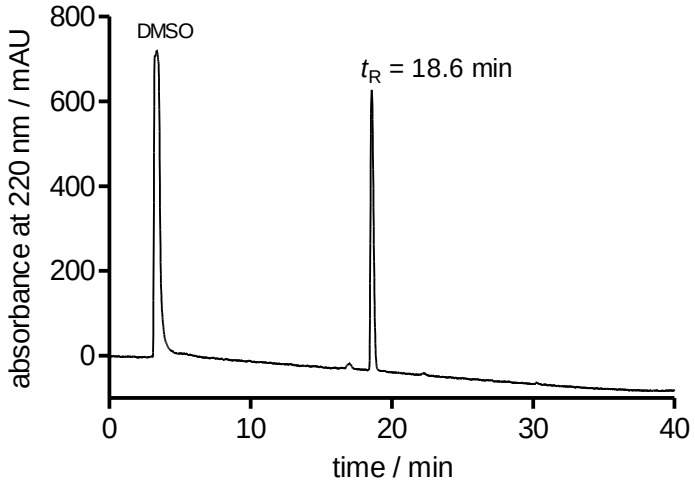

Figure App2.26. RP-HPLC analysis (purity control) of **3.35**.

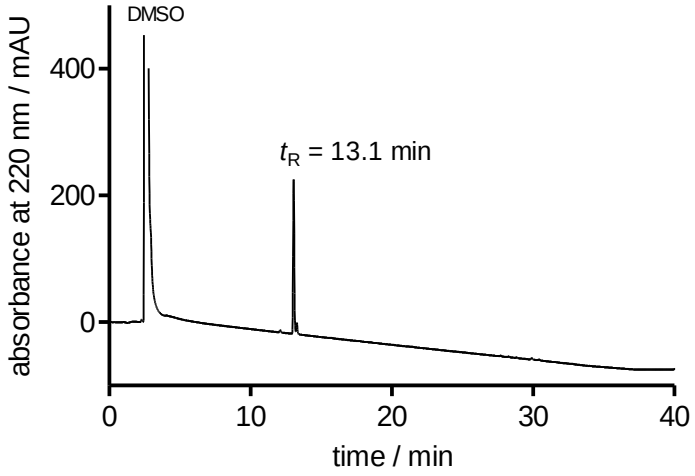

Figure App2.27. RP-HPLC analysis (purity control) of **3.36**.

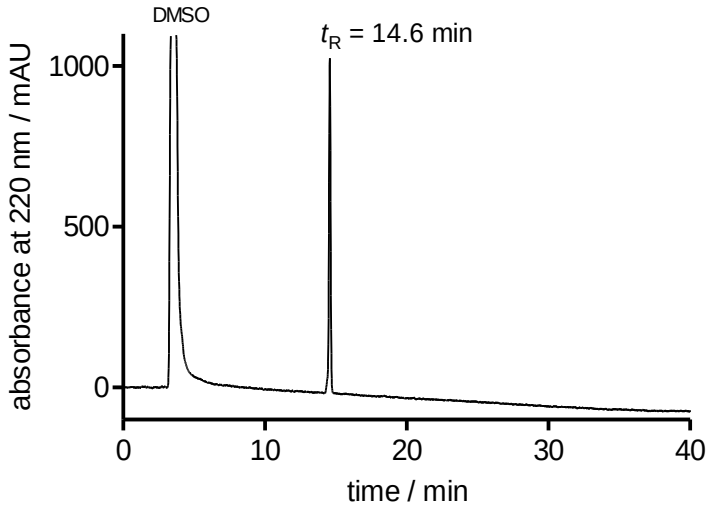

Figure App2.28. RP-HPLC analysis (purity control) of **3.37**.

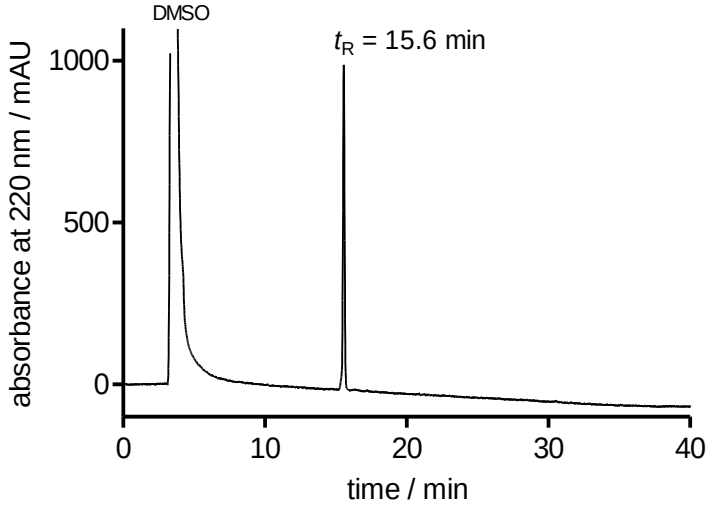

Figure App2.29. RP-HPLC analysis (purity control) of **3.38**.

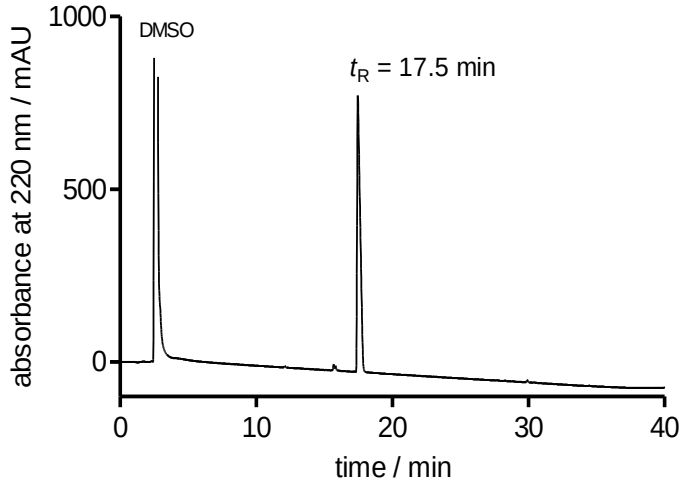

Figure App2.30. RP-HPLC analysis (purity control) of **3.39**.

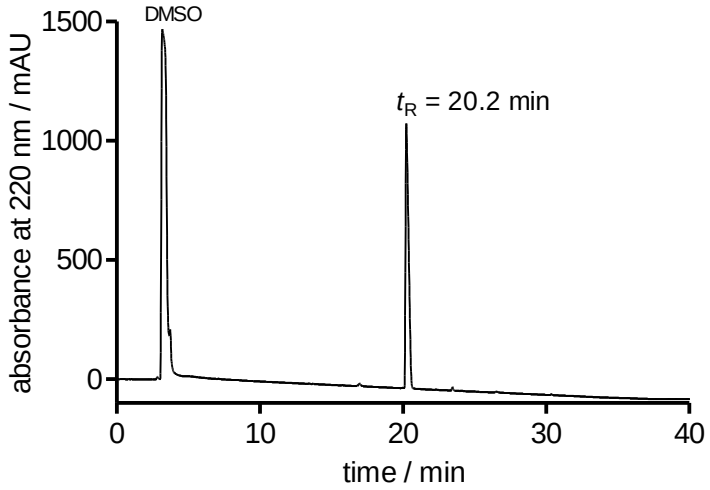

Figure App2.31. RP-HPLC analysis (purity control) of **3.40**.

App2.4 Absorption and Emission Spectra

Recording of absorption and emission spectra was performed with a FluoroMax-4 spectrofluorometer (HORIBA Scintific, Oberursel, Germany) and an Agilent Cary 60 UV-Vis spectrophotometer (Agilent Technologies). The resulting absorption and emission spectra are depicted in Figure App3.32 and the absorption and emission maxima are summarized in Table App2.1. Spectra were recorded in PBS (pH 7.4) and in PBS with 1% bovine serum albumin (BSA, SERVA Electrophoresis, Heidelberg, Germany) to simulate assay conditions and to study the influence of proteins on the fluorescence properties. In addition, the spectra were also recorded in ethanol to examine the influence of the polarity of the solvent. The fluorescent ligands were measured in a concentration range from 4-10 µM. The diluted samples were freshly prepared from 5 mM stock solutions in DMSO before the experiment. Blank spectra (in case of absorption spectra) were recorded with samples containing the respective solvent and the same amount of DMSO as those containing the fluorescent ligands. To avoid bleaching effects, the samples were protected from light between measurements. Recording of the spectra was performed in acryl cuvettes (10 x 10 mm, Sarstedt, Nümbrecht, Germany).

Table App2.1. Spectroscopic Characteristics (Absorption Maxima, λ_{abs} / nm, Emission Maxima, λ_{em} / nm) of Py-5, Py-5_Propyl, S0436, S0287, S0223, BODIPY 630/650-X NHS-Ester, 3.29, 3.32, 3.34-3.35 and 3.38-3.40 in Different Solvents

	EtOH		PBS		PBS + 1% BSA	
compd.	λ_{abs} / nm	λ_{em} / nm	λ_{abs} / nm	λ_{em} / nm	λ_{abs} / nm	λ_{em} / nm
Py-5	645*[4]	732*[4]	n.d.	n.d.	n.d.	n.d.
Py-5_propyl	484*[4]	671*[4]	n.d.	n.d.	n.d.	n.d.
3.29	498	671	431	672	483	622
S0436	644*[a]	666*[a]	n.d.	n.d.	n.d.	n.d.
3.32	648	665	644	661	661	672
3.34	647	666	644	660	657	671
3.35	648	668	644	661	660	671
S0387	646*[a]	669*[a]	n.d.	n.d.	n.d.	n.d.
3.38	650	666	647	661	653	663
S0223	642*[a]	663*[a]	n.d.	n.d.	n.d.	n.d.
3.39	644	662	641	658	657	668
BODIPY 630/650-X NHS Ester	628*[6] 646*[b]	643*[6] 664*[b]	629**[6]	646**[6]	n.d.	n.d.
3.40	628	640	657	644	638	645

[a]Data imported from www.few.de (Oct. 2020). [b]Data imported from www.spectra.arizona.edu (Oct. 2013). Ligand concentrations were 4-10 µM. The corresponding absorption and emission spectra are shown in Figure App2.32. *Measured in MeOH as solvent. **Measured in water as solvent.

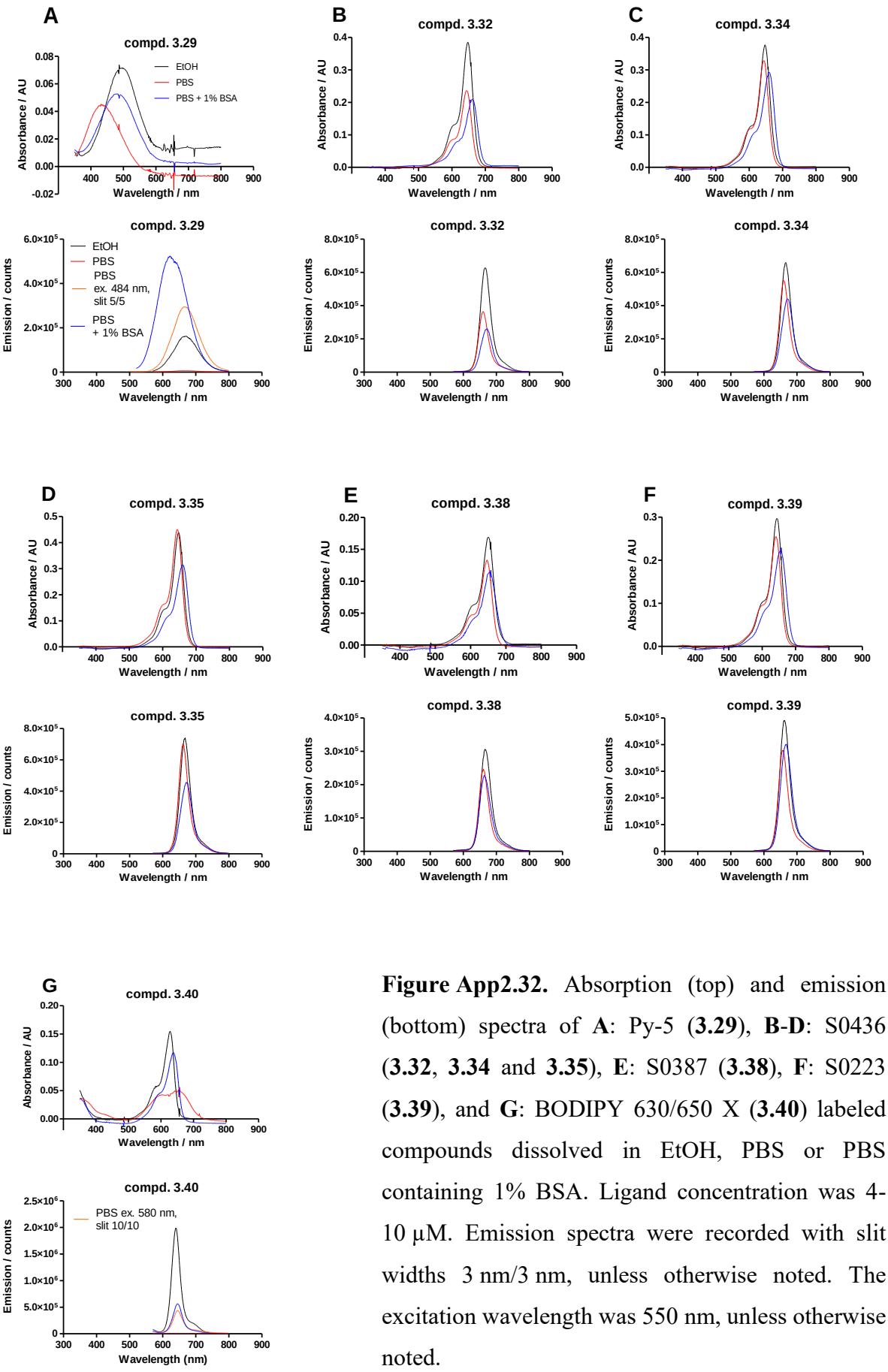

Figure App2.32. Absorption (top) and emission (bottom) spectra of **A**: Py-5 (**3.29**), **B-D**: S0436 (**3.32**, **3.34** and **3.35**), **E**: S0387 (**3.38**), **F**: S0223 (**3.39**), and **G**: BODIPY 630/650 X (**3.40**) labeled compounds dissolved in EtOH, PBS or PBS containing 1% BSA. Ligand concentration was 4-10 μM. Emission spectra were recorded with slit widths 3 nm/3 nm, unless otherwise noted. The excitation wavelength was 550 nm, unless otherwise noted.

App2.5 Saturation Binding Experiments of 3.28-3.31, 3.36-3.37 and 3.40 at HEK293T-hH$_2$R-qs5 Cells Studied by Flow Cytometry

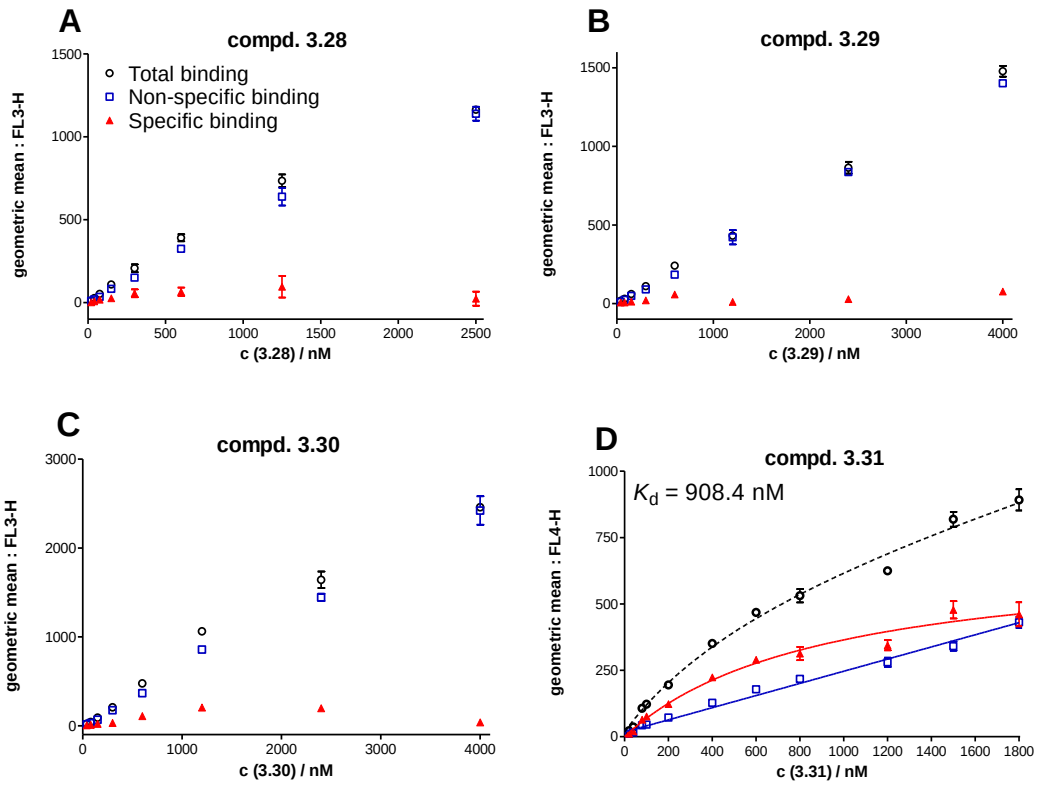

Figure App2.33. Representative flow cytometric saturation binding experiments performed with the fluorescent ligands **3.28-3.31** at intact HEK293T-hH$_2$R-qs5-HA cells. Non-specific binding was determined in the presence of famotidine (300-fold excess adjusted to the respective concentration of the fluorescent ligand). Cells were incubated with the fluorescent ligands at room temperature in the dark for 90 min. The Py-5-labeled compounds **3.28-3.30** (**A-C**) bound in a non-saturable manner. Compound **3.31** (**D**) showed a moderate non-specific binding. Error bars of specific binding represent propagated errors calculated according to the Gaussian law of error propagation. Error bars of total and unspecific binding represent the SEM. Experiments were performed in duplicate.

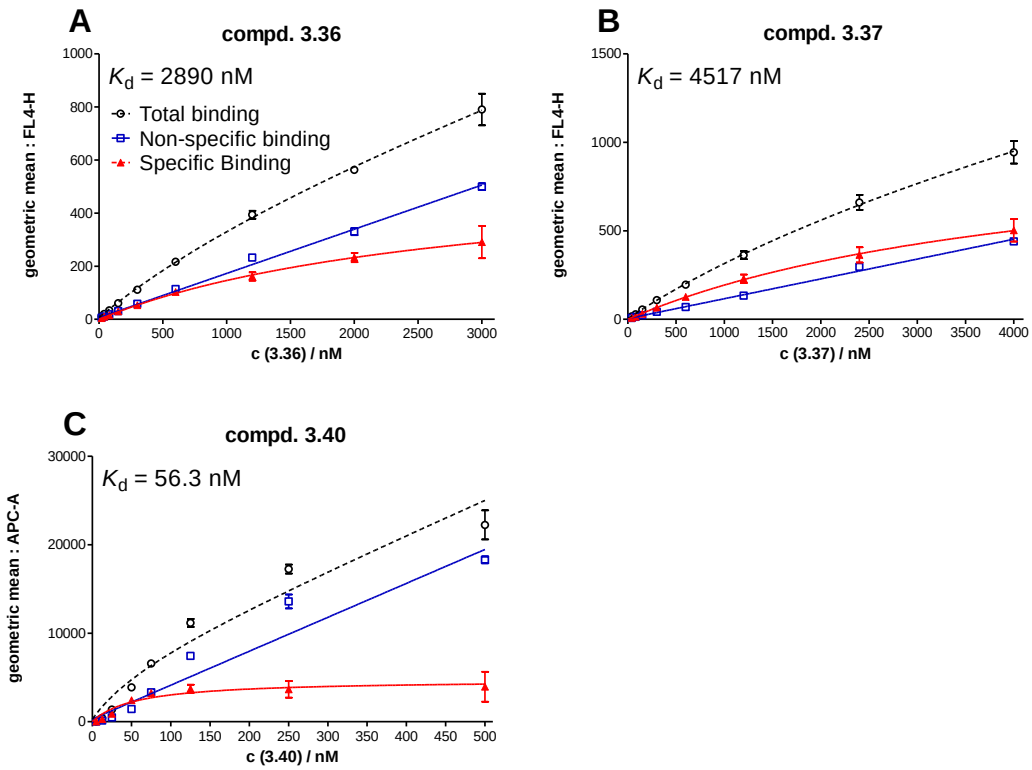

Figure App2.34. Representative flow cytometric saturation binding experiments performed with the fluorescent ligands **3.36**-**3.37** and **3.39** at intact HEK293T-hH_2R-qs5-HA cells. Unspecific binding was determined in the presence of famotidine (300-fold excess adjusted to the respective concentration of the fluorescent ligand). Cells were incubated with the fluorescent ligands at room temperature in the dark for 90 min. Compounds **3.36** (**A**), **3.37** (**B**) and **3.40** (**C**) showed a high non-specific binding. Error bars of specific binding represent propagated errors calculated according to the Gaussian law of error propagation. Error bars of total and unspecific binding represent the SEM. Experiments were performed in duplicate.

App2.6 Confocal Microscopy

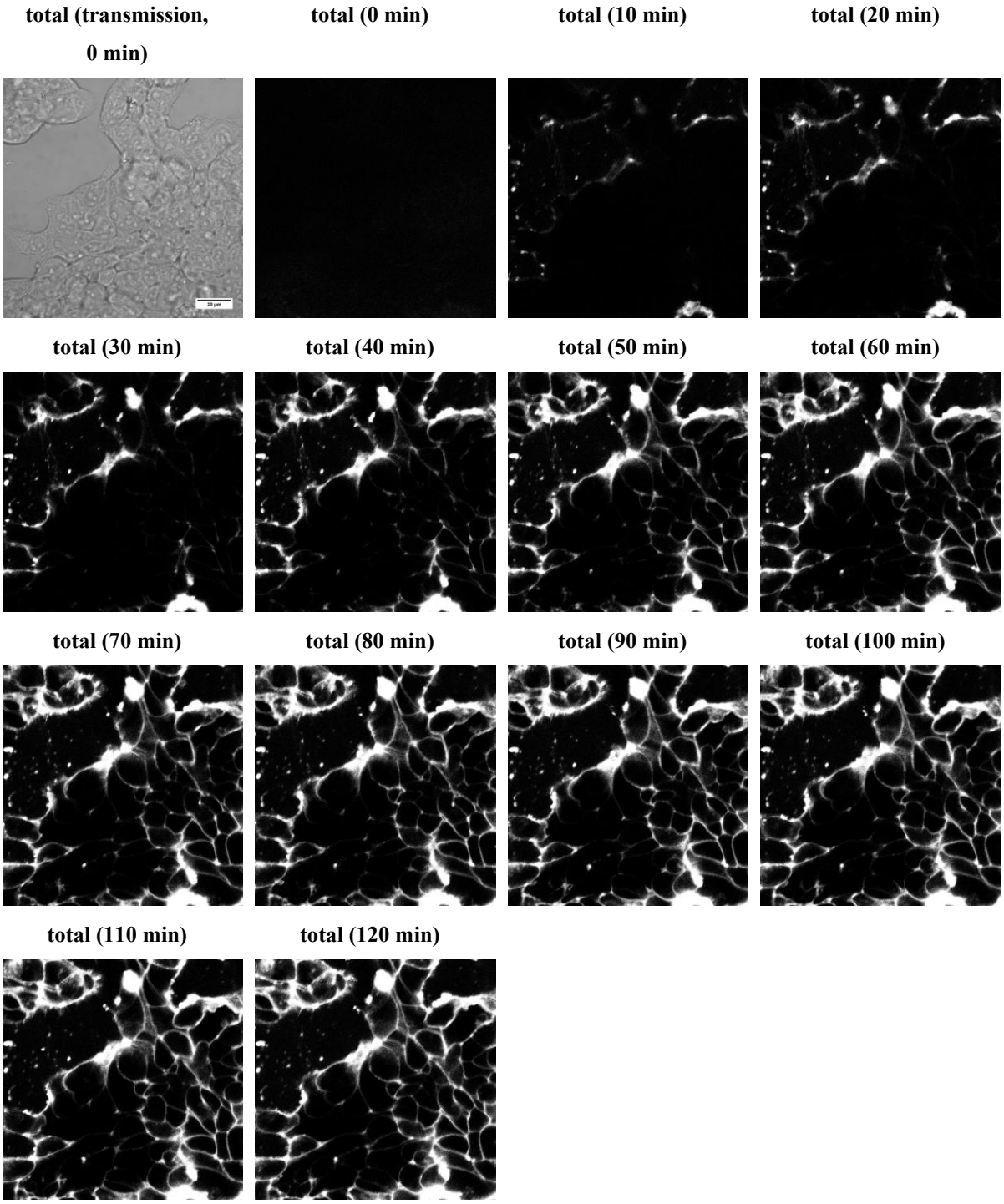

Figure App2.35. Selected frames from confocal microscopy experiments with **3.32** at HEK293T-hH_2R-qs5-HA cells. For total binding, association was started by the addition of **3.32** (c_{final} = 180 nM) to HEK293T-hH_2R-qs5-HA cells. Non-specific binding was recorded in the presence of famotidine (300-fold excess compared to **3.32**). Images were acquired with a Zeiss Axiovert 200M microscope equipped with LSM 510 Laser scanner. A 63x/1.40 oil immersion objective was used [excitation: 633 nm (7.0%), filter: LP650, pinhole: 248 μm].

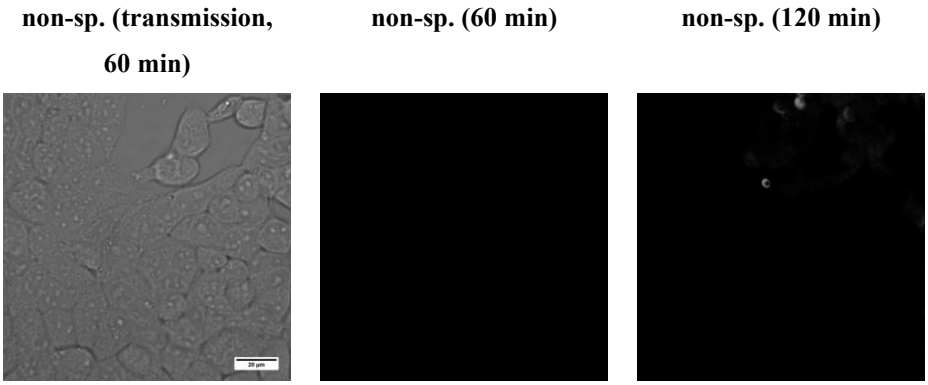

Figure App2.35. (continued)

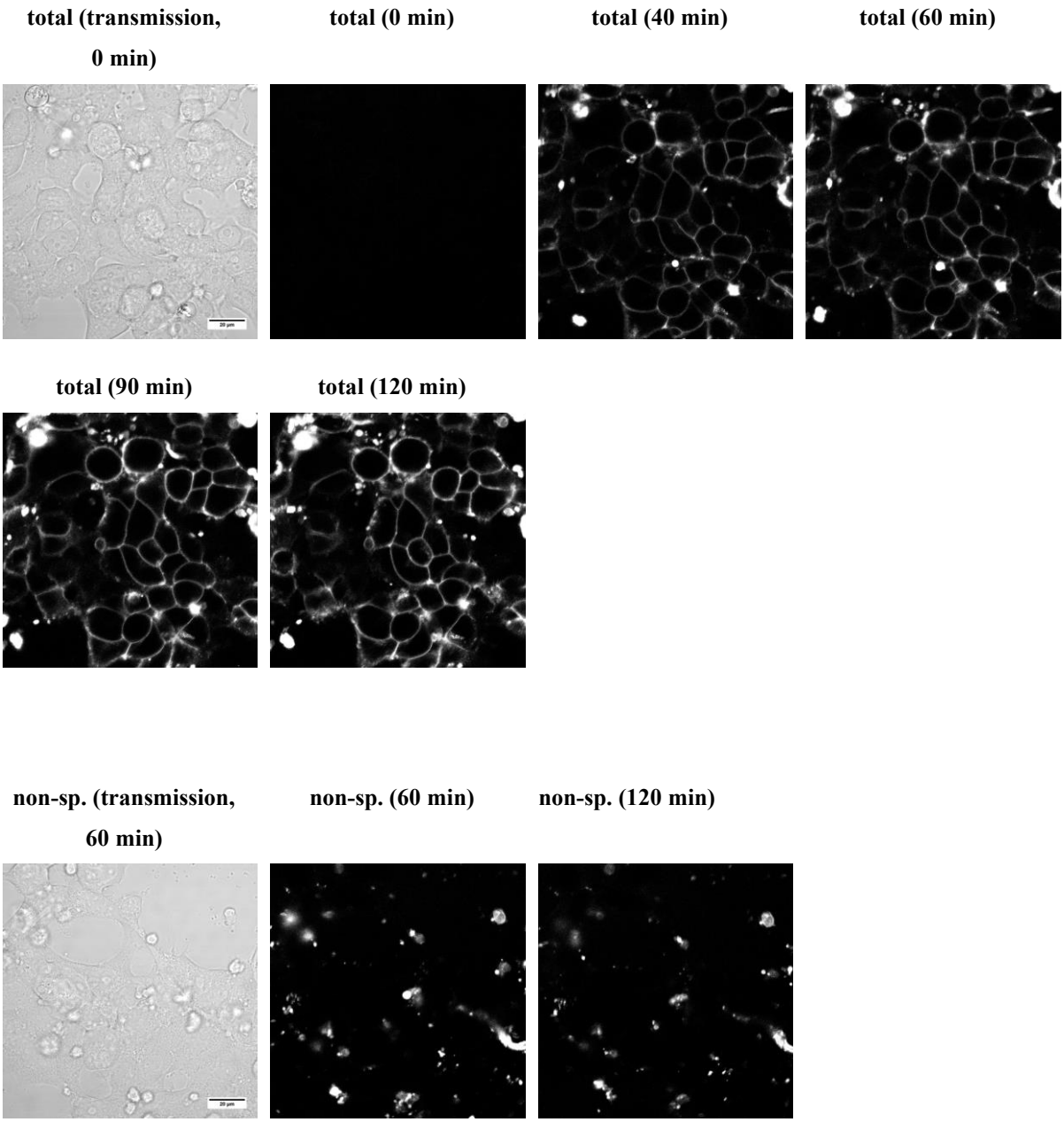

Figure App2.36. Selected frames from confocal microscopy experiments with **3.32** at HEK293T-SP-FLAG-hH_2R K33 cells. For total binding, association was started by the addition of **3.32** (c_{final} = 150 nM) to HEK293T-SP-FLAG-hH_2R K33 cells. Non-specific binding was recorded in the presence of famotidine (300-fold excess compared to **3.32**). Images were acquired with a Zeiss Axiovert 200M microscope equipped with LSM 510 Laser scanner. A 63x/1.40 oil immersion objective was used [excitation: 633 nm (10.0%), filter: LP650, pinhole: 244 µm].

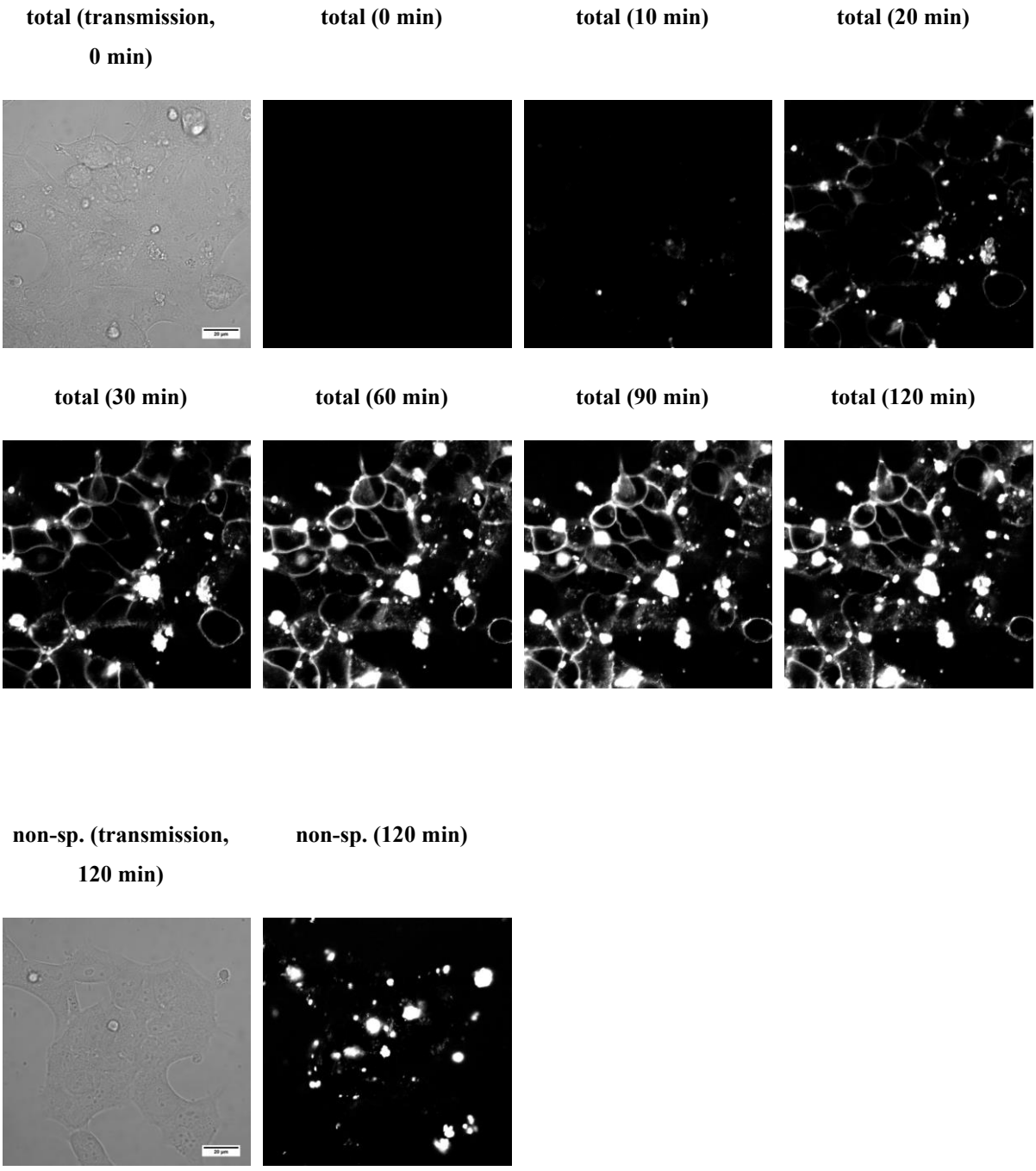

Figure App2.37. Selected frames from confocal microscopy experiments with **3.34** at HEK293T-hH$_2$R-qs5-HA cells. For total binding, association was started by the addition of **3.34** (c_{final} = 200 nM) to HEK293T-SP-FLAG-hH$_2$R K33 cells. Non-specific binding was recorded in the presence of famotidine (300-fold excess compared to **3.34**). Images were acquired with a Zeiss Axiovert 200M microscope equipped with LSM 510 Laser scanner. A 63x/1.40 oil immersion objective was used [excitation: 633 nm (7.0%), filter: LP650, pinhole: 248 µm].

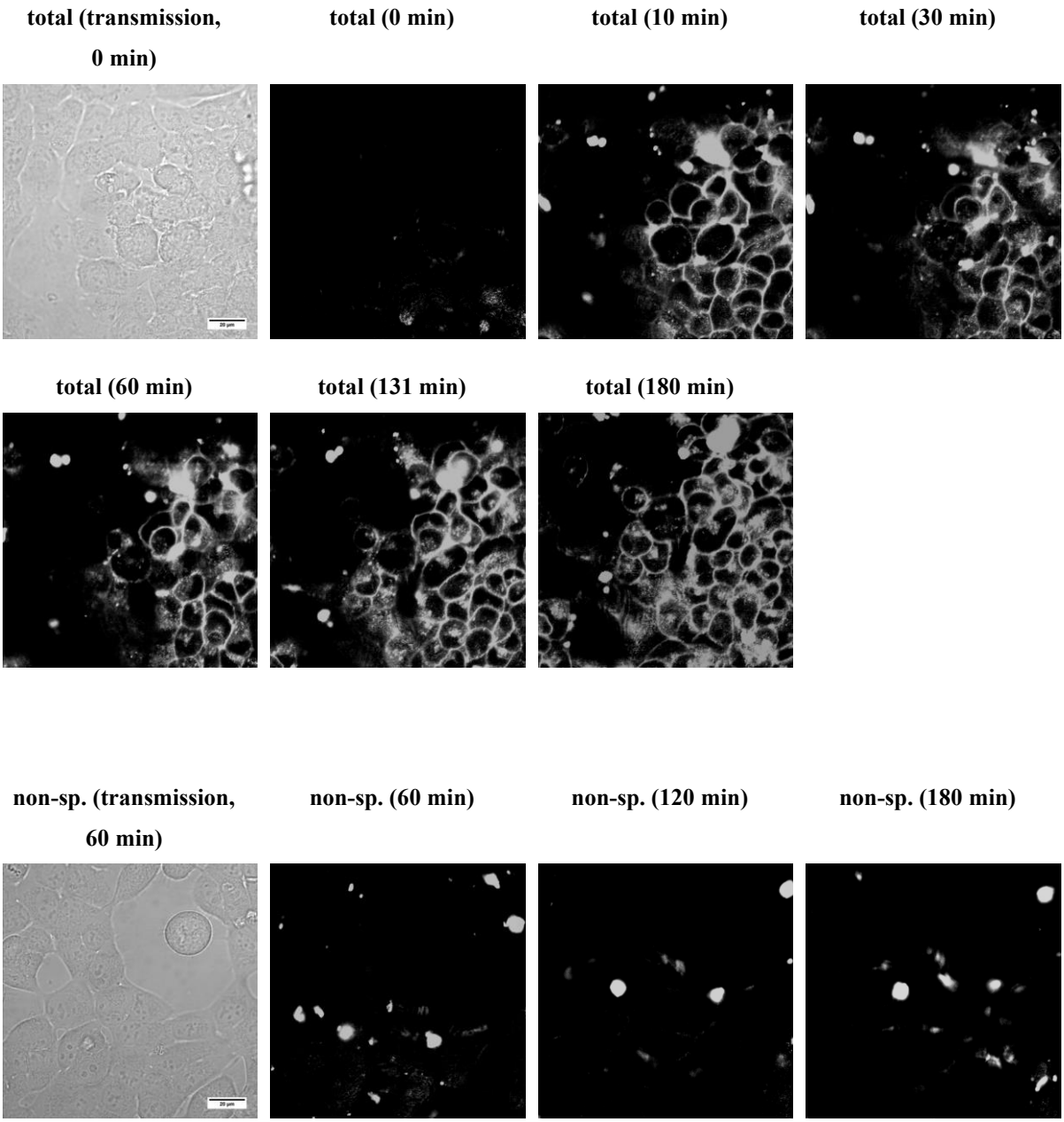

Figure App2.38. Selected frames from confocal microscopy experiments with **3.35** at HEK293T-hH_2R-qs5-HA cells. For total binding, association was started by the addition of **3.35** (c_{final} = 300 nM) to HEK293T-hH_2R-qs5-HA cells. Non-specific (non-sp.) binding was recorded in the presence of famotidine (300-fold excess compared to **3.35**). Images were acquired with a Zeiss Axiovert 200M microscope equipped with LSM 510 Laser scanner. A 63x/1.40 oil immersion objective was used [excitation: 633 nm (10%), filter: LP650, pinhole: 276 µm].

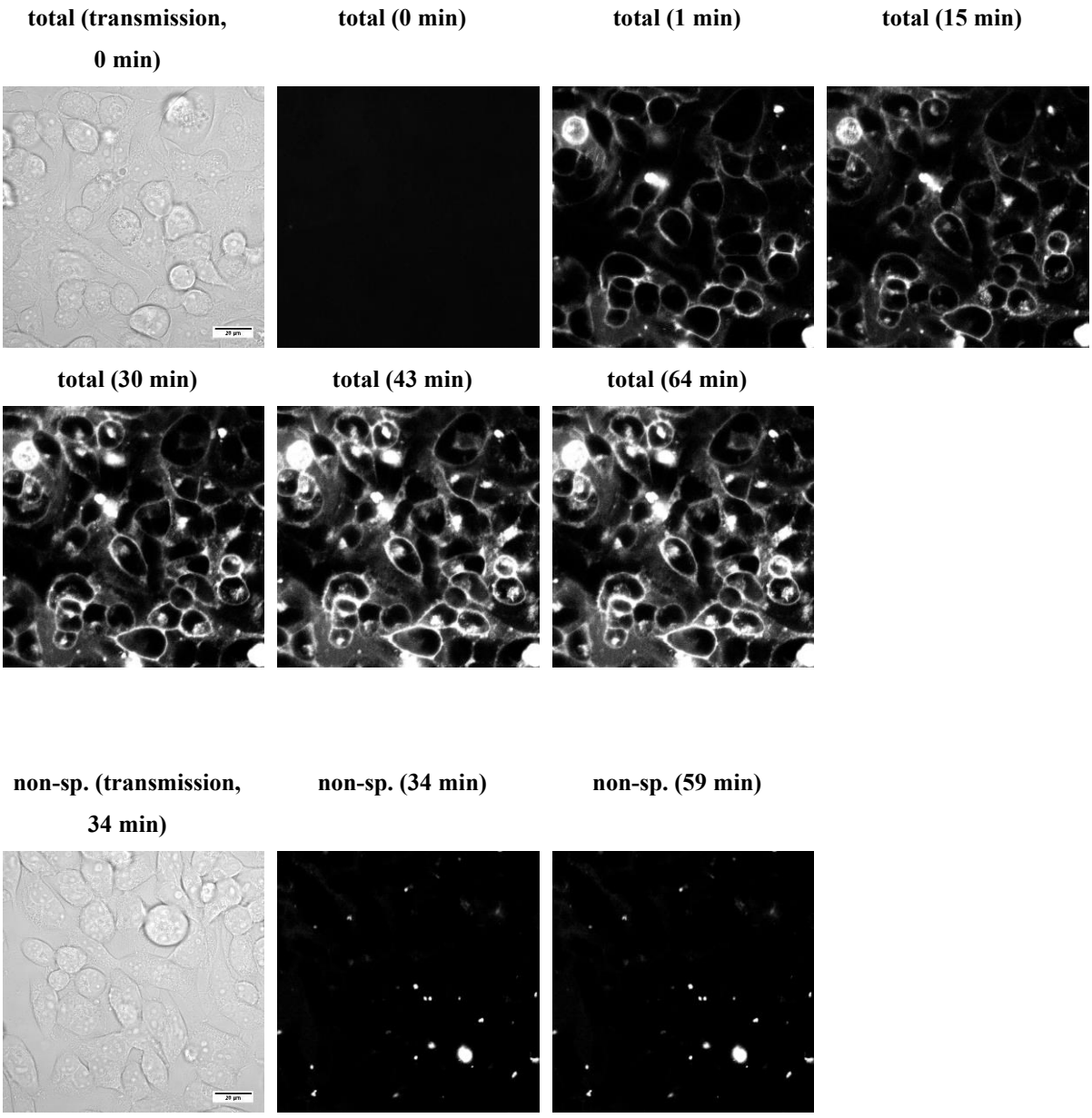

Figure App2.39. Selected frames from confocal microscopy experiments with **3.39** at HEK293T-hH_2R-qs5-HA cells. For total binding, association was started by the addition of **3.39** (c_{final} = 100 nM) to HEK293T-hH_2R-qs5-HA cells. Non-specific binding was recorded in the presence of famotidine (300-fold excess compared to **3.39**). Images were acquired with a Zeiss Axiovert 200M microscope equipped with LSM 510 Laser scanner. A 63x/1.40 oil immersion objective was used [excitation: 633 nM (10.0%), filter: LP650, pinhole: 244 µm].

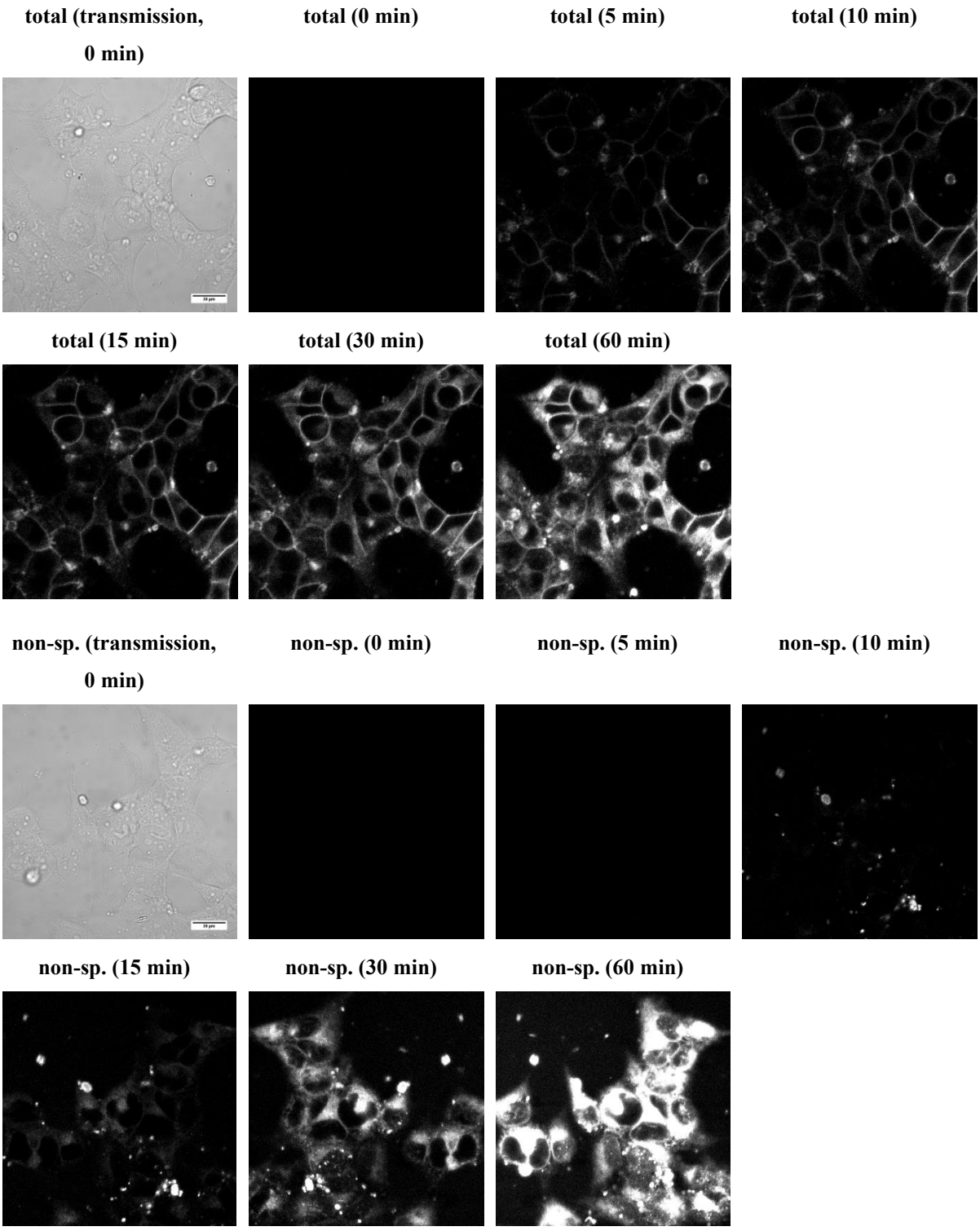

Figure App2.40. Selected frames from confocal microscopy experiments with **3.40** at HEK293T-hH_2R-qs5-HA cells. For total binding, association was started by the addition of **3.40** (c_{final} = 150 nM) to HEK293T-hH_2R-qs5-HA cells. Non-specific binding was recorded in the presence of famotidine (300-fold excess compared to **3.40**). Images were acquired with a Zeiss Axiovert 200M microscope equipped with LSM 510 Laser scanner. A 63x/1.40 oil immersion objective was used [excitation: 633 nM (7.0%), filter: LP650, pinhole: 248 µm].

App2.7 Bias Analysis

To test for biased agonism, we calculated bias factors (BF). To calculate the BF`s we either used efficacy BF (eBF) or potency BF (pBF).[7] Using this method, a biased agonist is defined as an agonist that has a statistically-significant different BF compared to the BF of the endogenous agonist histamine. The eBF for an agonist is calculated as the ratio between maximal responses (E_{max}) of two different signaling pathways ($pathway_1$:$pathway_2$).[7] The pBF of an agonist is calculated as the ratio between EC_{50} of two different signaling pathways ($pathway_1$:$pathway_2$).[7] However, for analysis of statistic difference between pBF of histamine and pBF of the agonist of interest we used the negative logarithm of the pBF or: $ppBF(pathway_1:pathway_2) = pEC_{50}(pathway_1) - pEC_{50}(pathway_2)$.[7] This is necessary since statistic information of SEM is only available for pEC_{50} and not for EC_{50}.

Table App2.2. Efficacy Bias Factors (eBF) and Negative Logarithm of the Potency Bias Factors (ppBF)

compd. / G protein assay	eBF	ppBF
His / [^{35}S]GTPγS	1.00 ± 0.00	1.52 ± 0.06
His / mGs	1.00 ± 0.00	0.59 ± 0.07
3.32 / [^{35}S]GTPγS	8.63 ± 0.34	0.51 ± 0.14
3.32 mGs	6.35 ± 0.33	0.93 ± 0.11
3.33 / [^{35}S]GTPγS	10.16 ± 0.27	0.33 ± 0.30
3.34 / [^{35}S]GTPγS	2.96 ± 0.08	0.45 ± 0.11
3.34 / mGs	3.74 ± 0.07	0.47 ± 0.06
3.35 / mGs	1.47 ± 0.06	0.60 ± 0.10
3.39 / [^{35}S]GTPγS	2.46 ± 0.14	1.31 ± 0.17
3.39 / mGs	2.15 ± 0.14	0.42 ± 0.17

eBF`s comparing efficacy and ppBF`s comparing potency in Gs and β-arrestin2 signaling pathways. The eBF for an agonist is calculated as the ratio between maximal responses (E_{max}) of Gs pathway and β-arrestin2 pathway [eBF = E_{max} (mGs or [^{35}S]GTPγS) / E_{max} (β-arrestin2)]. The ppBF of an agonist is calculated as the difference between pEC_{50} values between Gs pathway and β-arrestin2 pathway [ppBF = pEC_{50} (mGs or [^{35}S]GTPγS) – pEC_{50} (β-arrestin2)]. The E_{max} and pEC_{50} values used for these calculations are depicted in the Table 3.2 in the chapter 3.

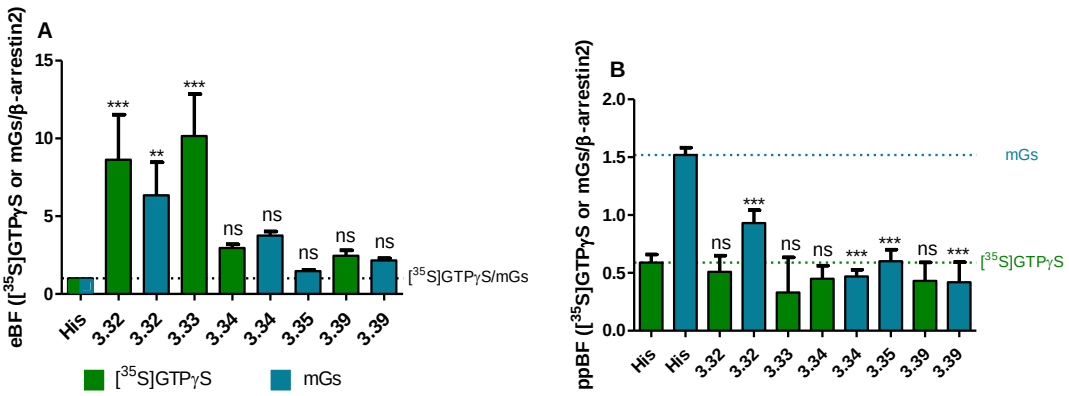

Figure App2.41. Histograms comparing the efficacy bias factors (eBF, **A**) and the negative logarithm of the potency bias factors (ppBF, **B**). Statistical comparison of values was performed by using a one-way ANOVA of BF for each agonist and Dunnett's post-tests were used to compare BF for **3.1** to BF`s for all other agonists (ns: not significant, ***p <0.001, **p<0.01, *p <0.05, as described by Thomsen et al.[7]).

App2.8 References

1. Tropmann, K.; Höring, C.; Plank, N.; Pockes, S., Discovery of a G protein biased radioligand for the histamine H_2 receptor with reversible binding properties. *J. Med. Chem.* **2020,** *63*, 13090-13102.
2. Tropmann, K.; Forster, L.; Bresinsky, M.; Buschauer, A.; Wittmann, H.-J.; Pockes, S; Strasser, A., Abolishing dopamine D_{2long}/D_3 receptor affinity of subtype-selective carbamoylguanidine-type histamine H_2 receptor agonists. *J. Med. Chem., submitted for publication* **2020**.
3. Ghorai, P.; Kraus, A.; Keller, M.; Götte, C.; Igel, P.; Schneider, E.; Schnell, D.; Bernhardt, G.; Dove, S.; Zabel, M.; Elz, S.; Seifert, R.; Buschauer, A., Acylguanidines as bioisosteres of guanidines: N^G-acylated imidazolylpropylguanidines, a new class of histamine H_2 receptor agonists. *J. Med. Chem.* **2008,** *51*, 7193-7204.
4. Höfelschweiger, B. K. The Pyrylium Dyes: A New Class of Biolabels. Synthesis, Spectroscopy, and Application as Labels and in General Protein Assay. Ph.D. Thesis. University Regensburg, 2005.
5. Bartole, E.; Grätz, L.; Littmann, T.; Wifling, D.; Seibel, U.; Buschauer, A.; Bernhardt, G., UR-DEBa242: A Py-5-Labeled Fluorescent Multipurpose Probe for Investigations on the Histamine H_3 and H_4 Receptors. *J. Med. Chem.* **2020,** *63*, 5297-5311.
6. Buschmann, V.; Weston, K. D.; Sauer, M., Spectroscopic study and evaluation of red-absorbing fluorescent dyes. *Bioconjug. Chem.* **2003,** *14*, 195-204.
7. Thomsen, A. R. B.; Hvidtfeldt, M.; Bräuner-Osborne, H., Biased agonism of the calcium-sensing receptor. *Cell Calcium* **2012,** *51*, 107-116. This model is only valid for ligands which are agonists in both pathways. The model can not be applied to ligands which are e.g. agonists in G protein and antagonists in arrestin pathway.

4 Synthesis and Pharmacological Characterization of 2-Arylbenzimidazole Derivatives as Histamine H_2 Receptor Ligands

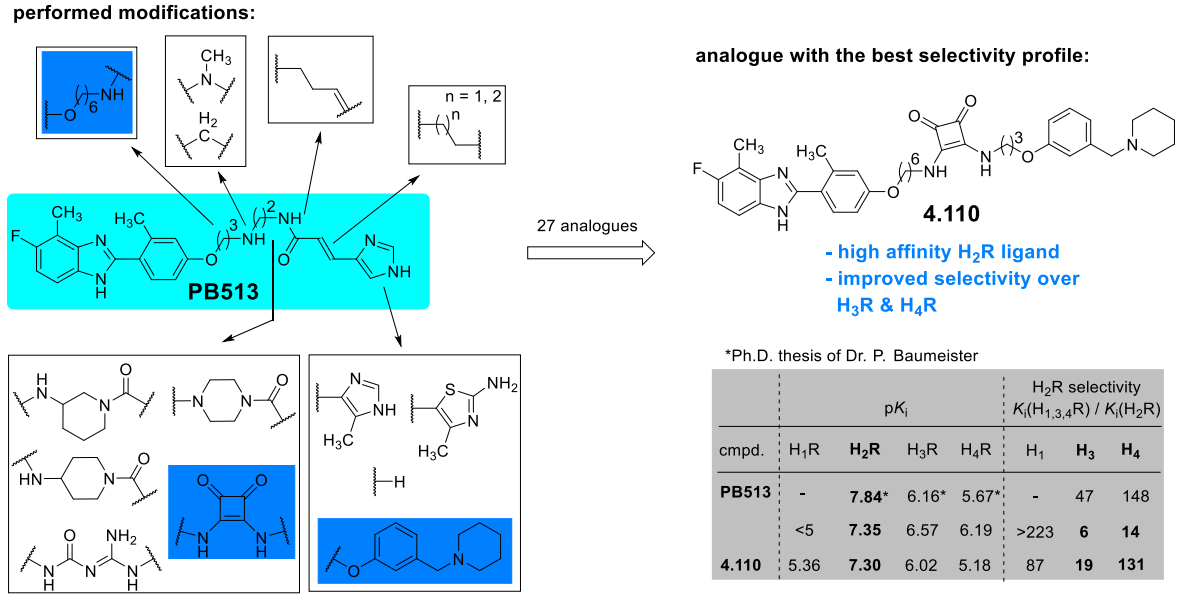

*Ph.D. thesis of Dr. P. Baumeister

	pKi				H_2R selectivity $K_i(H_{1,3,4}R) / K_i(H_2R)$		
cmpd.	H_1R	**H_2R**	H_3R	H_4R	H_1	**H_3**	**H_4**
PB513	-	**7.84***	6.16*	5.67*	-	47	148
	<5	**7.35**	6.57	6.19	>223	**6**	**14**
4.110	5.36	**7.30**	6.02	5.18	87	**19**	**131**

(*E*)-*N*-(2-((3-(4-(5-Fluoro-4-methyl-1*H*-benzo[*d*]imidazol-2-yl)-3-methylphenoxy)propyl)amino)ethyl)-3-(1*H*-imidazol-4-yl)acrylamide (PB513) is a high affinity (H_2R: pK_i = 7.84) 2-arylbenzimidazole-type histamine H_2 receptor (H_2R) inverse agonist / antagonist, showing a selectivity over the H_4R and the dopamine $D_{1\text{-}5}$ receptors, but only a preference over the H_3R. Aiming at an improved subtype selectivity for the H_2R, a series of 27 analogues related to PB513 was synthesized by variation of the linker and the basic head group. These new derivatives were investigated in radioligand binding and several functional assays ([^{35}S]GTPγS binding, mini-G and β-arrestin2 recruitment). The structural elements of PB513: 2-arylbenzimidazole, the secondary amine, the double bond, and the imidazole were identified as important for the H_2R affinity. On the other hand, the amide group was not of great importance for the affinity, but mainly influenced the subtype selectivity. Most of the synthesized compounds acted as inverse agonists / antagonists at the H_2R (like PB513), but also a few (biased) agonists were identified. Indeed, the mode of action [(inverse) agonist / antagonist] seemed to depend mainly on the basic head group. Although 27 analogues of PB513 were prepared and characterized, it was not possible to achieve a sufficient subtype selectivity [factor 100; compound with the best selectivity profile: **4.110**; H_2R: pK_i = 7.30; $K_i(H_{1,3,4})/K_i(H_2)$: H_1: 87; H_3: 19; H_4: 131]. In addition, PB513's previously reported selectivity for the H_4R (K_i (H_4) / K_i (H_2): reported: 148, obtained: 14) and preference for the H_3R (K_i (H_3) / K_i (H_2): reported: 47, obtained: 6) could not be reproduced. For this reason, the synthesized molecules were not employed in further studies at dopamine receptors.

4.1 Introduction

2-Arylbenzimidazole derivatives were published as high affinity hH_4R ligands by Lee-Dutra et al. (cf. Figure 4.1).[1] Structural variations of these molecules by Dr. P. Baumeister resulted in a H_4R ligand series including compound PB513 (Figure 4.1).[2] Surprisingly, PB513 bound to the hH_2R-$G_{s\alpha S}$ with high affinity ($pK_i = 7.8$) and had a 47-fold preference over the hH_3R ($pK_i = 6.2$) and a 148-fold selectivity over the hH_4R ($pK_i = 5.7$).[2] In the [^{35}S]GTPγS assay at hH_2R-$G_{s\alpha S}$ PB513 revealed a pK_b value of 7.7 ($\alpha = -0.20$[2]).[2]

Since our group is interested in subtype selective H_2R ligands, which are also selective over dopamine receptors, we tested PB513 for its affinity to dopamine receptors. PB513 bound to the dopamine receptors only with low affinity (pK_i 5.10-5.97, Figure 4.1), turning it into a promising starting point in the search for novel and selective (agonistic) H_2R ligands.

The aim of this work was to synthesize a small library of compounds related to PB513 (Figure 4.2A & B) and elucidate the structure-activity (H_2R) and structure-selectivity relationships (H_2R versus H_1R, H_3R and H_4R) using [^{35}S]GTPγS binding-, mini-G protein recruitment- and β-arrestin2 recruitment assays, as well as radioligand binding experiments. Furthermore, we investigated the feasibility to turn 2-arylbenzimidazoles from antagonistic into agonistic H_2R ligands.

To explore the structural requirements for hH_2R affinity and selectivity of PB513, the functional groups (secondary (sec.) amine, amide, double bound, heterocycle etc.) which deemed important, were gradually removed, replaced by a bioisoster, or rigidified by incorporation into a ring (Figure 4.2A). Moreover, the number and the nature (carbamoylguanidine, squaramide, amine) of basic centers was varied (Figure 4.2B). We did not include the acylguanidine group into the series (cf. UR-AK24[3], Figure 4.2B), because acylguanidines undergo hydrolytic cleavage upon long term storage in aqueous solution.[4] The imidazole-bearing moiety was modified with respect to typical H_2R ligand motifs which were published previously (cf. UR-AK24[3], UR-KAT523[5], BMY25368[6], Figure 4.2B), aiming at improved H_2R selectivity compared to the other histamine receptors. Moreover, the secondary amine in the spacer of PB513 was methylated to investigate this class of compounds for its potential application as radioligands.

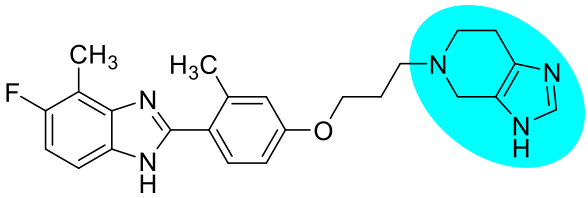

hH_xR	pK_i
1	<5[a]
2	<5[a], 5.9[b]
3	5.0[a], 4.7[b]
4	**8.5**[a], **8.3**[b]

hH_4R: pEC_{50} = 8.5 (E_{max} = 0.61)[a,c]

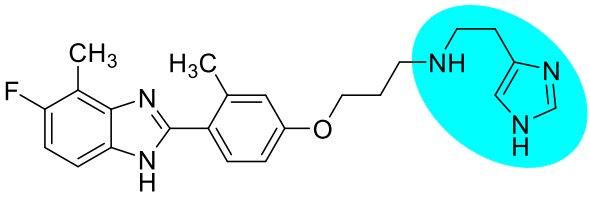

hH_xR	pK_i
1	<5[a]
2	6.9[a]
3	6.4[a]
4	**9.7**[a]

hH_4R: pEC_{50} = 9.3 (E_{max} = 0.96)[a]

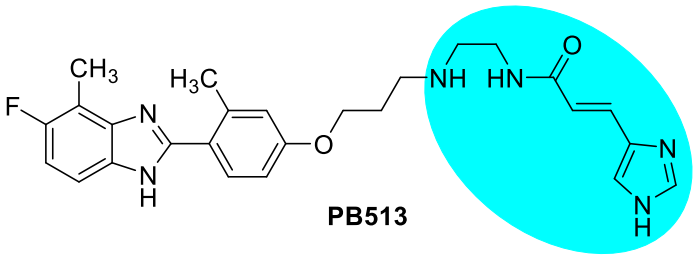

PB513

hH_xR	pK_i
1	n.d.
2	**7.8**[b]
3	6.2[b]
4	5.7[b]

hH_2R: pK_b = 7.7 (E_{max} = -0.20)[b,e]

hD_xR	pK_i
1	5.69 ± 0.06[d]
5	5.97 ± 0.13[d]
2long	5.12 ± 0.13[d]
2short	5.10 ± 0.08[d]
3	5.40 ± 0.01[d]
4	5.66 ± 0.03[d]

Figure 4.1. Structures of selected 2-arylbenzimidazole derivatives, including PB513 and their binding and functional data at histamine H_{1-4} receptors and in case of PB513 also at dopamine D_{1-5} receptors. The terminal amino moiety (shown in light blue) influences the HR selectivity. [a]Data from Savall et al.[7] [b]Data from the Ph.D. thesis of Dr. P. Baumeister.[2] [c]Luciferase reporter gene assay using SK-N-MC cells expressing the hH_4R. [d]Data from Dr. H. Hübner (Friedrich-Alexander University Erlangen-Nürnberg). [e][^{35}S]GTPγS binding assay on membrane preparations of Sf9 insect cells expressing the hH_2R-$G_{s\alpha S}$ fusion protein. n.d.: not dertermined.

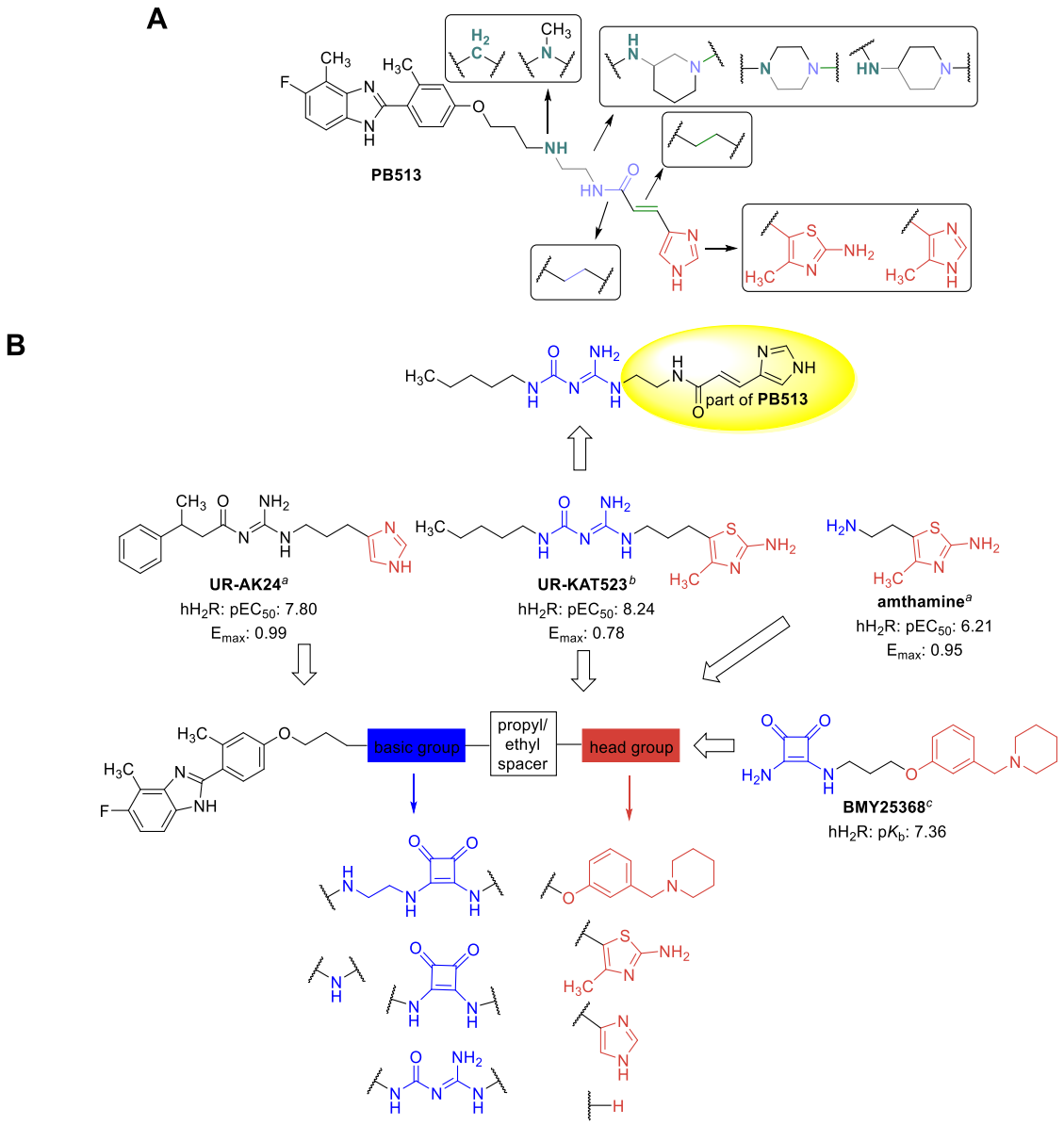

Figure 4.2. **A**: Overview of the performed structural variations of PB513[2]. **B**: Further variations, including modification of known H_2R ligands with a 2-arylbenzimidazole or urocanic acid amide moiety. [a]Data from Kraus et al.[3] [b]Data from Biselli et al.[5] [c]Data from Baumeister et al.[8] [a,b]Agonism measured on guinea pig right atrium. [c]Agonism measured in the steady-state GTPase assay.

4.2 Results and Discussion

4.2.1 Chemistry

Many different building blocks were synthesized as ligand precursors in multistep syntheses. Figure 4.3 offers an overview of these building blocks and is subdivided into sections containing the respective carboxylic acids, amines and mixed squaramates which were fused together with the corresponding *O*-alkylated 2-arylbenzimidzoles to form the desired bioactive compounds.

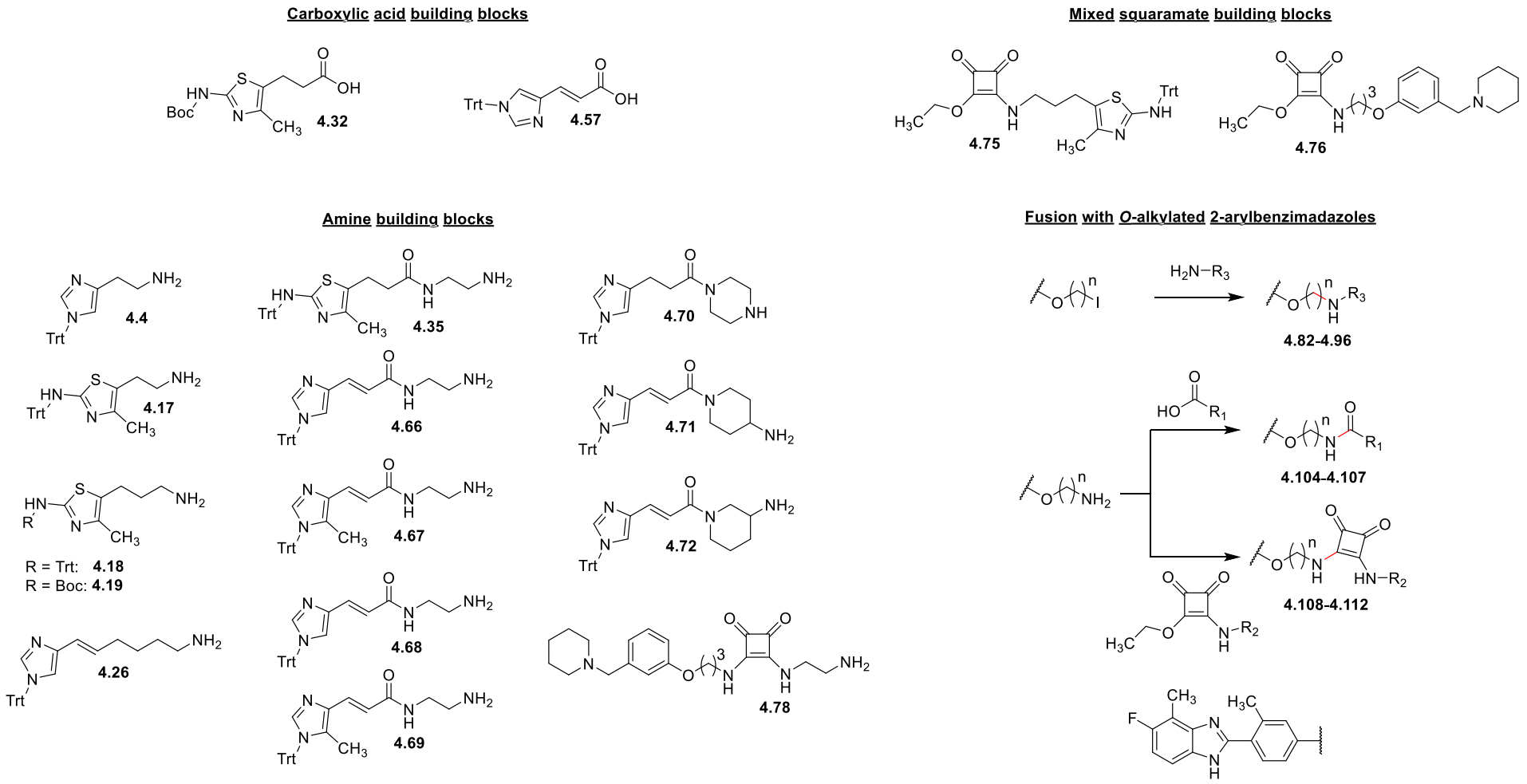

Figure 4.3. Structures of the synthesized carboxylic acid-, amine- and mixed squaramate building blocks and overview of their coupling reaction with *O*-alkylated 2-arylbenzimidazoles.

4.2.1.1 Synthesis of the Amine Building Block 4.4

Compound **4.2** was obtained from the reaction of histamine dihydrochloride (**4.1**) with Nefkens`reagent. Trityl (Trt) protection of the imidazole **4.2**, followed by hydrazinolysis of the phthalimide group afforded the 2-(1-trityl-1*H*-imidazol-4-yl)ethanamine (**4.4**).

Scheme 4.1. Synthesis of 4.4[a]

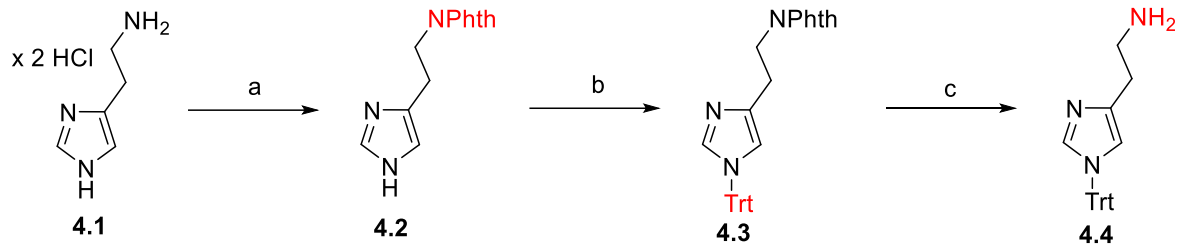

[a]Reagents and conditions: (a) Nefkens` reagent, K_2CO_3, H_2O, rt, 2 h, 97%; (b) Trt-Cl, NEt_3, MeCN, rt, 16 h, 97%; (c) hydrazine monohydrate (N_2H_4 x H_2O), EtOH, reflux, 2 h, 98%.

4.2.1.2 Synthesis of the Amine Building Blocks 4.17-4.19

The methyl ketones **4.8** and **4.9** were obtained from the reaction of either 5-chloro-2-pentanone (**4.5**) or 6-chloro-2-hexanone (**4.6**) with phthalimide (**4.7**). In case of **4.8**, regioselective bromination was achieved by employing Br_2, and glacial acetic acid as solvent according to Black et al.[9] In contrast, compound **4.9** was α-brominated with Br_2 in 1,4-dioxane and CH_2Cl_2 according to von Angerer et al.[10] Cyclization of the α-bromoketones **4.10** or **4.11** with thiourea gave the thiazoles **4.12** and **4.13**.[11] After trityl (**4.14-4.15**) or Boc (**4.16**)[12] protection of the aromatic amine function, the phthalimide group was cleaved by hydrazinolysis to give 5-(2-aminoethyl)-4-methyl-*N*-tritylthiazol-2-amine (**4.17**), 5-(3-aminopropyl)-4-methyl-*N*-tritylthiazol-2-amine (**4.18**) and *tert*-butyl 5-(3-aminopropyl)-4-methylthiazol-2-ylcarbamate (**4.19**), respectively (Scheme 4.2). Although the Boc protecting group is commonly employed,[3-4, 13-14] we decided to synthesize the Trt-protected derivatives, because the Trt protecting group proved to be more stable under the conditions of the nucleophilic substitution reaction in the microwave (this observation is based on personal and literature experience[15]).

Scheme 4.2. Synthesis of 4.17-4.19[a]

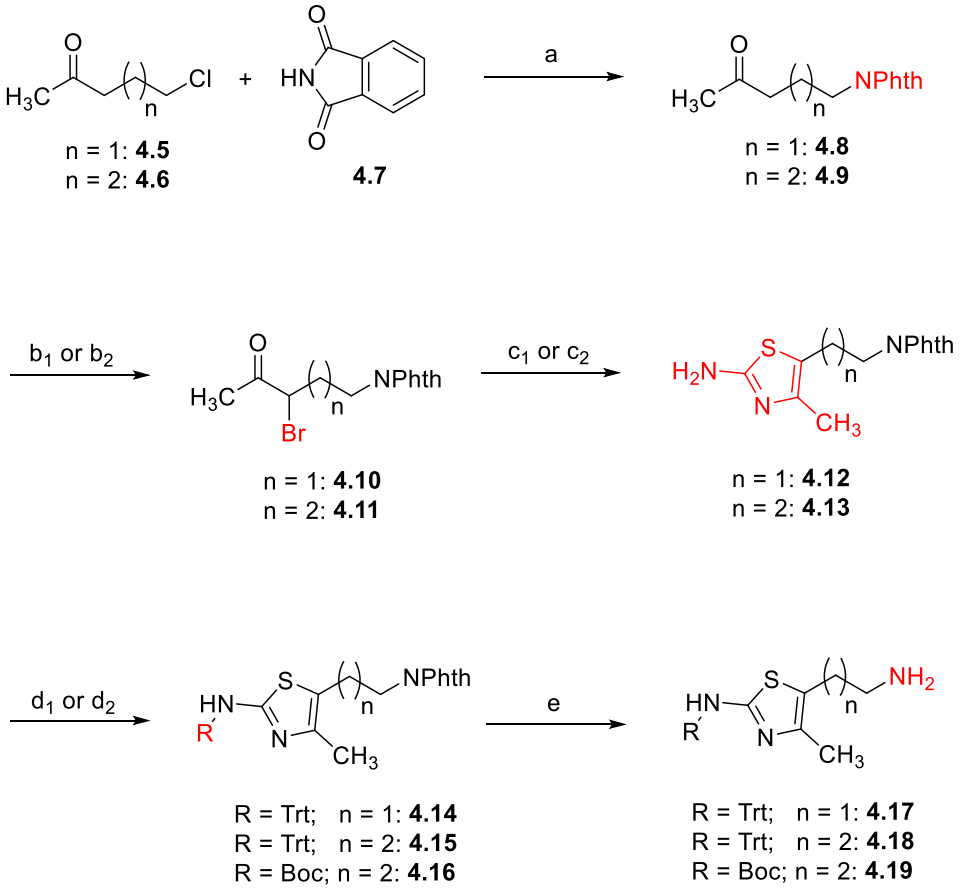

[a]Reagents and conditions: (a) K_2CO_3, KI (cat.), DMF, 95-110 °C, 12-24 h, **4.8**: 50% and **4.9**: 74%; (b_1) Br_2, glacial acetic acid, 10 °C to rt, 1 h, **4.10**: 57%; (b_2) Br_2, 1,4-dioxane/CH_2Cl_2, rt, 4 h, **4.11**: 93%; (c_1) (1) thiourea, DMF, 100 °C, 3 h, (2) MeOH/1 N HCl in MeOH, rt, 72 h, **4.12**: 79% over two steps; (c_2) thiourea, DMF, 100 °C, 3 h, **4.13**: 29%; (d_1) Trt-Cl, NEt_3, MeCN, rt, 16 h, **4.14**: 62% and **4.15**: 27%; (d_2) Boc_2O, NEt_3, DMAP (cat.), chloroform, rt, overnight, **4.16**: 69%; (e) N_2H_4 x H_2O, EtOH, *n*-BuOH or EtOH/*n*-BuOH, rt, 16-24 h, **4.17**: 99%, **4.18**: 68% and **4.19**: 100%.

4.2.1.3 Synthesis of the Amine Building Block 4.26

A synthetic approach similar to that described by Griffith et al.[16] was employed to prepare the $^{\tau}$*N*-Trt-protected amine **4.26** (Scheme 4.3). Potassium phthalimide (**4.20**) was first converted to *N*-(5-bromopentyl)phthalimide (**4.22**) using an excess of 1,5-dibromopentane (**4.21**). Treatment of **4.22** with Ph_3P in MeCN provided the corresponding phosphonium salt **4.23**, which was coupled with the $^{\tau}$*N*-Trt-protected imidazole aldehyde **4.24** to give the *Wittig* olefination product **4.25**. The following liberation of the primary amine with hydrazine provided the $^{\tau}$*N*-Trt-protected amine **4.26**.

Scheme 4.3. Synthesis of 4.26[a]

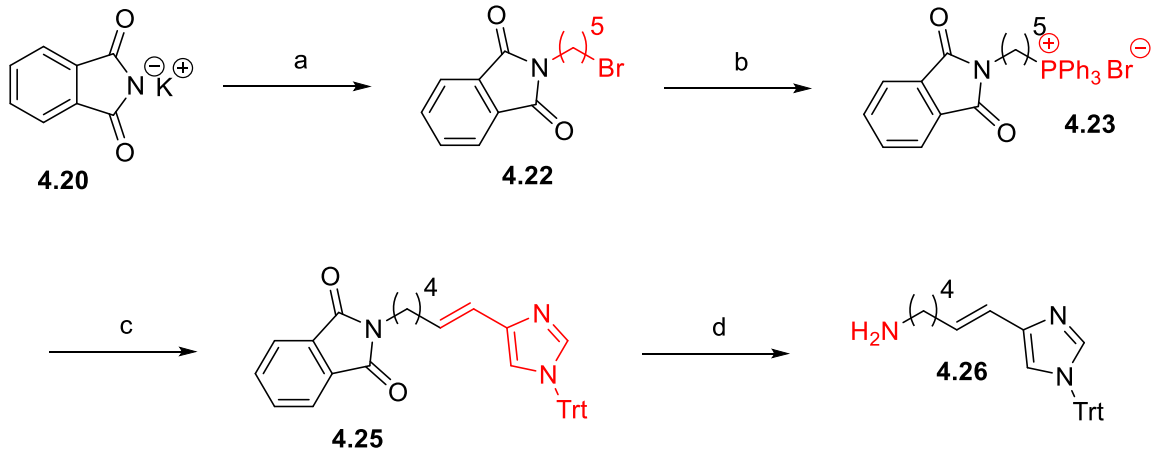

[a]Reagents and conditions: (a) 1,5-dibromopentane (**4.21**), DMF, rt, 24 h, 31%; (b) Ph_3P, MeCN, reflux, 48 h, 100%; (c) aldehyde **4.24**, *t*-BuOK, THF, 0 °C to reflux, 18 h; (d) N_2H_4 x H_2O, EtOH, rt, 48 h, 7% over 2 steps.

4.2.1.4 Synthesis of the Carboxylic Acid Building Block 4.32 and Amine Building Block 4.35

The carboxylic acid **4.32** and the amine **4.35** were prepared from commercially available γ-acetobutyric acid (**4.27**, Scheme 4.4). **4.27** was converted to ethyl γ-acetobutyrate (**4.28**) by esterification with EtOH. In an one pot reaction, **4.28** was α-brominated using Br_2, and the ring closure reaction was carried out with thiourea under solvent-free conditions as described by Dodson et al.[17] Subsequent Boc (**4.30**) or Trt (**4.31**) protection and ethyl ester hydrolysis gave the carboxylic acids **4.32** or **4.33**. The Trt-protected carboxylic acid **4.33** was coupled to mono-phthalimide protected ethylenediamine (**4.49**) using EDC/HOBt. The phthalimide group was removed using hydrazine to give the amine **4.35**.

Scheme 4.4. Synthesis of 4.32 and 4.35[a]

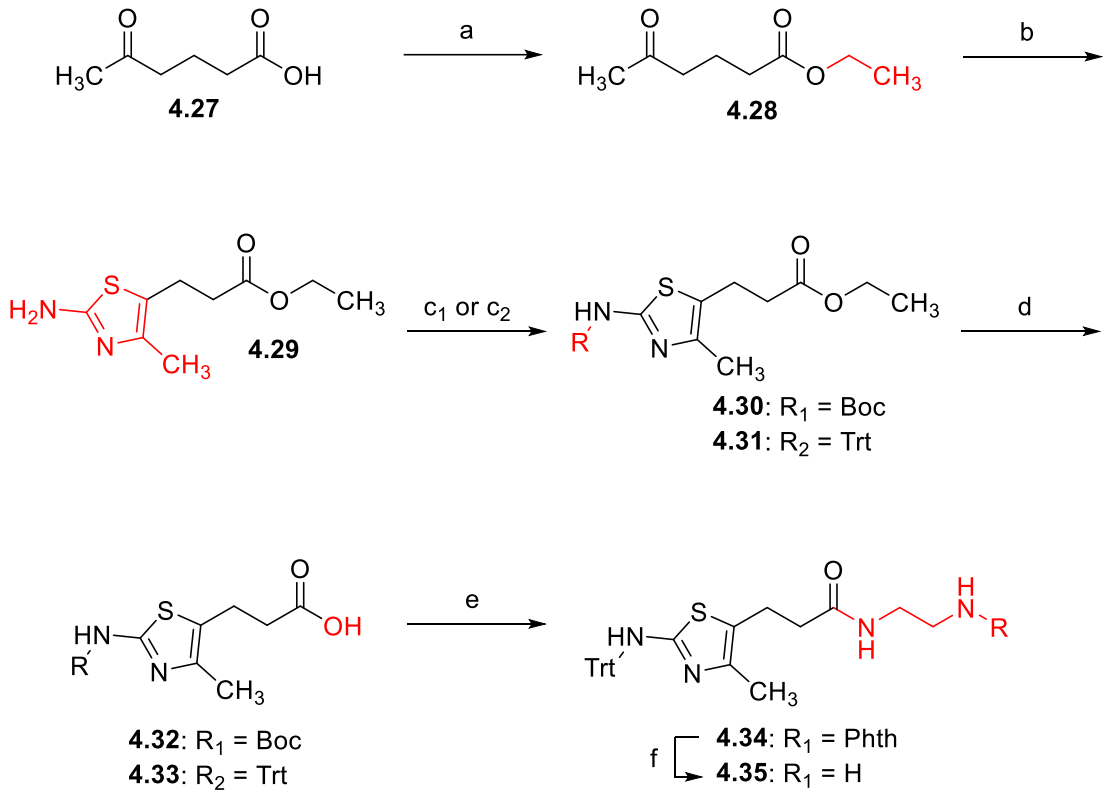

[a]Reagents and conditions: (a) (1) oxalyl chloride, DMF (cat.), CH_2Cl_2, 0 °C to rt, 2 h; (2) EtOH, NEt_3, rt, 30 min, 34%; (b) Br_2, thiourea, steam-bath, 3 h, 13%; (c_1) Boc_2O, NEt_3, DMAP (cat.), CH_2Cl_2, rt, 16 h, **4.30**: 63%; (c_2) Trt-Cl, NEt_3, DMF, rt, 16 h, **4.31**: 68%; (d) KOH, EtOH/H_2O, 0 °C to rt, 16 h, **4.32**: 89% and **4.33**: 100%; (e) 2-(2-aminoethyl)isoindoline-1,3-dione (**4.49**, Scheme 4.5C), EDC x HCl, HOBt x H_2O, DIPEA, DMF, 0 °C to rt, 16 h, 21%; (f) N_2H_4 x H_2O, EtOH, rt, 16 h, 89%.

4.2.1.5 Synthesis of the Amine Building Blocks 4.66-4.72

The carboxybenzyl (Cbz)- or phthalimide-protected amines **4.42-4.43**, **4.46** and **4.49** were synthesized as shown in Scheme 4.5. The synthesis started from the commercially available (RS)-3-hydroxypiperidine (**4.36**) or piperidin-4-ol (**4.37**, Scheme 4.5A). These compounds were transformed into the corresponding *N*-Boc derivatives and subsequently mesylated giving **4.38** and **4.39**. Compounds **4.38** and **4.39** were used for nucleophilic substitution with phthalimide. Cleavage of the Boc protecting group with TFA led to the free secondary amines (**4.42-4.43**).

The amines **4.46** and **4.49** were synthesized from mono-Boc-protected piperazine (**4.44**) or ethane-1,2-diamine (**4.47**) by Cbz (**4.45**) and phthalimide (**4.48**) protection and subsequent acidic Boc deprotection (Scheme 4.5B & C).

Scheme 4.5. Synthesis of Cbz- or Phthalimide-Protected Amines 4.42-4.43, 4.46 and 4.49[a]

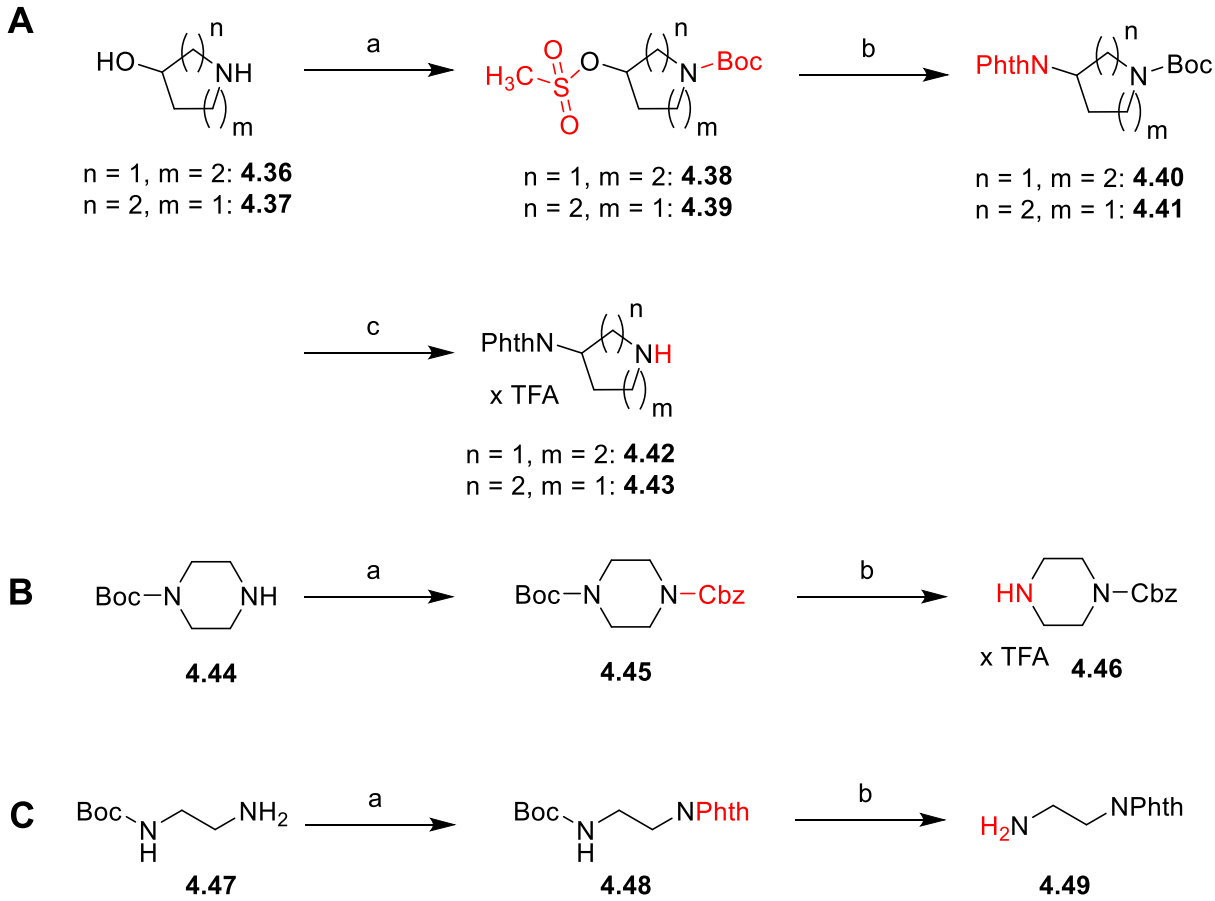

[a]Reagents and conditions: **A**: (a) (1) Boc_2O, NEt_3, CH_2Cl_2, 0 °C, 2 h; (2) mesityl chloride, NEt_3, 0 °C to rt, 3 h, **4.38**: 75% and **4.39**: 74%; (b) potassium phthalimide, DMF, 75 °C, 24 h, **4.40**: 10% and **4.41**: 21%; (c) TFA, CH_2Cl_2, rt, 8-16 h, **4.42** and **4.43**: 100%; **B**: (a) benzyl chloroformate, NEt_3, CH_2Cl_2, 0°C to rt, overnight, 61%; (b) TFA, CH_2Cl_2, rt, 7 h, 99%; **C**: (a) Nefkens`reagent, K_2CO_3, H_2O, rt, 16 h, 22%; (b) TFA, CH_2Cl_2, rt, 48 h, 100%.

The amine building blocks **4.66-4.72** were prepared as highlighted in Scheme 4.6. The carboxylic acid **4.54** was obtained *via* Horner-Wadsworth-Emmons reaction[18] of the Trt-protected aldehyde **4.51** with triethyl phosphonoacetate followed by saponification of the ethyl ester **4.52** with KOH in EtOH/H_2O. To obtain the hydrogenated derivative **4.55** the C=C double bound of **4.52** was reduced with H_2 and Pd/C.[19] To synthesize the non-methylated precursors (**4.57** and **4.58**), the imidazole of urocanic acid was *N*-Trt-protected. The corresponding reduced derivative (**4.58**) was obtained by hydrogenation of the C=C double bound. Then, the Cbz- or phthalimide-protected amines (**4.43-4.43**, **4.46** and **4.49**, cf. Scheme 4.5) were coupled to carboxylic acids **4.54-4.58** using EDC/HOBt followed by Cbz deprotection with H_2 and Pd/C (**4.63**) or phthalimide deprotection with N_2H_4 (**4.59-4.65**, except **4.63**) to give the amine building blocks **4.66-4.72**.

Scheme 4.6. Synthesis of Amine Building Blocks 4.66-4.72[a]

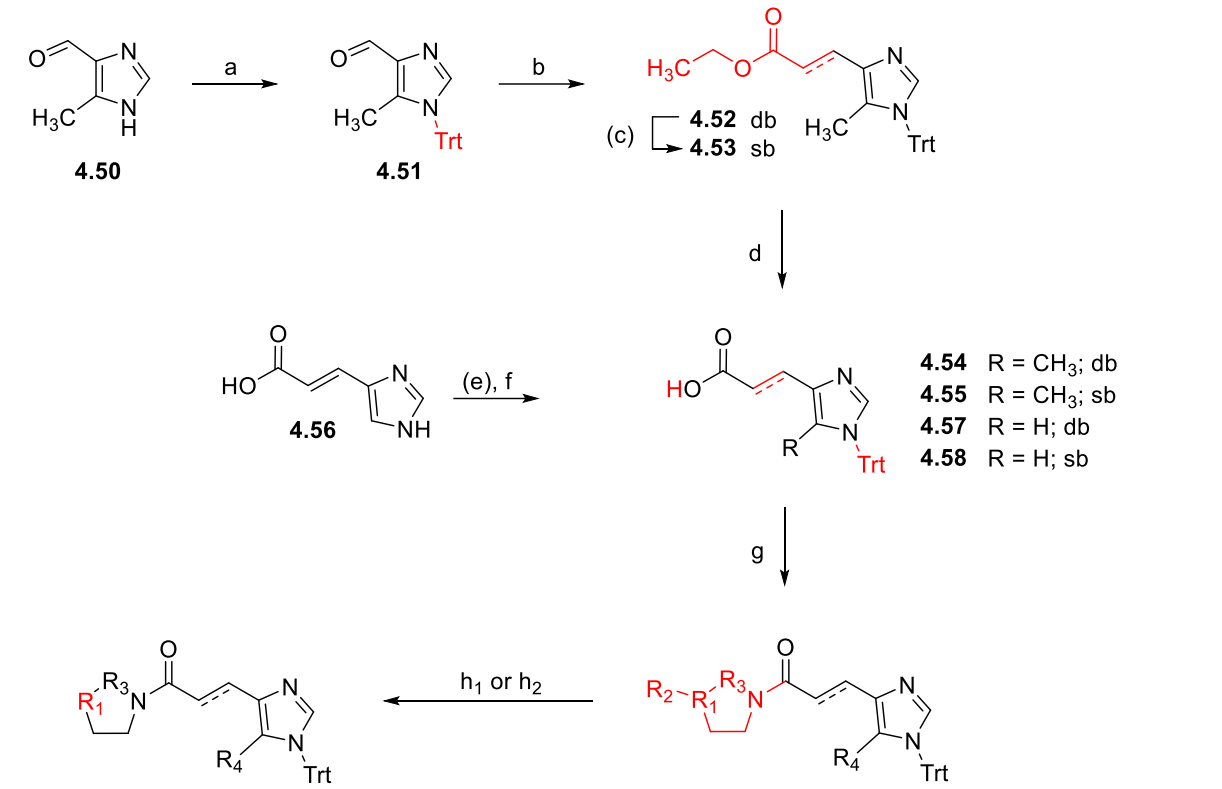

[a]Reagents and conditions: (a) Trt-Cl, NEt_3, MeCN, rt, 16 h, 43%; (b) NaH, triethyl phosphonoacetate, THF, reflux, 16 h, 18%; (c) Pd/C, H_2 (1 atm), EtOH, rt, overnight, 81%; (d) KOH, EtOH/H_2O, 0 °C to rt, 16-48 h, **4.54**: 79% and **4.55**: 54%; (e) Pd/C, H_2 (1 atm), MeOH, rt, 5 h, 100%; (f) Trt-Cl, NEt_3, DMF, rt, 14 h, **4.57**: 42% and **4.58**: 40%; (g) **4.42**, **4.43**, **4.46** or **4.49**, EDC x HCl, HOBt x H_2O, DIPEA, DMF, 0 °C to rt, 16 h, **4.59**: 34%, **4.60**: 48%, **4.61**: 98%, **4.62**: 79%, **4.63**: 100%, **4.64**: 99% and **4.65**: 55%; (h_1) N_2H_4 x H_2O, EtOH, rt, 16 h, **4.66**: 50%, **4.67**: 60%, **4.68**: 43%, **4.69**: 88%, **4.71**: 80% and **4.72**: 34%; (h_2) Pd/C, H_2 (1 atm), MeOH/THF, rt, 6 h, **4.70**: 62%. sb: single bond. db: double bond. n.a.: not available.

4.2.1.6 Synthesis of the Mixed Squaramate Building Blocks 4.75 and 4.76, the Amine Building Block 4.78 and the Squaramide 4.117

The synthesis of the mixed squaramates **4.75** and **4.76** was adapted from published procedures.[8, 20] The precursors **4.18** or **4.74** (synthesized as described previously[21]) and 3,4-diethoxycyclobut-3-ene-1,2-dione (**4.73**) were stirred in EtOH at rt for 3 h or overnight yielding the mixed squaramates **4.75** and **4.76** in very good to excellent yields (Scheme 4.7). The

following reaction, leading to squaramides **4.77** (Boc-protected) or **4.117**, was performed in EtOH at rt using *tert*-butyl 2-aminoethylcarbamate or propylamine. Cleavage of the Boc group with TFA led to the corresponding squaramide **4.78** (Scheme 4.7).

Scheme 4.7. Synthesis of Mixed Squaramates 4.75-4.76 & Squaramides 4.78 and 4.117[a]

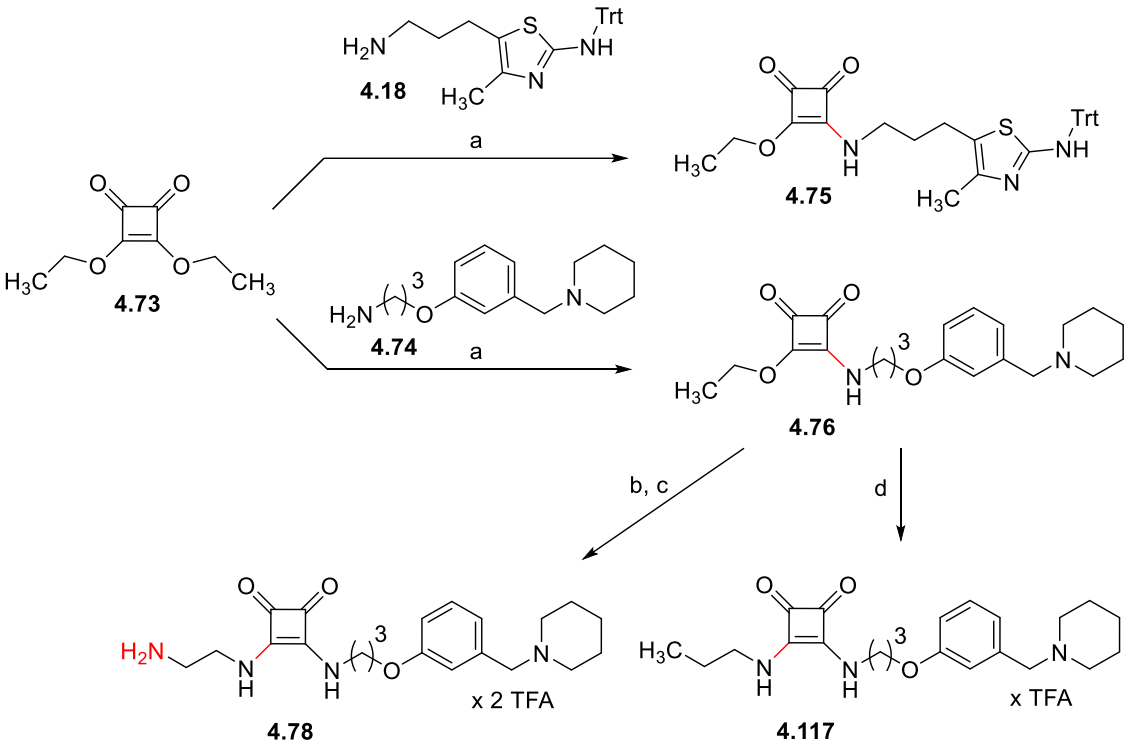

[a]Reagents and conditions: (a) EtOH, rt, 3 h or overnight, **4.75**: 90% and **4.76**: 100%; (b) *tert*-butyl 2-aminoethylcarbamate, EtOH, rt, overnight, **4.77**: 61%; (c) TFA, CH_2Cl_2, rt, overnight, 100%; (d) propylamine, EtOH, 70 °C, overnight, 69%.

4.2.1.7 Coupling of the Building Blocks with *O*-Alkylated 2-Arylbenzimidazoles

As shown in Scheme 4.8, the 2-arylbenzimidazoles **4.82-4.96** were synthesized according to the procedure of Savall et al.[22] The nucleophilic substitution reaction of the iodine derivatives (**4.79-4.81**) with the respective Trt-protected imidazole- (**4.4**, **4.26** and **4.66-4.72**), Trt-protected thiazole- (**4.17-4.18** and **4.35**), squaramide- (**4.78**) building blocks or 3-(3-(piperidin-1-ylmethyl)phenoxy)propan-1-amine (**4.74**) in the presence of K_2CO_3 in MeCN gave the secondary or tertiary amines. The iodine derivatives (**4.79-4.81**) were synthesized as published previously.[2] If necessary, the Trt protecting group was removed under acidic conditions. The purification by preparative HPLC led to the 2-arylbenzimidazoles **4.82-4.96** as TFA salts with purities ≥95%. The isolated yields were poor to moderate, ranging from 2-44%. The tertiary

amine **4.97** was synthesized from the secondary amine **4.86** by Eschweiler-Clarke reaction using an excess of formic acid and formaldehyde (Scheme 4.9).

Scheme 4.8. Synthesis of 2-Arylbenzimidazoles 4.82-4.96 [a]

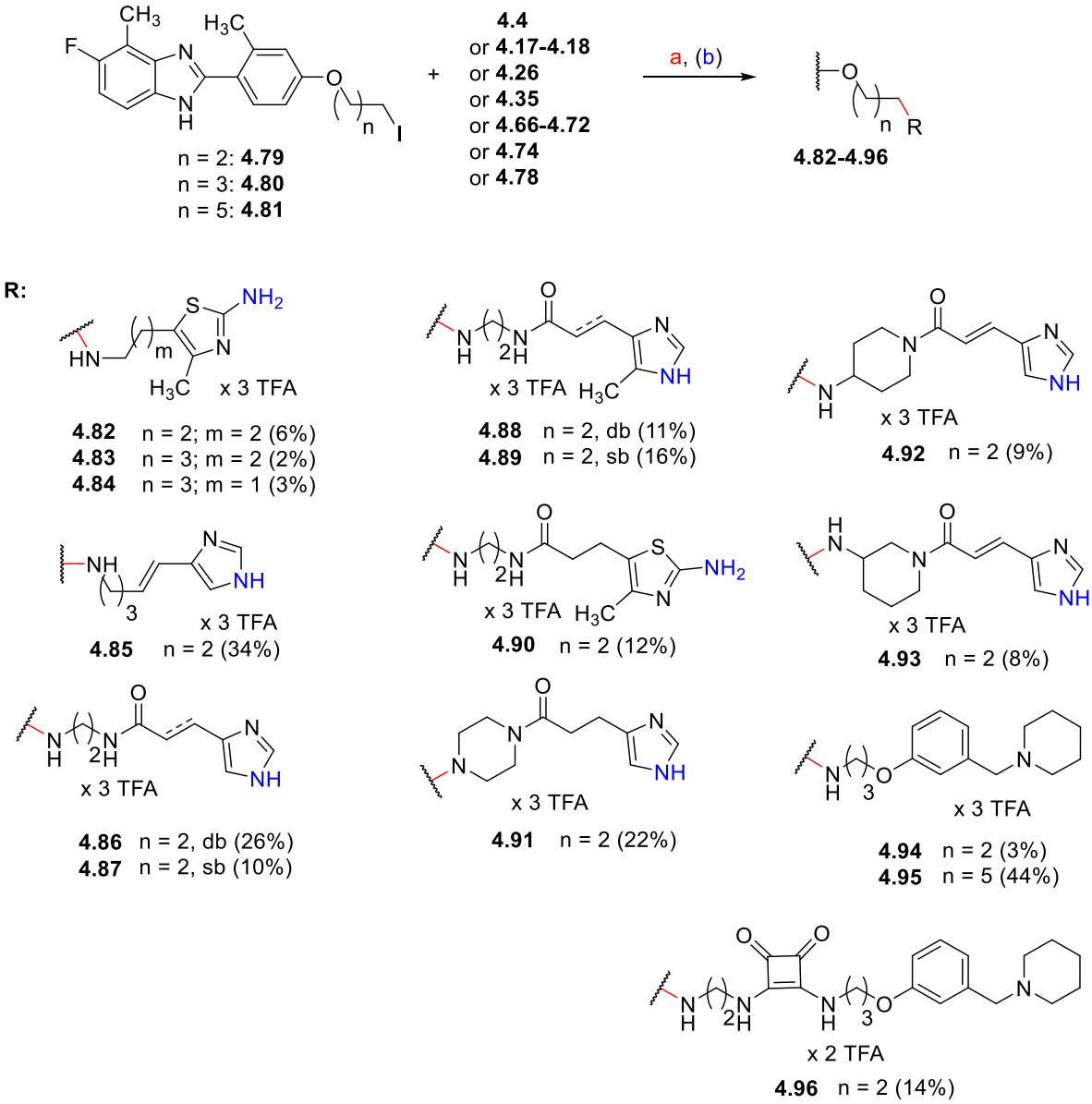

[a]Reagents and conditions: (a) K_2CO_3, MeCN, microwave, 130 °C, 20 min; (b) in case of **4.82-4.93**, TFA, CH_2Cl_2, rt, 7-18 h. db = double bound. sb = single bound. Isolated yields over one or two steps are given in brackets.

Scheme 4.9. Synthesis of 2-Arylbenzimidazole 4.97.[a]

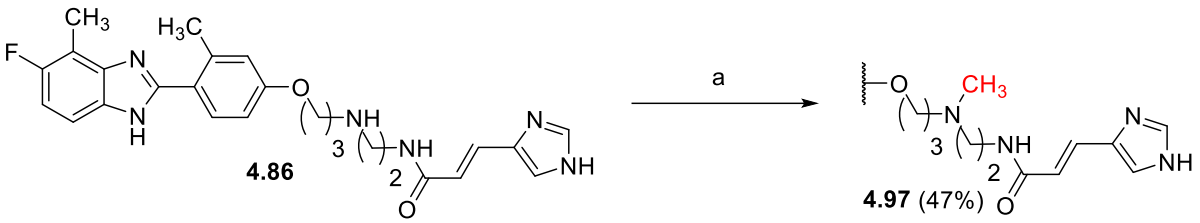

[a]Reagents and conditions: (a) formic acid, formaldehyde solution (37%, aq), 95 °C, 4 h. Isolated yield is given in brackets.

The synthesis of **4.102** and **4.103** followed the same alkylation principle (Scheme 4.10). *O*-Alkylation with Boc-protected 6-bromohexanamine **4.100** or Boc-protected 3-bromopropanamine **4.101** and the subsequent acidic deprotection of the Boc group yielded **4.102** and **4.103**, which were used as building blocks for further synthesis.

Scheme 4.10. Synthesis of 2-Arylbenzimidazoles 4.102-4.103.[a]

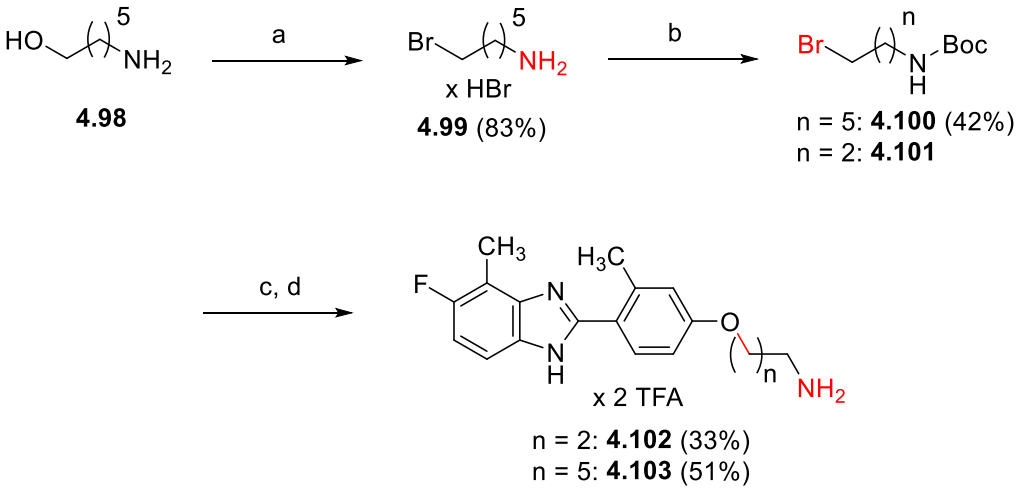

[a]Reagents and conditions: (a) HBr (48%, aq), reflux, 3 h, 83%; (b) Boc_2O, NaOH, H_2O/CH_2Cl_2, rt, 3 h, 42%; (c) 4-(5-fluoro-4-methyl-1*H*-benzo[*d*]imidazol-2-yl)-3-methylphenol[2], Cs_2CO_3, MeCN, microwave, 130 °C, 15 min; (d) TFA, CH_2Cl_2, rt, 7 h, **4.102**: 32%, **4.103**: 51%, over 2 steps.

The amines **4.102** and **4.103** were coupled to carboxylic acids **4.32** or **4.57** using EDC/HOBt followed by Trt- or Boc deprotection using TFA to give the amides **4.104**-**4.107** as TFA salts (cf. Scheme 4.11).

The amine **4.102** was treated with triphosgene to give the corresponding diisocyanate, which was allowed to react with mono-Boc-protected *S*-methylisothiourea[3] yielding the guanidinylating reagent **4.113** (cf. Scheme 4.11). The carbamoylguanidine-type ligands **4.114-4.116** were prepared by treating 3-(1-trityl-1*H*-imidazol-4-yl)-propylamine, **4.4** or **4.18** with the guanidinylating reagent **4.113** in the presence of $HgCl_2$ and NEt_3. The following acidic deprotection led to the 2-arylbenzimidazoles **4.114-4.116** as TFA salts (cf. Scheme 4.11).

The squaramides **4.108**-**4.110** were synthesized from the amines **4.102** or **4.103** and mixed squaramates **4.75** or **4.76** in EtOH at elevated temperature (Scheme 4.11). The reaction was very slow, so that the reaction mixture had to be stirred for up to 12 days to get the products in only acceptable yields (6-28%). **4.112** was synthesized in reverse. First, the amine **4.102** was reacted with **4.73** to the corresponding mixed squaramate **4.111**, which was then reacted with the propylamine. The reverse approach did not improve the yield over two steps (14%), and also did not shorten the reaction time.

Scheme 4.11. Synthesis of 2-Arylbenzimidazoles 4.104-4.110, 4.112 and 4.114-4.116.[a]

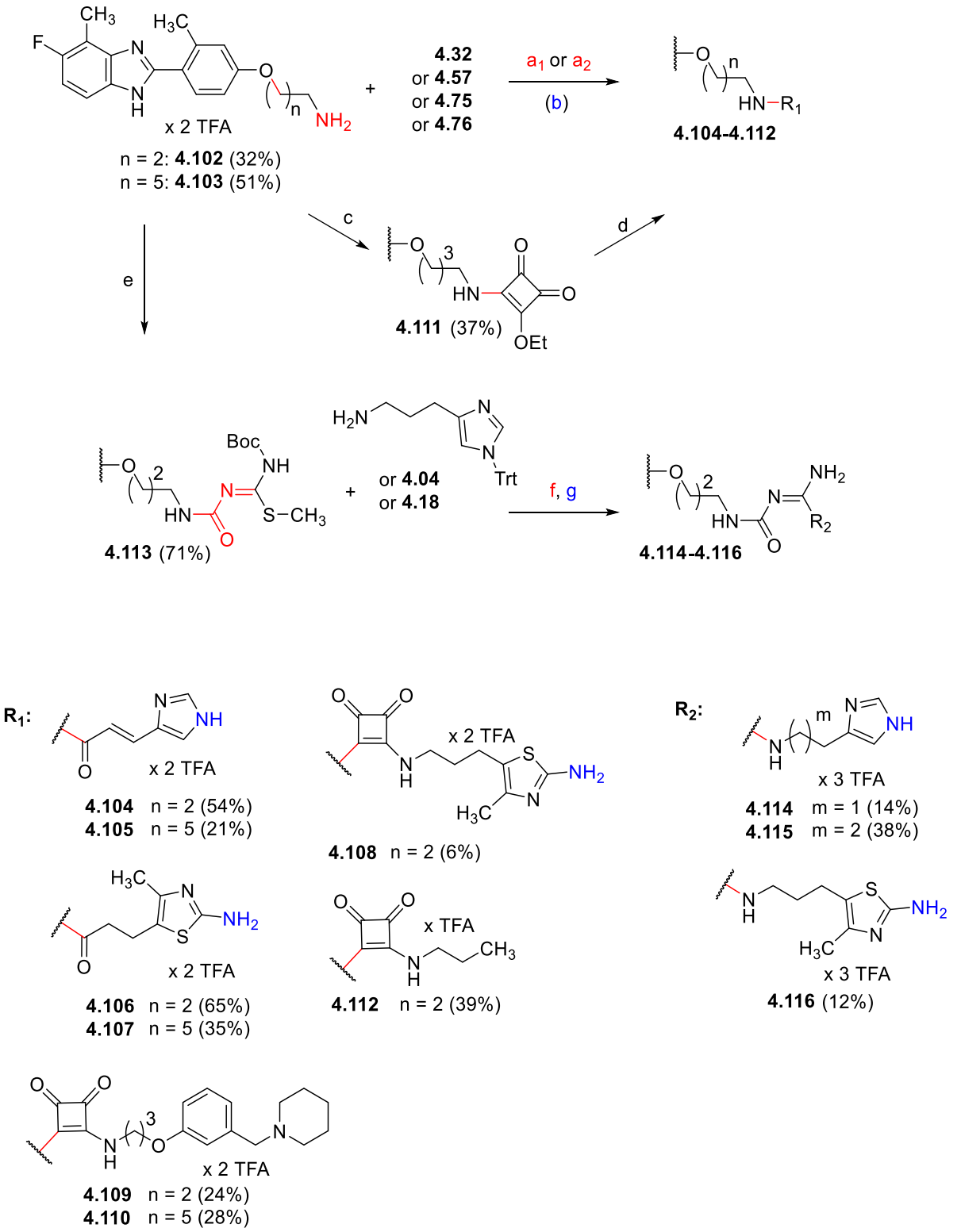

[a]Reagents and conditions: (a_1) **4.32** or **4.57**, EDC x HCl, HOBt x H_2O, DIPEA, DMF, 0 °C to rt, 14-18 h; (a_2) **4.75** or **4.76**, NEt_3, EtOH, 60 °C, 7-12 d; (b) TFA, CH_2Cl_2, rt, 7 h; (c) **4.73**, NEt_3, EtOH, rt, 18 d; (d) propylamine, EtOH, 70 °C, 24 h; (e) (1) triphosgene, DIPEA, CH_2Cl_2, 0 °C, 1 h; (2) *N*-*tert*-butoxycarbonyl-*S*-methylthiourea[3], CH_2Cl_2, 0 °C to rt, 3.5 h; (f) $HgCl_2$, NEt_3, CH_2Cl_2, rt, 4-18 h; (g) TFA, CH_2Cl_2, rt, 7-18 h. Isolated yields over one or two steps are given in brackets.

4.2.1.8 Synthesis of the Carbamoylguanidine 4.120

The protected carbamoylguanidine-type intermediate **4.119** was prepared by treating the building block PB506[2] (synthesized as described by Dr. Paul Baumeister[2]) with the guanidinylating reagent **4.118** (synthesized as described by Biselli et al.[5]) in the presence of $HgCl_2$ and NEt_3 (Scheme 4.12). Treating the protected carbamoylguanidine-type intermediate **4.119** first with H_2 and Pd/C and second with TFA gave compound **4.120**.

Scheme 4.12. Synthesis of Carbamoylguanidine-Type Ligand 4.120[a]

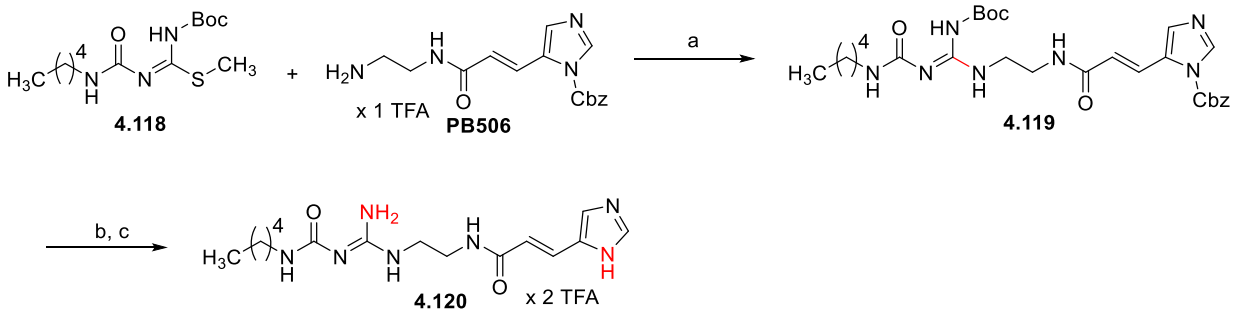

[a]Reagents and conditions: (a) NEt_3, $HgCl_2$, CH_2Cl_2, overnight, rt, 32%; (b) H_2 (8 bar), Pd/C, THF/MeOH, rt, 2 h; (c) TFA, CH_2Cl_2, 8 h, rt, 11% over 2 steps.

4.2.2 Covalent Binding Experiments

Bioactive compounds (e.g. afatanib, ibrutinib, AMG 510, VUF14480, cf. Figure 4.4) containing Michael acceptors are known to form irreversible addition products with cysteine residues in specific proteins.[23-30] Since PB513 also contains a Michael acceptor we wanted to investigate whether it is able to form a covalent adduct with glutathione or less sterically demanding L-cysteine in binding buffer at pH 7.4 (same conditions as in the binding assay) in a preliminary experiment. This is a literature known screening method to identify covalent modifiers.[25] For this purpose, PB513 was mixed with glutathione or L-cysteine in a 1:1 molar ratio and incubated for 5 h at 37 °C with shaking. Afterwards, the incubated mixtures were analyzed by LC-MS. PB513 did not react with either glutathione or L-cysteine in a covalent manner (Figures 4.5 & 4.6). Surprisingly, we observed a small peak with a mass of 479.2570 Da after the incubation of PB513 with L-cysteine, which equals the mass of the hydrogenated PB513 (cf. Figure 4.5B). This might be a side-product of the oxidation of L-cysteine to cystine (this was not investigated further). The reaction is known to occur in neutral to alkaline aqueous solution when air is admitted via a radical mechanism (thio-ene-reaction).[31-32]

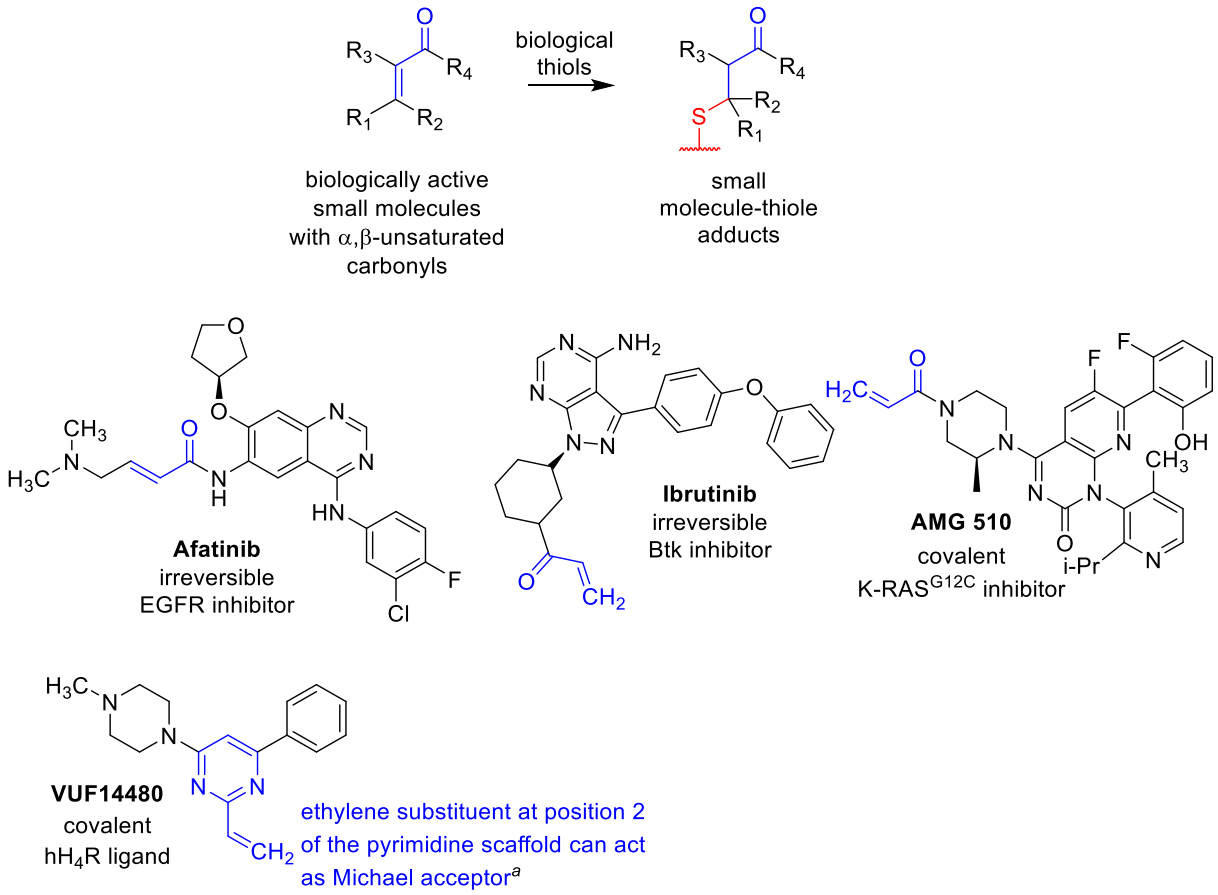

Figure 4.4. Published covalent ligands containing Michael acceptors.[23-25] [a]Karagiorguo et al.[33] & Liu et al.[34] EGFR: epidermal growth factor receptor. Btk: Brutons`s tyrosine kinase. KRAS^{G12C}: Kirsten rat sarcoma protein p.G12C mutant.

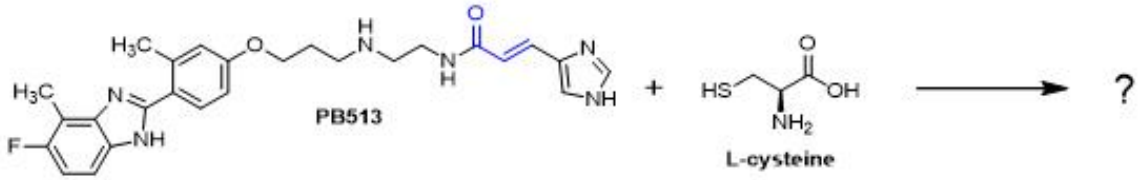

A

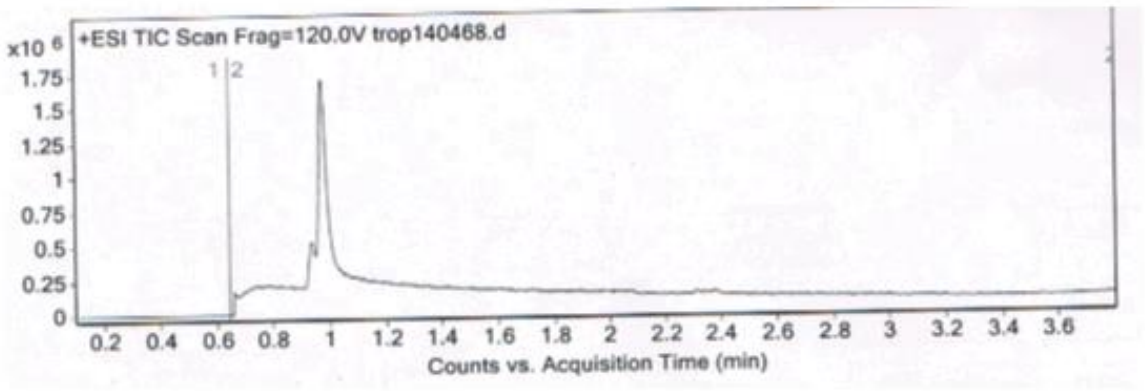

B

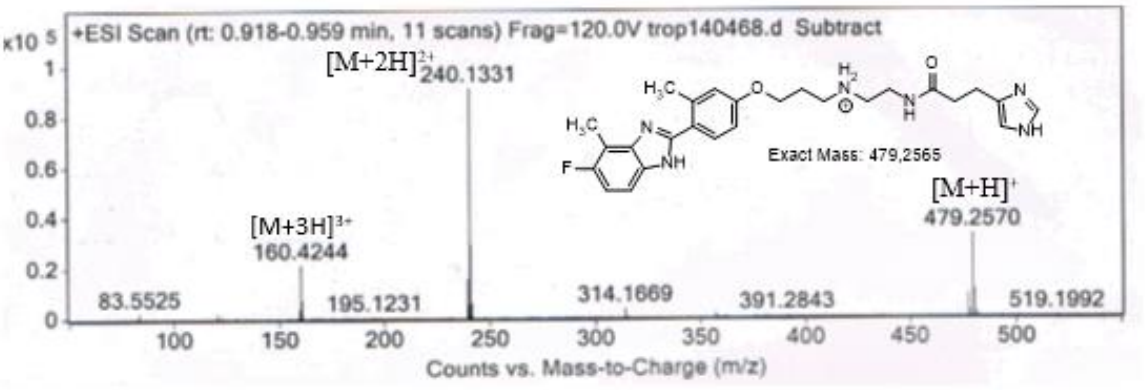

C

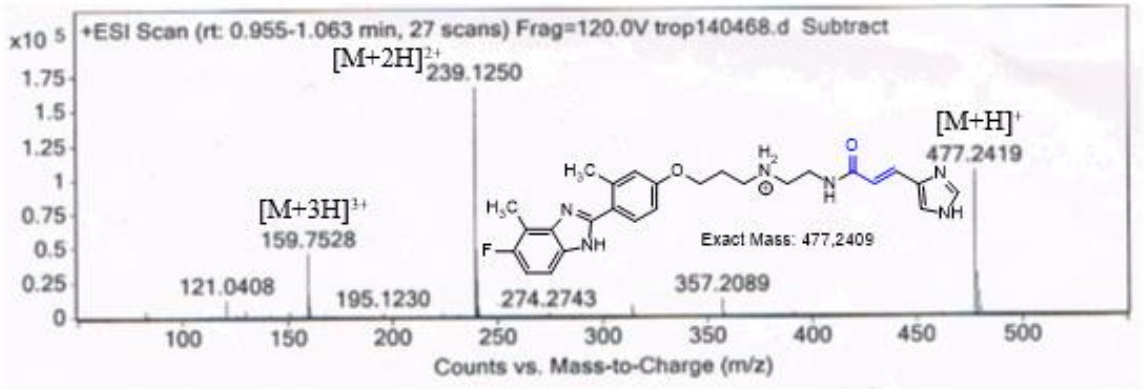

Figure 4.5. Reaction control of the L-cysteine addition to PB513 by LC-MS. **A**: + ESI total ion current scan. **B**: + ESI scan (t_R = 0.918-0.959 min). **C**: + ESI scan (t_R = 0.955-1.063 min).

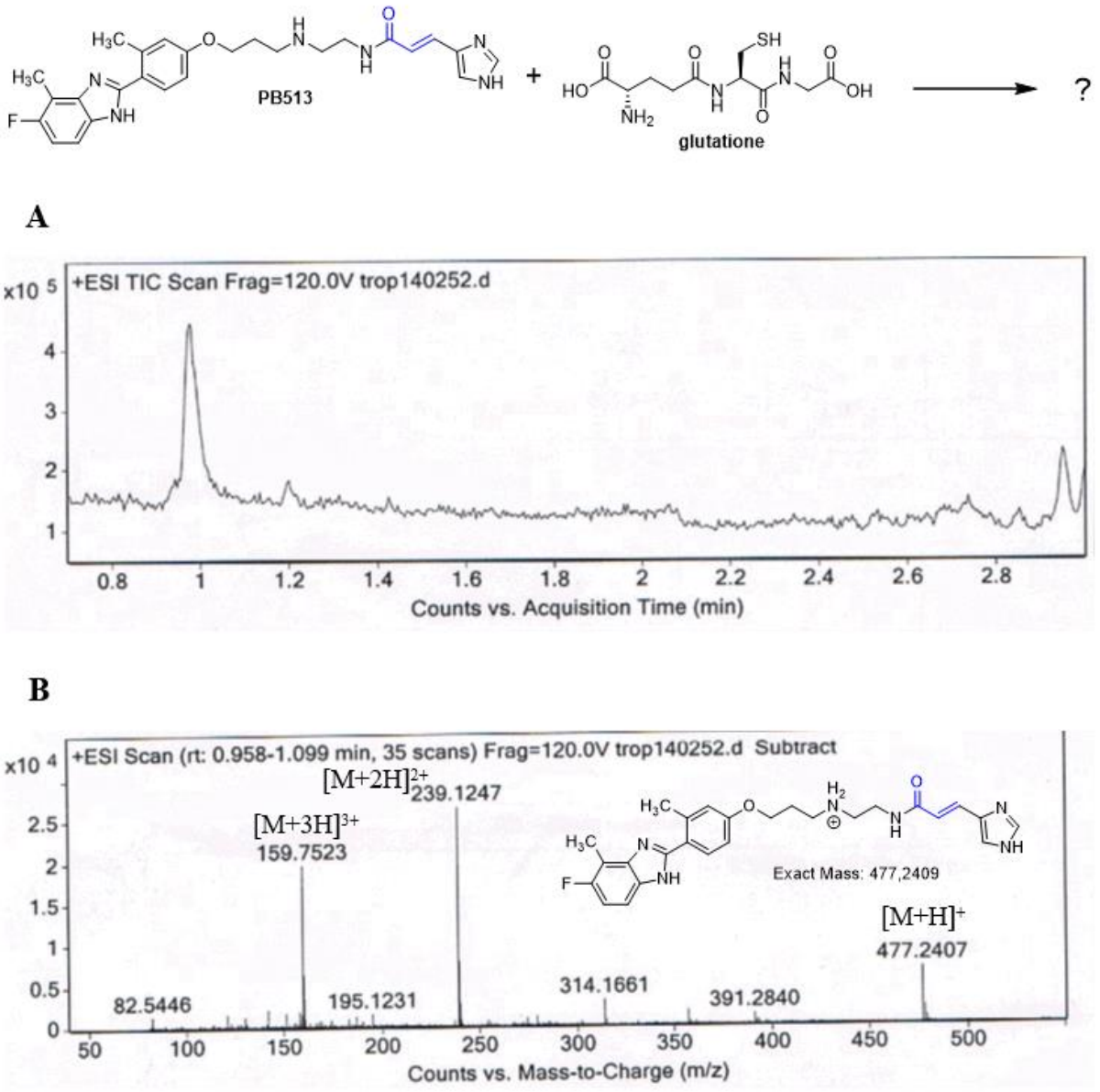

Figure 4.6. Reaction control of the glutathione addition to PB513 by LC-MS. **A**: + ESI total ion current scan. **B**: + ESI scan (t_R = 0.958-1.099 min).

4.2.3 Pharmacological Studies

The synthesized target compounds **4.82-4.97**, **4.104-4.110**, **4.112**, **4.114-4.117** and **4.120** (cf. Figure 4.7) were characterized with respect to binding at H_{1-4} receptors (cf. Table 4.1). Moreover, functional activity of compounds having a pK_i >6 was determined at the hH_2R using [^{35}S]GTPγS binding assay as well as mini-G protein and β-arrestin2 recruitment assays (cf. Table 4.2). Not all compounds (pK_i >6) could be investigated using the [^{35}S]GTPγS binding assay, because the [^{35}S]GTPγS reagent was no longer commercially available in sufficient purity and at an affordable price throughout the timeframe of this project.[35]

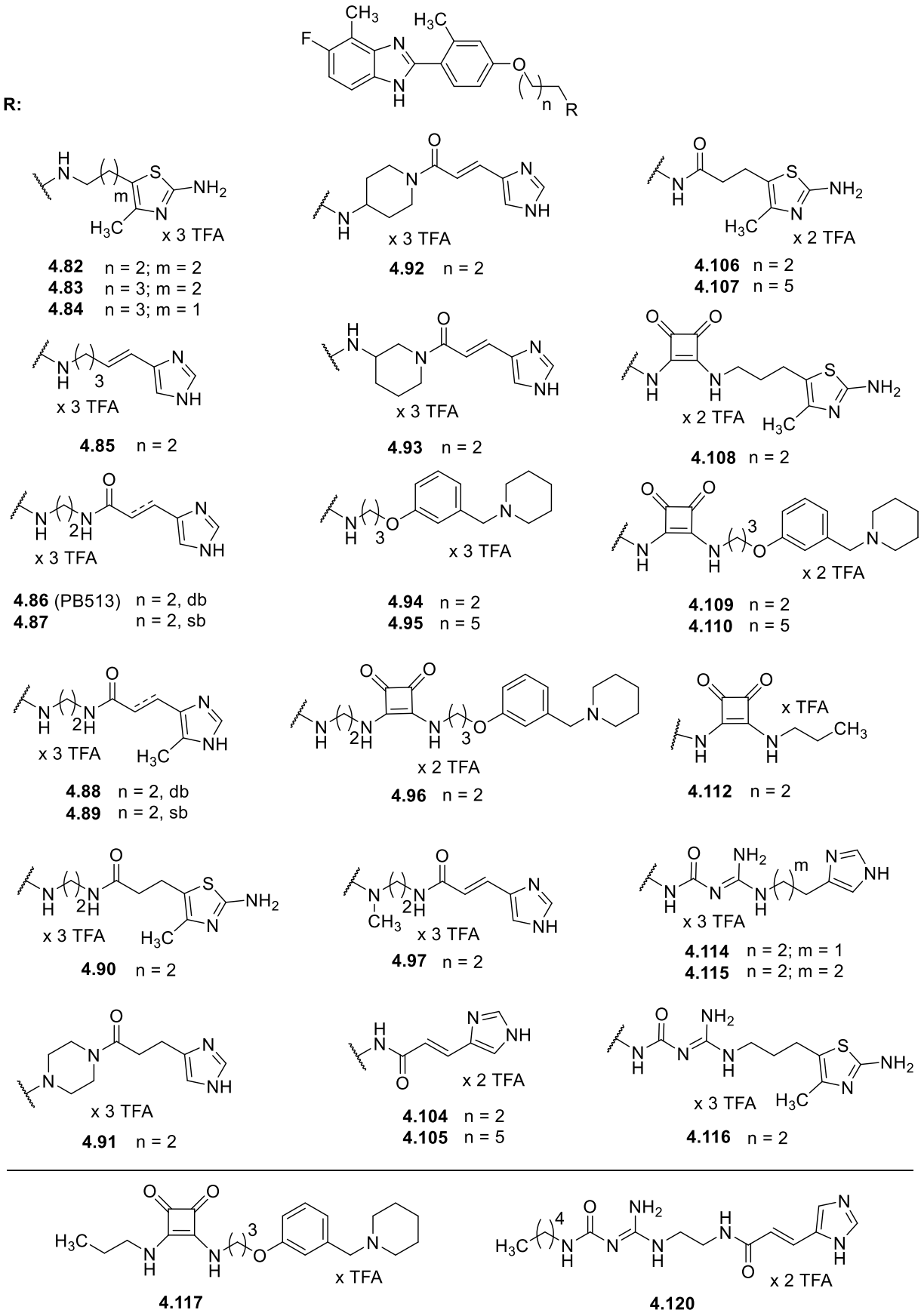

Figure 4.7. Structural overview of investigated 2-arylbenzimidazoles **4.82**-**4.97**, **4.104**-**4.110**, **4.112**, **4.114**-**1.116**, the squaramide **4.117**, and the carbamoylguanidine **4.120**.

4.2.3.1 H_2R Affinities and Receptor Subtype Selectivities

To study the subtype selectivity, the compounds **4.82-4.97**, **4.104-4.110**, **4.112**, **4.114-4.117** and **4.120** were tested at the $hH_{1\text{-}4}R$ in competition binding studies using membrane preparations of Sf9 insect cells expressing the hH_1R + RGS4, hH_2R-$G_{s\alpha S}$ fusion protein, hH_3R + $G_{\alpha i2}$ + $G_{\beta 1\gamma 2}$ or hH_4R + $G_{\alpha i2}$ + $G_{\beta 1\gamma 2}$, respectively.[4] The results are summarized in Table 4.1. Moreover, the resynthesized compound PB513 (H_2R-$G_{s\alpha S}$: pK_i: 7.35, cf. Table 4.1) was investigated again in the same assays, but it was not possible to reproduce the results obtained from Dr. P. Baumeister exactly (H_2R–$G_{s\alpha S}$: pK_i: 7.84[2]). The affinity of PB513 to the H_3R (pK_i: 6.57) and particularly to the H_4R (pK_i: 6.19) was higher as reported previously (H_3R pK_i: 6.16[2], H_4R pK_i: 5.67[2]). Nonetheless, due to the high H_2R-$G_{s\alpha S}$ affinity it was worth to further explore the SAR of 2-arylbenzimidazoles as H_2R ligands.

Removing (**4.105**, pK_i: <5) or methylation (**4.97**, pK_i: 5.98) of the secondary amine in the aliphatic chain of **4.86** (PB513, pK_i: 7.35) resulted in a dramatic affinity drop at the hH_2R-$Gs_{\alpha s}$ fusion protein. Therefore, the synthesis of a radioligand by methylation the secondary amine of PB513 would not be advised. The same observation regarding the H_2R-$Gs_{\alpha s}$ affinity was made by removing the double bound (**4.87**, pK_i: 6.18). The removal of the amide moiety (**4.85**) did not change the H_2R-$Gs_{\alpha s}$ affinity (pK_i: 7.55) but increased the hH_3- (pK_i: 7.50) and hH_4- (pK_i: 7.38) receptor affinities. The incorporation of the ethyl linker into an aliphatic ring **4.91** (piperazine, pK_i: 5.25), **4.92** (4-aminopiperidine, pK_i: 6.33), **4.93** (3-aminopiperidine, pK_i: 6.48) and the exchange of imidazole ring by 4-methylimidazole (**4.88** (pK_i: 6.30), **4.89** (pK_i: 6.42)) or 2-aminothiazole (**4.90**, pK_i: 5.60) had also a negative effect on the H_2R-$G_{s\alpha S}$ affinity. For a better visualization of the effects of the structural changes of PB513 on the H_2R affinity and subtype selectivity, the obtained results are also shown in a bar chart (Figure 4.8).

Moreover, introduction of 3-[3-(piperidin-1-ylmethyl)phenoxy)propan-1-amine (**4.74**, a well-known substructure of H_2R ligands, e.g. (iod)aminopotentidine[36], BMY25368[6], UR-DE257[8]) resulted in compounds **4.94** (propyl-spacer, pK_i: 6.39) and **4.95** (hexyl-spacer, pK_i: 6.77) with three-digit nanomolar affinity. The introduction of the squaramide- (e.g. **4.96**, **4.109**, **4.110**) or carbamoylguanidine-group (**4.114-4.116**) in the linker was well tolerated and resulted in some compounds with two-digit nanomolar affinity (pK_i: 7.07-7.76). In conclusion, squaramide **4.110** showed the best subtype selectivity profile (K_i $H_{1,3,4}R$/K_i H_2R; H_1:H_3:H_4 87:19:131), while having two-digit nanomolar H_2R-$G_{s\alpha S}$ affinity (pK_i: 7.30). However, since all of the compounds did not show acceptable (selectivity ratios > 100) subtype selectivity, we did not further investigate them for their binding affinity towards dopamine receptors.

Table 4.1. Binding Data (pK_i values) at Histamine Receptor Subtypes[a]

compd.	pK_i								H_2R selectivity $K_i(H_{1,3,4}R)/K_i(H_2R)$		
	hH_1R[a]	N	**hH_2R-$G_{s\alpha s}$**[b]	N	**hH_3R**[c]	N	**hH_4R**[d]	N	H_1	H_3	H_4
His	5.62 ± 0.03[37]	3	6.58 ± 0.04[13]	48	7.59 ± 0.01[13]	42	7.60 ± 0.01[13]	45	9	0.1	
4.82	5.13 ± 0.16*	2	6.32 ± 0.16	4	5.98 ± 0.08*	2	7.32 ± 0.13	3	16	2	0.1
4.83	<5	2	6.21 ± 0.17	4	5.66 ± 0.16*	2	6.06 ± 0.07	3	>16	4	1
4.84	4.96 ± 0.09*	2	6.53 ± 0.12	3	6.03 ± 0.02*	2	6.64 ± 0.13	3	37	3	0.8
4.85	5.49 ± 0.03*	2	7.55 ± 0.11	3	7.50 ± 0.08	3	7.38 ± 0.04	3	115	1	1
4.86 (PB513[2])	<5	2	7.35 ± 0.09	3	6.57 ± 0.07	3	6.19 ± 0.11	3	>223	6	14
4.87	<5	2	6.18 ± 0.14	3	7.37 ± 0.10	3	6.24 ± 0.13	3	>15	0.1	0.9
4.88	5.08 ± 0.10*	2	6.30 ± 0.15	3	6.60 ± 0.04	3	5.21 ± 0.01*	2	17	0.5	12
4.89	5.16 ± 0.01*	2	6.42 ± 0.04	3	6.04 ± 0.17*	2	6.23 ± 0.11	3	18	2	2
4.90	<5	2	5.60 ± 0.09	3	5.31 ± 0.14*	2	5.02 ± 0.12	3	>4	2	4
4.91	5.41 ± 0.12*	2	5.25 ± 0.04	3	6.55 ± 0.04	3	6.19 ± 0.14	3	0.7	0.1	0.1
4.92	4.98 ± 0.12*	2	6.33 ± 0.06	3	5.82 ± 0.02*	2	5.04 ± 0.03*	2	22	3	19
4.93	<5	2	6.48 ± 0.10	3	6.32 ± 0.08	3	5.04 ± 0.10	3	>30	1	28
4.94	5.66 ± 0.12	4	6.39 ± 0.17	4	7.38 ± 0.10	3	5.35 ± 0.19	3	5	0.1	11
4.95	6.29 ± 0.01	3	6.77 ± 0.17	4	7.45 ± 0.09	3	5.66 ± 0.12*	2	3	0.2	13
4.96	5.66 ± 0.11	4	7.51 ± 0.11	3	7.13 ± 0.10	3	5.32 ± 0.03*	2	70	2	155
4.97	<5	2	5.98 ± 0.10	3	6.64 ± 0.11	3	5.80 ± 0.03*	2	>10	0.2	1.5
4.104	<5	2	<5	2	4.92 ± 0.17*	2	5.06 ± 0.22*	2	-	-	-
4.105	<5	2	<5	2	<5	2	5.12 ± 0.19*	2	-	-	-
4.106	<5	2	5.35 ± 0.15	3	4.96 ± 0.10*	2	<5	2	>2	2	>2
4.107	<5	2	5.31 ± 0.12	3	4.97 ± 0.20*	2	<5	2	>2	2	>2
4.108	<5	2	6.45 ± 0.13	3	<5	2	<5	3	>28	>28	>28
4.109	5.35 ± 0.12*	2	7.38 ± 0.10	3	6.57 ± 0.10	3	5.48 ± 0.15*	2	107	6	79

Table 4.1. (continued)

4.110	5.36 ± 0.04*	2	7.30 ± 0.14	3	6.02 ± 0.10*	2	5.18 ± 0.04*	2	87	19	131
4.112	<5	2	<5	2	<5	2	4.90 ± 0.16*	2	-	-	-
4.114	5.89 ± 0.13	3	7.76 ± 0.10	3	8.24 ± 0.07	3	6.53 ± 0.16	3	74	0.3	17
4.115	6.06 ± 0.01*	2	7.76 ± 0.09	3	8.22 ± 0.01	3	7.34 ± 0.09	3	50	0.3	3
4.116	5.64 ± 0.06*	2	7.07 ± 0.09	3	6.02 ± 0.07	3	5.97 ± 0.14*	2	26	11	13
4.117	<5	3	7.55 ± 0.04	3	n.d.		n.d.		>355	-	-
4.120	n.d.		5.36 ± 0.12*	2	n.d.		n.d.		-	-	-

[a]Competition binding assay on membrane preparations of Sf9 insect cells expressing the hH_1R + RGS4, the hH_2R-$G_{s\alpha S}$, the hH_3R + $G_{\alpha i2}$ + $G_{\beta 1\gamma 2}$ or the hH_4R + $G_{\alpha i2}$ + $G_{\beta 1\gamma 2}$. [b]Displacement of [^{3}H]mepyramine (K_d = 4.5 nM[4], c = 5 nM). [c]Displacement of [^{3}H]UR-DE257[8] (K_d = 12.1 nM[38], c = 20 nM). [d]Displacement of [^{3}H]UR-PI294[39] (K_d = 3 nM[40], c = 2 nM). [e]Displacement of [^{3}H]histamine (K_d = 47.5 nM[41], c = 30 nM). Presented are mean values ± SEM (N ≥3) or SE (N = 2, indicated with *) of N (2-3 for pK_i values ≤ 6.25 or 3-4 for pK_i values > 6.25) independent experiments (each performed in duplicate or triplicate). n.d.: not determined. Displacement curves of representative 2-arylbenzimidazoles **4.85**, **4.86** (PB513), **4.88**, **4.108**, **4.110** and **4.114** are shown in Appendix 3 (Figure App3.97).

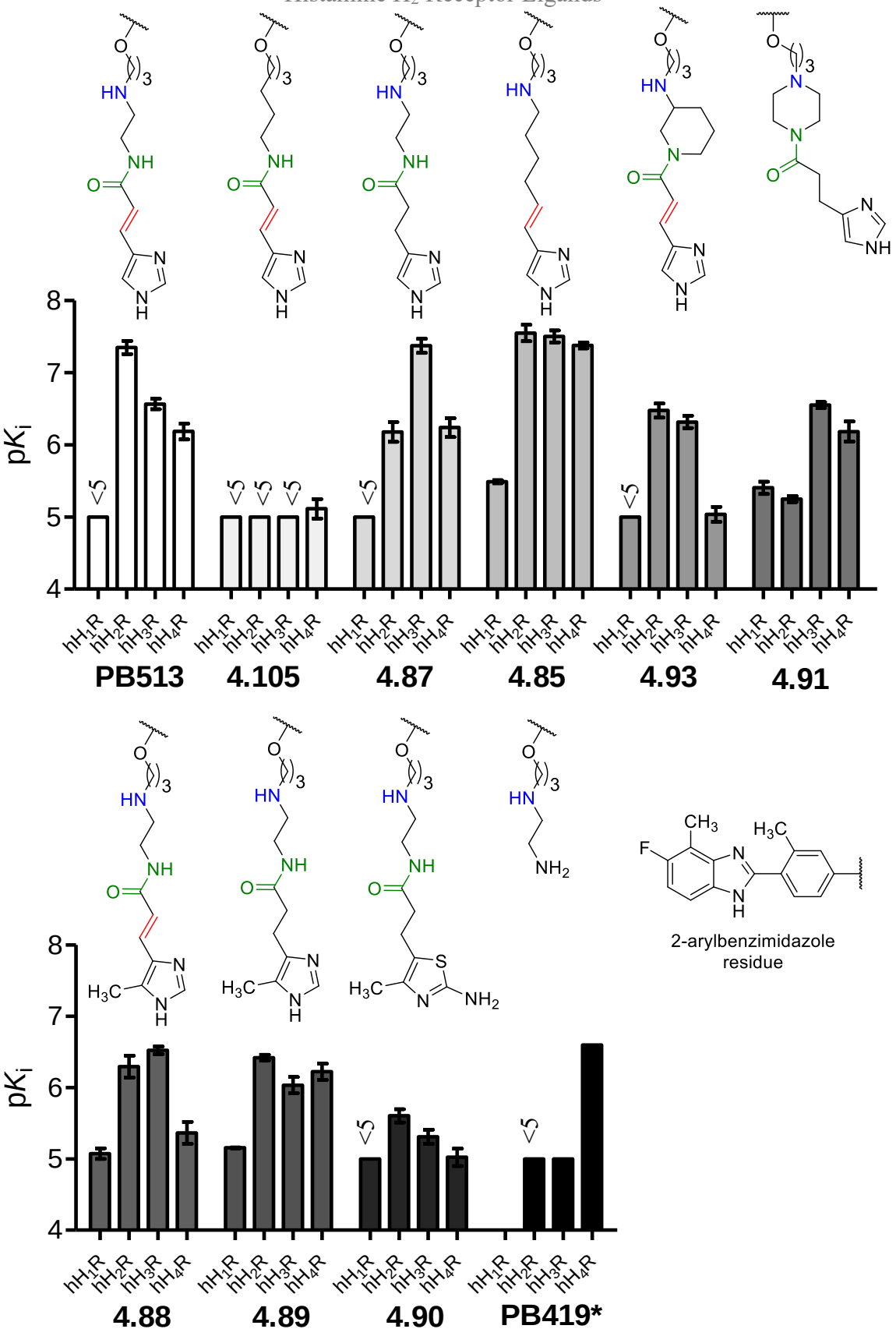

Figure 4.8. Selectivity profiles of selected 2-arylbenzimidazoles. *Binding data from PhD thesis of Dr. P. Baumeister.

4.2.3.2 Role of a 2-Arylbenzimidazole Motif for the hH2R Affinity in 4.109, 4.110 and PB513

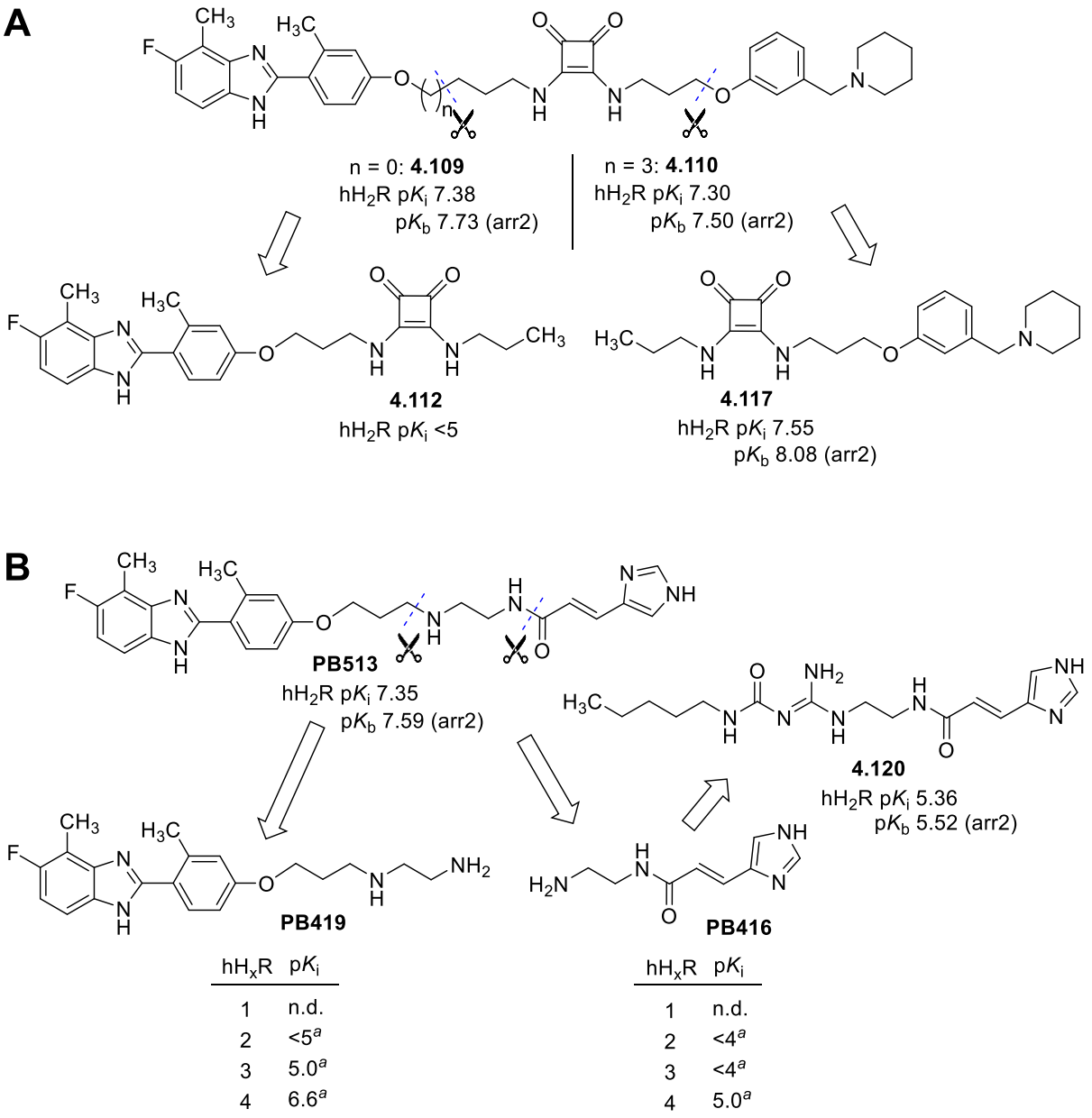

hH_xR	pK_i
1	n.d.
2	<5[a]
3	5.0[a]
4	6.6[a]

hH_xR	pK_i
1	n.d.
2	<4[a]
3	<4[a]
4	5.0[a]

Figure 4.9. An investigation into the importance of the role of a 2-arylbenzimidazole motif for the hH_2R affinity of **4.109**-**4.110** (**A**) & PB513 (**B**). [a]Data from the Ph.D. thesis of Dr. P. Baumeister.[2]

In order to investigate whether the 2-arylbenzimidazole motif in compounds **4.109** and **4.110** has any influence on H_2R-$G_{s\alpha S}$ affinity and subtype-selectivity, we synthesized and tested the two control compounds **4.112** and **4.117** (Figure 4.9A). The binding data indicate that the 2-arylbenzimidazole residue does apparently not contribute to the H_2R-$G_{s\alpha S}$ affinity because the control substance **4.117** (pK_i: 7.55), without the 2-arylbenzimidazole, had a slightly higher

affinity at the H_2R-$G_{s\alpha S}$ fusion protein (cf. pK_i: **4.109**: 7.38; **4.110**: 7.30). In addition, the substance **4.112** without the 3-(piperidin-1-ylmethyl)phenol showed no affinity within the investigated concentration range at the H_2R-$G_{s\alpha S}$. (pK_i <5).

In contrast to these observations, the combined molecule PB513 possessed a double-digit nanomolar affinity for H_2R-$G_{s\alpha S}$ (pK_i: 7.35), while the individual components PB416 and PB419 had no or only low affinity for the H_2R-$G_{s\alpha S}$ (pK_i: <5) (Figure 4.9B). Moreover, the urocanic acid amide PB416 was introduced in the general structure of a typical carbamoylguanidine-type ligand (**4.120**, cf. Figure 4.9B and Scheme 4.12). The resulting antagonist **4.120** showed also only low affinity for the H_2R-$G_{s\alpha S}$ (pK_i: 5.36, cf. Table 4.1 or Figure 4.9B). These results indicate that both the 2-arylbenzimidazole and the urocanic acid amide moiety are necessary for the high H_2R affinity of PB513 to the H_2R.

4.2.3.3 Functional Characterization of Selected 2-Arylbenzimidazoles at the Human H_2R in the [^{35}S]GTPγS Binding, mini-G Protein and β-Arrestin2 Recruitment Assays

The potencies (pEC_{50}), efficacies (E_{max}) and dissociation constants (pK_b, in case of antagonists or inverse agonists) of the selected 2-arylbenzimidazoles (pK_i >6) are presented in Table 4.2. Most of the synthesized 2-arylbanzimidazoles were antagonists (**4.85-4.86**, **4.93-4.96**, **4.109-4.110** and **4.117**) in the [^{35}S]GTPγS binding and the β-arrestin2 recruitment assays (Table 4.2). In the mini-G protein assay the same compounds showed inverse agonism. For this reason, both pEC_{50} (agonist mode) and the pK_b (antagonist mode) values were determined for these molecules (Table 4.2). However, due to the low signal to noise (S/N) ratio of 1.5 in the [^{35}S]GTPγS binding assay (cf. S/N 12 in the mini-G protein recruitment assay),[42] potential inverse agonism might not be detectable. The determined pK_b values of the antagonists ([^{35}S]GTPγS or β-arrestin2) or inverse agonists (mGs) were in good agreement with the pK_i values obtained from the radioligand competition binding assay (cf. Table 4.1). Exceptions were the squaramide-containing compounds **4.109**-**4.110**, which showed pK_b values (pK_b: 8.54-8.59, cf. Table 4.2) higher than the pK_i values (pK_i: 7.30-7.38, cf. Table 4.1) in the mini-G protein recruitment assay by more than one order of magnitude. It is likely that due to the above-mentioned low S/N, compounds **4.82**-**4.84** and **4.88** are antagonists in [^{35}S]GTPγS binding assay and at the same time show partial agonistic behavior in the mini-G protein recruitment assay. Compound **4.88** is specifically interesting since its additional methyl group in the 4-position of imidazole reverses inverse agonism (cf. PB513, Table 4.2) to weak agonism in mini-G protein recruitment assay. **4.89** and **4.92** were inactive in the mini-G protein and β-arrestin2 recruitment assays. The carbamoylguanidines **4.114**-**4.116** were agonists. Finally, the

synthesized aryl benzimidazole series incorporates a few G-protein biased H_2R partial agonists [e.g. **4.108**: $E_{max} = 0.56$ ([^{35}S]GTPγS), $E_{max} = 0.73$ (mGs), $E_{max} = 0.06$ at c = 10 µM (β-arrestin2), cf. Table 4.2] which could not be exploited further due to the lack of subtype selectivity.

As a result, (inverse) agonism or antagonism seem to depend on the basic head group and not on the 2-arylbenzimidazole or the type of basic center in the spacer. This observation could be confirmed since the introduction of a head group, which already lead to agonism in a different H_2R ligand class series, also results in agonists in this ligand class (**4.108**, cf. Table 4.2). The same is true for antagonism (**4.109** and **4.110**, cf. Table 4.2**)**.

Table 4.2. H_2R Agonist Potencies (pEC_{50}) and Efficacies (E_{max}) or Antagonism (pK_b)

	[^{35}S]GTPγS binding[a]				**mGs recruitment**[b]				**β-arrestin2 recruitment**[c]			
compd.	(pK_b) or pEC_{50}	N	E_{max}	N	(pK_b) or pEC_{50}	N	E_{max}	N	(pK_b) or pEC_{50}	N	E_{max}	N
His	5.85 ± 0.06[4]		1.00[4]	4	6.94 ± 0.06[42]	9	1.00[42]	9	5.42 ± 0.02[43]	4	1.00[43]	4
UR-DE257[8]	(7.42)[8]	-	0.08[8]	-	7.28 ± 0.08 (7.97 ± 0.10)	3 4	-0.11 ± 0.02	3	(8.03 ± 0.06)	3	0.00 ± 0.01†	3
4.82	(5.96 ± 0.29*)	2	-0.03 ± 0.17†*	2	5.73 ± 0.04	3	0.22 ± 0.01	3	(6.31 ± 0.17)	7	-0.02 ± 0.01†	3
4.83	(5.98 ± 0.11*)	2	-0.04 ± 0.07†*	2	5.51 ± 0.16	3	0.32 ± 0.04	3	(6.06 ± 0.09)	5	-0.04 ± 0.01†	3
4.84	n.d.	-	n.d.	-	6.15 ± 0.04	3	0.14 ± 0.02	3	(6.34 ± 0.06)	3	-0.02 ± 0.01†	3
4.85	(7.95 ± 0.05)	3	-0.12 ± 0.03†	3	6.55 ± 0.08 (6.95 ± 0.04)	3 3	-0.11 ± 0.02	3	(7.30 ± 0.05)	3	-0.03 ± 0.02†	3
4.86 (PB513[2])	(7.73)[2]	-	-0.20[2]	-	6.80 ± 0.09 (6.99 ± 0.09)	3 3	-0.09 ± 0.01	3	(7.59 ± 0.09)	3	-0.00 ± 0.01†	3
4.87	(5.27 ± 0.14)	3	-0.18 ± 0.01†*	2	(<5)	3	-0.03 ± 0.01†	3	(5.77 ± 0.03)	3	-0.02 ± 0.01†	3
4.88	n.d.	-	-0.19 ± 0.10†*	2	5.76 ± 0.10	3	0.16 ± 0.04†	3	(5.94 ± 0.07)	4	n.a.	3
4.89	n.d.	-	n.d.	-	(<5)	3	-0.03 ± 0.01†	4	(<5)	3	-0.05 ± 0.02†	3
4.92	n.d.	-	n.d.	-	(<5)	3	-0.02 ± 0.02†.	3	(<5)	3	0.00 ± 0.01†	3

Table 4.2. (continued)

4.93	(6.15 ± 0.29*)	2	-0.14 ± 0.05†*	2	6.25 ± 0.08 (6.62 ± 0.04)	4 3	-0.13 ± 0.02	4	(7.06 ± 0.04)	3	-0.01 ± 0.02†	3
4.94	(6.48 ± 0.06)	3	0.01 ± 0.17†*	2	<5 (6.18 ± 0.02)	3 3	-0.10 ± 0.02†	3	(6.25 ± 0.09)	3	-0.01 ± 0.01†	3
4.95	(6.78 ± 0.27)	3	-0.05 ± 0.08†*	2	5.87 ± 0.01 (6.25 ± 0.05)	4 3	-0.14 ± 0.01	3	(6.56 ± 0.13)	5	-0.04 ± 0.02†	3
4.96	(7.55 ± 0.04)	3	-0.03 ± 0.01†.	3	6.87 ± 0.08 (7.77 ± 0.06)	4 3	-0.12 ± 0.02	4	(7.75 ± 0.11)	3	-0.05 ± 0.03†	3
4.108	7.09 ± 0.05	3	0.56± 0.06	3	7.18 ± 0.04	3	0.73 ± 0.03	3	(6.80 ± 0.13)	4	0.06 ± 0.02†	5
4.109	(7.39 ± 0.13)	3	-0.14 ± 0.06†*	2	7.28 ± 0.17 (8.59 ± 0.05)	3 3	-0.10 ± 0.01	3	(7.73 ± 0.11)	3	-0.03 ± 0.04†	3
4.110	(7.80 ± 0.10)	3	-0.12 ± 0.06†*	2	7.03 ± 0.15 (8.54 ± 0.09)	5 3	-0.13 ± 0.01	5	(7.50 ± 0.16)	5	-0.02 ± 0.01†	3
4.114	n.d.	-	n.d.	-	6.59 ± 0.07	3	0.83 ± 0.03	3	6.38 ± 0.13	3	0.10 ± 0.02	4
4.115	7.53 ± 0.05	4	0.64 ± 0.04	4	7.70 ± 0.21	3	0.94 ± 0.04	3	6.58 ± 0.14	5	0.56 ± 0.10	5
4.116	7.45 ± 0.26	4	0.58 ± 0.09	4	7.36 ± 0.20	3	0.91 ± 0.05	3	6.68 ± 0.09	4	0.18 ± 0.04	4
4.117	n.d.	-	n.d.	-	7.16 ± 0.05 (8.13 ± 0.11)	3 4	-0.10 ± 0.01	3	(8.08 ± 0.02)	3	-0.02 ± 0.01†	3

Presented are mean values ± SEM (N ≥ 3) or SE (N = 2, indicated with *) of N independent experiments (each performed in duplicate or triplicate). Data were analyzed by nonlinear regression and best fitted to sigmoidal concentration-response curves. [a][^{35}S]GTPγS binding assays on membrane preparations of Sf9 insect cells expressing the hH_2R-$G_{s\alpha S}$.[4, 44] Antagonism was determined in the presence of 1 µM histamine. [b]Mini-G protein recruitment assay was performed using HEK293T NlucN-mGs/hH_2R-NlucC cell line.[42] Antagonism was determined in the presence of 1 µM histamine. [c]β-Arrestin2 recruitment assay was performed using HEK293T-ARRB2-hH_2R cell line.[38, 43] Antagonism was determined in the presence of 8 µM histamine. E_{max}: maximum response relative to histamine (E_{max} = 1.00 and buffer control (E_{max} = 0.00). †E_{max} at c = 10 µM; four-parameter logistic fits of the data from individual experiments failed. pK_b = -logK_b. The K_b value was calculated from the corresponding IC_{50} values by using the Cheng-Prusoff equation.[45] n.d.: not determined. Concentration-response curves of representative 2-arylbenzimidazoles **4.85**, **4.86** (PB513), **4.88**, **4.108**, **4.110** and **4.114** are shown in Appendix 3 (Figure App3.98-App3.100).

4.3 Summary and Conclusion

In search for new H_2R ligands which should not bind to dopamine receptors, we synthesized and tested 27 new 2-arylbenzimidazoles based on the recently reported high affinity H_2R antagonist PB513. The synthesized compounds showed low to high affinity to the H_2R-$G_{s\alpha S}$ fusion protein (pK_i: <5-7.76), depending on their structural features. We found that the following structural motifs in PB513 are important for the H_2R affinity: 2-arylbenzimidazole, sec. amine, double bond, and the imidazole. The amide group in PB513 is not important for H_2R affinity but for the subtype selectivity. We also observed that the mode of action ((inverse) agonism / antagonism) is strongly dependent on the basic head group. The squaramide **4.110** showed the best subtype selectivity profile (H_1:H_2:H_3:H_4 87:1:19:131), while having two-digit nanomolar H_2R affinity (pK_i = 7.30). However, **4.110** turned out to be an antagonist as expected from its basic head group. The synthesized series also contains some (biased) agonists, which are not subtype selective. Due to this overall lack of subtype selectivity we did not investigate these compounds for their selectivity at dopamine receptors. These results may contribute to a better understanding of the structure-activity and structure-selectivity relationships of H_2R ligands.

4.4 Experimental Section

4.4.1 General Experimental Section

Unless otherwise stated, chemicals and solvents were purchased from standard commercial suppliers (Merck, Sigma-Aldrich, Acros, Alfa, abcr) and were used as received. 3-(1-Trityl-1*H*-imidazol-4-yl)-propylamine was synthesized like published previously and kindly provided by Dr. S. Pockes.[46] *tert*-Butyl (*E*)-(2-(3-(1*H*-imidazol-4-yl)acrylamido)ethyl)carbamate was synthesized like published previously and kindly provided by Dr. M. Keller.[47] All of the solvents were of analytical grade or distilled prior to use. For column chromatography silica gel 60 (0.04-0.063 mm, Merck, Darmstadt, Germany) was used. Flash chromatography was performed on an Intelli Flash-310 workstation from Varian Deutschland GmbH (Darmstadt, Germany) with SuperFlash (SF) columns (Si50, 4-40 g) from Agilent Technologies (Santa Clara, CA, USA). Reactions were monitored by thin layer chromatography (TLC) on Merck silica gel 60 F254 aluminium sheets, and spots were visualized with UV light at 254 nm or ninhydrin staining. Melting points were determined with a B-540 apparatus (BÜCHI GmbH, Essen, Germany). NMR spectra were recorded on a Bruker Avance 300 (^{1}H: 300 MHz, ^{13}C: 75 MHz), 400 (^{1}H: 400 MHz, ^{13}C: 101 MHz) or 600 (^{1}H: 600 MHz, ^{13}C: 151 MHz) (Bruker,

Karlsruhe, Germany) with deuterated solvents from Deutero (Kastellaun, Germany). Multiplicities are specified with the following abbreviations: s (singlet), d (doublet), t (triplet), q (quartet), quint (quintet), m (multiplet), dd (doublet of doublet), and br (broad). The multiplicity of carbon atoms (^{13}C-NMR) was determined by distortionless enhancement by polarization transfer (DEPT) 135 and DEPT 90: "+" primary and tertiary carbon atom (positive DEPT signal), "-" secondary carbon atom (negative DEPT signal), "quat" quaternary carbon atom. In certain cases 2D-NMR techniques (COSY, HSQC, and HMBC) were used to assign ^{1}H and ^{13}C chemical shifts. The NMR spectra of target compounds are depicted in the Appendix 3, App3.1 ^{1}H-and/or ^{13}C-NMR Spectra of **4.82-4.97**, **4.104-4.110**, **4.112**, **4.114-4.117** and **4.120**. HRMS was performed on a Q-TOF 6540 UHD LC/MS system (Agilent Technologies) using an ESI source or on an AccuTOF GCX GC/MS system (Jeol, Peabody, MA, USA) using an EI source. Preparative HPLC was performed with a system from Waters (Milford, Massachusetts, USA) consisting of a 2524 binary gradient module, a 2489 detector, a prep inject injector, fraction collector III and the column was a Phenomenex Kinetex (250 x 21 mm, 5 µm) (Phenomenex, Aschaffenburg, Germany). As mobile phase mixtures of MeCN and 0.1% aqueous TFA were used. The UV detection was carried out at 220 nm. Freeze-drying was carried out using a ScanVac CoolSafe 4-15L freeze dryer from Labogene (LMS, Brigachtal, Germany), equipped with a RZ 6 rotary vane vacuum pump (Vacuubrand, Wertheim, Germany). Analytical HPLC experiments were performed on a 1100 HPLC system from Agilent Technologies equipped with Instant Pilot controller, a G1312A Bin Pump, a G1329A ALS autosampler, a G1379A vacuum degasser, a G1316A column compartment and a G1315B DAD detector. The column was a Phenomenex Kinetex XB-C18 column (250 x 4.6 mm, 5 µm) (Phenomenex, Aschaffenburg, Germany), tempered at 30 °C. As mobile phase, mixtures of MeCN and 0.05% aqueous TFA were used. Gradient mode: MeCN/TFA (0.05%) (v/v) 0 min: 10:90, 30 min: 90:10, 33 min: 95:5, 40 min: 95:5; flow rate: 0.8 mL/min, t_0 = 3.21 min; capacity factor $k = (t_R\text{-}t_0)/t_0$. Absorbance was detected at 220 nm. Compounds purities were calculated as the percentage peak area of the analyzed compound by UV detection at 220 nm. The purities of the ligands used for pharmacological investigation were ≥95% (exception: **4.117** (purity = 93%); chromatograms are shown in the Appendix 3, App3.2 RP-HPLC Chromatograms of **4.82-4.97**, **4.104-4.110**, **4.112**, **4.114-4.117** and **4.120**).

4.4.2 General Procedures

General Procedure A (Amide Coupling). The respective amine (1.2 equiv) was dissolved in anhydrous DMF (0.2-0.8 mL) and the solution was cooled to 0 °C. DIPEA (2 equiv) and

EDC x HCl (1 equiv, dissolved in 0.1-0.4 mL anhydrous DMF) as well as HOBt x H_2O (1 equiv, dissolved in 0.1-0.4 mL anhydrous DMF) were added. Subsequently, the respective carboxylic acid (1 equiv) and DIPEA (3 equiv) dissolved in anhydrous DMF (0.5-1 mL) were added in one portion. The solution was stirred for 14-18 h and was allowed to warm to rt. The solvent was evaporated under reduced pressure, the residue was purified by flash chromatography [eluent: CH_2Cl_2/(0.5% NH_3 in) MeOH] and dried under reduced pressure. If necessary, deprotection was performed by stirring with 20-40% TFA in CH_2Cl_2 at rt for 7-18 h (TLC control). After evaporation of the solvent under reduced pressure, the crude product was purified by preparative RP-HPLC.

General Procedure B (Hydrazinolysis of the Phthalimides). To a suspension of the respective phthalimide (1 equiv) in EtOH (10 mL) was added N_2H_4 x H_2O (5-6.8 equiv). After stirring at rt for 16-48 h, the mixture was cooled with an ice bath. The formed precipitate was removed by filtration and the filtrate was concentrated to dryness. If necessary, the crude product was subjected to flash chromatography (eluent: CH_2Cl_2/0.5% NH_3 in MeOH).

General Procedure C (Nucleophilic Substitution). The respective iodinated compound (1 equiv), the respective amine (1.8-3.0 equiv) and K_2CO_3 (6 equiv) in MeCN (2.5 mL) were heated under microwave irradiation at 130 °C for 20 min. Subsequently, the solvent was removed under reduced pressure. The crude, Boc- or Trt-protected intermediate was pre-purified by flash chromatographie (eluent: CH_2Cl_2/MeOH) and dried under reduced pressure. The residue was dissolved in CH_2Cl_2, TFA was added and the reaction mixture was stirred until the protection group was removed (approx. 7 h, TLC control). After evaporation of the solvent under reduced pressure, the crude product was purified by preparative RP-HPLC.

General Procedure D (Preparation of Squaramides). The respective mixed squaramate (1.0-1.1 equiv) was dissolved in EtOH (2 mL). After addition of the respective amine (1-1.1 equiv, dissolved in 3 mL EtOH), the solution was stirred at rt to 70 °C for overnight to 18 days (TLC control). The solvent was evaporated, and the residue was pre-purified by flash chromatography (eluent: CH_2Cl_2/0.5% NH_3 in MeOH). After evaporation of the solvent under reduced pressure, the crude product was purified by preparative RP-HPLC.

General Procedure E (Preparation of N^G-Carbamoylated Guanidines). 4.113 (1-1.1 equiv) and the respective amine (1-1.1 equiv) were dissolved in anhydrous CH_2Cl_2 (3 mL).

NEt_3 (2.5 equiv) and $HgCl_2$ (2 equiv) were added. The reaction mixture was stirred at rt for 4-18 h. The resulting suspension was filtered through Celite 545 in order to remove the mercury salt and the crude product was pre-purified by flash chromatography (eluent: PE/EtOAc). Removal of the solvent under reduced pressure afforded the Trt-/Boc-protected intermediate. Subsequently, the deprotection was performed by stirring the intermediate in a mixture of CH_2Cl_2 and TFA overnight at rt. The solvent was removed under reduced pressure and the product was purified by preparative HPLC.

4.4.3 Preparation of 2-(1-Trityl-1*H*-imidazol-4-yl)ethan-1-amine (4.4)

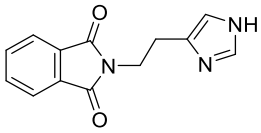

2-(2-(1*H*-Imidazol-4-yl)ethyl)isoindoline-1,3-dione (4.2).[41, 48] Nefkens` reagent (4.3 g, 19.6 mmol, 1.2 equiv) was added to a stirred solution of histamine dihydrochloride (**4.1**, 3.0 g, 16.3 mmol, 1 equiv) and K_2CO_3 (6.8 g, 48.9 mmol, 3 equiv) in H_2O (30 mL) at rt. The resulting white suspension was stirred vigorously at rt for 2 h. The solid was filtered off and thoroughly washed with ice-cold H_2O (3 x 5 mL). The solid was collected and dried under high vacuum to give the product as white solid (3.8 g, 97%). R_f = 0.21 (CH_2Cl_2/MeOH 9:1). M. p.: 189-191 °C (lit.: 189-191 °C)[49]. ^{1}H-NMR (300 MHz, DMSO-d_6) δ 11.88 (s, 1H), 7.89-7.76 (m, 4H), 7.50 (d, *J* = 1.2 Hz, 1H), 6.80 (s, 1H), 3.78 (t, *J* = 8.1 Hz, 2H), 2.82 (t, *J* = 7.4 Hz, 2H). ^{13}C-NMR (75 MHz, DMSO-d_6) δ 167.58 (2C), 134.79, 134.15 (2C), 133.87, 131.47 (2C), 122.81 (2C), 116.21, 37.60, 25.63. NMR data matches literature reference.[41] HRMS (ESI-MS): calcd. for $C_{13}H_{12}N_3O_2^+$: 242.0924, found: 242.0936. MF: $C_{13}H_{11}N_3O_2$. MW: 241.25.

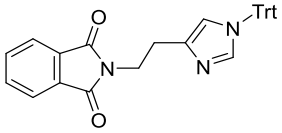

2-(2-(1-Trityl-1*H*-imidazol-4-yl)ethyl)isoindoline-1,3-dione (4.3).[41, 48] A mixture of **4.2** (1.75 g, 7.25 mmol, 1 equiv), NEt_3 (4.0 mL, 29.0 mmol, 4 equiv) and Trt-Cl (3.0 g, 10.9 mmol, 1.5 equiv) in MeCN (150 mL) was stirred at rt for 16 h. The solvent was removed by evaporation and the residue was purified by column chromatography (PE/EtOAc 50:50). The product was obtained as light-yellow solid (3.4 g, 97%). R_f = 0.22 (PE/EtOAc 1:1). ^{1}H-NMR (300 MHz, $CDCl_3$) δ 7.84-7.75 (m, 2H), 7.72-7.64 (m, 2H), 7.34-7.30 (m, 1H), 7.30-7.20 (m, 9H), 7.10-7.00 (m, 6H), 6.52 (d, *J* = 1.4 Hz, 1H), 3.97 (t, *J* = 7.0 Hz, 2H), 2.94 (t, *J* = 7.0 Hz,

2H). ^{13}C-NMR (75 MHz, $CDCl_3$) δ 168.23 (2C), 142.52 (3C), 138.79, 137.75, 133.83 (2C), 132.24 (2C), 129.83 (6C), 128.03 (6C), 128.00 (3C), 123.25 (2C), 118.74, 75.14, 38.10, 27.42. NMR data matches literature reference.[41] HRMS (ESI-MS): calcd. for $C_{32}H_{26}N_3O_2^+$: 484.2020, found: 484.2054. MF: $C_{32}H_{25}N_3O_2$. MW: 483.57.

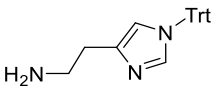

2-(1-Trityl-1*H*-imidazol-4-yl)ethan-1-amine (4.4).[41, 48, 50] A mixture of **4.3** (3.33 g, 6.9 mmol, 1 equiv) and N_2H_4 x H_2O (1.7 mL, 34.4 mmol, 5 equiv) in EtOH (70 mL) was refluxed for 2 h. After removal of insoluble material, the filtrate was evaporated giving a light-yellow solid, which was purified by column chromatography (CH_2Cl_2/MeOH 100:0-92:8) and afforded a yellow oil (2.4 g, 98%). R_f = 0.83 (CH_2Cl_2/MeOH 9:1). ^{1}H-NMR (400 MHz, MeOD) δ 7.40 (d, *J* = 1.4 Hz, 1H), 7.39-7.32 (m, 9H), 7.19-7.12 (m, 6H), 6.76-6.71 (m, 1H), 2.87 (t, *J* = 7.1 Hz, 2H), 2.66 (t, *J* = 7.0 Hz, 2H). ^{13}C-NMR (101 MHz, MeOD) δ 143.99 (3C), 140.06, 139.93, 131.13 (6C), 129.61 (3C), 129.53 (6C), 120.67, 77.09, 42.44, 32.12. NMR data matches literature reference.[41] HRMS (ESI-MS): calcd. for $C_{24}H_{24}N_3^+$: 354.1965, found: 354.1965. MF: $C_{24}H_{23}N_3$. MW: 353.47.

4.4.4 Preparation of the Amine Building Blocks 4.17-4.19

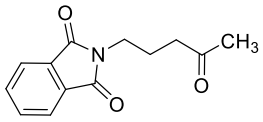

2-(4-Oxopentyl)isoindoline-1,3-dione (4.8).[51-52] A mixture of phthalimide (**4.7**, 27.3 g, 0.186 mol, 1 equiv), 5-chloropentan-2-one (**4.5**, 22.3 g, 0.185 mol, 1 equiv), ground K_2CO_3 (25.57 g, 0.185 mol, 1 equiv) and KI (0.1 g, cat.) in DMF (200 mL) was heated while stirring for a period of 12 h at 110°C. After cooling down the inorganic solids were filtered off and the filtrate was concentrated in vacuum. The residue was dissolved in EtOAc (50 mL) and after standing overnight in refrigerator the unreacted phthalimide was filtered off, the filtrate was concentrated in vacuum and the residue was purified by column chromatography (CH_2Cl_2/MeOH 95:5) yielding a light brown solid (21.4 g, 50%). R_f = 0.63 (PE/EtOAc 1:1). M. p.: 70 °C (lit.: 68-74 °C)[51-52]. ^{1}H-NMR (300 MHz, $CDCl_3$) δ 7.83-7.61 (m, 4H), 3.66 (t, *J* = 6.7 Hz, 2H), 2.46 (t, *J* = 7.2 Hz, 2H), 2.10 (s, 3H), 1.91 (quint, *J* = 7.0 Hz, 2H). ^{13}C-NMR (75 Hz, $CDCl_3$) δ 207.58, 168.48 (2C), 134.02 (2C), 132.02 (2C), 123.25 (2C), 40.55, 37.19,

29.98, 22.68. NMR data matches literature reference.[52] HRMS (ESI-MS): calcd. for $C_{13}H_{14}NO_3^+$: 232.0968, found: 232.0973. MF: $C_{13}H_{13}NO_3$. MW: 231.25.

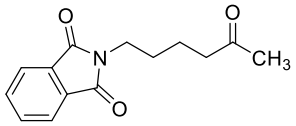

2-(5-Oxohexyl)isoindoline-1,3-dione (4.9).[3, 12, 52] 6-Chlorohexan-2-one (5.88 g, 43.7 mmol, 1 equiv), phthalimide (**4.7**, 6.55 g, 43.7 mmol, 1 equiv), K_2CO_3 (9.24 g, 65.6 mmol, 1 equiv) and KI (0.1 g, cat.) were dissolved in DMF (100 mL). The mixture was heated at 95 °C for 24 h. After cooling to rt, the solvent was evaporated in vacuum. The residue was suspended in H_2O (500 mL) and extracted with chloroform (2 x 200 mL). The combined organic layers were dried over Na_2SO_4 and evaporated in vacuum. The crude product was purified by column chromatography (CH_2Cl_2/MeOH 100:0-95:5) yielding the product as white solid (7.93 g, 74%). R_f = 0.78 (PE/EtOAc 1:1). M. p.: 58 °C (lit. 58-59 °C). ^{1}H-NMR (300 MHz, $CDCl_3$) δ 7.81-7.57 (m, 4H), 3.62 (t, *J* = 6.8 Hz, 2H), 2.43 (t, *J* = 7.0 Hz, 2H), 2.07 (s, 3H), 1.69-1.45 (m, 4H). ^{13}C-NMR (75 MHz, $CDCl_3$) δ 208.37, 168.35 (2C), 133.93 (2C), 132.02 (2C), 123.16 (2C), 42.82, 37.45, 29.95, 27.89, 20.74. NMR data matches literature reference. [3, 12, 52] HRMS (ESI-MS): calcd. for $C_{14}H_{16}NO_3^+$: 246.1125, found: 246.1152. MF: $C_{14}H_{15}NO_3$. MW: 245.28.

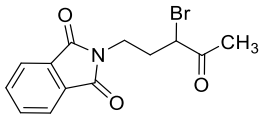

2-(3-Bromo-4-oxopentyl)isoindoline-1,3-dione (4.10).[53] A solution of **4.8** (5.0 g, 21.62 mmol, 1.08 equiv) in glacial acetic acid (55 mL) was cooled to 10 °C and Br_2 (1.01 mL, 20.02 mmol, 1 equiv) was added dropwise under stirring. The reaction mixture was allowed to warm up to rt and was stirred for additional 1 h. A mixture of ice-cold water (1 L)/chloroform (333 mL) was added to the reaction mixture. The organic phase was separated and concentrated in vacuum. The crude product was obtained as a brown oil (3.55 g, 57%) and used in the next step without further purification. R_f = 0.63 (PE/EtOAc 1:1). M. p.: 75-79 °C (lit. 73-75 °C)[53]. ^{1}H-NMR (300 MHz, $CDCl_3$) δ 7.82-7.75 (m, 2H), 7.71-7.63 (m, 2H), 4.30-4.22 (m, 1H), 3.76-3.70 (m, 2H), 2.53-2.38 (m, 2H), 2.33 (s, 3H). NMR data matches literature reference.[53] HRMS (ESI-MS): calcd. for $C_{13}H_{13}BrNO_3^+$: 310.0073, 312.0053, found: 310.0078, 312.0059. MF: $C_{13}H_{12}BrNO_3$. MW: 310.15.

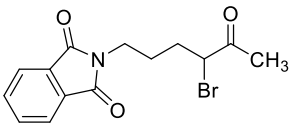

2-(4-Bromo-5-oxohexyl)-1,3-dihydro-2*H*-isoindol-1,3-dione (4.11).[3] To a solution of **4.9** (10.55 g, 43.0 mmol, 1.1 equiv) in 1,4-dioxane (218 mL) and CH_2Cl_2 (141 mL), Br_2 (2.00 mL, 39.1 mmol, 1 equiv) was added so that the brown color always disappeared and then stirred for 4 h at rt. Subsequently, the mixture was washed with H_2O (2 x 300 mL) and extracted with EtOAc (3 x 200 mL). The organic layer was dried over Na_2SO_4, and the solvent was removed in vacuum. The crude product was obtained as a yellow oil (11.78 g, 93%) and used in the next step without further purification. R_f = 0.55 (PE/EtOAc 2:1). ^{1}H-NMR (300 MHz, $CDCl_3$) δ 7.90-7.79 (m, 2H), 7.77-7.67 (m, 2H), 4.39-4.29 (m, 1H), 3.74 (t, *J* = 6.7 Hz, 2H), 2.37 (s, 3H), 2.09-1.54 (m, 4H). NMR data matches literature reference[3]. HRMS (ESI-MS): calcd. for $C_{14}H_{15}BrNO_3^+$: 324.0230, 326.0209, found: 324.0233, 326.0214. MF: $C_{14}H_{14}BrNO_3$. MW: 324.17.

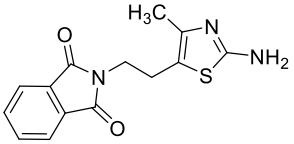

2-(2-(2-Amino-4-methylthiazol-5-yl)ethyl)isoindoline-1,3-dione (4.12).[54] To a stirred solution of **4.10** (1.5 g, 4.84 mmol, 1 equiv) in DMF (15 mL), a solution of thiourea (368 mg, 4.84 mmol, 1 equiv) in DMF (15 mL) was added and the mixture was heated at 100 °C for 3 h. After cooling and removing the solvent in vacuum, the crude product was purified by flash chromatography (gradient: 0-40 min: CH_2Cl_2/MeOH 100:0-90:10, SF 25 g) to obtain the formylated intermediate as yellow foam (1.23 g, 81%). ^{1}H-NMR (300 MHz, DMSO-d_6) δ 12.00 (s, 1H), 8.37 (s, 1H), 7.98-7.66 (m, 4H), 3.74 (t, *J* = 6.8 Hz, 2H), 3.02 (t, *J* = 6.8 Hz, 2H), 2.06 (s, 3H). ^{13}C-NMR (75 MHz, DMSO-d_6) δ 167.67 (q, 2C), 159.21 (+), 152.88 (q), 143.16 (q), 134.53 (+, 2C), 131.43 (q, 2C), 123.12 (+, 2C), 120.53 (q), 38.06 (-), 23.98 (-), 14.21 (+). HRMS (ESI-MS): calcd. for $C_{15}H_{14}N_3O_3S^+$: 316.0750, found: 316.0755. MF: $C_{15}H_{13}N_3O_3S$. MW: 315.35. The formylated intermediate (1.23 g, 3.9 mmol) was suspended in MeOH (22.3 mL), 1 N HCl in MeOH (14.5 mL) was added and the mixture was stirred at rt for 72 h. The mixture was neutralized (pH 7-8) using 1 N NaOH in MeOH, filtrated and the solvent was removed in vacuum. The crude product was purified by column chromatography (CH_2Cl_2/MeOH 90:10) yielding the product as yellow oil (1.1 g, 98%). R_f = 0.60 (CH_2Cl_2/MeOH 9:1). ^{1}H-NMR (300 MHz, DMSO-d_6) δ 7.93-7.78 (m, 4H), 6.60 (br s, 2H), 3.67 (t, *J* = 6.8 Hz, 2H), 2.85 (t,

J = 6.8 Hz, 2H), 1.88 (s, 3H). ^{13}C-NMR (75 MHz, DMSO-d$_6$) δ 167.69 (q, 2C), 165.23 (q), 143.59 (q), 134.50 (+, 2C), 131.50 (q, 2C), 123.09 (+, 2C), 112.96 (q), 38.36 (-), 24.18 (-), 14.31 (+). NMR data matches literature reference.[54] HRMS (ESI-MS): calcd. for $C_{14}H_{14}N_3O_2S^+$: 288.0801, found: 288.0818. MF: $C_{14}H_{13}N_3O_2S$. MW:287.34.

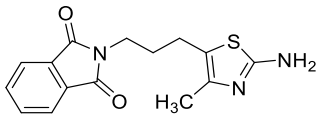

2-[3-(2-Amino-4-methylthiazol-5-yl)propyl]-1,3-dihydro-2*H*-isoindol-1,3-dione (4.13).[11] To a stirred solution of **4.11** (11.75 g, 36.25 mmol, 1 equiv) in DMF (50 mL), a solution of thiourea (2.76 g, 36.25 mmol, 1 equiv) in DMF (50 mL) was added and the mixture was heated at 100 °C for 3 h. After cooling and removing the solvent in vacuum, a mixture of EtOAc/MeOH (1:1 (v/v), 40 mL) was added, and the suspension was stirred for 30 min. Subsequently, the precipitate was filtered off, washed with EtOAc and diethyl ether and the solid was dried in vacuum (3.2 g, 29%). R_f = 0.45 (PE/EtOAc 1:4). ^{1}H-NMR (300 MHz, $CDCl_3$) δ 7.84 (m, 4H), 3.61 (t, *J* = 7.0 Hz, 2H), 2.71 (t, *J* = 7.5 Hz, 2H), 2.14 (s, 3H), 1.97-1.77 (m, 2H). NMR data matches literature reference.[11,55] HRMS (ESI-MS): calcd. for $C_{15}H_{16}N_3O_2S^+$: 302.0958, found: 302.0962. MF: $C_{15}H_{15}N_3O_2S$. MW: 301.36.

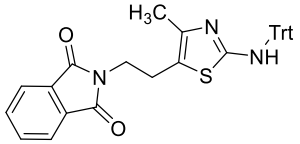

2-(2-(4-Methyl-2-(tritylamino)thiazol-5-yl)ethyl)isoindoline-1,3-dione (4.14). Trt-Cl (652 mg, 2.34 mmol, 1.2 equiv) was dissolved in MeCN (60 mL) and was added dropwise to a suspension of **4.12** (560 mg, 1.95 mmol, 1 equiv) and NEt_3 (487 µL, 3.51 mmol, 1.8 equiv) in MeCN (60 mL) at rt under stirring. After the addition, stirring was continued for 16 h. The solvent was removed in vacuum and the resulting solid was purified by flash chromatography (gradient: 0-20 min: PE/EtOAc 100:0-67:33, SF 12 g) yielding the product as yellow foam (0.64 g, 62%). R_f = 0.50 (PE/EtOAc 1:1). ^{1}H-NMR (300 MHz, $CDCl_3$) δ 7.84-7.75 (m, 2H), 7.74-7.65 (m, 2H), 7.38-7.16 (m, 15H), 6.79 (s, 1H), 3.65 (t, *J* = 7.2 Hz, 2H), 2.77 (t, *J* = 7.2 Hz, 2H), 2.08 (s, 3H). ^{13}C-NMR (75 MHz, $CDCl_3$) δ 168.02 (q, 2C), 165.74 (q), 143.68 (q, 3C), 142.76 (q), 133.97 (+, 2C), 132.08 (q, 2C), 129.31 (+, 6C), 128.18 (+, 6C), 127.46 (+, 3C), 123.35 (+, 2C), 116.21 (q), 71.77 (q), 38.65 (-), 24.85 (-), 14.28 (+). HRMS (ESI-MS): calcd. for $C_{33}H_{28}N_3O_2S^+$: 530.1897, found: 530.1902. MF: $C_{33}H_{27}N_3O_2S$. MW: 529.66.

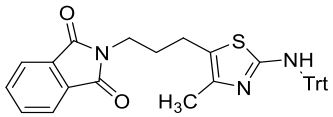

2-(3-(4-Methyl-2-(tritylamino)thiazol-5-yl)propyl)isoindoline-1,3-dione (4.15).[5] **4.13** (4.56 g, 15.1 mmol, 1 equiv) was dissolved in MeCN (120 mL) and Trt-Cl (5.07 g, 18.2 mmol, 1.2 equiv) and NEt_3 (3.77 mL, 27.2 mmol, 1.8 equiv) were added. The mixture was stirred for 16 h at rt. The solvent was removed in vacuum. The crude product was purified by flash chromatography (gradient: 0-20 min: PE/EtOAc 100:0-75:25, 40 min: 75:25, 60 min: 30:70 SF 12 g) to obtain the product as a yellow foam (2.18 g, 27%). ^{1}H-NMR (300 MHz, $CDCl_3$) δ 7.88-7.79 (m, 2H), 7.75-7.68 (m, 2H), 7.36-7.18 (m, 15H), 3.59 (t, *J* = 7.3 Hz, 2H), 2.49-2.41 (m, 2H), 2.07 (s, 3H), 1.77-1.65 (m, 2H). ^{13}C-NMR (75 MHz, $CDCl_3$) δ 168.33 (q, 2C), 165.10 (q), 143.81 (q, 3C), 134.03 (+, 2C), 132.13 (q, 2C), 129.28 (+, 6C), 128.18 (+, 6C), 127.44 (+, 3C), 123.30 (+, 2C), 120.02 (q), 71.84 (q), 37.53 (-), 30.36 (-), 23.83 (-), 14.47 (+), 1 C signal is missing. HRMS (ESI-MS): calcd. for $C_{34}H_{30}N_3O_2S^+$: 544.2053, found: 544.2082. MF: $C_{34}H_{29}N_3O_2S$. MW: 543.69.

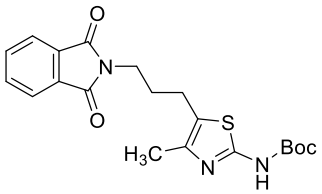

***tert*-Butyl 4-methyl-5-[3-(1,3-dioxo-1,3-dihydro-2*H*-isoindol-2-yl)propyl]thiazol-2-ylcarbamate (4.16).**[3, 12] **4.13** (3.14 g, 10.4 mmol, 1 equiv) was dissolved in chloroform (100 mL) and Boc_2O (2.45 g, 11.2 mmol, 1.08 equiv), NEt_3 (1.68 mL, 12.09 mmol, 1.16 equiv) and DMAP (0.1 g, cat.) were added. The mixture was stirred overnight at rt. The mixture was extracted with CH_2Cl_2, washed with 0.1 N HCl (2 x 50 mL), brine (50 mL) and H_2O (50 mL), dried over Na_2SO_4 and the solvent removed in vacuum. The crude product by purified by flash chromatography (gradient: 0-20 min: PE/EtOAc 100:0-66:34, 40 min: 66:34, SF 25 g) to obtain the product as a colorless foam (2.87 g, 69%). ^{1}H-NMR (300 MHz, $CDCl_3$) δ 7.81-7.73 (m, 2H), 7.69-7.60 (m, 2H), 3.74 (t, *J* = 7.1 Hz, 2H), 2.71 (t, *J* = 7.6 Hz, 2H), 2.22 (s, 3H), 1.98 (m, 2H), 1.51 (s, 9H). NMR data matches literature reference.[12,55] HRMS (ESI-MS): calcd. for $C_{20}H_{24}N_3O_4S^+$: 402.1482, found: 402.1486. MF: $C_{20}H_{23}N_3O_4S$. MW: 401.48.

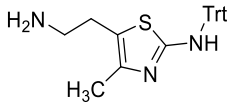

5-(2-Aminoethyl)-4-methyl-*N*-tritylthiazol-2-amine (4.17). To a suspension of **4.14** (0.64 g, 1.21 mmol, 1 equiv) in *n*-BuOH (25 mL) was added N_2H_4 x H_2O (293 µL, 6.04 mmol, 5 equiv). After stirring for 16 h at rt, the mixture was cooled in an ice bath, the precipitate was removed by filtration and the filtrate concentrated to dryness. The crude product (0.48 g, 99%) was used in the next step without further purification. R_f = 0.1 (CH_2Cl_2/MeOH). ^{1}H-NMR (300 MHz, MeOD) δ 7.43-7.15 (m, 15H), 2.64-2.52 (m, 4H), 2.05 (s, 3H). ^{13}C-NMR (75 MHz, MeOD) δ 167.80 (q), 145.38 (q, 3C), 143.52 (q), 130.53 (+, 6C), 129.21 (+, 6C), 128.56 (+, 3C), 118.79 (q), 73.24 (q), 43.55 (-), 29.29 (-), 14.41 (+). HRMS (ESI-MS): calcd. for $C_{25}H_{26}N_3S^+$: 400.1842, found: 400.1841. MF: $C_{25}H_{25}N_3S$. MW: 399.56.

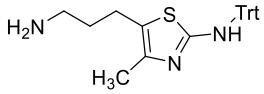

5-(3-Aminopropyl)-4-methyl-*N*-tritylthiazol-2-amine (4.18).[5] A mixture of **4.15** (1.73 g, 3.18 mmol, 1 equiv) and N_2H_4°x°H_2O (772 µL, 15.91 mmol, 5 equiv) in EtOH/*n*-BuOH (5:2 (v/v), 35 mL) was stirred at rt for 24 h. After removal of insoluble material, the filtrate was evaporated giving a pale yellowish oil (0.90 g, 68%), which was used in the next step without further purification. R_f = 0.33 (CH_2Cl_2/MeOH 9:1). ^{1}H-NMR (300 MHz, MeOD) δ 7.39-7.18 (m, 15H), 2.70 (t, *J* = 7.6 Hz, 2H), 2.52-2.41 (m, 2H), 2.01 (s, 3H), 1.69-1.54 (m, 2H). ^{13}C-NMR (75 MHz, MeOD) δ 161.18 (q), 145.23 (q, 3C), 142.44 (q), 130.34 (+, 6C), 129.04 (+, 6C), 128.38 (+, 3C), 120.82 (q), 73.03 (q), 40.47 (-), 31.97 (-), 23.87 (-), 14.26 (+). HRMS (ESI-MS): calcd. for $C_{26}H_{28}N_3S^+$: 414.1998, found: 414.1995. MF: $C_{26}H_{27}N_3S$. MW: 413.58.

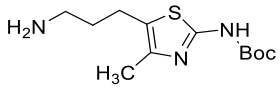

***tert*-Butyl 5-(3-aminopropyl)-4-methylthiazol-2-ylcarbamate (4.19).**[3, 12] To a suspension of **4.16** (2.87 g, 7.15 mmol, 1 equiv) in EtOH (35 mL) was added N_2H_4 x H_2O (1.73 mL, 35.74 mmol, 5 equiv) and the solution was stirred at rt for 16 h. The mixture was cooled by using an ice bath, the precipitate was removed by filtration and the filtrate concentrated to dryness. The crude product (1.94 g, 100%) was used in the next step without further purification. ^{1}H-NMR (400 MHz, MeOD) δ 2.93-2.87 (m, 2H), 2.74 (t, *J* = 7.6 Hz, 2H), 2.15 (s, 3H), 1.94-1.83 (m, 2H), 1.51 (s, 9H). ^{13}C-NMR (101 MHz, MeOD) δ 159.01, 154.69,

143.52, 124.42, 83.03, 40.83, 32.17, 28.78 (3C), 24.19, 14.76. NMR data matches literature reference.[12,55] HRMS (ESI-MS): calcd. for $C_{12}H_{22}N_3O_2S^+$: 272.1427, found: 272.1428; calcd. for $C_{24}H_{42}N_6NaO_4S_2^+$: 565.2601, found: 565.2602. MF: $C_{12}H_{21}N_3O_2S$. MW: 271.38.

4.4.5 Preparation of the Amine Building Block 4.26

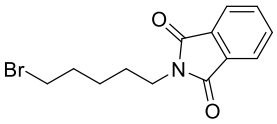

2-(5-Bromopentyl)isoindoline-1,3-dione (4.22).[56] To a solution of 1,5-dibromopentane (**4.21**, 5.0 mL, 36.71 mmol, 1 equiv) dissolved in DMF (50 mL) was added potassium phthalimide (**4.20**, 6.80 g, 36.71 mmol, 1 equiv) at rt, and the reaction mixture was stirred for 24 h. The solvent was removed in vacuum, and the residue was subjected to flash chromatography (gradient: 0-20 min: PE/EtOAc 100:0 to 75:25, SF 80 g) to give the product as transparent oil (3.37 g, 31%). R_f = 0.57 (PE/EtOAc 4:1). ^{1}H-NMR (300 MHz, $CDCl_3$) δ 7.83-7.76 (m, 2H), 7.71-7.64 (m, 2H), 3.65 (t, *J* = 7.2 Hz, 2H), 3.36 (t, *J* = 6.7 Hz, 2H), 1.95-1.80 (m, 2H), 1.76-1.60 (m, 2H), 1.55-1.39 (m, 2H). ^{13}C-NMR (75 MHz, $CDCl_3$) δ 168.38 (q, 2C), 133.95 (+, 2C), 132.10 (q, 2C), 123.22 (+, 2C), 37.67 (-), 33.47 (-), 32.22 (-), 27.76 (+), 25.42 (-). NMR data matches literature reference.[56] HRMS (ESI-MS): calcd. for $C_{13}H_{15}BrNO_2^+$: 296.0281, found: 296.0284. MF: $C_{13}H_{14}BrNO_2$. MW: 296.16.

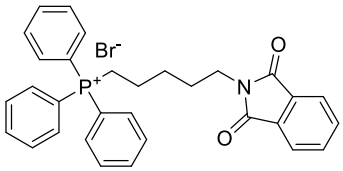

(5-(1,3-Dioxoisoindolin-2-yl)pentyl)triphenylphosphonium bromide (4.23).[57] To a solution of **4.22** (3.37 g, 11.38 mmol, 1 equiv) in MeCN (21 mL) was added PPh_3 (3.00 g, 11.42 mmol, 1 equiv). The mixture was refluxed for 48 h, and the solvent was removed at reduced pressure to give the phosphonium bromide (6.45 g, 100%) as beige foam. The product was used in the next step without further purification. R_f = 0.47 (CH_2Cl_2/MeOH 95:5). ^{1}H-NMR (300 MHz, MeOD) δ 7.94-7.69 (m, 19H), 3.63 (t, *J* = 6.7 Hz, 2H), 3.50–3.36 (m, 2H), 1.80-1.64 (m, 4H), 1.63-1.51 (m, 2H). ^{13}C-NMR (75 MHz, MeOD) δ 169.89 (2C), 136.33 (+, d, *J* = 3.1 Hz, 3C), 135.49 (+, 2C), 134.89 (+, d, *J* = 10.0 Hz, 6C), 133.36 (q, 2C), 131.61 (+, d, *J* = 12.60 Hz, 6C), 124.18 (+, 2C), 120 (q, d, *J* = 86.26 Hz, 3C), 38.17 (-), 28.73 (-, d, *J* = 3.6 Hz), 28.53 (-), 23.05 (-, d, *J* = 3.52 Hz), 22.35 (-). NMR data matches literature

reference.[57] HRMS (ESI-MS): calcd. for $C_{31}H_{29}NO_2P^+$: 478.1930, found: 478.1937. MF**:** $C_{31}H_{29}BrNO_2P$. MW: 558.46.

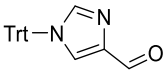

1-Trityl-1*H*-imidazole-4-carbaldehyde (4.24).[58] To a solution of 1*H*-imidazole-4-carbaldehyde (2.35 g, 24.5 mmol, 1.0 equiv) and Trt-Cl (7.50 g, 26.9 mmol, 1.1 equiv) in MeCN (80 mL), NEt_3 (6.11 mL, 44.1 mmol, 1.8 equiv) was added dropwise. After 20 h, *n*-hexane (8 mL) and H_2O (80 mL) were added and the mixture was stirred for 30 min. The precipitated product was filtered and washed with H_2O (2 x 20 mL). Recrystallization from EtOAc/n-hexane yielded a beige solid (8.11 g, 98%). R_f = 0.68 (CH_2Cl_2/0.5% NH_3 in MeOH 9:1). M. p.: 163-168 °C (lit. 162-165)[19]. ^{1}H-NMR (300 MHz, $CDCl_3$) δ 7.16-7.06 (m, 6H), 7.41-7.31 (m, 9H), 7.53 (d, *J* = 1.3 Hz, 1H), 7.61 (d, *J* = 1.3 Hz, 1H), 9.88 (s, 1H). ^{13}C-NMR (75 MHz, $CDCl_3$) δ 186.61 (q), 141.56 (q, 3C), 140.90 (q), 140.65 (+), 129.69 (+, 6C), 128.57 (+, 6C), 128.42 (+, 3C), 126.80 (+), 76.39 (q). NMR data matches literature reference.[58] HRMS (ESI-MS): calcd. for $C_{23}H_{18}N_2NaO^+$: 361.1311, found: 361.1319. MF: $C_{23}H_{18}N_2O$. MW: 338.41.

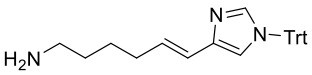

(*E*)-6-(1-Trityl-1*H*-imidazol-4-yl)hex-5-en-1-amine (4.26). The title compound was synthesized according to the procedure of Griffith et al.[16] To a stirred suspension of **4.23** (3.0 g, 5.37 mmol, 1 equiv) and **4.24** (1.82 g, 5.37 mmol, 1 equiv) in anhydrous THF (25 mL) under N_2 atmosphere at 0 °C was added *t*-BuOK (0.60 g, 5.37 mmol, 1 equiv) in one portion. The mixture was refluxed for 18 h and then filtered. The solvent was evaporated in vacuum and the residue was purified by flash chromatography (gradient: 0-20 min: CH_2Cl_2/EtOAc 100:0-95:5, SF 40 g) to afford mixture of product and the aldehyde as light beige solid (1.38 g). R_f = 0.7 (CH_2Cl_2/EtOAc 85:15). HRMS (ESI-MS): calcd. for $C_{36}H_{32}N_3O_2^+$: 538.2489, found: 538.2490. MF: $C_{36}H_{31}N_3O_2$. MW: 537.66. This mixture was dissolved in EtOH (50 mL) and N_2H_4 x H_2O (0.62 mL) was added. The reaction mixture was stirred at rt for 48 h. Then, the solvent was evaporated, and the residue was purified by flash chromatography (gradient: 0-20 min: CH_2Cl_2/MeOH 100:0-95:5, 35 min: 95:5, 55 min: 90:10, SF 12 g). The product was obtained as transparent oil (160 mg, 7% over 2 steps). R_f = 0.25 (CH_2Cl_2/MeOH 9:1). ^{1}H-NMR (300 MHz, $CDCl_3$) δ 7.46-7.40 (m, 1H), 7.37-7.29 (m, 9H), 7.18-7.09 (m, 7H), 6.77-6.70 (m,

1H), 6.24-6.16 (m, 1H), 2.72-2.57 (m, 2H), 2.41-2.29 (m, 2H), 1.52-1.41 (m, 4H). ^{13}C-NMR (75 MHz, $CDCl_3$) δ 142.27 (q, 3C), 138.71 (q), 138.50 (+), 130.53 (+), 129.77 (+, 6C), 128.08(+, 9C), 121.23 (+), 120.60 (+), 75.36 (q), 41.30 (-), 31.99 (-), 28.51 (-), 26.40 (-). HRMS (ESI-MS): calcd. for $C_{28}H_{30}N_3^+$: 408.2434, found: 408.2438. MF: $C_{28}H_{29}N_3$. MW: 407.56.

4.4.6 Preparation of the Building Blocks 4.32 and 4.35

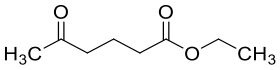

Ethyl 5-oxohexanoate (4.28).[59] Oxalyl chloride (1.98 mL, 23.1 mmol, 3 equiv) was added dropwise to a solution of 5-oxohexanoic acid (**4.27**, 0.92 mL, 7.7 mmol, 1 equiv), and DMF (0.2 mL, cat.) in anhydrous CH_2Cl_2 (10 mL) at 0 °C under stirring in an argon atmosphere. After a period of 2 h at rt, the solution was evaporated in vacuum, the yellowish liquid residue was taken up in CH_2Cl_2 (20 mL) and added dropwise to a mixture of EtOH (1.08 mL, 18.4 mmol, 2.4 equiv) and NEt_3 (3.20 mL, 23.1 mmol, 3 equiv) at rt. After stirring for 30 min, the mixture was concentrated in vacuum, taken up in Et_2O (100 mL) and extracted successively with aqueous HCl (2 x 70 mL), brine (50 mL). The organic layers were dried over Na_2SO_4, filtered and the filtrate was concentrated in vacuum. The residue was purified by flash chromatography (gradient: 0-20 min: PE/EtOAc 100:0-95:5, SF 12 g) yielding the product as yellow oil (0.41 g, 34%). R_f = 0.86 (PE/EtOAc 1:1, $KMnO_4$ stain). ^{1}H-NMR (300 MHz, $CDCl_3$) δ 4.07 (q, *J* = 6.7 Hz, 2H), 2.46 (t, *J* = 6.7 Hz, 2H), 2.27 (t, *J* = 6.7 Hz, 2H), 2.09 (s, 3H), 1.82 (quint, *J* = 7.7 Hz, 2H), 1.19 (t, *J* = 6.7 Hz, 3H). ^{13}C-NMR (75 MHz, $CDCl_3$) δ 207.94 (q), 172.66 (q), 60.23 (+), 42.42 (+), 33.17 (+), 29.80 (-), 18.71 (+), 14.16 (-). NMR data matches literature reference.[59] HRMS (EI-MS): calcd. for $C_8H_{14}O_3^{+\cdot}$: 158.0937, found: 158.0942. MF: $C_8H_{14}O_3$. MW: 158.20.

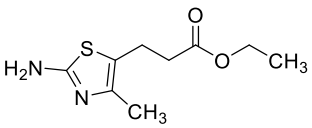

Ethyl 3-(2-amino-4-methylthiazol-5-yl)propanoate (4.29).[60] To a suspension of **4.28** (2.58 g, 16.3 mmol, 1 equiv) and thiourea (2.48 g, 32.6 mmol, 2 equiv) was added Br_2 (835 µL, 16.3 mmol, 1 equiv) under stirring. After Br_2 was added, the mixture was warmed on the steam bath for 3 h under stirring. The reaction mixture was cooled at rt and purified using flash chromatography (gradient: 0-20 min: PE/EtOAc 100:0 to 50:50, 40 min: 40:60, 60 min: 40:60, SF 12 g) yielding the product as greenish oil (0.45 g, 13%). R_f = 0.51 (CH_2Cl_2/0.5% NH_3 in

MeOH) ^{1}H-NMR (300 MHz, $CDCl_3$) δ 8.21 (br s, 2H), 4.07 (q, *J* = 6.9 Hz, 2H), 2.79 (t, *J* = 6.9 Hz, 2H), 2.47 (t, *J* = 7.0 Hz, 2H), 2.13 (s, 3H), 1.19 (t, *J* = 7.6 Hz, 3H). HRMS (ESI-MS): calcd. for $C_9H_{15}N_2O_2S^+$: 215.0849, found: 215.0881. MF: $C_9H_{14}N_2O_2S$. MW: 214.28.

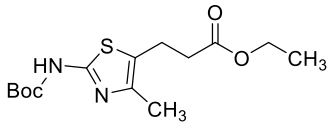

Ethyl 3-(2-((*tert*-butoxycarbonyl)amino)-4-methylthiazol-5-yl)propanoate (4.30). 4.29 (0.29 g, 1.35 mmol, 1 equiv) was dissolved in CH_2Cl_2 (10 mL). NEt_3 (218 µL, 1.56 mmol, 1.16 equiv), DMAP (25 mg, cat.) and Boc_2O (319 mg, 1.46 mmol, 1.08 equiv) were added. The reaction mixture was stirred at rt for 16 h. The solvent was removed in vacuum and the residue was purified by flash chromatography (gradient: 0-20 min: PE/EtOAc 100:0 to 75:25, SF 8 g) yielding the product as yellow oil (270 mg, 63%). R_f = 0.89 (CH_2Cl_2/0.5% NH_3 in MeOH 9:1). ^{1}H-NMR (300 MHz, $CDCl_3$) δ 10.55 (br s, 1H), 4.13 (q, *J* = 7.1 Hz, 2H), 3.02-2.93 (m, 2H), 2.61-2.52 (m, 2H), 2.25 (s, 3H), 1.51 (s, 9H), 1.24 (t, *J* = 7.2 Hz, 3H).^{13}C-NMR (75 MHz, $CDCl_3$) δ 172.35 (q), 158.00 (q), 152.84 (q), 142.43 (q), 122.43 (q), 82.35 (q), 60.75 (-), 35.94 (-), 28.40 (+, 3C), 21.62 (-), 14.61 (+), 14.33 (+). HRMS (ESI-MS): calcd. for $C_{14}H_{23}N_2O_4S^+$: 315.1373, found: 315.1381. MF: $C_{14}H_{22}N_2O_4S$. MW: 314.40.

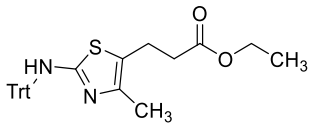

Ethyl 3-(4-methyl-2-(tritylamino)thiazol-5-yl)propanoate (4.31). Trt-Cl (3.1 g, 11.2 mmol, 1.2 equiv) was dissolved in DMF (25 mL) and added dropwise to a solution of **4.29** (2.0 g, 9.3 mmol, 1 equiv) and NEt_3 (3.9 mL, 27.9 mmol, 3 equiv) in DMF (25 mL). After the addition, the mixture was stirred at rt for 16 h. The solvent was removed in vacuum and the crude product was purified by flash chromatography (gradient: 0-30 min: PE/EtOAc 100:0-80:20, 50 min: 50:50, SF 12 g) yielding the product as yellow solid (2.9 g, 68%). R_f = 0.39 (PE/EtOAc 3:1). ^{1}H-NMR (300 MHz, $CDCl_3$) δ 7.36-7.22 (m, 15H), 6.51 (bs, 1H), 4.19-3.99 (m, 2H), 2.72 (t, *J* = 7.2 Hz, 2H), 2.37-2.29 (m, 2H), 2.10 (s, 3H), 1.29-1.13 (m, 2H). ^{13}C-NMR (75 MHz, $CDCl_3$) δ 172.84 (q), 165.25 (q), 143.90 (q, 3C), 142.11 (q), 129.36 (+, 6C), 128.24 (+, 6C), 127.51 (+, 3C), 119.29 (q), 71.81 (q), 60.63 (-), 51.80 (+), 35.84 (-), 21.76 (-), 14.52 (+). HRMS (ESI-MS): calcd. for $C_{28}H_{29}N_2O_2S^+$: 457.1944, found: 457.1945. MF: $C_{28}H_{28}N_2O_2S$. MW: 456.60.

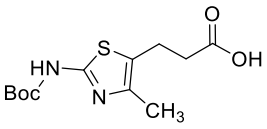

3-(2-((*tert*-Butoxycarbonyl)amino)-4-methylthiazol-5-yl)propanoic acid (4.32). To an ice-cold solution of KOH (145 mg, 2.58 mmol, 3 equiv) in EtOH/H_2O (95:5 (v/v), 7 mL) was added **4.30** (270 mg, 0.86 mmol, 1 equiv). The reaction mixture was stirred for 16 h during which it warmed to rt. The mixture was neutralized with 1 M HCl in MeOH. The solvent was removed in vacuum. The residue was taken up in H_2O (20 mL) and the solution was acidified to pH 3-4 with 1 M HCl in H_2O. The aqueous solution was extracted with EtOAc (2 x 20 mL) and CH_2Cl_2 (2 x 20 mL), the combined organic phases were dried over $MgSO_4$ and evaporated to dryness yielding the product as while solid (220 mg, 89%). ^{1}H-NMR (300 MHz, MeOD) δ 2.96 (t, *J* = 7.2 Hz, 2H), 2.56 (t, *J* = 7.3 Hz, 2H), 2.19 (s, 3H), 1.52 (s, 9H). ^{13}C-NMR (75 MHz, MeOD) δ 175.96 (q), 158.90 (q), 154.34 (q), 143.31 (q), 124.10 (q), 82.73 (q), 36.53 (-), 28.47 (+, 3C), 22.37 (-), 14.40 (+). HRMS (ESI-MS): calcd. for $C_{12}H_{19}N_2O_4S^+$: 287.1060; found: 287.1080. MF: $C_{12}H_{18}N_2O_4S$. MW: 286.35.

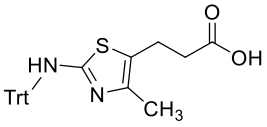

3-(4-Methyl-2-(tritylamino)thiazol-5-yl)propanoic acid (4.33). To an ice-cold solution of KOH (320 mg, 5.72 mmol, 3 equiv) in EtOH/H_2O (95:5 (v/v), 21 mL) was added **4.31** (870 mg, 1.91 mmol, 1 equiv). The reaction mixture was stirred for 16 h during which it warmed to rt. The mixture was neutralized with 1 M HCl in MeOH. The solvent was removed in vacuum. The residue was taken up in H_2O (20 mL) and the solution was acidified to pH 3-4 with 1 M HCl in H_2O. The precipitated white solid was filtered off, washed with H_2O (5 mL) and dried in vacuum (820 mg, 100%). R_f = 0.60 (CH_2Cl_2/MeOH 9:1). ^{1}H-NMR (300 MHz, DMSO-d_6) δ 12.14 (br s, 1H), 8.42 (br s, 1H), 7.34-7.18 (m, 15H), 2.61 (t, *J* = 7.3 Hz, 2H), 2.26 (t, *J* = 7.3 Hz, 2H), 1.85 (s, 3H). ^{13}C-NMR (75 MHz, DMSO-d_6) δ 173.29 (q), 163.69 (q), 144.29 (q, 4C), 128.90 (+, 6C), 127.64 (+, 6C), 126.71 (+, 3C), 118.15 (q), 71.52 (q), 35.40 (-), 20.95 (-), 14.17 (+). HRMS (ESI-MS): calcd. for $C_{26}H_{25}N_2O_2S^+$: 429.1631; found: 429.1662. MF: $C_{26}H_{24}N_2O_2S$. MW: 428.55.

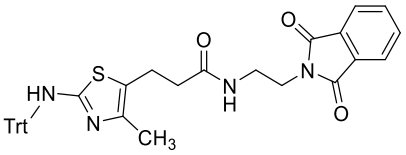

***N*-(2-(1,3-Dioxoisoindolin-2-yl)ethyl)-3-(4-methyl-2-(tritylamino)thiazol-5-yl)propenamide (4.34).** The title compound was prepared from **4.33** (235 mg, 0.55 mmol), **4.49** (200 mg, 0.66 mmol), EDC x HCl (126 mg, 0.66 mmol), HOBt x H_2O (101 mg, 0.66 mmol) and DIPEA (466 µL, 2.74 mmol) in DMF (2.6 mL) according to the general procedure A. The crude product was purified by flash chromatography (gradient: 0-20 min: CH_2Cl_2/0.5% NH_3 in MeOH 100:0 to 95:5, 40 min: 95:5, SF 8 g) yielding the product as yellow oil (70 mg, 21%). R_f = 0.12 (CH_2Cl_2/0.5% NH_3 in MeOH 9:1). ^{1}H-NMR (300 MHz, $CDCl_3$) δ 7.77-7.57 (m, 4H), 7.30-7.11 (m, 15H), 3.74-3.65 (m, 2H), 3.41-3.29 (m, 2H), 2.61-2.54 (m, 2H), 2.07-2.01 (m, 2H), 1.96 (s, 3H). HRMS (ESI-MS): calcd. for $C_{36}H_{33}N_4O_3S^+$: 601.2268, found: 601.2277. MF: $C_{36}H_{32}N_4O_3S$. MW: 600.74.

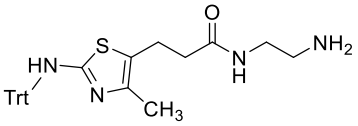

***N*-(2-Aminoethyl)-3-(4-methyl-2-(tritylamino)thiazol-5-yl)propenamide (4.35). 4.34** (70 mg, 0.12 mmol, 1 equiv) was dissolved in EtOH (5 mL) and N_2H_4 x H_2O (28 µL, 0.59 mmol, 5 equiv) was added. The mixture was stirred at rt for 16 h and then heated at 60 °C for 2 h. The mixture was cooled with an ice-bath, the precipitate was removed by filtration and the filtrate was concentrated to dryness yielding **4.35** as a yellow oil (50 mg, 89%). R_f = 0.12 (CH_2Cl_2/0.5% NH_3 in MeOH 9:1). The crude product was used in the next step without further purification. ^{1}H-NMR (400 MHz, MeOD) δ 7.41-7.23 (m, 15H), 3.29 (t, *J* = 6.2 Hz, 2H), 2.87-2.83 (m, 2H), 2.74 (t, *J* = 7.4 Hz, 2H), 2.26 (t, *J* = 7.4 Hz, 2H), 2.07 (s, 3H). HRMS (ESI-MS): calcd. for $C_{28}H_{31}N_4OS^+$: 471.6425, found: 471.2210. MF: $C_{28}H_{30}N_4OS$. MW: 470.64.

4.4.7 Preparation of the Cbz- or Phthalimide-Protected Amines 4.42-4.43, 4.46 and 4.49

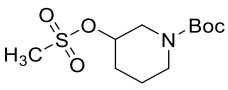

***tert*-Butyl 3-((methylsulfonyl)oxy)piperidine-1-carboxylate (4.38).**[61] Piperidin-3-ol (**4.36**, 2 g, 19.8 mmol, 1 equiv) was dissolved in CH_2Cl_2 (25 mL). NEt_3 (2.74 mL, 19.8 mmol, 1 equiv) was added and the mixture was cooled to 0 °C by using an ice-bath. Boc_2O (4.15 g,

19.0 mmol, 0.96 equiv) was dissolved in CH_2Cl_2 (15 mL) and added dropwise to the ice-cold piperidin-3-ol/NEt_3 mixture while stirring. The resulting mixture was stirred at 0 °C for 2 h. After 2 h, NEt_3 (3.27 mL, 24.0 mmol, 1.19 equiv) and mesityl chloride (2.31 g, 20.0 mmol, 1.02 equiv) were added. The ice-bath was removed, and the reaction mixture was stirred at rt for 3 h. After 3 h, the mixture was diluted with EtOAc/PE (1:1, 200 mL) and washed successively with aqueous citric acid (100 mL), saturated, aqueous $NaHCO_3$ (100 mL) and brine (100 mL). The combined organic phases were dried over Na_2SO_4. Na_2SO_4 was filtered off and the filtrate was evaporated. The product was purified by flash chromatography (gradient: 0-20 min: PE/EtOAc 100:0 to 80:20, 40 min: 60:40, SF 12 g). The product was obtained as a white solid (4.0 g, 75%). R_f = 0.76 (PE/EtOAc 1:1). ^{1}H-NMR (300 MHz, $CDCl_3$) δ 4.80-4.63 (m, 1H), 3.78-3.25 (m, 4H), 3.04 (s, 3H), 2.00-1.67 (m, 3H), 1.61-1.38 (m, 10H). ^{13}C-NMR (75 MHz, $CDCl_3$) δ 154.87 (q), 80.36 (q), 75.58 (+), 47.9 (-), 43.5 (-), 38.96 (+), 30.61 (-), 28.50 (+, 3C), 21.81 (-). NMR data matches literature reference.[62] HRMS (ESI-MS): calcd. for $C_{22}H_{42}N_2NaO_{10}S_2^+$: 581.2173, found: 581.2176. MF: $C_{11}H_{21}NO_5S$. MW: 279.35.

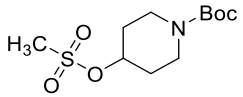

***tert*-Butyl 4-((methylsulfonyl)oxy)piperidine-1-carboxylate (4.39).**[61] Piperidin-4-ol (**4.37**, 2 g, 19.8 mmol, 1 equiv) was dissolved in CH_2Cl_2 (25 mL). NEt_3 (2.74 mL, 19.8 mmol, 1 equiv) was added and the mixture was cooled to 0 °C by using an ice-bath. Boc_2O (4.15 g, 19.0 mmol, 0.96 equiv) was dissolved in CH_2Cl_2 (15 mL) and added dropwise to the ice-cold piperidin-4-ol/NEt_3 mixture while stirring. The resulting mixture was stirred at 0 °C for 2 h. After 2 h, NEt_3 (3.27 mL, 24.0 mmol, 1.19 equiv) and mesityl chloride (2.31 g, 20.0 mmol, 1.02 equiv) were added. The ice-bath was removed, and the reaction mixture was stirred at rt for 3 h. After 3 h, the mixture was diluted with EA/PE 1:1 (200 mL) and washed successively with aqueous citric acid (100 mL), saturated, aqueous $NaHCO_3$ (100 mL) and brine (100 mL). The combined organic phases were dried over Na_2SO_4. Na_2SO_4 was filtered off and the filtrate was evaporated. The product was purified by flash chromatography (gradient: 0-20 min: PE/EtOAc 100:0 to 80:20, 40 min: 60:40, SF 12 g). The product was obtained as a white solid (3.93 g, 74%). R_f = 0.54 (PE/EtOAc 1:1). ^{1}H-NMR (300 MHz, $CDCl_3$) δ 4.91-4.81 (m, 1H), 3.76-3.61 (m, 2H), 3.34-3.22 (m, 2H), 3.02 (s, 3H), 2.00-1.73 (m, 4H), 1.44 (s, 9H). ^{13}C-NMR (75 MHz, $CDCl_3$) δ 154.69 (q), 80.11 (q), 60.51 (-), 40.61 (-, 2C), 38.96 (+), 31.77 (-, 2C), 28.51 (+, 3C). NMR data matches literature reference.[63-64] HRMS (ESI-MS): calcd. for $C_{22}H_{42}N_2NaO_{10}S_2^+$: 581.2173, found: 581.2172. MF: $C_{11}H_{21}NO_5S$. MW: 279.35.

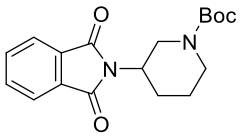

***tert*-Butyl 3-(1,3-dioxoisoindolin-2-yl)piperidine-1-carboxylate (4.40). 4.38** (3.9 g, 14.0 mmol, 1 equiv) and potassium phthalimide (3.1 g, 16.52 mmol, 1.18 equiv) were dissolved in DMF (70 mL). The mixture was stirred at 75 °C for 24 h. After 24 h, the mixture was diluted with H_2O (300 mL) and extracted with EtOAc (3 x 150 mL). The combines organic phases were extracted successively with H_2O (2 x 100 mL), brine (100 mL) and dried over Na_2SO_4. Na_2SO_4 was filtered off and the filtrate was evaporated. The product was purified by flash chromatography (gradient: 0-20 min: PE/EtOAc 100:0-90:10, SF 12 g) to give the product as oily solid (465 mg, 10%). R_f = 0.85 (PE/EtOAc 1:1). ^{1}H-NMR (400 MHz, $CDCl_3$) δ 7.87-7.77 (m, 2H), 7.76-7.66 (m, 2H), 4.26-3.89 (m, 3H), 3.48 (t, *J* = 12.1 Hz, 1H), 2.81-2.62 (m, 1H), 2.42-2.23 (m, 1H), 1.90-1.72 (m, 2H), 1.64-1.51 (m, 1H), 1.45 (s, 9H). ^{13}C-NMR (101 MHz, $CDCl_3$) δ 168.08, 154.61 (2C), 133.99 (2C), 131.79 (2C), 123.21 (2C), 79.82, 47.89, 46.07, 43.24, 28.37 (3C), 27.85, 24.95. HRMS (ESI-MS): calcd. for $C_{18}H_{22}N_2NaO_4^+$: 353.1472, found: 353.1472. MF: $C_{18}H_{22}N_2O_4$. MW: 330.38.

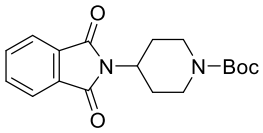

***tert*-Butyl 4-(1,3-dioxoisoindolin-2-yl)piperidine-1-carboxylate (4.41).**[65] **4.39** (2.1 g, 7.52 mmol, 1 equiv) and potassium phthalimide (1.64 g, 8.87 mmol, 1.18 equiv) were dissolved in DMF (70 mL). The mixture was stirred at 75 °C for 24 h. After 24 h, the mixture was diluted with H_2O (300 mL) and extracted with EtOAc (3 x 150 mL). The combines organic phases were extracted successively with H_2O (2 x 100 mL), brine (100 mL) and dried over Na_2SO_4. Na_2SO_4 was filtered off and the filtrate was evaporated. The product was purified by flash chromatography (gradient: 0-20 min: PE/EtOAc 100:0-80:20, SF 12 g) to give the product as white solid (530 mg, 21%). R_f = 0.83 (PE/EtOAc 1:1). ^{1}H-NMR (300 MHz, $CDCl_3$) δ 7.86-7.65 (m, 4H), 4.36-4.14 (m, 3H), 2.77 (t, *J* = 13.4 Hz, 2H), 2.50-2.28 (m, 2H), 1.72-1.60 (m, 2H), 1.47 (s, 9H). ^{13}C-NMR (75 MHz, $CDCl_3$) δ 168.29 (q), 154.74 (q), 134.13 (+, 2C), 131.99 (q, 2C), 123.34 (+, 2C), 79.87 (q), 49.19 (+), 43.51 (-, 2C), 29.08 (-, 2C), 28.59 (+, 3C). HRMS (ESI-MS): calcd. for $C_{18}H_{22}N_2NaO_4^+$: 353.1472, found: 353.1472. MF: $C_{18}H_{22}N_2O_4$. MW: 330.38.

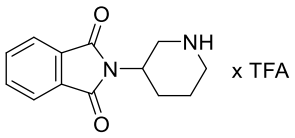

2-(Piperidin-3-yl)isoindoline-1,3-dione hydrotrifluoroacetate (4.42). 4.40 (465 mg, 1.41 mmol) was dissolved in CH_2Cl_2 (4 mL) and TFA (1 mL) was added under stirring at rt. After stirring for 16 h, the solvent was removed in vacuum. The product was obtained as beige solid (485 mg, 100%). ^{1}H-NMR (400 MHz, MeOD) δ 7.91-7.73 (m, 4H), 4.57-4.46 (m, 1H), 3.71 (t, *J* = 11.9 Hz, 1H), 3.50-3.35 (m, 2H), 3.11-2.99 (m, 1H), 2.45-2.32 (m, 1H), 2.15-2.05 (m, 1H), 2.03-1.94 (m, 1H), 1.93-1.80 (m, 1H). ^{13}C-NMR (101 MHz, MeOD) δ 169.14 (2C), 135.67 (2C), 132.94 (2C), 124.34 (2C), 46.23, 45.72, 44.83, 27.37, 22.93. HRMS (ESI-MS): calcd. for $C_{13}H_{15}N_2O_2^+$: 231.1128, found: 231.1138. MF: $C_{13}H_{14}N_2S_2$ x $C_2HF_3O_2$. MW: (230.27 + 114.02).

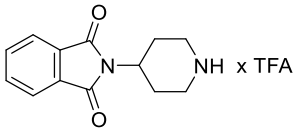

2-(Piperidin-4-yl)isoindoline-1,3-dione hydrotrifluoroacetate (4.43). 4.41 (520 mg, 1.57 mmol) was dissolved in CH_2Cl_2 (4 mL) and TFA (1 mL) was added under stirring at rt. After stirring for 16 h, the solvent was removed in vacuum. The product was obtained as beige solid (540 mg, 100%). R_f = 0.57 (CH_2Cl_2/0.5% NH_3 in MeOH 9:1). ^{1}H-NMR (300 MHz, MeOD) δ 7.89-7.73 (m, 4H), 4.54-4.37 (m, 1H), 3.59-3.44 (m, 2H), 3.29-3.07 (m, 2H), 2.77-2.58 (m, 2H), 2.09-1.93 (m, 2H). ^{13}C-NMR (75 MHz, $CDCl_3$) δ 169.20 (q, 2C), 160.09 (q, *J* = 39.6 Hz, TFA), 135.48 (+, 2C), 132.98 (q, 2C), 124.19 (+, 2C), 116.64 (q, *J* = 286.4 Hz, TFA), 47.16 (+), 45.01 (-, 2C), 22.16 (-, 2C). HRMS (ESI-MS): calcd. for $C_{13}H_{15}N_2O_2^+$: 231.1128, found: 231.1144. MF: $C_{13}H_{14}N_2O_2$ x $C_2HF_3O_2$. MW: (230.27 + 114.02).

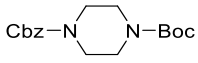

1-Benzyl 4-(*tert*-butyl) piperazine-1,4-dicarboxylate (4.45). *tert*-Butyl piperazine-1-carboxylate (**4.44**, 0.29 g, 1.02 mmol, 1 equiv) and NEt_3 (156 µL, 1.12 mmol, 1.1 equiv) were dissolved in CH_2Cl_2 (10 mL) and cooled to 0 °C by using an ice-bath. A solution of benzyl chloroformate (147 µL, 1.03 mmol, 1.01 equiv) in CH_2Cl_2 (5 mL) was added dropwise while stirring. After stirring the mixture overnight, the solvent was removed in vacuum and the residue was purified by flash chromatography (gradient: 0-20 min: PE/EtOAc 100:0-80:20, SF 8 g) to give the product as transparent oil (200 mg, 61%). R_f = 0.56 (PE/EtOAc 4:1). ^{1}H-NMR

(300 MHz, $CDCl_3$) δ 7.44-7.28 (m, 5H), 5.13 (s, 2H), 3.54-3.28 (m, 8H), 1.46 (s, 9H). ^{13}C-NMR (75 MHz, $CDCl_3$) δ 155.12 (q), 154.52 (q), 136.40 (q), 128.45 (+, 2C), 128.05 (+), 127.89 (+, 2C), 80.08 (q), 67.25 (-), 43.58 (-, 4C), 28.30 (+, 3C). HRMS (ESI-MS): calcd. for $C_{17}H_{28}N_3O_4^+$: 338.2074, found: 338.2076. MF: $C_{17}H_{24}N_2O_4$. MW: 320.39.

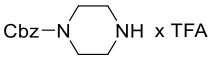

Benzyl piperazine-1-carboxylate hydrotrifluoroacetate (4.46). 4.45 (200 mg, 0.63 mmol) was dissolved in CH_2Cl_2 (3 mL) and TFA (2 mL) was added. The mixture was stirred for 7 h at rt. The solvent was evaporated to give the product as brown oil (208 mg, 99%.). R_f = 0.54 (CH_2Cl_2/0.5% NH_3 in MeOH 9:1). ^{1}H-NMR (300 MHz, MeOD) δ 7.44-7.19 (m, 5H), 5.14 (s, 2H), 3.73 (t, *J* = 4.3 Hz, 4H), 3.20 (t, *J* = 5.5 Hz, 4H). ^{13}C-NMR (75 MHz, MeOD) δ 156.30 (q), 137.59 (q), 129.59 (+, 2C), 129.33 (+), 129.16 (+, 2C), 68.92 (-), 44.22 (-, 2C), 41.78 (-, 2C). HRMS (ESI-MS): calcd. for $C_{12}H_{17}N_2O_2^+$: 221.1285, found: 221.1288. MF: $C_{12}H_{16}N_2O_2$ x $C_2HF_3O_2$. MW: (220.27 + 114.02).

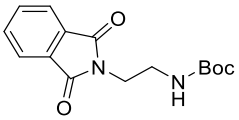

***tert*-Butyl (2-(1,3-dioxoisoindolin-2-yl)ethyl)carbamate (4.48).** A mixture of *tert*-butyl (2-aminoethyl)carbamate (**4.47**, 0.8 g, 5.0 mmol, 1 equiv), Nefkens` reagent (1.32 g, 6.0 mmol, 1.2 mmol) and K_2CO_3 (2.07 g, 15 mmol, 3 equiv) in H_2O (30 mL) was stirred at rt for 16 h. The precipitate was filtered off, washed with H_2O, and dried in vacuum (0.33 g, 22%). R_f = 0.22 (PE/EtOAc 3:1). ^{1}H-NMR (300 MHz, $CDCl_3$) δ 7.88-7.80 (m, 2H), 7.75-7.67 (m, 2H), 3.88-3.77 (m, 2H), 3.42 (q, *J* = 5.8 Hz, 2H), 1.33 (s, 9H). ^{13}C-NMR (75 MHz, $CDCl_3$) δ 168.61 (q, 2C), 156.09 (q), 134.10 (+, 2C), 132.19 (q, 2C), 123.44 (+, 2C), 79.55 (q), 39.70 (-), 38.21 (-), 28.36 (+, 3C). HRMS (ESI-MS): calcd. for $C_{15}H_{18}N_2NaO_4^+$: 313.1159, found: 313.1157. MF: $C_{15}H_{18}N_2O_4$. MW: 290.32.

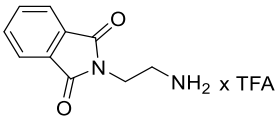

2-(2-Aminoethyl)isoindoline-1,3-dione hydrotrifluoroacetate (4.49). To a solution of **4.48** (1.93 g, 6.6 mmol) in CH_2Cl_2 (10 mL) was added TFA (5 mL) and the mixture was stirred at rt for 48 h. Subsequently, the solvent was removed in vacuum yielding a yellow oil (2.0 g, 100%). R_f = 0.55 (CH_2Cl_2/0.5% NH_3 in MeOH 9:1). ^{1}H-NMR (300 MHz, MeOD) δ 7.94-7.78 (m, 4H),

4.05-3.95 (m, 2H), 3.30-3.21 (m, 2H). ^{13}C-NMR (75 MHz, MeOD) δ 169.76 (q, 2C), 135.53 (+, 2C), 133.36 (q, 2C), 124.34 (+, 2C), 39.85 (-), 36.46 (-). HRMS (ESI-MS): calcd. for $C_{10}H_{11}N_2O_2^+$: 191.0815, found: 191.0820. MF: $C_{10}H_{10}N_2O_2$ x $C_2HF_3O_2$. MW: (190.20 + 114.02).

4.4.8 Preparation of the Amine Building Blocks 4.66-4.72

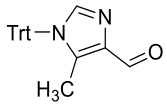

5-Methyl-1-trityl-1*H*-imidazole-4-carbaldehyde (4.51).[19, 66] To a solution of 5-methyl-1-trityl-1*H*-imidazole-4-carbaldehyde (**4.50**, 2.0 g, 18.2 mmol, 1 equiv) and Trt-Cl (5.6 g, 19.98 mmol, 1.1 equiv) in MeCN (80 mL), NEt_3 (4.54 mL, 32.8 mmol, 1.8 equiv) was added dropwise. After stirring at rt for 16 h, n-hexane (8 mL) and H_2O (80 mL) were added and the mixture was stirred for 30 min. The precipitated product was filtered and washed with H_2O. Recrystallization from EtOAc/n-hexane yielded a beige solid (2.75 g, 43%). R_f = 0.63 (PE/EtOAc 1:1). M. p.: 162-165 °C. ^{1}H-NMR (300 MHz, $CDCl_3$) δ 9.11 (s, 1H), 7.39-7.30 (m, 10H), 7.21-7.12 (m, 6H), 2.55 (s, 3H). ^{13}C-NMR (75 MHz, $CDCl_3$) δ 181.17 (q), 151.86 (q, 3C), 141.58 (q), 141.53 (+), 129.59 (+, 6C), 128.58 (q), 128.47 (+, 6C), 128.43 (+, 3C), 76.19 (q), 15.77 (+). NMR data matches literature reference.[19] HRMS (ESI-MS): calcd. for $C_{24}H_{21}N_2O^+$: 353.1648, found: 353.1681. MF: $C_{24}H_{20}N_2O$. MW: 352.44.

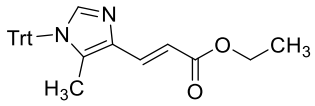

(*E*)-Ethyl 3-(5-methyl-1-trityl-1*H*-imidazol-4-yl)acrylate (4.52).[18-19] To a solution of triethyl phosphonoacetate (1.69 mL, 8.51 mmol, 1.5 equiv) in anhydrous THF (35 mL), NaH (60% dispersion in mineral oil, 204 mg, 8.51 mmol, 1.5 equiv) was added in portions. After stirring for 1 h at rt, a solution of **4.51** (2.0 g, 5.67 mmol, 1 equiv) in anhydrous THF (20 mL) was added dropwise. The mixture was refluxed for 16 h. The solvent was evaporated, and the crude product was dissolved in EtOAc (100 mL) and washed with water (3 x 100 mL). The organic layer was dried over Na_2SO_4, evaporated and the crude product purified by flash chromatography (gradient: 0-20 min: PE/EtOAc 100:0-90:10; 40 min: 90:10, SF 12 g) yielding the product as white solid (0.43 g, 18%). R_f = 0.24 (PE/EtOAc 4:1). M. p.: 175-176 °C. ^{1}H-NMR (300 MHz, $CDCl_3$) δ 7.56 (d, *J* = 15.4 Hz, 1H), 7.41-7.28 (m, 10H), 7.19-7.09 (m, 6H), 6.58 (d, *J* = 15.4 Hz, 1H), 4.22 (q, *J* = 7.1 Hz, 2H), 1.57 (s, 3H), 1.29 (t, *J* = 7.1 Hz, 3H). ^{13}C-

NMR (75 MHz, $CDCl_3$) δ 167.95 (q), 141.38 (q, 3C), 139.43 (+), 136.40 (q), 135.11 (+), 132.90 (q), 129.99 (+, 6C), 128.21 (+, 6C), 128.15 (+, 3C), 115.36 (+), 75.40 (q), 60.12 (-), 14.44 (+), 11.99 (+). NMR data matches literature reference.[19] HRMS (ESI-MS): calcd. for $C_{28}H_{27}N_2O_2^+$: 423.2067, found: 423.2072. MF: $C_{28}H_{26}N_2O_2$. MW: 422.53.

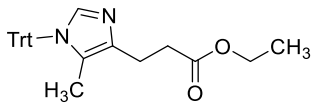

Ethyl 3-(5-methyl-1-trityl-1*H*-imidazol-4-yl)propanoate (4.53).[19] To a solution of **4.52** (430 mg, 1.02 mmol) in EtOH (10 mL), Pd/C (10 wt%, 50 mg) was added. After stirring overnight at rt under a hydrogen atmosphere (1 atm), the catalyst was removed by filtration over Celite 545 and the solvent was evaporated. The product was obtained as a white solid (350 mg, 81%). The crude product was used in the next reaction without further purification. R_f = 0.38 (PE/EtOAc 3:1). M. p.: 94-95 °C. ^{1}H-NMR (300 MHz, $CDCl_3$) δ 7.37-7.28 (m, 9H), 7.22 (s, 1H), 7.17-7.08 (m, 6H), 4.11 (q, *J* = 7.1 Hz, 2H), 2.79 (t, *J* = 7.4 Hz, 2H), 2.68 (t, *J* = 7.4 Hz, 2H), 1.39 (s, 3H), 1.24 (t, *J* = 7.1 Hz, 3H). ^{13}C-NMR (75 MHz, $CDCl_3$) δ 173.45 (q), 142.04 (q, 3C), 138.54 (q), 137.42 (+), 130.11 (+, 6C), 127.95 (+, 6C), 127.81 (+, 3C), 125.22 (q), 74.78 (q), 60.22 (-), 34.25 (-), 22.73 (-), 14.31 (+), 11.63 (+). NMR data matches literature reference.[19] HRMS (ESI-MS): calcd. for $C_{28}H_{29}N_2O_2^+$: 425.2224, found: 425.2224. MF: $C_{28}H_{28}N_2O_2$. MW: 424.54.

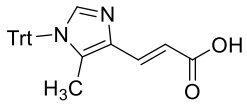

(*E*)-3-(5-Methyl-1-trityl-1*H*-imidazol-4-yl)acrylic acid (4.54). To an ice-cold solution of KOH (120 mg, 2.13 mmol, 3 equiv) in EtOH/H_2O (95:5 (v/v), 7 mL) was added **4.52** (300 mg, 0.71 mmol, 1 equiv). The resulting mixture was stirred for 48 h, meanwhile the mixture was allowed to warm up to rt. The mixture was neutralized with 1 M HCl in MeOH. The solvent was removed in vacuum. The residue was taken up in H_2O (20 mL) and the solution was acidified to pH 3-4 with 1 M HCl in H_2O. The precipitated white solid was filtered off, washed with H_2O (5 mL), and dried in vacuum (220 mg, 79%). R_f = 0.80 (CH_2Cl_2/MeOH 9:1). ^{1}H-NMR (300 MHz, $CDCl_3$) δ 7.60 (d, *J* = 15.4 Hz, 1H), 7.47 (s, 1H), 7.38-7.30 (m, 9H), 7.19-7.09 (m, 6H), 6.62 (d, *J* = 15.5 Hz, 1H), 1.57 (s, 3H). ^{13}C-NMR (75 MHz, $CDCl_3$) δ 171.83 (q), 141.11 (q, 3C), 139.46 (+), 135.94 (+), 135.77 (q), 133.32 (q), 129.90 (+, 6C), 128.20 (+, 6C),

128.17 (+, 3C), 115.48 (+), 75.56 (q), 11.98 (+). HRMS (ESI-MS): calcd. for $C_{26}H_{23}N_2O_2^+$: 395.1754, found: 395.1751. MF: $C_{26}H_{22}N_2O_2$. MW: 394.47.

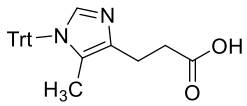

3-(5-Methyl-1-trityl-1*H*-imidazol-4-yl)propanoic acid (4.55). To an ice-cold solution of KOH (190 mg, 3.39 mmol, 3 equiv) in EtOH/H_2O (95:5 (v/v), 11.7 mL) was added **4.53** (480 mg, 1.13 mmol, 1 equiv) and stirred for 16 h and the reaction mixture was allowed to warm up to rt. The mixture was neutralized with 1 M HCl in MeOH. The solvent was removed in vacuum. The residue was taken up in H_2O (20 mL) and the solution was acidified to pH 3-4 with 1 M HCl in H_2O. The precipitated white solid was filtered off, washed with H_2O (5 mL), and dried in vacuum (240 mg, 54%). R_f = 0.44 (CH_2Cl_2/MeOH 9:1). ^{1}H-NMR (300 MHz, $CDCl_3$) δ 7.39-7.32 (m, 10H), 7.16-7.07 (m, 6H), 2.86-2.68 (m, 4H), 1.38 (s, 3H). ^{13}C-NMR (75 MHz, $CDCl_3$) δ 175.37 (q), 141.06 (q), 137.21 (q), 135.83 (+), 129.91 (+, 6C), 128.26 (+), 128.20 (+, 9C), 125.37 (q), 75.56 (q), 35.17 (-), 21.13 (-), 11.48 (+). HRMS (ESI-MS): calcd. for $C_{26}H_{25}N_2O_2^+$: 397.1911, found: 397.1920. MF: $C_{26}H_{24}N_2O_2$. MW: 396.49.

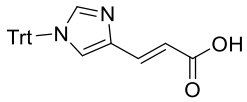

(*E*)-3-(1-Trityl-1*H*-imidazol-4-yl)acrylic acid (4.57). Trt-Cl (2.0 g, 7.17 mmol, 1 equiv) was dissolved in DMF (25 mL) and added dropwise to a mixture of urocanic acid (**4.56**, 1.0 g, 7.17 mmol, 1 equiv) and NEt_3 (2.97 mL, 21.7 mmol, 3 equiv) in DMF (25 mL). After the addition, the mixture was stirred for 14 h at rt. The solvent was removed in vacuum and the crude product was purified by flash chromatography (gradient: 0-20 min: PE/EtOAc 100:0-50:50, 30 min: 30:70, 40 min: 30:70, 60 min: 10:90, SF 12 g) to give white solid (1.14 g, 42%). R_f = 0.44 (CH_2Cl_2/MeOH 9:1). ^{1}H-NMR (300 MHz, $CDCl_3$) δ 12.08 (s, 1H), 7.51-7.33 (m, 12H), 7.17-7.08 (m, 6H), 6.30 (d, *J* = 15.6 Hz, 1H). ^{13}C-NMR (75 MHz, $CDCl_3$) δ 169.70 (q), 141.88 (q, 3C), 140.29 (+), 137.03 (q), 136.42 (+), 129.66 (+, 6C), 128.30 (+, 6C), 128.22 (+, 3C), 127.07 (+), 123.85 (q), 81.74 (q). HRMS (ESI-MS): calcd. for $C_{25}H_{20}N_2NaO_2^+$: 403.1417, found: 403.1412. MF: $C_{25}H_{20}N_2O_2$. MW: 380.45.

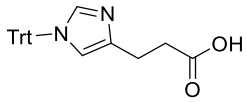

3-(1-Trityl-1*H*-imidazol-4-yl)propanoic acid (4.58).[67-68] Urocanic acid (**4.56**, 1.0 g, 7.24 mmol) was dissolved in MeOH (30 mL) and Pd/C (10 wt%, 217 mg) was added. H_2 gas was bubbled though the suspension for 5 h under stirring at rt. The mixture was filtered over Celite 545 and the solvent was evaporated to yield 3-(1*H*-imidazol-4-yl)propanoic acid (1.01 g, 100%). ^{1}H-NMR (300 MHz, DMSO-d_6) δ 14.70 (s, 2H), 9.02 (s, 1H), 7.39 (s, 1H), 2.84 (t, *J* = 7.1 Hz, 2H), 2.66 (t, *J* = 7.1 Hz, 2H). ^{13}C-NMR (75 MHz, DMSO-d_6) δ 172.97 (q), 133.21 (-), 132.27 (q), 115.42 (-), 32.26 (+), 19.55 (+). NMR data matches literature reference.[67] HRMS (ESI-MS): calcd. for $C_6H_9N_2O_2^+$: 141.0659, found: 141.0672. MF: $C_6H_8N_2O_2$. MW: 140.14. Trt-Cl (2.61 g, 9.35 mmol, 1 equiv) was dissolved in DMF (25 mL) and added dropwise to a mixture of 3-(1*H*-imidazol-4-yl)propanoic acid (1.31 mg, 9.35 mmol, 1 equiv) and NEt_3 (3.89 mL, 28.05 mmol, 3 equiv) in DMF (50 mL). After the addition, the mixture was stirred for 14 h at rt. The solvent was removed in vacuum and the crude product was purified by flash chromatography (gradient: 0-20 min: PE/EtOAc 100:0-50:50, 30 min: 30:70, 40 min: 10:90, SF 12 g) to give the product as beige solid (1.44 g, 40%). M. p.: 185 °C (ref. 188-190 °C). R_f = 0.77 (CH_2Cl_2/MeOH 9:1). ^{1}H-NMR (300 MHz, $CDCl_3$) δ 11.55 (s, 1H), 7.48 (d, *J* = 1.43 Hz, 1H), 7.38-7.28 (m, 9H), 7.15-7.06 (m, 6H), 6.58 (s, 1H), 2.87 (t, *J* = 6.96 Hz, 2H), 2.67 (t, *J* = 7.19 Hz, 2H). ^{13}C-NMR (75 MHz, $CDCl_3$) δ 175.6 (q), 141.89 (q, 3C), 139.25(q), 137.50 (+), 129.66 (+, 6C), 128.16 (+, 3C), 128.09 (+, 6C), 118.09 (+), 75.62 (q), 34.92 (-), 22.74 (-). NMR data matches literature reference.[55] HRMS (ESI-MS): calcd. for $C_{25}H_{23}N_2O_2^+$: 383.1754, found: 383.1762 MF: $C_{25}H_{22}N_2O_2$. MW: 382.46.

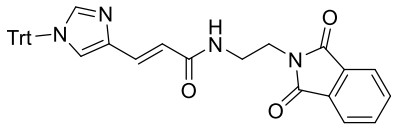

(*E*)-*N*-(2-(1,3-Dioxoisoindolin-2-yl)ethyl)-3-(1-trityl-1*H*-imidazol-4-yl)acrylamide (4.59). The title compound was prepared from **4.57** (261 mg, 0.69 mmol), **4.49** (250 mg, 0.82 mmol), EDC x HCl (158 mg, 0.82 mmol), HOBt x H_2O (126 mg, 0.82 mmol) and DIPEA (699 µL, 4.11 mmol) in DMF (2.2 mL) according to the general procedure A. The crude product was purified by flash chromatography (gradient: 0-20 min: CH_2Cl_2/0.5% NH_3 in MeOH 100:0-95:5; 40 min: 95:5, SF 12 g) yielding yellow oil (130 mg, 34%). R_f = 0.87 (CH_2Cl_2/0.5% NH_3 in MeOH 9:1). ^{1}H-NMR (300 MHz, $CDCl_3$) δ 7.97 (s, 1H), 7.80-7.73 (m, 2H), 7.69-7.62 (m, 2H), 7.45-7.18 (m, 16H), 6.91 (s, 1H), 6.49 (d, *J* = 15.2 Hz, 1H), 3.86 (t,

J = 5.4 Hz, 2H), 3.64-3.56 (m, 2H), NH signal is missing. HRMS (ESI-MS): calcd. for $C_{35}H_{29}N_4O_3^+$: 553.2234, found: 553.2238. MF: $C_{35}H_{28}N_4O_3$. MW: 552.63.

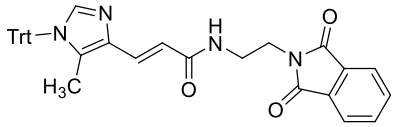

(*E*)-*N*-(2-(1,3-Dioxoisoindolin-2-yl)ethyl)-3-(5-methyl-1-trityl-1*H*-imidazol-4-yl)acrylamide (4.60). The title compound was prepared from **4.54** (216 mg, 0.55 mmol), **4.49** (200 mg, 0.66 mmol), EDC x HCl (126 mg, 0.66 mmol), HOBt x H_2O (101 mg, 0.66 mmol) and DIPEA (466 µL, 2.74 mmol) in DMF (2.2 mL) according to the general procedure A. The crude product was purified by flash chromatography (gradient: 0-20 min: CH_2Cl_2/0.5% NH_3 in MeOH 100:0-95:5; 40 min: 95:5, SF 8 g) yielding yellow oil (150 mg, 48%). R_f = 0.79 (CH_2Cl_2/0.5% NH_3 in MeOH 9:1). ^{1}H-NMR (300 MHz, $CDCl_3$) δ 8.73 (br s, 1H), 7.72-7.65 (m, 2H), 7.61-7.54 (m, 2H), 7.44 (d, *J* = 15.3 Hz, 1H), 7.31 (s, 1H), 7.28-7.20 (m, 15H), 6.56-6.49 (m, 1H), 3.85-3.75 (m, 2H), 3.61-3.52 (m, 2H), 1.43 (s, 3H). HRMS (ESI-MS): calcd. for $C_{36}H_{31}N_4O_3^+$: 567.2391, found: 567.2402. MF: $C_{36}H_{30}N_4O_3$. MW: 566.66.

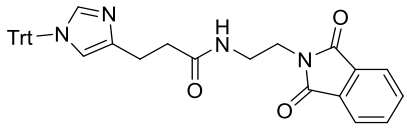

***N*-(2-(1,3-Dioxoisoindolin-2-yl)ethyl)-3-(1-trityl-1*H*-imidazol-4-yl)propanamide (4.61).** The title compound was prepared from **4.58** (346 mg, 0.90 mmol), **4.49** (330 mg, 1.09 mmol), EDC x HCl (208 mg, 1.09 mmol), HOBt x H_2O (166 mg, 1.09 mmol) and DIPEA (768 µL, 4.52 mmol) in DMF (2.2 mL) according to the general procedure A. The crude product was purified by flash chromatography (gradient: 0-20 min: CH_2Cl_2/0.5% NH_3 in MeOH 100:0-95:5; 40 min: 95:5, SF 8 g) yielding yellow oil (490 mg, 98%). R_f = 0.70 (CH_2Cl_2/0.5% NH_3 in MeOH 9:1). ^{1}H-NMR (300 MHz, $CDCl_3$) δ 11.05 (br s, 1H), 7.77-7.70 (m, 2H), 7.66-7.57 (m, 2H), 7.45-7.40 (m, 1H), 7.34-7.23 (m, 9H), 7.07-6.97 (m, 6H), 6.50 (d, *J* = 1.4 Hz, 1H), 3.80-3.74 (m, 2H), 3.44-3.32 (m, 2H), 2.74 (t, *J* = 5.6 Hz, 2H), 2.44 (t, *J* = 7.2 Hz, 2H). HRMS (ESI-MS): calcd. for $C_{35}H_{31}N_4O_3^+$: 555.2391, found: 555.2404. MF: $C_{35}H_{30}N_4O_3$. MW: 554.65.

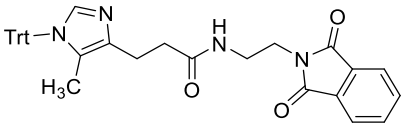

***N*-(2-(1,3-Dioxoisoindolin-2-yl)ethyl)-3-(5-methyl-1-trityl-1*H*-imidazol-4-yl)propanamide (4.62).** The title compound was prepared from **4.54** (217 mg, 0.55 mmol), **4.49** (200 mg, 0.66 mmol), EDC x HCl (126 mg, 0.66 mmol), HOBt x H_2O (101 mg, 0.66 mmol) and DIPEA (466 µL, 2.74 mmol) in DMF (2.2 mL) according to the general procedure A. The crude product was purified by flash chromatography (gradient: 0-20 min: CH_2Cl_2/0.5% NH_3 in MeOH 100:0-95:5; 40 min: 95:5, SF 8 g) yielding yellow oil (247 mg, 79%). R_f = 0.62 (CH_2Cl_2/0.5% NH_3 in MeOH 9:1). ^{1}H-NMR (300 MHz, $CDCl_3$) δ 10.97 (br s, 1H), 7.85 (s, 1H), 7.70-7.53 (m, 4H), 7.38-7.28 (m, 9H), 7.14-7.02 (m, 6H), 3.79-3.70 (m, 2H), 3.56-3.45 (m, 2H), 2.87 (t, *J* = 7.0 Hz, 2H), 2.61 (t, *J* = 7.2 Hz, 2H), 1.45 (s, 3H). HRMS (ESI-MS): calcd. for $C_{36}H_{33}N_4O_3^+$: 569.2547, found: 569.2560. MF: $C_{36}H_{32}N_4O_3$. MW: 568.68.

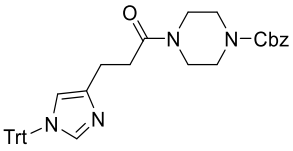

Benzyl 4-(3-(1-trityl-1*H*-imidazol-4-yl)propanoyl)piperazine-1-carboxylate (4.63). The title compound was prepared from **4.58** (199 mg, 0.52 mmol), **4.46** (209 mg, 0.63 mmol), EDC x HCl (120 mg, 0.63 mmol), HOBt x H_2O (96 mg, 0.63 mmol) and DIPEA (532 µL, 3.13 mmol) in DMF (2.2 mL) according to the general procedure A. The crude product was purified by flash chromatography (gradient: 0-20 min: CH_2Cl_2/0.5% NH_3 in MeOH 100:0-95:5, 40 min: 90:10, SF 8 g) yielding the product as a yellow foam (305 mg, 100%). R_f = 0.83 (CH_2Cl_2/0.5% NH_3 in MeOH 9:1). ^{1}H-NMR (300 MHz, $CDCl_3$) δ 7.61 (s, 1H), 7.39-7.28 (m, 14H), 7.15-7.02 (m, 6H), 6.66 (s, 1H), 5.14 (s, 2H), 3.58-3.33 (m, 8H), 2.89 (t, *J* = 7.6 Hz, 2H), 2.65 (t, *J* = 7.6 Hz, 2H). ^{13}C-NMR (75 MHz, $CDCl_3$) δ 170.59 (q), 155.23 (q), 143.66 (q, 3C), 141.48 (q), 137.29 (+), 136.52 (q), 129.75 (+), 128.69 (+), 128.62 (+), 128.44 (+), 128.32 (+), 128.17 (+), 126.32 (+), 124.12 (+), 119.40 (+), 109.91 (+), 76.50 (q), 67.56 (-), 45.29 (-), 44.06 (-), 43.65 (-), 41.48 (-), 32.47 (-), 22.79 (-). HRMS (ESI-MS): calcd. for $C_{37}H_{37}N_4O_3^+$: 585.2860, found: 585.2909. MF: $C_{37}H_{36}N_4O_3$. MW: 584.72.

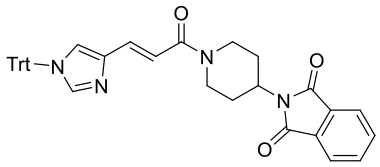

(*E*)-2-(1-(3-(1-Trityl-1*H*-imidazol-4-yl)acryloyl)piperidin-4-yl)isoindoline-1,3-dione (4.64). The title compound was prepared from **4.57** (249 mg, 0.65 mmol), **4.43** (270 mg, 0.79 mmol), EDC x HCl (150 mg, 0.79 mmol), HOBt x H_2O (120 mg, 0.79 mmol) and DIPEA (556 µL, 3.27 mmol) in DMF (2.2 mL) according to the general procedure A. The crude product was purified by flash chromatography (gradient: 0-20 min: CH_2Cl_2/0.5% NH_3 in MeOH 100:0-90:10, SF 8 g) yielding the product as yellowish oil (380 mg, 99%). R_f = 0.69 (CH_2Cl_2/0.5% NH_3 in MeOH 9:1). ^{1}H-NMR (300 MHz, $CDCl_3$) δ 7.83-7.74 (m, 2H), 7.72-7.63 (m, 2H), 7.52-7.44 (m, 1H), 7.43-7.40 (m, 1H), 7.36-7.28 (m, 9H), 7.16-7.06 (m, 7H), 6.95 (d, *J* = 1.3 Hz, 1H), 4.44-4.23 (m, 2H), 3.19-3.03 (m, 1H), 2.51-2.28 (m, 2H), 1.82-1.66 (m, 2H). ^{13}C-NMR (75 MHz, $CDCl_3$) δ 168.12, 165.83, 142.03, 139.99 (+), 137.75, 134.31 (+), 134.09 (+, 2C), 131.89, 129.75 (+, 6C), 128.35 (+, 3C), 128.29 (+, 6C), 123.79 (+), 123.30 (+, 2C), 115.19 (+), 75.76, 49.05 (+), 36.58 (+), 31.51 (+). HRMS (ESI-MS): calcd. for $C_{38}H_{33}N_4O_3^+$: 593.2547, found: 593.2553. MF: $C_{38}H_{32}N_4O_3$. MW: 592.70.

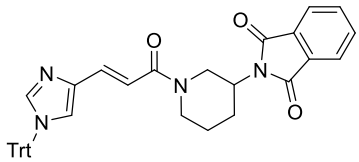

(*E*)-2-(1-(3-(1-Trityl-1*H*-imidazol-4-yl)acryloyl)piperidin-3-yl)isoindoline-1,3-dione (4.65). The title compound was prepared from **4.57** (223 mg, 0.59 mmol), **4.42** (162 mg, 0.70 mmol), EDC x HCl (135 mg, 0.70 mmol), HOBt x H_2O (108 mg, 0.70 mmol) and DIPEA (498 µL, 2.93 mmol) in DMF (2.2 mL) according to the general procedure A. The crude product was purified by flash chromatography (gradient: 0-40 min: CH_2Cl_2/MeOH 100:0-90:10, SF 8 g) yielding **4.65** as yellowish oil (190 mg, 55%). R_f = 0.71 (CH_2Cl_2/MeOH 95:5). ^{1}H-NMR (400 MHz, $CDCl_3$) δ 7.87-7.65 (m, 4H), 7.52-7.30 (m, 10H), 7.29-7.28 (m, 1H), 7.26-7.25 (m, 1H), 7.18-7.03 (m, 6H), 6.96 (s, 1H), 4.84-4.65 (m, 1H), 4.30-4.07 (m, 2H), 3.58-3.34 (m, 1H), 3.17-3.00 (m, 1H), 2.46-2.28 (m, 1H), 1.97-1.78 (m, 2H), 1.68-1.52 (m, 1H). ^{13}C-NMR (101 MHz, $CDCl_3$) δ 167.97 (2C), 165.84, 141.89 (3C), 137.54, 134.18, 133.99 (2C), 131.76 (2C), 129.64 (6C), 128.69, 128.16 (6C), 127.81 (3C), 126.85, 123.72, 123.22 (2C), 81.90, 48.61, 45.66, 43.91, 28.21, 25.90. HRMS (ESI-MS): calcd. for $C_{38}H_{33}N_4O_3^+$: 593.2547, found: 593.2562. MF: $C_{38}H_{32}N_4O_3$. MW: 592.70.

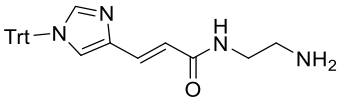

(*E*)-*N*-(2-Aminoethyl)-3-(1-trityl-1*H*-imidazol-4-yl)acrylamide (4.66). The title compound was prepared from **4.59** (180 mg, 0.33 mmol) and N_2H_4 x H_2O (79 µL, 1.63 mmol) in EtOH (10 mL) according to the general procedure B. The crude product was purified by flash chromatography (gradient: 0-40 min: CH_2Cl_2/0.5% NH_3 in MeOH 100:0-80:20, SF 12 g) yielding **4.66** as a white solid (70 mg, 50%). R_f = 0.21 (CH_2Cl_2/0.5% NH_3 in MeOH 9:1). ^{1}H-NMR (300 MHz, MeOD) δ 7.58 (d, *J* = 1.3 Hz, 1H), 7.46-7.36 (m, 12H), 7.26 (d, *J* = 1.3 Hz, 1H), 7.23-7.13 (m, 7H), 6.60 (d, *J* = 15.5 Hz, 1H), 3.50 (t, *J* = 6.1 Hz, 2H), 2.99 (t, *J* = 6.1 Hz, 2H). HRMS (ESI-MS): calcd. for $C_{27}H_{27}N_4O^+$: 423.2179, found: 423.2190. MF: $C_{27}H_{26}N_4O$. MW: 422.53.

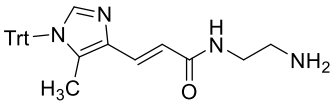

(*E*)-*N*-(2-Aminoethyl)-3-(5-methyl-1-trityl-1*H*-imidazol-4-yl)acrylamide (4.67). The title compound was prepared from **4.60** (150 mg, 0.27 mmol) and N_2H_4 x H_2O (64 µL, 1.32 mmol) in EtOH (10 mL) according to the general procedure B yielding **4.67** as a yellow oil (71 mg, 60%). The crude product was used in the next step without further purification. R_f = 0.11 (CH_2Cl_2/0.5% NH_3 in MeOH 9:1). ^{1}H-NMR (400 MHz, MeOD) δ 8.03-8.00 (m, 1H), 7.50 (d, *J* = 15.3 Hz, 1H), 7.44-7.35 (m, 9H), 7.20-7.12 (m, 6H), 6.62 (d, *J* = 15.3 Hz, 1H), 3.59 (t, *J* = 6.0 Hz, 2H), 3.13 (t, *J* = 5.9 Hz, 2H), 1.59 (s, 3H). HRMS (ESI-MS): calcd. for $C_{28}H_{29}N_4O^+$: 437.2336, found: 437.2348. MF: $C_{28}H_{28}N_4O$. MW: 436.56.

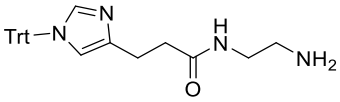

***N*-(2-Aminoethyl)-3-(1-trityl-1*H*-imidazol-4-yl)propanamide (4.68).** The title compound was prepared from **4.61** (460 mg, 0.83 mmol) and N_2H_4 x H_2O (202 µL, 4.15 mmol) in EtOH (10 mL) according to the general procedure B. The crude product was purified by flash chromatography (gradient: 0-30 min: CH_2Cl_2/0.5% NH_3 in MeOH 100:0-90:10, 50 min: 80:20, SF 4 g) yielding **4.68** as a yellow oil (150 mg, 43%). R_f = 0.22 (CH_2Cl_2/0.5% NH_3 in MeOH 9:1). ^{1}H-NMR (400 MHz, MeOD) δ 7.40 (d, *J* = 1.4 Hz, 1H), 7.37-7.30 (m, 9H), 7.16-7.07 (m, 6H), 6.68 (d, *J* = 1.4 Hz, 1H), 3.38-3.33 (m, 2H), 2.89 (t, *J* = 6.0 Hz, 2H), 2.83 (t, *J* = 7.2 Hz, 2H), 2.48 (t, *J* = 7.2 Hz, 2H). ^{13}C-NMR (101 MHz, MeOD) δ 176.10 (q), 143.61 (q, 3C), 140.93

(q), 139.36 (+), 130.80 (+, 6C), 129.31 (+, 3C), 129.22 (+, 6C), 119.80 (+), 76.74 (q), 41.49 (-), 39.99 (-), 36.76 (-), 24.94 (-). HRMS (ESI-MS): calcd. for $C_{27}H_{29}N_4O^+$: 425.2336, found: 425.2340. MF: $C_{27}H_{28}N_4O$. MW: 424.55.

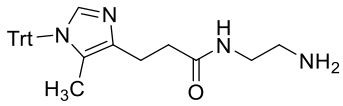

***N*-(2-Aminoethyl)-3-(5-methyl-1-trityl-1*H*-imidazol-4-yl)propanamide (4.69).** The title compound was prepared from **4.62** (247 mg, 0.43 mmol) and N_2H_4 x H_2O (144 µL, 2.97 mmol) in EtOH (10 mL) according to the general procedure B. The crude product was purified by flash chromatography (gradient: 0-20 min: CH_2Cl_2/0.5% NH_3 in MeOH 100:0-90:10, SF 8 g) yielding **4.69** as a yellow oil (167 mg, 88%). R_f = 0.19 (CH_2Cl_2/0.5% NH_3 in MeOH 9:1). ^{1}H-NMR (400 MHz, MeOD) δ 7.44-7.37 (m, 9H), 7.35 (s, 1H), 7.21-7.12 (m, 6H), 3.53 (t, *J* = 5.7 Hz, 2H), 3.13 (t, *J* = 5.7 Hz, 2H), 2.85 (t, *J* = 7.1 Hz, 2H), 2.54 (t, *J* = 7.1 Hz, 2H), 1.45 (s, 3H). ^{13}C-NMR (101 MHz, MeOD) δ 176.96 (q), 143.16 (q, 3C), 139.27 (q), 138.36 (+), 131.40 (+, 6C), 129.55 (+, 9C), 127.62 (q), 76.86 (q), 41.46 (-), 38.27 (-), 37.14 (-), 23.98 (-), 12.25 (+). HRMS (ESI-MS): calcd. for $C_{28}H_{31}N_4O^+$: 439.2492, found: 439.2494. MF: $C_{28}H_{30}N_4O$. MW: 438.58.

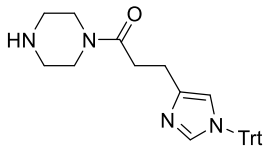

1-(Piperazin-1-yl)-3-(1-trityl-1*H*-imidazol-4-yl)propan-1-one (4.70). Pd/C (10 wt%, 60 mg) was added to a solution of **4.63** (280 mg, 0.48 mmol) in THF/MeOH (1 mL:1.5 mL), and the mixture was stirred under a H_2 atmosphere (1 amt) at rt for 6 h. The mixture was filtered through Celite 545, the filtrate was evaporated, and the residue was purified by flash chromatography (gradient: 0-40 min: CH_2Cl_2/0.5% NH_3 in MeOH 100:0-90:10, SF 4 g) to give the product as a yellow oil (134 mg, 62%). R_f = 0.35 (CH_2Cl_2/0.5% NH_3 in MeOH 9:1). ^{1}H-NMR (300 MHz, MeOD) δ 7.35 (d, *J* = 1.4 Hz, 1H), 7.34-7.25 (m, 9H), 7.14-7.05 (m, 6H), 6.67 (d, *J* = 1.4 Hz, 1H), 3.56-3.39 (m, 4H), 2.83-2.61 (m, 8H). ^{13}C-NMR (75 MHz, MeOD) δ 172.99 (q), 143.75 (q, 3C), 141.12 (q), 139.36 (+), 130.96 (+, 6C), 129.43 (+, 3C), 129.37 (+, 6C), 120.03 (+), 76.84 (q), 47.60 (-), 46.82 (-), 46.38 (-), 43.50 (-), 33.51 (-), 24.96 (-). HRMS (ESI-MS): calcd. for $C_{29}H_{31}N_4O^+$: 451.2492, found: 451.2498. MF: $C_{29}H_{30}N_4O$. MW: 450.59.

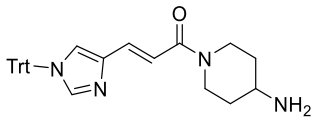

(*E*)-1-(4-Aminopiperidin-1-yl)-3-(1-trityl-1*H*-imidazol-4-yl)prop-2-en-1-one (4.71). The title compound was prepared from **4.64** (321 mg, 0.54 mmol) and N_2H_4 x H_2O (180 µL, 3.71 mmol) in EtOH (10 mL) according to the general procedure B. The crude product was purified by flash chromatography (gradient: 0-20 min: CH_2Cl_2/0.5% NH_3 in MeOH 100:0-90:10, 25 min: 90:10, 40 min: 80:20, SF 4 g) yielding **4.71** as a yellow oil (220 mg, 80%). R_f = 0.21 (CH_2Cl_2/0.5% NH_3 in MeOH 9:1). ^{1}H-NMR (300 MHz, MeOD) δ 7.56-7.53 (m, 1H), 7.42 (s, 1H), 7.40-7.30 (m, 9H), 7.26 (d, *J* = 1.3 Hz, 1H), 7.20-7.07 (m, 6H), 6.71 (d, *J* = 1.4 Hz, 1H), 4.65-4.51 (m, 2H), 4.32-4.12 (m, 2H), 3.13-3.03 (m, 1H), 2.07-1.83 (m, 2H), 1.50-1.21 (m, 2H). HRMS (ESI-MS): calcd. for $C_{30}H_{31}N_4O^+$: 463.2492, found: 463.2488. MF: $C_{30}H_{30}N_4O$. MW: 462.60.

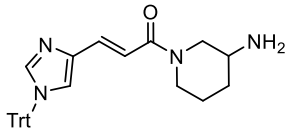

(*E*)-1-(3-Aminopiperidin-1-yl)-3-(1-trityl-1*H*-imidazol-4-yl)prop-2-en-1-one (4.72). The title compound was prepared from **4.65** (190 mg, 0.32 mmol) and N_2H_4 x H_2O (82 µL, 1.69 mmol) in EtOH (10 mL) according to the general procedure B. The crude product was purified by flash chromatography (gradient: 0-20 min: CH_2Cl_2/0.5% NH_3 in MeOH 100:0-90:10, SF 8 g) yielding **4.72** as a white solid (50 mg, 34%). R_f = 0.55 (CH_2Cl_2/0.5% NH_3 in MeOH 9:1). ^{1}H-NMR (400 MHz, MeOD) δ 7.55 (s, 1H), 7.44-7.32 (m, 10H), 7.26 s (1H), 7.20-7.05 (7H), 4.53-3.79 (m, 4H), 3.02-2.76 (m, 1H), 2.14-1.35 (m, 4H). HRMS (ESI-MS): calcd. for $C_{30}H_{31}N_4O^+$: 463.2492, found: 463.2495. MF: $C_{30}H_{30}N_4O$. MW: 462.60.

4.4.9 Preparation of the Mixed Squaramate Building Blocks 4.75 and 4.76 as well as the Amine Building Block 4.78

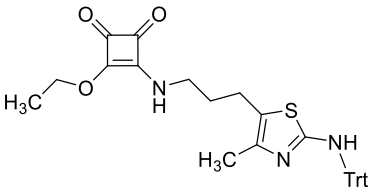

3-Ethoxy-4-((3-(4-methyl-2-(tritylamino)thiazol-5-yl)propyl)amino)cyclobut-3-ene-1,2-dione (4.75). The title compound was synthetized according to the procedure of Dr. D. Erdmann.[20] Diethoxycyclobut-3-ene-1,2-dione (**4.73**, 187 mg, 1.1 mmol, 1.1 equiv) was dissolved in EtOH (10 mL) and slowly added to a solution of **4.18** (414 mg, 1.0 mmol, 1 equiv) in EtOH (10 mL). The yellow solution was stirred at rt overnight. The solvent was evaporated under reduced pressure. The residue was dissolved in EtOAc (30 mL) and washed with H_2O (3 x 20 mL). After drying over Na_2SO_4, EtOAc was evaporated and the product dried in vacuum to give brown foam (484 mg, 90%). R_f = 0.86 (CH_2Cl_2/0.5% NH_3 in MeOH 9:1). ^{1}H-NMR (300 MHz, $CDCl_3$) δ 7.36-7.21 (m, 15H), 4.77-4.67 (m, 2H), 3.41-3.14 (m, 2H), 2.45 (t, *J* = 7.5 Hz, 2H), 2.06 (s, 3H), 1.65 (quint, *J* = 7.2 Hz, 2H), 1.47 (t, *J* = 7.1 Hz, 3H). ^{13}C-NMR (75 MHz, $CDCl_3$) δ 184.40 (q, 2C), 172.50 (q), 171.39 (q), 165.37 (q), 143.86 (q, 3C), 141.68 (q), 129.41 (+, 6C), 128.32 (+, 6C), 127.62 (+, 3C), 119.51 (q), 71.97 (q), 69.91 (-), 60.62 (-), 44.01 (-), 23.02 (-), 15.82 (+), 14.57 (+). HRMS (ESI-MS): calcd. for $C_{32}H_{32}N_3O_3S^+$: 538.2159, found: 538.2186. MF: $C_{32}H_{31}N_3O_3S$. MW: 537.68.

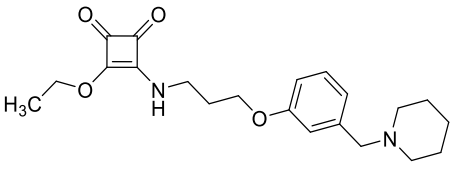

3-Ethoxy-4-((3-(3-(piperidin-1-ylmethyl)phenoxy)propyl)amino)cyclobut-3-ene-1,2-dione (4.76).[20] The title compound was synthetized according to the procedure of Dr. D. Erdmann.[20] 3,4-Diethoxycyclobut-3-ene-1,2-dione (**4.73**, 0.24 g, 0.97 mmol, 1 equiv), dissolved in EtOH (10 mL), was slowly added to a solution of **4.74** (0.18 g, 1.1 mmol, 1.1 equiv) in EtOH (10 mL). The yellow solution was stirred at rt for 3 h before the solvent was evaporated under reduced pressure. The residue was dissolved in EtOAc (30 mL) and washed with H_2O (3 x 20 mL). After drying over Na_2SO_4, the EtOAc phase was evaporated and dried in vacuum to give the product as sticky yellow oil (0.36 g, 100%). R_f = 0.66 (CH_2Cl_2/0.5% NH_3 in MeOH 9:1). ^{1}H-NMR (300 MHz, $CDCl_3$) δ 7.21 (t, *J* = 8.0 Hz, 1H), 6.95-6.86 (m, 2H), 6.80-

6.73 (m, 1H), 4.72 (q, *J* = 7.1 Hz, 2H), 4.12-4.01 (m, 2H), 3.98-3.80 (m, 1H), 3.75-3.62 (m, 1H), 3.47 (s, 2H), 2.49-2.33 (m, 4H), 2.10 (quint, *J* = 6.06 Hz, 2H), 1.59 (quint, *J* = 5.5 Hz, 4H), 1.50-1.36 (m, 5H). ^{13}C-NMR (101 MHz, $CDCl_3$) δ 188.52, 182.03, 176.66, 171.67, 157.60, 139.59, 128.31, 121.23, 114.13, 112.11, 68.83, 64.13, 62.86, 53.69 (2C), 41.63, 29.20, 25.08 (2C), 23.49, 14.97. NMR data matches literature reference.[20] HRMS (ESI-MS): calcd. for $C_{21}H_{29}N_2O_4^+$: 373.2122, found: 373.2136. MF: $C_{21}H_{28}N_2O_4$. MW: 372.47.

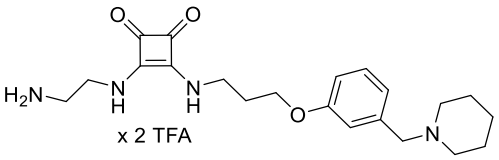

3-((2-Aminoethyl)amino)-4-((3-(3-(piperidin-1-ylmethyl)phenoxy)propyl)amino)cyclobut-3-ene-1,2-dione dihydrotrifluoroacetate (4.78). [20] The title compound was synthetized according to the procedure of Dr. D. Erdmann.[20] **4.76** (0.23 g, 0.62 mmol, 1 equiv) and *tert*-butyl 2-aminoethylcarbamate (0.12 g, 0.73 mmol, 1.1 equiv) were dissolved in EtOH (30 mL) and stirred at rt overnight. After evaporation of the solvent the product was purified by flash chromatography (eluent CH_2Cl_2/0.5% NH_3 in MeOH; gradient: 0-20 min: CH_2Cl_2/MeOH 100:0 to 97:3, 40 min: 95:5, 60 min: 95:5; 80 min: 90:10, SF 8 g) leading to a yellow foam (**4.77**, 184 mg, 61%). R_f = 0.49 (CH_2Cl_2/0.5% NH_3 in MeOH 9:1). ^{1}H-NMR (300 MHz, $CDCl_3$) δ 7.17 (t, *J* = 7.8 Hz, 1H), 6.95-6.81 (m, 2H), 6.74 (dd, *J* = 8.2, 2.5 Hz, 1H), 4.04 (t, *J* = 5.9 Hz, 2H), 3.92-3.75 (m, 2H), 3.73-3.52 (m, 1H), 3.40 (s, 2H), 3.34-3.22 (m, 2H), 2.44-2.26 (m, 4H), 2.20-2.04 (m, 2H), 1.55 (quint, *J* = 5.4 Hz, 4H), 1.48-1.33 (m, 11H). ^{13}C-NMR (75 MHz, $CDCl_3$) δ 167.86, 158.66, 140.10, 129.06, 121.91, 115.42, 112.81, 64.86, 63.80, 54.52 (2C), 41.66, 30.71 (2C), 28.36 (3C), 25.86, 24.30, 2 C`s not detected. NMR data matches literature reference.[20] HRMS (ESI-MS): calcd. for $C_{26}H_{39}N_4O_5^+$: 487.2915, found: 487.2927. MF: $C_{26}H_{38}N_4O_5$. MW: 486.61. The Boc-protected intermediate (180 mg, 0.37 mmol) was dissolved in CH_2Cl_2 (4 mL) and TFA (1 mL) was added. The solution was stirred at rt overnight. The solvent was evaporated to give the product as yellow solid (230 mg, 100%). R_f = 0.18 (CH_2Cl_2/0.5% NH_3 in MeOH 9:1). ^{1}H-NMR (300 MHz, MeOD) δ 7.37 (dd, *J* = 8.4, 7.2 Hz, 1H), 7.09-7.00 (m, 3H), 4.23 (s, 2H), 4.13 (t, *J* = 5.9 Hz, 2H), 3.85 (t, *J* = 6.0 Hz, 4H), 3.49-3.38 (m, 3H), 3.18 (t, *J* = 6.0 Hz, 2H), 3.03-2.87 (m, 2H), 2.11 (quint, *J* = 6.4 Hz, 2H), 2.00-1.65 (m, 4H), 1.59-1.45 (m, 2H). ^{13}C-NMR (75 MHz, MeOD) δ 161.27 (2C), 132.21, 131.92 (2C), 124.95, 120.66, 118.91, 117.62, 115.75, 66.64, 62.21, 54.57 (2C), 42.95, 41.99, 32.13, 28.23, 24.61 (2C), 23.24. NMR data matches

literature reference.[20] HRMS (ESI-MS): calcd. for $C_{21}H_{31}N_4O_3^+$: 387.2391, found: 387.2396. MF: $C_{21}H_{30}N_4O_3$ x $C_4H_2F_6O_4$. MW: (386.50 + 228.05).

4.4.10 Preparation of the 2-Arylbenzimidazoles 4.82-4.97, 4.104-4.110, 4.112 and 4.114-4.116, the Squaramide 4.117 as well as Carbamoylguanidine 4.120

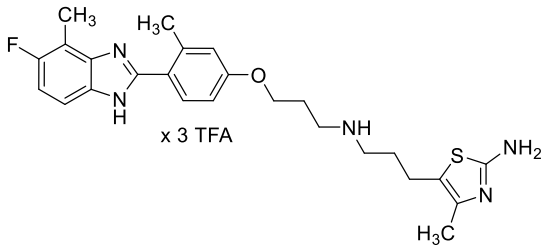

5-(3-((3-(4-(5-Fluoro-4-methyl-1*H*-benzo[*d*]imidazol-2-yl)-3-methylphenoxy)propyl)amino)propyl)-4-methylthiazol-2-amine trihydrotrifluoroacetate (4.82). The title compound was synthesized from **4.79** (50 mg, 0.115 mmol), K_2CO_3 (95 mg, 0.684 mmol) and **4.18** (109 mg, 0.264 mmol) in MeCN (2.5 mL) according to the general procedure C. Deprotection in CH_2Cl_2 (3 mL) and TFA (2 mL) followed by preparative RP-HPLC afforded a white, foamlike and hygroscopic solid (5.34 mg, 5.8%). R_f = 0.10 (CH_2Cl_2/MeOH 9:1). RP-HPLC (220 nm): 100% (t_R = 9.3 min, k = 1.90). ^{1}H-NMR (300 MHz, MeOD) δ 7.76-7.54 (m, 2H), 7.33 (dd, J = 10.1, 9.0 Hz, 1H), 7.16-7.01 (m, 2H), 4.22 (t, J = 5.8 Hz, 2H), 3.30-3.23 (m, 2H, overlapped with MeOH signal), 3.18-3.01 (m, 2H), 2.74 (t, J = 7.7 Hz, 2H), 2.64-2.48 (m, 6H), 2.34-2.13 (m, 5H), 1.96 (quint, J = 8.1 Hz, 2H). ^{1}H-NMR (600 MHz, DMSO-d_6) δ 9.04 (s, 2H), 8.64 (s, 2H), 7.72 (d, J = 8.3 Hz, 1H), 7.51-7.43 (m, 1H), 7.14 (t, J = 9.6 Hz, 1H), 7.02-6.95 (m, 2H), 4.15 (t, J = 6.1 Hz, 2H), 3.14-3.07 (m, 2H), 3.00-2.93 (m, 2H), 2.65 (t, J = 7.5 Hz, 2H), 2.57 (s, 3H), 2.49 (d, J = 1.7 Hz, 3H, overlapped with DMSO signal), 2.12–2.07 (m, 5H), 1.80 (quint, J = 7.7 Hz, 2H). ^{13}C-NMR (151 MHz, DMSO-d_6) δ 167.75, 159.63 (HMBC), 159.0 (q, J = 32.8 Hz, TFA),156.90 (HMBC), 152.11, 141.24, 139.30, 134.65 (HMBC), 131.60, 126.31, 120.46 (HMBC), 117.03, 116.68 (q, J = 296.7 Hz, TFA), 115.93, 112.01, 111.31 (HSQC), 110.75 (HMBC), 64.80, 45.92, 44.27, 26.74, 25.53, 21.97, 20.75, 11.55, 9.38, 1 C signal is missing. HRMS (ESI-MS): calcd. for $C_{25}H_{31}FN_5OS^+$: 468.2228, found: 468.2227. MF: $C_{25}H_{30}FN_5OS$ x $C_6H_3F_9O_6$. MW: (467.61 + 342.07).

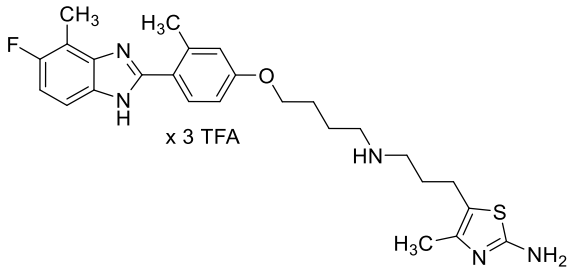

5-(3-((4-(4-(5-Fluoro-4-methyl-1*H*-benzo[*d*]imidazol-2-yl)-3-methylphenoxy)butyl)amino)propyl)-4-methylthiazol-2-amine trihydrotrifluoroacetate (4.83). The title compound was synthesized from **4.80** (50 mg, 0.114 mmol), K_2CO_3 (95 mg, 0.684 mmol) and **4.18** (141 mg, 0.341 mmol) in MeCN (2.5 mL) according to the general procedure C. Deprotection in CH_2Cl_2 (3 mL) and TFA (2 mL) followed by preparative RP-HPLC afforded a white, foamlike and hygroscopic solid (2.0 mg, 2.2%). R_f = 0.10 (CH_2Cl_2/MeOH 9:1). RP-HPLC (220 nm): 97% (t_R = 9.9 min, k = 2.08). ^{1}H-NMR (300 MHz, MeOD) δ 7.67 (d, J = 8.5 Hz, 1H), 7.60 (dd, J = 8.9, 4.2 Hz, 1H), 7.40-7.29 (m, 1H), 7.11-7.00 (m, 2H), 4.19-4.12 (m, 2H), 3.16-3.05 (m, 4H), 2.74 (t, J = 7.7 Hz, 2H), 2.56 (d, J = 1.8 Hz, 3H), 2.51 (s, 3H), 2.19 (s, 3H), 2.01-1.88 (m, 6H). HRMS (ESI-MS): calcd. for $C_{26}H_{33}FN_5OS^+$: 482.2384, found: 482.2386. MF: $C_{26}H_{32}FN_5OS$ x $C_6H_3F_9O_6$. MW: (481.63 + 342.07).

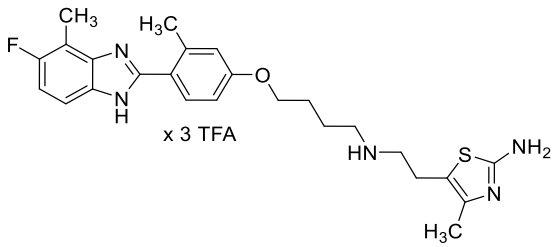

5-(2-((4-(4-(5-Fluoro-4-methyl-1*H*-benzo[*d*]imidazol-2-yl)-3-methylphenoxy)butyl)amino)ethyl)-4-methylthiazol-2-amine trihydrotrifluoroacetate (4.84). The title compound was synthesized from **4.80** (50 mg, 0.114 mmol), K_2CO_3 (95 mg, 0.684 mmol) and **4.17** (137 mg, 0.342 mmol) in MeCN (2.5 mL) according to the general procedure C. Deprotection in CH_2Cl_2 (3 mL) and TFA (2 mL) followed by preparative RP-HPLC afforded a white, foamlike and hygroscopic solid (2.4 mg, 2.6%). R_f = 0.13 (CH_2Cl_2/MeOH 9:1). RP-HPLC (220 nm): 96% (t_R = 10.5 min, k = 2.27). ^{1}H-NMR (300 MHz, MeOD) δ 7.71-7.58 (m, 2H), 7.35 (dd, J = 10.1, 9.0 Hz, 1H), 7.11-7.00 (m, 2H), 4.19-4.11 (m, 2H), 3.28-3.21 (m, 2H), 3.19-3.11 (m, 2H), 3.06-2.97 (m, 2H), 2.57 (d, J = 1.8 Hz, 3H), 2.50 (s, 3H), 2.25-2.20 (m, 3H), 2.00-1.89 (m, 4H). HRMS (ESI-MS): calcd. for $C_{25}H_{31}FN_5OS^+$: 468.2228, found: 468.2228. MF: $C_{25}H_{30}FN_5OS$ x $C_6H_4F_9O_6$. MW: 467.61 + 342.07.

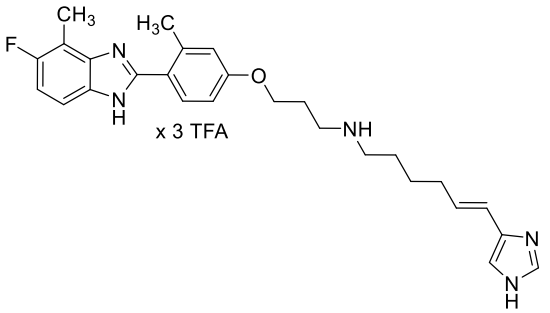

(*E*)-*N*-(3-(4-(5-Fluoro-4-methyl-1*H*-benzo[*d*]imidazol-2-yl)-3-methylphenoxy)propyl)-6-(1*H*-imidazol-4-yl)hex-5-en-1-amine trihydrotrifluoroacetate (4.85). The title compound was synthesized from **4.79** (40 mg, 0.094 mmol), K_2CO_3 (78 mg, 0.57 mmol) and **4.26** (115 mg, 0.28 mmol) in MeCN (2.5 mL) according to the general procedure C. Deprotection in CH_2Cl_2 (3 mL) and TFA (2 mL) followed by preparative RP-HPLC afforded a white, foamlike and hygroscopic solid (27.3 mg, 34%). R_f = 0.21 (CH_2Cl_2/0.5% NH_3 in MeOH 9:1). RP-HPLC (220 nm): 98% (t_R = 10.7 min, k = 2.33). ^{1}H-NMR (300 MHz, MeOD) δ 8.87 (d, J = 1.3 Hz, 1H), 7.74-7.54 (m, 3H), 7.34 (dd, J = 10.2, 9.0 Hz, 1H), 7.14-6.99 (m, 2H), 6.44-6.28 (m, 1H), 6.10-5.96 (m, 1H), 4.22 (t, J = 5.8 Hz, 2H), 3.30-3.19 (m, 2H, overlapped with MeOH signal), 3.15-3.03 (m, 2H), 2.56 (d, J = 1.8 Hz, 3H), 2.51 (s, 3H), 2.48-2.34 (m, 2H), 2.30-2.15 (m, 2H), 1.89-1.71 (m, 2H), 1.71-1.55 (m, 2H). ^{1}H-NMR (600 MHz, DMSO-d_6) δ 9.06 (d, J = 1.2 Hz, 1H), 8.77 (br s, 2H), 7.75-7.70 (m, 2H), 7.56 (dd, J = 8.9, 4.3 Hz, 1H), 7.23 (t, J = 9.5 Hz, 1H), 7.05-6.98 (m, 2H), 6.34-6.30 (m, 1H), 5.95-5.88 (m, 1H), 4.17 (t, J = 6.1 Hz, 2H), 3.17-3.06 (m, 2H), 3.03-2.95 (m, 2H), 2.55 (s, 3H), 2.50 (s, 3H, overlapped with DMSO signal), 2.34-2.28 (m, 2H), 2.14-2.08 (m, 2H), 1.67 (quint, J = 7.7 Hz, 2H), 1.53 (quint, J = 7.4 Hz, 2H), 2 H signals missing. ^{13}C-NMR (151 MHz, DMSO-d_6) δ 160.20, 158.63 (q, J = 32.9 Hz, TFA), 157.23 (d, J = 236.0 Hz), 151.69, 139.55, 136.29, 135.55, 133.78, 132.05, 131.07, 129.27, 118.90, 117.06, 116.70 (q, J = 296.3 Hz, TFA), 116.69, 114.60, 112.52–111.77 (m, 3C), 110.75 (d, J = 22.8 Hz), 64.95, 46.68, 44.16, 28.35, 25.48, 25.42, 25.21, 20.41, 9.35. HRMS (ESI-MS): calcd. for $C_{27}H_{33}FN_5O^+$: 462.2664, found: 462.2665. MF: $C_{27}H_{32}FN_5O$ x $C_6H_3F_9O_6$. MW: (461.59 + 342.06).

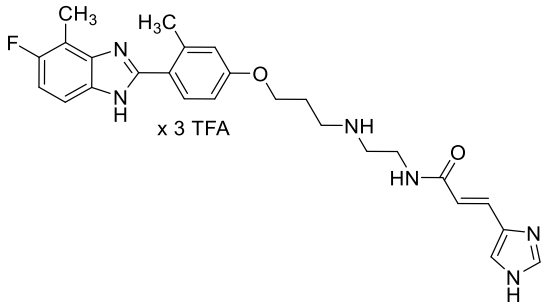

(*E*)-*N*-(2-((3-(4-(5-Fluoro-4-methyl-1*H*-benzo[*d*]imidazol-2-yl)-3-methylphenoxy)propyl)amino)ethyl)-3-(1*H*-imidazol-4-yl)acrylamide trihydrotrifluoroacetate (4.86, PB513). The title compound was synthesized from **4.79** (35 mg, 0.083 mmol), K_2CO_3 (69 mg, 0.50 mmol) and **4.66** (70 mg, 0.17 mmol) in MeCN (2.5 mL) according to the general procedure C. Deprotection in CH_2Cl_2 (3 mL) and TFA (2 mL) followed by preparative RP-HPLC afforded a white, foamlike and hygroscopic solid (17.5 mg, 26%). R_f = 0.3 (CH_2Cl_2/0.5% NH_3 in MeOH 8:2). RP-HPLC (220 nm): 97% (t_R = 10.0 min, k = 2.12). ^{1}H-NMR (600 MHz, DMSO-d_6) δ 9.03-8.93 (m, 1H), 8.87-8.69 (m, 2H), 8.57 (t, J = 5.8 Hz, 1H), 7.91 (s, 1H), 7.72 (d, J = 8.4 Hz, 1H), 7.55 (dd, J = 8.8, 4.3 Hz, 1H), 7.40 (d, J = 15.9 Hz, 1H), 7.25-7.18 (m, 1H), 7.08-6.97 (m, 2H), 6.66 (d, J = 15.8 Hz, 1H), 4.17 (t, J = 6.1 Hz, 2H), 3.51 (q, J = 6.2 Hz, 2H), 3.23–3.07 (m, 4H), 2.54 (s, 3H), 2.50 (3H, overlapped with DMSO signal), 2.15–2.07 (m, 2H), 1 NH signal is missing. ^{13}C-NMR (151 MHz, DMSO-d_6) δ 165.14, 160.12, 158.55 (q, J = 32.7 Hz, TFA), 157.18 (d, J = 236.0 Hz), 151.73, 139.50, 136.36, 135.78, 131.98, 131.22, 129.93, 125.58, 123.01, 120.39, 119.09, 117.09, 116.69 (q, J = 297.3 Hz, TFA), 110.66 (d, J = 21.9 Hz), 112.41–112.09 (m, 2C), 111.88 (d, J = 26.4 Hz), 65.00, 46.52, 44.46, 35.64, 25.47, 20.45, 9.37. HRMS (ESI-MS): calcd. for $C_{26}H_{30}FN_6O_2^+$: 477.2409, found: 477.2405; calcd. for $C_{26}H_{31}FN_6O_2^{2+}$: 239.1241, found: 239.1247; calcd. for $C_{26}H_{32}FN_6O_2^{3+}$: 159.7518, found: 159.7522. MF: $C_{26}H_{29}FN_6O_2$ x $C_6H_3F_9O_6$. MW: (476.56 + 342.06).

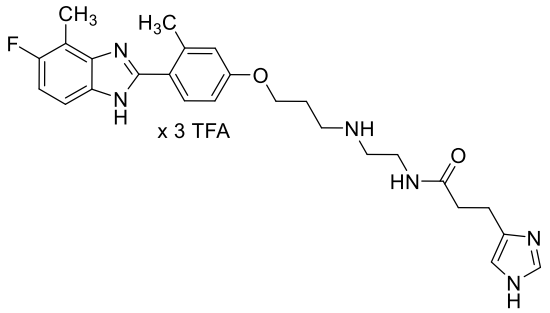

***N*-(2-((3-(4-(5-Fluoro-4-methyl-1*H*-benzo[*d*]imidazol-2-yl)-3-methylphenoxy)propyl)amino)ethyl)-3-(1*H*-imidazol-4-yl)propanamide trihydrotrifluoroacetate (4.87).** The title compound was synthesized from **4.79** (50 mg, 0.118 mmol), K_2CO_3 (98 mg, 0.71 mmol) and **4.68** (150 mg, 0.35 mmol) in MeCN (2.5 mL) according to the general procedure C. Deprotection in CH_2Cl_2 (3 mL) and TFA (2 mL) followed by preparative RP-HPLC afforded a white, foamlike and hygroscopic solid (9.8 mg, 10%). R_f = 0.20 (CH_2Cl_2/0.5% NH_3 in MeOH 9:1). RP-HPLC (220 nm): 99% (t_R = 9.9 min, k = 2.08). ^{1}H-NMR (300 MHz, MeOD) δ 8.78 (d, J = 1.4 Hz, 1H), 7.67 (d, J = 8.6 Hz, 1H), 7.58 (dd, J = 8.9, 4.1 Hz, 1H), 7.40-7.23 (m, 2H), 7.19-6.97 (m, 2H), 4.23 (t, J = 5.7 Hz, 2H), 3.53 (t, J = 5.9 Hz, 2H), 3.30-3.24 (m, 2H), 3.21 (t, J = 5.9 Hz, 2H), 3.03 (t, J = 7.3 Hz, 2H), 2.66 (t, J = 7.3 Hz, 2H), 2.56 (d, J = 1.8 Hz, 3H), 2.51 (s, 3H), 2.24 (quint, J = 6.1 Hz, 2H). ^{1}H-NMR (600 MHz, DMSO-d_6) δ 14.39 (s, 1H), 8.97 (d, J = 1.4 Hz, 1H), 8.79-8.64 (m, 2H), 8.26 (t, J = 5.7 Hz, 1H), 7.72 (d, J = 8.4 Hz, 1H), 7.56-7.48 (m, 1H), 7.37 (s, 1H), 7.18 (t, J = 9.6 Hz, 1H), 7.05-6.97 (m, 2H), 4.15 (t, J = 6.0 Hz, 2H), 3.37 (q, J = 6.2 Hz, 2H), 3.13 (quint, J = 6.1 Hz, 2H), 3.04 (t, J = 5.9 Hz, 2H), 2.89 (t, J = 7.5 Hz, 2H), 2.56 (s, 3H), 2.51-2.53 (m, 2H, overlapped with DMSO signal), 2.50 (s, 3H, overlapped with DMSO signal), 2.14-2.05 (m, 2H). ^{13}C-NMR (151 MHz, DMSO-d_6) δ 171.35, 159.85, 158.34 (q, J = 32.8 Hz, TFA), 157.02 (d, J = 237.2 Hz), 151.92, 139.38, 133.68, 132.70, 131.77, 119.94 (HMBC), 117.06, 116.63 (q, J = 296.5 Hz, TFA), 115.50, 112.08 (2C, HSQC), 111.46 (2C, HSQC), 110.73, 64.92, 46.43, 44.34, 35.22, 33.46, 25.47, 20.61, 19.83, 9.38, 1 C signal is missing. HRMS (ESI-MS): calcd. for $C_{26}H_{32}FN_6O_2^+$: 479.2565, found: 479.2563. MF: $C_{26}H_{31}FN_6O_2$ x $C_6H_3F_9O_6$. MW: (478.57 + 342.06).

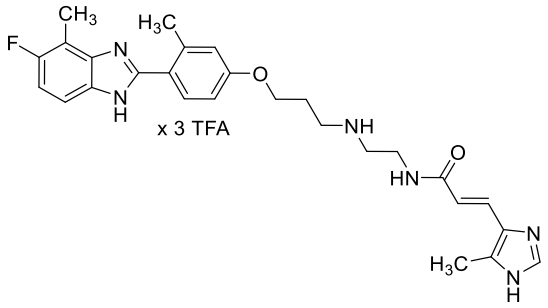

(*E*)-*N*-(2-((3-(4-(5-Fluoro-4-methyl-1*H*-benzo[*d*]imidazol-2-yl)-3-methylphenoxy)propyl)amino)ethyl)-3-(5-methyl-1*H*-imidazol-4-yl)acrylamide trihydrotrifluoroacetate (4.88). The title compound was synthesized from **4.79** (17 mg, 0.039 mmol), K_2CO_3 (32 mg, 0.23 mmol) and **4.67** (31 mg, 0.071 mmol) in MeCN (2.5 mL) according to the general procedure C. Deprotection in CH_2Cl_2 (3 mL) and TFA (2 mL) followed by preparative RP-HPLC afforded a white, foamlike and hygroscopic solid (3.6 mg, 11%). R_f = 0.10 (CH_2Cl_2/0.5% NH_3 in MeOH 9:1). RP-HPLC (220 nm): 99% (t_R = 9.9 min, k = 2.08). ^{1}H-NMR (600 MHz, DMSO-d_6) δ 8.90 (s, 1H), 8.63 (s, 2H), 8.51 (t, J = 5.8 Hz, 1H), 7.71 (d, J = 8.3 Hz, 1H), 7.50-7.43 (m, 1H), 7.36 (d, J = 5.8 Hz, 1H), 7.13 (t, J = 9.6 Hz, 1H), 7.02-6.97 (m, 2H), 6.56 (d, J = 15.8 Hz, 1H), 4.16 (t, J = 6.0 Hz, 2H), 3.50 (q, J = 6.2 Hz, 2H), 3.21-3.07 (m, 4H), 2.57 (s, 3H), 2.48 (d, J = 1.6 Hz, 3H), 2.38 (s, 3H), 2.14-2.07 (m, 2H), 1 NH signal is missing. HRMS (ESI-MS): calcd. for $C_{27}H_{32}FN_6O_2^+$: 491.2565, found: 491.2561; calcd. for $C_{27}H_{33}FN_6O_2^{2+}$: 246.1319, found: 246.1326; calcd. for $C_{27}H_{34}FN_6O_2^{3+}$: 164.4237, found: 164.4244. MF: $C_{27}H_{31}FN_6O_2$ x $C_6H_3F_9O_6$. MW: (490.58 + 342.06).

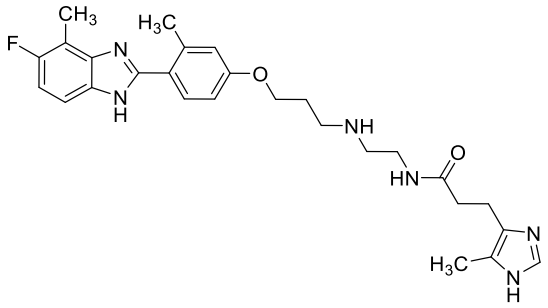

***N*-(2-((3-(4-(5-Fluoro-4-methyl-1*H*-benzo[*d*]imidazol-2-yl)-3-methylphenoxy)propyl)amino)ethyl)-3-(5-methyl-1*H*-imidazol-4-yl)propanamide trihydrotrifluoroacetate (4.89).** The title compound was synthesized from **4.79** (70 mg, 0.166 mmol), K_2CO_3 (138 mg, 0.996 mmol) and **4.69** (167 mg, 0.381 mmol) in MeCN (2.5 mL) according to the general procedure C. Deprotection in CH_2Cl_2 (3 mL) and TFA (2 mL) followed by preparative RP-HPLC afforded a white, foamlike and hygroscopic solid (22.5 mg, 16%). R_f = 0.1 (CH_2Cl_2/0.5% NH_3 in MeOH 9:1). RP-HPLC (220 nm): 97% (t_R = 10.1 min,

k = 2.15). ^{1}H-NMR (300 MHz, MeOD) δ 8.66 (s, 1H), 7.75-7.57 (m, 2H), 7.36 (dd, *J* = 10.1, 9.0 Hz, 1H), 7.16-7.04 (m, 2H), 4.23 (t, *J* = 5.8 Hz, 2H), 3.52 (t, *J* = 5.8 Hz, 2H), 3.33-3.25 (m, 2H, overlapped with MeOH signal), 3.20 (t, *J* = 5.9 Hz, 2H), 2.97 (t, *J* = 7.2 Hz, 2H), 2.64-2.55 (m, 5H), 2.52 (s, 3H), 2.33-2.17 (m, 5H). ^{1}H-NMR (600 MHz, DMSO-d_6) δ 14.29 (s, 2H), 8.89-8.76 (m, 3H), 8.27 (t, *J* = 5.7 Hz, 1H), 7.73 (d, *J* = 8.5 Hz, 1H), 7.56 (dd, *J* = 8.9, 4.3 Hz, 1H), 7.22 (t, *J* = 9.5 Hz, 1H), 7.05-6.99 (m, 2H), 4.16 (t, *J* = 6.1 Hz, 2H), 3.36 (q, *J* = 6.2 Hz, 2H), 3.17-3.09 (m, 2H), 3.05-2.99 (m, 2H), 2.83 (t, *J* = 7.4 Hz, 2H), 2.55 (s, 3H), 2.50 (s, 3H), 2.45 (t, *J* = 7.4 Hz, 2H), 2.21 (s, 3H), 2.14-2.06 (m, 2H). ^{13}C-NMR (151 MHz, DMSO-d_6) δ 171.45, 160.16, 158.60 (q, *J* = 32.5 Hz, TFA), 157.21 (d, *J* = 236.3 Hz), 151.72, 139.52, 135.81, 132.08, 132.00, 131.13, 127.57, 124.62, 119.03, 117.08, 116.76 (q, *J* = 296.4 Hz, TFA), 112.61–111.74 (m, 3C), 110.70 (d, *J* = 16.7 Hz), 64.98, 46.39, 44.31, 35.22, 34.05, 25.46, 20.44, 18.88, 9.36, 8.51. HRMS (ESI-MS): calcd. for $C_{27}H_{34}FN_6O_2^+$: 493.2722, found: 493.2728; calcd. for $C_{27}H_{35}FN_6O_2^{2+}$: 247.1397, found: 247.1407; calcd. for $C_{27}H_{36}FN_6O_2^{3+}$: 165.0956, found: 165.0967. MF: $C_{27}H_{33}FN_6O_2$ x $C_6H_3F_9O_6$. MW: (492.60 + 342.06).

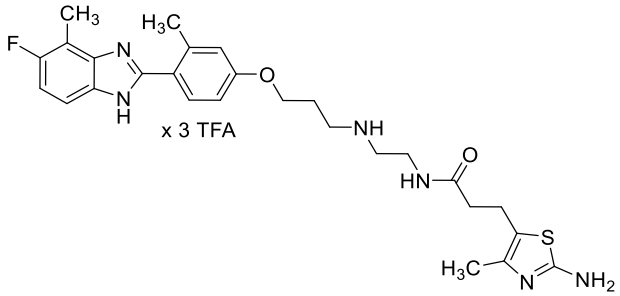

3-(2-Amino-4-methylthiazol-5-yl)-*N*-(2-((3-(4-(5-fluoro-4-methyl-1*H*-benzo[*d*]imidazol-2-yl)-3-methylphenoxy)propyl)amino)ethyl)propanamide trihydrotrifluoroacetate (4.90). The title compound was synthesized from **4.79** (24 mg, 0.056 mmol), K_2CO_3 (46 mg, 0.336 mmol) and **4.35** (50 mg, 0.106 mmol) in MeCN (2.5 mL) according to the general procedure C. Deprotection in CH_2Cl_2 (3 mL) and TFA (2 mL) followed by preparative RP-HPLC afforded a white, foamlike and hygroscopic solid (6.0 mg, 12%). R_f = 0.10 (CH_2Cl_2/0.5% NH_3 in MeOH 9:1). RP-HPLC (220 nm): 95% (t_R = 10.4 min, *k* = 2.24). ^{1}H-NMR (300 MHz, MeOD) δ 7.68 (d, *J* = 8.5 Hz, 1H), 7.60 (dd, *J* = 8.9, 4.1 Hz, 1H), 7.33 (dd, *J* = 10.1, 8.9 Hz, 1H), 7.15-7.04 (m, 2H), 4.23 (t, *J* = 5.7 Hz, 2H), 3.52 (t, *J* = 5.8 Hz, 2H), 3.30-3.25 (m, 2H, overlapped with MeOH signal), 3.20 (t, *J* = 5.9 Hz, 2H), 2.91 (t, *J* = 7.0 Hz, 2H), 2.61-2.46 (m, 7H), 2.24 (quint, *J* = 6.3 Hz, 2H), 2.17 (s, 3H). ^{1}H-NMR (600 MHz, DMSO-d_6) δ 8.95 (s, 2H), 8.57 (s, 2H), 8.21 (t, *J* = 5.6 Hz, 1H), 7.72 (d, *J* = 8.3 Hz, 1H), 7.45 (s, 1H), 7.17-7.06 (m, 1H), 7.03-6.95 (m, 2H), 4.15 (t, *J* = 6.0 Hz, 2H), 3.36 (q, *J* = 6.3 Hz, 2H), 3.13 (quint,

J = 6.8 Hz, 2H), 3.02 (quint, *J* = 6.3 Hz, 2H), 2.78 (t, *J* = 7.0 Hz, 2H), 2.58 (s, 3H), 2.48 (d, *J* = 1.6 Hz, 3H), 2.37 (q, *J* = 7.0 Hz, 2H), 2.08 (d, *J* = 7.6 Hz, 5H). HRMS (ESI-MS): calcd. for $C_{27}H_{34}FN_6O_2S^+$: 525.2442, found: 525.2441; calcd. for $C_{27}H_{35}FN_6O_2S^{2+}$: 263.1258, found: 263.1266; calcd. for $C_{27}H_{36}FN_6O_2S^{3+}$: 175.7529, found: 175.7538. MF: $C_{27}H_{33}FN_6O_2S$ x $C_6H_3F_9O_6$. MW: (524.66 + 342.06).

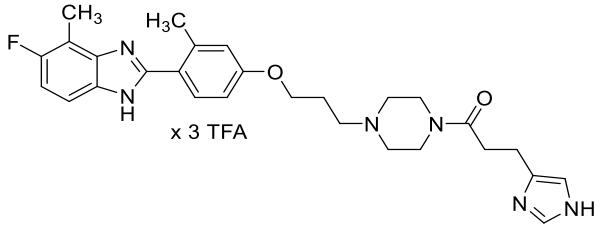

1-(4-(3-(4-(5-Fluoro-4-methyl-1*H*-benzo[*d*]imidazol-2-yl)-3-methylphenoxy)propyl)piperazin-1-yl)-3-(1*H*-imidazol-4-yl)propan-1-one trihydrotrifluoroacetate (4.91). The title compound was prepared from **4.79** (50 mg, 0.12 mmol), K_2CO_3 (98 mg, 0.71 mmol) and **4.70** (134 mg, 0.30 mmol) in MeCN (2.5 mL) according to the general procedure C. Deprotection in CH_2Cl_2 (4 mL) and TFA (2 mL) followed by preparative RP-HPLC afforded the product as a white, foamlike and hygroscopic solid (22.2 mg, 22%). R_f = 0.18 (CH_2Cl_2/1.75°N NH_3 in MeOH 9:1). RP-HPLC (220 nm): 99%, (t_R = 10.1 min, k = 2.15). ^{1}H-NMR (300 MHz, MeOD) δ 8.77 (d, *J* = 1.5 Hz, 1H), 7.68 (d, *J* = 8.5 Hz, 1H), 7.60 (dd, *J* = 8.9, 4.1 Hz, 1H), 7.38-7.29 (m, 2H), 7.11-6.99 (m, 2H), 4.23 (t, *J* = 5.7 Hz, 2H), 4.14-3.55 (br s, 4H), 3.46-3.36 (m, 4H), 3.35-3.28 (m, 2H, overlapped with MeOH signal), 3.04 (t, *J* = 7.0 Hz, 2H), 2.88 (t, *J* = 7.0 Hz, 2H), 2.56 (d, *J* = 1.9 Hz, 3H), 2.52 (s, 3H), 2.38-2.26 (m, 2H). ^{1}H-NMR (400 MHz, DMSO-d_6) δ 14.40 (br s, 2H), 10.39 (br s, 1H), 8.96 (d, *J* = 1.2 Hz, 1H), 7.72 (d, *J* = 8.3 Hz, 1H), 7.52 (dd, *J* = 8.7, 4.1 Hz, 1H), 7.42 (s, 1H), 7.26-7.13 (m, 1H), 7.06-6.95 (m, 2H), 4.69-2.69 (m, 16H), 2.54 (s, 3H), 2.49 (s, 3H, overlapped with DMSO signal), 2.24-2.12 (m, 2H). ^{13}C-NMR (101 MHz, DMSO-d_6) δ 169.89, 160.39, 157.57 (d, *J* = 248.4 Hz, HMBC), 152.27, 139.94, 136.54 (HMBC), 133.93, 133.68 (HMBC), 133.34, 132.36, 119.96 (HMBC), 117.53, 116.15, 112.59, 112.07 (HSQC), 111.28 (HMBC), 65.48, 53.60, 51.44, 51.22, 42.18, 38.66, 31.05, 23.84, 21.00, 20.00, 9.83 (d, *J* = 3.2 Hz), 1 C signal is missing. HRMS (ESI-MS): calcd. for $C_{28}H_{34}FN_6O_2^+$: 505.2722, found: 479.2563; calcd. for $C_{28}H_{35}FN_6O_2^{2+}$: 253.1397, found: 253.1406; calcd. for $C_{28}H_{36}FN_6O_2^{3+}$: 169.0956, found: 169.0961. MF: $C_{28}H_{33}FN_6O_2$ x $C_6H_3F_9O_6$. MW: (504.61 + 342.06).

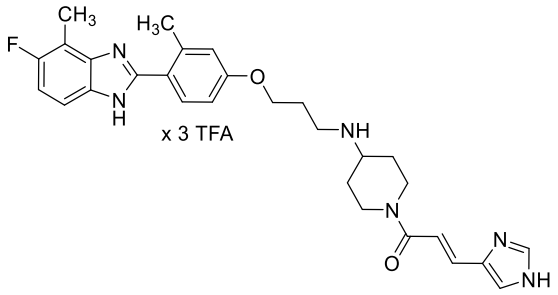

(*E*)-1-(4-((3-(4-(5-Fluoro-4-methyl-1*H*-benzo[*d*]imidazol-2-yl)-3-methylphenoxy)propyl)amino)piperidin-1-yl)-3-(1*H*-imidazol-4-yl)prop-2-en-1-one trihydrotrifluoroacetate (4.92). The title compound was synthesized from **4.79** (67 mg, 0.159 mmol), K_2CO_3 (131 mg, 0.951 mmol) and **4.71** (220 mg, 0.476 mmol) in MeCN (2.5 mL) according to the general procedure C. Deprotection in CH_2Cl_2 (4 mL) and TFA (2 mL) followed by preparative RP-HPLC afforded a white, foamlike and hygroscopic solid (12.3 mg, 9%). R_f = 0.20 (CH_2Cl_2/0.5% NH_3 in MeOH 9:1). RP-HPLC (220 nm): 99% (t_R = 10.2 min, k = 2.18). ^{1}H-NMR (300 MHz, MeOD) δ 8.88 (d, J = 1.0 Hz, 2H), 7.83 (d, J = 1.0 Hz, 1H), 7.69 (d, J = 8.4 Hz, 1H), 7.62 (dd, J = 8.6, 3.8 Hz, 1H), 7.55-7.47 (m, 1H), 7.40-7.29 (m, 2H), 7.13-7.03 (m, 2H), 4.83-4.68 (m, 1H), 4.45-4.33 (m, 1H), 4.24 (t, J = 5.8 Hz, 3H), 3.58-3.45 (m, 1H), 3.37-3.13 (m, 3H), 2.92-2.75 (m, 1H), 2.56 (d, J = 1.6 Hz, 3H), 2.52 (s, 3H), 2.34-2.15 (m, 4H), 1.72-1.49 (m, 2H). ^{1}H-NMR (600 MHz, DMSO-d_6) δ 9.08 (s, 1H), 8.93-8.79 (br s, 2H), 7.97 (s, 1H), 7.73 (d, J = 8.4 Hz, 1H), 7.55-7.50 (m, 1H), 7.45-7.35 (m, 2H), 7.20 (t, J = 9.5 Hz, 1H), 7.04-6.97 (m, 2H), 4.60-4.50 (m, 1H), 4.29-4.14 (m, 3H), 3.47-3.38 (m, 1H), 3.24-3.12 (m, 3H), 2.79-2.68 (m, 1H), 2.50 (s, 3H, overlapped with DMSO signal), 2.18-2.04 (m, 4H), 1.56-1.38 (m, 2H). ^{13}C-NMR (151 MHz, DMSO-d_6) δ 163.38, 159.99, 158.48 (q, J = 32.4 Hz, TFA), 157.15 (d, J = 235.8 Hz), 151.83, 139.47, 136.16, 131.89, 131.54 (HMBC), 129.97, 127.13, 120.58, 119.78, 119.53, 117.06, 116.72 (q, J = 298.2 Hz, TFA), 112.11 (2C, HSQC), 111.67 (d, J = 28.7 Hz), 110.60, 64.88, 53.97, 43.18, 41.18, 39.92 (HSQC), 28.90, 27.83, 25.62, 20.53, 9.37, 1 C signal is missing. HRMS (ESI-MS): calcd. for $C_{29}H_{34}FN_6O_2^+$: 517.2722, found: 517.2721. MF: $C_{29}H_{33}FN_6O_2$ x $C_6H_3F_9O_6$. MW: (516.62 + 342.06).

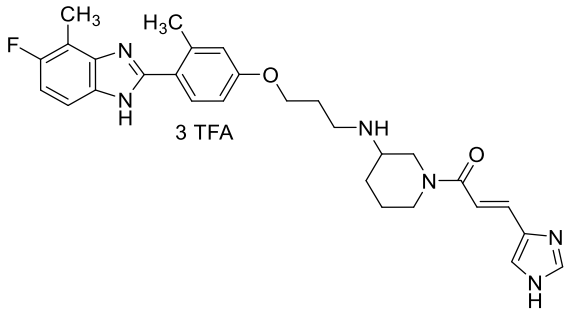

(*E*)-1-(3-((3-(4-(5-Fluoro-4-methyl-1*H*-benzo[*d*]imidazol-2-yl)-3-methylphenoxy)propyl)amino)piperidin-1-yl)-3-(1*H*-imidazol-4-yl)prop-2-en-1-one trihydrotrifluoroacetate (4.93). The title compound was synthesized from **4.79** (19 mg, 0.057 mmol), K_2CO_3 (50 mg, 0.36 mmol) and **4.72** (50 mg, 0.11 mmol) in MeCN (2.5 mL) according to the general procedure C. Deprotection in CH_2Cl_2 (4 mL) and TFA (2 mL) followed by preparative RP-HPLC afforded a white, foamlike and hygroscopic solid (3.8 mg, 8%). R_f = 0.1 (CH_2Cl_2/0.5% NH_3 in MeOH 9:1). RP-HPLC (220 nm): 98% (t_R = 10.3 min, k = 2.21). ^{1}H-NMR (300 MHz, MeOD) δ 8.72 (s, 1H), 7.78 (s, 1H), 7.69 (d, J = 8.5 Hz, 1H), 7.64-7.47 (m, 2H), 7.40-7.30 (m, 1H), 7.31-7.23 (m, 1H), 7.15-7.03 (m, 2H), 4.51-4.41 (m, 1H), 4.25 (t, J = 5.7 Hz, 2H), 4.03-3.91 (m, 1H), 3.59-3.34 (m, 5H), 2.57 (d, J = 1.9 Hz, 3H), 2.52 (s, 3H), 2.35-2.19 (m, 3H), 2.01-1.59 (m, 3H). ^{1}H-NMR (600 MHz, DMSO-d_6) δ 8.92 (s, 1H), 8.77-8.58 (m, 2H), 7.90 (s, 1H), 7.71 (d, J = 8.3 Hz, 1H), 7.50-7.38 (m, 2H), 7.29 (d, J = 15.5 Hz, 1H), 7.10 (t, J = 9.6 Hz, 1H), 7.04-6.90 (m, 2H), 4.39 (d, J = 12.3 Hz, 1H), 4.16 (t, J = 6.0 Hz, 2H), 3.88 (d, J = 13.5 Hz, 1H), 3.38-3.29 (m, 1H), 3.28-3.11 (m, 4H), 2.57 (s, 3H), 2.47 (d, J = 1.5 Hz, 3H), 2.15-2.04 (m, 3H), 1.91-1.80 (m, 1H), 1.71-1.62 (m, 1H), 1.55-1.40 (m, 1H), 1 NH signal is missing. HRMS (ESI-MS): calcd. for $C_{29}H_{34}FN_6O_2^+$: 517.2722, found: 517.2720; calcd. for $C_{29}H_{35}FN_6O_2^{2+}$: 259.1397, found: 259.1404; calcd. for $C_{29}H_{36}FN_6O_2^{3+}$: 173.0956, found: 173.0963. MF: $C_{29}H_{33}FN_6O_2$ x $C_6H_3F_9O_6$. MW: (516.62 + 342.06).

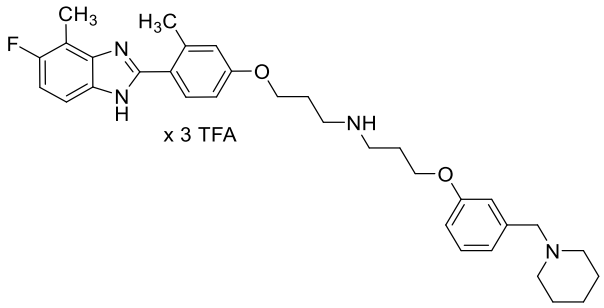

3-(4-(5-Fluoro-4-methyl-1*H*-benzo[*d*]imidazol-2-yl)-3-methylphenoxy)-*N*-(3-(3-(piperidin-1-ylmethyl)phenoxy)propyl)propan-1-amine trihydrotrifluoroacetate (4.94). The title compound was prepared from **4.79** (50 mg, 0.12 mmol), K_2CO_3 (100 mg, 0.72 mmol)

and **4.76** (90 mg, 0.36 mmol) in MeCN (2.5 mL) according to the general procedure C. The crude product was purified by preparative RP-HPLC and afforded a white, foamlike and hygroscopic solid (3.4 mg, 3.2%). R_f = 0.23 (CH_2Cl_2/MeOH 95:5). RP-HPLC (220 nm): 99% (t_R = 12.4 min, k = 2.86). ^{1}H-NMR (300 MHz, MeOD) δ 7.69 (d, J = 8.5 Hz, 1H), 7.61 (dd, J = 8.9, 4.2 Hz, 1H), 7.48-7.30 (m, 2H), 7.21-7.03 (m, 5H), 4.38-4.10 (m, 6H), 3.52-3.38 (m, 2H), 2.95 (t, J = 12.1 Hz, 2H), 2.69-2.47 (m, 6H), 2.40-2.17 (m, 4H), 2.02-1.41 (m, 6H), 4 H´s are overlapped with MeOH signal. ^{1}H-NMR (600 MHz, DMSO-d_6) δ 9.69 (s, 1H), 8.71 (s, 2H), 7.72 (d, J = 8.2 Hz, 1H), 7.50–7.35 (m, 2H), 7.15–7.07 (m, 3H), 7.06–7.02 (m, 1H), 7.00–6.95 (m, 2H), 4.24 (d, J = 4.6 Hz, 2H), 4.17 (t, J = 6.0 Hz, 2H), 4.10 (t, J = 6.0 Hz, 2H), 3.30 (d, J = 12.2 Hz, 2H), 3.18–3.12 (m, 4H), 2.91–2.81 (m, 2H), 2.58 (s, 3H), 2.48 (d, J = 1.6 Hz, 3H, overlapped with DMSO signal), 2.15–2.08 (m, 4H), 1.85–1.76 (m, 2H), 1.72-1.60 (m, 3H). HRMS (ESI-MS): calcd. for $C_{33}H_{42}FN_4O_2^+$: 545.3286, found: 545.3289; calcd. for $C_{33}H_{43}FN_4O_2^{2+}$: 273.1680, found: 273.1688; calcd. for $C_{33}H_{44}FN_6O_2^{3+}$: 182.4477, found: 182.4485. MF: $C_{33}H_{41}FN_4O_2$ x $C_6H_3F_9O_6$. MW: (544.72 + 342.07).

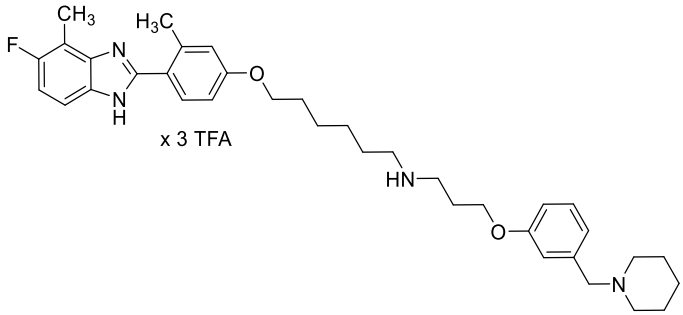

6-(4-(5-Fluoro-4-methyl-1*H*-benzo[*d*]imidazol-2-yl)-3-methylphenoxy)-*N*-(3-(3-(piperidin-1-ylmethyl)phenoxy)propyl)hexan-1-amine trihydrotrifluoroacetate (**4.95**)**.** The title compound was prepared from **4.81** (50 mg, 0.11 mmol), K_2CO_3 (89 mg, 0.64 mmol) and **4.76** (80 mg, 0.32 mmol) in MeCN (2.5 mL) according to the general procedure C. The crude product was purified by preparative RP-HPLC and afforded a white, foamlike and hygroscopic solid (44.9 mg, 44%). R_f = 0.21 (CH_2Cl_2/MeOH 9:1). RP-HPLC (220 nm): 99% (t_R = 13.1 min, k = 3.08). ^{1}H-NMR (300 MHz, MeOD) δ 7.71-7.58 (m, 2H), 7.43-7.31 (m, 2H), 7.14-6.98 (m, 5H), 4.25 (s, 2H), 4.18-4.06 (m, 4H), 3.50-3.38 (m, 2H), 3.24 (t, J = 7.6 Hz, 2H), 3.13-3.02 (m, 2H), 3.01-2.86 (m, 2H), 2.57 (d, J = 1.8 Hz, 3H), 2.52 (s, 3H), 2.27-2.14 (m, 2H), 2.01-1.68 (m, 9H), 1.65-1.37 (m, 5H). ^{1}H-NMR (600 MHz, DMSO-d_6) δ 10.02 (s, 1H), 8.80 (quint, J = 6.1 Hz, 2H), 7.70 (d, J = 8.5 Hz, 1H), 7.57 (dd, J = 8.8, 4.3 Hz, 1H), 7.37 (t, J = 7.9 Hz, 1H), 7.27-7.22 (m, 1H), 7.11 (t, J = 2.0 Hz, 1H), 7.09-7.05 (m, 1H), 7.04-6.98 (m, 3H), 4.24 (d, J = 4.2 Hz, 2H), 4.07 (t, J = 6.3 Hz, 4H), 3.30 (d, J = 12.0 Hz, 2H), 3.12-3.06 (m,

2H), 2.99–2.93 (m, 2H), 2.90-2.81 (m, 2H), 2.53 (s, 3H), 2.13-2.05 (m, 2H), 1.84-1.72 (m, 4H), 1.70-1.60 (m, 5H), 1.50-1.31 (m, 5H). ^{13}C-NMR (151 MHz, DMSO-d_6) δ 160.72, 158.56 (q, *J* = 33.1 Hz, TFA), 158.42, 157.29 (d, *J* = 236.5 Hz), 151.71, 139.56, 135.42, 132.10, 131.20, 130.82, 129.96, 123.49, 117.10, 117.05, 116.74 (q, *J* = 297.5 Hz, TFA), 115.45, 112.54–111.83 (m, 3C), 110.67 (d, *J* = 19.61 Hz), 67.59, 64.70, 58.91, 51.76 (2C), 46.79, 44.17, 28.35, 25.66, 25.50, 25.46, 25.01, 22.28 (2C), 21.34, 20.33, 9.34. HRMS (ESI-MS): calcd. for $C_{36}H_{48}FN_4O_2^+$: 587.3756, found: 587.3758. MF: $C_{36}H_{47}FN_4O_2$ x $C_6H_3F_9O_6$. MW: (586.80 + 342.06).

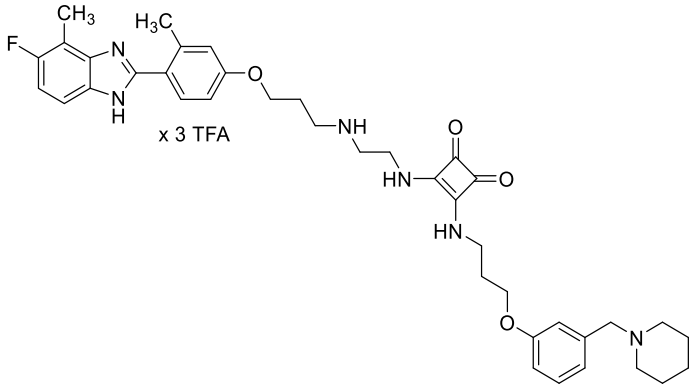

3-((2-((3-(4-(5-Fluoro-4-methyl-1*H*-benzo[*d*]imidazol-2-yl)-3-methylphenoxy)propyl)amino)ethyl)amino)-4-((3-(3-(piperidin-1-ylmethyl)phenoxy)propyl)amino)cyclobut-3-ene-1,2-dione trihydrotrifluoroacetate (4.96). The title compound was prepared from **4.79** (40 mg, 0.094 mmol), K_2CO_3 (78 mg, 0.566 mmol) and **4.78** (174 mg, 0.283 mmol) in MeCN (2.5 mL) according to the general procedure C. The crude product was purified by preparative RP-HPLC and afforded a white, foamlike and hygroscopic solid (13.8 mg, 14%). R_f = 0.20 (CH_2Cl_2/0.5% NH_3 in MeOH 9:1). RP-HPLC (220 nm): 98% (t_R = 11.9 min, *k* = 2.71). ^{1}H-NMR (300 MHz, MeOD) δ 7.68 (d, *J* = 8.5 Hz, 1H), 7.64-7.56 (m, 1H), 7.43-7.30 (m, 2H), 7.15-6.98 (m, 5H), 4.32-4.18 (m, 4H), 4.12 (t, *J* = 5.9 Hz, 2H), 3.95 (t, *J* = 5.9 Hz, 2H), 3.89-3.74 (m, 2H), 3.50-3.38 (m, 2H), 3.37-3.30 (m, 4H, overlapped with MeOH signal), 2.94 (t, *J* = 12.2 Hz, 2H), 2.56 (d, *J* = 1.8 Hz, 3H), 2.52 (s, 3H), 2.25 (quint, *J* = 6.3 Hz, 2H), 2.11 (quint, *J* = 6.4 Hz, 2H), 2.02-1.43 (m, 6H). ^{1}H-NMR (600 MHz, DMSO-d_6) δ 9.63 (s, 1H), 8.82 (s, 2H), 8.18-7.90 (m, 2H), 7.72 (d, *J* = 8.5 Hz, 1H), 7.54 (dd, *J* = 8.7, 4.3 Hz, 1H), 7.36 (t, *J* = 7.9 Hz, 1H), 7.21 (t, *J* = 9.5 Hz, 1H), 7.09 (t, *J* = 2.0 Hz, 1H), 7.06-6.97 (m, 4H), 4.23 (d, *J* = 4.5 Hz, 2H), 4.16 (t, *J* = 6.1 Hz, 2H), 4.06 (t, *J* = 6.2 Hz, 2H), 3.81 (q, *J* = 6.2 Hz, 2H), 3.75-3.63 (m, 2H), 3.34-3.26 (m, 2H), 3.24-3.13 (m, 4H), 2.91-2.79 (m, 2H), 2.55 (s, 3H), 2.50 (s, 3H, overlapped with DMSO signal), 2.15-2.08 (m, 2H), 2.01 (quint, *J* = 6.5 Hz, 2H), 1.86-1.76 (m, 2H), 1.71-1.56 (m, 3H), 1.40-1.29 (m, 1H).

^{13}C-NMR (151 MHz, DMSO-d_6) δ 182.78, 182.44, 168.50, 167.81, 160.05, 158.59, 158.49 (q, *J* = 33.0 Hz, TFA), 157.12 (d, *J* = 237.8 Hz), 151.78, 139.49, 135.66 (HMBC), 131.92, 131.05, 129.95, 123.33, 119.40 (HMBC), 117.34, 117.07, 116.64 (q, *J* = 296.6 Hz, TFA), 115.31, 112.13 (2C), 111.90 (HSQC), 110.80 (HMBC), 64.92, 64.75, 58.96, 51.81 (2C), 47.48, 44.38, 40.49, 39.71 (overlapped with DMSO signal, HSQC), 30.32, 25.44, 22.32 (2C), 21.31, 20.48, 9.37, 1 C signal is missing. HRMS (ESI-MS): calcd. for $C_{39}H_{48}FN_6O_4^+$: 683.3716, found: 683.3718. MF: $C_{39}H_{47}FN_6O_4$ x $C_6H_3F_9O_6$. MW: (682.84 + 342.06).

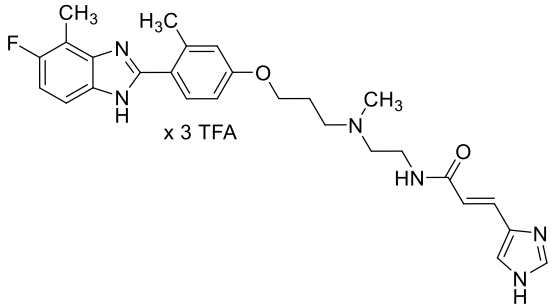

(*E*)-*N*-(2-((3-(4-(5-Fluoro-4-methyl-1*H*-benzo[*d*]imidazol-2-yl)-3-methylphenoxy)propyl)(methyl)amino)ethyl)-3-(1*H*-imidazol-4-yl)acrylamide trihydrotrifluoroacetate (4.97). Formic acid (100 µL) and formaldehyde solution (37% aq, 100 µL) were added to **4.86** (15.29 mg, 18.7 µmol) and the resulting mixture was stirred at 95 °C for 4 h. Then, 1 mL MeCN/1% aq TFA (95:5, 1 mL) was added and the resulting solution was purified by preparative RP-HPLC and afforded a white, foamlike and hygroscopic solid (7.3 mg, 47%). RP-HPLC (220 nm): 98% (t_R = 9.6 min, *k* = 1.99). ^{1}H-NMR (300 MHz, MeOD) δ 8.86 (d, *J* = 1.3 Hz, 1H), 7.80 (d, *J* = 1.2 Hz, 1H), 7.70 (d, *J* = 8.5 Hz, 1H), 7.63 (dd, *J* = 9.0, 4.1 Hz, 1H), 7.49 (d, *J* = 15.9 Hz, 1H), 7.37 (dd, *J* = 10.1, 9.0 Hz, 1H), 7.15-7.04 (m, 2H), 6.72 (d, *J* = 15.9 Hz, 1H), 4.24 (t, *J* = 5.8 Hz, 2H), 3.75 (t, *J* = 5.9 Hz, 2H), 3.57-3.38 (m, 4H), 3.04 (s, 3H), 2.57 (d, *J* = 1.8 Hz, 3H), 2.52 (s, 3H), 2.32 (quint, *J* = 7.3 Hz, 2H). HRMS (ESI-MS): calcd. for $C_{27}H_{32}FN_6O_2^+$: 491.2565, found: 491.2560; calcd. for $C_{27}H_{33}FN_6O_2^{2+}$: 246.1319, found: 246.1322; calcd. for $C_{27}H_{34}FN_6O_2^{3+}$: 164.4237, found: 164.4241. MF: $C_{27}H_{31}FN_6O_2$ x $C_6H_3F_9O_6$. MW: (490.58 + 342.06).

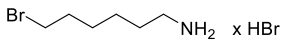

6-Bromohexan-1-amine hydrobromide (4.99).[69] The mixture of 6-aminohexan-1-ol (**4.98**, 599 µL, 4.65 mmol) and 48% HBr, aq (5 mL) was refluxed for 3 h with stirring. Evaporating of the mixture gave the product (1.0 g, 83%) as a brown oil. R_f = 0.46 (CH_2Cl_2/MeOH 9:1). ^{1}H-

NMR (300 MHz, MeOD) δ 3.47 (t, *J* = 6.7 Hz, 2H), 2.94 (t, *J* = 7.5 Hz, 2H), 1.97-1.81 (m, 2H), 1.75-1.61 (m, 2H), 1.59-1.34 (m, 4H). ^{13}C-NMR (75 MHz, MeOD) δ 40.64 (-), 34.22 (-), 33.60 (-), 28.61 (-), 28.35 (-), 26.56 (-). NMR data matches literature reference.[69] HRMS (ESI-MS): calcd. for $C_6H_{15}BrN^+$: 180.0382, found: 180.0391. MF: $C_6H_{14}BrN$ x HBr. MW: 180.09 + 80.91.

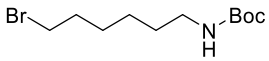

***tert*-Butyl (6-bromohexyl)carbamate (4.100).**[70] A solution of NaOH (306 mg, 7.66 mmol, 2 equiv) in H_2O (15 mL), was added dropwise to a vigorously stirring biphasic mixture consisting of **4.99** (1.0 g, 3.83 mmol, 1 equiv) in H_2O (25 mL) and Boc_2O (585 mg, 2.68 mmol, 0.7 mmol) in CH_2Cl_2 (50 mL). After 3 h, the organic phase was separated and washed with 2 N HCl, aqueous (50 mL) and brine (50 mL). The organic phase was dried over Na_2SO_4 and concentrated under reduced pressure. The solvent was removed in vacuum to give the product as yellow oil (450 mg, 42%). R_f = 0.95 (CH_2Cl_2/MeOH 9:1). ^{1}H-NMR (300 MHz, $CDCl_3$) δ 3.38 (t, *J* = 6.8 Hz, 2H), 3.09 (q, *J* = 6.6 Hz, 2H), 1.93-1.73 (m, 2H), 1.53-1.27 (m, 15H). ^{13}C-NMR (75 MHz, $CDCl_3$) δ 156.07 (q), 79.15 (q), 40.53 (-), 33.88 (-), 32.75 (-), 30.04 (-), 28.52 (+, 3C), 27.92 (-), 26.04 (-). NMR data matches literature reference.[70] HRMS (ESI-MS): calcd. for $C_{11}H_{22}BrNNaO_2^+$: 302.0726, found: 302.0724. MF: $C_{11}H_{22}BrNO_2$. MW: 280.21.

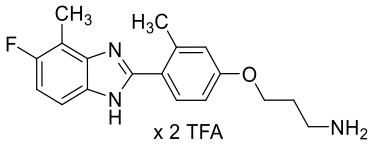

3-(4-(5-Fluoro-4-methyl-1*H*-benzo[*d*]imidazol-2-yl)-3-methylphenoxy)propan-1-amine dihydrotrifluoroacetate (4.102).[2] A suspension of 4-(5-fluoro-4-methyl-1*H*-benzo[*d*]imidazol-2-yl)-3-methylphenol (807 mg, 3.15 mmol, 1.5 equiv), and Cs_2CO_3 (889 mg, 2.73 mmol, 1.3 equiv) in MeCN (16 mL) was treated with *tert*-butyl (3-bromopropyl)carbamate (**4.101**, 500 mg, 2.10 mmol, 1 equiv) and heated under microwave irradiation at 130 °C for 15 min. The reaction mixture was cooled to rt, diluted with chloroform, and filtered through a glass fritted funnel to remove inorganic solid. The filtrate was concentrated under reduced pressure and purified by flash chromatography (gradient: 0-20 min: PE/EtOAc 100:0-67:33, 30 min: 67:33) yielding yellow oil (590 mg, 68%). R_f = 0.27 (PE/EtOAc 2:1). ^{1}H-NMR (300 MHz, $CDCl_3$) δ 7.24-7.18 (m, 1H), 6.97-6.89 (m, 1H), 6.65-6.55 (m, 1H), 6.51-6.34 (m, 2H), 3.87 (t, *J* = 5.9 Hz, 2H), 3.22 (q, *J* = 6.6 Hz, 2H), 2.52-2.46 (m, 3H), 2.35 (s, 3H), 1.95-1.77 (m, 2H), 1.41 (s, 9H). HRMS (ESI-MS): calcd. for $C_{23}H_{29}FN_3O_3^+$: 414.2187, found:

414.2210. MF: $C_{23}H_{28}FN_3O_3$. MW: 413.49. The Boc-protected intermediate (560 mg, 1.35 mmol) was dissolved in CH_2Cl_2 (3 mL), TFA (1 mL) was added and the reaction mixture was stirred at rt until the protection group was removed (7 h, TLC control). After evaporation of the solvent in vacuum, the crude product was recrystallized from isopropyl alcohol/diethyl ether yielding a beige solid (0.35 g, 48%). R_f = 0.13 (CH_2Cl_2/MeOH 9:1). ^{1}H-NMR (300 MHz, MeOD) δ 7.74-7.60 (m, 2H), 7.37 (dd, *J* = 10.1, 8.9 Hz, 1H), 7.15-7.04 (m, 2H), 4.24 (t, *J* = 5.8 Hz, 2H), 3.20 (t, *J* = 7.4 Hz, 2H), 2.58 (d, *J* = 1.8 Hz, 3H), 2.53 (s, 3H), 2.29-2.14 (m, 2H). ^{13}C-NMR (75 MHz, MeOD) δ 163.43, 152.62, 141.52, 133.61, 129.45, 118.44, 117.05, 115.73 (d, *J* = 27.6 Hz), 113.96, 113.30 (d, *J* = 10.0 Hz), 112.37 (d, *J* = 23.7 Hz), 66.57, 38.37, 28.26, 20.11, 9.36 (d, *J* = 3.8 Hz), 2C`s are missing. NMR data matches literature reference.[2] HRMS (ESI-MS): calcd. for $C_{18}H_{21}FN_3O^+$: 314.1663, found: 314.1663. MF: $C_{18}H_{20}FN_3O$ x $C_4H_2F_6O_4$. MW: (313.38 + 228.05).

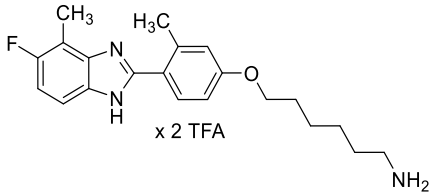

6-(4-(5-Fluoro-4-methyl-1*H*-benzo[*d*]imidazol-2-yl)-3-methylphenoxy)hexan-1-amine dihydrotrifluoroacetate (4.103). A suspension of 4-(5-fluoro-4-methyl-1*H*-benzo[*d*]imidazol-2-yl)-3-methylphenol (516 mg, 2.01 mmol, 1.5 equiv), and Cs_2CO_3 (568 mg, 1.74 mmol, 1.3 equiv) in MeCN (12 mL) was treated with **4.100** (376 mg, 1.34 mmol, 1 equiv) and heated under microwave irradiation at 130 °C for 15 min. The reaction mixture was cooled to rt, diluted with $CHCl_3$, and filtered through a glass fritted funnel to remove inorganic solid. The filtrate was concentrated under reduced pressure and purified by flash chromatography (gradient: 0-20 min: PE/EtOAc 100:0-75:25, 30 min: 75:25) yielding yellow oil (410 mg, 67%). R_f = 0.42 (PE/EtOAc 2:1). ^{1}H-NMR (300 MHz, $CDCl_3$) δ 7.43 (d, *J* = 8.5 Hz, 1H), 6.95 (dd, *J* = 10.2, 8.7 Hz, 1H), 6.76 (d, *J* = 2.5 Hz, 1H), 6.67 (dd, *J* = 8.5, 2.5 Hz, 2H), 3.94 (t, *J* = 6.4 Hz, 2H), 3.16–3.01 (m, 2H), 2.49 (s, 3H), 2.03 (s, 3H), 1.76 (quint, *J* = 6.5 Hz, 2H), 1.55–1.29 (m, 15H). ^{13}C-NMR (75 MHz, $CDCl_3$) δ 159.88, 154.72 (d, *J* = 225.7 Hz), 138.94, 130.95, 122.53, 116.98, 111.82, 110.39 (d, *J* = 27.1 Hz), 79.17, 67.75, 60.44, 30.00, 29.09, 28.43 (3C), 26.51, 25.71, 21.00, 14.20, 6C`s are missing. HRMS (ESI-MS): calcd. for $C_{26}H_{35}FN_3O_3^+$: 456.2657, found: 456.2659. MF: $C_{26}H_{34}FN_3O_3$. MW: 455.57. The Boc-protected intermediate (410 mg, 0.90 mmol) was dissolved in CH_2Cl_2 (4 mL). TFA (1 mL) was added and the reaction mixture was stirred at rt until the protection group was removed (7 h, TLC control). After evaporation

of the solvent in vacuum, the crude product was recrystallized from isopropyl alcohol/diethyl ether yielding a beige solid (0.40 g, 76%). R_f = 0.21 (CH_2Cl_2/MeOH 9:1). ^{1}H-NMR (300 MHz, MeOD) δ 7.72-7.58 (m, 2H), 7.41-7.32 (m, 1H), 7.09-6.98 (m, 2H), 4.11 (t, *J* = 6.3 Hz, 2H), 2.95 (t, *J* = 7.6 Hz, 2H), 2.58 (d, *J* = 1.9 Hz, 3H), 2.52 (s, 3H), 1.93-1.81 (m, 2H), 1.78-1.66 (m, 2H), 1.63-1.41 (m, 4H). ^{13}C-NMR (75 MHz, MeOD) δ 164.11, 152.75, 141.42, 133.58, 129.31, 118.42, 116.31, 115.76 (d, *J* = 27.3 Hz), 113.93, 113.25 (d, *J* = 10.2 Hz), 112.33 (d, *J* = 23.6 Hz), 69.24, 40.65, 29.98, 28.53, 27.21, 26.66, 20.11, 9.35 (d, *J* = 3.9 Hz), 2C`s are missing. HRMS (ESI-MS): calcd. for $C_{21}H_{27}FN_3O^+$: 356.2133, found: 356.2131. MF: $C_{21}H_{26}FN_3O$ x $C_4H_2F_6O_4$. MW: (355.46 + 228.05).

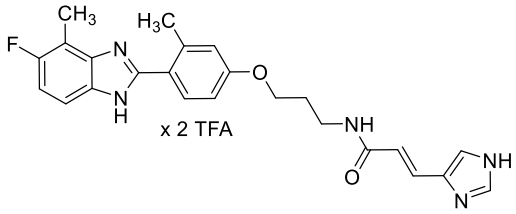

(*E*)-*N*-(3-(4-(5-Fluoro-4-methyl-1*H*-benzo[*d*]imidazol-2-yl)-3-methylphenoxy)propyl)-3-(1*H*-imidazol-4-yl)acrylamide dihydrotrifluoroacetate (4.104). The title compound was prepared from **4.102** (65 mg, 0.12 mmol), **4.57** (38 mg, 0.10 mmol), EDC x HCl (23 mg, 0.12 mmol), HOBt x H_2O (18 mg, 0.12 mmol) and DIPEA (85 µL, 0.50 mmol) in DMF (0.9 mL) according to the general procedure A. Deprotection in CH_2Cl_2 (4 mL) and TFA (1 mL) followed by preparative RP-HPLC afforded a white, foamlike and hygroscopic solid (35.4 mg, 54%). R_f = 0.42 (CH_2Cl_2/MeOH 9:1). RP-HPLC (220 nm): 99% (t_R = 12.2 min, *k* = 2.80). ^{1}H-NMR (300 MHz, MeOD) δ 8.86 (d, *J* = 1.2 Hz, 1H), 7.79 (d, *J* = 1.2 Hz, 1H), 7.74–7.58 (m, 2H), 7.52–7.32 (m, 2H), 7.19–7.02 (m, 2H), 6.68 (d, *J* = 15.8 Hz, 1H), 4.17 (t, *J* = 6.1 Hz, 2H), 3.53 (t, *J* = 6.9 Hz, 2H), 2.67–2.48 (m, 6H), 2.10 (quint, *J* = 6.4 Hz, 2H). ^{1}H-NMR (600 MHz, DMSO-d_6) δ 9.05 (s, 1H), 8.44 (t, *J* = 5.7 Hz, 1H), 7.92 (d, *J* = 1.6 Hz, 1H), 7.71 (d, *J* = 8.5 Hz, 1H), 7.59 (dd, *J* = 8.8, 4.2 Hz, 1H), 7.36 (d, *J* = 15.9 Hz, 1H), 7.27 (dd, *J* = 10.3, 8.8 Hz, 1H), 7.06–6.99 (m, 2H), 6.67 (d, *J* = 15.9 Hz, 1H), 4.16–4.10 (m, 2H), 3.37 (q, *J* = 6.5 Hz, 2H), 2.52 (s, 3H), 2.50 (s, 3H), 1.96 (quint, *J* = 6.6 Hz, 2H). ^{13}C-NMR (151 MHz, DMSO-d_6) δ 164.20, 160.81, 158.62 (q, *J* = 33.3 Hz, TFA), 157.40 (d, *J* = 236.9 Hz), 151.57, 139.64, 136.10, 134.79, 132.23, 130.41, 129.72, 124.50, 124.16, 119.91, 117.93, 117.11, 116.68 (q, *J* = 297.0 Hz, TFA), 112.45 (d, *J* = 26.7 Hz), 112.27 (2C), 110.68 (d, *J* = 22.5 Hz), 65.61, 35.92, 28.76, 20.25, 9.36. HRMS (ESI-MS): calcd. for $C_{24}H_{25}FN_5O_2^+$: 434.1987, found: 434.1995. MF: $C_{24}H_{24}FN_5O_2$ x $C_4H_2F_6O_4$. MW: (433.49 + 228.05).

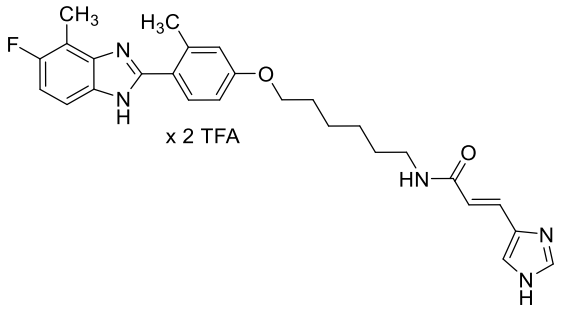

(*E*)-*N*-(6-(4-(5-Fluoro-4-methyl-1*H*-benzo[*d*]imidazol-2-yl)-3-methylphenoxy)hexyl)-3-(1*H*-imidazol-4-yl)acrylamide dihydrotrifluoroacetate (4.105). The title compound was prepared from **4.103** (74 mg, 0.13 mmol), **4.57** (40 mg, 0.10 mmol), EDC x HCl (24 mg, 0.13 mmol), HOBt x H_2O (19 mg, 0.13 mmol) and DIPEA (90 µL, 0.53 mmol) in DMF (0.9 mL) according to the general procedure A. Deprotection in CH_2Cl_2 (4 mL) and TFA (1 mL) followed by preparative RP-HPLC afforded a white, foamlike and hygroscopic solid (14.9 mg, 21%). R_f = 0.21 (CH_2Cl_2/MeOH 9:1). RP-HPLC (220 nm): 98% (t_R = 14.1 min, k = 3.39). ^{1}H-NMR (300 MHz, MeOD) δ 8.82 (d, J = 1.3 Hz, 1H), 7.77 (d, J = 1.4 Hz, 1H), 7.72–7.56 (m, 2H), 7.50–7.30 (m, 2H), 7.14–6.99 (m, 2H), 6.64 (d, J = 15.9 Hz, 1H), 4.10 (t, J = 6.3 Hz, 2H), 3.37–3.32 (m, 2H, overlapped with MeOH signal), 2.64–2.47 (m, 6H), 1.94–1.78 (m, 2H), 1.71–1.41 (m, 6H). ^{1}H-NMR (600 MHz, DMSO-d_6) δ 9.02 (s, 1H), 8.29 (t, J = 5.7 Hz, 1H), 7.90 (s, 1H), 7.69 (d, J = 8.5 Hz, 1H), 7.56 (dd, J = 8.8, 4.3 Hz, 1H), 7.34 (d, J = 15.9 Hz, 1H), 7.28–7.22 (m, 1H), 7.05–6.97 (m, 2H), 6.64 (d, J = 15.9 Hz, 1H), 4.07 (t, J = 6.5 Hz, 2H), 3.19 (q, J = 6.6 Hz, 2H), 2.52 (s, 3H), 2.50 (s, 3H), 1.75 (quint, J = 6.8 Hz, 2H), 1.55–1.42 (m, 4H), 1.41–1.32 (m, 2H). ^{13}C-NMR (151 MHz, DMSO-d_6) δ 163.95, 160.73, 158.40 (q, J = 33.1 Hz, TFA), 158.06, 156.49, 151.73, 139.53, 136.06, 135.29, 132.07, 130.83, 129.85, 124.41, 124.22, 119.79, 118.26, 117.07, 116.78 (q, J = 298.0 Hz, TFA), 112.65–111.73 (m, 3C), 110.64 (d, J = 22.5 Hz), 67.71, 38.80, 29.04, 28.55, 26.23, 25.23, 20.34, 9.37. HRMS (ESI-MS): calcd. for $C_{27}H_{31}FN_5O_2^+$: 476.2456, found: 476.2462. MF: $C_{27}H_{30}FN_5O_2$ x $C_4H_2F_6O_4$. MW: (475.57 + 228.05).

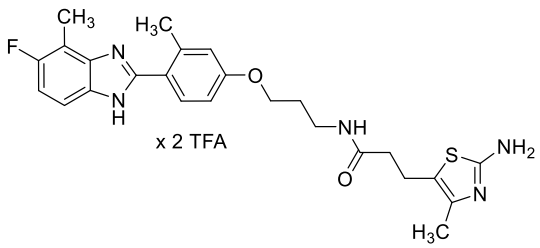

3-(2-Amino-4-methylthiazol-5-yl)-*N*-(3-(4-(5-fluoro-4-methyl-1*H*-benzo[*d*]imidazol-2-yl)-3-methylphenoxy)propyl)propanamide dihydrotrifluoroacetate (4.106). The title

compound was prepared from **4.102** (72 mg, 0.17 mmol), **4.32** (40 mg, 0.14 mmol), EDC x HCl (32 mg, 0.17 mmol), HOBt x H_2O (26 mg, 0.17 mmol) and DIPEA (134 µL, 0.78 mmol) in DMF (1.1 mL) according to the general procedure A. The crude product was purified by preparative RP-HPLC and afforded a white, foamlike and hygroscopic solid (65.5 mg, 65%). R_f = 0.36 (CH_2Cl_2/0.5% NH_3 in MeOH 9:1). RP-HPLC (220 nm): 95% (t_R = 12.0 min, k = 2.74). ^{1}H-NMR (300 MHz, MeOD) δ 7.71–7.60 (m, 2H), 7.37 (dd, J = 10.2, 9.0 Hz, 1H), 7.12–7.00 (m, 2H), 4.12 (t, J = 6.1 Hz, 2H), 3.44-3.36 (d, J = 6.7 Hz, 3H), 2.91 (t, J = 6.8 Hz, 2H), 2.63–2.42 (m, 8H), 2.18 (s, 3H), 2.08–1.96 (m, 2H). ^{13}C-NMR (101 MHz, MeOD) δ 172.45, 168.99, 162.53, 161.25 (q, J = 34.6 Hz, TFA), 158.80 (d, J = 141.7 Hz), 151.29 (d, J = 1.6 Hz), 140.07, 132.21, 132.13 (d, J = 9.7 Hz), 131.20, 127.87, 117.09, 116.97, 116.42 (q, J = 296.5 Hz, TFA), 115.07, 114.43 (d, J = 27.4 Hz), 112.53, 111.87, (d, J = 10.1 Hz), 10.98 (d, J = 23.7 Hz), 65.58, 36.05, 35.38, 28.70, 21.01, 18.70, 10.03, 7.95 (d, J = 3.8 Hz). HRMS (ESI-MS): calcd. for $C_{25}H_{29}FN_5O_2S^+$: 482.2021, found: 482.2027. MF: $C_{25}H_{28}FN_5O_2S$ x $C_4H_2F_6O_4$. MW: (481.59 + 228.05).

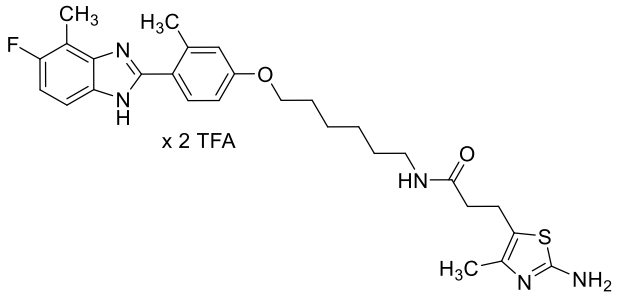

3-(2-Amino-4-methylthiazol-5-yl)-*N*-(6-(4-(5-fluoro-4-methyl-1*H*-benzo[*d*]imidazol-2-yl)-3-methylphenoxy)hexyl)propenamide dihydrotrifluoroacetate (4.107). The title compound was prepared from **4.103** (89 mg, 0.15 mmol), **4.32** (36 mg, 0.127 mmol), HOBt x H_2O (23 mg, 0.153 mmol), EDC x HCl (29 mg, 0.153 mmol) and DIPEA (108 µL, 0.638 mmol) in DMF (1.1 mL) according to the general procedure A. The crude product was purified by preparative RP-HPLC and afforded a white, foamlike and hygroscopic solid (33.0 mg, 35%). R_f = 0.32 (CH_2Cl_2/0.5% NH_3 in MeOH 9:1). RP-HPLC (220 nm): 95% (t_R = 14.3 min, k = 3.45). ^{1}H-NMR (300 MHz, MeOD) δ 7.71-7.59 (m, 2H), 7.37 (dd, J = 10.1, 9.0 Hz, 1H), 7.08-7.00 (m, 2H), 4.10 (t, J = 6.3 Hz, 2H), 3.19 (t, J = 6.9 Hz, 2H), 2.90 (t, J = 6.8 Hz, 2H), 2.57 (d, J = 1.8 Hz, 3H), 2.52 (s, 3H), 2.48-2.42 (m, 2H), 2.18 (s, 3H), 1.83 (quint, J = 7.2 Hz, 2H), 1.61-1.46 (m, 4H), 1.45-1.34 (m, 2H). ^{13}C-NMR (101 MHz, MeOD) δ 172.18, 168.97, 162.64, 158.66 (d, J = 248.9 Hz), 151.48 (HMBC), 139.95, 132.07 (2C, HMBC), 131.27, 128.30, 117.09, 117.01, 115.34, 114.15 (d, J = 28.1 Hz), 112.50, 111.83 (d,

J = 10.3 Hz), 110.92 (d, *J* = 23.3 Hz), 67.99, 39.00, 35.37, 28.93, 28.78, 26.33, 25.41, 21.06, 18.71, 10.06, 7.94 (d, *J* = 3.9 Hz). HRMS (ESI-MS): calcd. for $C_{28}H_{35}FN_5O_2S^+$: 524.2490, found: 524.2498. MF: $C_{28}H_{34}FN_5O_2S$ x $C_4H_2F_6O_4$ MW: (523.67 + 228.05).

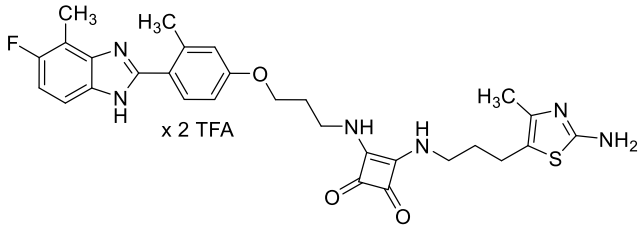

3-((3-(2-Amino-4-methylthiazol-5-yl)propyl)amino)-4-((3-(4-(5-fluoro-4-methyl-1*H*-benzo[*d*]imidazol-2-yl)-3-methylphenoxy)propyl)amino)cyclobut-3-ene-1,2-dione dihydrotrifluoroacetate (4.108). The title compound was prepared from **4.102** (84 mg, 0.155 mmol), **4.75** (100 mg, 0.186 mmol) and NEt_3 (43 µL, 0.31 mmol) in EtOH (5 mL) according to the general procedure D. Deprotection in CH_2Cl_2 (3 mL) and TFA (2 mL) followed by preparative RP-HPLC afforded the product as a white, foamlike and hygroscopic solid (7.18 mg, 6%). R_f = 0.17 (CH_2Cl_2/0.5% NH_3 in MeOH 9:1). HPLC: 97% (t_R = 12.1 min, *k* = 2.77). ^{1}H-NMR (300 MHz, MeOD) δ 7.69-7.56 (m, 2H), 7.34 (dd, *J* = 10.1, 8.9 Hz, 1H), 7.11-6.99 (m, 2H), 4.21 (t, *J* = 5.8 Hz, 2H), 3.93-3.78 (m, 2H), 3.65 (t, *J* = 6.8 Hz, 2H), 2.70 (t, *J* = 7.4 Hz, 2H), 2.57 (d, *J* = 1.8 Hz, 3H), 2.50 (s, 3H), 2.22-2.07 (m, 4H), 1.99-1.80 (m, 2H). ^{1}H-NMR (600 MHz, DMSO-d_6) δ 9.09 (s, 2H), 7.75-7.48 (m, 4H), 7.21 (t, *J* = 9.6 Hz, 1H), 7.04-6.97 (m, 2H), 4.14 (t, *J* = 6.1 Hz, 2H), 3.75-3.64 (m, 2H), 3.57-3.46 (m, 2H), 2.63-2.59 (m, 2H), 2.53 (s, 3H), 2.07-2.00 (m, 5H), 1.75 (quint, *J* = 7.1 Hz, 2H), 2 NH signals are missing. ^{13}C-NMR (151 MHz, DMSO-d_6) δ 182.40 (2C), 167.74, 160.31, 158.34 (q, *J* = 33.6 Hz, TFA), 157.13 (d, *J* = 236.1 Hz), 151.83, 139.42, 135.88 (HMBC), 131.88, 131.12, 119.23 (HMBC), 117.05, 116.69, 112.15 (2C), 111.80 (HSQC), 110.68 (HMBC), 65.03, 42.30, 40.41, 31.26, 30.32, 21.82, 20.48, 11.33, 9.38, 3 C signals are missing. HRMS (ESI-MS): calcd. for $C_{29}H_{32}FN_6O_3S^+$: 563.2235, found: 563.2237; calcd. for $C_{29}H_{33}FN_6O_3S^{2+}$: 282.1154, found: 282.1162. MF: $C_{29}H_{31}FN_6O_3S$ x $C_4H_2F_6O_4$. MW: (562.66 + 228.05).

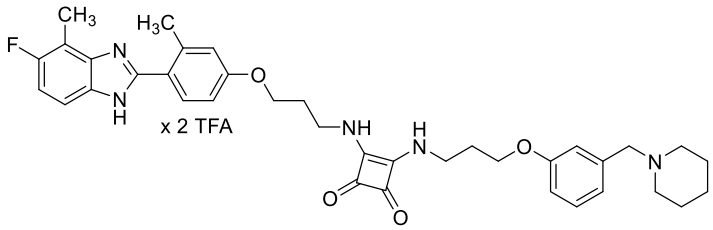

3-((3-(4-(5-Fluoro-4-methyl-1*H*-benzo[*d*]imidazol-2-yl)-3-methylphenoxy)propyl)amino)-4-((3-(3-(piperidin-1-ylmethyl)phenoxy)propyl)amino)cyclobut-3-ene-1,2-dione dihydrotrifluoroacetate (4.109). The title compound was prepared from **4.102** (25 mg, 0.067 mmol), **4.76** (30 mg, 0.055 mmol) and NEt_3 (15.4 µL, 0.111 mmol) in EtOH (5 mL) according to the general procedure D. The crude product was purified by preparative RP-HPLC and afforded a white, foamlike and hygroscopic solid (11.4 mg, 24%). R_f = 0.42 (CH_2Cl_2/0.5% NH_3 in MeOH 9:1). RP-HPLC (220 nm): 100% (t_R = 14.1 min, k = 3.39). ^{1}H-NMR (600 MHz, DMSO-d_6) δ 9.50 (s, 1H), 7.86-7.65 (m, 3H), 7.54 (dd, J = 8.9, 4.3 Hz, 1H), 7.36 (t, J = 7.9 Hz, 1H), 7.23 (t, J = 9.6 Hz, 1H), 7.11-7.08 (m, 1H), 7.06-6.98 (m, 4H), 4.22 (d, J = 3.8 Hz, 2H), 4.14 (t, J = 6.2 Hz, 2H), 4.06 (t, J = 6.1 Hz, 2H), 3.69 (s, 4H), 3.30 (d, J = 12.0 Hz, 2H), 2.85 (q, J = 11.5, 10.9 Hz, 2H), 2.53 (s, 3H), 2.06-1.98 (m, 4H), 1.85-1.77 (m, 2H), 1.71-1.57 (m, 3H), 1.42-1.30 (m, 1H). ^{13}C-NMR (151 MHz, DMSO-d_6) δ 182.43 (2C), 167.97 (2C), 160.39, 158.58, 158.25 (q, J = 33.2 Hz, TFA), 157.17 (d, J = 236.6 Hz), 151.78, 139.46, 135.53, 131.95, 131.02, 129.95, 123.31, 119.36, 117.31, 117.06, 116.65 (q, J = 297.9 Hz, TFA), 115.36, 112.18 (3C), 100.59, 65.06, 64.81, 58.99, 51.83 (2C), 40.46, 40.41, 30.36, 30.30, 22.33 (2C), 21.29, 20.43, 9.37. HRMS (ESI-MS): calcd. for $C_{37}H_{43}FN_5O_4^+$: 640.3294, found: 640.3294; calcd. for $C_{37}H_{44}FN_5O_4^{2+}$: 320.6689, found: 320.6683. MF: $C_{37}H_{42}FN_5O_4$x $C_4H_2F_6O_4$. MW: (639.77 + 228.05).

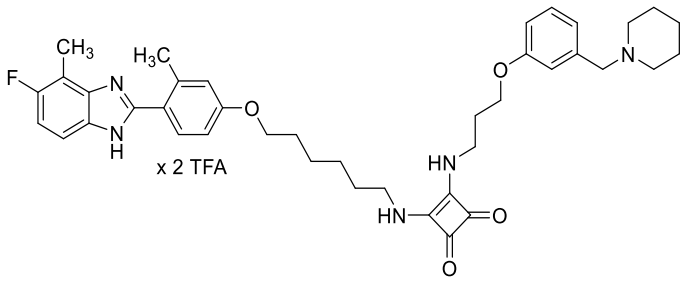

3-((6-(4-(5-Fluoro-4-methyl-1*H*-benzo[*d*]imidazol-2-yl)-3-methylphenoxy)hexyl)amino)-4-((3-(3-(piperidin-1-ylmethyl)phenoxy)propyl)amino)cyclobut-3-ene-1,2-dione dihydrotrifluoroacetate (4.110). The title compound was prepared from **4.103** (38 mg, 0.103 mmol), **4.76** (50 mg,

0.086 mmol) and NEt_3 (23.8 µL, 0.171 mmol) in EtOH (7 mL) according to the general procedure D The crude product was purified by preparative RP-HPLC and afforded a white, foamlike and hygroscopic solid (21.8 mg, 28%). R_f = 0.40 (CH_2Cl_2/0.5% NH_3 in MeOH 95:5). RP-HPLC (220 nm): 100% (t_R = 15.9 min, k = 3.95). ^{1}H-NMR (300 MHz, MeOD) δ 7.70-7.58 (m, 2H), 7.42-7.35 (m, 2H), 7.10-6.99 (m, 5H), 4.23 (s, 2H), 4.19-4.05 (m, 4H), 3.91-3.77 (m, 2H), 3.68-3.53 (m, 2H), 3.50-3.39 (m, 2H), 2.94 (t, J = 12.6 Hz, 2H), 2.61-2.48 (m, 6H), 2.10 (quint, J = 6.3 Hz, 2H), 2.02-1.40 (m, 14H). ^{1}H-NMR (600 MHz, DMSO-d_6) δ 9.64 (s, 1H), 7.84-7.67 (m, 3H), 7.60 (dd, J = 8.8, 4.2 Hz, 1H), 7.36 (t, J = 7.9 Hz, 1H), 7.29 (t, J = 9.5 Hz, 1H), 7.10 (t, J = 2.0 Hz, 1H), 7.06-7.00 (m, 4H), 4.23 (d, J = 4.2 Hz, 2H), 4.06 (q, J = 6.3 Hz, 4H), 3.74-3.64 (m, 2H), 3.59-3.45 (m, 2H), 3.30 (d, J = 12.0 Hz, 2H), 2.91-2.80 (m, 2H), 2.52 (s, 3H), 2.50 (s, 3H), 2.01 (quint, J = 6.5 Hz, 2H), 1.84-1.78 (m, 2H), 1.75 (quint, J = 6.7 Hz, 2H), 1.71-1.51 (m, 5H), 1.49-1.30 (m, 5H). ^{13}C-NMR (151 MHz, DMSO-d_6) δ 182.44, 182.24, 167.98, 167.83, 160.98, 158.60, 158.46 (q, J = 33.2 Hz, TFA), 156.66 (d, J = 238.0 Hz), 151.51, 139.65, 134.64, 132.27, 131.04, 130.14, 129.93, 123.31, 117.28, 117.08, 116.48 (q, J = 296.8 Hz, TFA), 115.39, 112.77–112.05 (m, 3C), 110.60 (d, J = 22.1 Hz), 67.73, 64.80, 58.99, 51.82 (2C), 43.21, 40.42, 30.73, 30.35, 28.48, 25.60, 25.10, 22.33 (2C), 21.31, 20.18, 9.36. HRMS (ESI-MS): calcd. for $C_{40}H_{49}FN_5O_4^+$: 682.3763, found: 682.3769. MF: $C_{40}H_{48}FN_5O_4$ x $C_4H_2F_6O_4$. MW: (681.85 + 228.05).

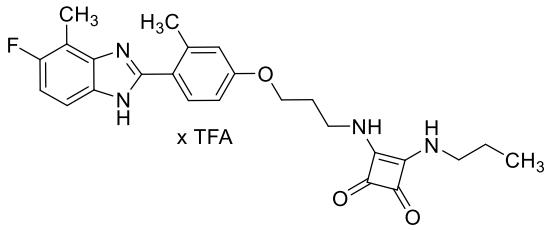

3-((3-(4-(5-Fluoro-4-methyl-1*H*-benzo[*d*]imidazol-2-yl)-3-methylphenoxy)propyl)amino)-4-(propylamino)cyclobut-3-ene-1,2-dione hydrotrifluoroacetate (4.112). The title compound was synthetized according to the procedure of D. Erdmann.[20] Diethoxycyclobut-3-ene-1,2-dione (**4.73**, 30 µL, 0.203 mmol, 1.1 equiv) was dissolved in EtOH (5 mL) and slowly added to a solution of **4.102** (100 mg, 0.185 mmol, 1 equiv) and NEt_3 (28 µL, 0.203 mmol, 1.1 equiv) in EtOH (5 mL). The yellow solution was stirred overnight at rt. The solvent was evaporated in vacuum. The residue was purified by flash chromatography (gradient: 0-20 min: CH_2Cl_2/MeOH 100:0-95:5) yielding the mixed squaramate **4.111** as a yellow oil (30 mg, 37%). R_f = 0.61 (CH_2Cl_2/MeOH 9:1). HRMS (ESI-MS): calcd. for $C_{24}H_{25}FN_3O_4^+$: 438.1824, found: 438.1861; calcd. for $C_{48}H_{49}F_2N_6O_8^+$:

875.3574, found: 875.3585. MF: $C_{24}H_{24}FN_3O_4$. MW: 437.47. The mixed squaramate **4.111** (30 mg, 0.069 mmol, 1 equiv) was dissolved in EtOH (1 mL). After addition of propan-1-amine (28 µL, 0.34 mmol, 5 equiv), the solution was stirred at 70 °C for 24 h. The solvent was evaporated, and the residue was purified by preparative RP-HPLC and afforded a white, foamlike and hygroscopic solid (15.1 mg, 39%). R_f = 0.67 (CH_2Cl_2/0.5% NH_3 in MeOH 95:5). RP-HPLC (220 nm): 99% (t_R = 14.1 min, k = 3.39). ^{1}H-NMR (300 MHz, MeOD) δ 7.71-7.59 (m, 2H), 7.44-7.34 (m, 1H), 7.10-7.00 (m, 2H), 4.23 (t, J = 5.8 Hz, 2H), 3.86 (t, J = 6.5 Hz, 2H), 3.62-3.47 (m, 2H), 2.58 (d, J = 1.8 Hz, 3H), 2.51 (s, 3H), 2.24-2.09 (m, 2H), 1.73-1.55 (m, 2H), 0.97 (t, J = 7.4 Hz, 3H). HRMS (ESI-MS): calcd. for $C_{25}H_{28}FN_4O_3^+$: 451.2140, found: 451.2149; calcd. for $C_{25}H_{29}FN_4O_3^{2+}$: 226.1106, found: 226.1113. MF: $C_{25}H_{27}FN_4O_3$ x $C_2HF_3O_2$. MW: (450.51 + 114.02).

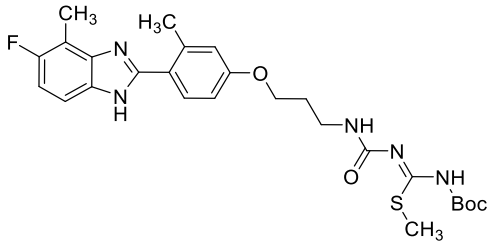

***N*-*tert*-Butoxycarbonyl-*N*'-[*N*-(3-(4-(5-fluoro-4-methyl-1*H*-benzo[*d*]imidazol-2-yl)-3-methylphenoxy)propyl)aminocarbonyl]-*S*-methylisothiourea (4.113).** The reaction was performed under argon atmosphere. Triphosgene (55 mg, 0.185 mmol, 1 equiv) was dissolved in CH_2Cl_2 (1 mL) and the solution was cooled to 0 °C by using an ice-bath. A solution of **4.102** (100 mg, 0.185 mmol, 1 equiv) and DIPEA (245 µL, 1.403 mmol, 7.6 equiv) in CH_2Cl_2 (2 mL) was added dropwise to the triphosgene solution over a period of 30 min. Then, the reaction mixture was stirred at 0 °C for additional 30 min. After 30 min, *N*-*tert*-butoxycarbonyl-*S*-methylthiourea (39 mg, 0.204 mmol, 1.1 equiv) was added, the ice-bath was removed, and the reaction mixture was stirred at rt for 3.5 h. The solvent was removed in vacuum and the residue was purified by flash chromatography (gradient: 0-20 min: PE/EtOAc 100:0-50:50) yielding yellow oil (70 mg, 71%). R_f = 0.66 (PE/EtOAc 1:2). ^{1}H-NMR (300 MHz, $CDCl_3$) δ 12.20 (s, 1H), 7.34-7.21 (m, 3H), 6.93 (dd, J = 10.2, 8.8 Hz, 1H), 6.68 (d, J = 2.6 Hz, 1H), 6.56 (dd, J = 8.5, 2.6 Hz, 1H), 6.02 (t, J = 6.0 Hz, 1H), 4.02-3.91 (m, 2H), 3.44-3.36 (m, 2H), 2.47 (d, J = 1.8 Hz, 3H), 2.39 (s, 3H), 2.26 (s, 3H), 2.05–1.95 (m, 2H), 1.44 (s, 9H). HRMS (ESI-MS): calcd. for $C_{26}H_{33}FN_5O_4S^+$: 530.2232, found: 530.2271; calcd. for $C_{26}H_{34}FN_5O_2S^{2+}$: 215.5890, found: 215.5890. MF: $C_{26}H_{32}FN_5O_4S$. MW: 529.63.

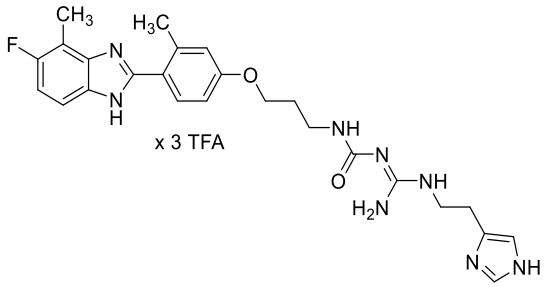

1-(Amino{[2-(1*H*-imidazol-4-yl)ethyl]amino}methylene)-3-(3-(4-(5-fluoro-4-methyl-1*H*-benzo[*d*]imidazol-2-yl)-3-methylphenoxy)propyl)urea trihydrotrifluoroacetate (4.114). The title compound was prepared from **4.113** (117 mg, 0.22 mmol), **4.4** (71 mg, 0.20 mmol), NEt_3 (69 µL, 0.50 mmol) and $HgCl_2$ (109 mg, 0.40 mmol) in CH_2Cl_2 (3 mL) according to the general procedure E. The crude product was purified by preparative RP-HPLC and afforded a white, foamlike and hygroscopic solid (24.1 mg, 14%). R_f = 0.26 (CH_2Cl_2/0.5% NH_3 in MeOH 9:1). HPLC: 100% (t_R = 10.8 min, k = 2.36). ^{1}H-NMR (600 MHz, DMSO-d_6) δ 10.75 (s, 1H), 9.14 (s, 1H), 9.01 (s, 1H), 8.67 (s, 2H), 7.71 (d, J = 8.4 Hz, 1H), 7.66 (s, 1H), 7.58 (dd, J = 8.9, 4.3 Hz, 1H), 7.51-7.46 (m, 1H), 7.25 (t, J = 9.5 Hz, 1H), 7.05-6.99 (m, 2H), 4.12 (t, J = 6.1 Hz, 2H), 3.58 (q, J = 6.7 Hz, 2H), 3.31 (q, J = 6.5 Hz, 2H), 2.93 (t, J = 6.8 Hz, 2H), 2.53 (s, 3H), 2.50 (s, 3H, overlapped with DMSO signal),1.95 (quint, J = 6.5 Hz, 2H), 1 NH is missing. ^{13}C-NMR (151 MHz, DMSO-d_6) δ 160.60, 158.99 (q, J = 33.1 Hz, TFA), 157.33 (d, J = 236.9 Hz), 154.04, 153.84, 151.66, 139.58, 135.22 (HMBC), 134.03, 132.12, 130.72, 129.93, 118.39, 117.06, 116.66 (q, J = 296.2 Hz, TFA), 116.62, 112.03–112.51 (m, 3C), 110.69 (d, J = 19.1 Hz), 65.51, 40.06, 36.49, 28.65, 23.49, 20.31, 9.37 (d, J = 3.4 Hz). HRMS (ESI-MS): calcd. for $C_{25}H_{30}FN_8O_2^+$: 493.2470, found: 493.2471. MF: $C_{25}H_{29}FN_8O_2$ x $C_6H_3F_9O_6$. MW: (492.24 + 342.06).

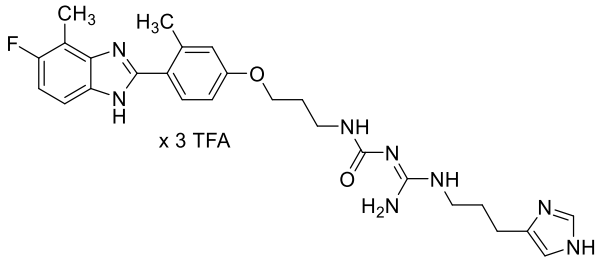

1-(Amino{[3-(1*H*-imidazol-4-yl)propyl]amino}methylene)-3-(3-(4-(5-fluoro-4-methyl-1*H*-benzo[*d*]imidazol-2-yl)-3-methylphenoxy)propyl)urea trihydrotrifluoroacetate (4.115). The title compound was prepared from **4.113** (35 mg, 0.066 mmol), 3-(1-trityl-1*H*-imidazol-4-yl)-propylamine (27 mg, 0.073 mmol), NEt_3 (23 µL, 0.165 mmol) and $HgCl_2$ (36 mg, 0.132 mmol) in CH_2Cl_2 (3 mL) according to the general procedure E. The crude

product was purified by preparative RP-HPLC and afforded a white, foamlike and hygroscopic solid (21.3 mg, 38%). RP-HPLC (220 nm): 100% (t_R = 11.2 min, k = 2.49). ^{1}H-NMR (300 MHz, MeOD) δ 8.80 (d, J = 1.4 Hz, 1H), 7.73-7.56 (m, 2H), 7.4-7.27 (m, 2H), 7.15-6.99 (m, 2H), 4.16 (t, J = 6.0 Hz, 2H), 3.44 (t, J = 6.7 Hz, 2H), 3.37 (t, J = 6.9 Hz, 2H), 2.84 (t, J = 7.7 Hz, 2H), 2.57 (d, J = 1.8 Hz, 3H), 2.51 (s, 3H), 2.13-1.92 (m, 4H). ^{1}H-NMR (600 MHz, DMSO-d_6) δ 10.74 (s, 1H), 9.14 (s, 1H), 8.99 (d, J = 1.4 Hz, 1H), 8.57 (s, 2H), 7.73-7.61 (m, 2H), 7.55 (dd, J = 8.9, 4.3 Hz, 1H), 7.44 (d, J = 1.3 Hz, 1H), 7.26-7.19 (m, 1H), 7.05-6.97 (m, 2H), 4.11 (t, J = 6.1 Hz, 2H), 3.36-3.26 (m, 4H), 2.69 (t, J = 7.6 Hz, 2H), 2.53 (s, 3H), 1.95 (quint, J = 6.5 Hz, 2H), 1.87 (quint, J = 7.3 Hz, 2H). ^{13}C-NMR (151 MHz, DMSO-d_6) δ 160.42, 158.91 (q, J = 32.7 Hz, TFA), 157.20 (d, J = 236.3 Hz), 153.91, 151.80, 139.50, 135.83, 133.89, 132.39, 131.97, 131.18, 118.82, 117.06, 116.74 (q, J = 297.4 Hz, TFA), 115.70, 112.56–111.66 (m, 3C), 110.67 (d, J = 22.0 Hz), 65.49, 40.06, 36.50, 28.67, 26.73, 21.08, 20.42, 9.38, 1 C signal is missing. HRMS (ESI-MS): calcd. for $C_{26}H_{32}FN_8O_2^+$: 507.2627, found: 507.2630. MF: $C_{26}H_{31}FN_8O_2$ x $C_6H_3F_9O_6$. MW: (506.59 + 342.06).

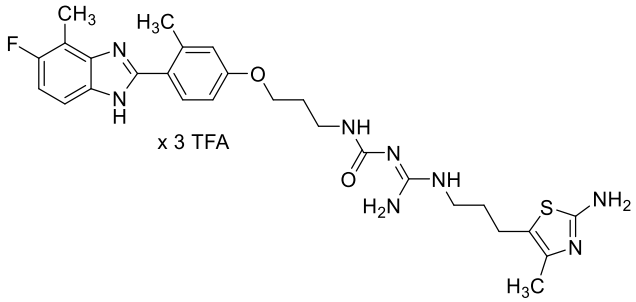

1-(Amino{[3-(2-amino-4-methylthiazol-5-yl)propyl]amino}methylene)-3-(3-(4-(5-fluoro-4-methyl-1*H*-benzo[*d*]imidazol-2-yl)-3-methylphenoxy)propyl)urea trihydrotrifluoroacetate (4.116). The title compound was prepared from **4.113** (92 mg, 0.174 mmol), **4.18** (65 mg, 0.158 mmol), NEt_3 (55 µL, 0.395 mmol) and $HgCl_2$ (86 mg, 0.316 mmol) in CH_2Cl_2 (3 mL) according to the general procedure E. The crude product was purified by preparative RP-HPLC and afforded a white, foamlike and hygroscopic solid (18.5 mg, 13%). R_f = 0.19 (CH_2Cl_2/0.5% NH_3 in MeOH 9:1). RP-HPLC (220 nm): 96% (t_R = 11.7 min, k = 2.64). ^{1}H-NMR (300 MHz, MeOD) δ 7.72-7.59 (m, 2H), 7.37 (dd, J = 10.1, 9.0 Hz, 1H), 7.12-7.01 (m, 2H), 4.17 (t, J = 6.0 Hz, 2H), 3.44 (t, J = 6.7 Hz, 2H), 3.37-3.31 (m, 2H), 2.72 (t, J = 7.6 Hz, 2H), 2.57 (d, J = 1.8 Hz, 3H), 2.51 (s, 3H), 2.18 (s, 3H), 2.06 (d, J = 6.3 Hz, 2H), 1.90 (quint, J = 7.1 Hz, 2H). ^{1}H-NMR (600 MHz, DMSO-d_6) δ 10.68 (s, 1H), 9.26 (s, 2H), 9.06 (s, 1H), 8.57 (s, 2H), 7.70 (d, J = 8.4 Hz, 1H), 7.63 (s, 1H), 7.57 (dd, J = 8.8, 4.2 Hz, 1H), 7.25 (t, J = 9.5 Hz, 1H), 7.04-7.00 (m, 2H), 4.12 (t, J = 6.1 Hz, 2H), 3.31 (q,

J = 6.5 Hz, 2H), 3.25 (q, *J* = 6.7 Hz, 2H), 2.60 (t, *J* = 7.5 Hz, 2H), 2.53 (s, 3H), 2.50 (s, 3H, overlapped with DMSO signal), 2.09 (s, 3H), 1.95 (quint, *J* = 6.5 Hz, 2H), 1.73 (quint, *J* = 7.3 Hz, 2H). ^{13}C-NMR (151 MHz, DMSO-d_6) δ 168.05, 160.58, 159.08 (q, *J* = 33.5 Hz, TFA), 157.31 (d, *J* = 237.0 Hz), 153.87 (2C), 151.65, 139.56, 135.21 (HMBC), 132.10, 131.23, 130.76, 118.41, 117.06, 116.55 (q, *J* = 295.9 Hz, TFA), 116.28, 112.22 (3C), 110.66 (d, *J* = 20.7 Hz), 65.51, 40.06, 36.48, 28.76, 28.65, 21.96, 20.32, 11.24, 9.36 (d, *J* = 3.3 Hz). HRMS (ESI-MS): calcd. for $C_{27}H_{34}FN_8O_2S^+$: 553.2504, found: 553.2507. MF: $C_{27}H_{33}FN_8O_2S$ x $C_6H_3F_9O_6$. MW: (552.67 + 342.06).

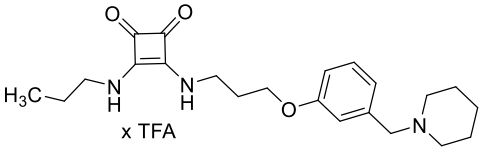

3-((3-(3-(Piperidin-1-ylmethyl)phenoxy)propyl)amino)-4-(propylamino)cyclobut-3-ene-1,2-dione hydrotrifluoroacetate (4.117). The title compound was prepared from **4.76** (130 mg, 0.297 mmol) and propylamine (122 µL, 1.49 mmol) in EtOH (5 mL) according to the general procedure D. The crude product was purified by preparative RP-HPLC and afforded a white, foamlike and hygroscopic solid (102 mg, 69%). R_f = 0.45 (CH_2Cl_2/0.5% NH_3 in MeOH 9:1). RP-HPLC (220 nm): 93% (t_R = 11.1 min, *k* = 2.46). ^{1}H-NMR (400 MHz, MeOD) δ 7.42-7.32 (m, 1H), 7.09-6.97 (m, 3H), 4.22 (s, 2H), 4.11 (t, *J* = 5.9 Hz, 2H), 3.83 (t, *J* = 6.4 Hz, 2H), 3.64-3.48 (m, 2H), 3.48-3.40 (m, 2H), 3.04-2.86 (m, 2H), 2.09 (quint, *J* = 6.3 Hz, 2H), 2.01-1.37 (m, 8H), 0.94 (t, *J* = 7.4 Hz, 3H). ^{13}C-NMR (101 MHz, MeOD) δ 183.61, 183.55, 169.76, 169.56, 162.28 (q, *J* = 33.7 Hz, TFA), 160.84, 131.86, 131.47, 124.60, 118.36, 117.84 (q, *J* = 290.9 Hz, TFA), 117.35, 66.39, 61.81, 54.18 (2C), 47.08, 42.58, 31.76, 25.61, 24.21 (2C), 22.85, 11.28. HRMS (ESI-MS): calcd. for $C_{22}H_{32}N_3O_3^+$: 386.2438, found: 386.2451. MF: $C_{22}H_{31}N_3O_3$ x $C_2HF_3O_2$. MW: (385.51 + 114.02).

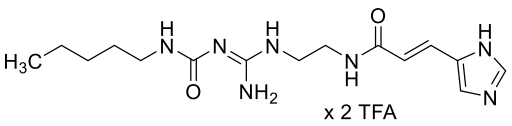

(*E*)-3-(1*H*-Imidazol-5-yl)-*N*-(2-((*E*)-2-(pentylcarbamoyl)guanidino)ethyl)acrylamide dihydrotrifluoroacetate (4.120). The guanidinylating reagent **4.118** (50 mg, 0.165 mmol, 1.0 equiv) and the amine PB506 (53 mg, 0.18 mmol, 1.1 equiv) were dissolved in CH_2Cl_2 (2 mL). NEt_3 (57 µL, 0.41 mmol, 2.5 equiv) and $HgCl_2$ (90 mg, 0.33 mmol, 2 equiv) were assess to the mixture. The mixture was stirred at rt overnight. The reaction mixture was diluted with

CH_2Cl_2 (10 mL). The precipitate was removed by filtration through Celite 545 and washed with CH_2Cl_2 (20 mL) and EtOAc (20 mL). The filtrate was concentrated in vacuum and the crude product was purified by column chromatography on silica gel (gradient: 0-20 min: CH_2Cl_2/MeOH 100:0-94:6) to obtain the fully protected intermediate **4.119** as yellow oil (30 mg, 32%). R_f = 0.56 (CH_2Cl_2/MeOH 9:1). HRMS (ESI-MS): calcd. for $C_{28}H_{40}N_7O_2^+$: 570.3035, found: 570.3038. MF: $C_{28}H_{39}N_7O_6$. MW: 569.66. To a stirred solution of the fully protected intermediate (**4.119**, 30 mg, 0.053 mmol) in THF/MeOH (1:1 (v/v), 5 mL) was added Pd/C (10 wt%, 10 mg). The mixture was stirred in a steel autoclave under a hydrogen atmosphere of 8 bar for 2 h at rt. The mixture was diluted with MeOH (10 mL). Pd/C was removed by filtration through Celite 545 and washed with MeOH (10 mL) and THF (10 mL). The filtrate was concentrated in vacuum. The residue was dissolved in CH_2Cl_2 (4 mL), TFA (1 mL) was added and the mixture was stirred at rt for 8 h. The solvent was removed in vacuum and the residue was purified by preparative HPLC to get white, foamlike and hygroscopic solid (3.15 mg, 11%). RP-HPLC (220 nm): 96% (t_R = 10.1 min, k = 2.15). ^{1}H-NMR (300 MHz, MeOD) δ 8.77 (s, 1H), 7.76 (d, J = 1.4 Hz, 1H), 7.48 (d, J = 15.9 Hz, 1H), 6.65 (d, J = 15.8 Hz, 1H), 3.61-3.41 (m, 4H), 3.18 (t, J = 7.1 Hz, 2H), 1.52 (quint, J = 7.1 Hz, 2H), 1.43-1.21 (m, 4H), 0.97-0.84 (m, 3H). ^{1}H-NMR (600 MHz, DMSO-d_6) δ 9.89 (s, 1H), 9.13-8.91 (m, 1H), 8.82-8.44 (m, 3H), 8.41 (t, J = 5.4 Hz, 1H), 7.78 (s, 1H), 7.47 (s, 1H), 7.36 (d, J = 15.7 Hz, 1H), 6.58 (d, J = 15.8 Hz, 1H), 3.42-3.32 (m, 4H), 3.08 (q, J = 6.6 Hz, 2H), 1.43 (quint, J = 7.2 Hz, 2H), 1.32-1.19 (m, 4H), 0.86 (t, J = 7.1 Hz, 3H). HRMS (ESI-MS): calcd. for $C_{15}H_{26}N_7O_2^+$: 336.2142, found: 336.2144; calcd. for $C_{15}H_{27}N_7O_2^{2+}$: 168.6108, found: 168.6111. MF: $C_{15}H_{25}N_7O_2$ x $C_4H_2F_6O_4$. MW: (335.21 + 228.05).

4.4.11 Radioligand Binding Experiments

Competition binding experiments were performed using membrane preparations of Sf9 insect cells expressing the hH_1R + RGS4[71], hH_2R-$G_{s\alpha S}$ fusion protein[72], hH_3R + $G_{\alpha i2}$ + $G_{\beta 1\gamma 2}$[73] or the hH_4R + $G_{\alpha i2}$ + $G_{\beta 1\gamma 2}$[74]. General procedures for the generation of recombinant baculoviruses, culture of Sf9 cells and membrane preparations have been described elsewhere.[75] The competition binding experiments were performed as previously described in detail[4, 13] with one minor modification: PBS (8 g NaCl, 0.2 g KCl, 1.0 g Na_2HPO_4 x 2 H_2O, 0.15 g NaH_2PO_4 x H_2O, 0.1 g KH_2PO_4 in 1 L Millipore H_2O; pH 7.4; 4 °C) was used as washing buffer while harvesting instead of the previously used binding buffer[4, 13]. [^{3}H]mepyramine (specific activity: 20.0 or 87 Ci/mmol) was from Hartmann analytics (Braunschweig, Germany) or Novandi Chemistry AB (Södertälje, Sweden), [^{3}H]histamine (specific activity: 25.0 Ci/mmol)

and [^{3}H]N^{α}-methylhistamine (specific activity: 85.3 Ci/mmol) were from Hartmann analytics (Braunschweig, Germany). [^{3}H]UR-DE257[8] (specific activity: 63.0 Ci/mmol) and [^{3}H]UR-PI294[39] (specific activity: 41.8 Ci/mmol) were synthesized and characterized in our laboratories.

4.4.12 Functional Assays

The [^{35}S]GTPγS assay was performed on Sf9 membranes expressing the hH_2R-$G_{s\alpha S}$ fusion protein as previously described[4, 44] with one minor modification: PBS (8 g NaCl, 0.2 g KCl, 1.0 g Na_2HPO_4 x 2 H_2O, 0.15 g NaH_2PO_4 x H_2O, 0.1 g KH_2PO_4 in 1 L Millipore H_2O; pH 7.4; 4 °C) was used as washing buffer while harvesting instead of the previously used binding buffer. The [^{35}S]GTPγS binding assay was evaluated as described in detail by Biselli et al.[44]

Functional studies in the mini-G protein or β-arrestin2 recruitment assays using HEK293T NlucN-mGs/hH_2R-NlucC[42]-, HEK293T-ARRB2-H_2R[38, 43]-, HEK293T-ARRB1-H_2R[43] cells were performed as previously described.

4.5 References

1. Lee-Dutra, A.; Arienti, K.; Buzard, D. J.; Hack, M. D.; Khatuya, H.; Desai, P. J.; Nguyen, R. L.; Thurmond, R. L.; Karlsson, L.; Edwards, J.; Breitenbucher, J. G., Identification of 2-arylbenzimidazoles as potet human histamine H_4 receptor ligand. *Bioorg. Med. Chem. Lett.* **2006,** *16*, 6043-6048.
2. Baumeister, P. Molecular Tools for G-Protein Coupled Receptors: Synthesis, Pharmacological Characterization and [^{3}H]-Labeling of Subtype-Selective Ligands for Histamine H_4 and NPY Y_2 Receptors. Ph. D. Thesis. University of Regensburg, 2014.
3. Kraus, A.; Ghorai, P.; Birnkammer, T.; Schnell, D.; Elz, S.; Seifert, R.; Dove, S.; Bernhardt, G.; Buschauer, A., N^G-Acylated aminothiazolylpropylguanidines as potent and selective histamine H_2 receptor agonists. *ChemMedChem* **2009,** *4*, 232-240.
4. Kagermeier, N.; Werner, K.; Keller, M.; Baumeister, P.; Bernhardt, G.; Seifert, R.; Buschauer, A., Dimeric carbamoylguanidine-type histamine H_2 receptor ligands: a new class of potent and selective agonists. *Bioorg. Med. Chem.* **2015,** *23*, 3957-3969.
5. Biselli, S.; Bresinsky, M.; Tropmann, K.; Forster, L.; Honisch, C.; Buschauer, A.; Bernhardt, G.; Pockes, S., Pharmacological characterization of a new series of carbamoylguanidines reveals potent agonism at the H_2R and D_3R. *Eur. J. Med. Chem.* **2021,** *214*, 113190.
6. Cavanagh, R. L.; Buyniski, J. P., Effect of BMY-25368, a potent and long-acting histamine H_2-receptor antagonist, on gastric secretion and aspirin-induced gastric lesions in the dog. *Aliment. Pharmacol. Ther.* **1989,** *3*, 299-313.
7. Savall, B. M.; Edwards, J. P.; Venable, J. D.; Buzard, D. J.; Thurmond, R.; Hack, M. D.; McGovern, P., Agonist/antagonist modulation in a series of 2-aryl benzimidazole H_4 receptor ligands. *Bioorg. Med. Chem. Lett.* **2010** *20*, 3367-3371.
8. Baumeister, P.; Erdmann, D.; Biselli, S.; Kagermeier, N.; Elz, S.; Bernhardt, G.; Buschauer, A., [^{3}H]UR-DE257: development of a tritium-labeled squaramide-type selective histamine H_2 receptor antagonist. *ChemMedChem* **2015,** *10*, 83-93.

9. Black, J. W.; Duncan, W. A. M.; Durant, G. J.; Ganellin, C. R.; Parsons, M. E., Definition and antagonism of histamine H_2-receptors. *Nature* **1972,** *236*, 385-390.
10. von Angerer, E.; Prekajac, J.; Strohmeier, J., 2-Phenylindoles. Relationship between structure, estrogen receptor affinity, and mammary tumor inhibiting activity in the rat. *J. Med. Chem.* **1984,** *27*, 1439-1447.
11. Eriks, J. C.; van der Goot, H.; Sterk, G. J.; Timmerman, H., Synthesis, in vitro pharmacology, and qualitative structure-activity relationships of substituted 4- and 5-(2-aminoethyl)thiazoles. *J. Med. Chem.* **1992,** *35*, 3239-3246.
12. Ghorai, P. Arpromidine-related acylguanidines: synthesis and structure activity relationships of a new class of guanidine-type histamine H_2 receptor agonists with reduced basicity. Ph.D. Thesis. University of Regensburg, 2005.
13. Pockes, S.; Wifling, D.; Keller, M.; Buschauer, A.; Elz, S., Highly potent, stable, and selective dimeric hetarylpropylguanidine-type histamine H_2 receptor agonists. *ACS Omega* **2018,** *3*, 2865-2882.
14. Pockes, S.; Wifling, D.; Buschauer, A.; Elz, S., Structure-activity relationship of hetarylpropylguanidines aiming at the development of selective histamine receptor ligands. *ChemistryOpen* **2019,** *8*, 285-297.
15. Green, T. W.; Wuts, P. G. M., Protection for the Amino Group. In *Protective Groups in Organic Synthesis*, Green, T. W.; Wuts, P. G. M., Eds. 1999; pp 494-653.
16. Griffith, R. K.; Dipietro, A. D., Improved syntheses of vinylimidazoles. *Synth. Commun.* **1986,** *16*, 1761-1770.
17. Dodson, R. M.; King, L. C., The reaction of ketones with halogens and thiourea1. *J. Am. Chem. Soc.* **1945,** *67*, 2242-2243.
18. Bermudez, J.; King, F. D.; Sanger, G. J., Indazole and indoline as aromatic bioisosteres in the imidazole class of serotonin 5-HT_3 receptor antagonists. *Bioorg. Med. Chem. Lett.* **1992,** *2*, 1509-1512.
19. Igel, P. Synthesis and Structure-Activity Relationships of N^G-Acylated Arylalkylguanidines and Related Compounds as Histamine Receptor Ligands: Searching for Selective H_4R Agonists. Ph. D. Thesis. University of Regensburg, 2008.
20. Erdmann, D. Histamine H_2 and H_3 - Receptor Antagonists Synthesis and Characterization of Radiolabelled and Fluorescent Pharmacological Tools. Ph. D. Thesis. University of Regensburg, 2010.
21. Buschauer, A.; Postius, S.; Szelenyi, I.; Schunack, W., Isohistamine und Homologe als Bausteine von H_2-Antagonisten. *Arzneim.-Forsch.* **1985,** *35*, 1025-1029.
22. Savall, B. M.; Fontimayor, J. R.; Edwards, J. P., Selective phenol alkylation for an improved synthesis of 2-arylbenzimidazole H_4 receptor ligands. *Tetrahedron Lett.* **2009,** *50*, 2490-2492.
23. Jackson, P. A.; Widen, J. C.; Harki, D. A.; Brummond, K. M., Covalent modifiers: a chemical perspective on the reactivity of α,β-unsaturated carbonyls with thiols via hetero-Michael addition reactions. *J. Med. Chem.* **2017,** *60*, 839-885.
24. Lanman, B. A.; Allen, J. R.; Allen, J. G.; Amegadzie, A. K.; Ashton, K. S.; Booker, S. K.; Chen, J. J.; Chen, N.; Frohn, M. J.; Goodman, G.; Kopecky, D. J.; Liu, L.; Lopez, P.; Low, J. D.; Ma, V.; Minatti, A. E.; Nguyen, T. T.; Nishimura, N.; Pickrell, A. J.; Reed, A. B.; Shin, Y.; Siegmund, A. C.; Tamayo, N. A.; Tegley, C. M.; Walton, M. C.; Wang, H.-L.; Wurz, R. P.; Xue, M.; Yang, K. C.; Achanta, P.; Bartberger, M. D.; Canon, J.; Hollis, L. S.; McCarter, J. D.; Mohr, C.; Rex, K.; Saiki, A. Y.; San Miguel, T.; Volak, L. P.; Wang, K. H.; Whittington, D. A.; Zech, S. G.; Lipford, J. R.; Cee, V. J., Discovery of a covalent inhibitor of KRASG12C (AMG 510) for the treatment of solid tumors. *J. Med. Chem.* **2020,** *63*, 52-65.
25. Nijmeijer, S.; Engelhardt, H.; Schultes, S.; van de Stolpe, A. C.; Lusink, V.; de Graaf, C.; Wijtmans, M.; Haaksma, E. E. J.; de Esch, I. J. P.; Stachurski, K.; Vischer, H. F.; Leurs, R., Design and pharmacological characterization of VUF14480, a covalent partial agonist that

interacts with cysteine 98(3.36) of the human histamine H_4 receptor. *Br. J. Pharmacol.* **2013,** *170*, 89-100.
26. Ekici, Ö. D.; Götz, M. G.; James, K. E.; Li, Z. Z.; Rukamp, B. J.; Asgian, J. L.; Caffrey, C. R.; Hansell, E.; Dvořák, J.; McKerrow, J. H.; Potempa, J.; Travis, J.; Mikolajczyk, J.; Salvesen, G. S.; Powers, J. C., Aza-peptide Michael acceptors: a new class of inhibitors specific for caspases and other clan CD cysteine proteases. *J. Med. Chem.* **2004,** *47*, 1889-1892.
27. Tsou, H.-R.; Overbeek-Klumpers, E. G.; Hallett, W. A.; Reich, M. F.; Floyd, M. B.; Johnson, B. D.; Michalak, R. S.; Nilakantan, R.; Discafani, C.; Golas, J.; Rabindran, S. K.; Shen, R.; Shi, X.; Wang, Y.-F.; Upeslacis, J.; Wissner, A., Optimization of 6,7-disubstituted-4-(arylamino)quinoline-3-carbonitriles as orally active, irreversible inhibitors of human epidermal growth factor receptor-2 kinase activity. *J. Med. Chem.* **2005,** *48*, 1107-1131.
28. Klutchko, S. R.; Zhou, H.; Winters, R. T.; Tran, T. P.; Bridges, A. J.; Althaus, I. W.; Amato, D. M.; Elliott, W. L.; Ellis, P. A.; Meade, M. A.; Roberts, B. J.; Fry, D. W.; Gonzales, A. J.; Harvey, P. J.; Nelson, J. M.; Sherwood, V.; Han, H.-K.; Pace, G.; Smaill, J. B.; Denny, W. A.; Showalter, H. D. H., Tyrosine kinase inhibitors. 19. 6-Alkynamides of 4-anilinoquinazolines and 4-anilinopyrido[3,4-d]pyrimidines as irreversible inhibitors of the erbB family of tyrosine kinase receptors. *J. Med. Chem.* **2006,** *49*, 1475-1485.
29. Pan, Z.; Scheerens, H.; Li, S. J.; Schultz, B. E.; Sprengeler, P. A.; Burrill, L. C.; Mendonca, R. V.; Sweeney, M. D.; Scott, K. C.; Grothaus, P. G.; Jeffery, D. A.; Spoerke, J. M.; Honigberg, L. A.; Young, P. R.; Dalrymple, S. A.; Palmer, J. T., Discovery of selective irreversible inhibitors for Bruton's tyrosine kinase. *ChemMedChem* **2007,** *2*, 58-61.
30. Garuti, L.; Roberti, M.; Bottegoni, G., Irreversible protein kinase inhibitors. *Curr. Med. Chem.* **2011,** *18*, 2981-2994.
31. Williams, M., *The Merck Index - An Encyclopedia of Chemicals, Drugs, and Biologicals. 15th Edition*. Royal Society of Chemistry, Cambridge, UK: Royal Society of Chemistry: 2013.
32. Hoyle, C. E.; Bowman, C. N., Thiol–ene click chemistry. *Angew. Chem. Int. Ed. Engl.* **2010,** *49*, 1540-1573.
33. Karagiorgou, O.; Patsis, G.; Pelecanou, M.; Raptopoulou, C. P.; Terzis, A.; Siatra-Papastaikoudi, T.; Alberto, R.; Pirmettis, I.; Papadopoulos, M., (S)-(2-(2'-Pyridyl)ethyl)cysteamine and (S)-(2-(2'-pyridyl)ethyl)-D,L-homocysteine as ligands for the "fac-$[M(CO)_3]^+$" (M = Re, ^{99m}Tc) core. *Inorg. Chem.* **2005,** *44*, 4118-4120.
34. Liu, F.; Dalhus, B.; L.-L., G.; Rise, F., Addition andcycloaddition to 2- and 8-vinylpurines. *Acta Chem. Scand.* **1999,** *53*, 269-279.
35. In the [^{35}S]GTPγS binding assay GTPγS labelled with ^{35}S is used. The half-life of this sulfur isotope is 87.37 d, so that the reagent can only be used for a limited time. Therefore, several batches have to be ordered in the course of a project. At the beginning of the project, our supplier still delivered the reagent in good quality, so we were able to perform this assay without any problems. However, the batches ordered towards the end of the project were of inadequate quality (was self-tested in our radiology lab with inadequate purity results). Since we did not find an alternative supplier with sufficient reagent quality, we could not perform this assay anymore. Thus, not all compounds could be characterized in the [^{35}S]GTPγS assay. All data given in the manuscript are comparable and have been performed with [^{35}S]GTPγS batches of high quality.
36. Ruat, M.; Traiffort, E.; Bouthenet, M. L.; Schwartz, J. C.; Hirschfeld, J.; Buschauer, A.; Schunack, W., Reversible and irreversible labeling and autoradiographic localization of the cerebral histamine H_2 receptor using [^{125}I]iodinated probes. *Proc. Natl. Acad. Sci. USA* **1990,** *87*, 1658-1662.
37. Pertz, H. H.; Görnemann, T.; Schurad, B.; Seifert, R.; Straßer, A., Striking differences of action of lisuride stereoisomers at histamine H_1 receptors. *N.-S. Arch. Pharmacol.* **2006,** *374*, 215-222.

38. Grätz, L.; Tropmann, K.; Bresinsky, M.; Müller, C.; Bernhardt, G.; Pockes, S., NanoBRET binding assay for histamine H_2 receptor ligands using live recombinant HEK293T cells. *Sci. Rep.* **2020,** *10, e13288*.
39. Igel, P.; Schnell, D.; Bernhardt, G.; Seifert, R.; Buschauer, A., Tritium-labeled N^1-[3-(1H-imidazol-4-yl)propyl]-N^2-propionylguanidine ([^{3}H]UR-PI294), a high-affinity histamine H_3 and H_4 receptor radioligand. *ChemMedChem* **2009,** *4*, 225-231.
40. Tropmann, K.; Höring, C.; Plank, N.; Pockes, S., Discovery of a G protein biased radioligand for the histamine H_2 receptor with reversible binding properties. *J. Med. Chem.* **2020,** *63*, 13090-13102.
41. Bartole, E.; Littmann, T.; Tanaka, M.; Ozawa, T.; Buschauer, A.; Bernhardt, G., [^{3}H]UR-DEBa176: a 2,4-diaminopyrimidine-type radioligand enabling binding studies at the human, mouse, and rat histamine H_4 receptors. *J. Med. Chem.* **2019,** *62*, 8338-8356.
42. Höring, C.; Seibel, U.; Tropmann, K.; Grätz, L.; Mönnich, D.; Pitzl, S.; Bernhardt, G.; Pockes, S.; Strasser, A., A dynamic, split-luciferase-based mini-G protein sensor to functionally characterize ligands at all four histamine receptor subtypes. *Int. J. Mol. Sci.* **2020,** *21, 8440*.
43. Felixberger, J. Luciferase Complementation for the Determination of Arrestin Recruitment: Investigation of Histamine and NPY receptors. Ph.D. Thesis. University of Regensburg, 2014.
44. Biselli, S.; Alencastre, I.; Tropmann, K.; Erdmann, D.; Chen, M.; Littmann, T.; Maia, A. F.; Gomez-Lazaro, M.; Tanaka, M.; Ozawa, T.; Keller, M.; Lamghari, M.; Buschauer, A.; Bernhardt, G., Fluorescent H_2 receptor squaramide-type antagonists: synthesis, characterization and applications. *ACS Med. Chem. Lett.* **2020,** *11*, 1521-1528.
45. Yung-Chi, C.; Prusoff, W. H., Relationship between the inhibition constant (K_i) and the concentration of inhibitor which causes 50 per cent inhibition (I_{50}) of an enzymatic reaction. *Biochem. Pharmacol.* **1973,** *22*, 3099-3108.
46. Ghorai, P.; Kraus, A.; Birnkammer, T.; Geyer, R.; Bernhardt, G.; Dove, S.; Seifert, R.; Elz, S.; Buschauer, A., Chiral N^G-acylated hetarylpropylguanidine-type histamine H_2 receptor agonists do not show significant stereoselectivity. *Bioorg. Med. Chem. Lett.* **2010,** *20*, 3173-3176.
47. Keller, M.; Tränkle, C.; She, X.; Pegoli, A.; Bernhardt, G.; Buschauer, A.; Read, R. W., M2 Subtype preferring dibenzodiazepinone-type muscarinic receptor ligands: Effect of chemical homo-dimerization on orthosteric (and allosteric?) binding. *Bioorg. Med. Chem.* **2015,** *23*, 3970-3990.
48. Lee, Y.; Park, G. Y.; Lucas, H. R.; Vajda, P. L.; Kamaraj, K.; Vance, M. A.; Milligan, A. E.; Woertink, J. S.; Siegler, M. A.; Narducci Sarjeant, A. A.; Zakharov, L. N.; Rheingold, A. L.; Solomon, E. I.; Karlin, K. D., Copper(I)/O_2 chemistry with imidazole containing tripodal tetradentate ligands leading to μ-1,2-peroxo-dicopper(II) species. *Inorg Chem* **2009,** *48*, 11297-11309.
49. Windsor, W. T.; Weber, P. C.; Wang, J. H.-S.; Strickland, C.; Njoroge, F.; George, G.; Timothy, J.; Girijavallabhan, V. M.; Ferreira, J. A.; Cooper, A. B.; Gelb, M. Treatment of malaria with farnesyl protein transferase inhibitors and preparation of tricyclic compounds for said treatment. WO 2002/056884, Jul 25, 2002, *Chem. Abstr.* **2002**, *137*, 125178.
50. Ghorai, P.; Kraus, A.; Keller, M.; Götte, C.; Igel, P.; Schneider, E.; Schnell, D.; Bernhardt, G.; Dove, S.; Zabel, M.; Elz, S.; Seifert, R.; Buschauer, A., Acylguanidines as bioisosteres of guanidines: N^G-acylated imidazolylpropylguanidines, a new class of histamine H_2 receptor agonists. *J. Med. Chem.* **2008,** *51*, 7193-7204.
51. Price, C. C.; Kabas, G.; Nakata, I., Some Amino and Ammonio Nitrogen Mustard Analogs. *J. Med. Chem.* **1965,** *8* (5), 650-655.
52. Geyer, R.; Kaske, M.; Baumeister, P.; Buschauer, A., Synthesis and functional characterization of imbutamine analogs as histamine H_3 and H_4 receptor ligands. *Arch. Pharm.* **2014,** *347*, 77-88.

53. Elz, S., An Alternative Synthesis of Homohistamine and Structurally Related (Imidazole-4-yl)alkylamines. *Z. Naturforsch.* **1987,** *42b*, 238-241.
54. Eriks, J. C.; van der Goot, H.; Sterk, G. J.; Timmerman, H., Histamine H_2-receptor agonists. Synthesis, in vitro pharmacology, and qualitative structure-activity relationships of substituted 4- and 5-(2-aminoethyl)thiazoles. *J. Med. Chem.* **1992,** *35*, 3239-3246.
55. Kraus, A. Highly Potent, Selective Acylguanidine-Type Histamine H_2 Receptor Agonists: Synthesis and Structure-Activity Relationships. PhD Thesis. University of Regensburg, 2007.
56. Lee, J. Y.; Choo, D. J.; Kim, Y. D.; Oh, C. R. Preparation of 3,4-dihydroquinazolines as T-type calcium channel blockers and anticancer drugs. WO 2008/136631, Nov 13, 2008, *Chem. Abstr.* **2008**, *135*, 9943.
57. Yoneyama, H.; Magata, T.; Uemura, K.; Usami, Y.; Tanaka, S.; Takaoka, M.; Harusawa, S., Efficient synthesis of *N*-[4-(4-chlorophenyl)butyl]-*S*-(3-piperidinopropyl)isothiourea (OUP-186) and its analogues using 2-nitrophenylacetyl isothiocyanate: application to novel histamine H_3R antagonists. *Synthesis* **2015,** *47*, 1291-1302.
58. Chen, B.-C.; Skoumbourdis, A. P.; Sundeen, J. E.; Rovnyak, G. C.; Traeger, S. C., Efficient molar-scale synthesis of 1-methyl-5-acylimidazole triflic acid salts. *Org. Process Res. Dev.* **2000,** *4*, 613-614.
59. Lin, Z.; Li, J.; Huang, Q.; Huang, Q.; Wang, Q.; Tang, L.; Gong, D.; Yang, J.; Zhu, J.; Deng, J., Chiral surfactant-type catalyst: enantioselective reduction of long-chain aliphatic ketoesters in water. *J. Org. Chem.* **2015,** *80*, 4419-4429.
60. Albertson, N. F., Alkylation with non-ketonic Mannich bases. Aminothiazoles and pyrrole *J. Am. Chem. Soc.* **1948,** *70*, 669-670.
61. Nakao, A.; Suzuki, H.; Tatsumi, R.; Seki, M.; Tanaka, M.; Setsuta, T.; Iwasaki, H. Preparation of N^2-(aryl or heteroaryl)-N^2-(carbamoylmethyl)glycinamides as homocysteine synthase inhibitors. WO 2009/125853, Oct 15, 2009, *Chem. Abst.* **2009**, *126*, 3140.
62. Kovačková, S.; Dračínský, M.; Rejman, D., The synthesis of piperidine nucleoside analogs—a comparison of several methods to access the introduction of nucleobases. *Tetrahedron* **2011,** *67* (7), 1485-1500.
63. Sangshetti, J. N.; Nagawade, R. R.; Shinde, D. B., Synthesis of novel 3-(1-(1-substituted piperidin-4-yl)-1H-1,2,3-triazol-4-yl)-1,2,4-oxadiazol-5(4H)-one as antifungal agents. *Bioorg. Med. Chem. Lett.* **2009,** *19*, 3564-3567.
64. Mühlhausen, U.; Sihver, W.; Ermert, J.; Coenen, H. H., Synthesis, radiofluorination and first evaluation of [^{18}F]fluorophenylsulfonyl- and [^{18}F]fluorophenylsulfinyl-piperidines as serotonin 5-HT_{2A} receptor antagonists for PET. *Nucl. Med. Biol.* **2010,** *37*, 605-614.
65. Ding, Z.; Lai, G.; Chen, S.; Yan, X. Preparation of hydrazine compounds as blood coagulation factor Xa inhibitor. CN 105085515, Nov 25, 2015, *Chem. Abstr.* **2015**, *190*, 9909, 2014.
66. Geerts, J.-P.; Motte, G.; Differding, E.; Henichart, J.-P. Preparation of substituted 4-(1,2,3,4-tetrahydro-1-naphthalenyl)-1H-imidazoles and 4-(2,3-dihydro-1H-inden-1-yl)-1H-imidazoles and their formulations as antiischemics and antihypertensives. EP 717037, Jun 19, 1996, *Chem. Abstr.* **1996**, *125*, 114632.
67. Higuchi, T.; Omiya, H.; Umezawa, N.; Kim, H.-S.; Wataya, Y. Preparation of azoles as antimalarial drugs. WO 2007/097450, Aug 30, 2007, *Chem. Abstr.* **2007**, *147*, 322987.
68. Menghin, S.; Pertz, H. H.; Kramer, K.; Seifert, R.; Schunack, W.; Elz, S., N_α-Imidazolylalkyl and pyridylalkyl derivatives of histaprodifen: synthesis and in vitro evaluation of highly potent histamine H_1-receptor agonists. *J. Med. Chem.* **2003,** *46*, 5458-5470.
69. Kai, K.; Fujii, H.; Ikenaka, R.; Akagawa, M.; Hayashi, H., An acyl-SAM analog as an affinity ligand for identifying quorum sensing signal synthases. *Chem. Comm.* **2014,** *50*, 8586-8589.

70. Mamedov, I.; Canals, S.; Henig, J.; Beyerlein, M.; Murayama, Y.; Mayer, H. A.; Logothetis, N. K.; Angelovski, G., In vivo characterization of a smart MRI agent that displays an inverse response to calcium concentration. *ACS Chem. Neurosci.* **2010,** *1*, 819-828.
71. Houston, C.; Wenzel-Seifert, K.; Bürckstümmer, T.; Seifert, R., The human histamine H_2-receptor couples more efficiently to Sf9 insect cell G_s-proteins than to insect cell G_q-proteins: limitations of Sf9 cells for the analysis of receptor/G_q-protein coupling. *J. Neurochem.* **2002,** *80*, 678-696.
72. Kelley, M. T.; Bürckstürmmer, T.; Wenzel-Seifert, K.; Dove, S.; Buschauer, A.; Seifert, R., Distinct interaction of human and guinea pig histamine H_2-receptor with guanidine-type agonists. *Mol. Pharmacol.* **2001,** *60*, 1210-1225.
73. Schnell, D.; Strasser, A.; Seifert, R., Comparison of the pharmacological properties of human and rat histamine H_3-receptors. *Biochem. Pharmacol.* **2010,** *80*, 1437-1449.
74. Schneider, E. H.; Schnell, D.; Papa, D.; Seifert, R., High constitutive activity and a G-protein-independent high-affinity state of the human histamine H_4-receptor. *Biochemistry* **2009,** *48*, 1424-1438.
75. Pop, N.; Igel, P.; Brennauer, A.; Cabrele, C.; Bernhardt, G.; Seifert, R.; Buschauer, A., Functional reconstitution of human neuropeptide Y (NPY) Y_2 and Y_4 receptors in Sf9 insect cells. *J. Recept. Signal Transduct.* **2011,** *31*, 271-285.

Appendix 3 Synthesis and Pharmacological Characterization of 2-Arylbenzimidazole Derivatives as Histamine H_2 Receptor Ligands

App3.1 ^{1}H- and/or ^{13}C-NMR Spectra of 4.82-4.97, 4.104-4.110, 4.112, 4.114-4.117 and 4.120

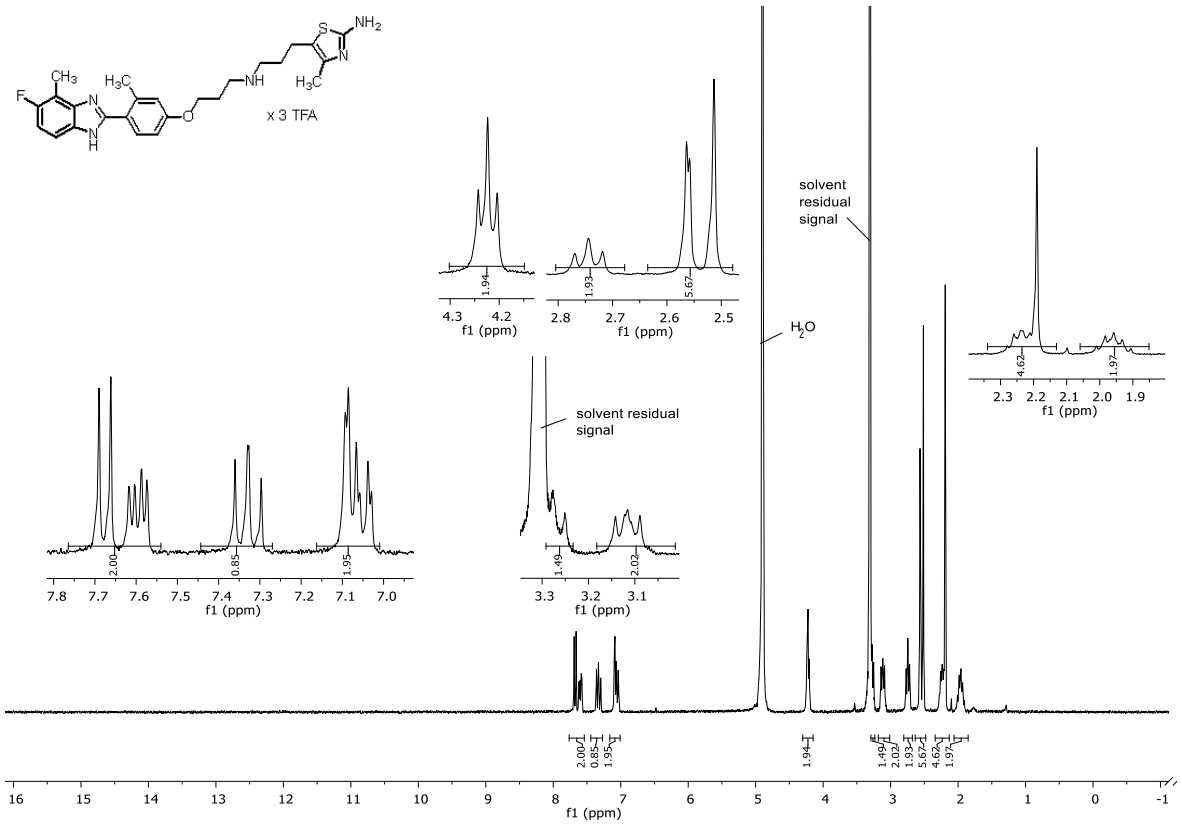

Figure App3.1. ^{1}H-NMR spectrum (300 MHz, MeOD) of compound **4.82**.

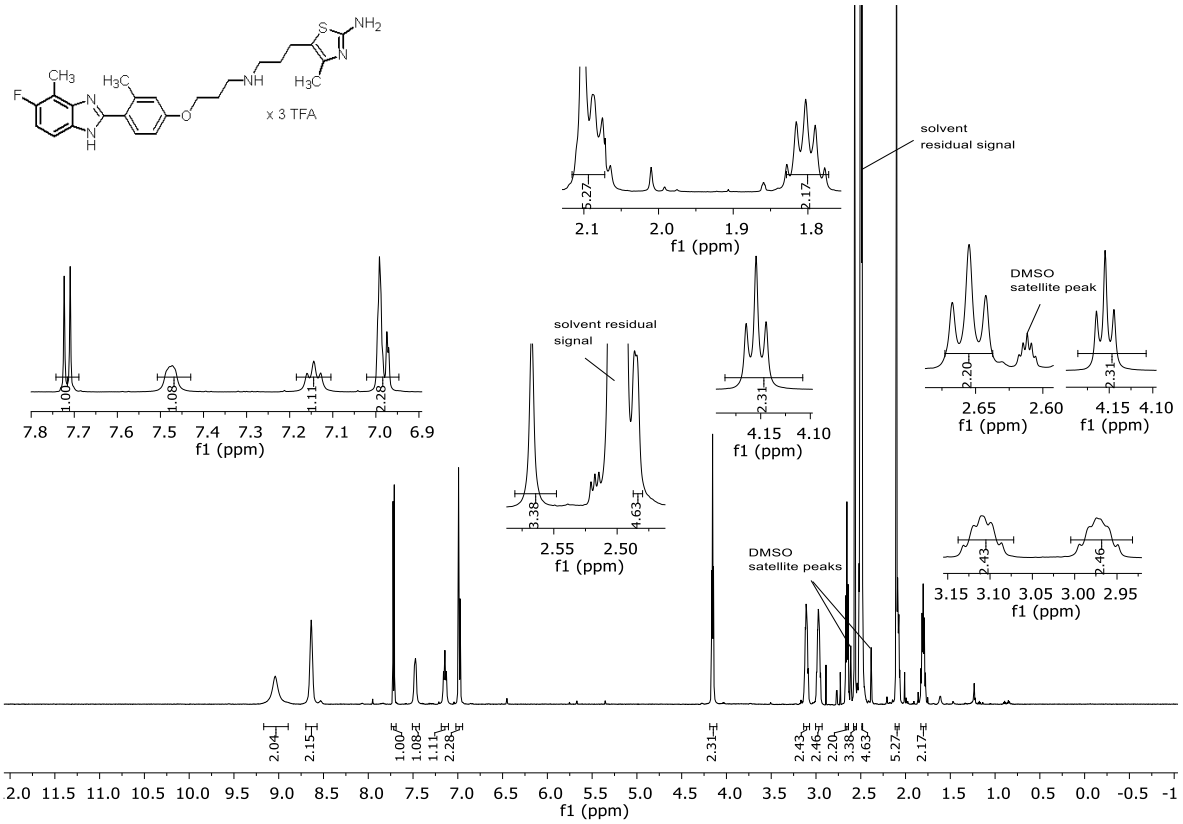

Figure App3.2. ^{1}H-NMR spectrum (600 MHz, DMSO-d_6) of compound **4.82**.

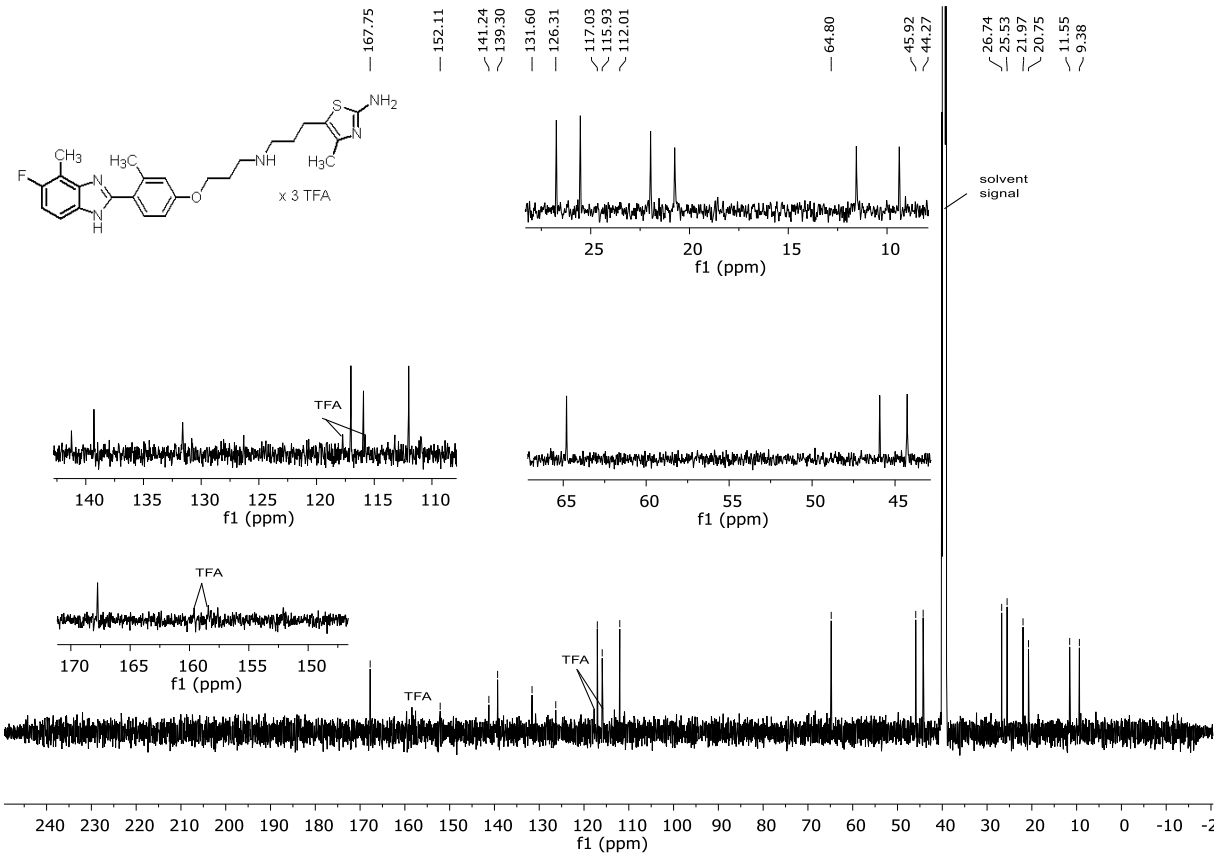

Figure App3.3. ^{13}C-NMR spectrum (151 MHz, DMSO-d_6) of compound **4.82**.

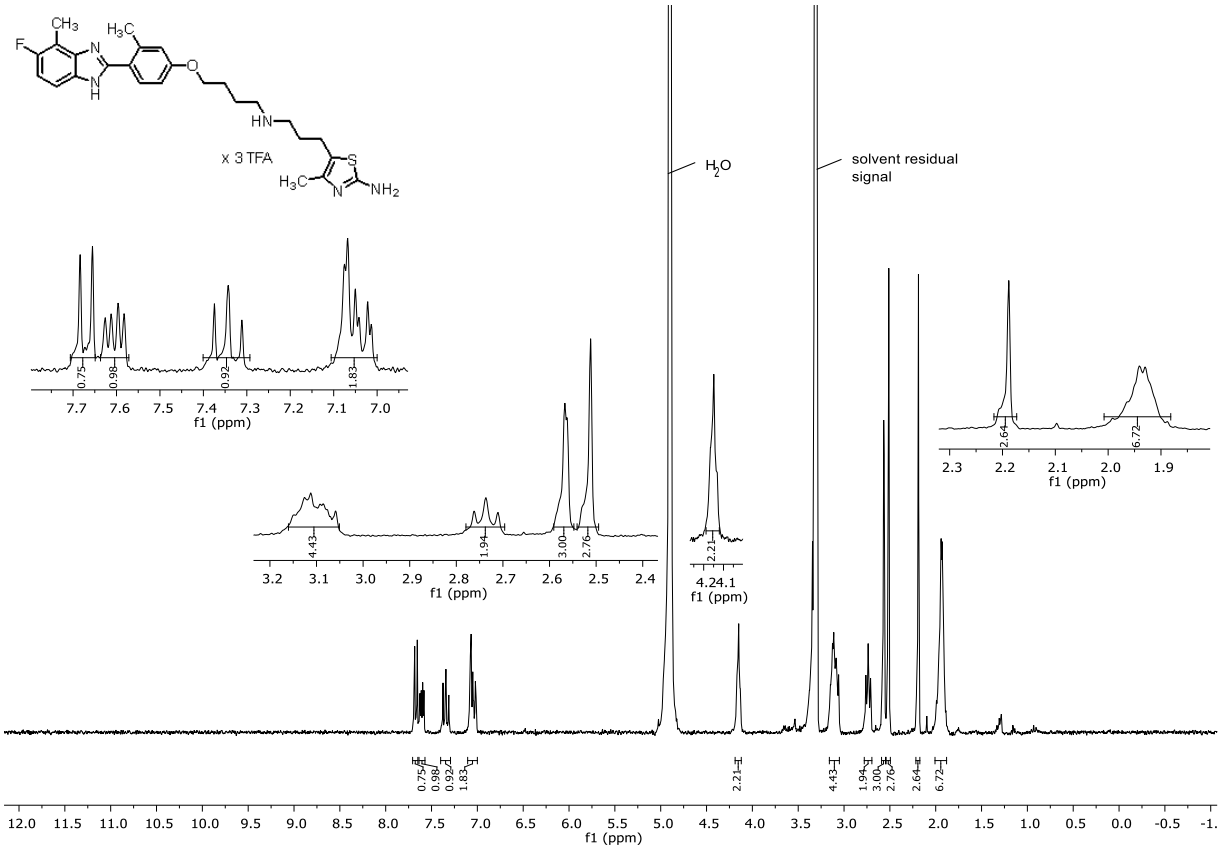

Figure App3.4. ^{1}H-NMR spectrum (300 MHz, MeOD) of compound **4.83**.

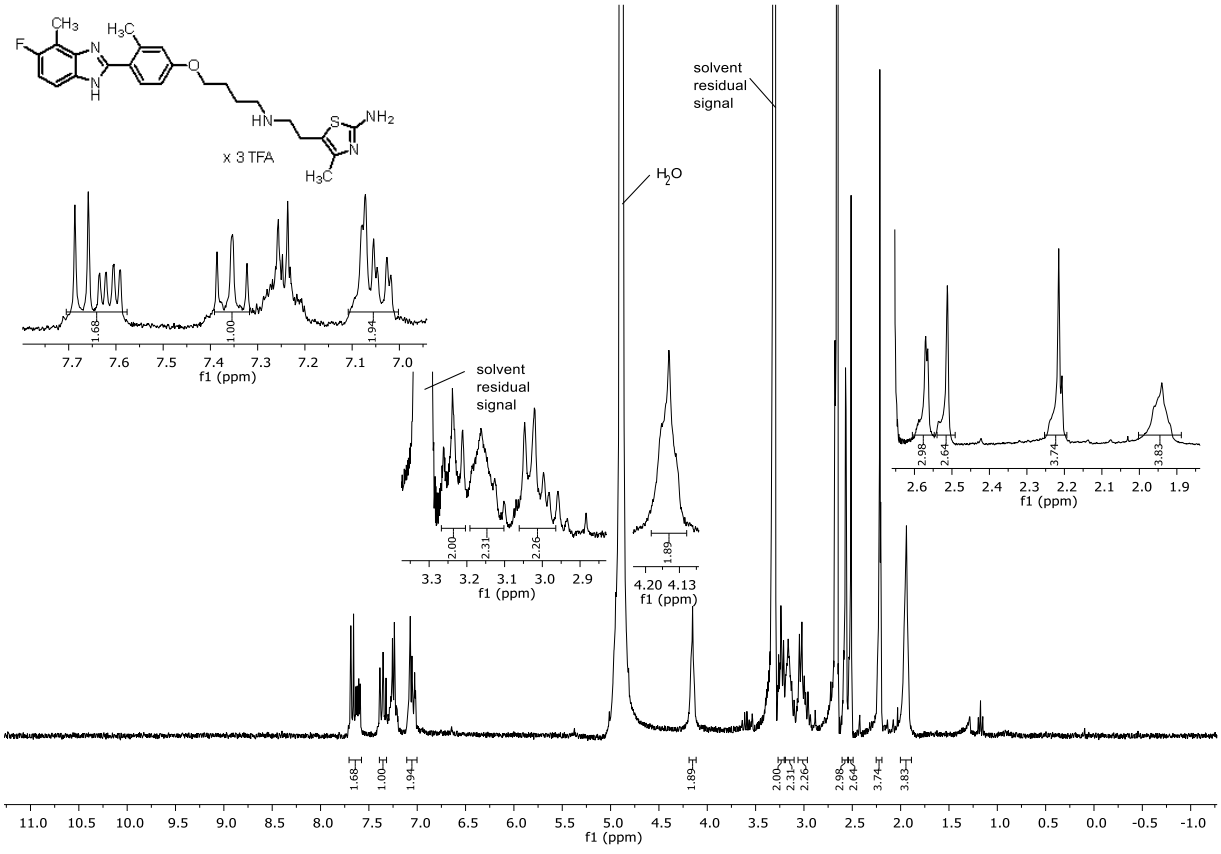

Figure App3.5. ^{1}H-NMR spectrum (300 MHz, MeOD) of compound **4.84**.

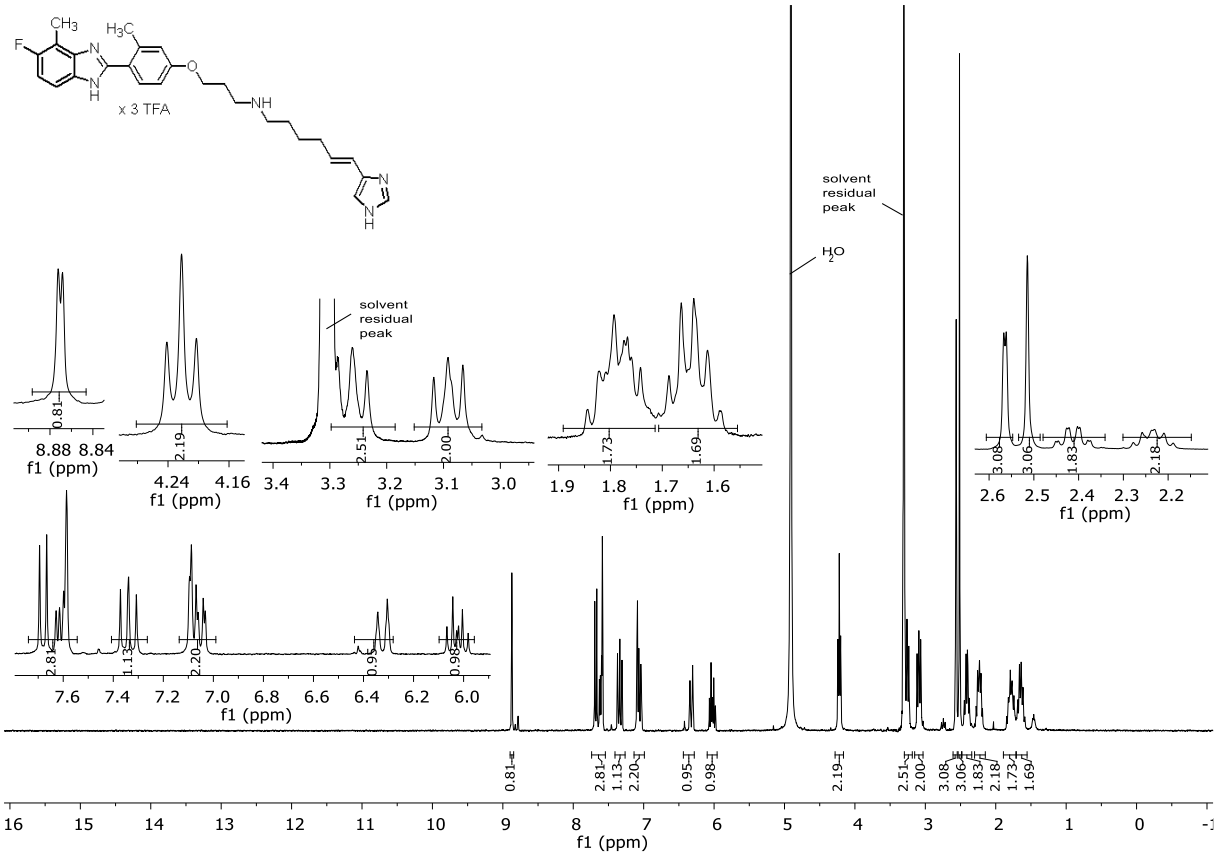

Figure App3.6. ^{1}H-NMR spectrum (300 MHz, MeOD) of compound **4.85**.

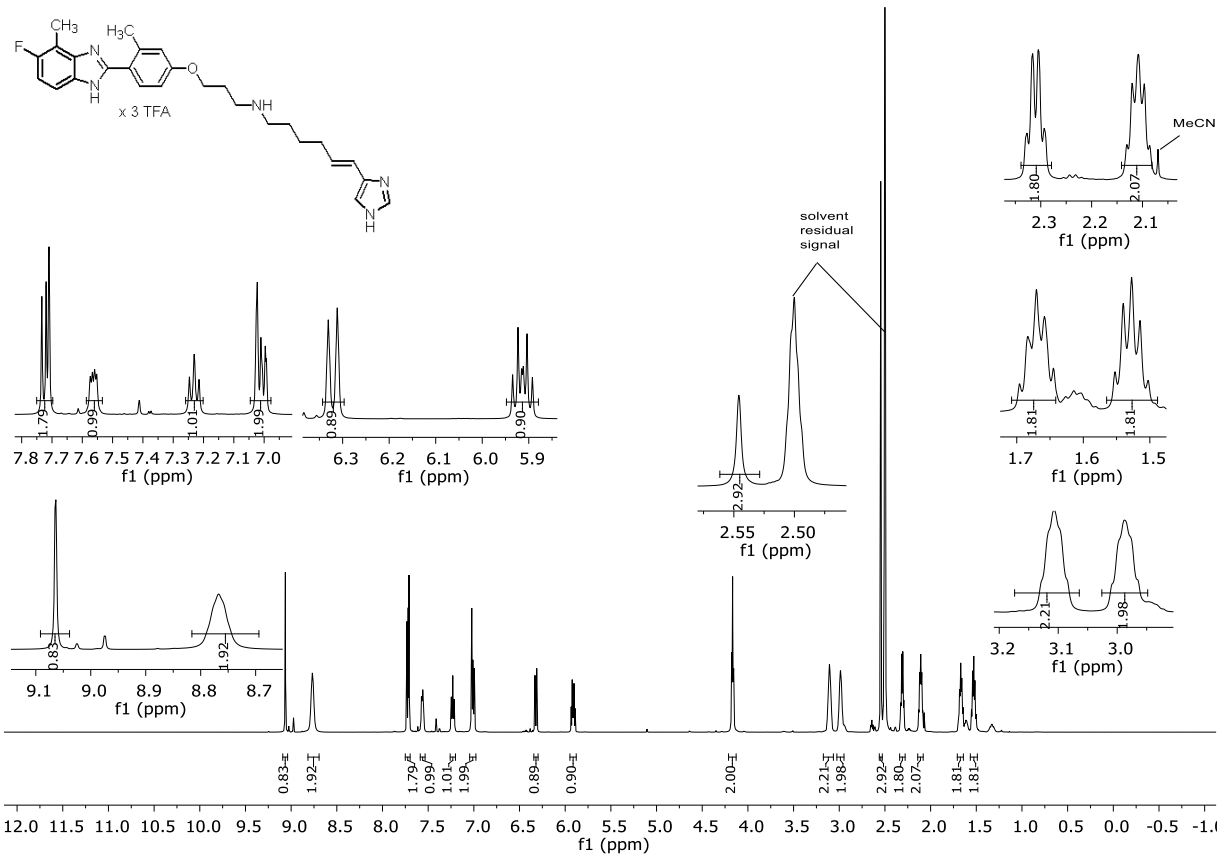

Figure App3.7. ^{1}H-NMR spectrum (600 MHz, DMSO-d_6) of compound **4.85**.

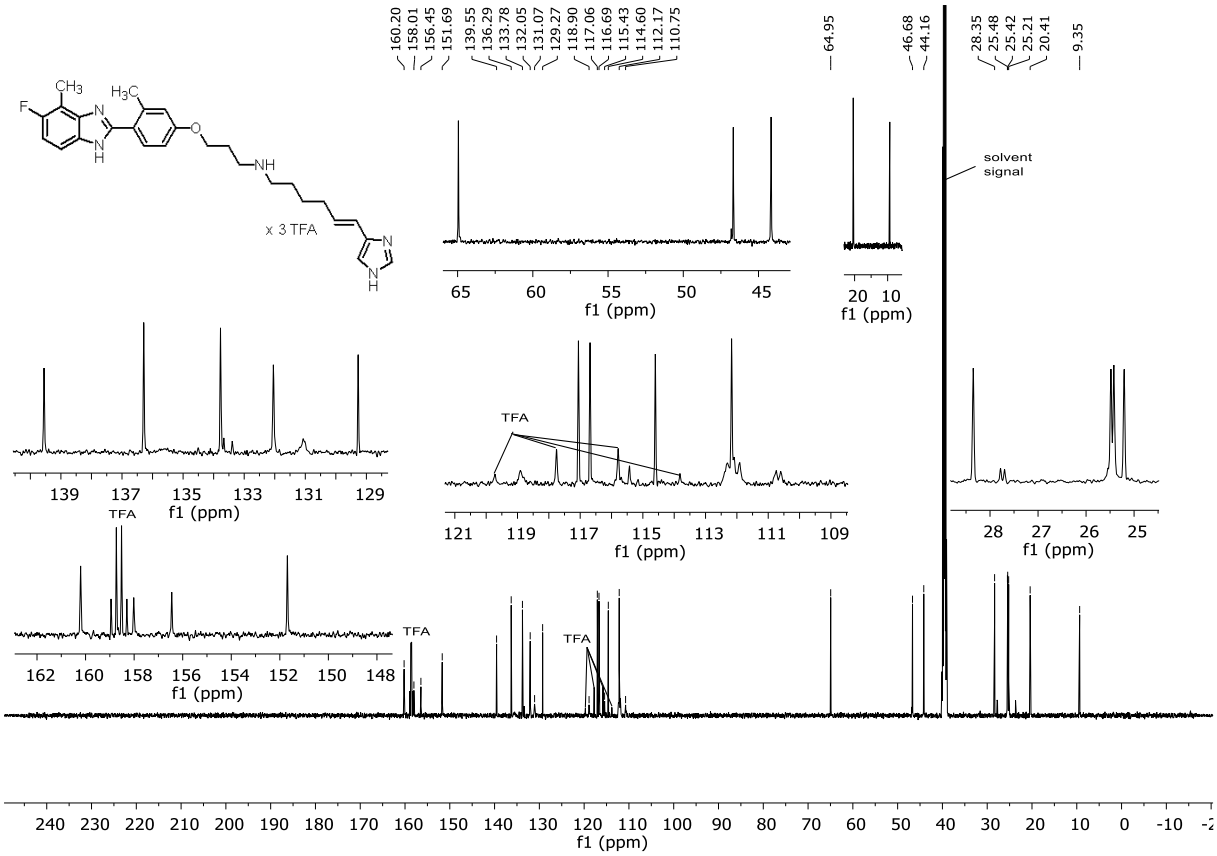

Figure App3.8. ^{13}C-NMR spectrum (151 MHz, DMSO-d_6) of compound **4.85**.

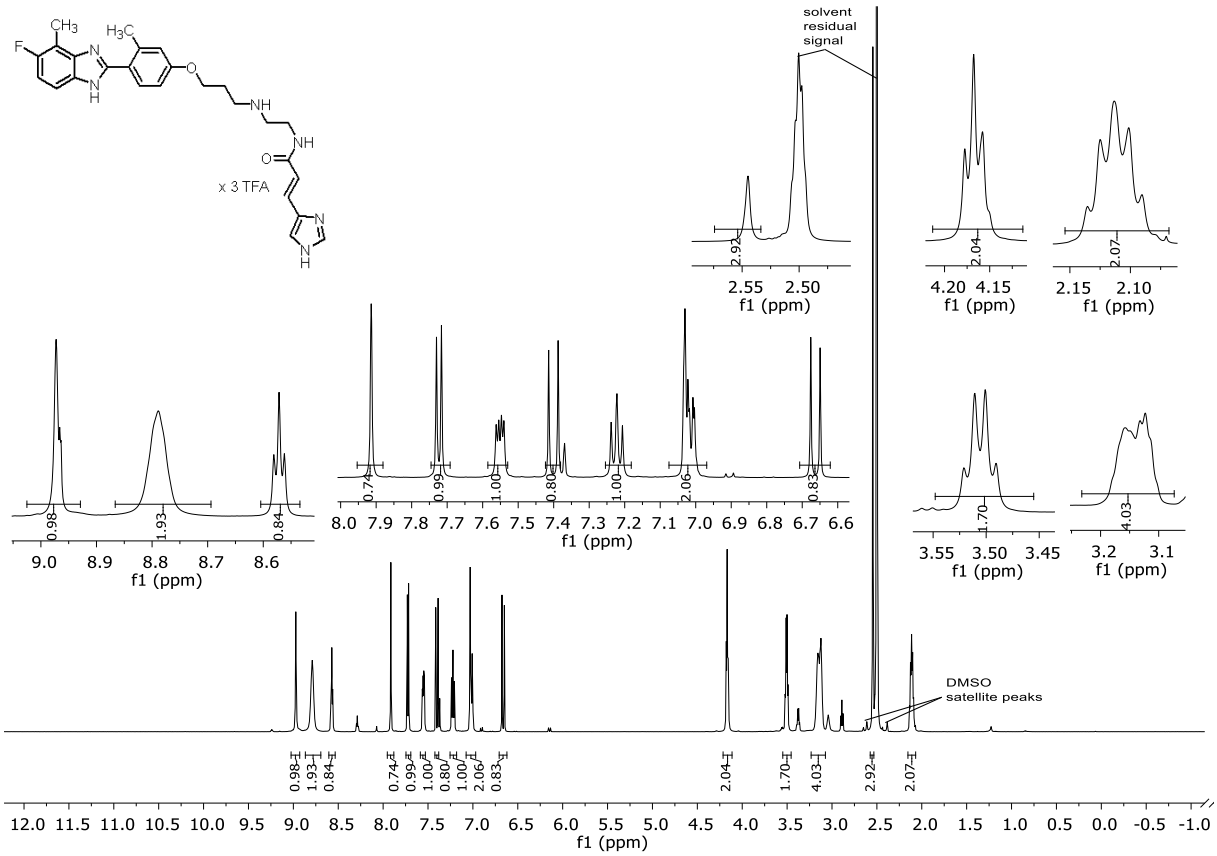

Figure App3.9. ^{1}H-NMR spectrum (600 MHz, DMSO-d_6) of compound **4.86**, PB513.

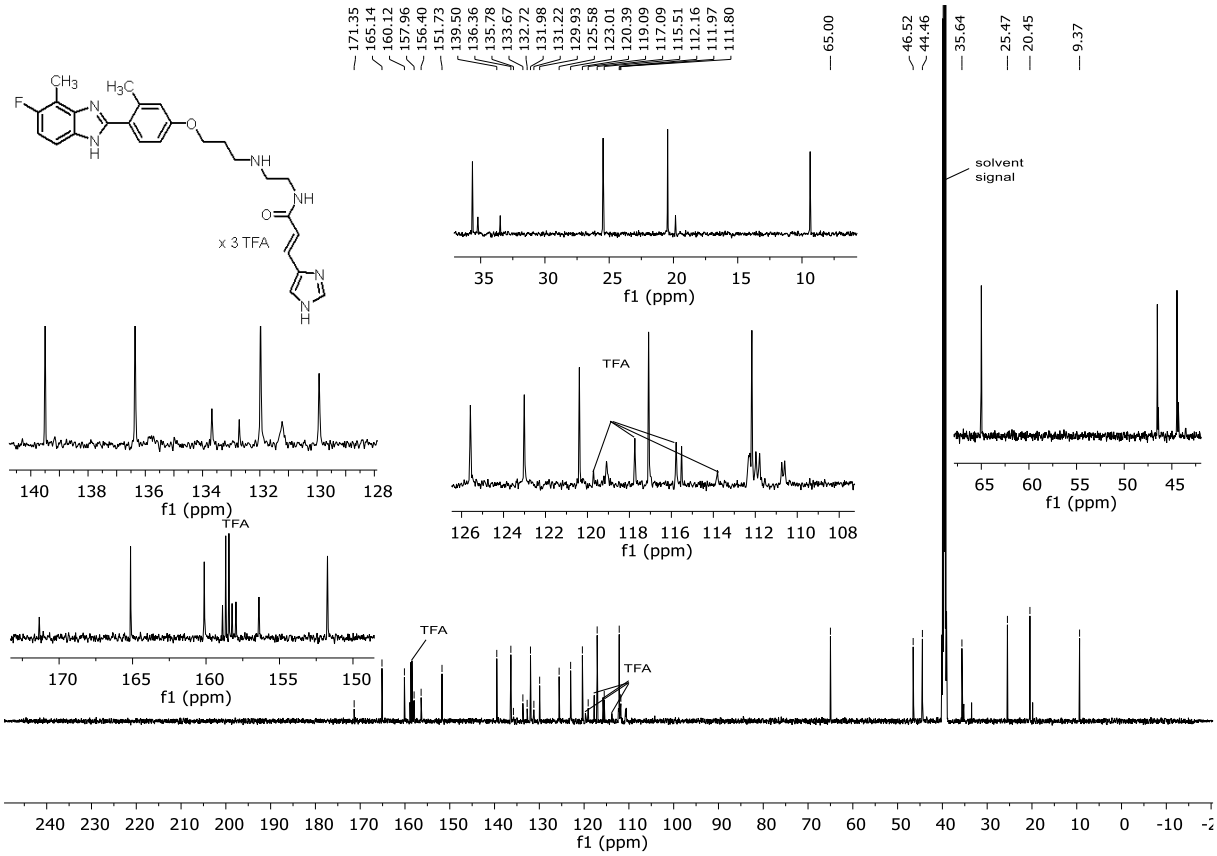

Figure App3.10. ^{13}C-NMR spectrum (151 MHz, DMSO-d_6) of compound **4.86**, PB513.

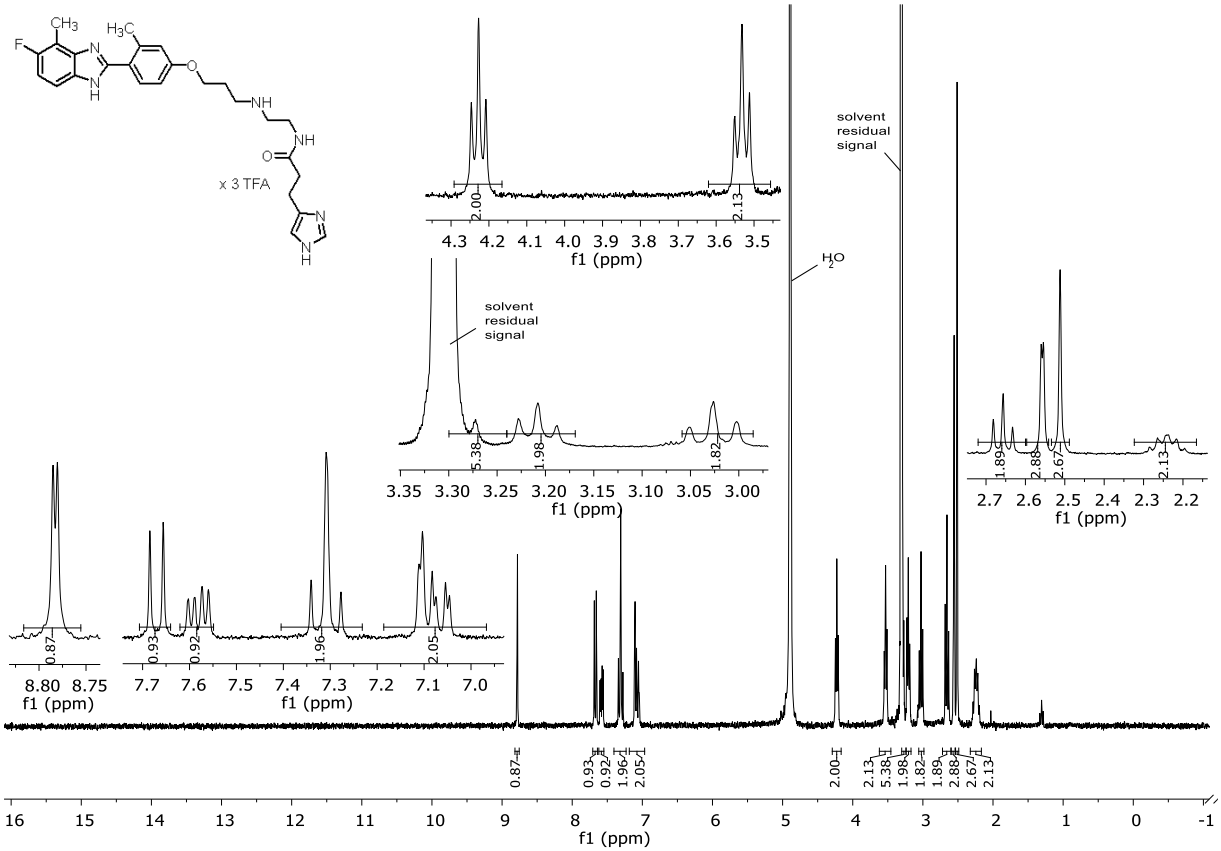

Figure App3.11. ^{1}H-NMR spectrum (300 MHz, DMSO-d_6) of compound **4.87**.

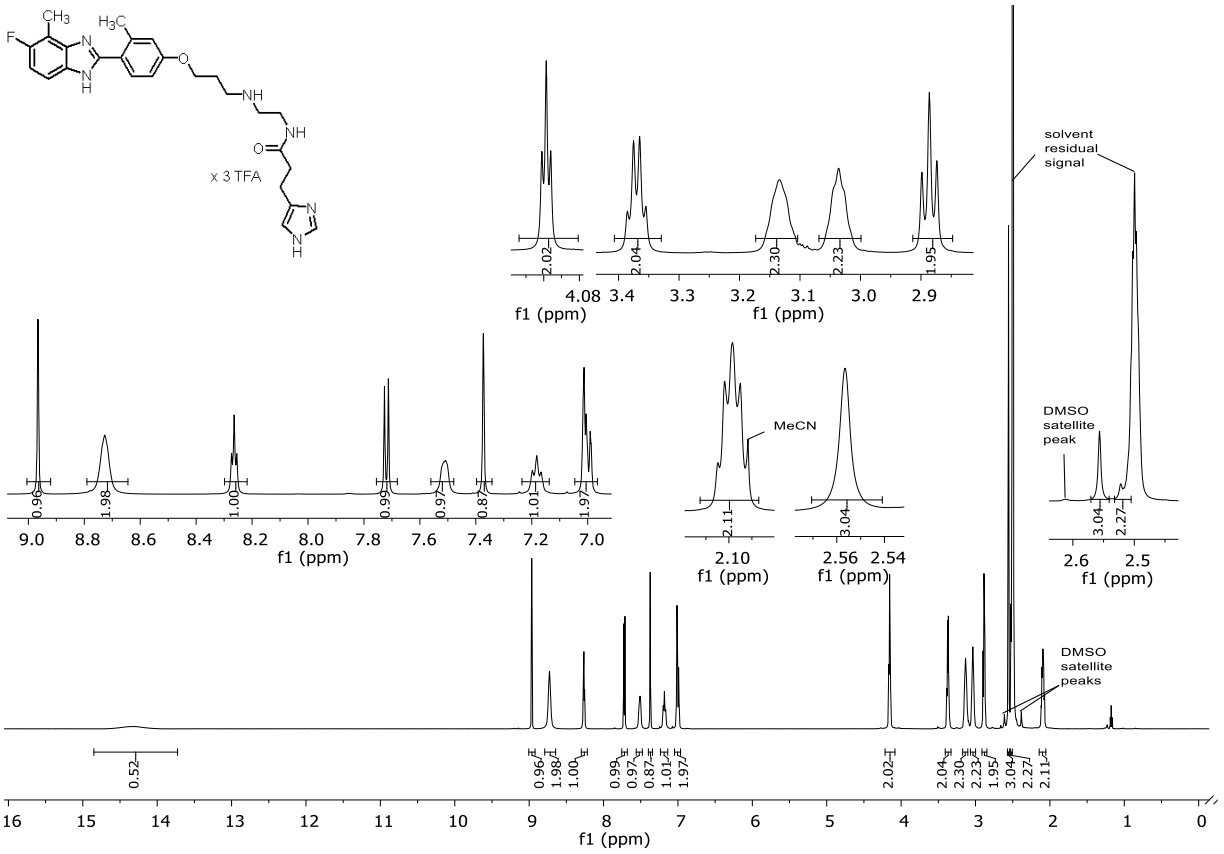

Figure App3.12. ^{1}H-NMR spectrum (600 MHz, DMSO-d_6) of compound **4.87**.

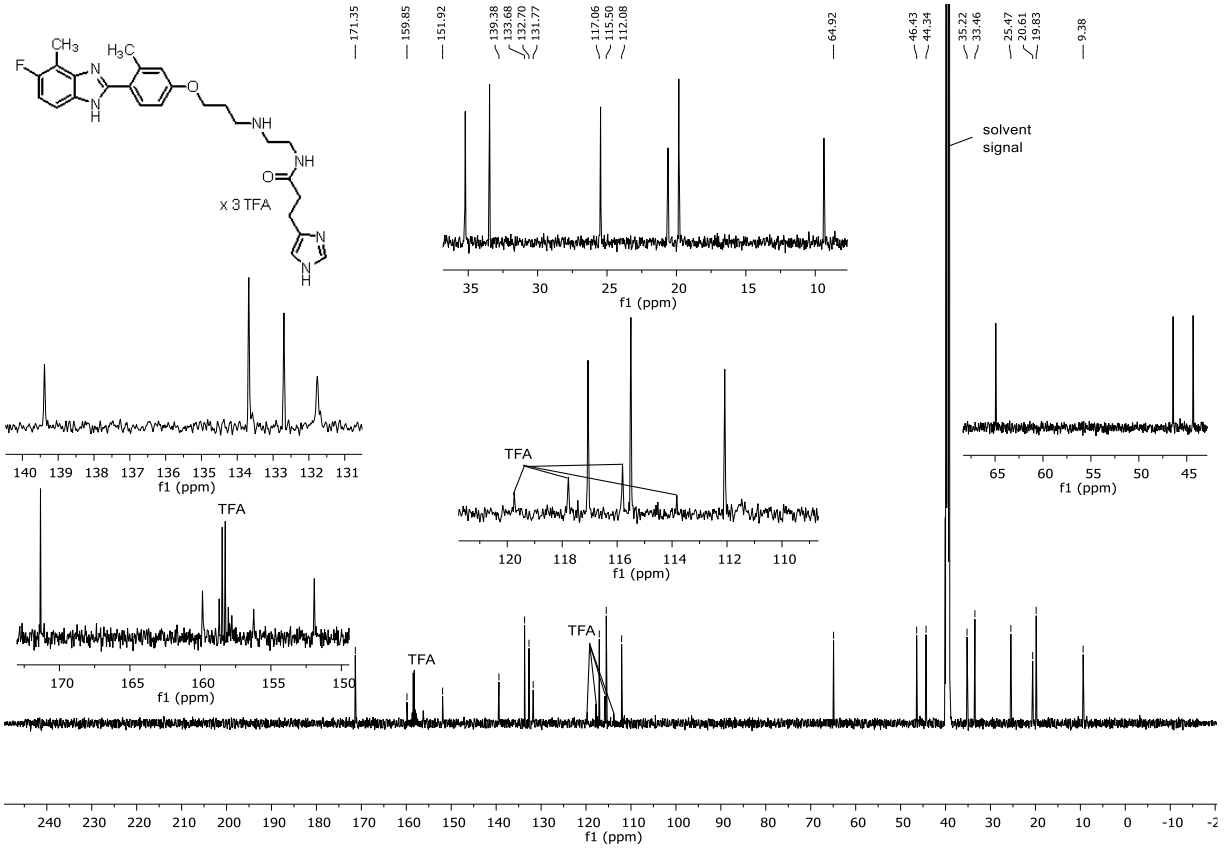

Figure App3.13. ^{13}C-NMR spectrum (151 MHz, DMSO-d_6) of compound **4.87**.

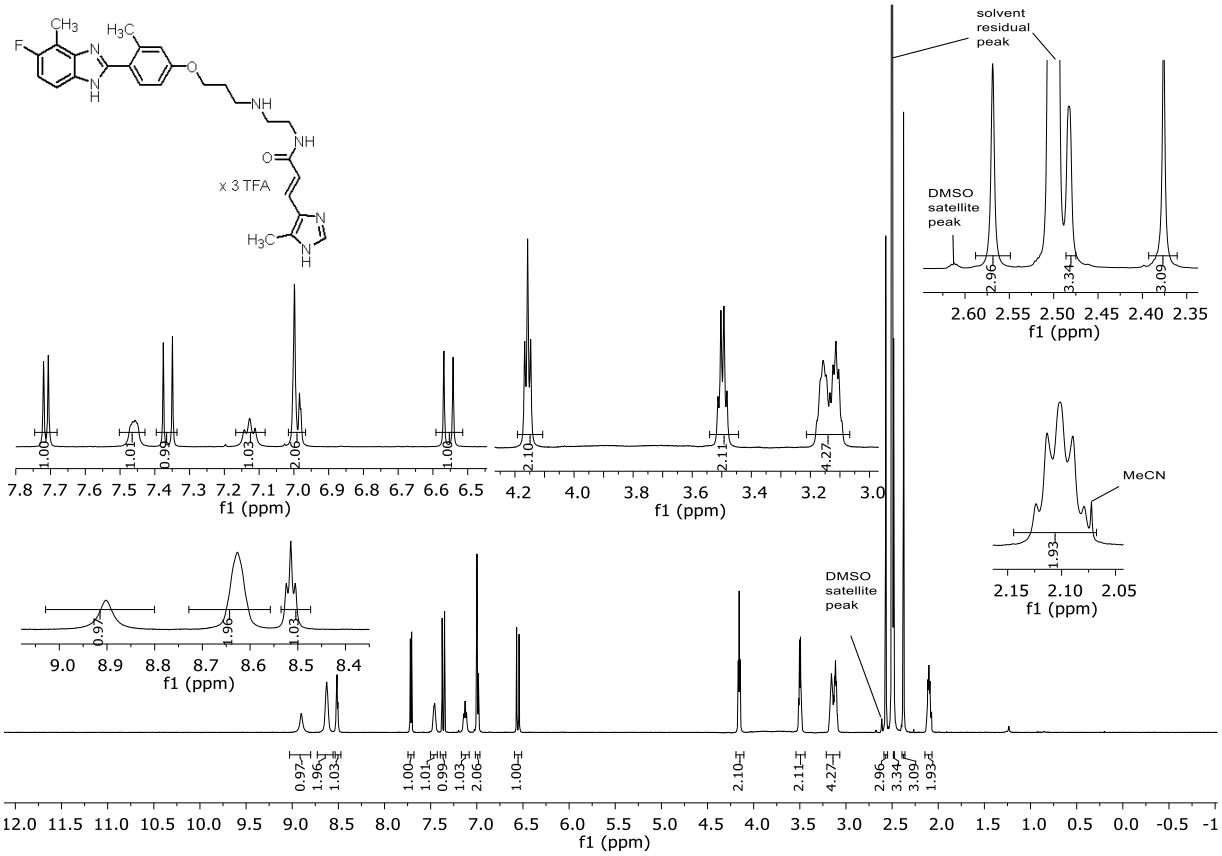

Figure App3.14. ^{1}H-NMR spectrum (600 MHz, DMSO-d_6) of compound **4.88**.

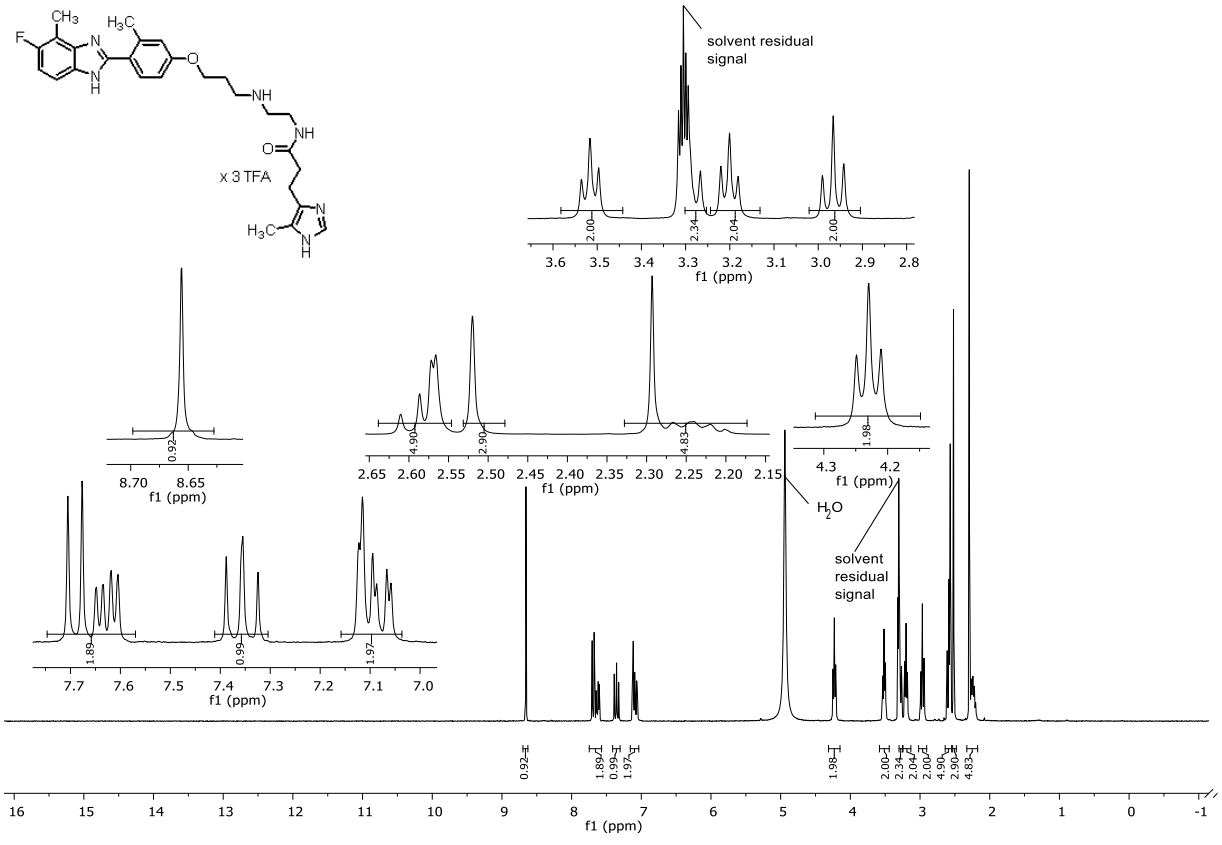

Figure App3.15. ^{1}H-NMR spectrum (300 MHz, MeOD) of compound **4.89**.

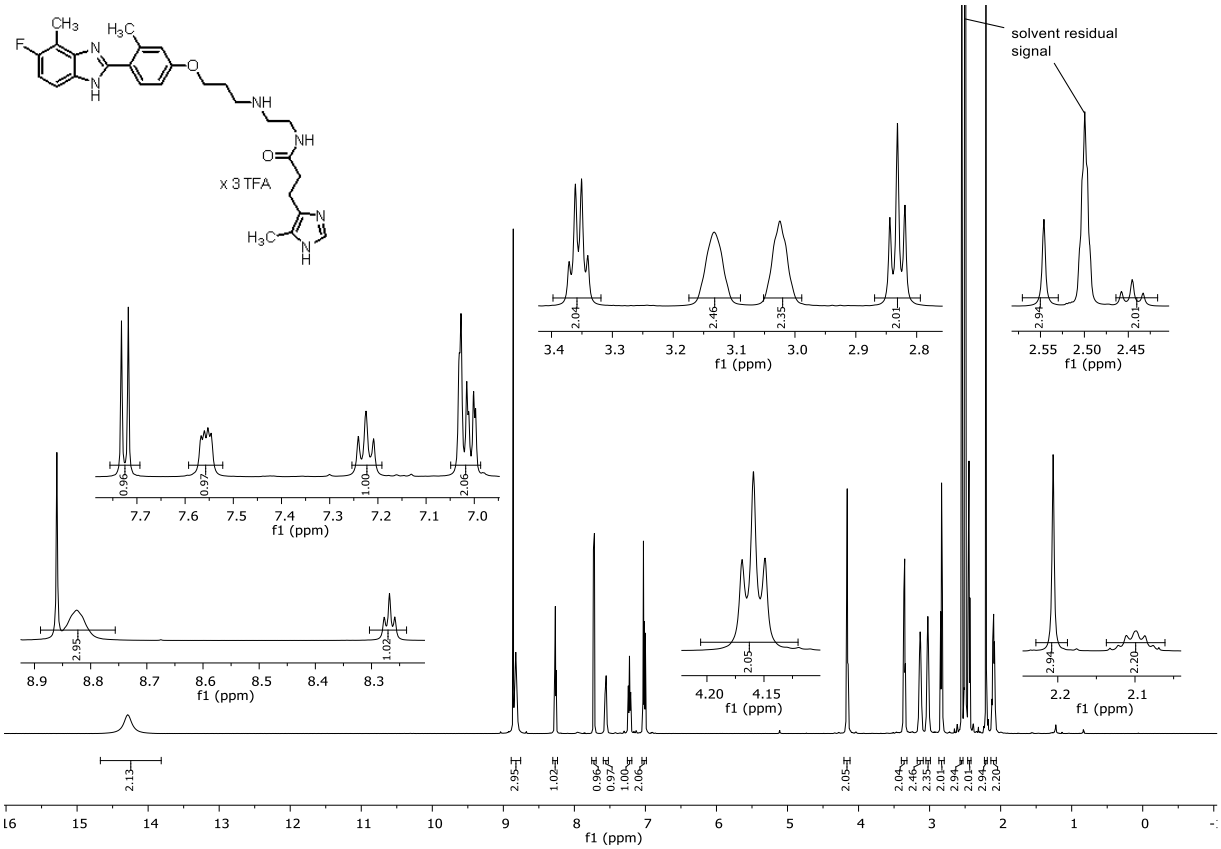

Figure App3.16. ^{1}H-NMR spectrum (600 MHz, DMSO-d_6) of compound **4.89**.

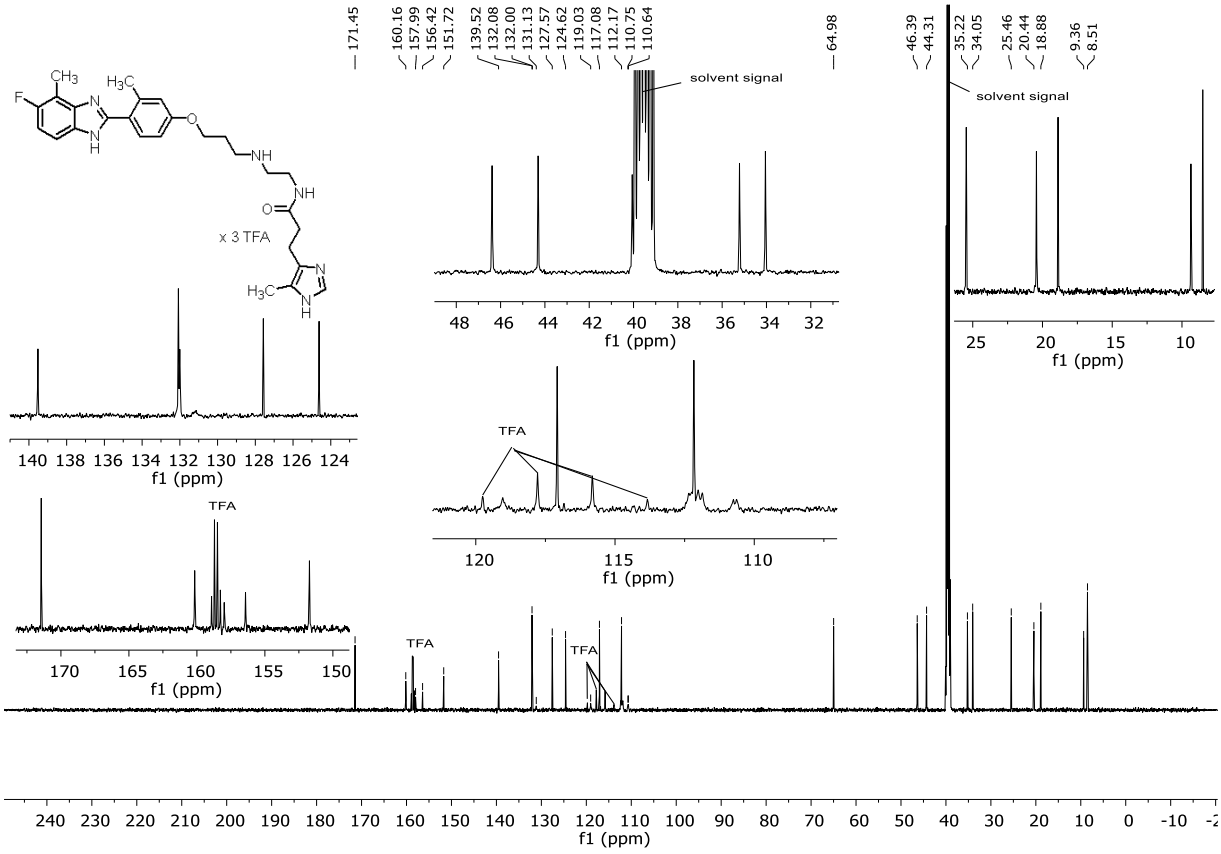

Figure App3.17. ^{13}C-NMR spectrum (151 MHz, DMSO-d_6) of compound **4.89**.

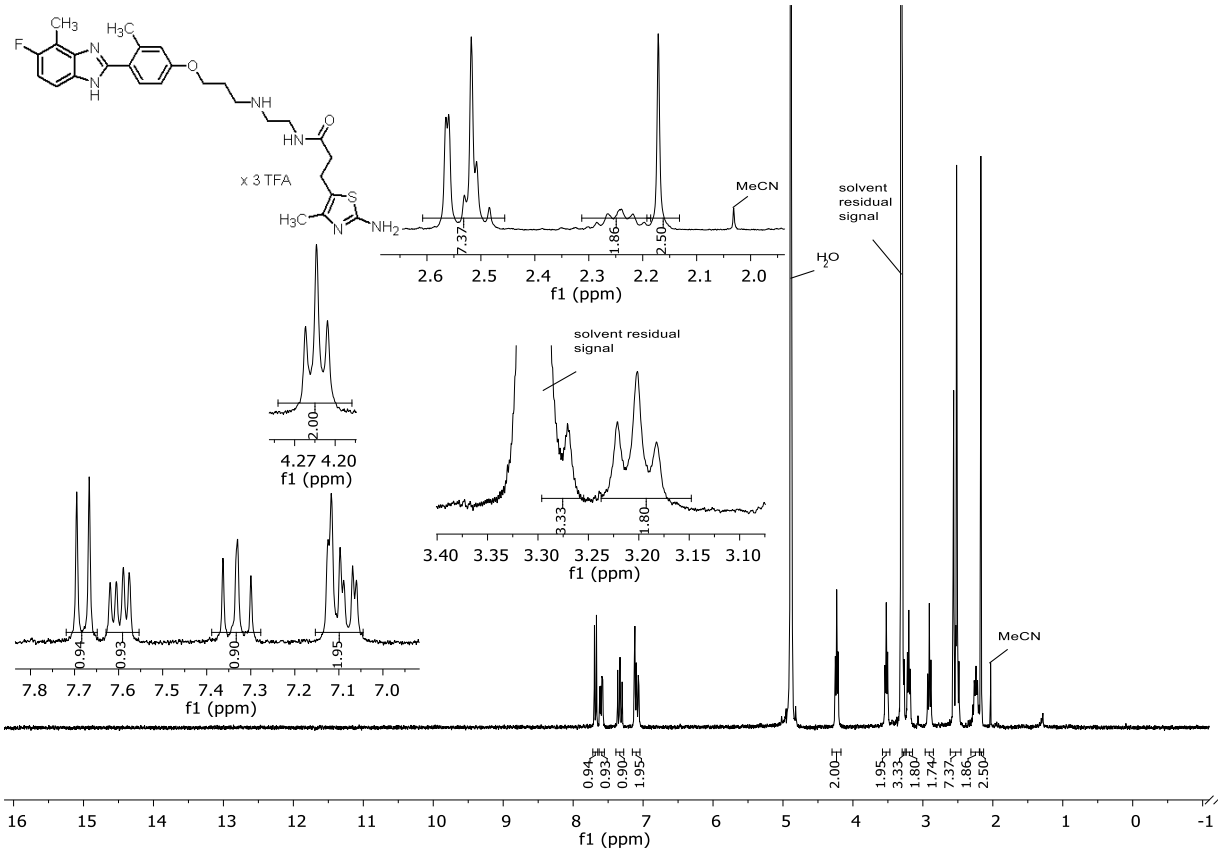

Figure App3.18. ^{1}H-NMR spectrum (300 MHz, MeOD) of compound **4.90**.

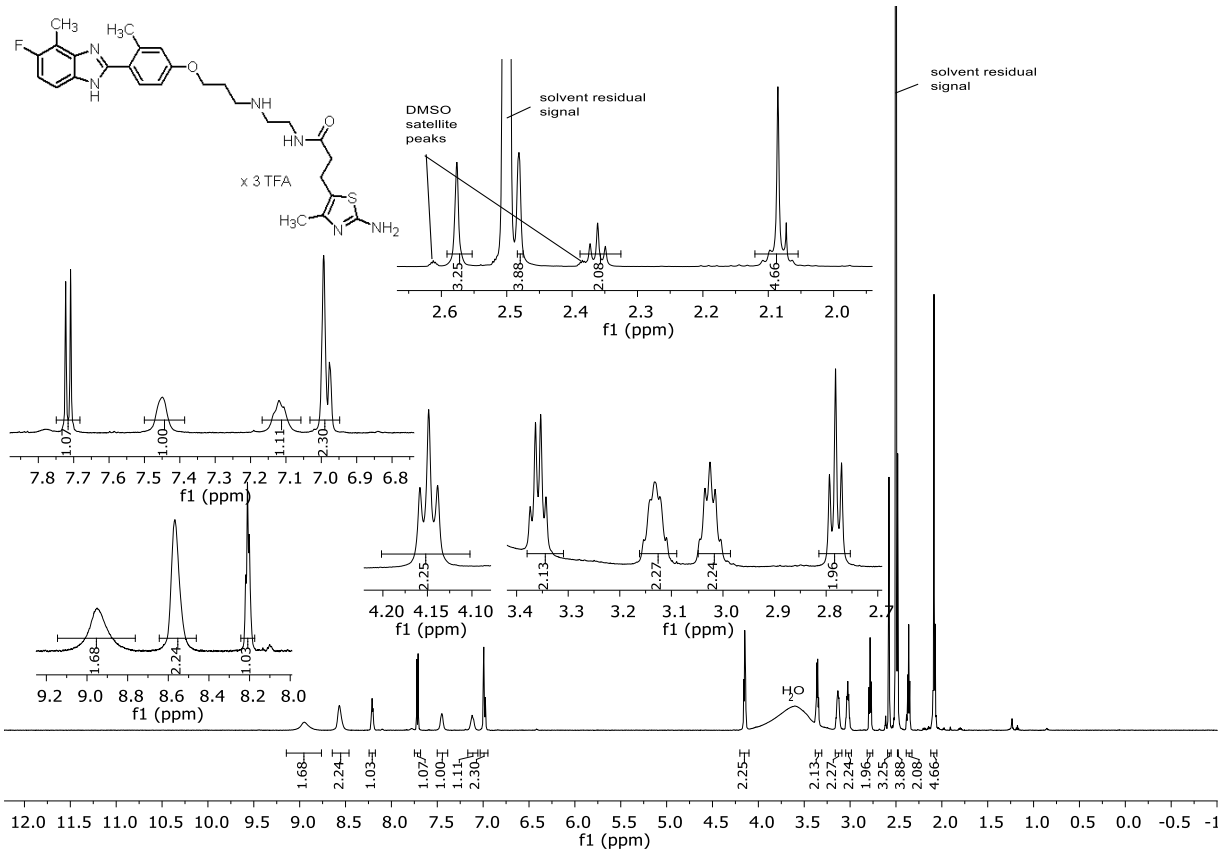

Figure App3.19. ^{1}H-NMR spectrum (600 MHz, DMSO-d_6) of compound **4.90**.

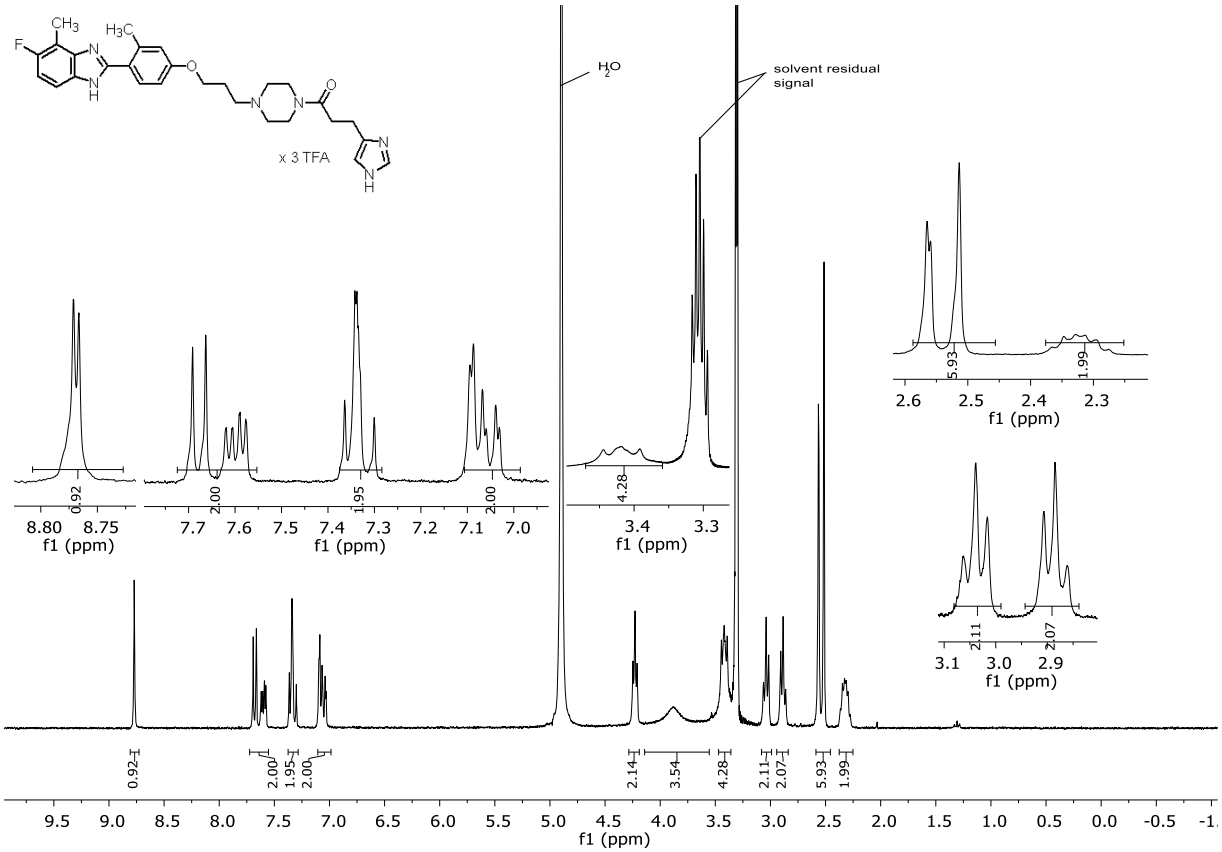

Figure App3.20. ^{1}H-NMR spectrum (300 MHz, MeOD) of compound **4.91**.

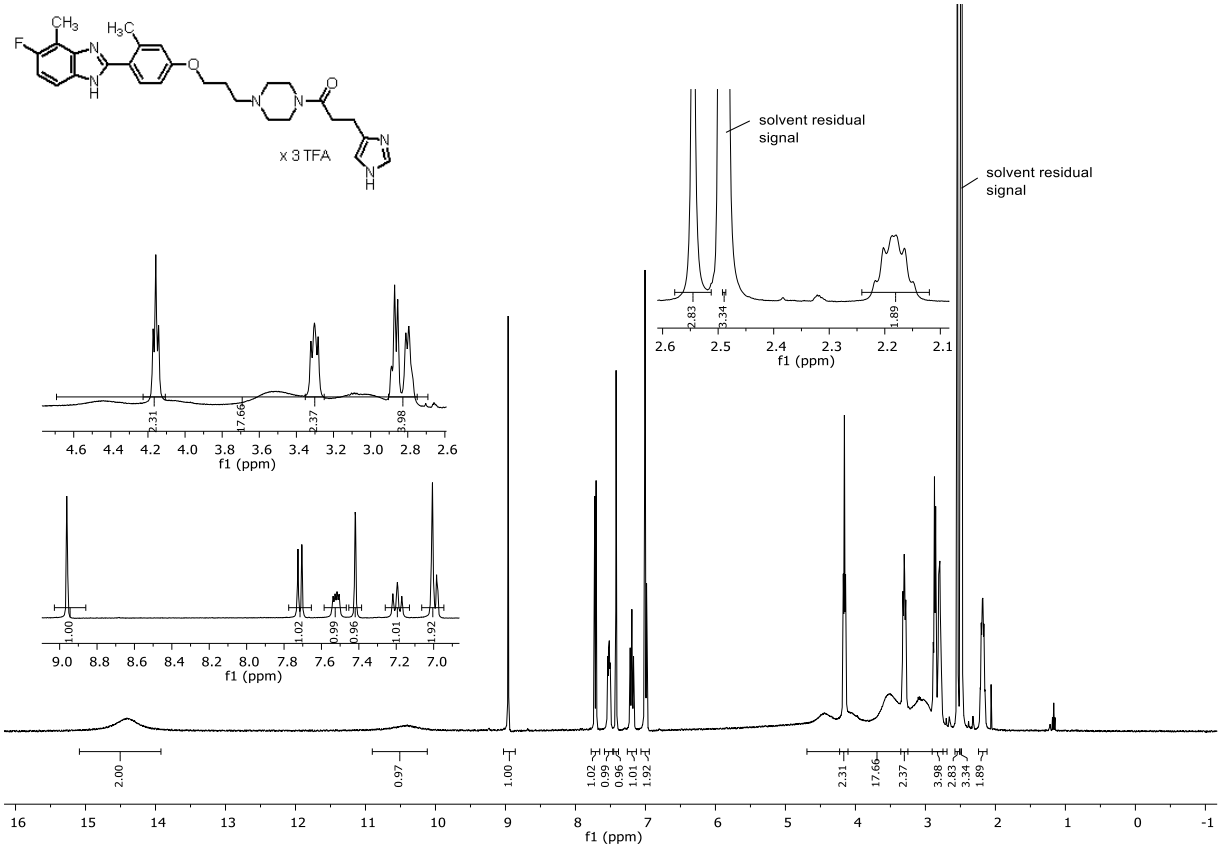

Figure App3.21. ^{1}H-NMR spectrum (400 MHz, DMSO-d_6) of compound **4.91**.

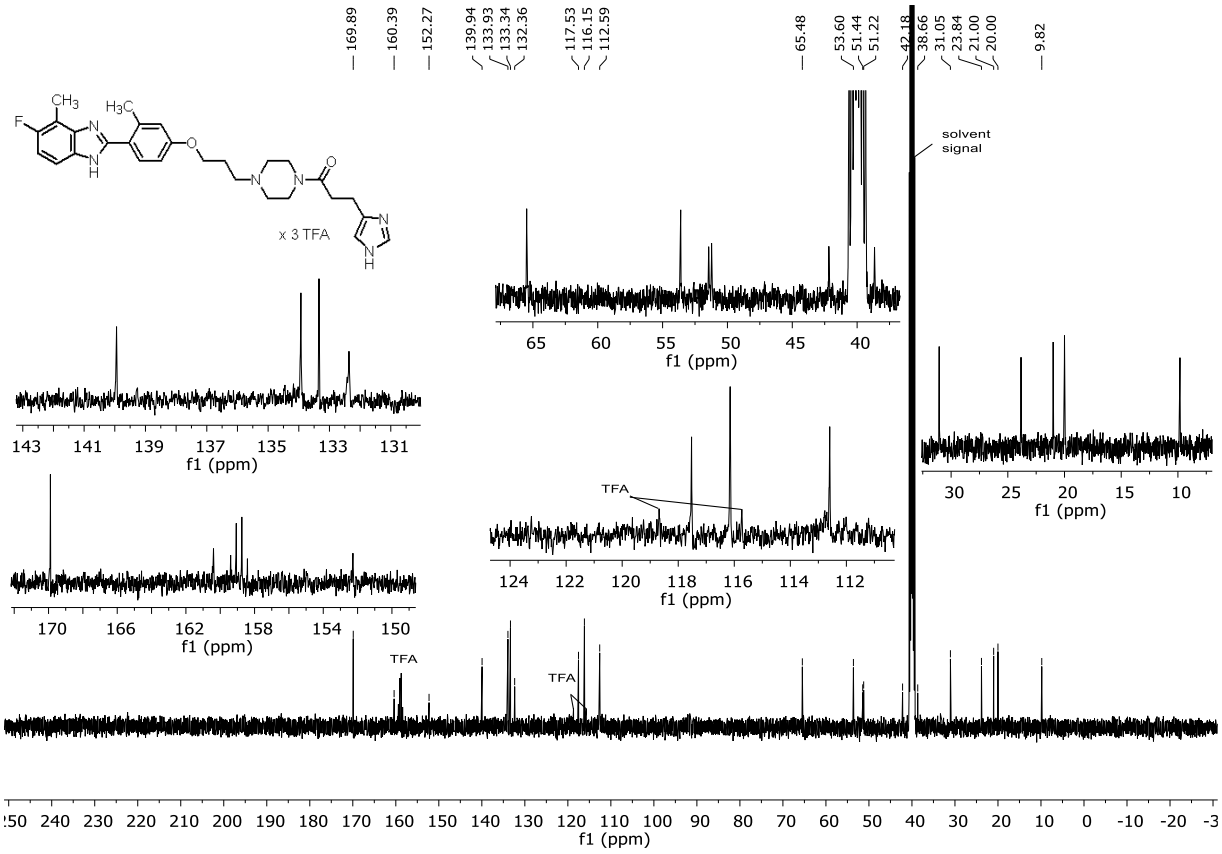

Figure App3.22. ^{13}C-NMR spectrum (101 MHz, DMSO-d_6) of compound **4.91**.

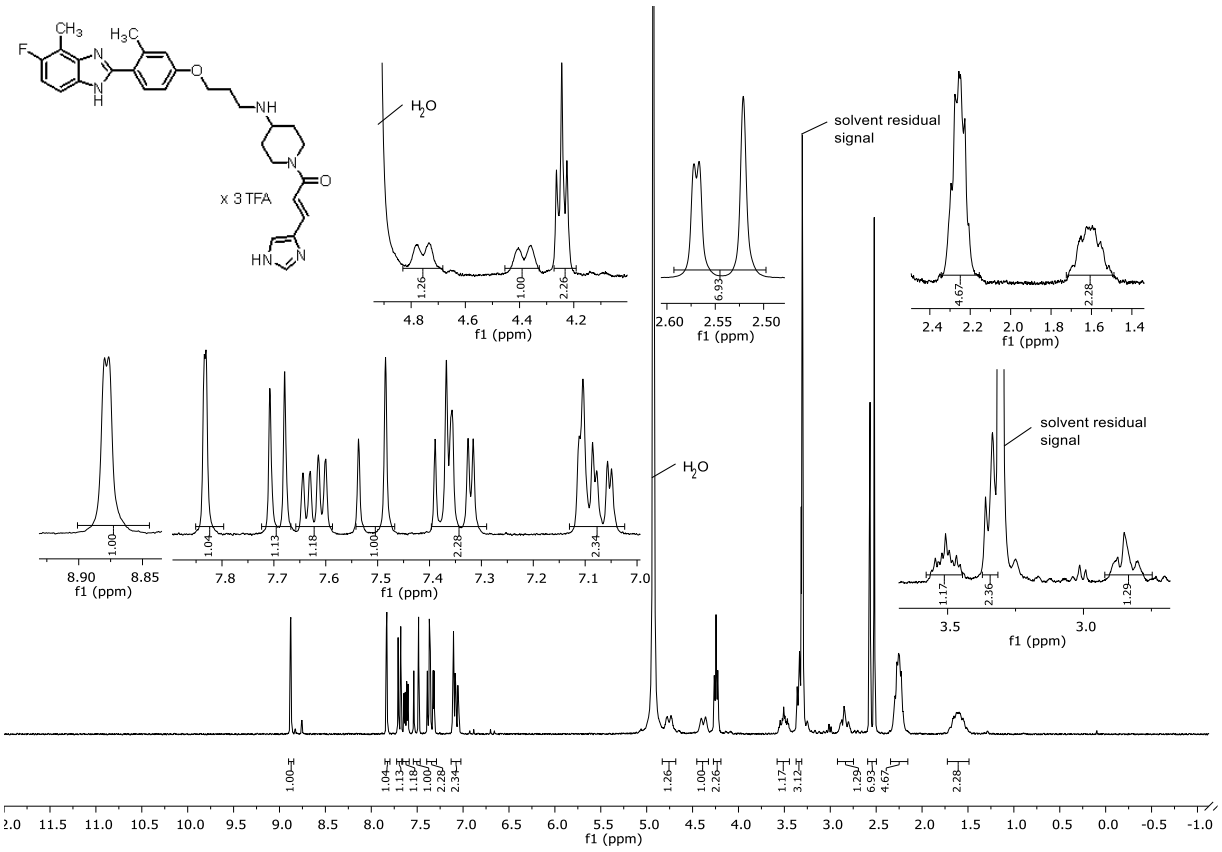

Figure App3.23. ^{1}H-NMR spectrum (300 MHz, MeOD) of compound **4.92**.

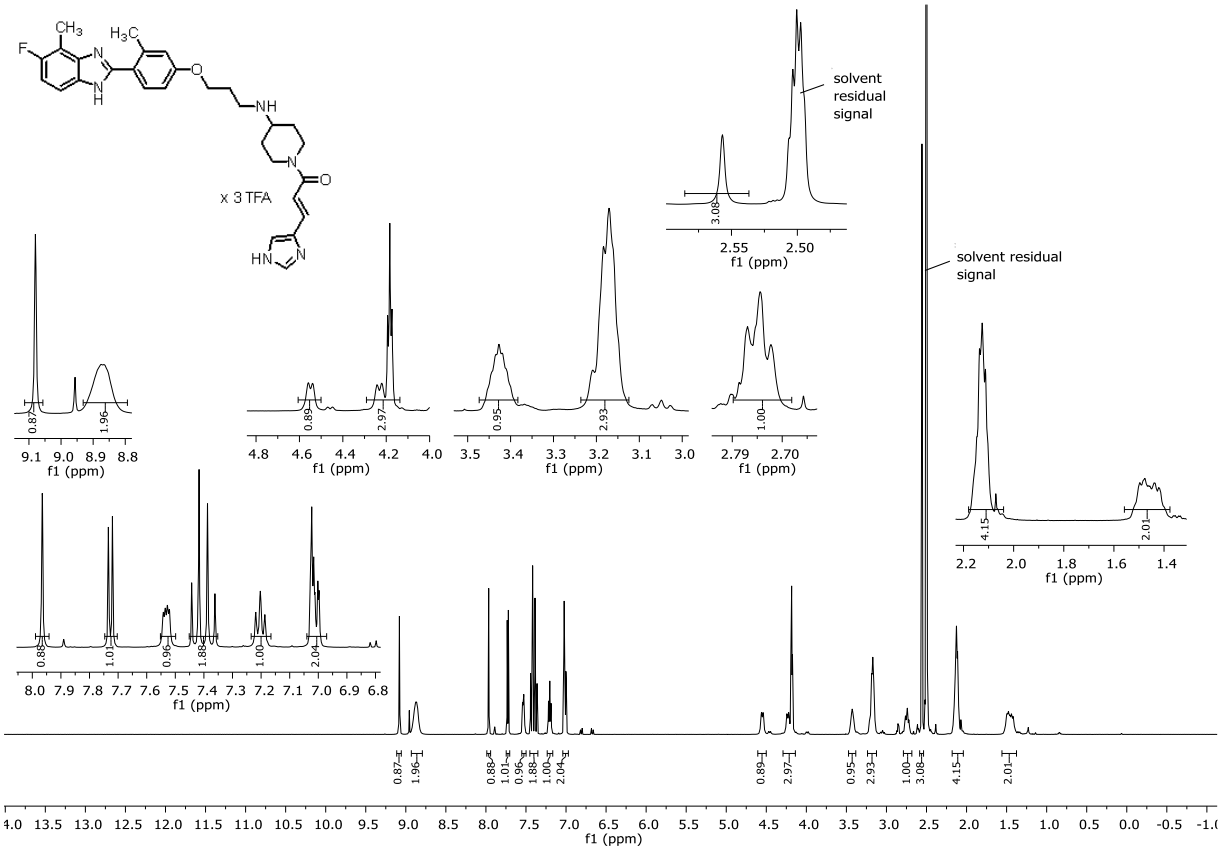

Figure App3.24. ^{1}H-NMR spectrum (600 MHz, DMSO-d_6) of compound **4.92**.

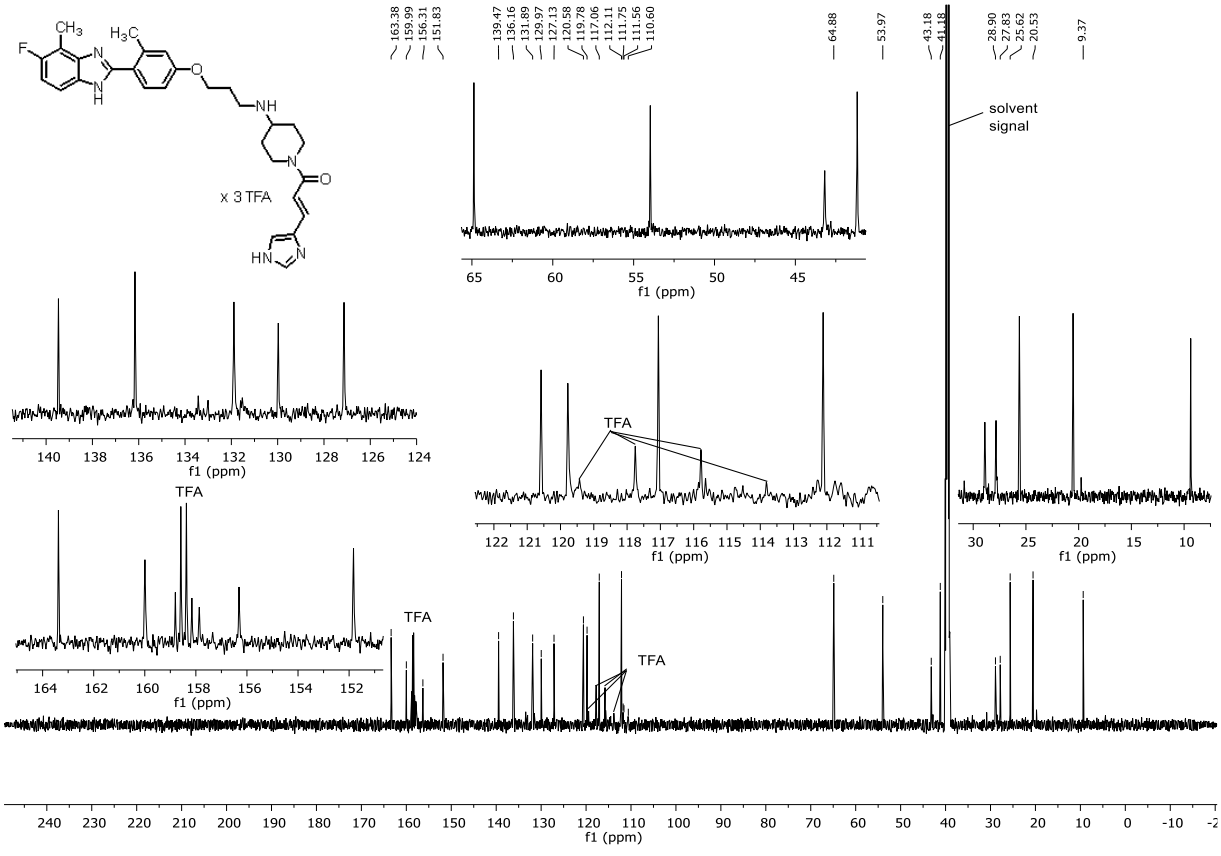

Figure App3.25. ^{1}H-NMR spectrum (151 MHz, DMSO-d_6) of compound **4.92**.

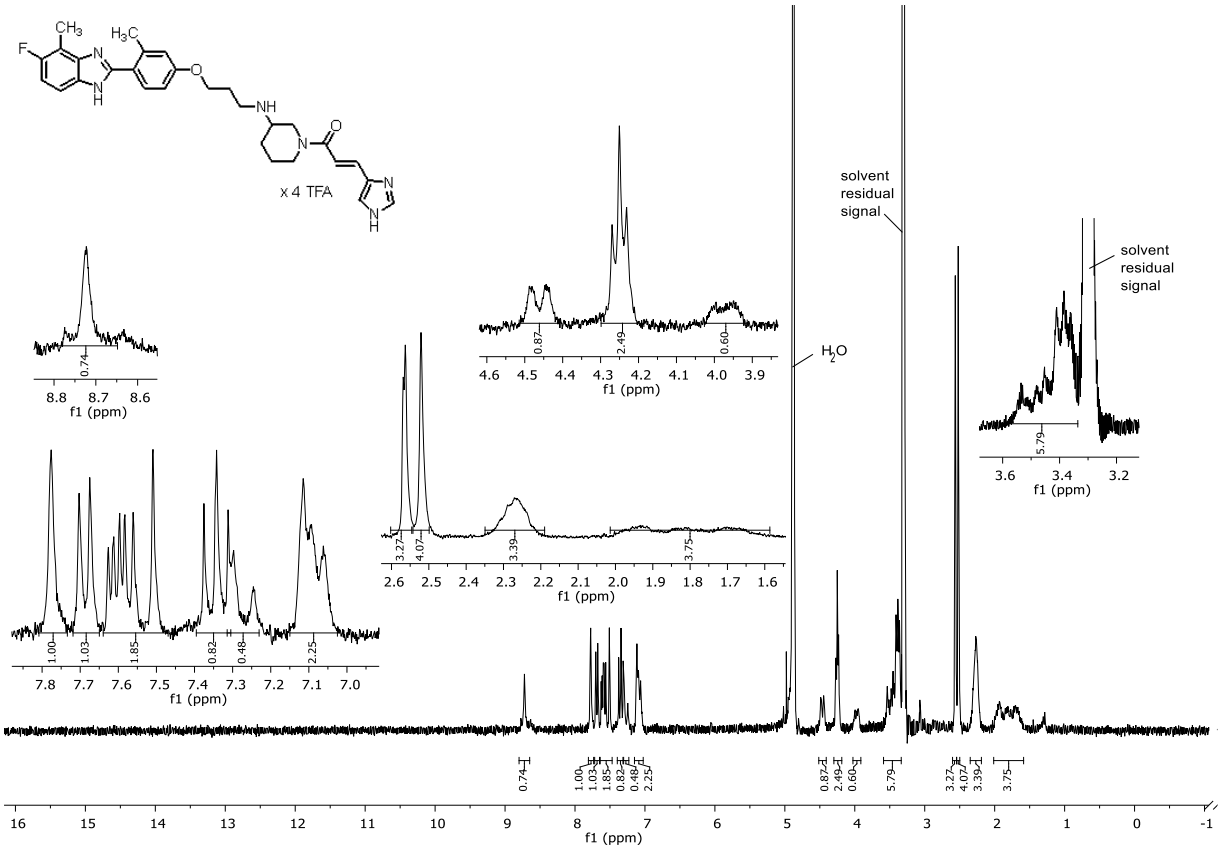

Figure App3.26. ^{1}H-NMR spectrum (300 MHz, MeOD) of compound **4.93**.

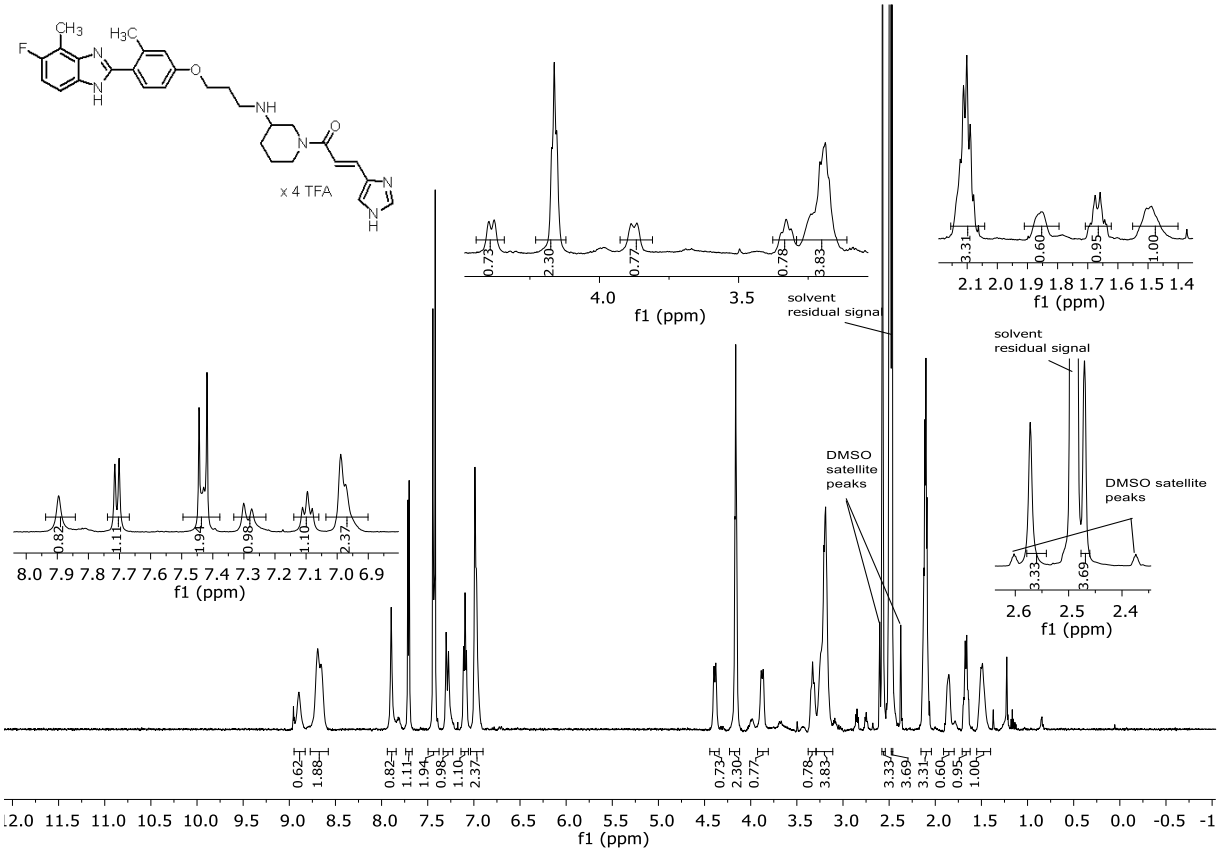

Figure App3.27. ^{1}H-NMR spectrum (600 MHz, DMSO-d_6) of compound **4.93**.

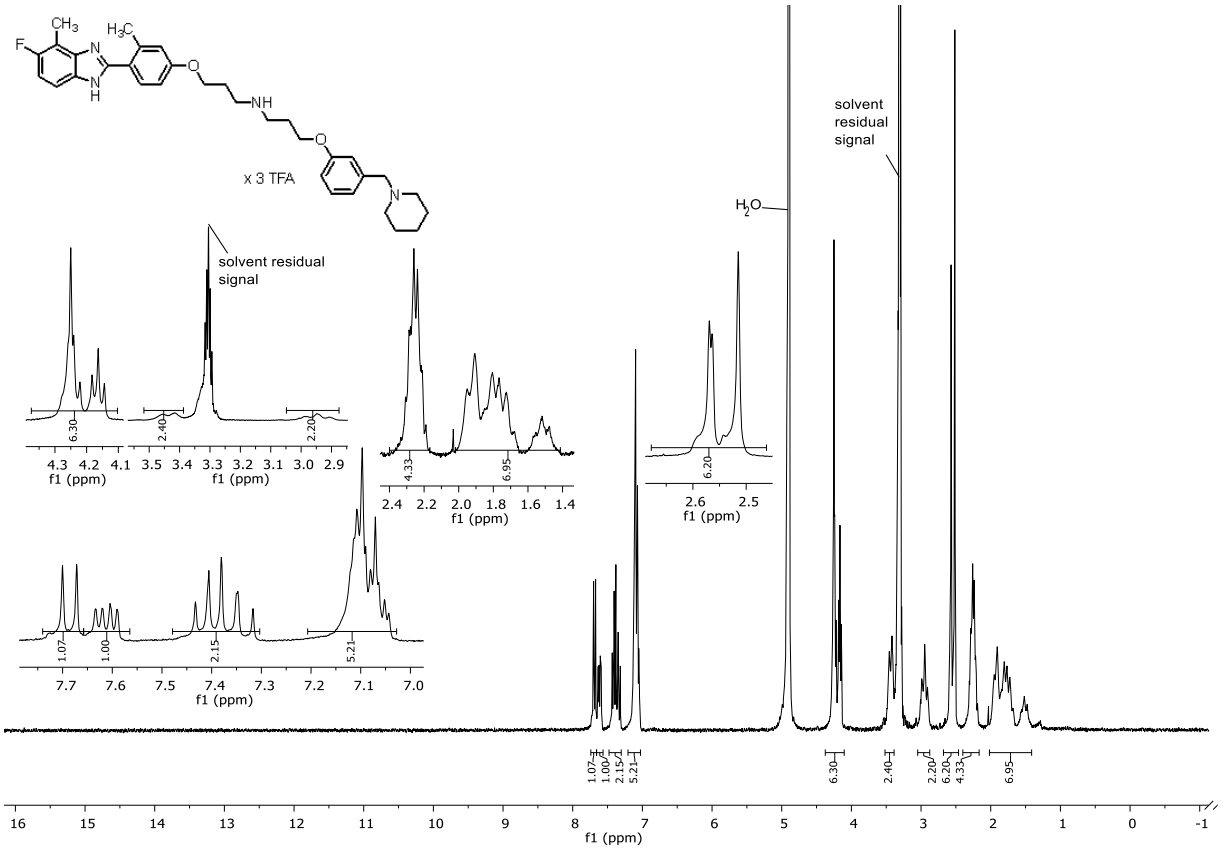

Figure App3.28. ^{1}H-NMR spectrum (300 MHz, MeOD) of compound **4.94**.

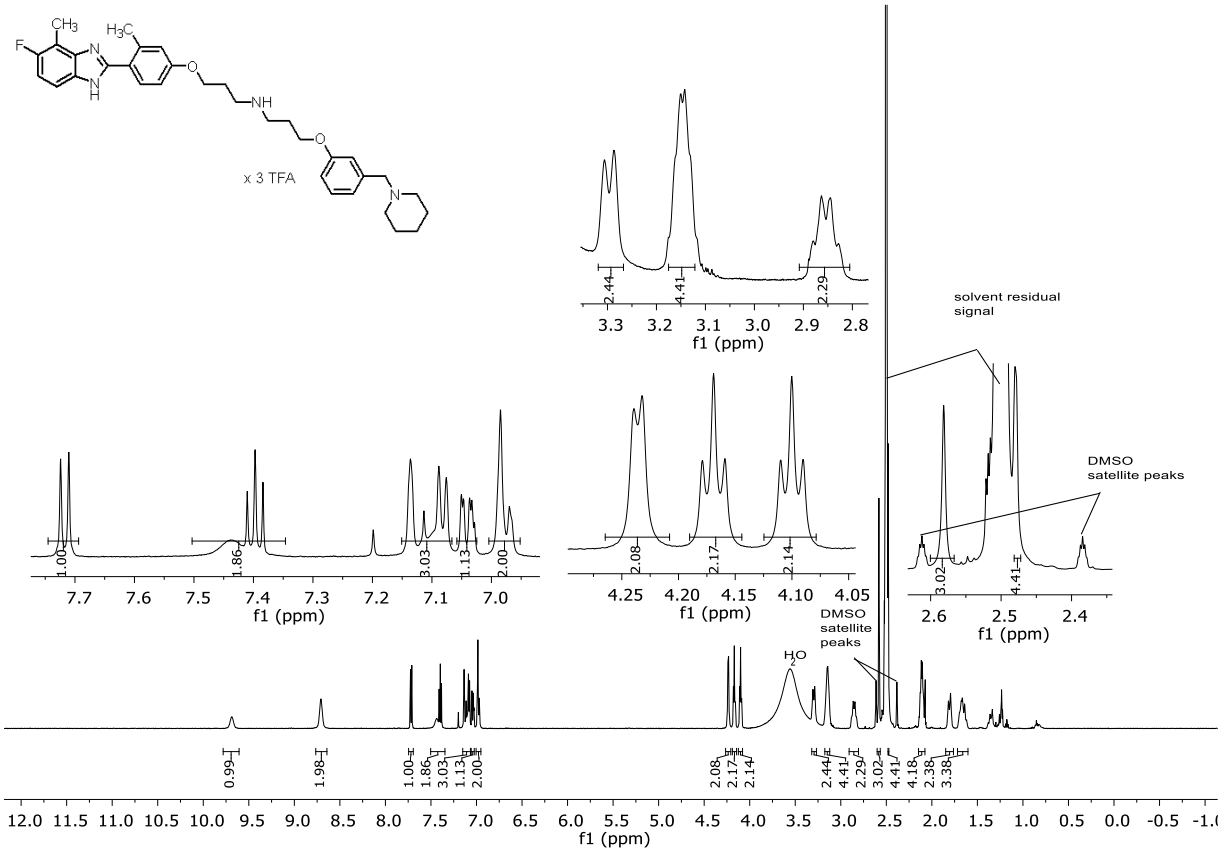

Figure App3.29. ^{1}H-NMR spectrum (600 MHz, DMSO-d_6) of compound **4.94**.

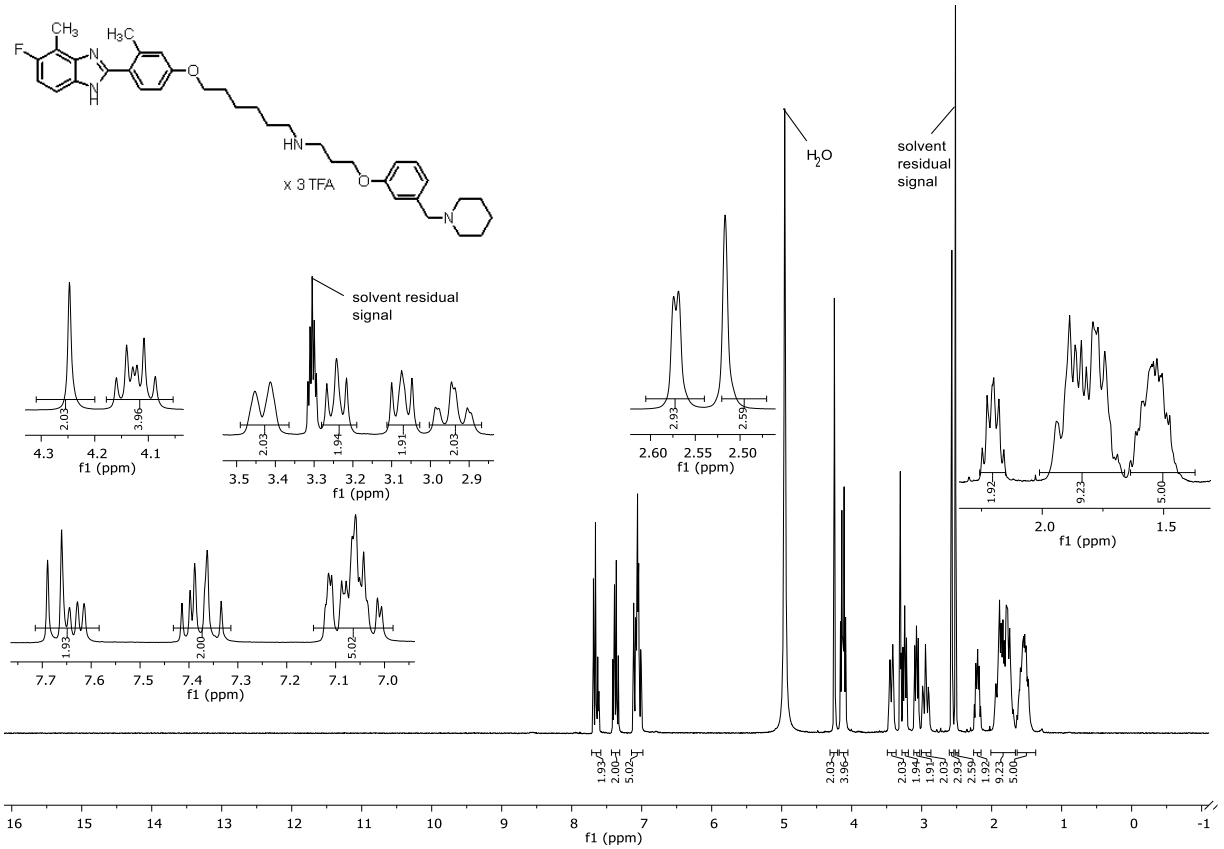

Figure App3.30. ^{1}H-NMR spectrum (300 MHz, MeOD) of compound **4.95**.

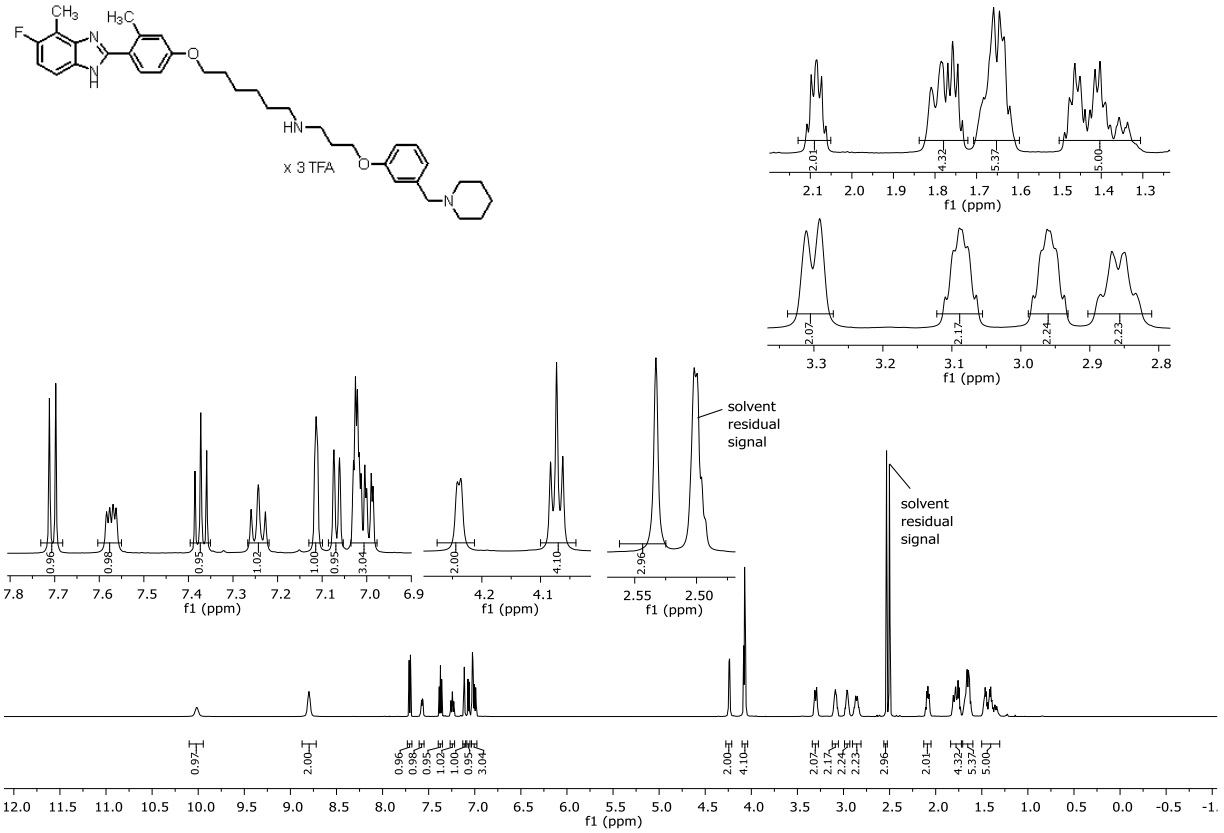

Figure App3.31. ^{1}H-NMR spectrum (600 MHz, DMSO-d_6) of compound **4.95**.

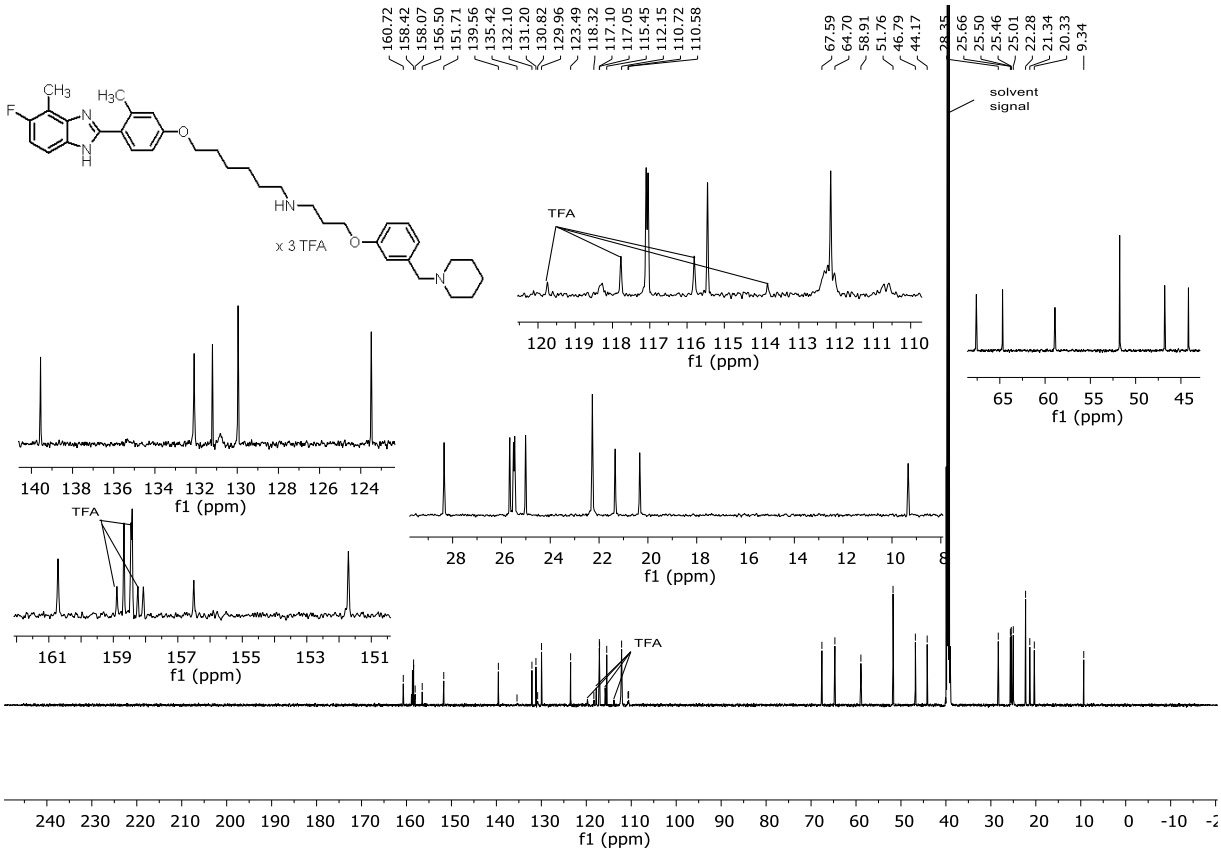

Figure App3.32. ^{13}C-NMR spectrum (151 MHz, DMSO-d_6) of compound **4.95**.

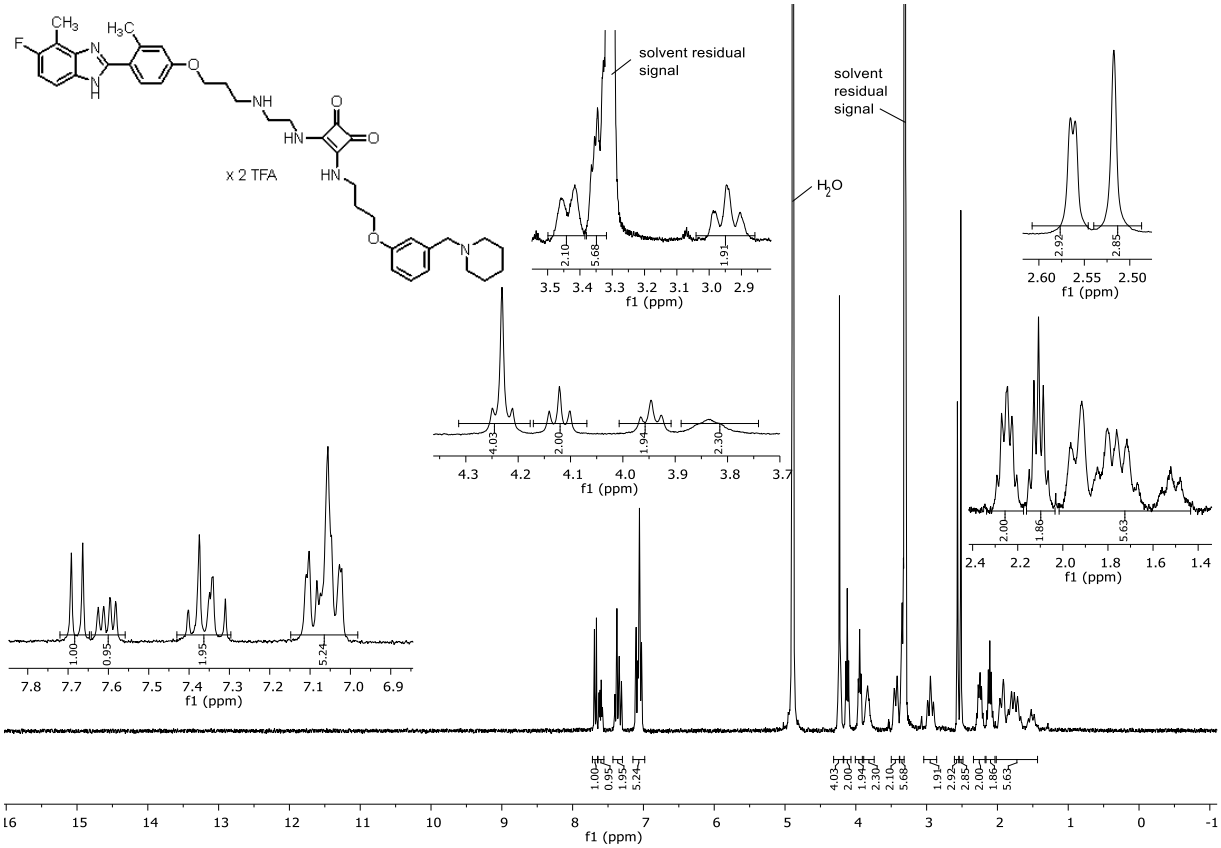

Figure App3.33. ^{1}H-NMR spectrum (300 MHz, MeOD) of compound **4.96**.

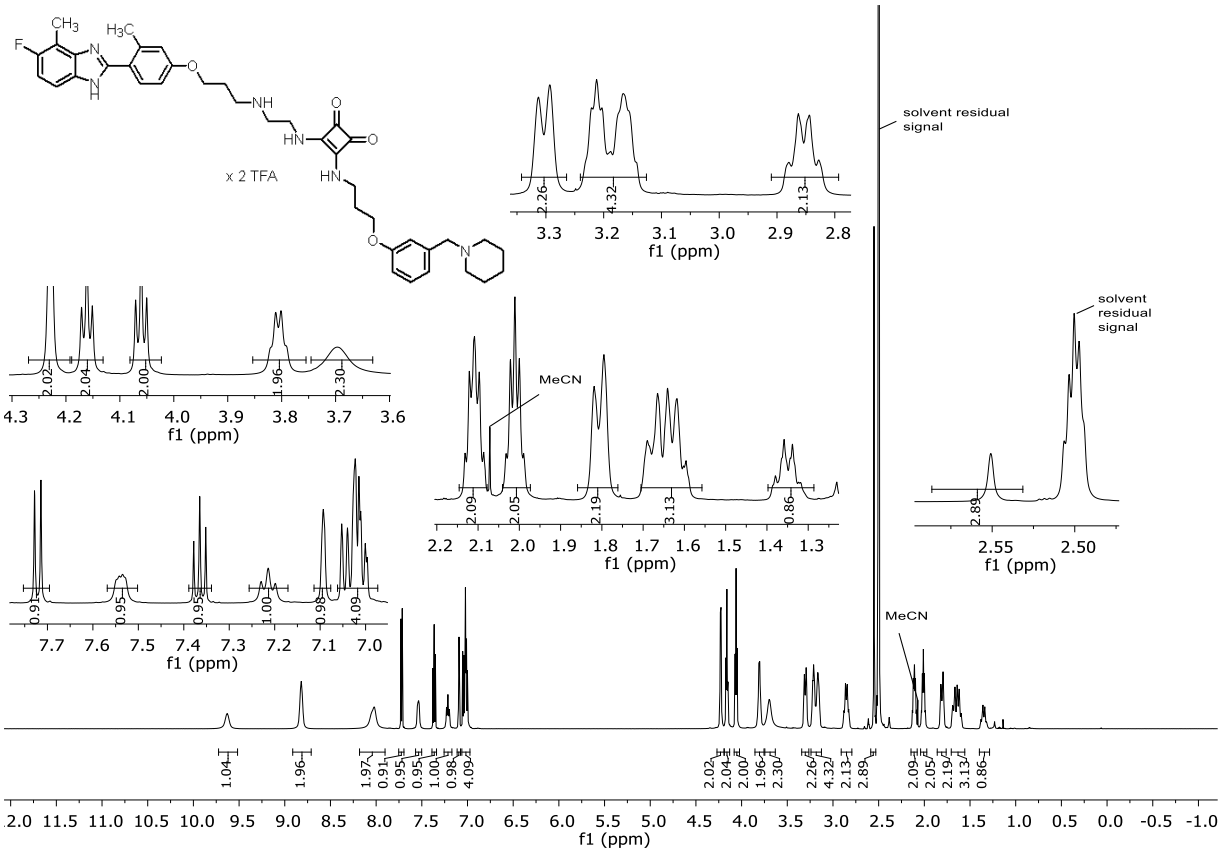

Figure App3.34. ^{1}H-NMR spectrum (600 MHz, DMSO-d_6) of compound **4.96**.

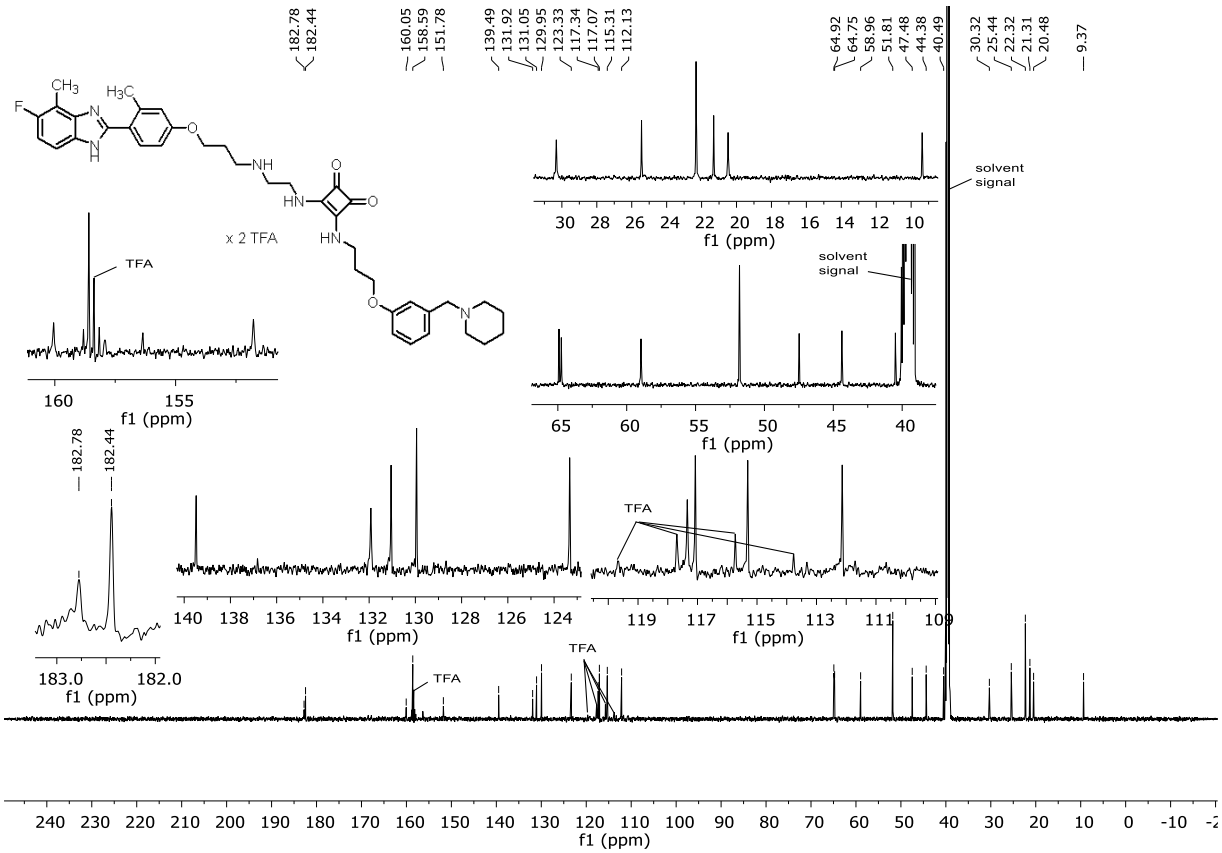

Figure App3.35. ^{13}C-NMR spectrum (151 MHz, DMSO-d_6) of compound **4.95**.

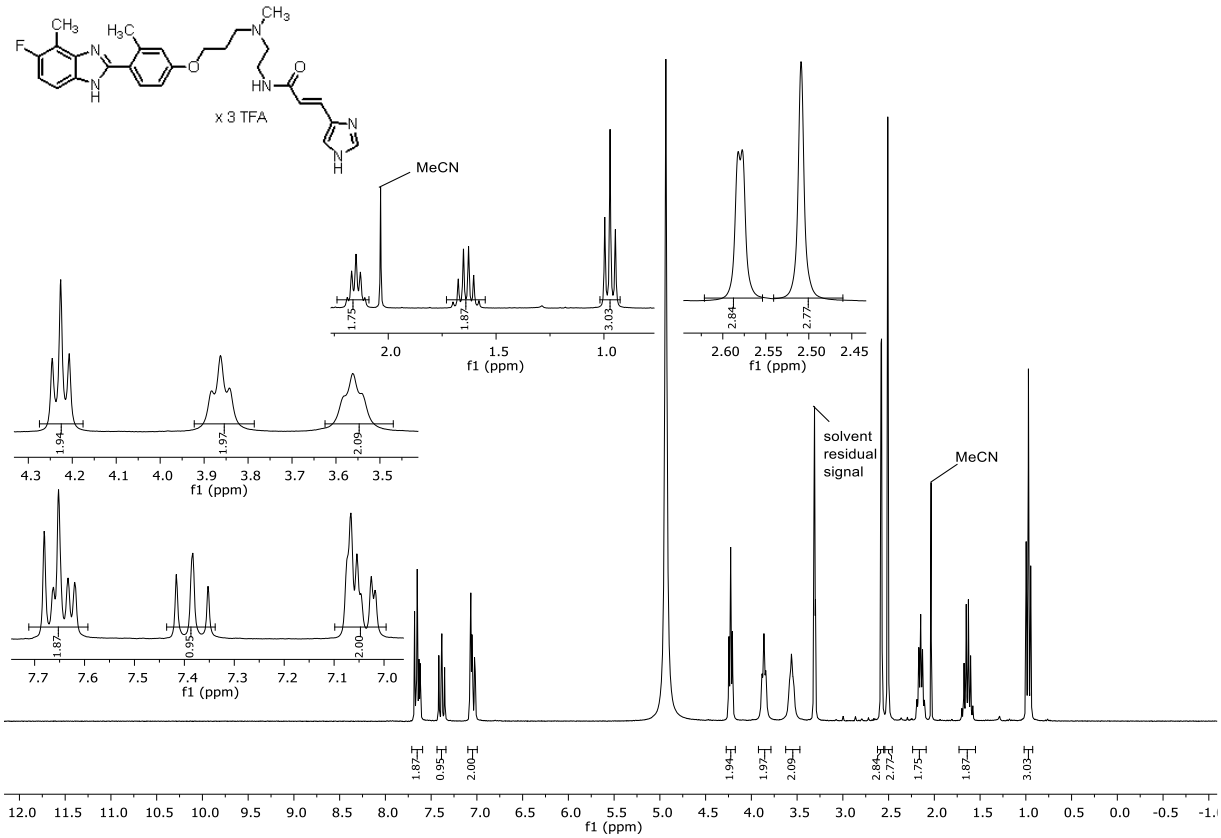

Figure App3.36. ^{1}H-NMR spectrum (300 MHz, MeOD) of compound **4.98**.

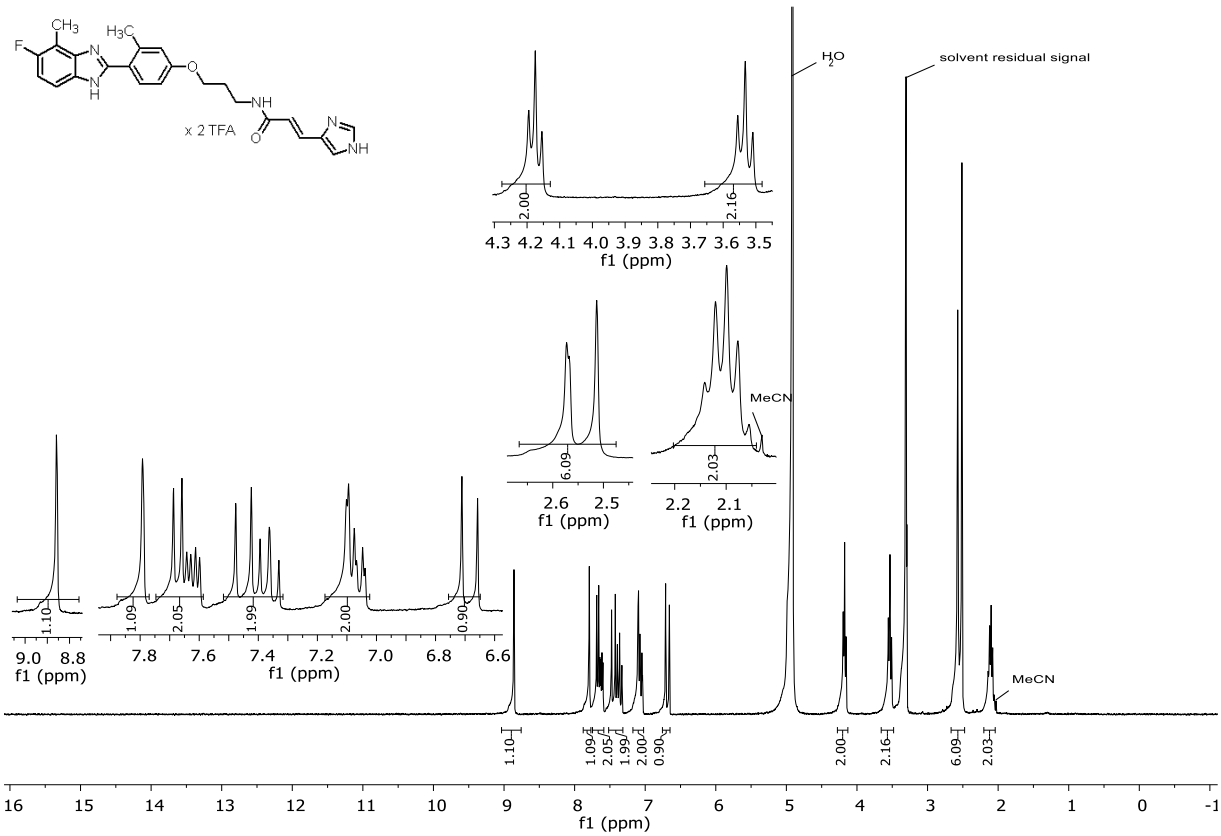

Figure App3.37. ^{1}H-NMR spectrum (300 MHz, MeOD) of compound **4.104**.

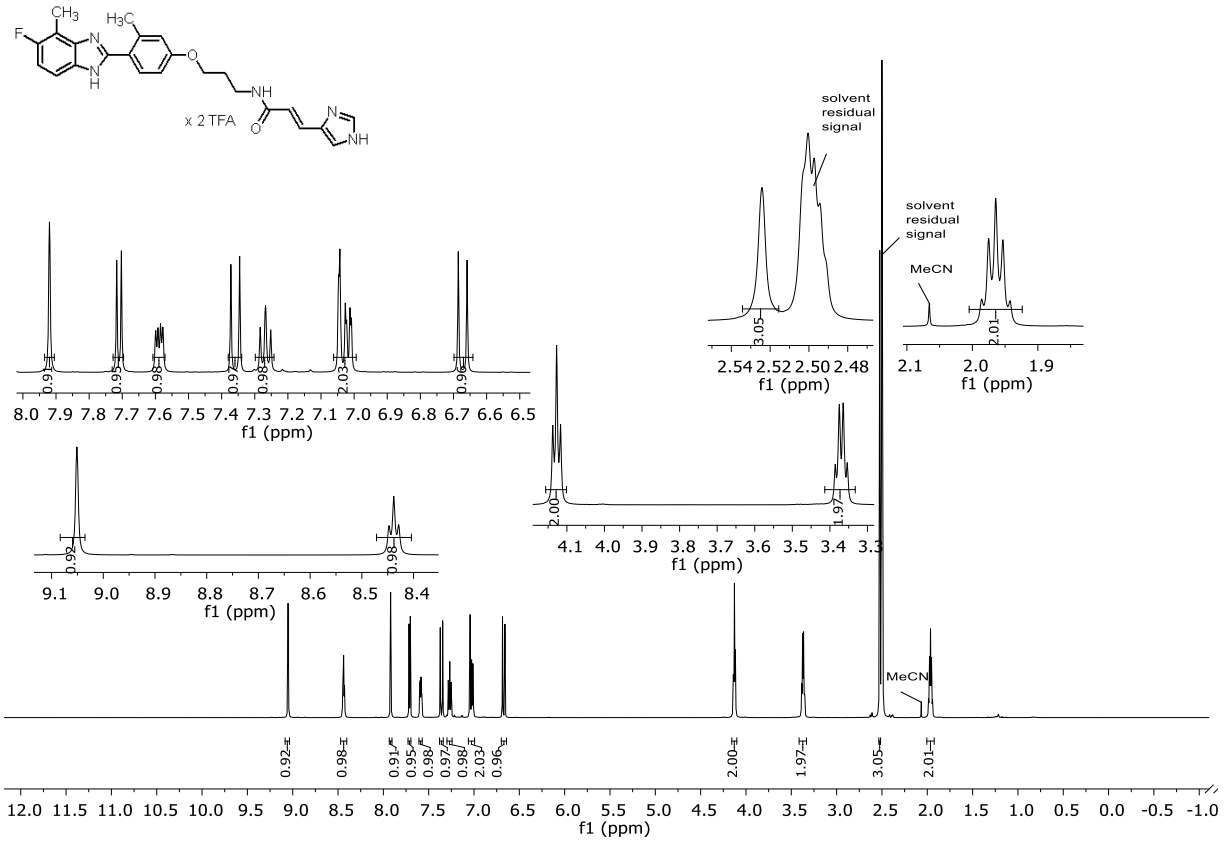

Figure App3.38. ^{1}H-NMR spectrum (600 MHz, DMSO-d_6) of compound **4.104**.

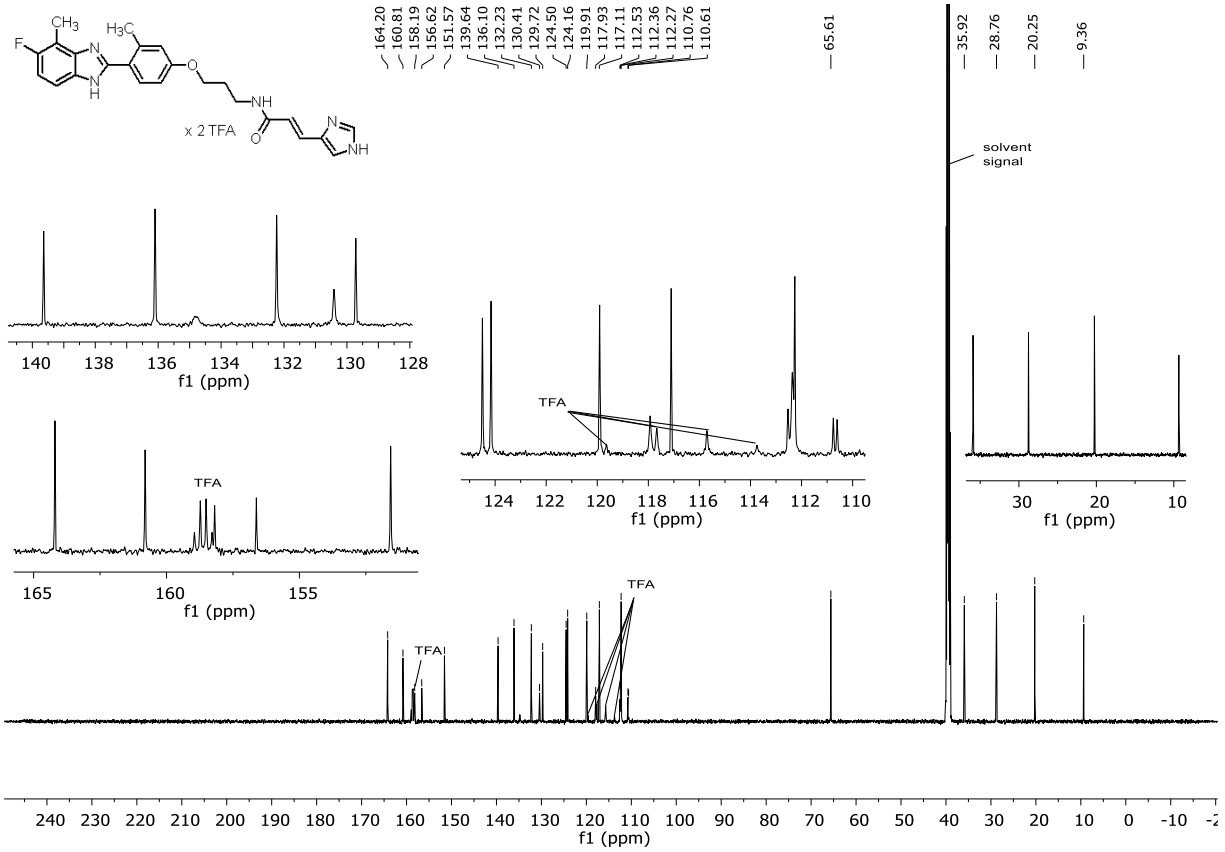

Figure App3.39. ^{13}C-NMR spectrum (151 MHz, DMSO-d_6) of compound **4.104**.

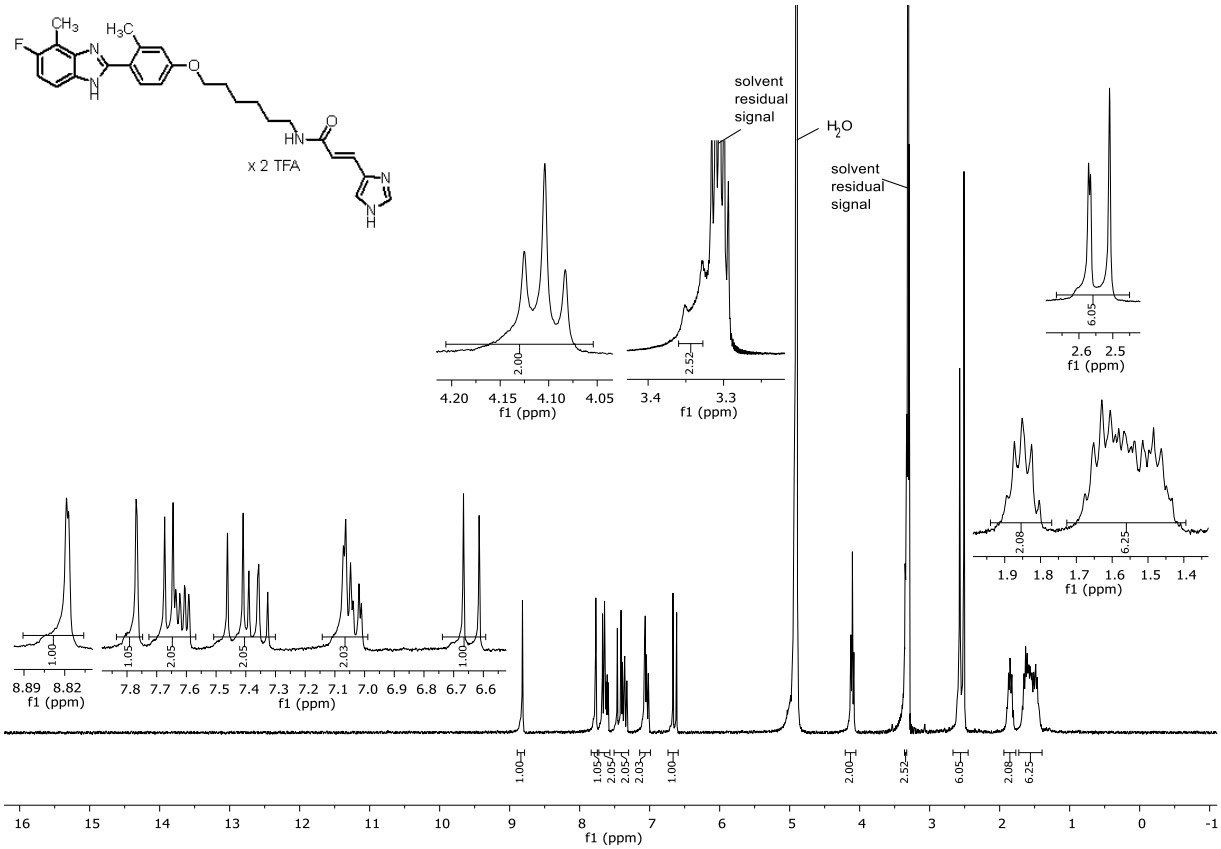

Figure App3.40. ^{1}H-NMR spectrum (300 MHz, MeOD) of compound **4.105**.

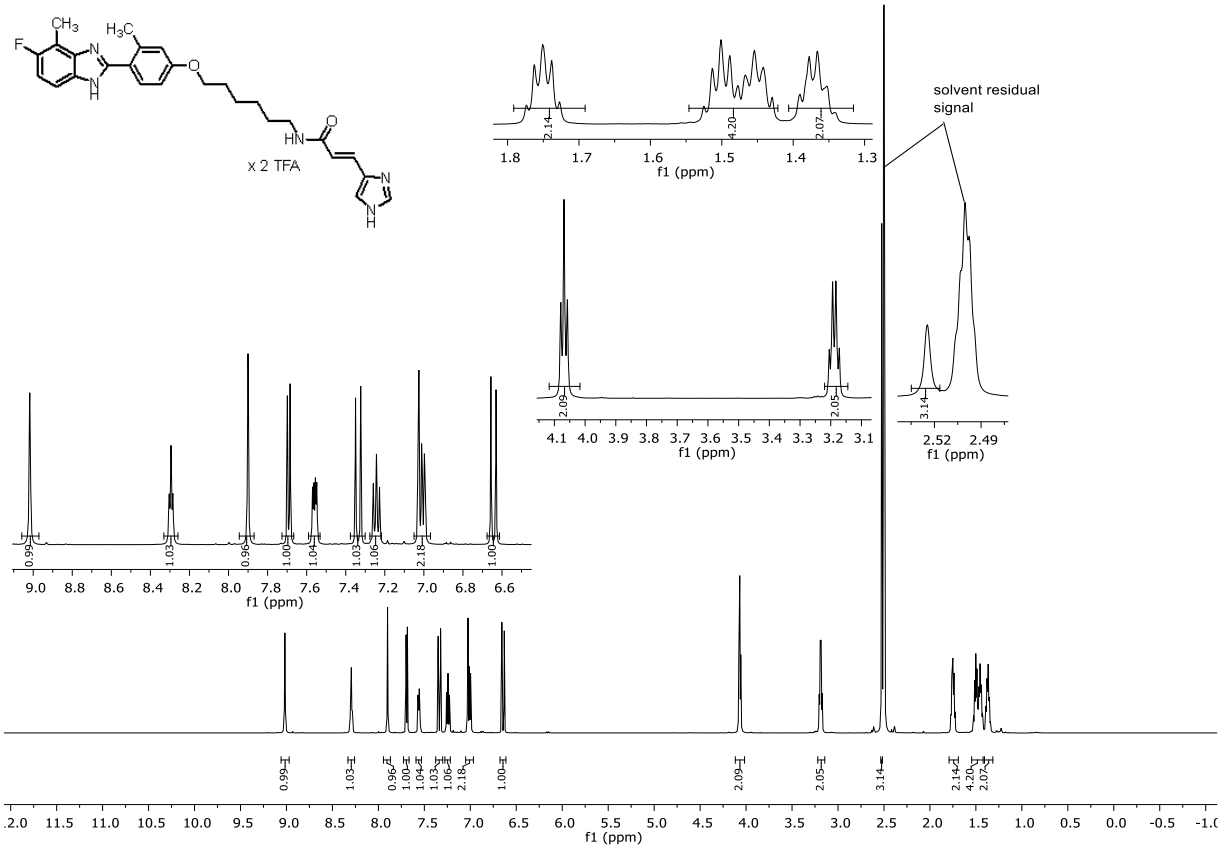

Figure App3.41. ^{1}H-NMR spectrum (600 MHz, DMSO-d_6) of compound **4.105**.

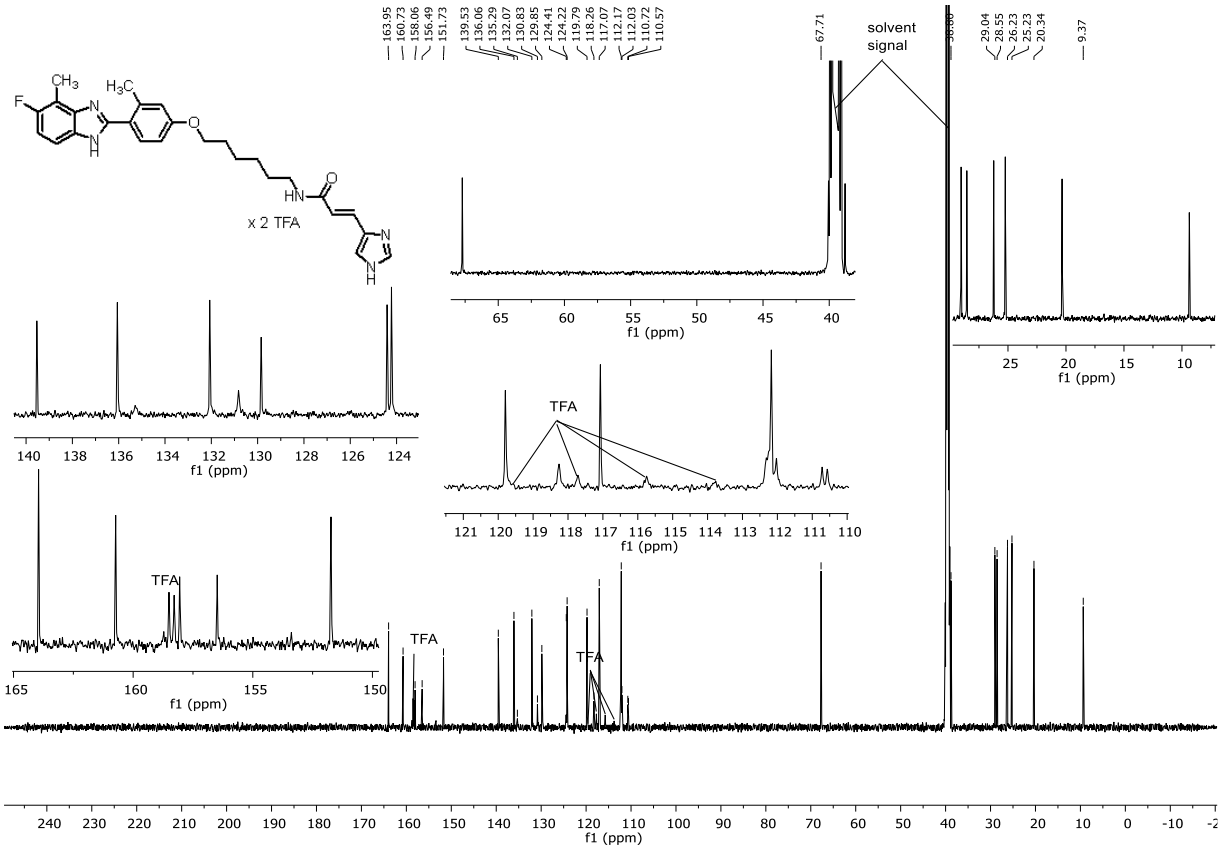

Figure App3.42. ^{13}C-NMR spectrum (151 MHz, DMSO-d_6) of compound **4.105**.

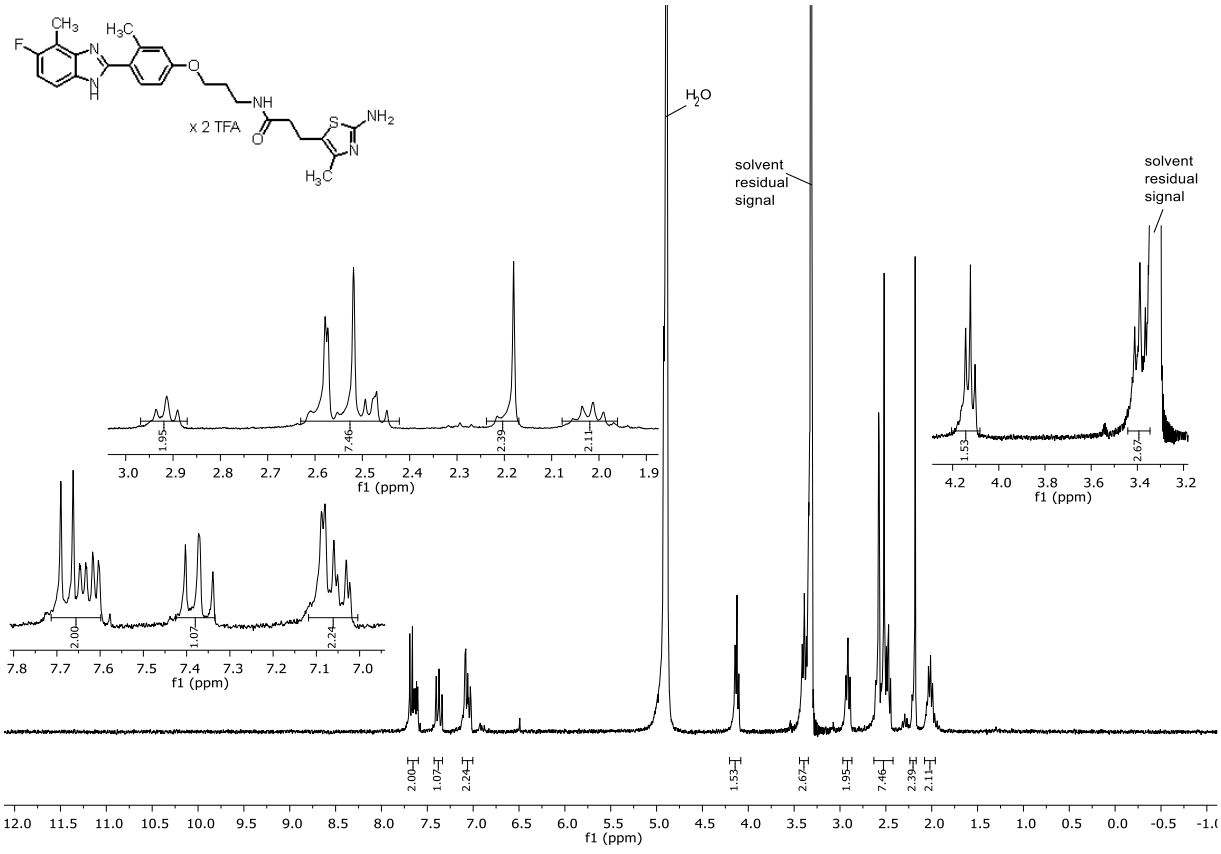

Figure App3.43. ^{1}H-NMR spectrum (300 MHz, MeOD) of compound **4.106**.

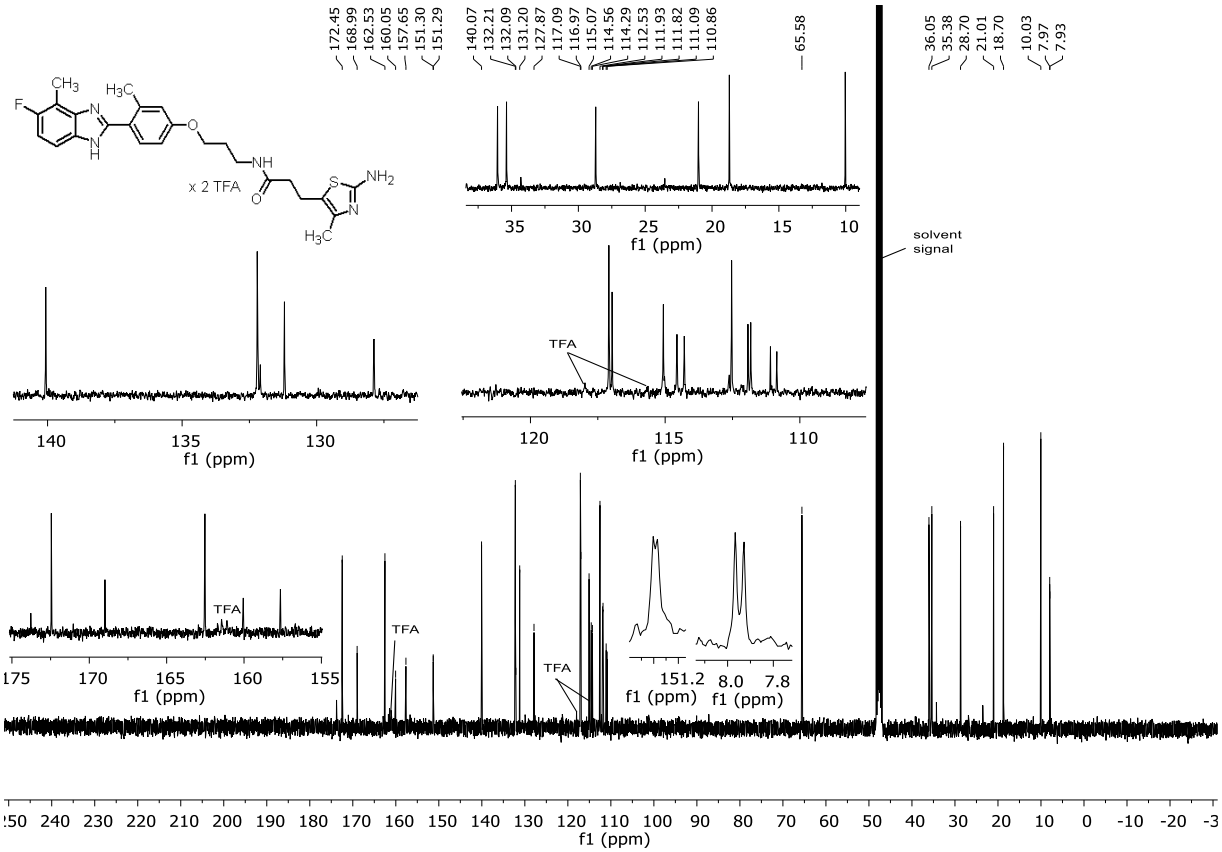

Figure App3.44. ^{13}C-NMR spectrum (101 MHz, MeOD) of compound **4.106**.

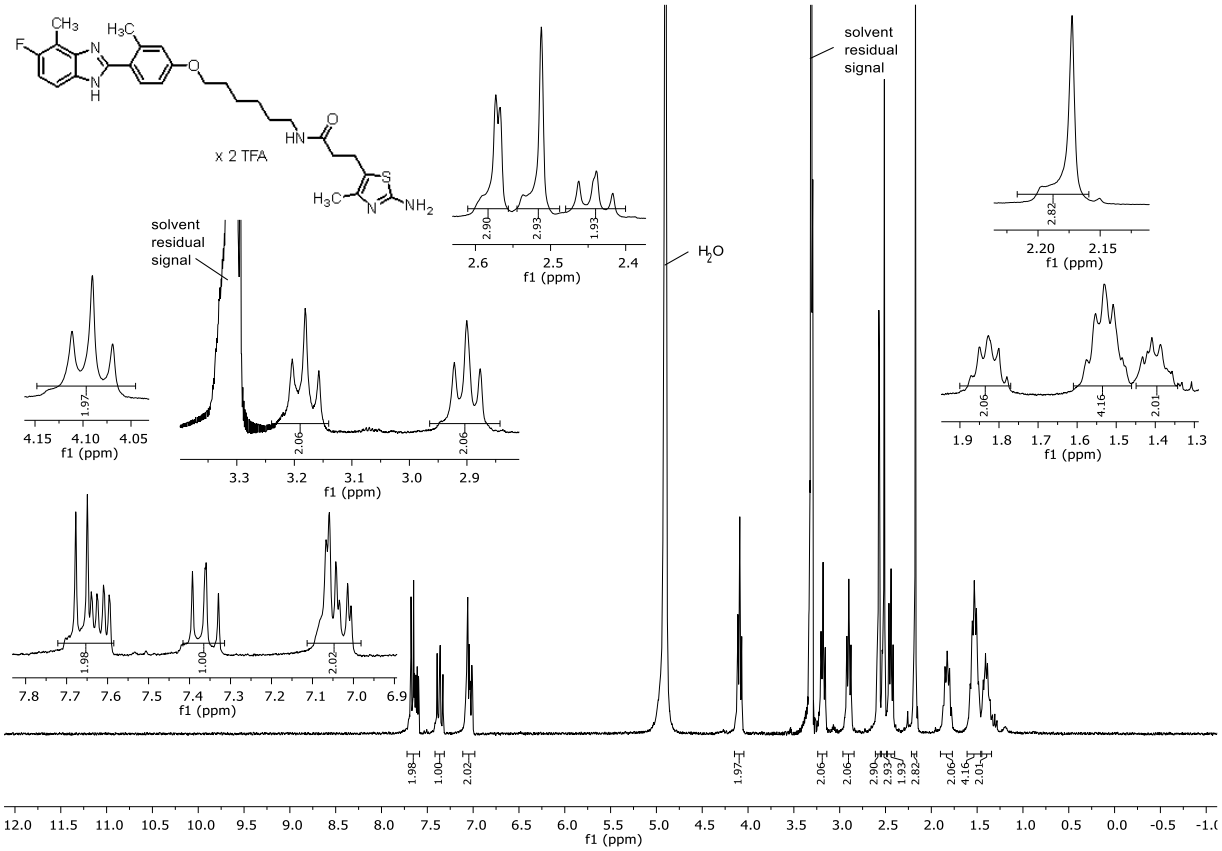

Figure App3.45. ^{1}H-NMR spectrum (300 MHz, MeOD) of compound **4.107**.

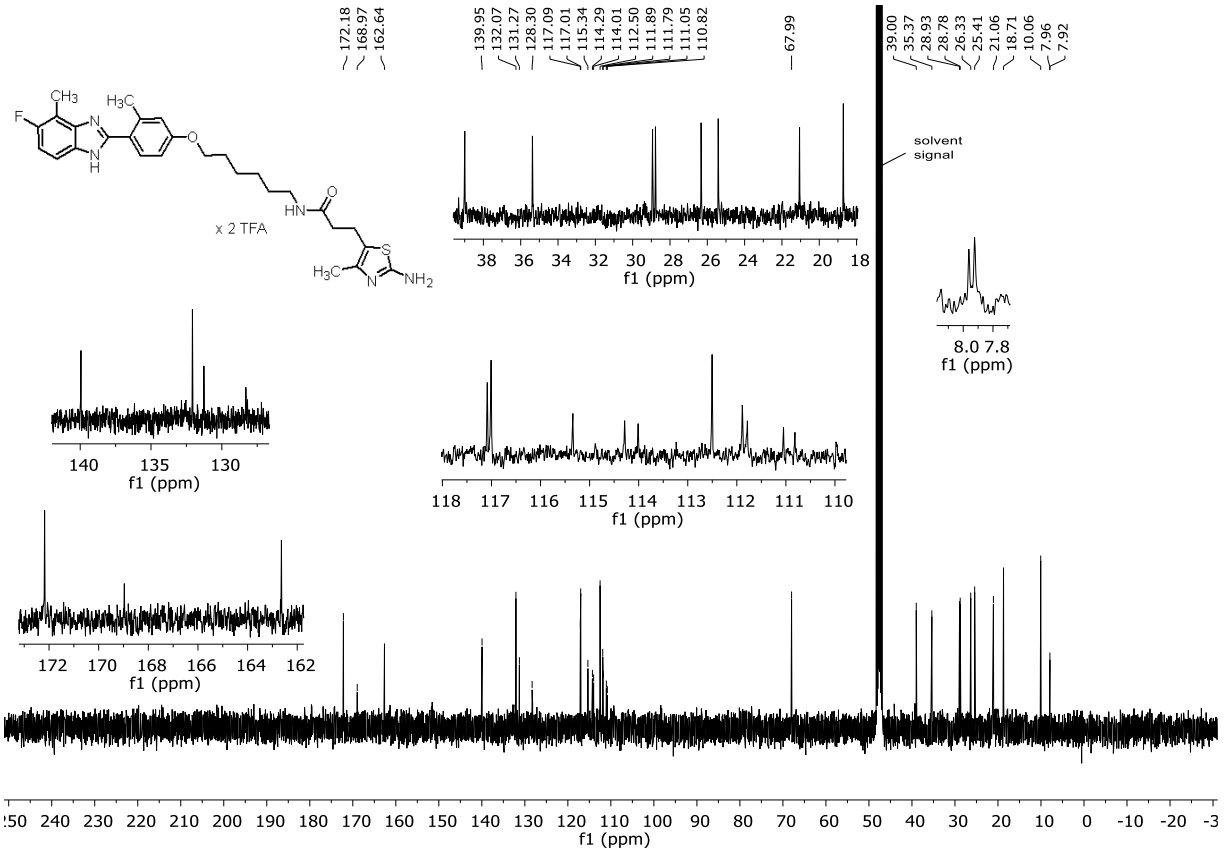

Figure App3.46. ^{13}C-NMR spectrum (101 MHz, MeOD) of compound **4.107**.

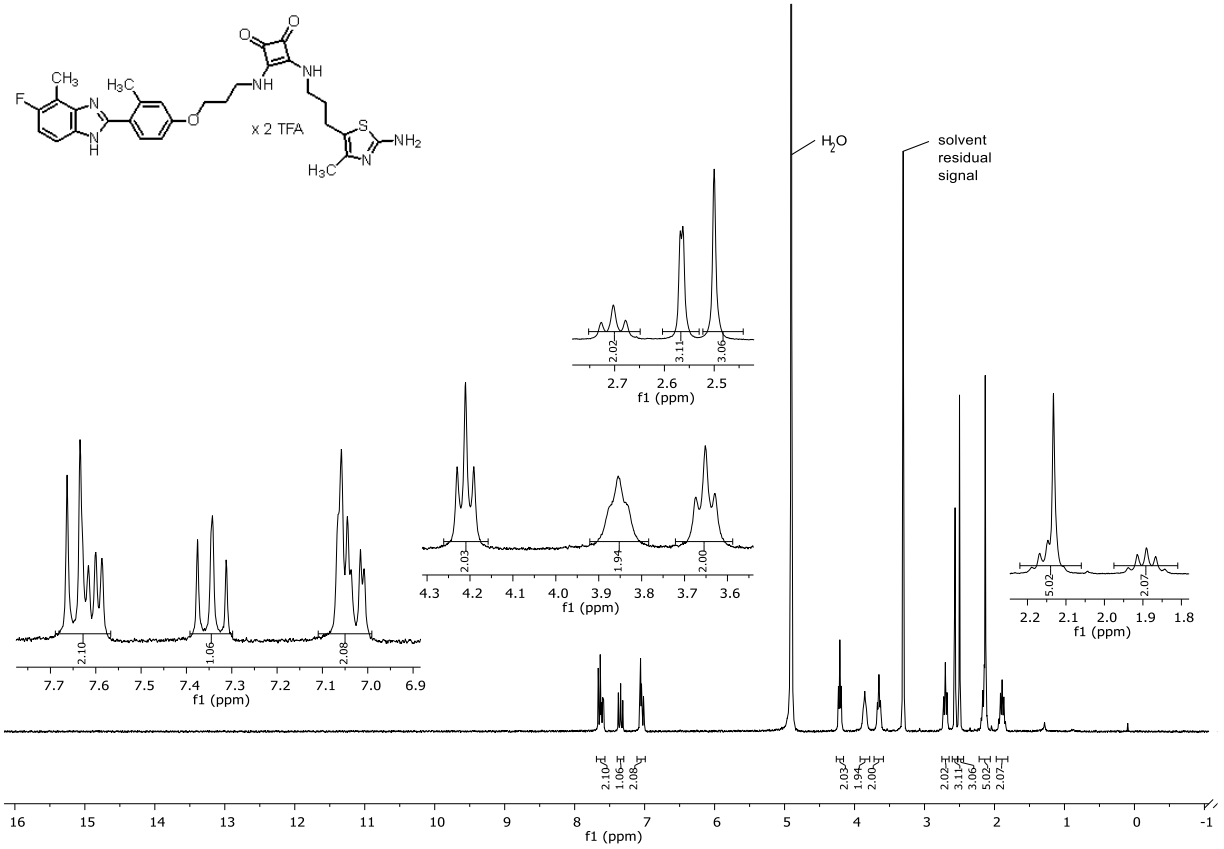

Figure App3.47. ^{1}H-NMR spectrum (300 MHz, MeOD) of compound **4.108**.

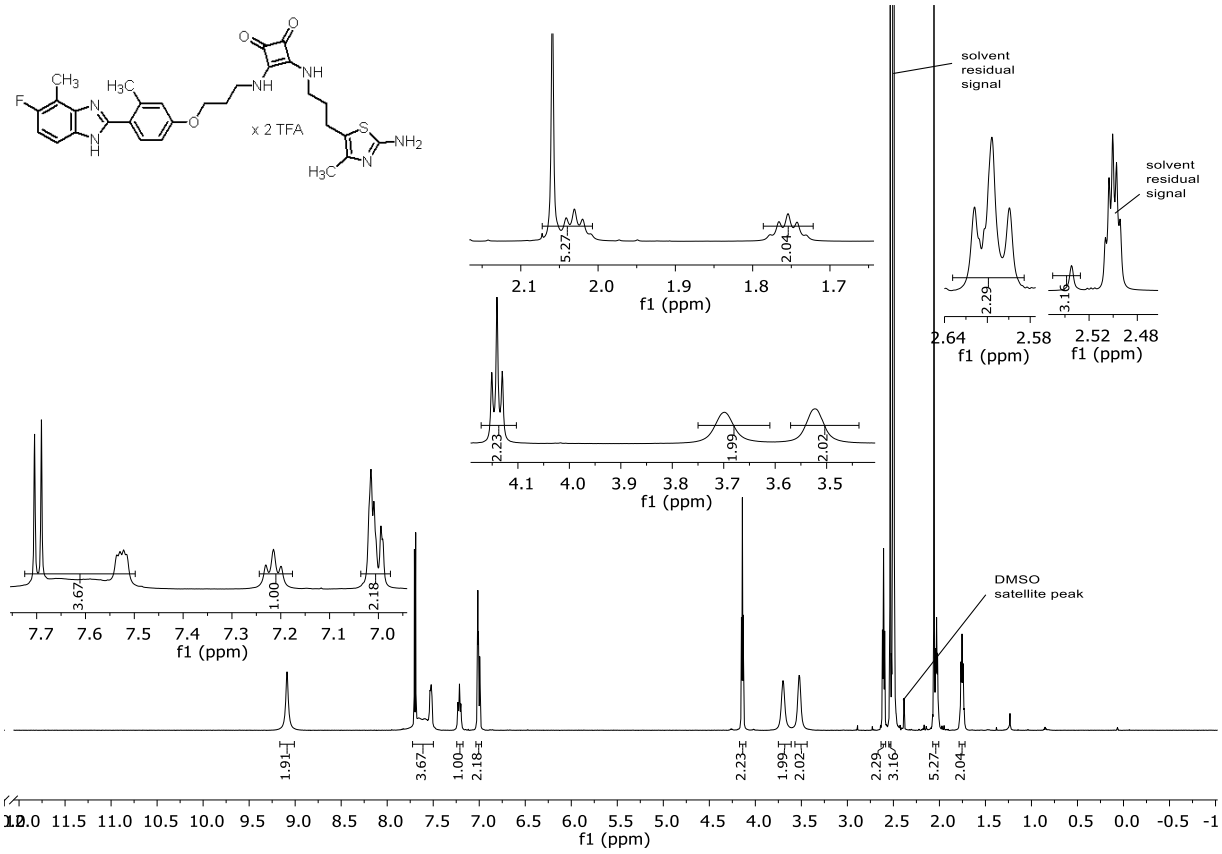

Figure App3.48. ^{1}H-NMR spectrum (600 MHz, DMSO-d_6) of compound **4.108**.

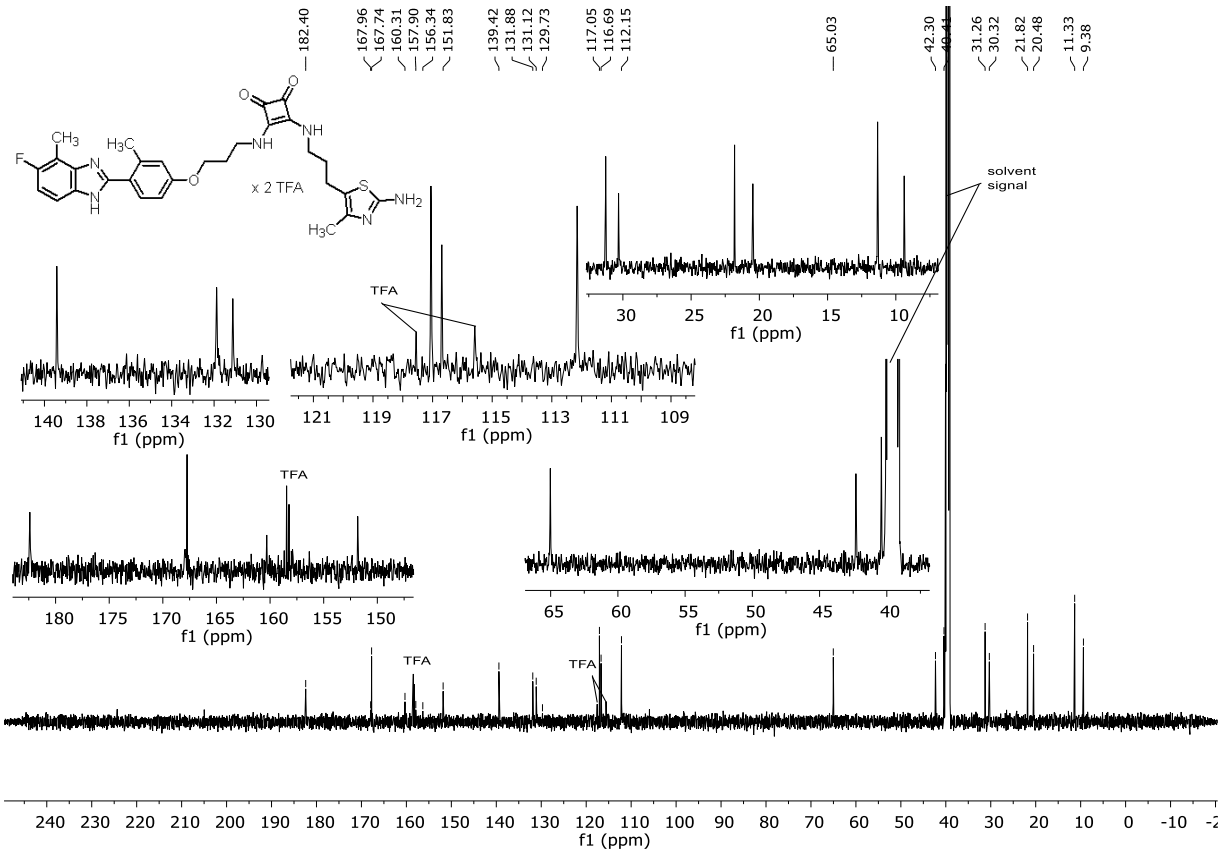

Figure App3.49. ^{13}C-NMR spectrum (151 MHz, DMSO-d_6) of compound **4.108**.

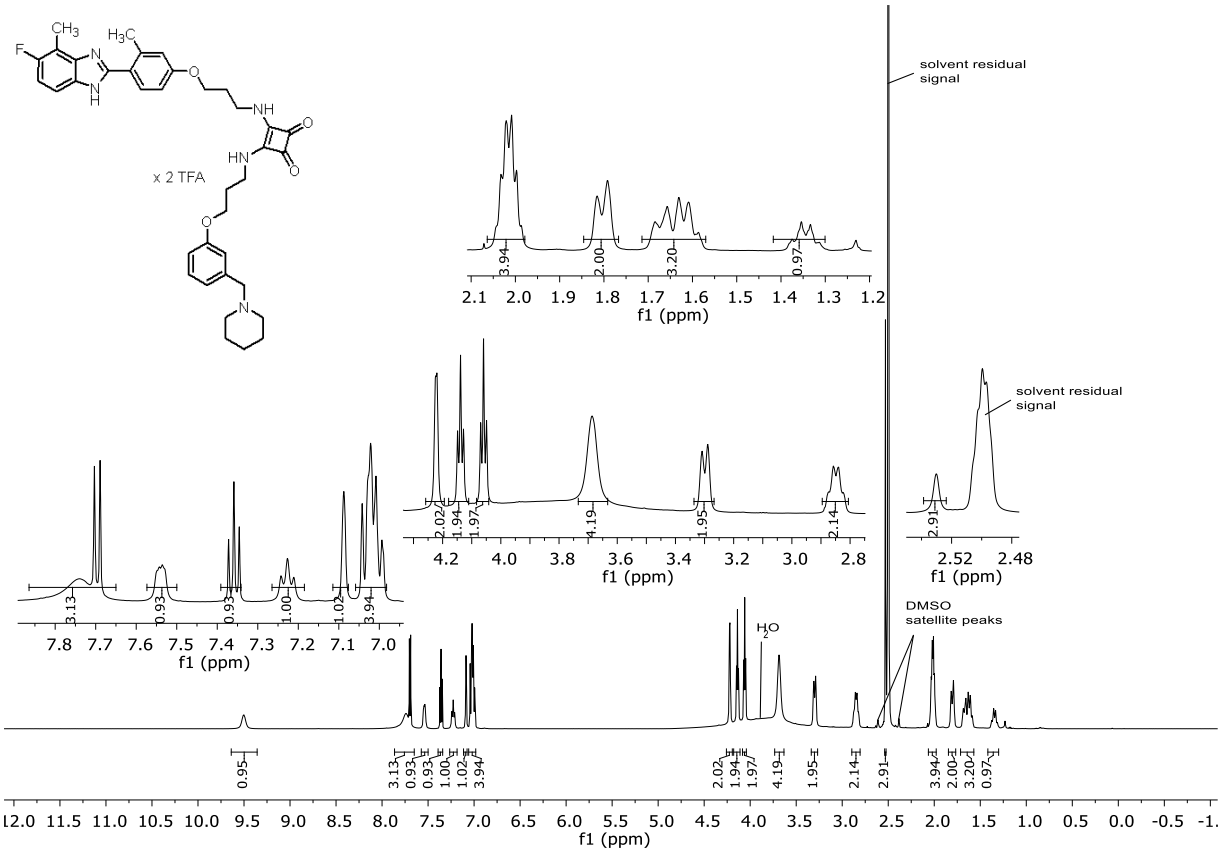

Figure App3.50. ^{1}H-NMR spectrum (600 MHz, DMSO-d_6) of compound **4.109**.

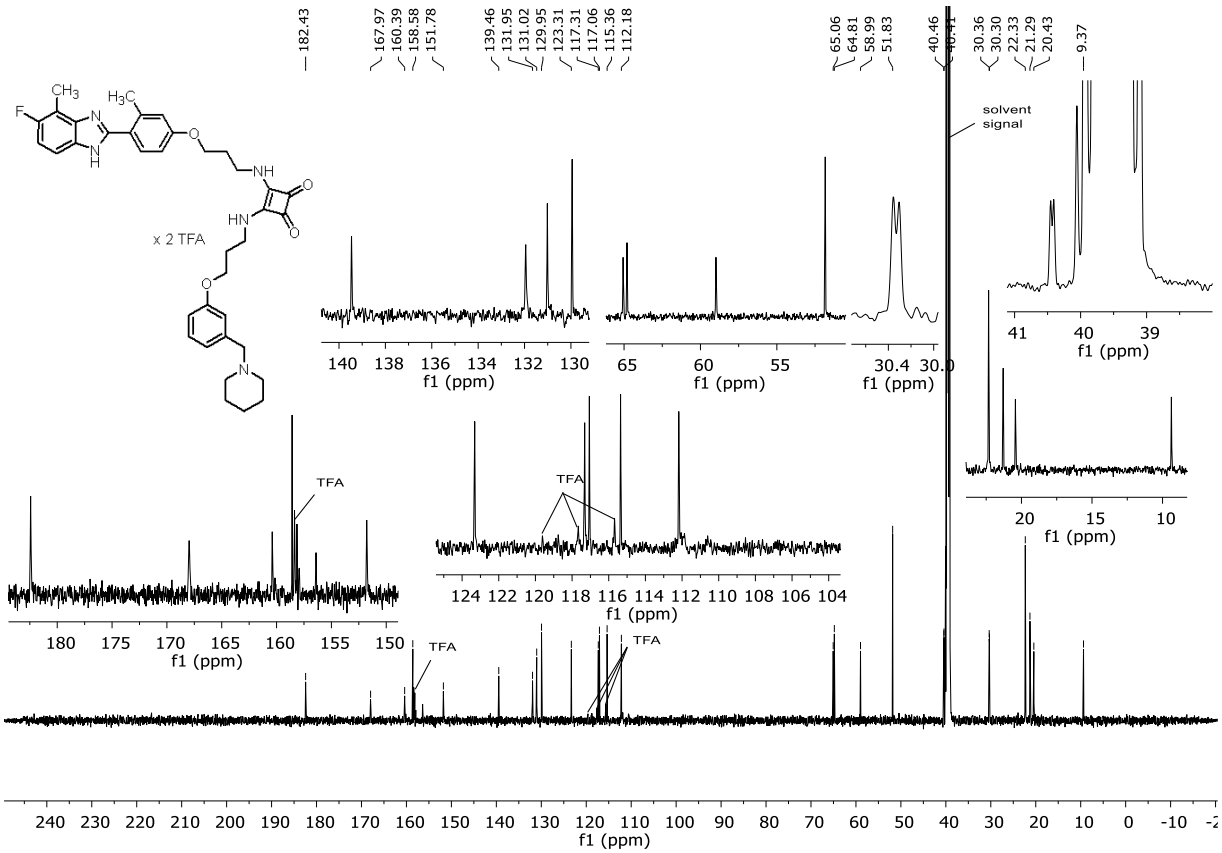

Figure App3.51. ^{13}C-NMR spectrum (151 MHz, DMSO-d_6) of compound **4.109**.

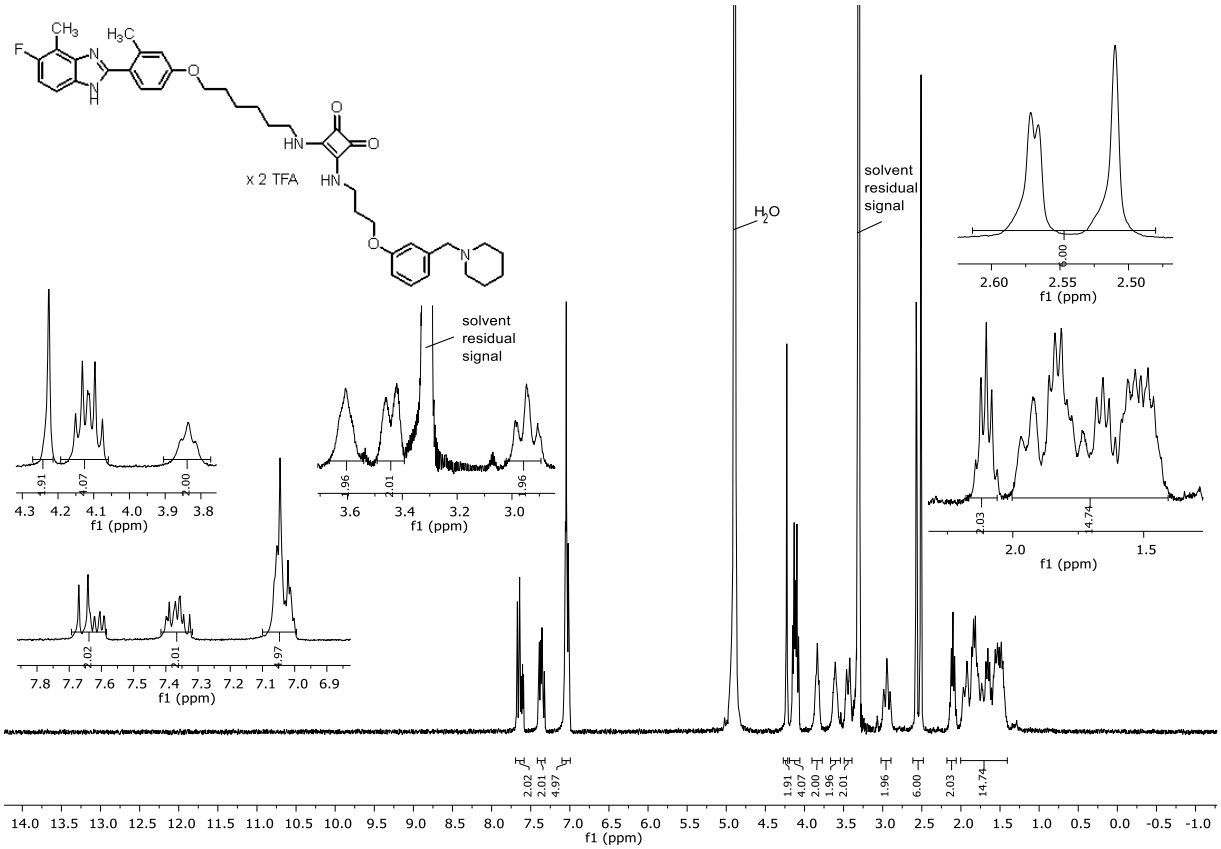

Figure App3.52. ^{1}H-NMR spectrum (300 MHz, MeOD) of compound **4.110**.

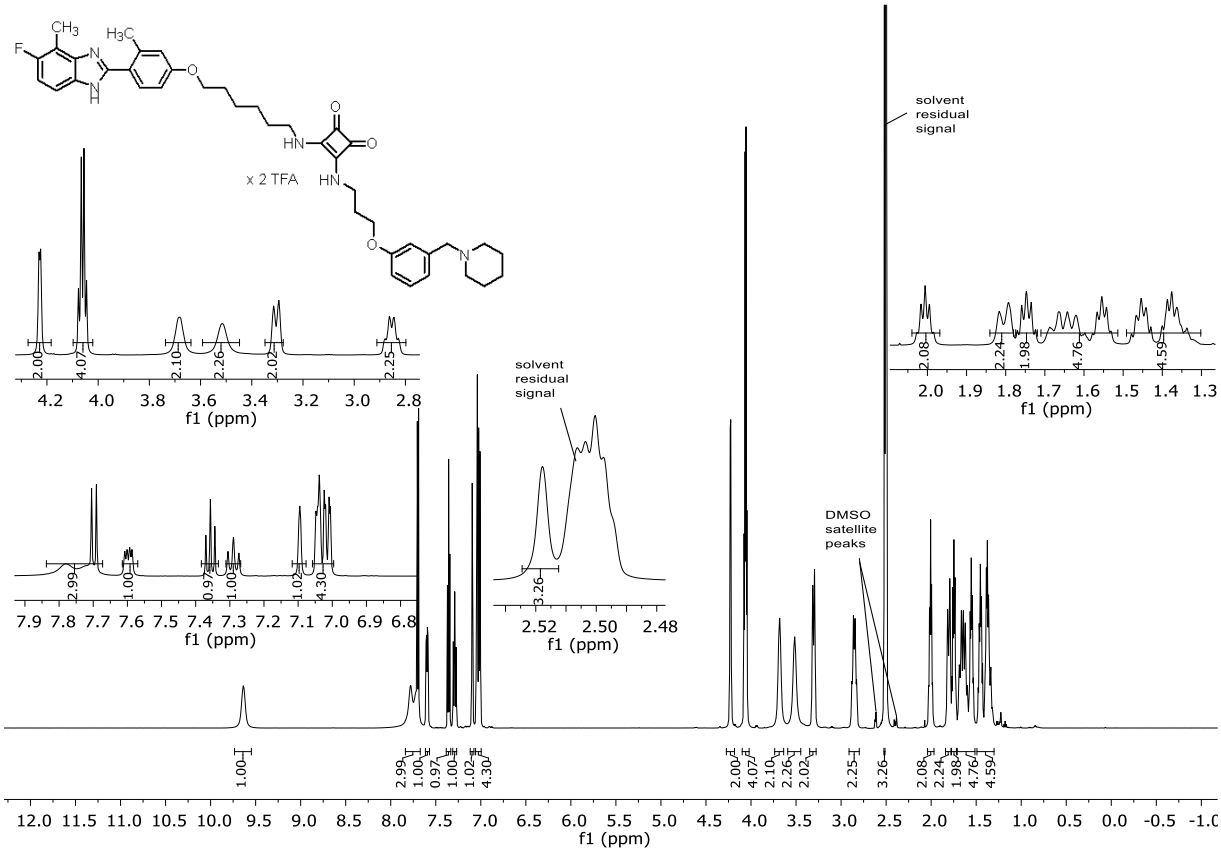

Figure App3.53. ^{1}H-NMR spectrum (600 MHz, DMSO-d_6) of compound **4.110**.

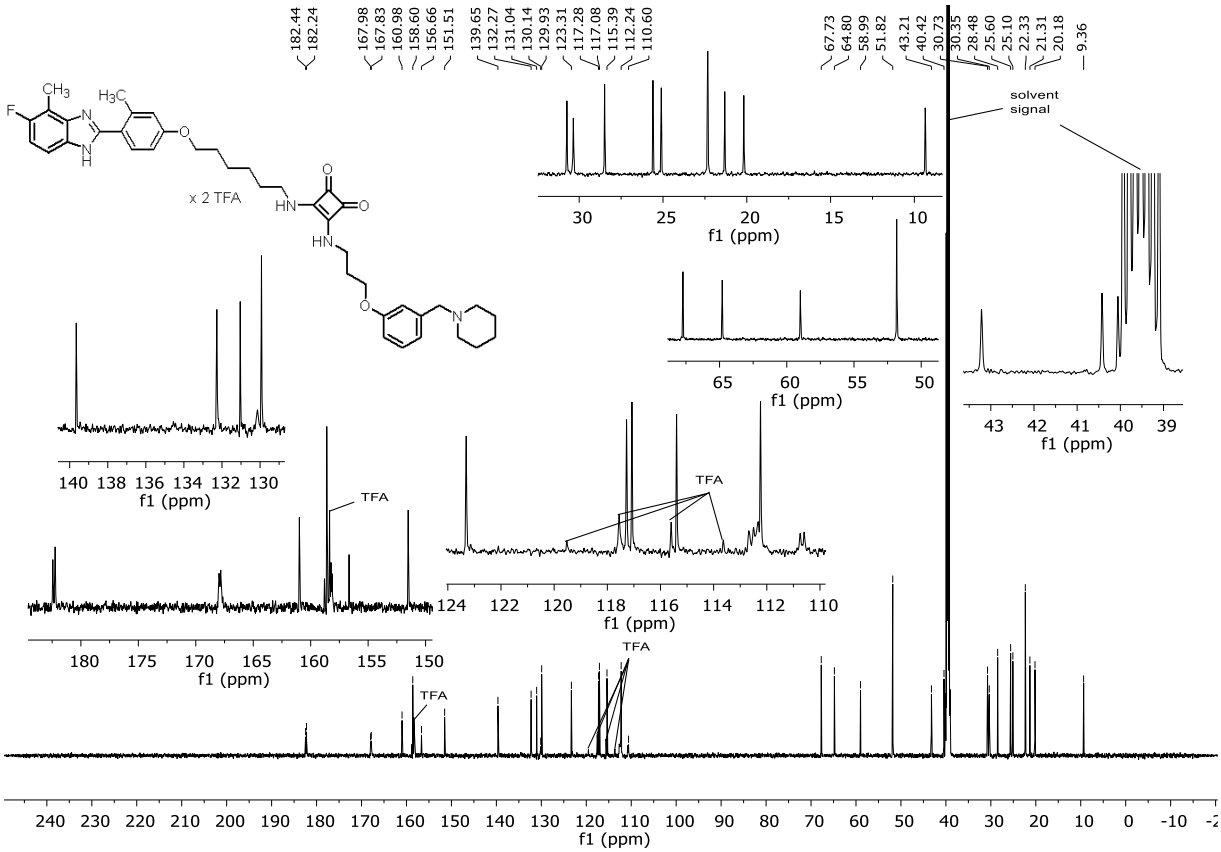

Figure App3.54. ^{13}C-NMR spectrum (151 MHz, DMSO-d_6) of compound **4.110**.

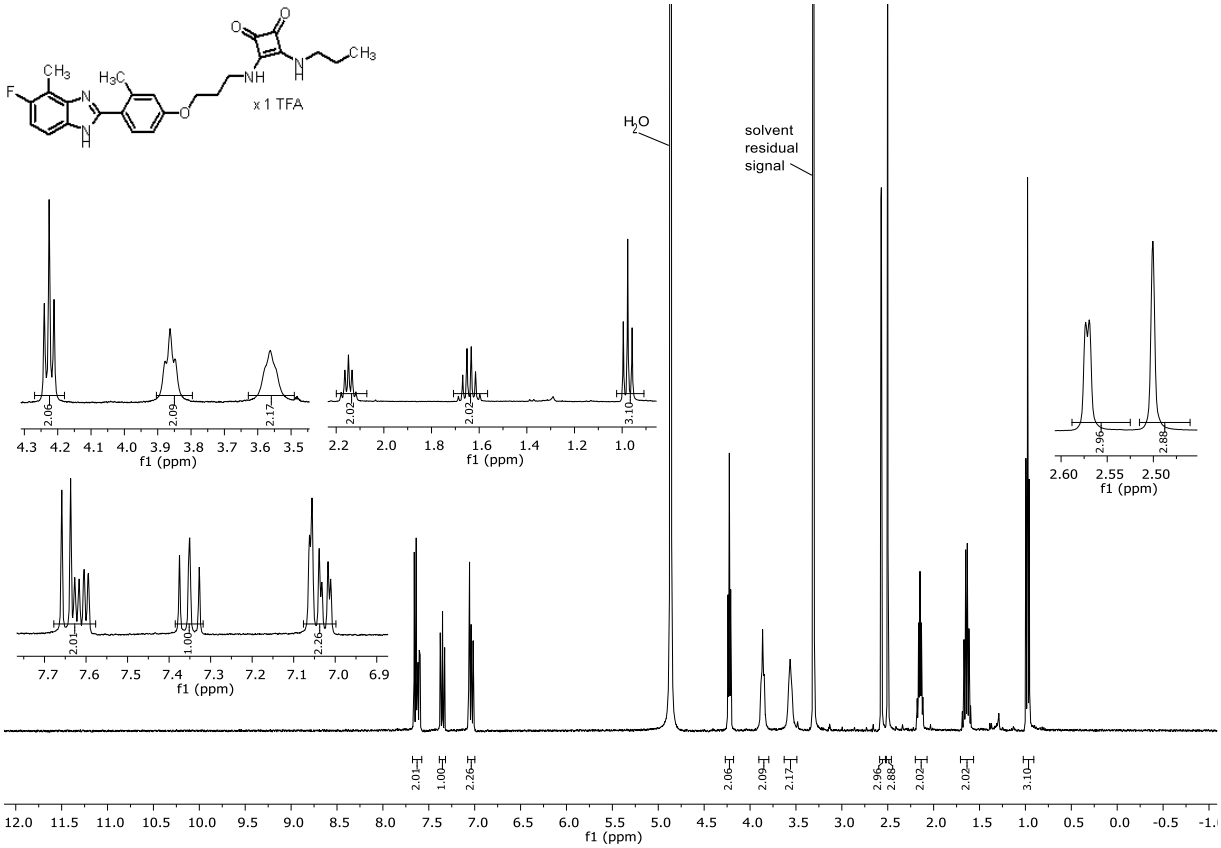

Figure App3.55. ^{1}H-NMR spectrum (300 MHz, MeOD) of compound **4.112**.

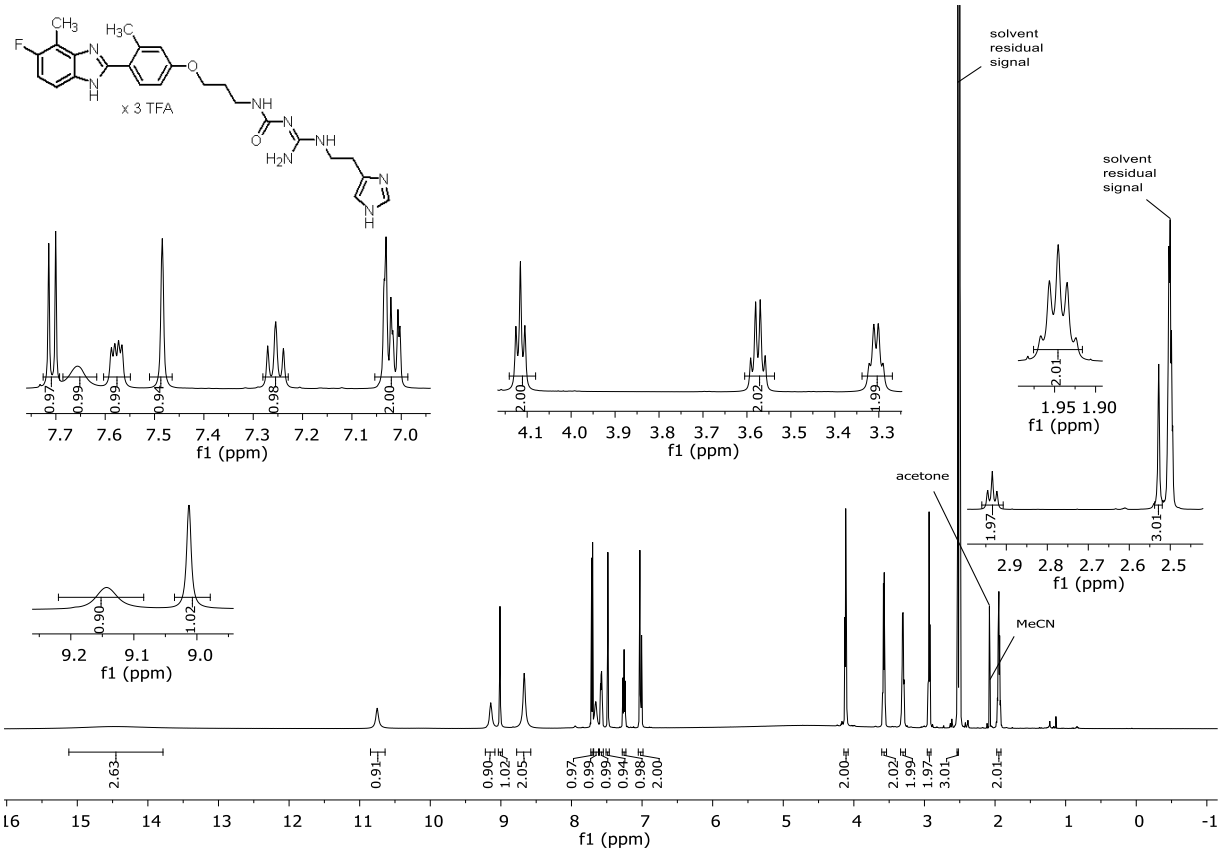

Figure App3.56. ^{1}H-NMR spectrum (600 MHz, DMSO-d_6) of compound **4.114**.

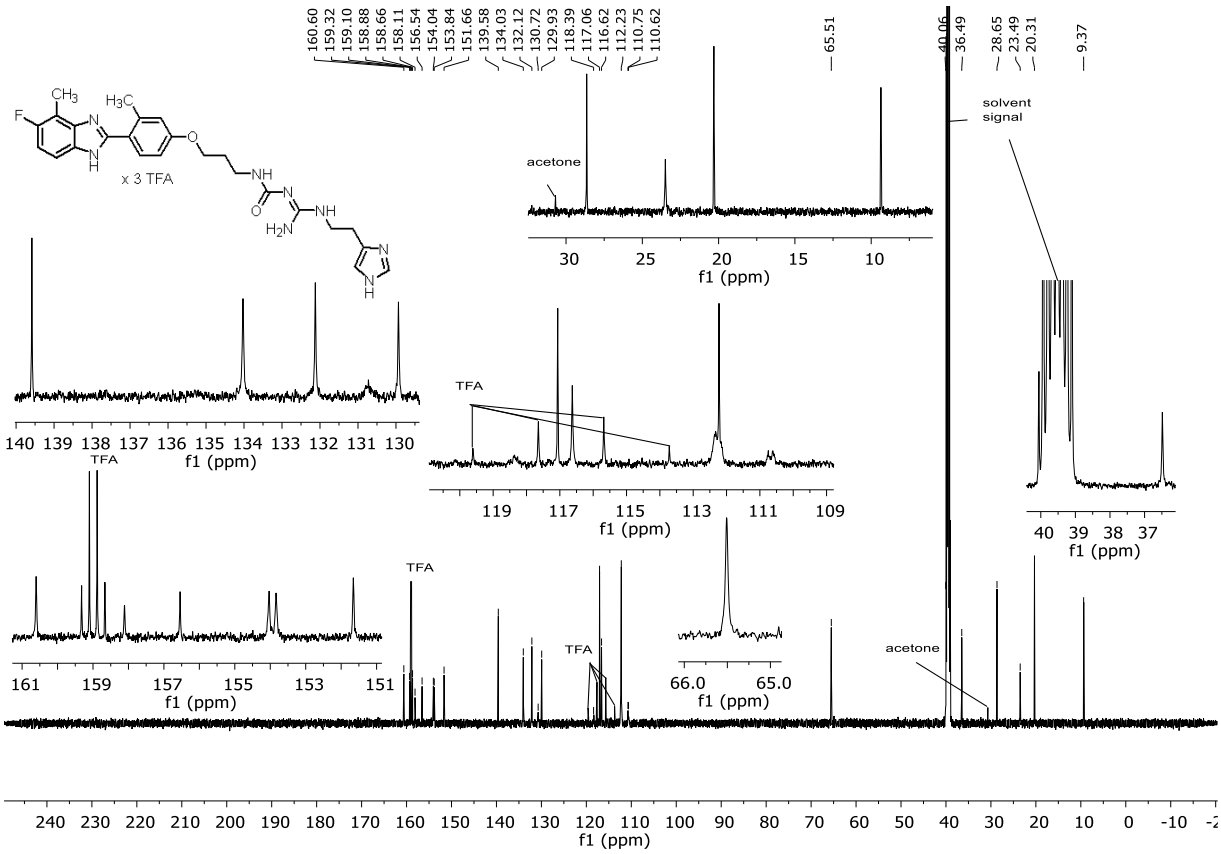

Figure App3.57. ^{13}C-NMR spectrum (151 MHz, DMSO-d_6) of compound **4.114**.

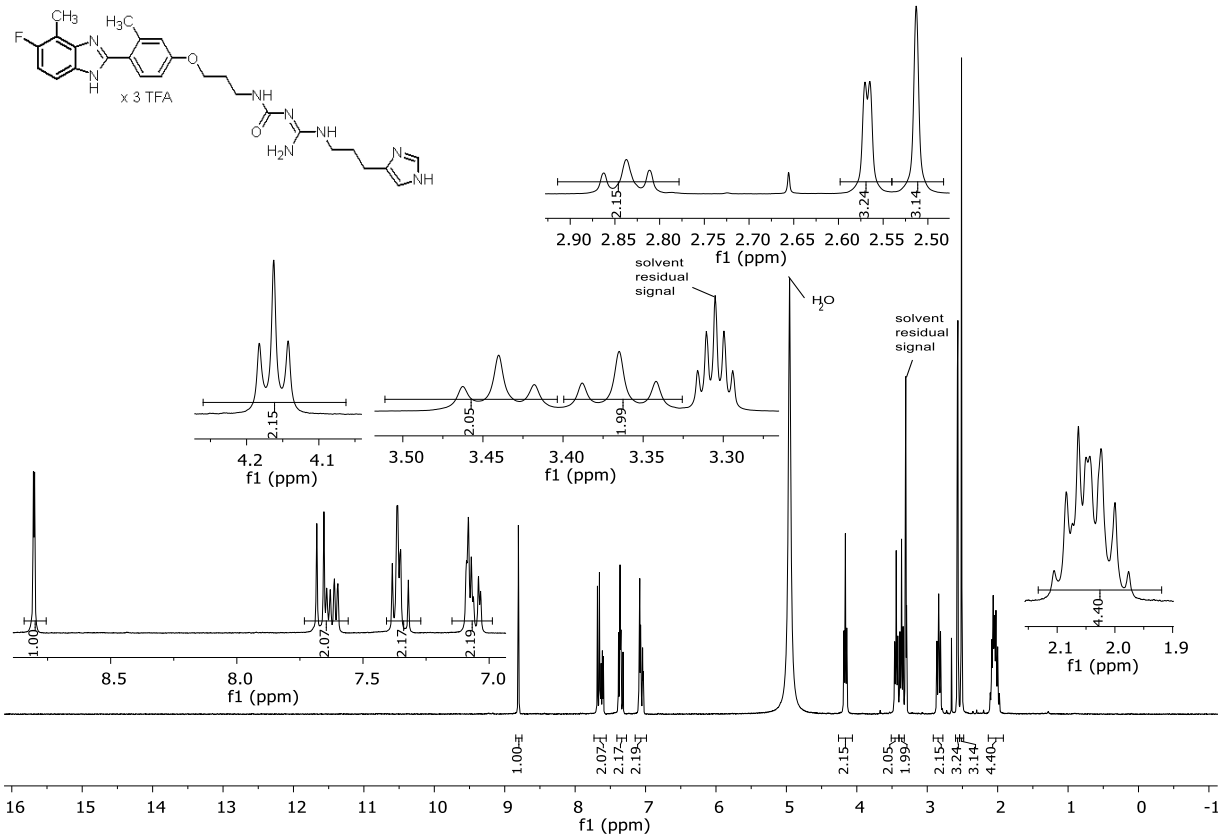

Figure App3.58. ^{1}H-NMR spectrum (300 MHz, MeOD) of compound **4.115**.

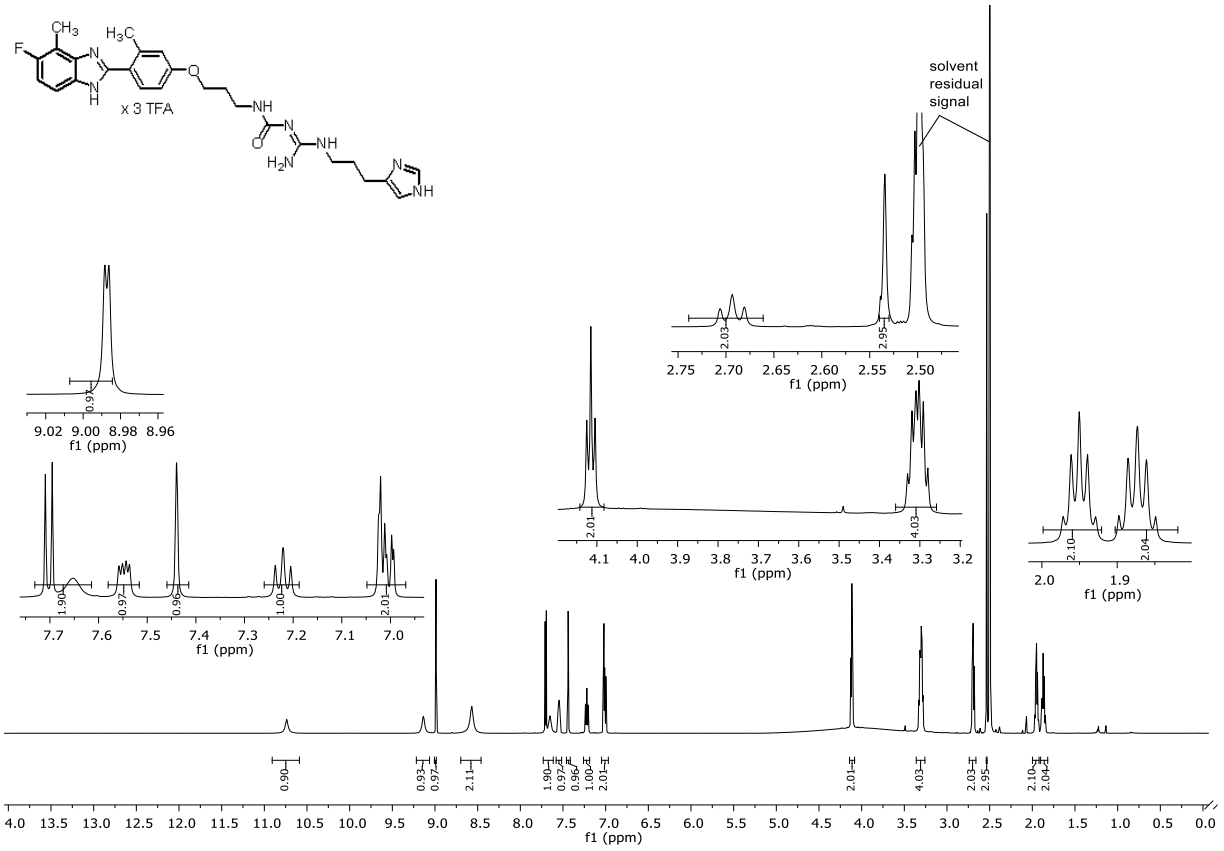

Figure App3.59. ^{1}H-NMR spectrum (600 MHz, DMSO-d_6) of compound **4.115**.

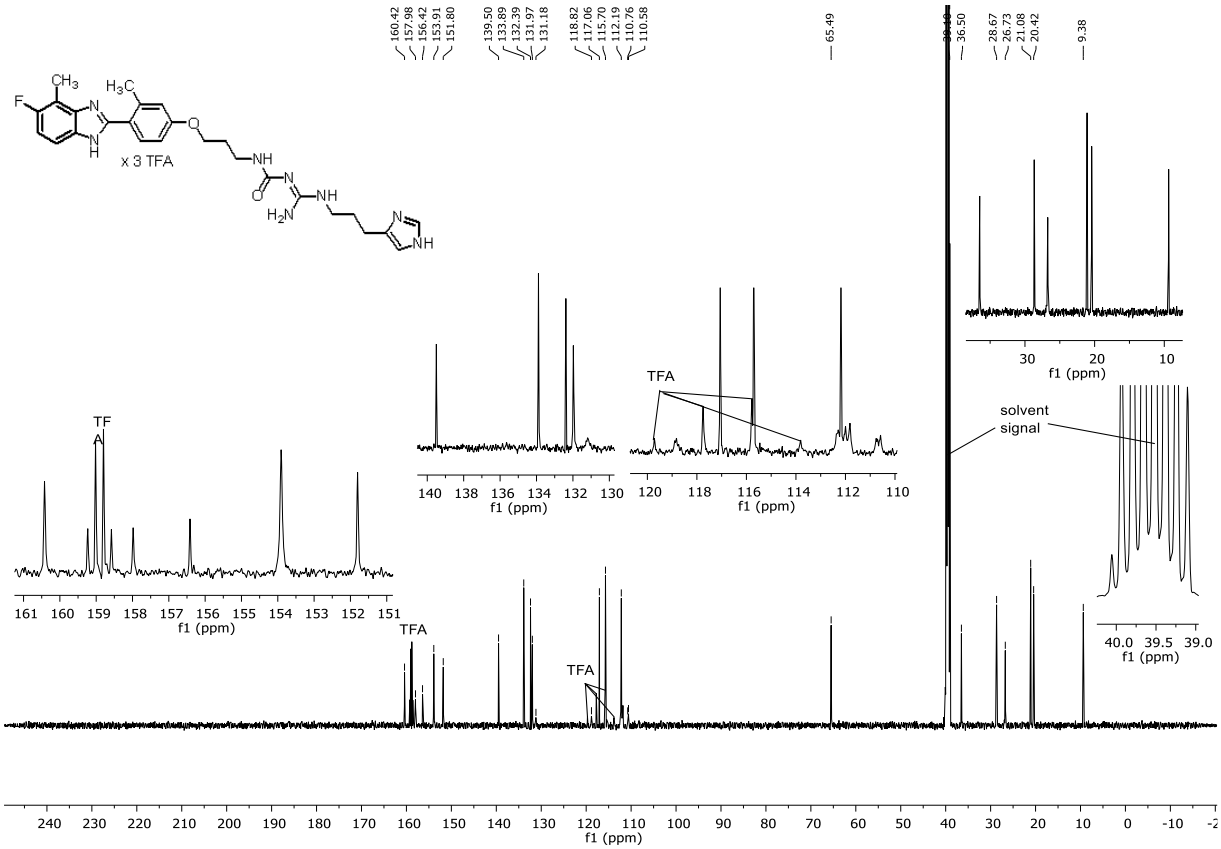

Figure App3.60. ^{13}C-NMR spectrum (151 MHz, DMSO-d_6) of compound **4.115**.

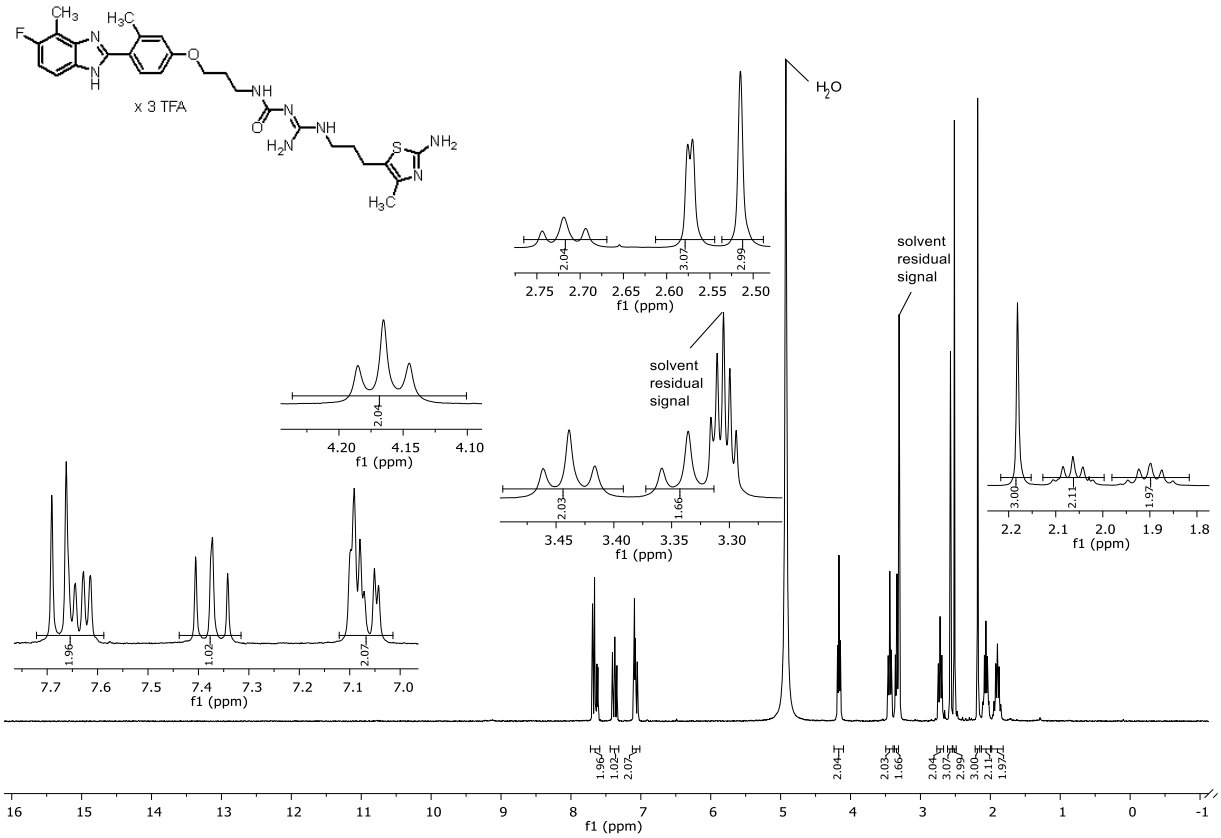

Figure App3.61. ^{1}H-NMR spectrum (300 MHz, MeOD) of compound **4.116**.

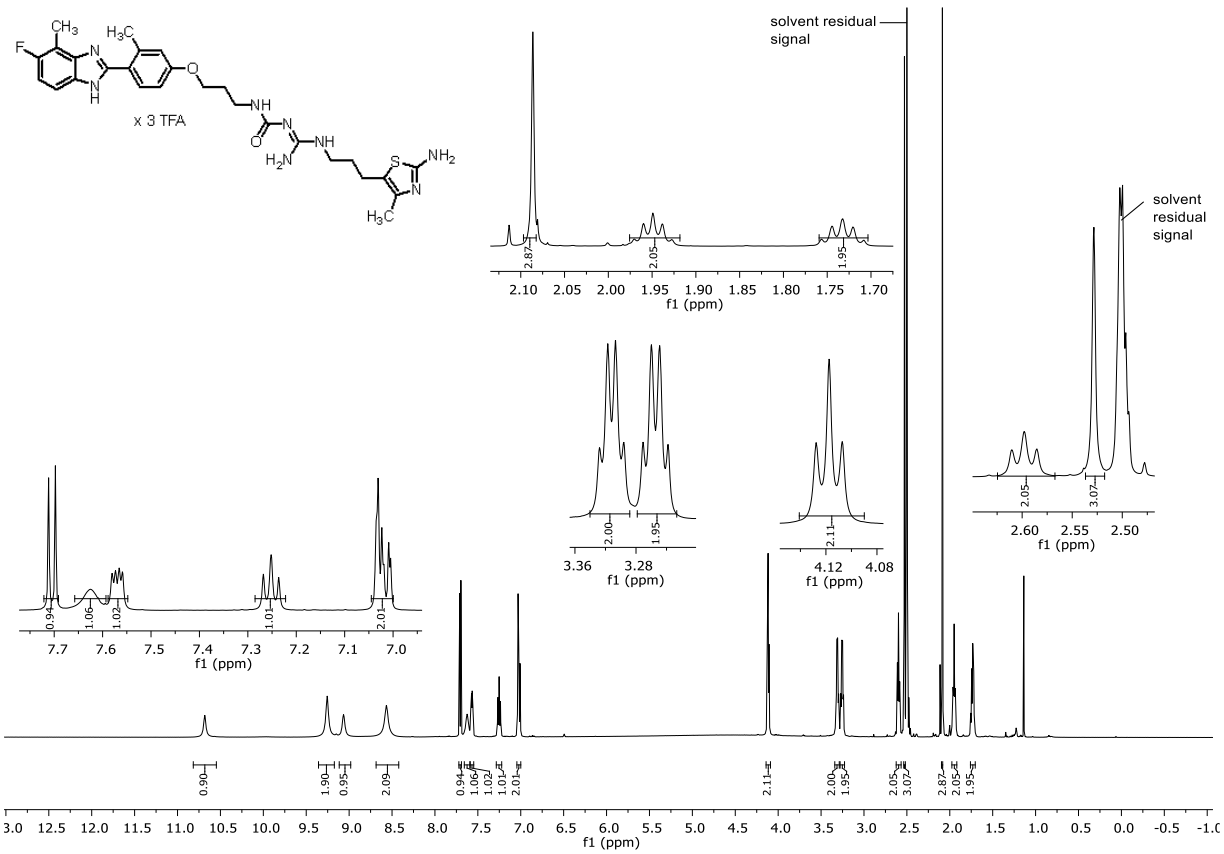

Figure App3.62. ^{1}H-NMR spectrum (600 MHz, DMSO-d_6) of compound **4.116**.

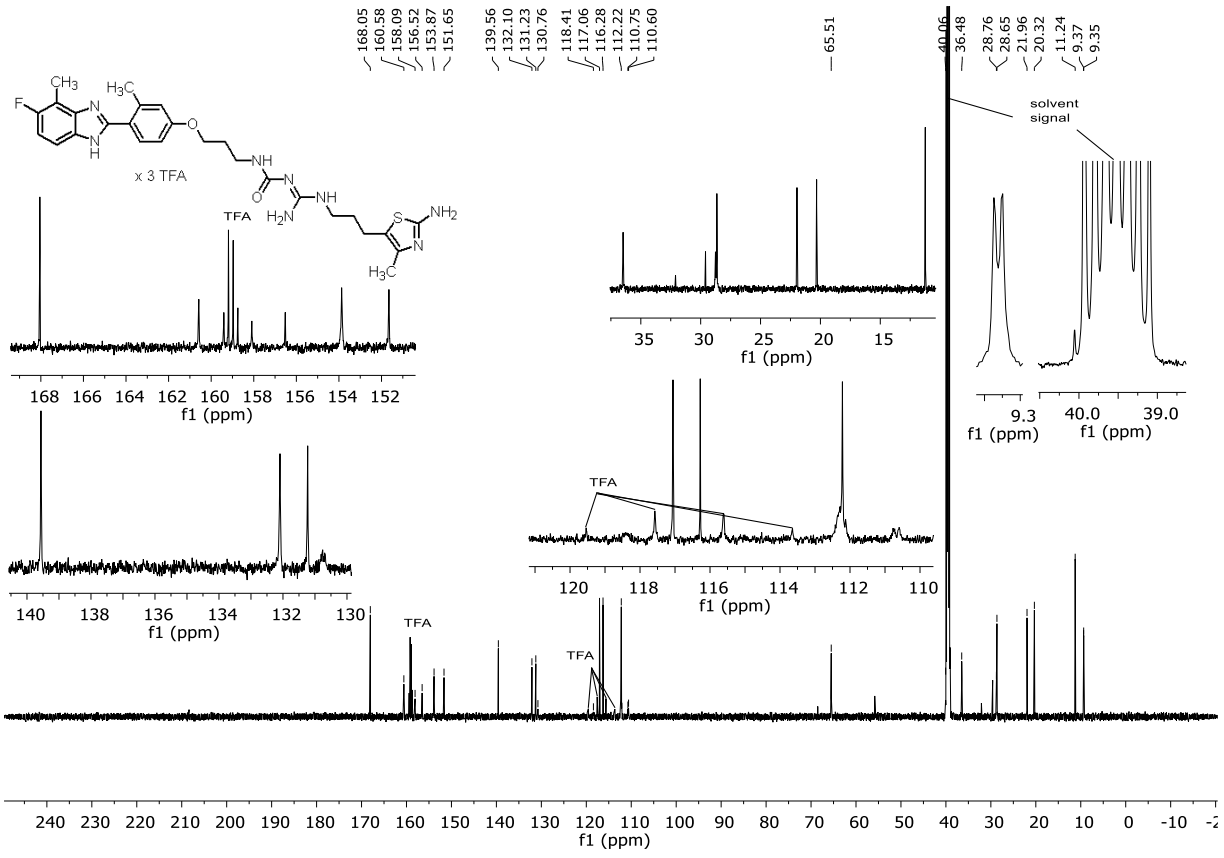

Figure App3.63. ^{13}C-NMR spectrum (151 MHz, DMSO-d_6) of compound **4.116**.

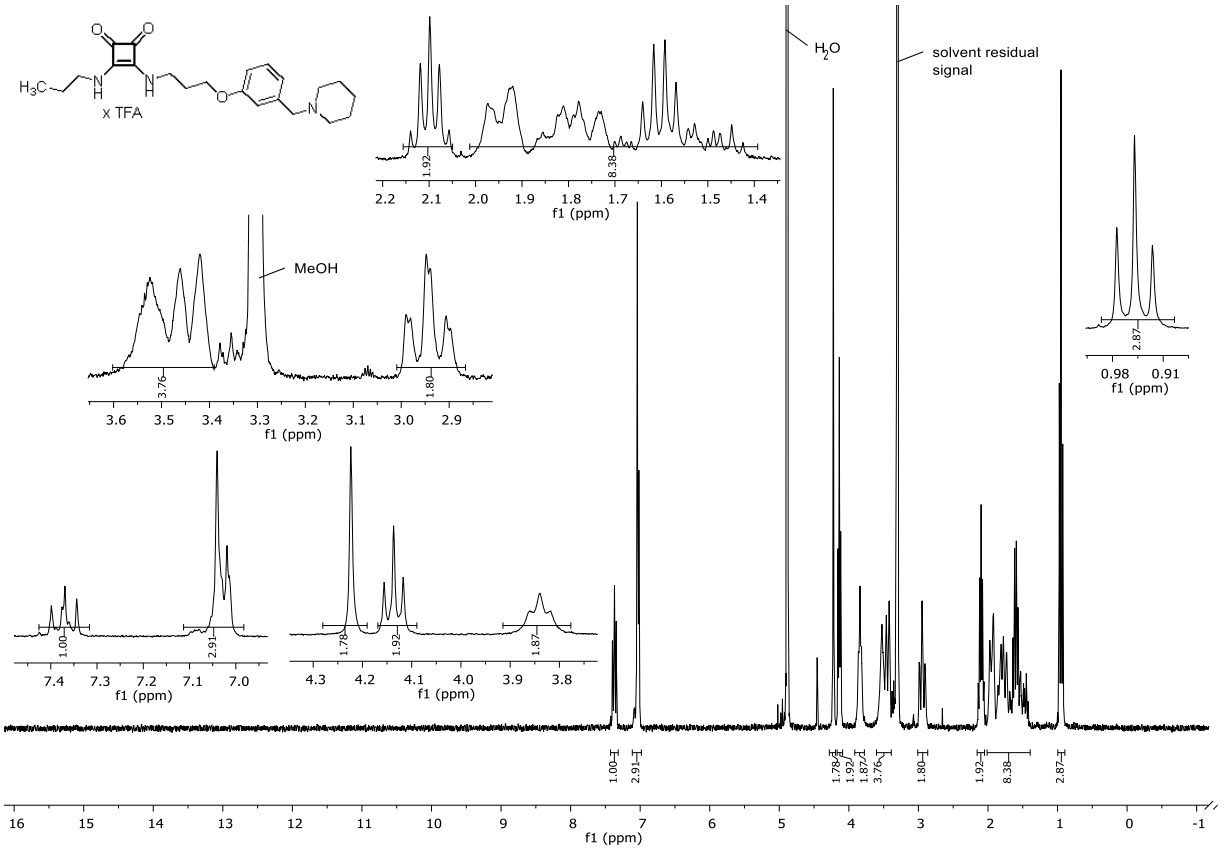

Figure App3.64. ^{1}H-NMR spectrum (400 MHz, MeOD) of compound **4.117**.

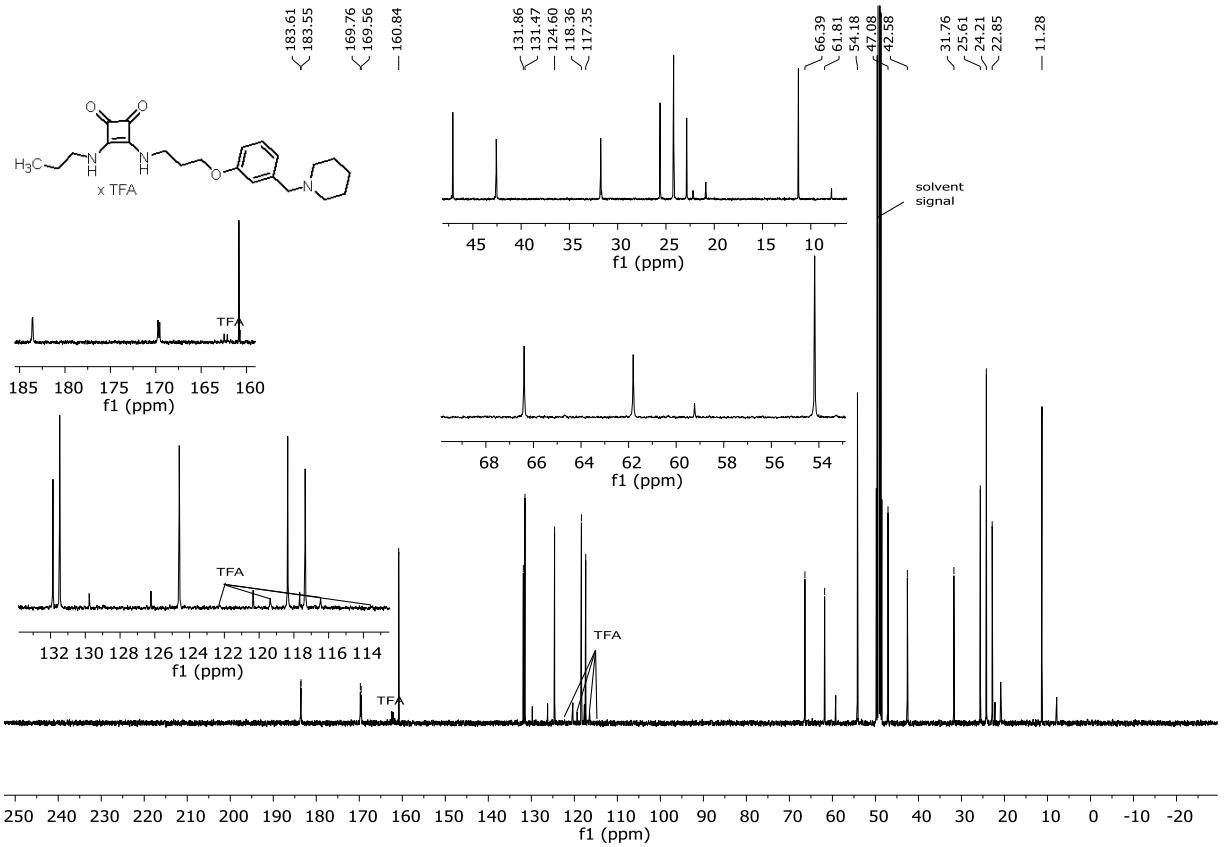

Figure App3.65. ^{13}C-NMR spectrum (101 MHz, MeOD) of compound **4.117**.

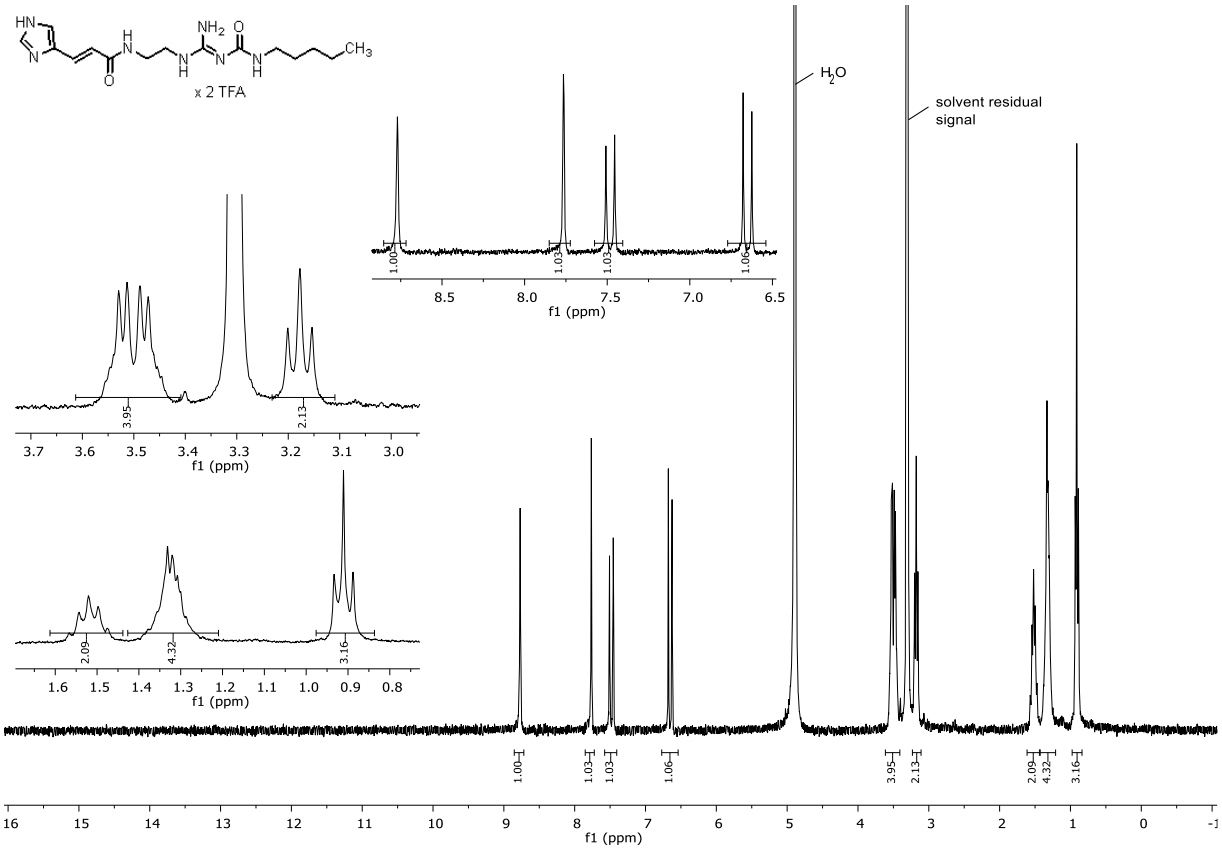

Figure App3.66. [1]H-NMR spectrum (300 MHz, MeOD) of compound **4.120**.

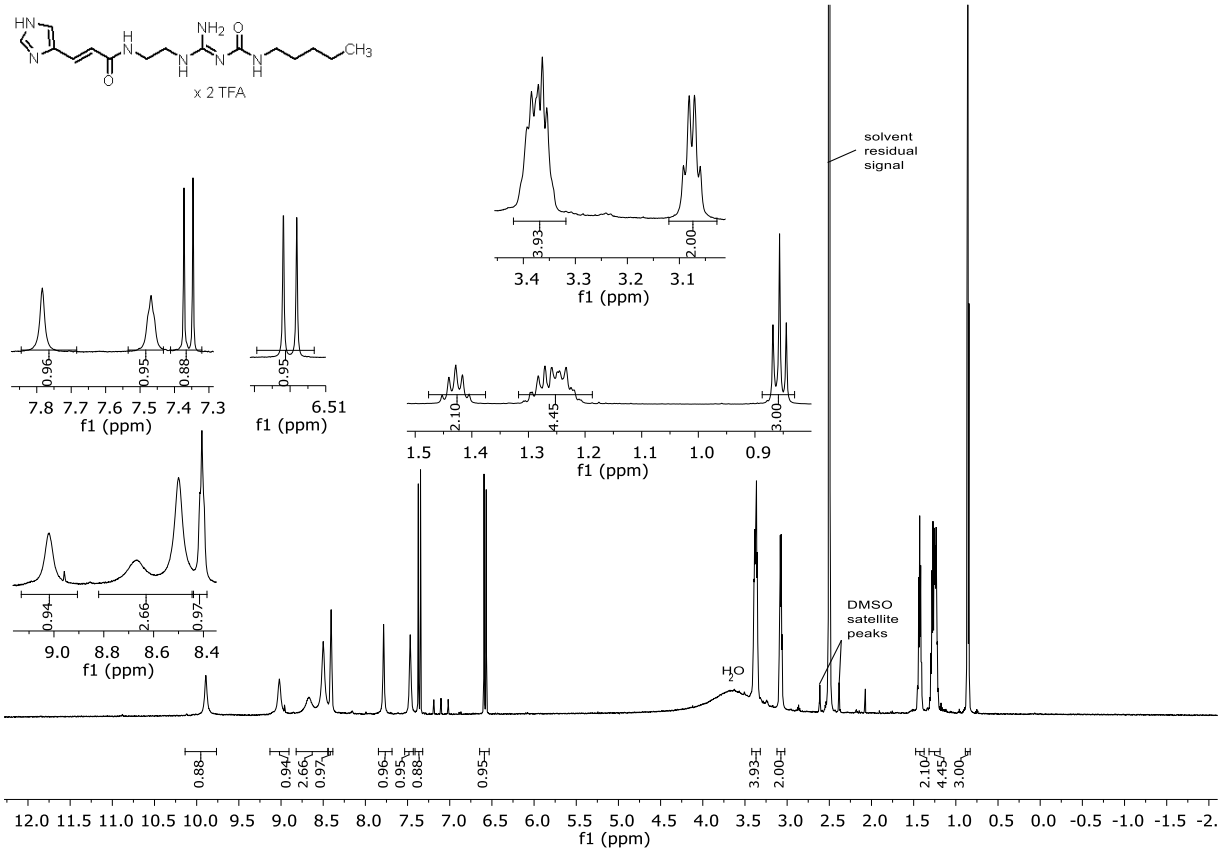

Figure App3.67. [1]H-NMR spectrum (600 MHz, DMSO-d_6) of compound **4.120**.

App3.2 RP-HPLC Chromatograms of 4.82-4.97, 4.104-4.110, 4.112, 4.114-4.117 and 4.120

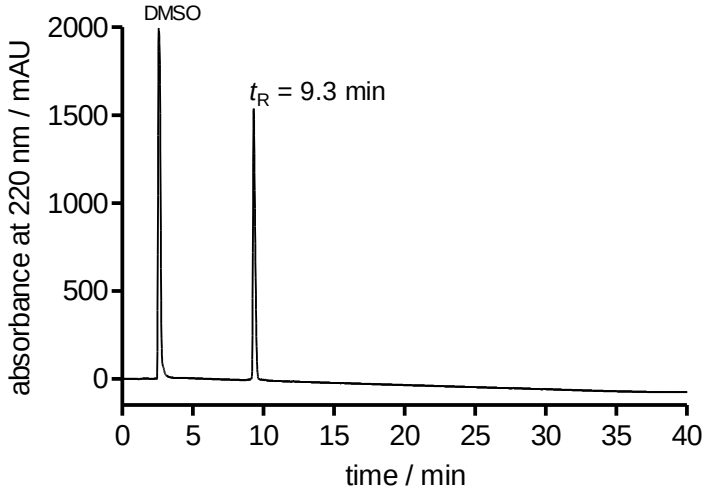

Figure App3.68. RP-HPLC analysis (purity control) of **4.82** (100%, 220 nm).

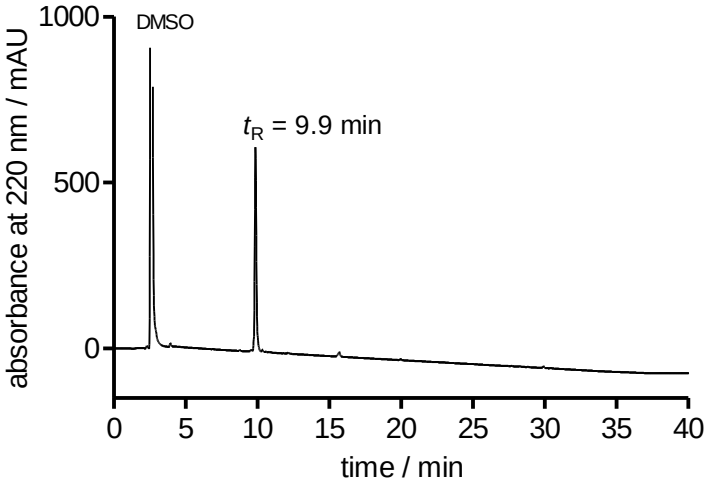

Figure App3.69. RP-HPLC analysis (purity control) of **4.83** (97%, 220 nm).

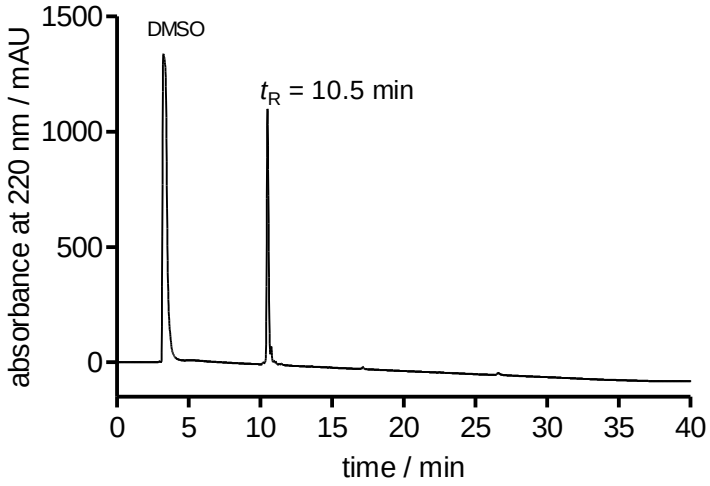

Figure App3.70. RP-HPLC analysis (purity control) of **4.84** (96%, 220 nm).

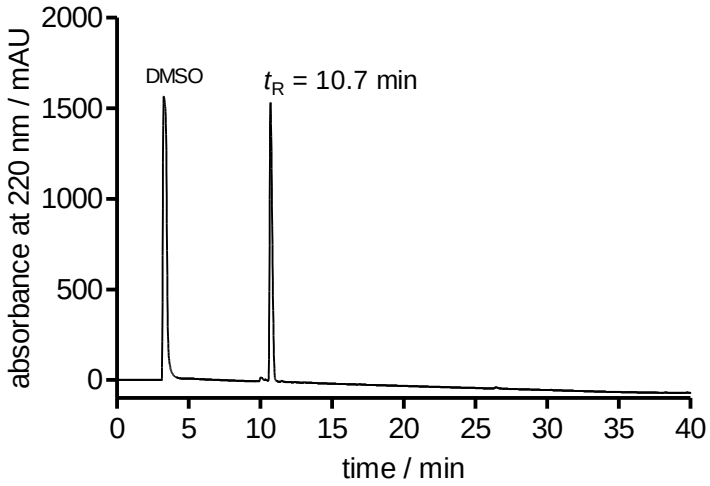

Figure App3.71. RP-HPLC analysis (purity control) of **4.85** (98%, 220 nm).

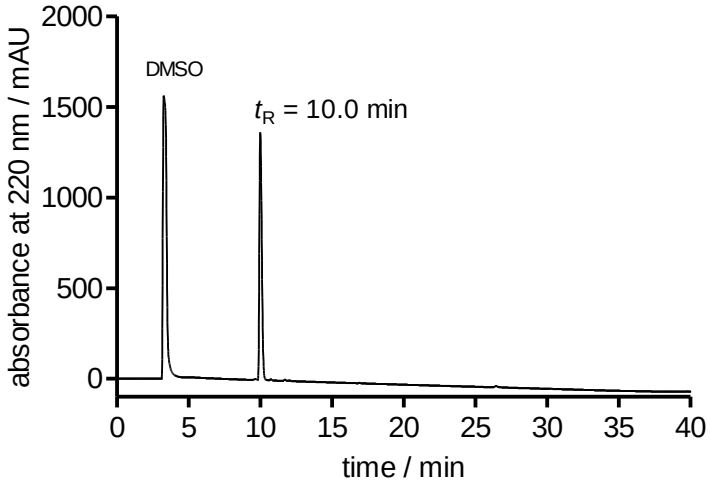

Figure App3.72. RP-HPLC analysis (purity control) of **4.86** (97%, 220 nm).

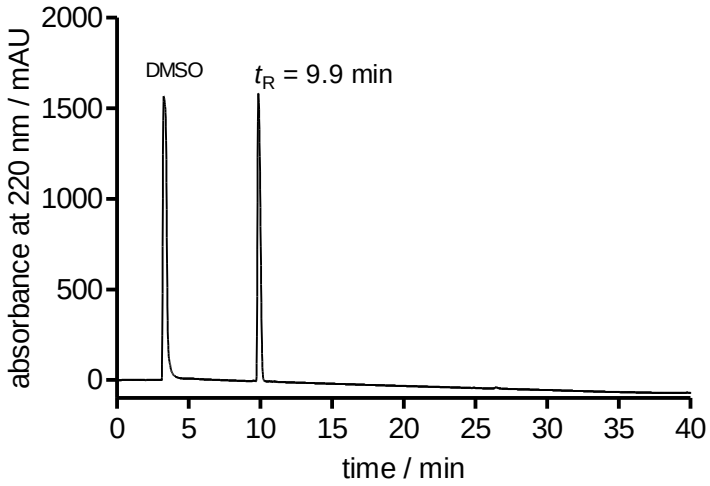

Figure App3.73. RP-HPLC analysis (purity control) of **4.87** (99%, 220 nm).

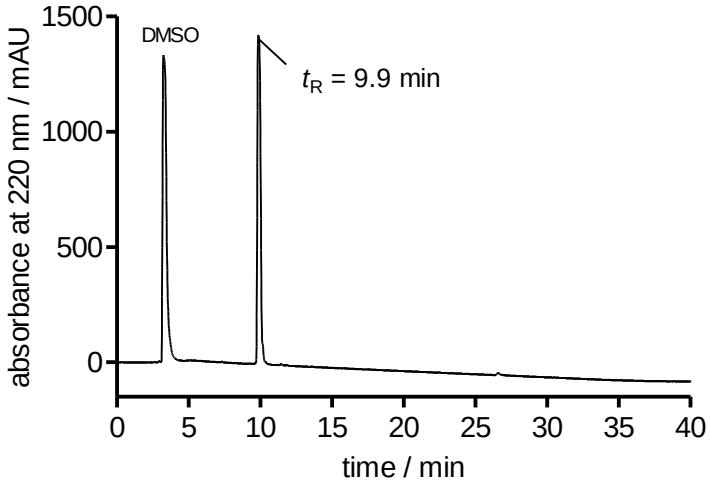

Figure App3.74. RP-HPLC analysis (purity control) of **4.88** (99%, 220 nm).

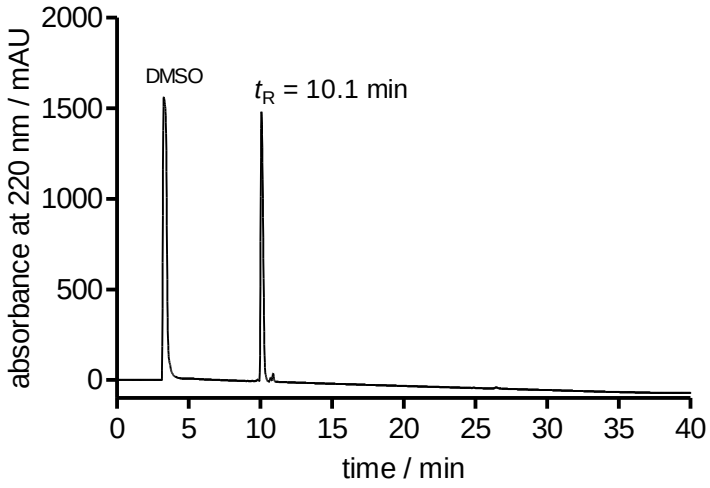

Figure App3.75. RP-HPLC analysis (purity control) of **4.89** (97%, 220 nm).

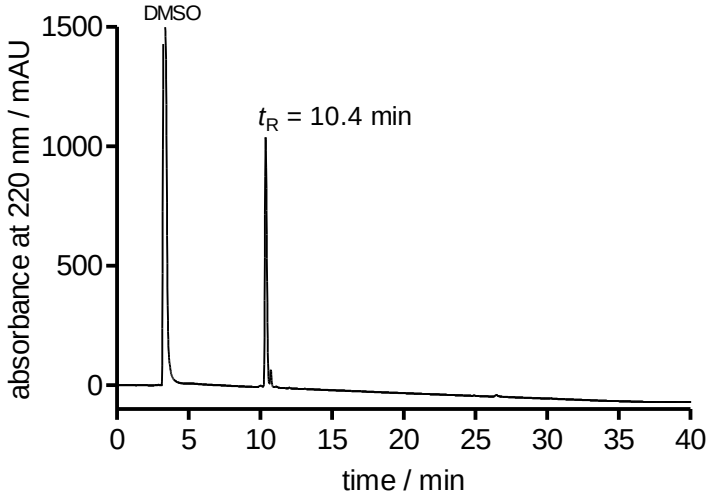

Figure App3.76. RP-HPLC analysis (purity control) of **4.90** (95%, 220 nm).

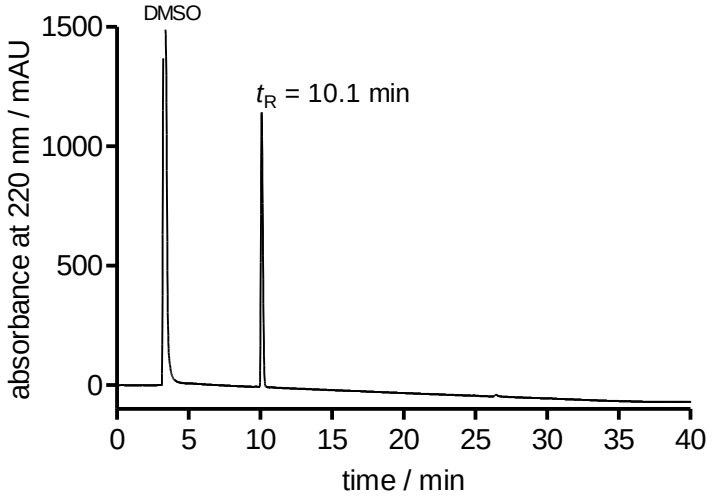

Figure App3.77. RP-HPLC analysis (purity control) of **4.91** (99%, 220 nm).

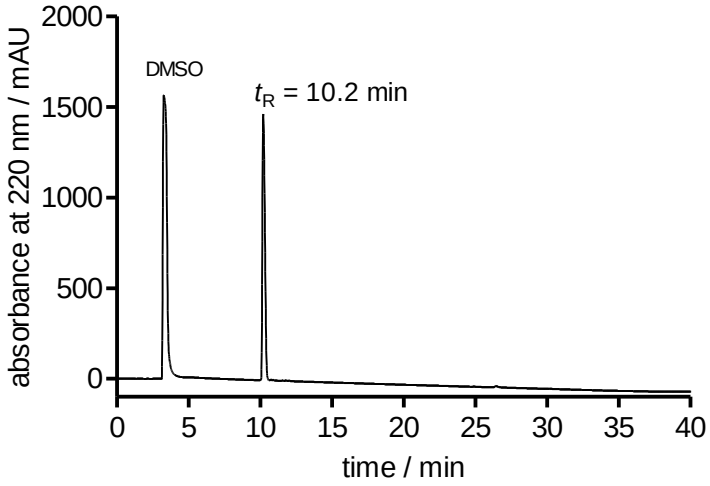

Figure App3.78. RP-HPLC analysis (purity control) of **4.92** (99%, 220 nm).

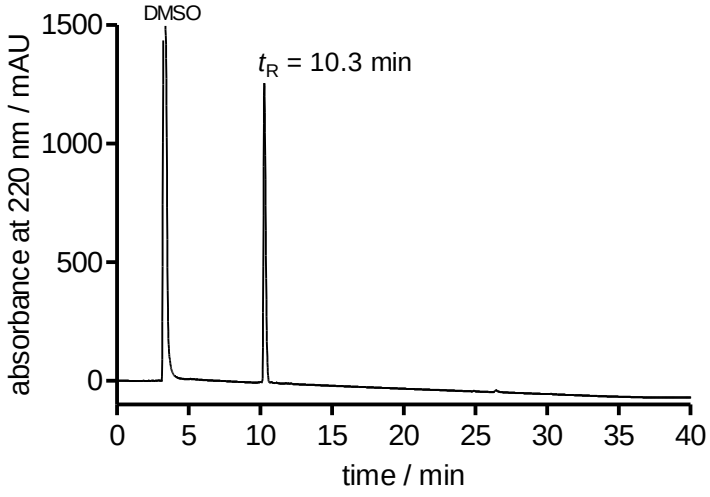

Figure App3.79. RP-HPLC analysis (purity control) of **4.93** (98%, 220 nm).

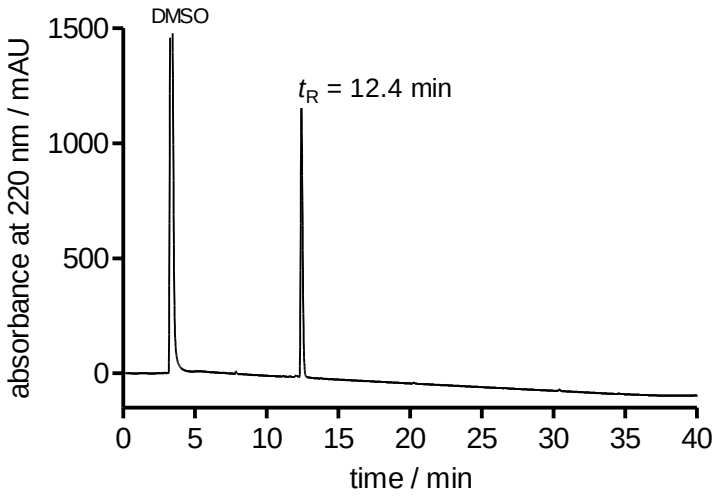

Figure App3.80. RP-HPLC analysis (purity control) of **4.94** (99%, 220 nm).

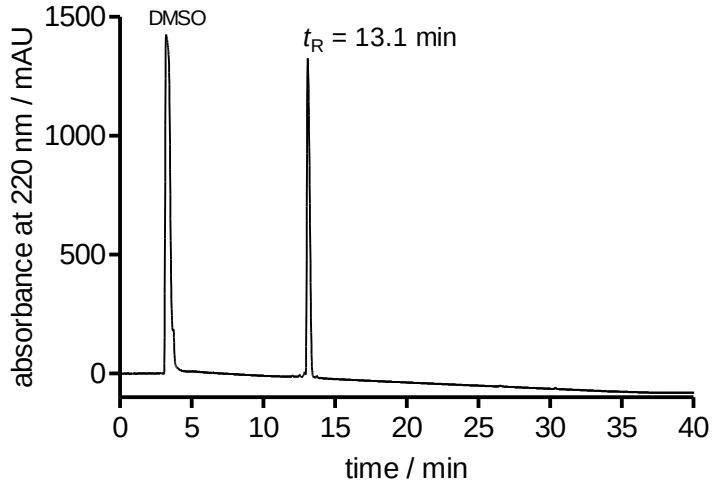

Figure App3.81. RP-HPLC analysis (purity control) of **4.95** (99%, 220 nm).

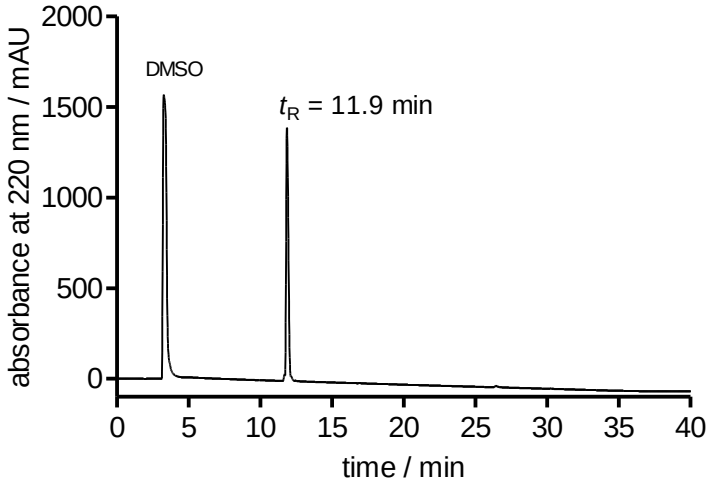

Figure App3.82. RP-HPLC analysis (purity control) of **4.96** (98%, 220 nm).

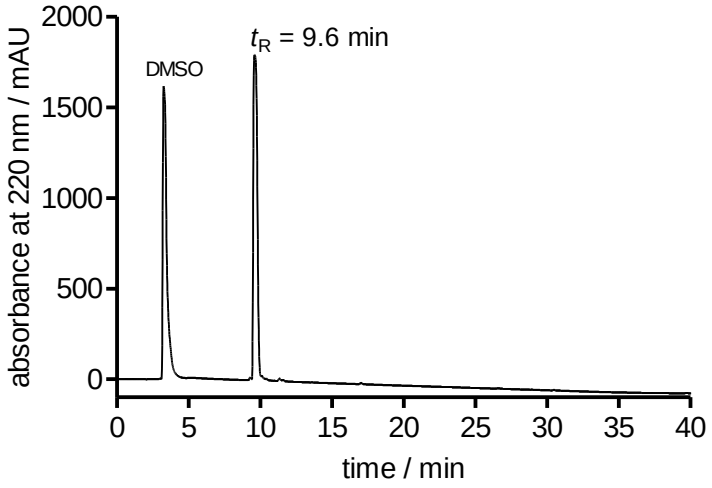

Figure App3.83. RP-HPLC analysis (purity control) of **4.98** (98%, 220 nm).

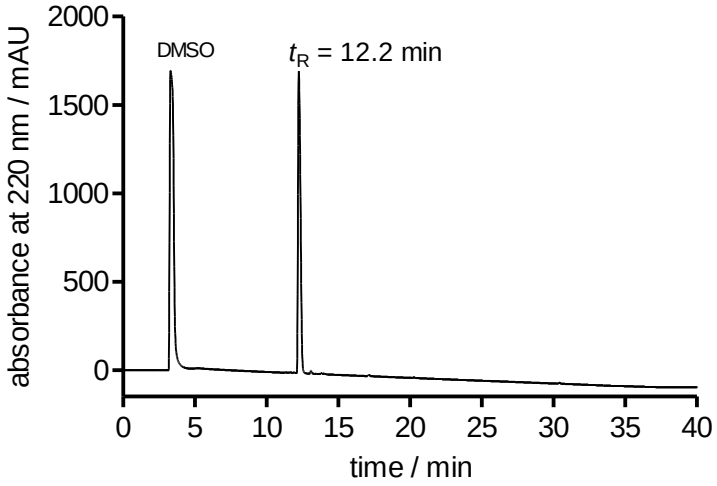

Figure App3.84. RP-HPLC analysis (purity control) of **4.104** (99%, 220 nm).

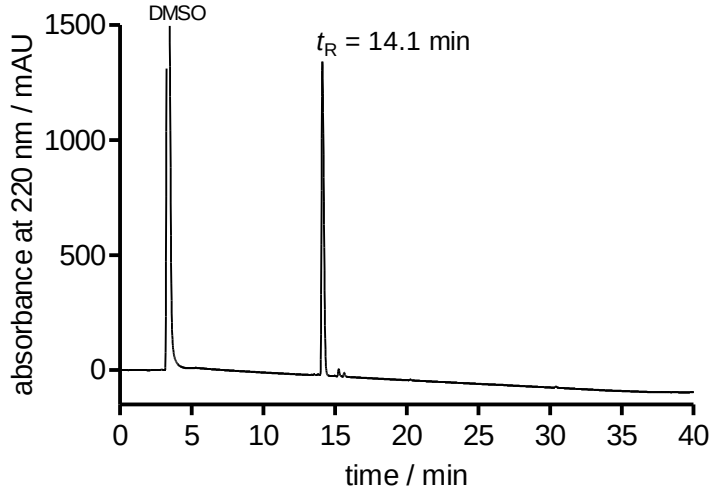

Figure App3.85. RP-HPLC analysis (purity control) of **4.105** (98%, 220 nm).

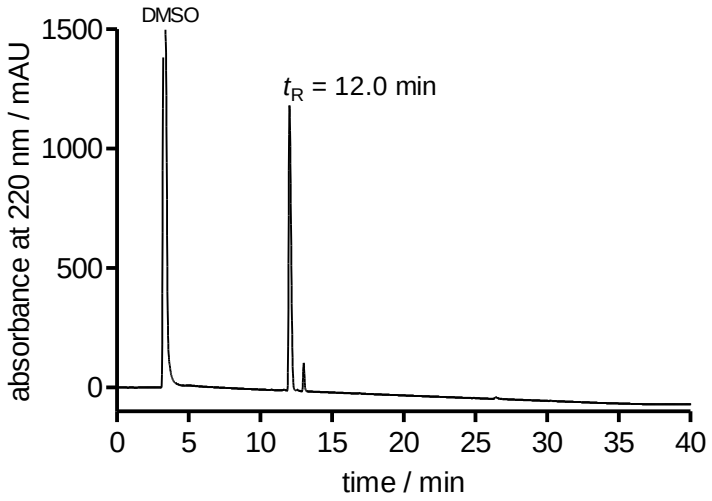

Figure App3.86. RP-HPLC analysis (purity control) of **4.106** (95%, 220 nm).

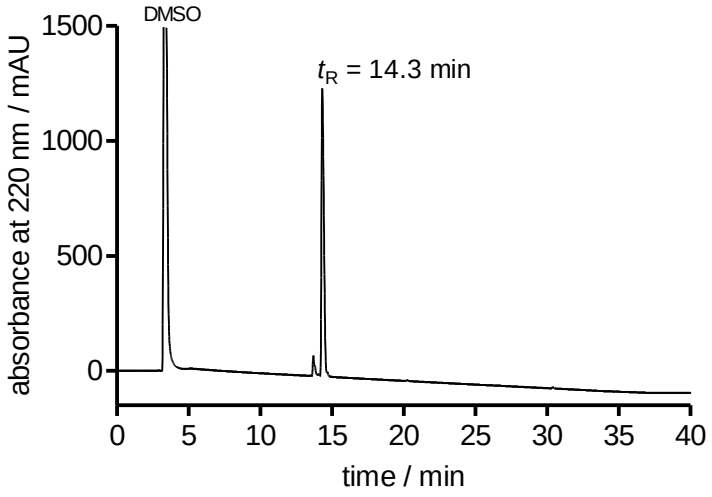

Figure App3.87. RP-HPLC analysis (purity control) of **4.107** (95%, 220 nm).

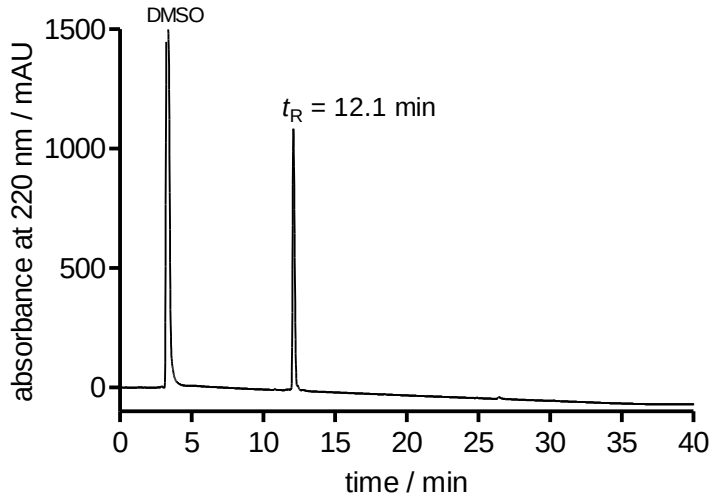

Figure App3.88. RP-HPLC analysis (purity control) of **4.108** (97%, 220 nm).

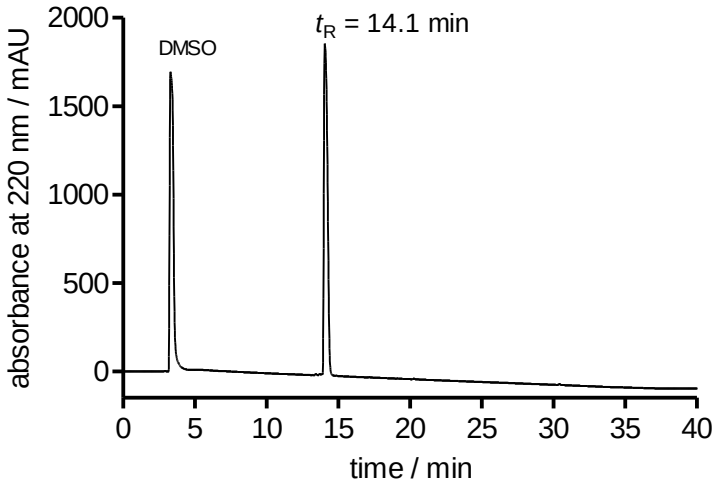

Figure App3.89. RP-HPLC analysis (purity control) of **4.109** (100%, 220 nm).

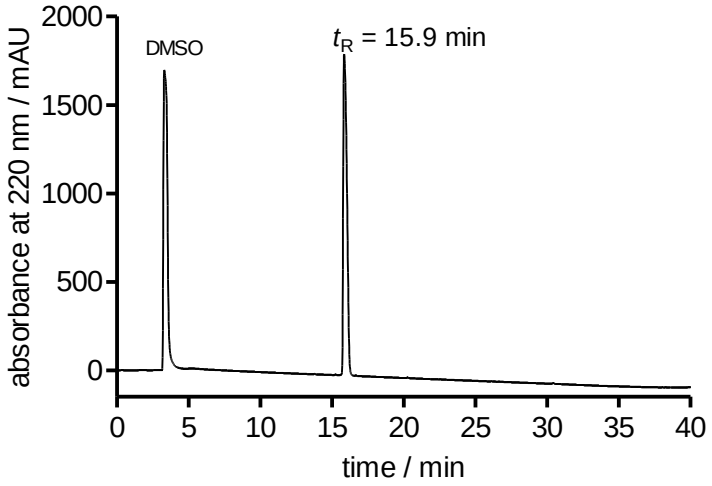

Figure App3.90. RP-HPLC analysis (purity control) of **4.110** (100%, 220 nm).

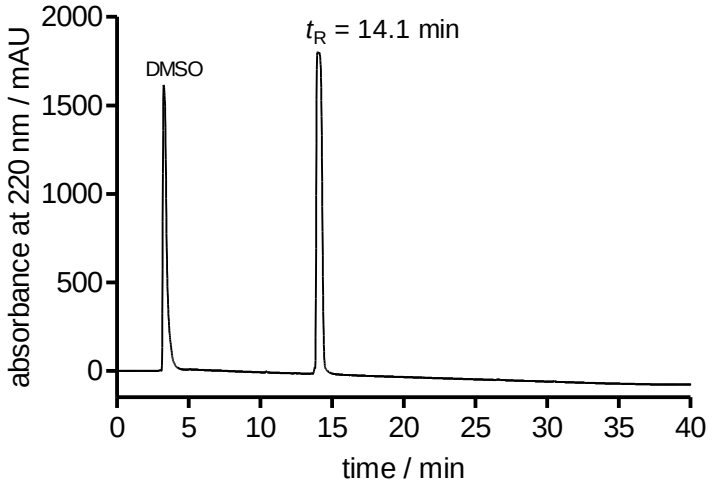

Figure App3.91. RP-HPLC analysis (purity control) of **4.112** (99%, 220 nm).

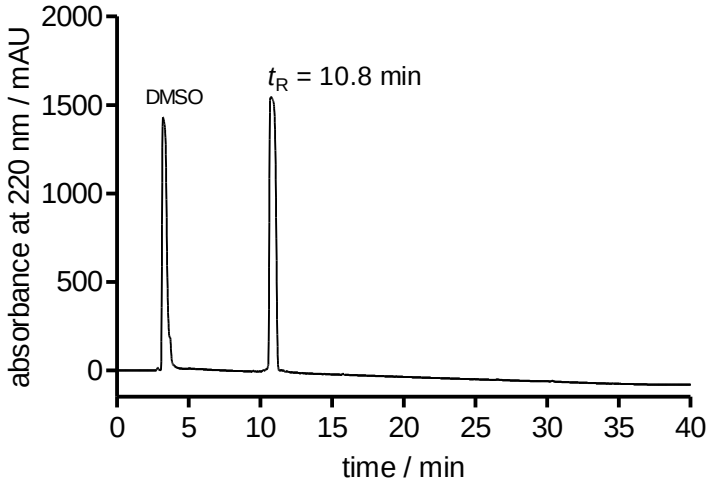

Figure App3.92. RP-HPLC analysis (purity control) of **4.114** (100%, 220 nm).

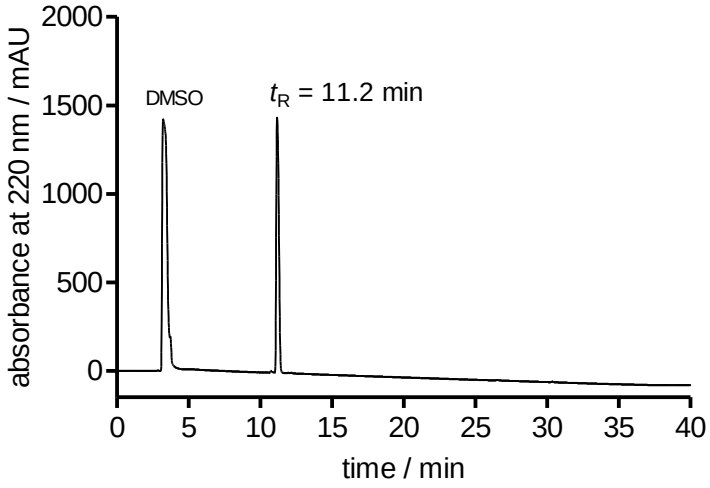

Figure App3.93. RP-HPLC analysis (purity control) of **4.115** (100%, 220 nm).

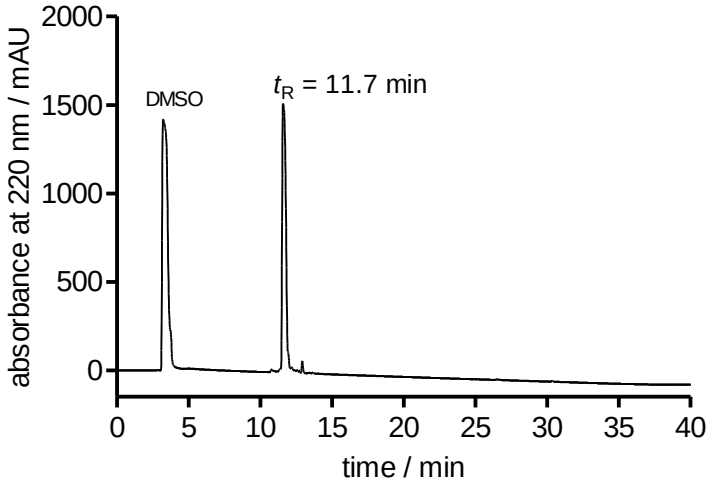

Figure App3.94. RP-HPLC analysis (purity control) of **4.116** (96%, 220 nm).

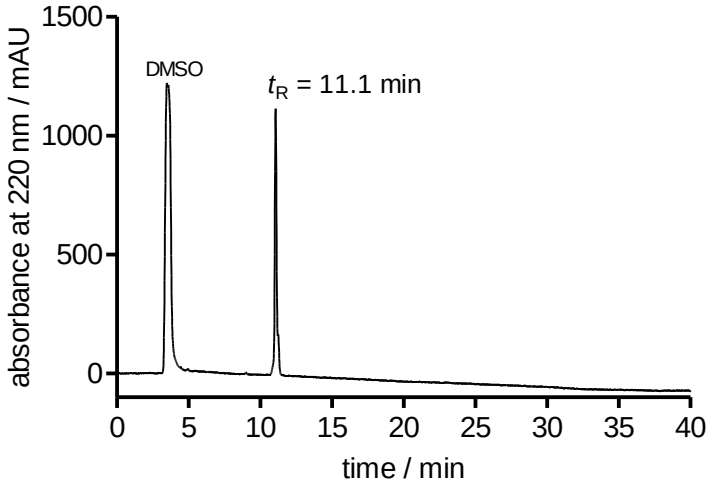

Figure App3.95. RP-HPLC analysis (purity control) of **4.117** (93%, 220 nm).

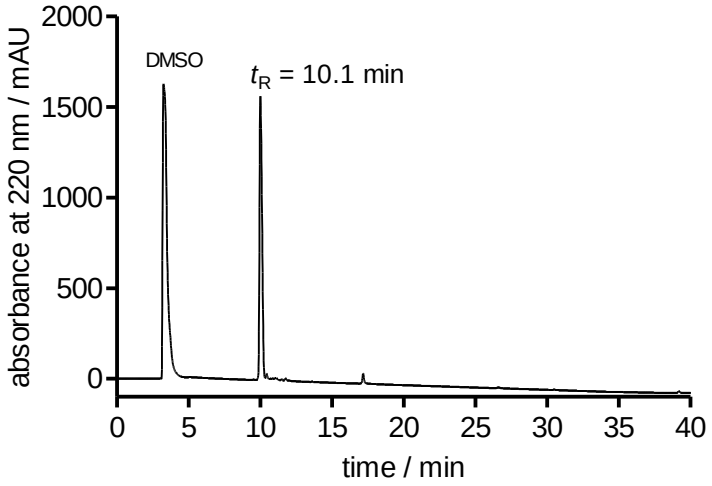

Figure App3.96. RP-HPLC analysis (purity control) of **4.120** (96%, 220 nm).

App3.3 Assay Curves of Selected Ligands 4.85, 4.86 (PB513), 4.88, 4.108, 4.110 and 4.114 (Radioligand Binding-, Mini-G Recruitment-, [^{35}S]GTPγS Binding- and β-Arrestin2 Recruitment Assays)

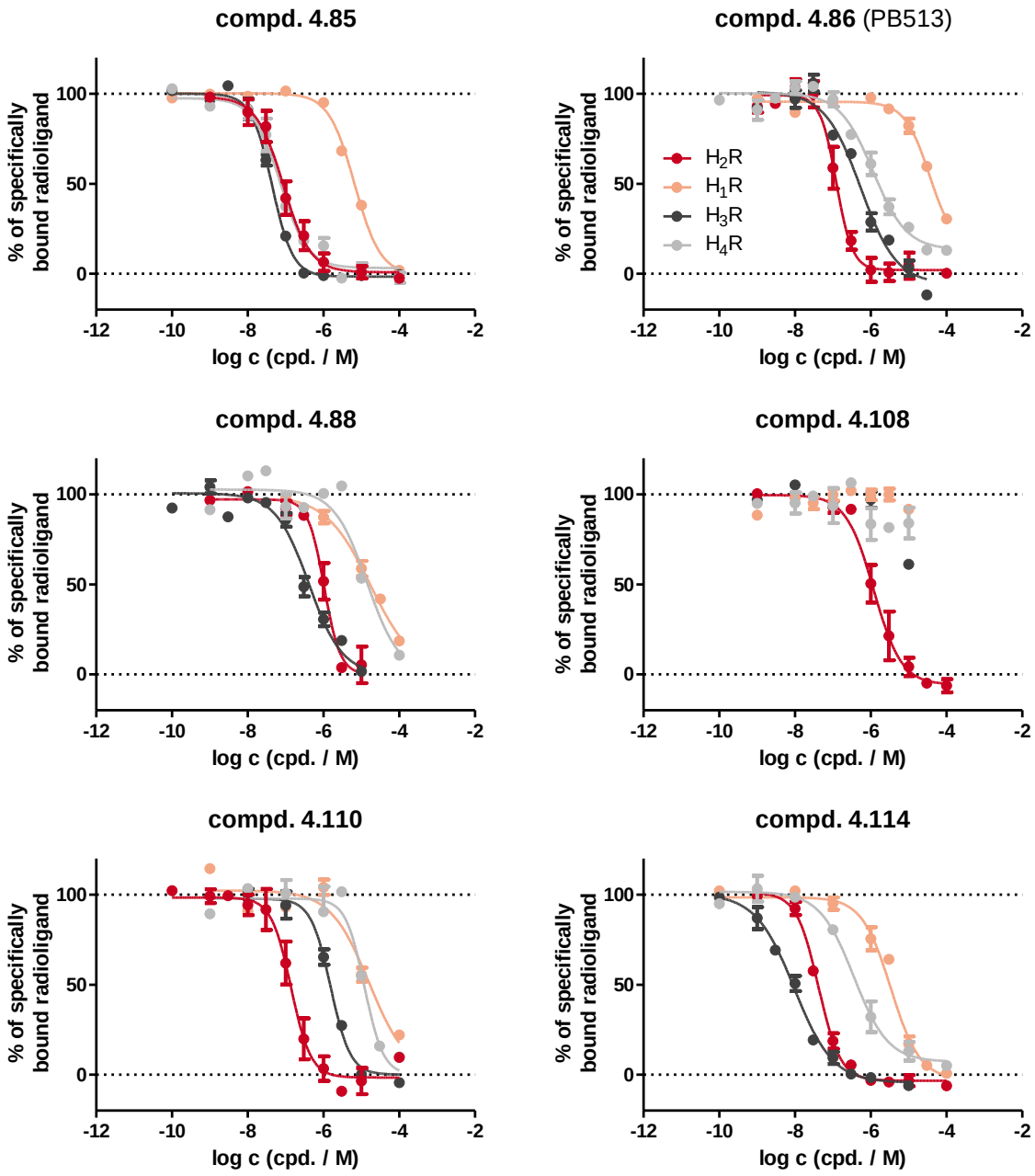

Figure App3.97. Displacement curves obtained from competition binding experiments with [^{3}H]mepyramine (hH$_1$R, c = 5 nM, K_d = 4.5 nM[1]), [^{3}H]UR-DE257[2] (hH$_2$R, c = 20 nM, K_d = 11.2 nM[3]), [^{3}H]UR-PI294[4] (hH$_3$R, c = 2 nM, K_d = 3 nM[5]) or [^{3}H]histamine (hH$_4$R, c = 30 nM, K_d = 47.5 nM[6]) and **4.85**, **4.86** (PB513), **4.88**, **4.108**, **4.110** and **4.114** at membranes of Sf9 cells expressing the hH$_1$R + RGS4, the hH$_2$R-G$_{s\alpha S}$, the hH$_3$R + G$_{\alpha i2}$ + G$_{\beta 1\gamma 2}$ or the hH$_4$R + G$_{\alpha i2}$ + G$_{\beta 1\gamma 2}$. Data represent mean values ± SEM from at least three independent experiments (performed in triplicate).

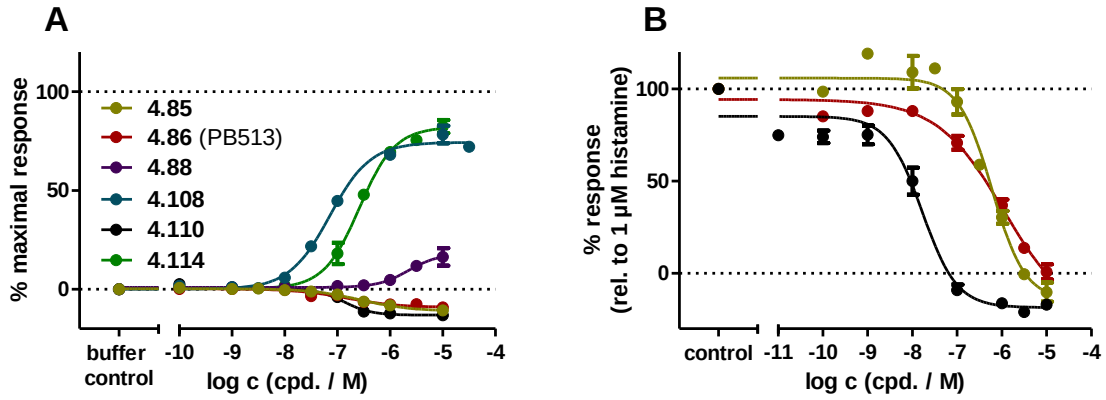

Figure App3.98. Concentration-response curves of representative 2-arylbenzimidazoles **4.85**, **4.86** (PB513[7]), **4.88**, **4.108**, **4.110** and **4.114** on hH_2R determined by mini-G protein recruitment assay using HEK293T NlucN-mGs/hH_2R-NlucC cells. **A**: The response was normalized to the maximum effect induced by 100 µM histamine (maximum response: 100%) and buffer control (maximum response: 0%). **B**: The response was normalized to the effect induced by 1 µM histamine (response: 100%) and buffer control (response: 0%). Data are presented as means ± SEM from at least three independent experiments, each performed in duplicate or triplicate.

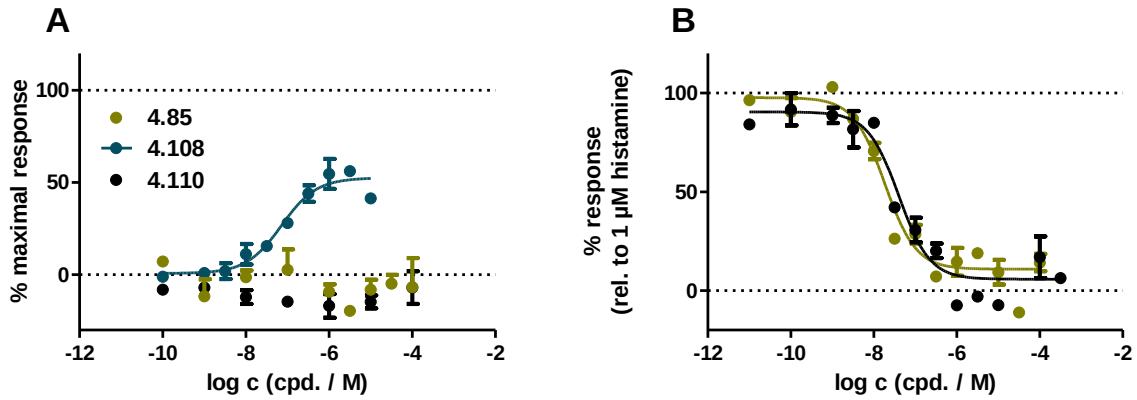

Figure App3.99. Concentration-response curves of representative 2-arylbenzimidazoles **4.85**, **4.108**, **4.110** and **4.114** on hH_2R determined by [^{35}S]GTPγS binding assay using membrane preparations of Sf9 insect cells expressing the hH_2R-$G_{s\alpha S}$ fusion protein. **A**: The response was normalized to the maximum effect induced by histamine (maximum response: 100%) and buffer control (maximum response: 0%). **B**: The response was normalized to the effect induced by 1 µM histamine (response: 100%) and buffer control (response: 0%). Data are presented as means ± SEM from at least three independent experiments, each performed in triplicate.

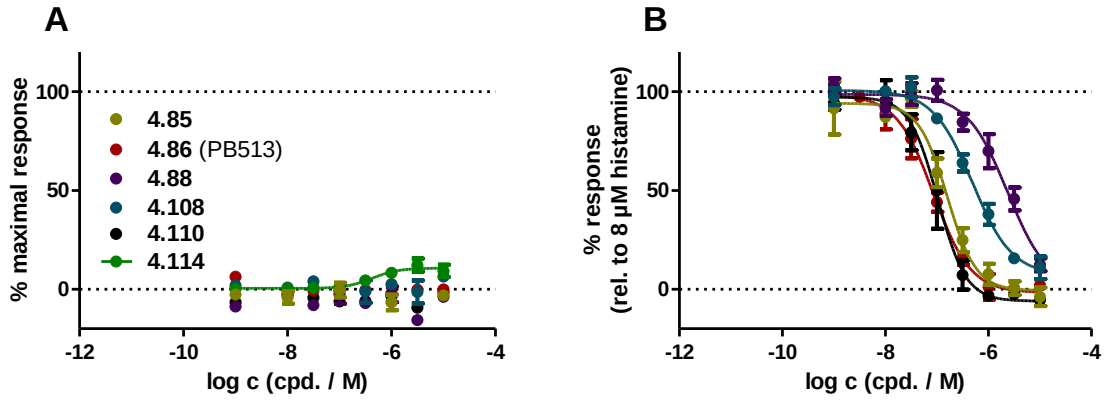

Figure App3.100. Concentration-response curves of representative 2-arylbenzimidazoles **4.85**, **4.86** (PB513[7]), **4.88**, **4.108**, **4.110** and **4.114** on hH_2R determined by β-arrestin2 recruitment assay using HEK293T-ARRB2-hH_2R cells. **A**: The response was normalized to the maximum effect induced by 100 µM histamine (maximum response: 100%) and buffer control (maximum response: 0%). **B**: The response was normalized to the effect induced by 8 µM histamine (response: 100%) and buffer control (response: 0%). Data are presented as means ± SEM from at least three independent experiments, each performed in duplicate or triplicate.

App3.4 References

1. Kagermeier, N.; Werner, K.; Keller, M.; Baumeister, P.; Bernhardt, G.; Seifert, R.; Buschauer, A., Dimeric carbamoylguanidine-type histamine H_2 receptor ligands: a new class of potent and selective agonists. *Bioorg. Med. Chem.* **2015,** *23*, 3957-3969.
2. Baumeister, P.; Erdmann, D.; Biselli, S.; Kagermeier, N.; Elz, S.; Bernhardt, G.; Buschauer, A., [^{3}H]UR-DE257: development of a tritium-labeled squaramide-type selective histamine H_2 receptor antagonist. *ChemMedChem* **2015,** *10*, 83-93.
3. Grätz, L.; Tropmann, K.; Bresinsky, M.; Müller, C.; Bernhardt, G.; Pockes, S., NanoBRET binding assay for histamine H_2 receptor ligands using live recombinant HEK293T cells. *Sci. Rep.* **2020,** *10, e13288*.
4. Igel, P.; Schnell, D.; Bernhardt, G.; Seifert, R.; Buschauer, A., Tritium-labeled N^1-[3-(1H-imidazol-4-yl)propyl]-N^2-propionylguanidine ([^{3}H]UR-PI294), a high-affinity histamine H_3 and H_4 receptor radioligand. *ChemMedChem* **2009,** *4*, 225-231.
5. Tropmann, K.; Höring, C.; Plank, N.; Pockes, S., Discovery of a G protein biased radioligand for the histamine H_2 receptor with reversible binding properties. *J. Med. Chem.* **2020,** *63*, 13090-13102.
6. Bartole, E.; Littmann, T.; Tanaka, M.; Ozawa, T.; Buschauer, A.; Bernhardt, G., [^{3}H]UR-DEBa176: a 2,4-diaminopyrimidine-type radioligand enabling binding studies at the human, mouse, and rat histamine H_4 receptors. *J. Med. Chem.* **2019,** *62*, 8338-8356.
7. Baumeister, P. Molecular Tools for G-Protein Coupled Receptors: Synthesis, Pharmacological Characterization and [^{3}H]-Labeling of Subtype-Selective Ligands for Histamine H_4 and NPY Y_2 Receptors. Ph. D. Thesis. University of Regensburg, 2014.

5 Abolishing Dopamine D_{2long}/D_3 Receptor Affinity of Subtype-Selective Carbamoylguanidine-Type Histamine H_2 Receptor Agonists

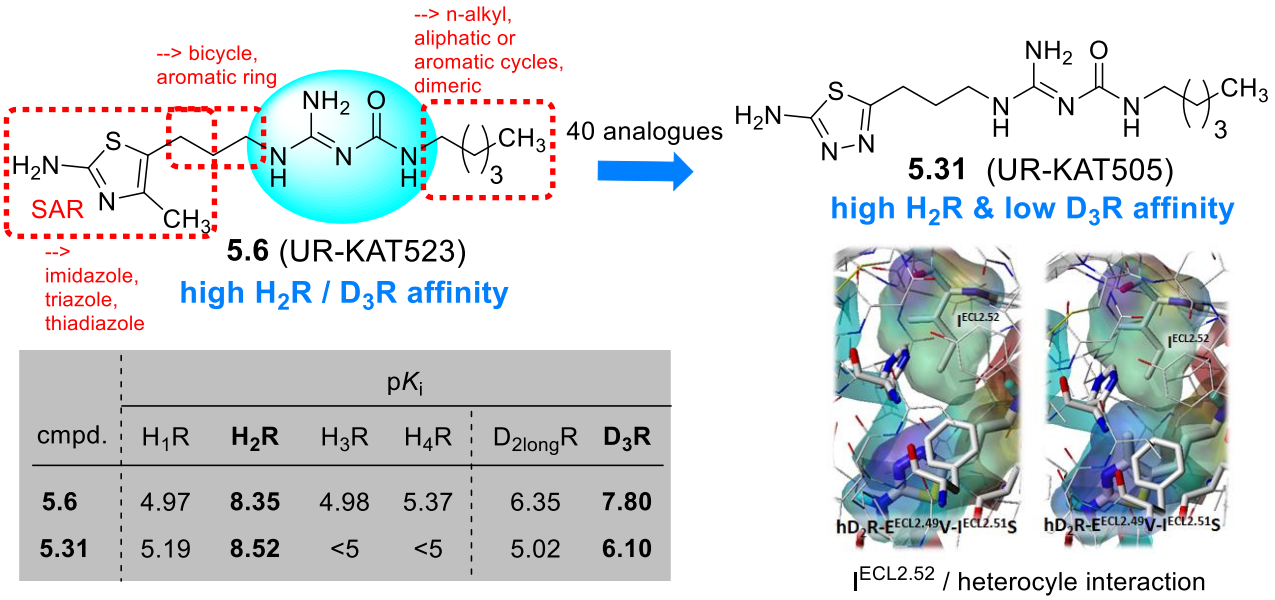

	pK_i					
cmpd.	H_1R	**H_2R**	H_3R	H_4R	$D_{2long}R$	**D_3R**
5.6	4.97	**8.35**	4.98	5.37	6.35	**7.80**
5.31	5.19	**8.52**	<5	<5	5.02	**6.10**

3-(2-Amino-4-methylthiazol-5-yl)propyl substituted carbamoylguanidines are potent, subtype-selective histamine H_2 receptor (H_2R) agonists, but their applicability as pharmacological tools to elucidate the largely unknown H_2R functions in the central nervous system (CNS) is compromised by their concomitantly high affinity towards dopamine D_2-like receptors (especially dopamine D_3 receptor (D_3R)). To improve the selectivity, a series of carbamoylguanidine-type ligands containing various heterocycles, spacers and side residues was rationally designed, synthesized, and tested in binding and/or functional assays at histamine H_{1-4} and dopamine $D_{2long/3}$ receptors. We observed that the selectivity of the ligands mainly depended on the heterocycle and on the type of the side residue which eventually led to the discovery of two promising candidate molecules (UR-KAT505 (**5.31**) and UR-KAT533 (**5.47**)). Docking studies suggest that the amino acid residues (3.28, 3.32, ECL2.49, ECL2.51, 5.42 and 7.35) are responsible for the different affinities at the H_2- and $D_{2long/3}$-receptors. These results provide a solid base for the exploration of the H_2R functions in the brain in further studies.

Prior to the submission of this thesis, this chapter has been submitted for publication: K. Tropmann, M. Bresinsky, L. Forster, A. Buschauer, H.-J. Wittmann, S. Pockes, and A. Strasser, Abolishing dopamine D_{2long}/D_3 receptor affinity of subtype-selective carbamoylguanidine-type histamine H_2 receptor agonists. *J. Med. Chem.* **2021**, submitted for publication.

Author contributions:

K.T. (**5.9-5.10**, **5.11** (Procedure A), **5.12**, **5.15-5.23**, **5.26-5.51** and **5.57-5.70**) and M.B. (**5.8**, **5.11** (Procedure B), **5.13-5.14**, **5.24-5.25** and **5.52-5.56**) performed the synthesis and analytical characterization of chemical compounds. K.T. performed the investigation of the chemical stability. M.B. determined the pK_a value for the 2-aminothiadiazole. K.T. (**5.30-5.51** and **5.57-5.70**) and M.B. (**5.52-5.56**) performed radioligand competition binding experiments at H_{1-4}Rs and analyzed the data. L.F. performed radioligand competition binding experiments at $D_{2long/3}$Rs and analyzed the data. K.T. performed the functional studies at H_2R and analyzed the data, with exception of guinea right atrium experiments, which were performed and analyzed by M.B. L.F. (**5.52-5.56**) and K.T. (**5.30-5.51** and **5.57-5.70**) performed and analyzed functional studies at $D_{2long/3}$Rs. H.J.W. and A.S. performed molecular docking and processed the data. A.B. and A.S. initiated and planned the project. S.P. and A.S. supervised the research. K.T., S.P. and A.S. wrote the manuscript.

5.1 Introduction

The histamine H_2 receptor (H_2R) has been subject of many research studies due to its versatile physiological properties.[5-6] The H_2R belongs to the class A G-protein-coupled receptors (GPCRs) and is expressed throughout the whole human body, most importantly in the stomach, heart, and central nervous system (CNS).[5-8] Activation of the H_2R by its endogenous ligand histamine (**5.1**, Figure 5.1A) leads to adenylyl cyclase activation by coupling to the Gs protein.[6] The central role of the H_2R in the stimulation of gastric acid secretion[6, 9] is the basis for the therapeutic use of H_2R antagonists to treat the gastroesophageal reflux disease and gastroduodenal ulcers.[5, 10] The function of the H_2R in the CNS is largely unknown, but includes, e.g. modulation of cognitive processes and circadian rhythm.[11] Furthermore, positive effects of the H_2-antagonist famotidine (**5.2**, Figure 5.1A) in schizophrenia and an improvement in L-DOPA-induced dyskinesia are reported in the literature.[11-19]

Starting from the H_2R agonists of the arpromidine (**5.3**, Figure 5.1A) series, several highly potent (up to 3000 times the potency of histamine) monomeric and dimeric H_2R agonists with acylguanidine or carbamoylguanidine partial structure were developed (**5.4**-**5.6**, Figure 5.1A).[2, 20-24] In contrast to acylguanidines, the carbamoylguanidines are chemically stable and possess an excellent selectivity over the other three histamine receptors ($H_{1,3,4}$) if a 2-aminothiazole ring is used for bioisosteric replacement of the imidazole ring (**5.5**-**5.6**, Figure 5.1A).[1, 22-23] Based on the existing knowledge about the physicochemical and/or pharmacokinetic properties of acyl- and carbamoylguanidines, we assume that carbamoylguanidines are also able to overcome the blood-brain barrier.[2, 20, 23, 25] This advantage over previously reported H_2R agonists (cf. guanidines, e.g. **5.3**, Figure 5.1A) should enable access to the H_2R in the CNS.[2, 20]

However, the 2-aminothiazole structural motif is also part of the dopamine receptor agonist pramipexole (**5.7**, Figure 5.1A), which is employed as a drug for the treatment of Parkinson's disease.[26-27] Due to these similarities, we assumed that H_2R agonists containing the 2-aminothiazole motif, might also bind to dopamine receptors. Indeed, we could prove this assumption during previous studies with radioligand binding experiments and we found that such H_2R agonists revealed a considerable affinity to dopamine receptors of the D_2-like family, in particular to the D_3 receptor.[23-24]

In order to use carbamoylguanidines as pharmacological tools to elucidate the H_2R functions in the CNS, we addressed the need to develop improved molecules which bind exclusively selective to the H_2 receptor. Thus, we herein report the synthesis and pharmacological characterization of these novel, subtype-selective H_2R ligands by variation of the carbamoylguanidine-based scaffold with different heterocycles, spacers, and side residues (Figure 5.1B).

The synthesized compounds were investigated for their functional activity at the H_2R and/or $D_{2long/3}R$ in minimal G (mini-G) protein- and/or β-arrestin2-recruitment assays as well as on the isolated spontaneously beating guinea pig (gp) right atrium in a more complex, but well-established standard model for the characterization of H_2R ligands.[5, 28] The selectivity for the human (h) H_2R over $hH_{1/3/4}R$ and $hD_{2long/3}R$ was evaluated in radioligand competition binding experiments. To support our investigations in silico, molecular docking studies were performed. We compared the binding of selected (4-methyl)thiazolyl- or thiadiazolyl-containing carbamoylguanidines to identify the amino acid residues that might be responsible for the different binding affinities of these ligands at the H_2- and $D_{2long/3}$-receptors.

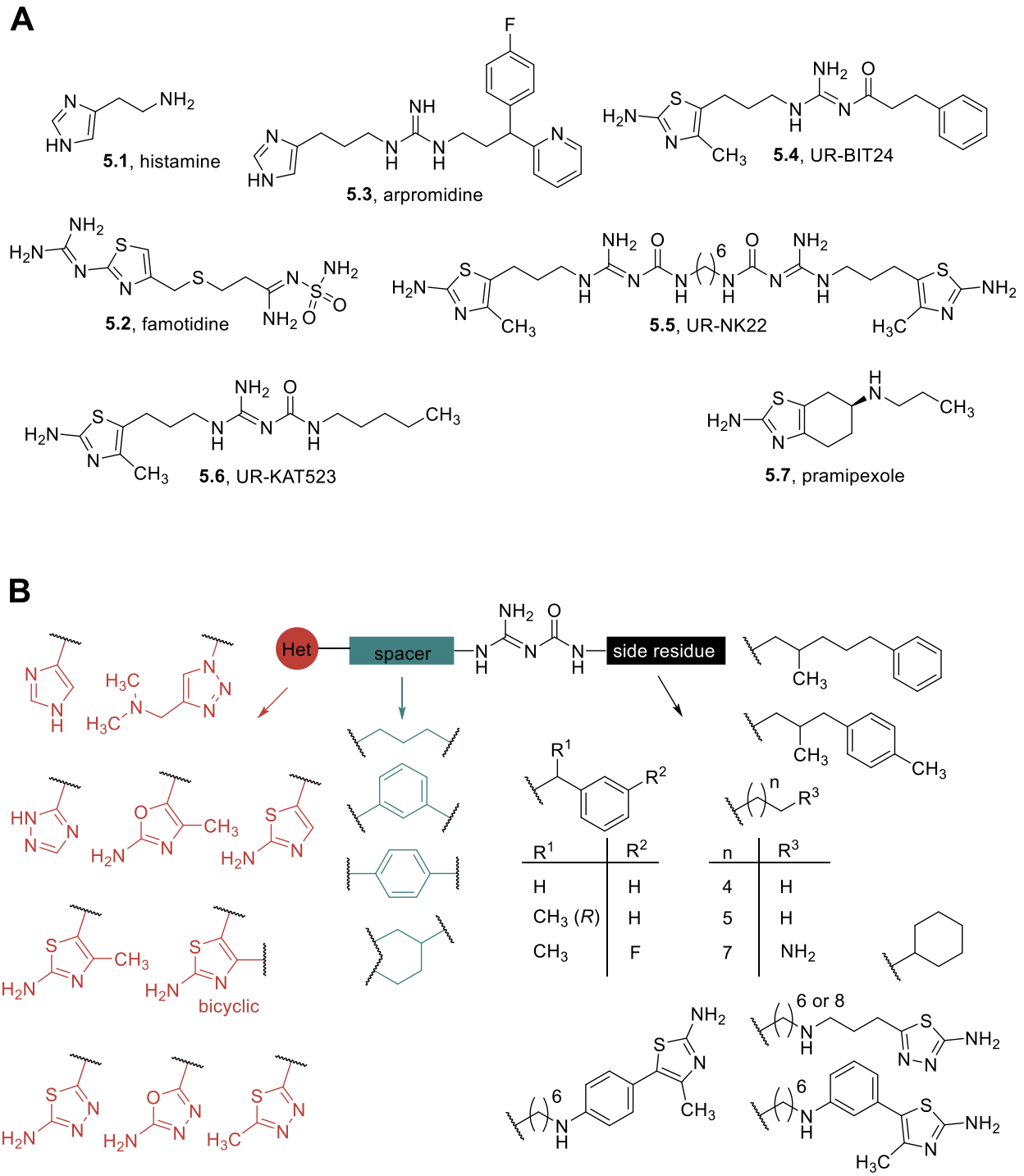

Figure 5.1. **A**: Structures of histamine (**5.1**), famotidine (**5.2**), arpromidine (**5.3**) and related prototypical acylguanidine-type (**5.4**) and carbamoylguanidine-type (**5.5-5.6**) H_2R agonists, as well as the D_2-like receptor agonist pramipexole (**5.7**). **B**: Structural modifications of N^G-carbamoylated guanidines resulting in the title compounds. Het: heterocycle.

5.2 Results and Discussion

5.2.1 Chemistry

The amines **5.8**-**5.17**[2, 20, 29-31] (Figure 5.2) and the guanidinylating reagents **5.18**-**5.29**[22-25] (Schemes 5.1 and 5.2) were synthesized as reported in the Appendix 4, App4.1 Experimental Details for the Amines **5.8**-**5.17** and the Guanidinylating Reagent **5.18**-**5.29** or in the literature. We chose several different side residues for the guanidinylating reagents **5.18**-**5.29**, which performed well in our recent studies about 2-aminothiazoles.[2, 20-25] The monomeric (Scheme 5.1) or dimeric (Scheme 5.2) carbamoylguanidine-type ligands were prepared by reacting the amines **5.8**-**5.17** with the guanidinylating reagents **5.18**-**5.29** in the presence of $HgCl_2$ and triethylamine (NEt_3).[32] Finally, the protected carbamoylguanidine-type intermediates were treated with TFA giving compounds **5.30**-**5.36**, **5.38**-**5.57** and **5.59**-**5.70** (Schemes 5.1 and 5.2), which were purified by preparative HPLC (acetonitrile (MeCN)/0.1% TFA in H_2O) or column chromatography (CH_2Cl_2/7 N NH_3 in MeOH) and subsequent recrystallization into the corresponding HCl salts. **5.37** and **5.58** were synthesized using a modified synthetic procedure (for details see the Experimental Section & the Appendix 4, Scheme App4.11).

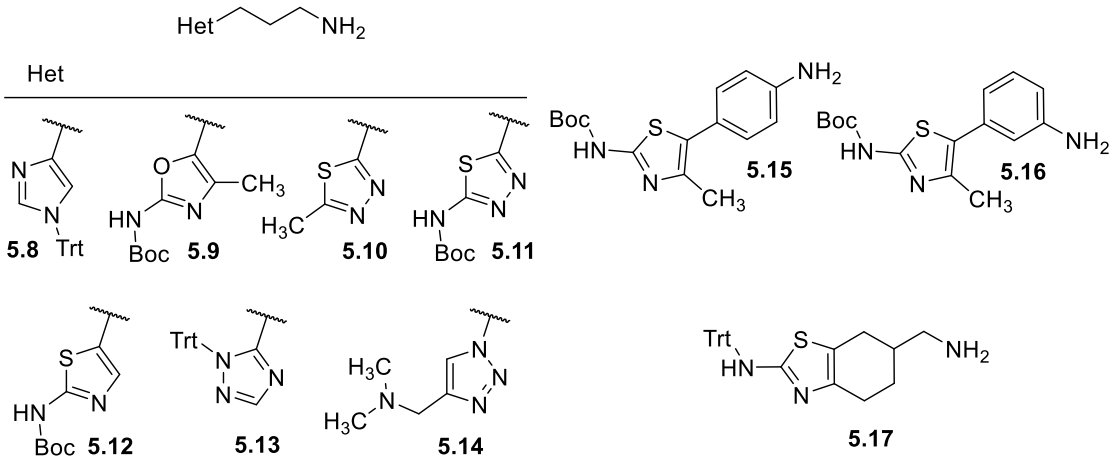

Figure 5.2. Structures of amines **5.8**-**5.17** used for the synthesis of monomeric (**5.30**-**5.36**, **5.38**-**5.57** and **5.59**-**5.66**) and dimeric (**5.67**-**5.70**) carbamoylguanidines. Het: heterocycle. For more details regarding **5.8**-**5.17** see Appendix 4, App4.1 Experimental Details for the Amines **5.8**-**5.17** and the Guanidinylating Reagent **5.18**-**5.29**.

Scheme 5.1. Synthesis of Monomeric Carbamoylguanidines 5.30-5.66[a]

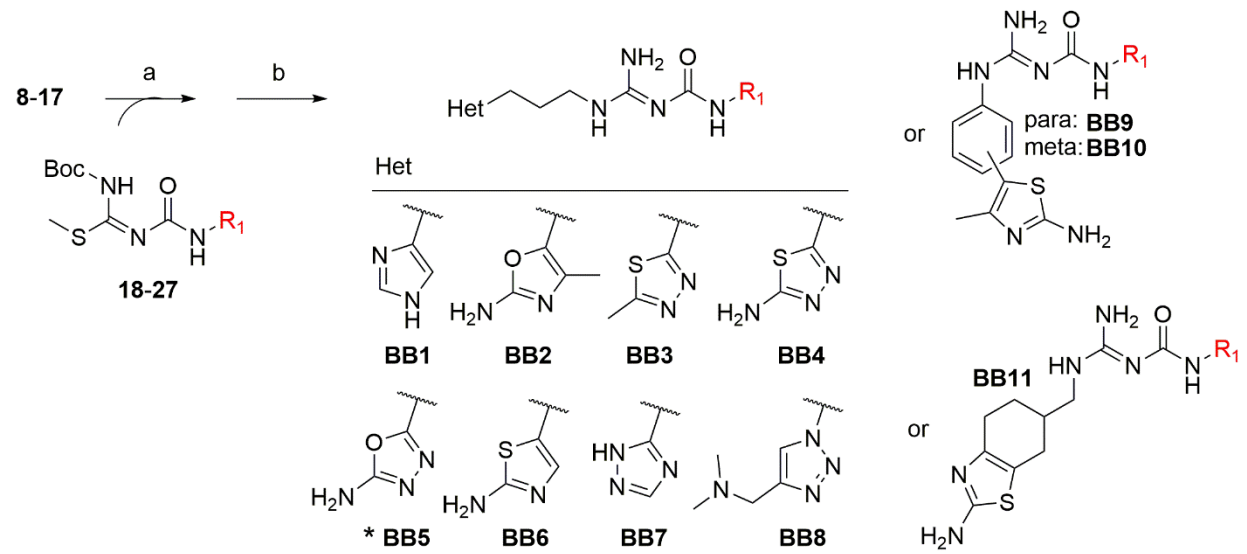

R_1:

- : **18**
BB3: **30** (34%)
BB4: **31** (19%)
BB6: **32** (26%)
BB9: **33** (45%)
BB10: **34** (48%)
BB11: **35** (22%)

- : **19**
BB4: **36** (18%)
BB5: **37** (6%)*

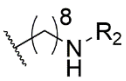

- , R_2 = Boc: **20**
BB3, R_2 = H: **38** (37%)
BB4, R_2 = H: **39** (26%)

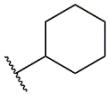

- : **21**
BB9: **40** (53%)

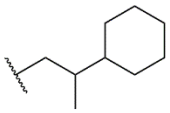

- : **22**
BB2: **41** (24%)
BB3: **42** (19%)
BB4: **43** (17%)
BB9: **44** (64%)

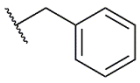

- : **23**
BB2: **45** (27%)
BB3: **46** (20%)
BB4: **47** (23%)
BB6: **48** (30%)
BB9: **49** (48%)
BB10: **50** (44%)
BB11: **51** (38%)

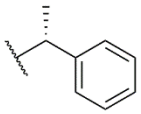

- : **24**
BB1: **52** (37%)
BB4: **53** (8%)
BB7: **54** (47%)
BB8: **55** (5%)

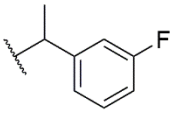

- : **25**
BB4: **56** (32%)

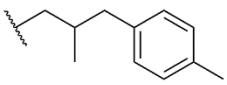

- : **26**
BB4: **57** (18%)
BB5: **58** (61%)*
BB6: **59** (23%)
BB9: **60** (55%)
BB10: **61** (34%)
BB11: **62** (16%)

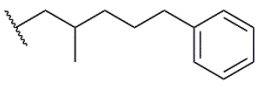

- : **27**
BB4: **63** (12%)
BB9: **64** (41%)
BB10: **65** (38%)
BB11: **66** (14%)

[a]Reagents and conditions: a) NEt_3, $HgCl_2$, CH_2Cl_2, rt, 4-48 h; (b) 30-70% TFA, CH_2Cl_2, rt, 7-18 h, 4-64% over two steps. Isolated yields over two steps are given in brackets. For more details regarding **5.8**-**5.27** see Appendix 4, App4.1 Experimental Details for the Amines **5.8**-**5.17** and the Guanidinylating Reagent **5.18**-**5.29**. *Modified synthetic procedure (see Experimental Section and Appendix 4, Scheme App4.11). BB: building block. Het: heterocycle. The target compounds **5.30**-**5.52**, **5.55** and **5.57**-**5.66** were obtained as TFA salts and **5.53**-**5.54** and **5.56** as HCl salts.

Scheme 5.2. Synthesis of the Dimeric N^G-Carbamoylated Guanidines 5.67-5.70[a]

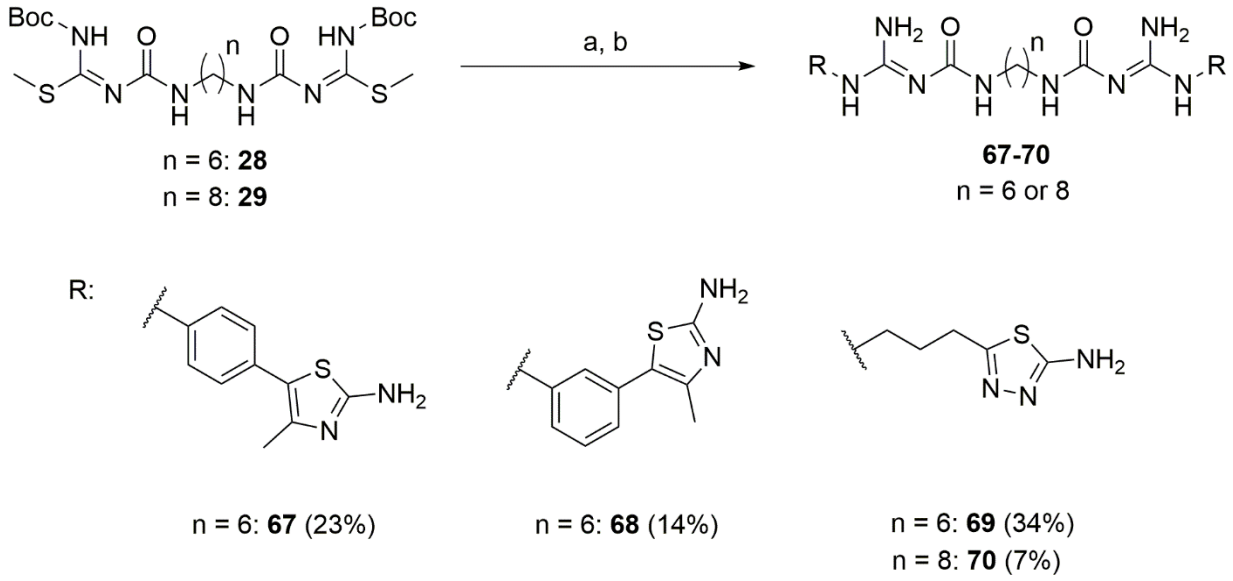

[a]Reagents and conditions: a) **5.11**, **5.15** or **5.16**, NEt_3, $HgCl_2$, CH_2Cl_2, rt, 8 h; (b) TFA, CH_2Cl_2, rt, 6-16 h, 7-23% over two steps. Isolated yields over two steps are given in brackets. For more details regarding **5.11**, **5.15**, **5.16** and **5.28**-**5.29** see Appendix 4, App4.1 Experimental Details for the Amines **5.8**-**5.17** and the Guanidinylating Reagent **5.18**-**5.29**.

5.2.2 Chemical Stability of Carbamoylguanidines

The chemical stability of selected compounds (**5.30-5.35**, **5.37**, **5.41** and **5.57**) was investigated in binding buffer[22] (pH 7.4) at room temperature (rt) over a time period of two weeks. Under these conditions, the investigated N^G-carbamoylated guanidines proved to be stable (for graphs see Figures 5.3 & 5.4, for details see Experimental Section).

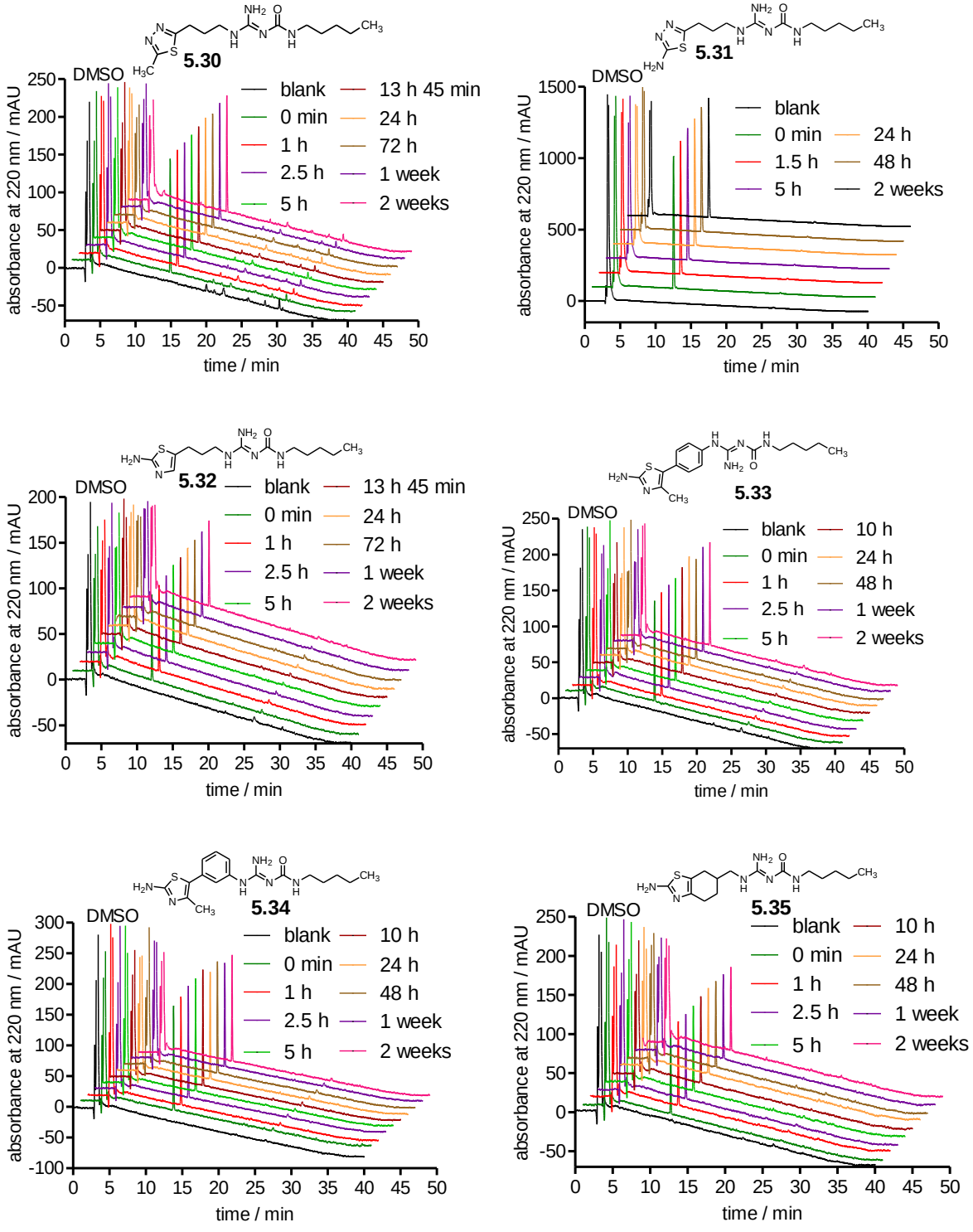

Figure 5.3. RP-HPLC chromatograms (chemical stability at room temperature in binding buffer) of **5.30**-**5.35** at 220 nm.

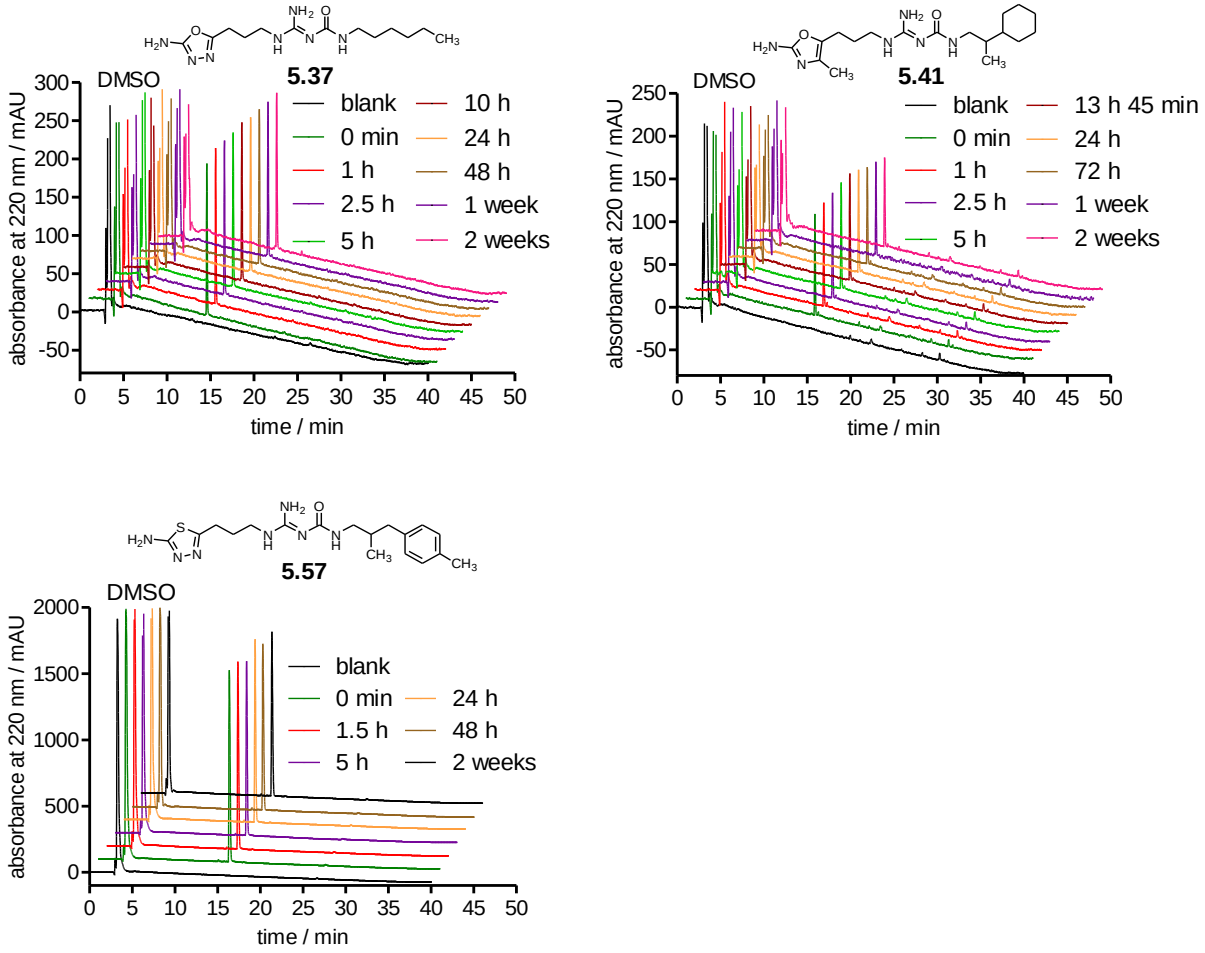

Figure 5.4. RP-HPLC chromatograms (chemical stability at room temperature in binding buffer) of **5.37**, **5.41** and **5.57** at 220 nm.

5.2.3 H_2R Affinity and Receptor Subtype Selectivity

The pK_i values of all target compounds were determined in competition binding studies on membrane preparations of Sf9 cells expressing the hH_2R-$G_{s\alpha S}$ fusion protein using the radioligand [^{3}H]UR-DE257[33] (Table 5.1). At first, we investigated the influence of the linker on the binding affinity. The conformationally restricted compounds (e.g. **5.33** (para, pK_i = 6.34), **5.34** (meta, pK_i = 6.72) and **5.35** (bicyclic, pK_i = 6.81), Table 5.1) bind well to the hH_2R albeit with lower affinities compared to their flexible (propyl linker) counterparts (e.g. **5.6**[23] (pK_i = 8.32[23]), Table 5.1).

Next, we investigated the influence of the heterocycle. The replacement of the sulfur atom in the 2-amino-4-methylthiazole by an oxygen atom resulted in decreased hH_2R affinity (e.g. oxazole: **5.45** ($pK_i = 6.41$) vs. thiazole UR-CH22[23-24] ($pK_i = 7.16$[23-24]), Table 5.1). The omission of the methyl group in position 4 of the heterocyclic ring did not cause a significant change in hH_2R affinity (**5.32**, **5.48** and **5.59** vs. **5.6**[23], UR-CH22[23-24] and UR-SB257[23-24], Table 5.1). However, the replacement of the amino(methyl)thiazole by a 2-amino-1,3,4-thiadiazole was favorable: the K_i-values of compounds **5.31** ($pK_i = 8.52$), **5.36** ($pK_i = 8.29$), **5.47** ($pK_i = 8.30$), **5.56** ($pK_i = 8.09$), and **5.57** ($pK_i = 8.19$) were in the single-digit nanomolar range (cf. Table 5.1). Also in case of the diazoles the substitution of the sulfur atom by an oxygen atom resulted in decreased hH_2R affinity (e.g. oxadiazole: **5.58** ($pK_i = 6.17$) vs. thiadiazole **5.57** ($pK_i = 8.19$), Table 5.1). The replacement of the free amine group in the 2-amino-1,3,4-thiadiazole by a methyl group (**5.30**, **5.38**, **5.42** and **5.46**) resulted in a dramatic decrease of hH_2R affinity (cf. Table 5.1), indicating that the heteroaromatic amine group is extremely important for high affinity. This observation was also supported by docking experiments (see molecular docking studies). Finally, using the reported 1H-1,2,4-triazole[31] or a more explorative 4-(dimethylamino)methyl-1,2,3-triazole instead of the 2-amino-4-methylthiazole resulted in decreased hH_2R affinities (1,2,4-triazole **5.54** ($pK_i = 7.27$) and 1,2,3-triazole **5.55** ($pK_i = 5.35$) vs. thiazole UR-Po563[23] ($pK_i = 7.75$[23]), Table 5.1).

It is literature known that dimeric ligands possess a significantly increased H_2R affinity (human or guinea pig).[1, 22] Therefore, we also synthesized several dimeric compounds, e.g. the 2-amino-1,3,4-thiadiazole heterocycle containing ligands **5.69** (hexyl-spacer, $pK_i = 8.28$, Table 5.1) and **5.70** (octyl-spacer, $pK_i = 8.32$, Table 5.1). However, no further increase in affinity could be achieved compared to the monomeric compounds **5.31** (pentyl, $pK_i = 8.52$, Table 5.1) and **5.36** (hexyl, $pK_i = 8.29$, Table 5.1).

The pK_i values of all synthesized compounds were also determined at the hH_1, hH_3 and hH_4 receptors on membranes of Sf9 cells expressing the respective histamine receptor using the radioligands [^{3}H]mepyramine (hH_1R), [^{3}H]N^{α}-methylhistamine or [^{3}H]UR-PI294[34] (hH_3R) and [^{3}H]**5.1** (hH_4R, cf. Table 5.1). The imidazole-containing ligand **5.52** was synthesized as control compound to showcase that the subtype selectivity is largely influenced by the heterocycle. Unsurprisingly, despite a high affinity at the H_2R, it bound similarly well or even better to the H_3R and H_4R. In contrast, neither of the 2-amino-1,3,4-thiadiazoles (**5.31**, **5.36**, **5.43**, **5.47**, **5.53**, **5.56**, **5.57**, **5.63**, **5.69** and **5.70**) displayed remarkable affinity to the hH_1, hH_3, or hH_4 receptors leading

to at least 100-fold selectivity for the hH_2R (cf. Table 5.1). The only exception among the thiadiazoles was observed for compound **5.39**, which contains the 8-aminooctyl side chain. Within the synthesized series, compound **5.31** showed the highest affinity (pK_i = 8.52, Table 5.1) and subtype selectivity (ratio of K_i $H_1R/H_3R/H_4R$ of 2138 : >3311 : >3311, Table 5.1).

Table 5.1. Binding Data of the Compounds 5.30-5.70 on Human Histamine Receptor Subtypes[a]

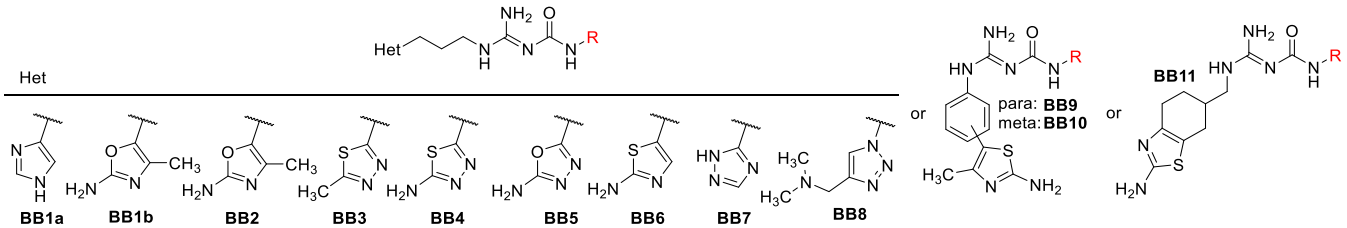

compd.	structure		pK_i								H_2R selectivity $K_i(H_xR)/K_i(H_2R)$, x=1,3,4		
	BB	R	hH_1R[b]	N	hH_2R[c]	N	hH_3R[d,e]	N	hH_4R[f]	N	H_1	H_3	H_4
5.1	-	-	5.62 ± 0.03[35]	4	6.58 ± 0.04[36]	48	7.59 ± 0.01[35]	42	7.60 ± 0.01[35]	45	9	0.1	0.1
5.7	-	-	n.d.	-	4.86 ± 0.07[23]	-	n.d.	-	n.d.	-	-	-	-
5.6[23]	1b		4.97 ± 0.10[23]	3	8.35 ± 0.08[23]	3	4.98 ± 0.17[23]	3	5.37 ± 0.09[23]	3	2399	2344	955
5.30	3		<5	3	5.66 ± 0.15	3	<5[e]	3	<5	3	>5	>5	>5
5.31 (UR-KAT505)	4		5.19 ± 0.05	3	8.52 ± 0.16	3	<5[e]	3	<5	3	2138	>3311	>3311
5.32 (UR-KAT583)	6	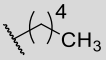	5.02 ± 0.03	3	7.64 ± 0.07	3	<5[e]	3	<5	3	417	>437	>437
5.33	9		5.43 ± 0.09	3	6.34 ± 0.06	3	4.94 ± 0.06 [d,e]	3	5.11 ± 0.04	3	8	25	17
5.34	10		5.18 ± 0.09	3	6.72 ± 0.03	3	5.02 ± 0.07[e]	3	5.13 ± 0.05	3	35	50	39
5.35	11		5.28 ± 0.10	3	6.81 ± 0.07	3	5.18 ± 0.15[d,e]	3	5.23 ± 0.04	3	34	43	38
UR-CH20[23-24]	1b		5.11 ± 0.03[23-24]	3	7.54 ± 0.07[23-24]	4	5.25 ± 0.02[23-24]	3	5.09 ± 0.02[23-24]	2	269	195	282
5.36	4	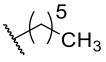	5.30 ± 0.09	3	8.29 ± 0.20	3	<5[e]	3	<5	3	977	>1950	>1950
5.37	5		5.05 ± 0.06	3	6.41 ± 0.01	3	<5[e]	3	<5	3	23	>26	>26

Table 5.1. (continued)

5.38	3	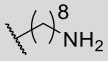	6.51 ± 0.19	3	5.74 ± 0.14	3	4.93 ± 0.18[e]	3	<5	3	0.2	7	>5
5.39	4		6.28 ± 0.09	3	7.48 ± 0.14	3	<5[e]	3	<5	3	16	>302	>302
5.40	9		5.26 ± 0.17	3	6.26 ± 0.14	3	4.91 ± 0.09 [d,e]	3	5.16 ± 0.07	3	10	22	13
UR-SB291[23-24]	1b		5.63 ± 0.06[23-24]	3	7.40 ± 0.01[23-24]	2	5.00 ± 0.08[23-24]	3	5.72 ± 0.05[23-24]	3	59	251	48
5.41	2		5.22 ± 0.04	3	6.61 ± 0.08	3	5.08 ± 0.11[e]	3	5.12 ± 0.07	3	25	34	31
5.42	3		5.15 ± 0.01	3	5.98 ± 0.12	3	4.94 ± 0.06	3	<5	3	7	11	>10
5.43	4		5.13 ± 0.06	3	7.71 ± 0.14	4	5.56 ± 0.10[e]	3	4.90 ± 0.12	3	380	141	646
5.44	9		5.54 ± 0.13	3	6.51 ± 0.10	3	5.25 ± 0.05[e]	3	5.11 ± 0.04	3	9	18	25
UR-CH22[23-24]	1b		5.21 ± 0.02[23-24]	3	7.16 ± 0.05[23-24]	3	4.71 ± 0.05[23-24]	3	4.72 ± 0.09[23-24]	2	89	282	275
5.45	2		5.05 ± 0.06	3	6.41 ± 0.11	3	<5[e]	3	<5	3	23	>26	>26
5.46	3		4.97 ± 0.08	3	5.25 ± 0.15	3	<5[e]	3	<5	3	2	>2	>2
5.47 (UR-KAT533)	4		5.27 ± 0.12	3	8.30 ± 0.07	3	<5[e]	3	<5	3	1072	>1995	>1995
5.48	6		5.25 ± 0.01	3	7.57 ± 0.07	3	<5[e]	3	<5	3	209	>372	>372
5.49	9		5.89 ± 0.03	3	6.67 ± 0.05	3	5.07 ± 0.10[d,e]	3	4.92 ± 0.14	3	6	40	56
5.50	10		5.14 ± 0.14	3	6.52 ± 0.13	3	<5[e]	3	<5	3	24	>33	>33
5.51	11		5.41 ± 0.12	3	6.52 ± 0.02	3	4.95 ± 0.06[d]	3	5.23 ± 0.02	3	13	37	19
UR-Po563[23]	1b		5.06 ± 0.05[23]	3	7.75 ± 0.05[23]	3	4.36 ± 0.04[23]	3	4.87 ± 0.01[23]	3	490	2455	759
5.52	1a		5.40 ± 0.04	3	8.21 ± 0.09	3	8.77 ± 0.02[e]	3	8.07 ± 0.06	3	646	0.3	1
5.53	4		<5	3	7.89 ± 0.06	3	<5[e]	3	<5	3	>776	>776	>776
5.54	7		5.10 ± 0.05	3	7.27 ± 0.07	3	<5[e]	3	<5	3	148	>186	>186

Table 5.1. (continued)

5.55	8		<5	3	5.35 ± 0.02	3	4.99 ± 0.02[e]	3	<5	3	>2	2	>2
UR-MB-69[23]	1b		5.11 ± 0.10[23]	3	8.69 ± 0.10[23]	3	4.41 ± 0.06[23]	3	4.88 ± 0.01[23]	3	3802	19055	6457
5.56 (UR-MB-165)	4		4.98 ± 0.02	3	8.09 ± 0.03	3	<5[e]	3	<5	3	1288	>1230	>1230
UR-SB257[23-24]	1b	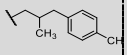	5.78 ± 0.13[23-24]	3	7.14 ± 0.08[23-24]	2	5.49 ± 0.01[23-24]	3	5.44 ± 0.02[23-24]	3	23	45	50
5.57	4		5.87 ± 0.12	3	8.19 ± 0.11	3	5.63 ± 0.11[e]	3	5.16 ± 0.11	3	209	363	1072
5.58	5		5.57 ± 0.09	3	6.17 ± 0.08	3	5.04 ± 0.03[e]	3	<5	3	4	13	>15
5.59	6		5.60 ± 0.05	3	7.19 ± 0.14	3	5.32 ± 0.11[e]	3	5.35 ± 0.11	3	39	74	69
5.60	9		5.74 ± 0.14	4	6.48 ± 0.04	3	5.08 ± 0.07[d,e]	3	5.20 ± 0.03	3	5	25	19
5.61	10		5.28 ± 0.18	3	6.63 ± 0.06	3	4.89 ± 0.13[e]	3	5.13 ± 0.06	3	22	45	32
5.62	11		6.74 ± 0.12	3	6.97 ± 0.03	3	5.71 ± 0.10[d]	3	5.47 ± 0.10	3	2	18	32
UR-KAT527[2][3-24]	1b		5.15 ± 0.07[23-24]	3	7.22 ± 0.05[23-24]	3	5.64 ± 0.08[23-24]	3	6.11 ± 0.13[23-24]	3	117	38	13
5.63	4		5.29 ± 0.08	3	7.82 ± 0.11	3	5.40 ± 0.13[e]	3	5.31 ± 0.16	3	339	263	324
5.64	9	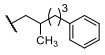	5.12 ± 0.11	3	6.50 ± 0.05	3	5.10 ± 0.11[d,e]	3	5.22 ± 0.03	3	24	25	19
5.65	10		4.88 ± 0.15	3	6.63 ± 0.07	3	4.97 ± 0.10[e]	3	5.15 ± 0.03	3	56	46	30
5.66	11		5.41 ± 0.08	3	6.96 ± 0.19	3	5.76 ± 0.13[d,e]	3	5.39 ± 0.11	3	35	16	37
5.5[22]	1b		6.06 ± 0.05[22]	-	8.07 ± 0.05[22]	-	5.94 ± 0.16[22]	-	5.69 ± 0.07[22]	-	102	135	240
5.67	9	dimeric 	5.67 ± 0.14	3	6.46 ± 0.18	3	5.71 ± 0.09[e]	3	5.67 ± 0.10	3	6	6	6
5.68	10		5.84 ± 0.03	3	6.42 ± 0.02	3	6.15 ± 0.04[e]	3	5.63 ± 0.04	3	4	2	6
5.69	4		5.45 ± 0.08	3	8.28 ± 0.13	3	5.00 ± 0.06[e]	3	<5	3	676	1905	>1905
5.70	4	dimeric 	5.74 ± 0.08	3	8.32 ± 0.11	3	5.16 ± 0.06[e]	3	5.05 ± 0.07	3	380	1445	1862

Table 5.1. (continued)

[a]Radioligand competition binding assay using membrane preparations of Sf9 cells expressing the hH_1R + RGS4, the hH_2R-$G_{s\alpha S}$, the hH_3R + $G_{\alpha i2}$ + $G_{\beta 1\gamma 2}$ or the hH_4R + $G_{\alpha i2}$ + $G_{\beta 1\gamma 2}$. Data represent mean values ± SEM of N independent experiments, each performed in triplicate. [b]Displacement of 5 nM [^{3}H]mepyramine (K_d = 4.5 nM[22]). [c]Displacement of 20 nM [^{3}H]UR-DE257[33] (K_d = 12.1 nM[37]). [d]Displacement of 8.6 nM [^{3}H]N^{α}-methylhistamine (K_d = 3 nM[35]). [e]Displacement of 2 nM [^{3}H]UR-PI294[34] (K_d = 3 nM[25]). [f]Displacement of 15 nM [^{3}H]**5.1** (K_d = 16 nM[35]). n.d.: not determined.

5.2.4 $D_{2long}R$ and D_3R Affinities of N^G-Carbamoylated Guanidines

N^G-carbamoylated guanidines with a pK_i value >7.0 at the hH_2R were investigated for their affinities to the hD_{2long}- and hD_3 receptors in radioligand binding assays on homogenates of HEK293T-CRE-Luc cells co-expressing the respective receptor (Table 5.2). Compounds containing the 2-aminothiazole heterocycle without a methyl group in position 4 (**5.32**, **5.48** and **5.59**) still showed high to moderate affinities to the $hD_{2long/3}$ receptors, especially to the hD_3R (cf. Table 5.2). The determined $hD_{2long/3}$ receptor affinities were comparable to affinities published for 2-amino(4-methyl)thiazoles.[23] Fortunately, compounds containing the 2-amino-1,3,4-thiadiazole or the 1*H*-1,2,4-triazole heterocycle displayed only low affinity to the hD_{2long}- and hD_3 receptors. We observed that some of them (**5.31**, **5.36**, **5.47**, **5.53**-**5.54** and **5.57**) showed even more than a 100-fold selectivity for the hH_2R over the hD_{2long} and hD_3 receptors (cf. Table 5.2). This trend indicates that the nitrogen in the 4 position might be responsible for the lower affinity to the hD_3R (for more details see docking results; Figure 5.6D). In addition to the effect of the heterocycle, the side residue played an important role for the dopamine $hD_{2long/3}$ receptor affinities. For example, thiadiazoles **5.43** (2-cyclohexylpropyl side residue) and **5.63** (2-methyl-5-phenylpentyl side residue) still had a moderate affinity for the $hD_{2long/3}$ receptors, which might indicate an additional (hydrophobic) interaction in the binding pocket of $D_{2long/3}$ receptors (not further investigated). Finally, the dimeric ligand **5.69** also possessed a high hD_{2long}- and hD_3 receptor affinity compared to the corresponding monomeric ligands **5.31** and **5.36** (cf. Table 5.2). Therefore, **5.70**, being also a dimeric ligand, was not further investigated. **5.39** and **5.52** were, despite their high H_2R affinity, also excluded from additional experiments due to their low subtype selectivity (cf. Table 5.1).

In summary, although many ligands (**5.31**, **5.36**, **5.47**, **5.53**-**5.54** and **5.57**) showed a decent selectivity for the hH_2R over the hD_{2long}- and hD_3 receptors (ratios of K_i >100), **5.31** and **5.47** turned out to be the most promising candidates due to their excellent selectivity profiles.

Table 5.2. Binding Data of the Selected N^G-Carbamoylated Guanidines on Human Dopamine D_{2long} and D_3 Receptors[a]

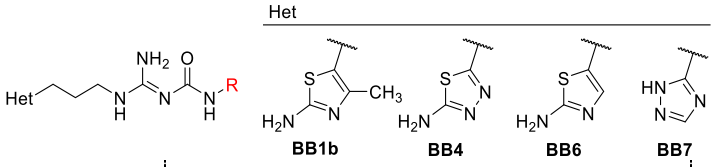

compd.	structure BB	R	pK_i $hD_{2long}R$[b]	N	hD_3R[c]	N	H_2R selectivity $K_i(D_xR)/K_i(H_2R)$ x = 2long, 3 $D_{2long}R$	D_3R
pramipexole (**5.7**)	-	-	hi 7.59 ± 0.12[38] low 6.00 ± 0.03[38]	3	9.18 ± 0.06[38]	3	0.002*	0.00005
5.6[23]	1b	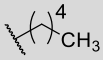	6.35 ± 0.01[23]	3	7.80 ± 0.09[23]	3	100	4
5.31	4		5.02 ± 0.15	3	6.10 ± 0.05	4	3162	263
5.32	6		5.46 ± 0.07	3	7.50 ± 0.02	3	151	1
5.36	4	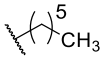	<5	3	6.23 ± 0.02	3	>1950	115
5.43	4		5.79 ± 0.01	3	6.63 ± 0.08	3	83	12
5.47	4		5.20 ± 0.04	3	5.58 ± 0.17	3	1259	525
5.48	6		5.34 ± 0.07	3	7.13 ± 0.04	3	170	3
5.53	4		<5	3	5.49 ± 0.10	3	>776	251
5.54	7		<5	3	<5	3	>186	>186
5.56	4		<5	3	6.18 ± 0.10	3	>1230	81
5.57	4	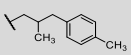	5.97 ± 0.07	3	5.69 ± 0.11	4	166	316
5.59	6		6.31 ± 0.07	3	6.64 ± 0.01	3	8	4
5.63	4	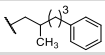	6.35 ± 0.06	3	6.49 ± 0.02	3	30	21
5.5[22]	1b	dimeric	7.09 ± 0.07	3	8.70 ± 0.04	3	10	0.2
5.69	4		6.02 ± 0.10	3	7.22 ± 0.07	3	182	12

[a]Data represent mean values ± SEM from N independent experiments, each performed in triplicate. Radioligand competition binding assay with [^{3}H]*N*-methylspiperone ([b]$hD_{2long}R$: K_d = 0.0149 nM, c = 0.05 nM or [c]hD_3R: K_d = 0.0258 nM, c = 0.05 nM) using homogenates of [b]HEK293T-CRE-Luc-$hD_{2long}R$ or [c]HEK293T-CRE-Luc-hD_3R cells.[38] *Calculated using pK_i high value.

5.2.5 Functional Studies at the Human H_2R

To get further insights into the general structure activity relationship of the N^G-carbamoylated guanidines, all target compounds (**30**-**70**) and the reference compounds (only mini-G) were investigated for hH_2R agonism and antagonism in the β-arrestin2- and mini-G protein-recruitment assays using genetically engineered HEK293T cells, respectively. The results are presented in Table 5.3. The responses in both assays were normalized to the maximum effect induced by 100 µM histamine (**5.1**, E_{max} = 1.00) and buffer control (E_{max} = 0). Thus, **5.1** is defined as a full, unbiased agonist in either readouts. **5.1** exhibits a significantly lower potency in the β-arrestin2 recruitment assay compared to the mini-G protein recruitment assay (pEC_{50} (β-arrestin2) = 5.42[39]; pEC_{50} (mGs (minimal $G_{\alpha s}$ protein)) = 6.94[40]; cf. Table 5.3). Similarly, the potencies of the investigated N^G-carbamoylated guanidines were also lower in the β-arrestin2 recruitment assay (cf. Table 5.3). A possible explanation for this trend could be the use of the mGs protein, since it is known that mG proteins stabilize active states of GPCRs, which favors the binding of agonists.[40-43]

The most interesting compounds (**5.31**-**5.32**, **5.36**, **5.43**, **5.47**-**5.48**, **5.53**-**5.54**, **5.56**-**5.57**, **5.59**, **5.63** and **5.69**) proved to be strong partial agonists (E_{max} = 0.83 to 0.95, cf. Table 5.3) in the mini-G protein recruitment assay with pEC_{50} values >7.0. The determined pEC_{50} values agree in most cases very well with the pK_i values from the radioligand binding assay. Compound **5.47**, containing the benzyl side residue, showed the highest hH_2R potency with a pEC_{50} of 8.48, but also **5.31** (pentyl side residue, pEC_{50} = 8.22) showed an excellent potency in the single-digit nanomolar range (cf. Table 5.3). The incorporation of a ring system (cf. Scheme 5.1, BB9-11) in the spacer resulted in either antagonists or partial agonists depending on the side residue (for details see Table 5.3). Surprisingly, some of the tested compounds revealed a completely different functional profile in the β-arrestin2 recruitment assay (cf. Table 5.3). Almost all tested 2-aminothiazoles **5.6**[23], UR-CH20[23-24], UR-CH22[23-24], UR-Po563[23], UR-MB-69[23], UR-SB257[23-24], UR-KAT527[23], **5.32**, **5.48** and **5.59** and some thiadiazoles **5.57** and **5.63**, containing a propyl spacer, as well as triazole-containing **5.54** exhibited a certain degree of efficacy bias towards G-protein activation. The compounds acted as strong partial agonists (E_{max} = 0.73 to 0.94, cf. Table 5.3) in the mini-G protein recruitment assay but were only partial agonists in the β-arrestin2 recruitment assay (E_{max} = 0.10 to 0.73, cf. Table 5.3). The efficacy bias was confirmed by the determination of efficacy bias factors (eBF, for details see in the Appendix 4, App4.4 Bias Analysis). The dimeric

ligands (e.g. thiazole: **5.5**[22], thiadiazole: **5.69**) exhibited similar characteristics as their monomeric counterparts. All compounds containing a rigidized spacer (cf. Scheme 5.1, BB9-11) acted as antagonists in the β-arrestin2 recruitment assay (see Table 5.3).

Table 5.3. Potencies and Efficacies of the Selected N^G-Carbamoylated Guanidines in the β-Arrestin2 and Mini-G Protein Recruitment Assays at the hH_2R[a]

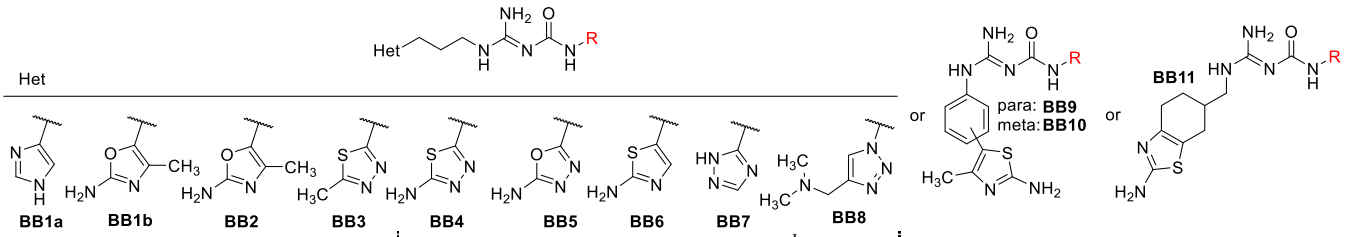

compd.	structure		β-arrestin2 recruitment[b]			mGs recruitment[c]		
	BB	R	pEC_{50} or (pK_b)[d]	E_{max}[e]	N	pEC_{50} or (pK_b)[d]	E_{max}[e]	N
5.1	-	-	5.42 ± 0.02[39]	1.00[39]	3	6.94 ± 0.06[40]	1.00[40]	9
5.7	-	-	4.40 ± 0.10[23]	0.35 ± 0.03[23]	3	6.78 ± 0.01	0.95 ± 0.01	
5.6[23]	1b		6.75 ± 0.12[23]	0.15 ± 0.02[23]	4	8.34 ± 0.05	0.88 ± 0.01	3
5.30	3		(5.70 ± 0.18)	0.01 ± 0.02‡	4	5.61 ± 0.02	0.62 ± 0.01	3
5.31**	4		6.63 ± 0.08	0.94 ± 0.06	6	8.24 ± 0.22	0.93 ± 0.01	3
5.32	6	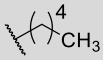	7.25 ± 0.04	0.64 ± 0.04	4	8.22 ± 0.04	0.89 ± 0.01	3
5.33	9		(7.27 ± 0.05)	0.00 ± 0.01‡	3	(6.96 ± 0.03)	0.00 ± 0.01‡	3
5.34	10		(7.27 ± 0.11)	0.00 ± 0.13‡	3	7.25 ± 0.10	0.43 ± 0.01	3
5.35**	11		(7.81 ± 0.13)	0.01 ± 0.03‡	3	7.24 ± 0.05	0.74 ± 0.04	3
UR-CH20[23-24]	1b	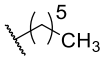	7.07 ± 0.02[23-24]	0.28 ± 0.03[23-24]	3	8.04 ± 0.04	0.87 ± 0.01	3
5.36	4		5.97 ± 0.04	1.16 ± 0.05	5	8.22 ± 0.06	0.95 ± 0.02	3
5.37	5		5.78 ± 0.05	0.61 ± 0.02	5	7.00 ± 0.04	0.93 ± 0.02	3
5.38	3	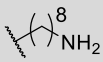	(5.51 ± 0.10)	-0.03 ± 0.01‡	4	<5	0.34 ± 0.06*	4
5.39	4		6.70 ± 0.14	0.87 ± 0.04	5	8.13 ± 0.05	0.93 ± 0.01	3
5.40	9		(6.65 ± 0.08)	-0.02 ± 0.01‡	3	(6.79 ± 0.02)	-0.04 ± 0.01‡	3
UR-SB291[23-24]	1b		6.65 ± 0.09[23-24]	0.40 ± 0.06[23-24]	3	7.52 ± 0.11	0.84 ± 0.01	3
5.41	2		(7.05 ± 0.04)	0.03 ± 0.02‡	3	7.08 ± 0.05	0.49 ± 0.02	3
5.42	3		(6.13 ± 0.12)	0.01 ± 0.01‡	4	5.97 ± 0.02	0.19 ± 0.01	3
5.43**	4		6.87 ± 0.09	0.90 ± 0.04	6	7.97 ± 0.03	0.88 ± 0.03	3
5.44	9		(6.87 ± 0.10)	-0.02 ± 0.01‡	4	(6.79 ± 0.03)	-0.12 ± 0.02‡	3
UR-CH22[23-24]	1b		7.00 ± 0.08[23-24]	0.33 ± 0.03[23-24]	3	8.14 ± 0.03	0.89 ± 0.01	3
5.45	2		(6.89 ± 0.20)	-0.02 ± 0.01‡	4	7.24 ± 0.07	0.86 ± 0.02	3
5.46	3		(5.43 ± 0.14)	0.01 ± 0.01‡	4	5.63 ± 0.07	0.71 ± 0.02	3
5.47	4		6.86 ± 0.13	0.94 ± 0.06	5	8.48 ± 0.07	0.92 ± 0.01	4

Table 5.3. (continued)

5.48	6		7.31 ± 0.05	0.73 ± 0.03	4	8.31 ± 0.14	0.94 ± 0.03	4
5.49	9		(7.81 ± 0.11)	0.01 ± 0.01‡	5	7.30 ± 0.04	0.08 ± 0.01	3
5.50	10		(7.13 ± 0.10)	-0.10 ± 0.09‡	3	7.16 ± 0.10	0.67 ± 0.02	4
5.51**	11		(7.35 ± 0.08)	0.03 ± 0.04‡	3	7.19 ± 0.05	0.73 ± 0.02	3
UR-Po563[23]	1b		7.34 ± 0.11[23]	0.34 ± 0.03[23]	4	8.04 ± 0.01	0.88 ± 0.01	3
5.52***	1a		7.13 ± 0.04	0.72 ± 0.06	3	8.17 ± 0.01	0.93 ± 0.01	3
5.53	4		6.55 ± 0.09	0.87 ± 0.02	5	7.70 ± 0.04	0.91 ± 0.02	3
5.54	7		6.49 ± 0.10	0.37 ± 0.02	4	7.59 ± 0.04	0.90 ± 0.02	3
5.55***	8		(<5)	-0.02 ± 0.01‡	3	<5"	0.03 ± 0.01‡	3
UR-MB-69[23]	1b		7.19 ± 0.11[23]	0.30 ± 0.01[23]	4	8.07 ± 0.01	0.89 ± 0.01	3
5.56	4		7.12 ± 0.05	1.04 ± 0.03	6	8.09 ± 0.04	0.95 ± 0.01	3
UR-SB257[23-24]	1b		6.9 ± 0.1[23-24]	0.10 ± 0.01[23-24]	3	7.43 ± 0.02	0.73 ± 0.02	3
5.57**	4		6.89 ± 0.17	0.53 ± 0.04	5	7.21 ± 0.09	0.91 ± 0.01	4
5.58	5	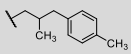	(6.31 ± 0.14)	0.04 ± 0.05‡	4	6.58 ± 0.05	0.74 ± 0.02	3
5.59	6		6.63 ± 0.08	0.16 ± 0.01	4	7.11 ± 0.04	0.83 ± 0.01	4
5.60	9		(6.80 ± 0.06)	-0.03 ± 0.02‡	4	(6.73 ± 0.05)	-0.07 ± 0.01‡	3
5.61	10		(7.32 ± 0.10)	0.01 ± 0.02‡	4	(7.09 ± 0.01)	-0.08 ± 0.01‡	3
5.62**	11		(7.39 ± 0.07)	-0.01 ± 0.02‡	4	(6.96 ± 0.03)	0.02 ± 0.01‡	3
UR-KAT527[23]	1b		5.60 ± 0.11[23]	0.13 ± 0.02[23]	4	7.28 ± 0.09	0.76 ± 0.04	3
5.63	4		6.54 ± 0.17	0.38 ± 0.04	5	7.62 ± 0.09	0.84 ± 0.02	4
5.64	9	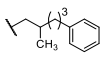	(6.57 ± 0.03)	-0.00 ± 0.01‡	3	(6.86 ± 0.03)	-0.08 ± 0.01‡	3
5.65	10		(7.02 ± 0.11)	-0.08 ± 0.11‡	3	(7.31 ± 0.01)	-0.05 ± 0.01‡	3
5.66**	11		(7.30 ± 0.11)	-0.01 ± 0.01‡	3	6.69 ± 0.04 (6.96 ± 0.03)	-0.04 ± 0.01	3
5.5[22]	1b		6.80 ± 0.14	0.30 ± 0.04	6	7.62 ± 0.02	0.89 ± 0.01	3
5.67	9	dimeric	(7.86 ± 0.12)	-0.03 ± 0.07‡	4	6.13 ± 0.12	0.44 ± 0.05	4
5.68	10		(7.10 ± 0.04)	-0.05 ± 0.13‡	3	6.59 ± 0.12	0.19 ± 0.02	3
5.69**	4		6.39 ± 0.07	0.82 ± 0.06	4	7.70 ± 0.12	0.94 ± 0.01	3
5.70	4	dimeric 	6.66 ± 0.03	0.81 ± 0.07	4	8.06 ± 0.02	0.94 ± 0.01	3

Table 5.3. (continued)

[a]Data represent mean values ± SEM from N independent experiments, each performed in triplicate. [b]β-arrestin2 recruitment assay was performed using HEK293T-ARRB2-H_2R cells.[37, 39] [c]Mini-G protein recruitment assay was performed using HEK293T NlucN-mGs/hH_2R-NlucC cells.[40] [d]pK_b = -logK_b. K_b values were calculated from the IC_{50} values according to the Cheng-Prusoff equation.[44] The K_b values of antagonists or inverse agonists were determined in the antagonist mode versus **5.1** (8 µM **5.1** for the β-arrestin2 recruitment assay or 1 µM **5.1** for the mini-G protein recruitment assay). [e]The response in both assays was normalized to the maximal effect induced by 100 µM **5.1** (E_{max} = 1.00) and buffer control (E_{max} = 0.00). n.a.: not applicable, silent antagonist. ": inactive as agonist as well as antagonist. ‡E_{max} at c = 10 µM. **Selected compounds were investigated for functional activity in the [^{35}S]GTPγS binding assay at the hH_2R-$G_{s\alpha S}$ fusion protein.[122] The response was normalized to the maximal effect induced by **5.1** (E_{max} = 1.00) and buffer control (E_{max} = 0.00). The pIC_{50} values of antagonists or inverse agonists were determined in the antagonist mode versus **5.1** (c = 1 µM, EC_{50} = 5.85 ± 0.06) and converted to the corresponding K_b values by using the Cheng-Prusoff equation[44], pK_b = -logK_b. The obtained results were in good agreement with the results from the mini-G protein recruitment assay. **5.31**: pEC_{50} = 7.59 ± 0.11, E_{max} = 0.84 ± 0.04 (N = 3); **5.35**: pEC_{50} = 7.23 ± 0.10, E_{max} = 0.31 ± 0.05 (N = 3); **5.43**: pEC_{50} = 7.88 ± 0.09, E_{max} = 0.78 ± 0.07 (N = 3); **5.51**: pEC_{50} = 6.91 ± 0.07, E_{max} = 0.26 ± 0.03 (N = 3); **5.57**: pEC_{50} = 7.89 ± 0.11, E_{max} = 0.88 ± 0.06 (N = 4); **5.62**: pK_b = 6.79 ± 0.18 (N = 2, ± SE); E_{max} = -0.06 ± 0.06‡ (N = 2, ± SE); **5.66**: pK_b = 6.96 ± 0.04 (N = 2, ± SE); E_{max} = -0.07 ± 0.04‡ (N = 2, ± SE). **5.69**: pEC_{50} = 7.46 ± 0.09, E_{max} = 0.71 ± 0.06 (N = 3). ***Compounds **5.52** and **5.55** were also investigated on isolated spontaneously beating guinea pig right atrium [35]: **5.52**: pEC_{50} = 8.88 ± 0.12, E_{max} = 1.14 ± 0.17 (N = 3); **5.55**: not active, E_{max} = 0 (N = 3).

5.2.6 Functional Studies at the Guinea Pig H_2R

Furthermore, a selection of compounds (with a pK_i >7.0 at the hH_2R and a selectivity over the h$D_{2long/3}$ receptors) was investigated on the isolated spontaneously beating guinea pig right atrium as a more complex, well established standard model for the characterization of H_2R ligands (Table 5.4).[5, 28] All compounds turned out to be full agonists in this assay (E_{max} = 0.98 to 1.15, cf. Table 5.4). The obtained data are generally comparable with the results from the gpH_2R mini-G protein recruitment assay in terms of potency and efficacy (Table 5.4). Noteworthily, **5.53**, **5.56** and **5.57** showed the highest discrepancies regarding the potency in both assays. While **5.53** and **5.56** showed higher potencies by about one logarithmic unit on the guinea pig right atrium, **5.57** behaved exactly the opposite (Table 5.4). The thiadiazole **5.56** (pEC_{50} = 9.04) showed the highest potency on the guinea pig right atrium whereas **5.47** was the most potent compound in the mini-G protein recruitment assay (pEC_{50} = 8.66). In general, a comparison of the mini-G protein recruitment assay data at the guinea pig and human H_2Rs showed that the potencies at the gpH_2R were slightly better for all substances tested, while the efficacies were pretty much the same. A similar observation was already published for the [^{35}S]GTPγS assay and the steady state GTPase assay.[1-4]

Table 5.4. Potencies and Efficacies of the Tested N^G-Carbamoylated Guanidines Determined in the Mini-G Protein Recruitment Assay at the gpH_2R or by Organ Bath Studies at the Spontaneously Beating Guinea Pig Right Atrium[a]

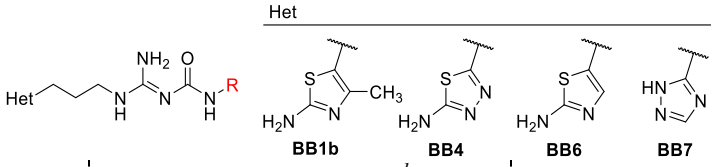

compd.	structure		mGs recruitment[b]			atrium[d]		
	BB	R	pEC_{50}	E_{max}[c]	N	pEC_{50}[e]	E_{max}[f]	N
5.1	-	-	6.60 ± 0.07[25]	1.00[25]	3	6.16 ± 0.01[35]	1.00[35]	225
5.6[23]	1b	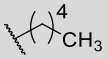	n.d.	n.d.	-	8.24 ± 0.03[23]	0.78 ± 0.03[23]	3
5.31	4		8.36 ± 0.07	0.94 ± 0.01	3	8.25 ± 0.11	1.09 ± 0.02	3
5.36	4	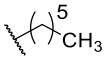	8.64 ± 0.05	0.96 ± 0.01	3	8.32 ± 0.06	1.06 ± 0.05	3
5.47	4		8.66 ± 0.04	0.94 ± 0.01	3	8.88 ± 0.03	1.05 ± 0.01	3
5.53	4		7.60 ± 0.03	0.90 ± 0.02	3	8.54 ± 0.09	0.98 ± 0.04	3
5.54	7		7.79 ± 0.02	0.86 ± 0.03	3	7.42 ± 0.10	1.15 ± 0.11	3
5.56	4		8.16 ± 0.03	0.93 ± 0.02	3	9.04 ± 0.10	1.10 ± 0.05	3
5.57	4	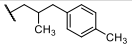	7.83 ± 0.09	0.92 ± 0.01	3	7.02 ± 0.08	1.02 ± 0.10	3

[a]Data represent mean values ± SEM from N independent experiments, each performed in triplicate. [b]Mini-G protein recruitment assay was performed using HEK293T NlucN-mGs/gpH_2R-NlucC cells.[25] [c]The response was normalized to the maximal effect induced by 100 µM **5.1** (E_{max} = 1.00) and buffer control (E_{max} = 0.00). [d]Organ bath studies using the isolated, spontaneously beating guinea pig right atrium.[35] [e]pEC_{50} was calculated from the mean corrected shift ΔEC_{50} of the agonist curve relative to the histamine reference curve by equation: $pEC_{50} = 6.16 + \Delta pEC_{50}$. [f]$E_{max}$: maximal response relative to the maximal increase in heart rate induced by 30 µM **5.1** (E_{max} = 1.00). n.d.: not determined.

5.2.7 Functional Studies at the Human $D_{2long/3}$ Receptors

Although the relevant N^G-carbamoylated guanidines (**5.31-5.32**, **5.36**, **5.47**, **5.53-5.54** and **5.56-5.57**) bind to the $hD_{2long/3}$ receptors only with low affinity (pK_i <6.5 (only **5.32** has a pK_i >6.5 at the D_3R), see Table 5.2), we decided to characterize these ligands in the β-arrestin2 assay which is already established in our lab.[38] In addition, the data of **5.5**[22], **5.43**, **5.48**, **5.59**, **5.63** and **5.69** were collected for a broader comparison of the compounds. The measured potencies and efficacies are presented in Table 5.5. All tested compounds showed agonistic activities in the β-arrestin2 recruitment assay at the hD_3R. In the β-arrestin2 recruitment assay at the $hD_{2long}R$, **5.47** and **5.54** were inactive (up to a tested concentration of 10 µM, cf. Table 5.5). The remaining compounds

(**5.5**[22], **5.31**-**5.32**, **5.36**, **5.43**, **5.48**, **5.53**, **5.56**, **5.59** and **5.69**) acted as agonists with exception of **5.57** and **5.63**, which were antagonists. Some compounds (**5.31**, **5.36**, **5.43**, **5.53** and **5.56** at the $hD_{2long}R$ and **5.54** and **5.57** at the hD_3R) showed only very weak partial agonism at the highest tested concentration of 10 µM, which could not be fitted. In general, thiadiazoles showed lower potencies and efficacies at the $hD_{2long/3}$ receptors than their thiazole counterparts (cf. Table 5.5).

Table 5.5. Potencies and Efficacies of Selected N^G-Carbamoylated Guanidines Determined in the β-Arrestin2 Recruitment Assay at the $hD_{2long}R$ or hD_3R[a]

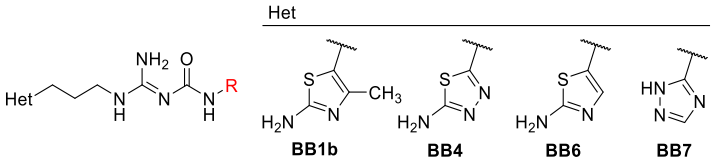

compd.	structure		$hD_{2long}R$[b]			hD_3R[c]		
	BB	R	$pEC_{50}/(pK_b)$[d]	E_{max}[e]	N	pEC_{50}	E_{max}[e]	N
quinpirole	-	-	7.55 ± 0.07[38]	1.00[38]	5	8.75 ± 0.07[38]	1.00[38]	6
5.7	-	-	8.19 ± 0.05[38]	0.86 ± 0.04[38]	4	9.09 ± 0.06[38]	0.99 ± 0.04[38]	4
5.6[23]	1b		5.98 ± 0.02[23]	0.41 ± 0.05[23]	4	7.80 ± 0.05[23]	0.96 ± 0.05[23]	3
5.31	4	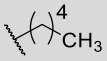	<5	0.11 ± 0.01‡	3	5.55 ± 0.18	0.74 ± 0.08	3
5.32	6		5.85 ± 0.07	0.56 ± 0.05	4	7.40 ± 0.01	0.87 ± 0.01	3
5.36	4	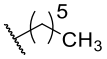	<5	0.15 ± 0.01‡	3	6.09 ± 0.09	0.73 ± 0.07	4
5.43	4		<5	0.17 ± 0.05‡	3	5.87 ± 0.10	0.26 ± 0.05	3
5.47	4		<5	0.05 ± 0.02‡	5	5.92 ± 0.14	0.43 ± 0.02	4
5.48	6		5.47 ± 0.08	0.23 ± 0.04	3	7.17 ± 0.03	0.87 ± 0.04	3
5.53	4		<5	0.06 ± 0.01‡	3	5.97 ± 0.16	0.71 ± 0.04	3
5.54	7		<5	0.00 ± 0.01‡	3	<5	0.18 ± 0.05‡	3
5.56	4		<5	0.07 ± 0.01‡	3	5.72 ± 0.07	0.73 ± 0.11	3
5.57	4	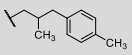	(5.69 ± 0.01)	0.06 ± 0.03‡	3	<5	0.12 ± 0.01‡	3
5.59	6		5.35 ± 0.06	0.31 ± 0.04	3	5.98 ± 0.02	0.71 ± 0.02	4
5.63	4	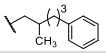	(5.42 ± 0.01)	-0.02 ± 0.02‡	4	6.33 ± 0.07	0.56 ± 0.05	3
5.5[22]	1b	dimeric	6.67 ± 0.09	0.88 ± 0.07	4	7.70 ± 0.08	1.01 ± 0.06	6
5.69	4		5.95 ± 0.05	0.32 ± 0.05	3	6.53 ± 0.12	0.80 ± 0.03	3

[a]Data represent mean values ± SEM from N independent experiments, each performed in triplicate. β-arrestin2 recruitment assay was performed using HEK293T ElucN-βarr2 $hD_{2long}R$-ElucC[b] or HEK293T ElucN-βarr2 hD_3R-ElucC[c] cells.[38] [d]$pK_b = -\log K_b$. K_b values were calculated according to the Cheng-Prusoff equation.[44] The IC_{50} values of antagonists were determined in the antagonist mode versus quinpirole (50 nM, $D_{2long}R$). [e]The response in both assays was normalized to the maximal effect induced by 10 µM (E_{max} = 1.00) and buffer control (E_{max} = 0.00). ‡E_{max} at c = 10 µM.

5.2.8 Molecular Docking Studies

To shed light on the binding modes of the amino(methyl)thiazole- and the aminothiadiazole-containing carbamoylguanidines and to get insight into the specific molecular interactions leading to the differences in hH_2R, hD_2R and hD_3R affinities, we performed molecular docking studies (Figure 5.6). We chose to investigate compounds **5.6** (2-amino-4-methylthiazole), **5.31** (2-aminothiadiazole) and **5.32** (2-aminothiazole) on the active-state receptor models of the hH_2R (homology model based on the β_2 adrenergic receptor-Gs protein complex crystal structure 3SN6[45]; sequence identity of about 37%[20]) and the hD_2R (based on the D_2R-G protein complex crystal structure 6VMS[46]). Since **5.6**, **5.31** and **5.32** act as agonists at the hD_3-receptor (β-arrestin2 assay, Table 5.5), they should be docked into its active-state receptor model. However, to the best of our knowledge, an active-state model of the D_3R has not been reported yet. To investigate the binding mode at the hD_3R despite this drawback, we decided to create mutants of the active-state hD_2R model, containing amino acid(s) (aa(s)) of hD_3R.

First of all, we studied and analyzed literature data regarding mutagenesis studies at aminergic GPCRs (primarily histamine and dopamine receptors) focusing onto the different amino acids of the orthosteric binding pocket at the hH_2R, the hD_2R and hD_3R.

At the hD_2R, the $V^{2.61}F$ mutation led to an approx. 50-fold decrease in K_i of clozapine, compared to the human dopamine D_4 receptor (hD_4R).[47] Furthermore, multiple mutations at the hD_2R and hD_4R suggest that the amino acid at position 2.61 is part of a microdomain (including the amino acids at 3.28, 3.29, 7.35), which is partially accountable for the selectivity between hD_2R and hD_4R.[47] At the hH_1R, the mutation $N^{2.61}S$ ($hH_1R \rightarrow gpH_1R$) had no or only a small influence onto the binding affinities of small compounds, like mepyramine, cetirizine or histamine, while the pK_i of more voluminous partial agonists (e.g. suprahistaprodifen and dimeric histaprodifen) increased towards gpH_1R.[48] However, another study indicates that this amino acid is not the only responsible amino acid for the observed species differences between hH_1R and gpH_1R.[49] Besides, the influence of distinct amino acids (ECL2.49, ECL2.51 and ECL2.52, Figure 5.5) of the extracellular loop 2 (ECL2) onto binding affinity of ligands at the hD_2R and hD_3R was shown by mutagenesis.[50-53] The position 5.42 is highly important for ligand binding at several aminergic GPCRs: for example, the $S^{5.42}A$ mutation at the hD_1R[54], mouse D_2R, hD_2R[55-56] or hD_3R[57] led to a ≥10-fold alteration of the affinity of different ligands. Additionally, also the $S^{5.46}A$ mutant at several aminergic GPCRs, e.g.

at the hD_1R, led to a ≥10-fold alteration of affinity for selected ligands[54, 58-59] and the amino acid at 5.46 is suggested to influence the subtype selectivity.[60] Moreover, for other mutants, e.g. $N^{5.46}A$ at gpH_1R[61-62] or $E^{5.46}D,Q$ at hH_4R[63-64] a ≥10-fold alteration of ligand-affinity was reported. Although the single mutations $S^{5.42}A$ and $S^{5.46}A$ did not significantly reduce the binding affinity for e.g. (-)-epinephrine, the double mutation $S^{5.42}A/S^{5.46}A$ led to an approx. 100-fold reduced affinity compared to the wild-type rat (r) α_1-adrenergic receptor[65], indicating that both amino acids affect each other. Furthermore, it was shown that the mutation of the amino acid at position 6.51 may affect the affinity up to 1000-fold, e.g. for the $F^{6.51}A,L,Y$ mutants at the hD_2R.[66] The mutation $I^{6.53}V$ at hH_1R was described to increase the K_d of [^{3}H]mepyramine by approx. 10-fold[67], while in another study a slight decrease was reported.[48] Several further studies showed that mutations of the amino acid at position 6.55 may lead to an up to 25-fold alteration of the binding affinity, e.g. for the gpH_1R-$F^{6.55}A$[68], rD_2R-$H^{6.55}L$[69], hD_3R-$H^{6.55}L$[70] and rD_2R-$H^{6.55}N$[71]. However, these studies also suggest that the amino acid at position 6.55 may affect the binding affinity not only by a direct interaction with the ligand, but also by changing the interaction network within the receptor. Also the amino acid 7.35 was described to affect ligand affinity, as shown by the $W^{7.35}A,F$ mutants of the human muscarinic receptor M_1.[72]

The docking studies of **5.31** and **5.32** suggest that the heterocyclic 5-membered ring (BB4 or BB6, respectively), particularly if surrounded by the amino acids $C^{3.36}$, $T^{3.37}$, $D^{5.42}$, $T^{5.46}$ and $F^{6.55}$, fits well into the orthosteric binding pocket of the hH_2R (Figure 5.6A, shown for **5.31**). However, both heterocycles are suggested to bind in a conformation with the sulfur being located near to $C^{3.36}$ and $T^{3.37}$. Additionally, **5.31** and **5.32** are stabilized by an electrostatic interaction between the aspartate of the $D^{5.42}$-$T^{5.46}$ motif and the NH_2-group of the heterocycle (Figure 5.6A, shown for **5.31**). The carbamoylguanidine moiety of both **5.31** and **5.32** forms an electrostatic interaction network with the amino acids $Y^{3.28}$, $D^{3.32}$ and $E^{7.35}$ (Figure 5.6A, shown for **5.31**). **5.31** and **5.32** could also be docked into the analog binding pocket of the hD_2R. In contrast to the hH_2R, there is a serine instead of an aspartate at position 5.42, which results in a reduced electrostatic interaction of the hD_2R and the NH_2 moiety of the heterocycle (BB4 or BB6, respectively) (Figure 5.6B, shown for **5.31**). As roughly estimated by calculation of the docking energy between the hH_2R or the hH_2R-$D^{5.42}S$ mutant and **5.31** or **5.32**, respectively, the interaction energy is considerably reduced for the hH_2R-$D^{5.42}S$ mutant. Thus, this missing interaction is probably one reason for the reduced affinity of **5.31** or **5.32** at hD_2R and hD_3R, compared to hH_2R. For the hD_2R, no compensating interaction between the heterocycle (BB4 or BB6, respectively) and the receptor could be identified.

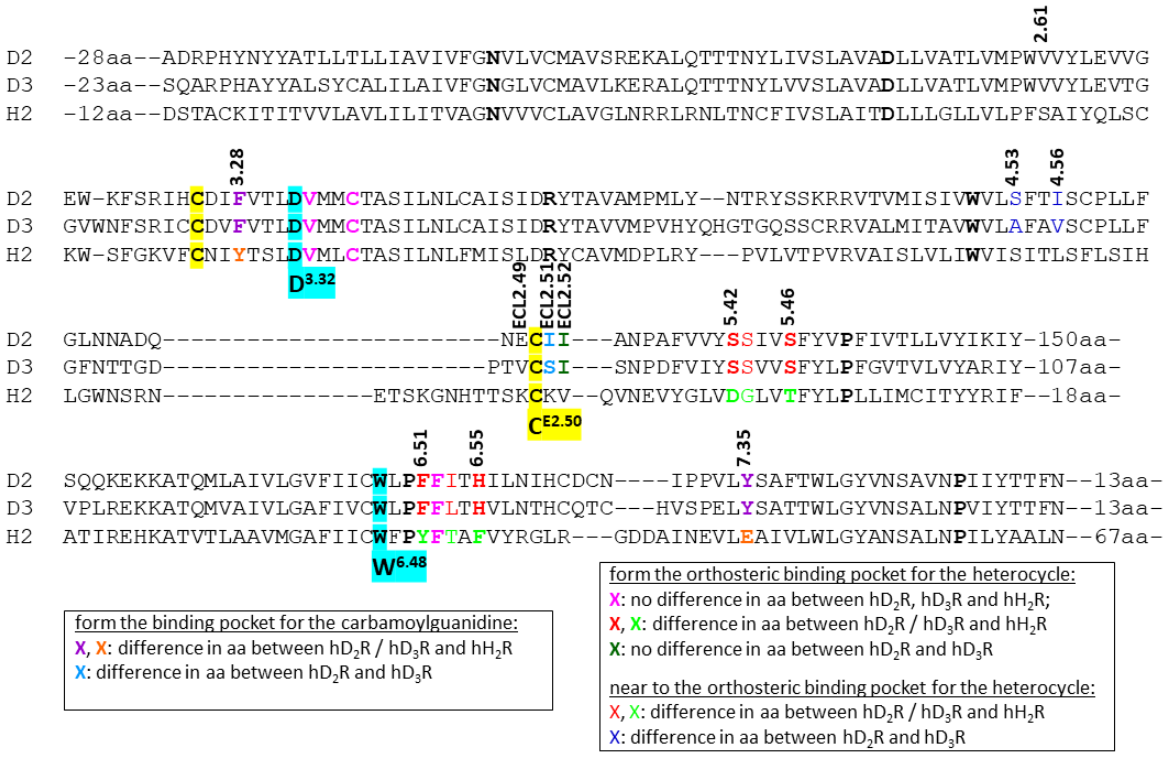

Figure 5.5. Comparison of the amino acid sequence of hH_2R, hD_2R and hD_3R. The amino acid sequences are given in the one-letter code. Colored and/or bold letters were used to indicate the amino acids, which form and/or are in close proximity to the binding pockets for the heterocycle and the carbamoylguanidine.

Next, we performed further investigations to elucidate why the compounds **5.31** and **5.32** have a higher affinity to hD_3R than to hD_2R. Concerning the 5.42-5.46 motif, the situation at the hD_3R is identical compared to the hD_2R. Although a comparison of the amino acid sequence between hD_2R and hD_3R revealed two differences at the positions 4.53 and 4.56 (hD_2R: $S^{4.53}$, $I^{4.56}$; hD_3R: $A^{4.53}$, $V^{4.56}$), which are in close proximity to the 5.42-5.46 motif, subsequent docking studies at the hD_2R-$S^{4.53}A$-$I^{4.56}V$ mutant suggested that these amino acids are not responsible for the subtype selectivity between hD_2R and hD_3R. Therefore, we performed an analysis of the interaction between the carbamoylguanidine moiety and the hD_2R or hD_3R. We observed that at position 7.35 the glutamate (hH_2R) is exchanged into a tyrosine, which is not able to establish an as strong electrostatic interaction as the glutamate. Furthermore, the $Y^{3.28}$, which also interacts at the hH_2R with the carbamoylguanidine by an electrostatic interaction, is a phenylalanine at the hD_2R and

hD_3R, resulting in a deficit in electrostatic interaction. These two reduced interactions between hD_2R and the carbamoylguanidine constitute probably another reason for the reduced affinity of **5.31** or **5.32** at hD_2R or hD_3R compared to hH_2R. An advanced comparison of the amino acid sequence between hD_2R and hD_3R revealed another two differences in the ECL2 in neighborhood to the highly conserved cysteine (hD_2R: $E^{ECL2.49}C^{ECL2.50}I^{ECL2.51}$; hD_3R: $V^{ECL2.49}C^{ECL2.50}S^{ECL2.51}$) (for amino-acid alignment see Figure 5.5). In case of the hD_2R, the $E^{ECL2.49}$ is too far away from the carbamoylguanidine moiety of the ligand and is not able to establish an electrostatic interaction (Figure 5.6C, right). In contrast, at the hD_3R, the $S^{ECL2.51}$ is able to form a hydrogen bond with the carbamoylguanidine (cf. hD_2R-$E^{ECL2.49}V$-$I^{ECL2.51}S$, Figure 5.6C, center). Thus, the reduced interaction between the receptor and the carbamoylguanidine moiety in the series $hH_2R \rightarrow hD_3R \rightarrow hD_2R$ will explain the reduced affinity, obtained by competition binding studies, within the same sequence. However, this effect could only be observed for the double mutant hD_2R-$E^{ECL2.49}V$-$I^{ECL2.51}S$, not for the single mutant hD_2R-$I^{ECL2.51}S$. As suggested by the modelling studies, in case of the single mutant, the $S^{ECL2.51}$ interacts with $E^{ECL2.49}$ and not with the carbamoylguanidine moiety of the ligand. Thus, the double mutation is suggested to be essential for the reduced affinity of the compounds at the hD_2R compared to the hD_3R. Furthermore, the experimental studies show a decrease in affinity to the hD_3R in the series **5.6** → **5.32** → **5.31**. Here, the docking studies suggest that an isoleucine of the ECL2 ($I^{ECL2.52}$) is responsible for that trend (Figure 5.6D). This isoleucine is in close contact with the methyl group of the heterocycle of compound **6** establishing an additional van-der-Waals interaction between **6** and the receptor (Figure 5.6D, right). For **5.32**, this contact, and therefore the van-der-Waals interaction, is reduced due to the replacement of the methyl group with a proton at the heterocycle (Figure 5.6D, center). For **5.31**, this interaction is completely missing due to the presence of an additional nitrogen atom in the ring (Figure 5.6D, left). In summary, the docking studies at the active state models of the hH_2R and the hD_2R suggest, that the amino acids at the positions 3.28, 3.32, ECL2.49, ECL2.51, 5.42 and 7.35 are responsible for different affinities of **5.6**, **5.31** and **5.32** at hH_2R, hD_2R and hD_3R. However, this participation has to be verified in detail by the corresponding mutagenesis experiments in futures studies.

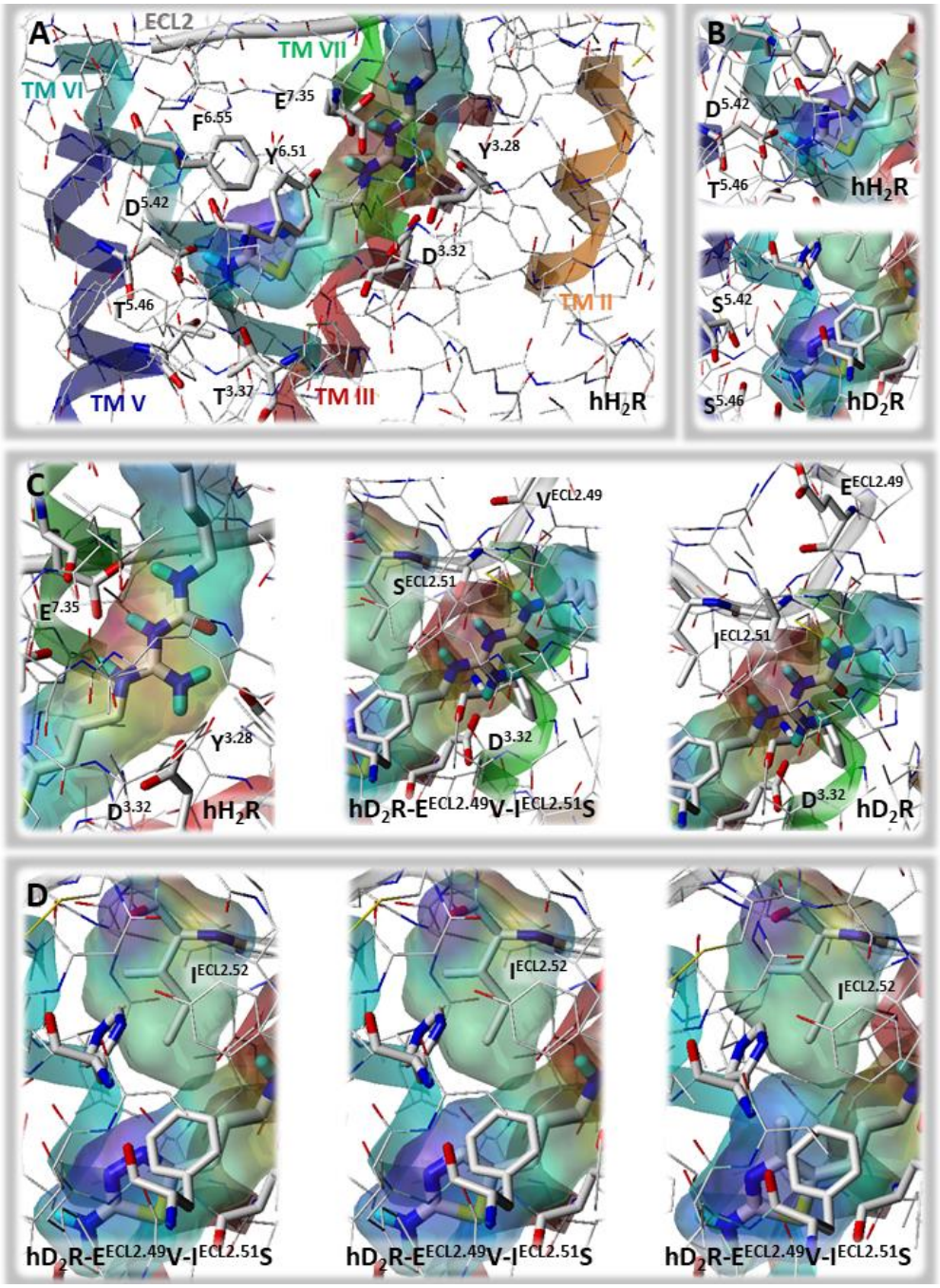

Figure 5.6. A: Active-state model of the hH_2R with **5.31** in the binding pocket. The most important amino acids interacting with **5.31** are highlighted. **B**: Differences between the interaction sites of the aminothiadiazole moiety of **5.31** and the hH_2R or the hD_2R, respectively. **C**: The most important amino acids of hH_2R (left), hD_2R-$E^{ECL2.49}V$-$I^{ECL2.51}S$ (center) and hD_2R (right), interacting with the carbamoylguanidine moiety of **5.31**. **D**: The influence of the isoleucine at position ECL2.52 of the ECL2 onto the interaction with the heterocycle of **5.31** (left), **5.32** (center) and **5.6** (right).

5.3 Summary and Conclusion

In summary, we aimed for the development of novel, subtype-selective H_2R ligands, which also have a selectivity over dopamine $D_{2long/3}$ receptors. To achieve this goal, we synthesized and characterized a series of 40 compounds containing a carbamoylguanidine as key motif, as well as varying heterocycles, spacers, and side residues. We observed that the replacement of the thiazole by a thiadiazole ring in N^G-carbamoylated thiazolylpropylguanidines resulted in potent H_2R agonists with affinities in the low one-digit nanomolar range. Furthermore, ligands containing this modification possess a significantly increased selectivity for the hH_2R over dopamine $hD_{2long/3}$ receptors. To identify the molecular interactions leading to this selectivity towards the $hD_{2long/3}$ receptors, molecular docking studies with **5.6**[23], **5.31** (UR-KAT505) and **5.32** (UR-KAT583) on the active state models of the hH_2R and the hD_2R were performed. We found that 3.28, 3.32, ECL2.49, ECL2.51, 5.42 and 7.35 are most likely the responsible amino acids, which will be confirmed in future receptor mutagenesis experiments. Within the synthesized thiadiazole-containing ligand series, compounds **5.31** and **5.47** (UR-KAT533) turned out to be the most promising candidates reaching up to 1000-fold selectivity over the other three receptor subtypes ($hH_{1,3,4}R$). **5.31** showed the highest selectivity for hH_2R over $hD_{2long}R$ (>2000-fold) and 260-fold selectivity for hH_2R over hD_3R. **5.47** on the other hand, showed a very good selectivity for hH_2R over $hD_{2long}R$ (>1000-fold) and the highest selectivity for hH_2R over hD_3R (>520-fold). These key characteristics render **5.31** and **5.47** the most affine and selective monomeric carbamoylguanidine-type agonists known so far. Therefore, we plan to employ them as pharmacological tools for further investigations on the physiological and pathophysiological role of the H_2R and hope that those studies can contribute to clarify the largely unknown function of H_2 receptors in the CNS.

5.4 Experimental Section

5.4.1 General Experimental Section

Unless otherwise stated, chemicals and solvents were from commercial suppliers and were used as received. All the solvents were of analytical grade or were distilled prior to use. For column chromatography silica gel 60 (0.04-0.063 mm, Merck, Darmstadt, Germany) was used. Flash chromatography was performed on an Intelli Flash-310 workstation from Varian Deutschland GmbH (Darmstadt, Germany) with SuperFlash (SF) columns (Si50, 4-40 g) from Agilent Technologies (Santa Clara, CA, USA). Reactions were monitored by thin layer chromatography

(TLC) on Merck silica gel 60 F254 aluminium sheets, and spots were visualized with UV light at 254 nm or ninhydrin staining. NMR spectra were recorded on a Bruker Avance 300 (^{1}H: 300 MHz, ^{13}C: 76 MHz), a Bruker Avance 400 (^{1}H: 400 MHz, ^{13}C: 101 MHz) and a Bruker Avance 600 (^{1}H: 600 MHz, ^{13}C: 151 MHz) (Bruker, Karlsruhe, Germany) NMR spectrometer with deuterated solvents from Deutero (Kastellaun, Germany). All chemical shifts are reported in δ-scale as parts per million (ppm, multiplicity, coupling constant (*J*), number of protons) relative to the solvent residual peaks as the internal standard.[73-74] The spectra were analyzed by first order and coupling constants are given in Hertz (Hz). Abbreviations for the multiplicities of the signals are s (singlet), d (doublet), t (triplet), q (quartet), quint (quintet), m (multiplet), dd (double of doublets), br s (broad singlet). HRMS was performed on a Q-TOF 6540 UHD LC/MS system (Agilent Technologies) using an ESI source or on an AccuTOF GCX GC/MS system (Jeol, Peabody, MA, USA) using an EI source. Preparative HPLC was performed with a system from Knauer (Berlin, Germany) consisting of two K-1800 pumps, a K-2001 detector and the column was a Phenomenex Kinetex (250 x 21 mm, 5 µm) (Phenomenex, Aschaffenburg, Germany). As mobile phase mixtures of MeCN and 0.1% aqueous TFA were used. The UV detection was carried out at 220 nm. Prior to lyophilization (ScanVac CoolSafe 4-15L freeze dryer from Labogene (LMS, Brigachtal, Germany), equipped with a RZ 6 rotary vane vacuum pump (Vacuubrand, Wertheim, Germany)), MeCN was removed under reduced pressure. Analytical HPLC experiments were performed on a 1100 HPLC system from Agilent Technologies equipped with Instant Pilot controller, a G1312A binary pump, a G1329A ALS autosampler, a G1379A vacuum degasser, a G1316A column compartment and a G1315B DAD detector. The column was a Phenomenex Kinetex XB-C18 column (250 x 4.6 mm, 5 µm) (Phenomenex, Aschaffenburg, Germany), tempered at 30 °C. As mobile phase, mixtures of MeCN/aqueous TFA were used. The following linear gradients were applied. Compounds **5.30**-**5.51** and **5.57**-**5.70**: MeCN/TFA (0.05 %) (v/v) 0 min: 10:90, 30 min: 90:10, 33 min: 95:5, 40 min: 95:5; flow rate: 0.8 mL/min, t_0 = 3.21 min. Compounds **5.52**-**5.56**: MeCN/TFA (0.05 %) (v/v) 0 min: 10:90, 25 min: 95:5, 35 min: 95:5; flow rate: 1.0 mL/min, t_0 = 2.67 min. The injection volume was 5-50 µL. Absorbance was detected at 220 nm. Compound concentration was between 100-1000 µM.

5.4.2 Compound Characterization

Target compounds (**5.30-5.70**) were characterized by ^{1}H-NMR, ^{13}C-NMR, and 2D NMR (COSY, HSQC, HMBC) spectroscopy, HRMS, and RP-HPLC analysis. The corresponding ^{1}H- and ^{13}C-NMR spectra as well as RP-HPLC chromatograms are shown in the Supporting Information of the published manuscript (submitted for publication). The purities of the H_2R ligands used for pharmacological investigation were ≥95%. All stock solutions were prepared in DMSO or water/DMSO 1:1 (v/v) or 20 mM HCl/DMSO 1:1 (v/v).

5.4.3 Synthesis and Analytical Data

General procedure for the synthesis of the carbamoylguanidine-type ligands (5.30-5.36, 5.38-5.57 and 5.59-5.70). The reaction was performed in analogy to the published procedure for bivalent carbamoylguanidine-type ligands.[22] In this general procedure, mercuric chloride ($HgCl_2$) is used as a reagent, which is very toxic and potentially carcinogenic. It should be used only in a well-ventilated fume hood after reading the safety precautions and wearing proper lab safety equipment (gloves, safety googles and lab coat). Future synthetic work should consider replacements for $HgCl_2$. The guanidinylating reagents **5.18**-**5.29** (1-1.1 equiv) and 1-2 equiv of the respective amines **5.8**-**5.17** were dissolved in CH_2Cl_2 (3-20 mL). NEt_3 (2.5-3 equiv) and $HgCl_2$ (1.1-2 equiv) were added to the mixture and stirring was continued for 4-48 h. The precipitate was removed by filtration through Celite 545 or centrifugation (4000 x *g*, 5 min). In the case of **5.52**-**5.56** the reaction was quenched with 7 N NH_3 (5 mL) in MeOH prior to filtration. The solvent was removed in vacuum. The crude product was purified by flash or column chromatography on silica gel (gradient: 0-20 min: petroleum ether/ethyl acetate (PE/EtOAc) 100:0-50:50, SF 8-12 g, gradient: CH_2Cl_2/MeOH 90:10 to CH_2Cl_2/MeOH/25% NH_3 in H_2O 50:50:1, or isocratic: CH_2Cl_2/7 N NH_3 in MeOH 99:1) and dried in vacuum. The Trt- and/or Boc-protected intermediates were analyzed using LC-MS (data not shown). Subsequently, the deprotection was performed by stirring the respective compound with 30-70% TFA in CH_2Cl_2 (5-14 mL) for 7-18 h. The obtained carbamoylguanidines (cf. **5.30**-**5.36**, **5.38**-**52**, **55**, **57** and **59**-**70**) were purified by preparative HPLC. In case of **5.53**-**5.54** and **5.56**, the HCl salts were synthesized according to the following procedure. After deprotection with TFA, the ligands were purified by column chromatography (isocratic: CH_2Cl_2/7 N NH_3 in MeOH 90:10) yielding the free base. The free base was dissolved in 1,4-dioxane (10 mL) and 1-2 N HCl (5 mL) in diethyl ether (Et_2O) was added

dropwise, so that the HCl salt precipitated. The suspension was concentrated in vacuum and the solid was washed with Et_2O (3 x 15 mL). After removing of the solvent in vacuum, compounds **5.53**-**5.54** and **5.56** were obtained as HCl salts.

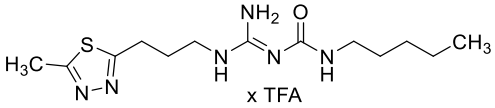

1-(Amino{[3-(5-methyl-1,3,4-thiadiazol-2-yl)propyl]amino}methylene)-3-(pentyl)urea hydrotrifluoroacetate (5.30) was prepared from amine **5.10** (29 mg, 0.19 mmol, 1.1 equiv), **5.18** (51 mg, 0.17 mmol, 1 equiv), NEt_3 (58 µL, 0.42 mmol, 2.5 equiv) and $HgCl_2$ (91 mg, 0.34 mmol, 2 equiv) according to the general procedure yielding the product as a white, foamlike and hygroscopic solid (25 mg, 34%). $R_f = 0.01$ (PE/EtOAc 3:7). RP-HPLC: 98%, (t_R = 13.5 min, k = 3.21). ^{1}H-NMR (600 MHz, DMSO-d_6): δ 10.46 (br s, 1H), 9.06 (br s, 1H), 8.54 (br s, 2H), 7.51 (br s, 1H), 3.37-3.29 (m, 2H), 3.12-3.04 (m, 4H), 2.68 (s, 3H), 1.96 (quint, J = 7.4 Hz, 2H), 1.44 (quint, J = 7.2 Hz, 2H), 1.32-1.20 (m, 4H), 0.86 (t, J = 7.1 Hz, 3H). ^{13}C-NMR (151 MHz, DMSO-d_6): δ 169.15, 165.01, 159.81 (q, J = 31.9 Hz, TFA), 153.89, 153.69, 117.36 (q, J = 299.5 Hz, TFA), 40.02, 19.11, 28.61, 28.39, 27.94, 26.31, 21.75, 15.10, 13.85. HRMS (ESI-MS): calcd. for $C_{13}H_{25}NOS^+$: 313.1805; found: 313.1827. MF: $C_{13}H_{24}N_6OS$ x $C_2HF_3O_2$. MW: (312.44 + 114.02).

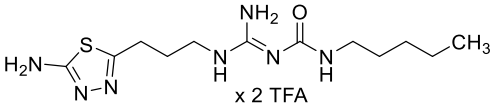

1-(Amino{[3-(5-amino-1,3,4-thiadiazol-2-yl)propyl]amino}methylene)-3-(pentyl)urea dihydrotrifluoroacetate (5.31) was prepared from amine **5.11** (53 mg, 0.18 mmol, 1 equiv), **5.18** (50 mg, 0.19 mmol, 1.1 equiv), NEt_3 (61 µL, 0.44 mmol, 2.5 equiv) and $HgCl_2$ (96 mg, 0.35 mmol, 2 equiv) according to the general procedure yielding the product as a white, foamlike and hygroscopic solid (19 mg, 19%). $R_f = 0.49$ (CH_2Cl_2/MeOH 9:1). RP-HPLC: 99%, (t_R = 11.4 min, k = 2.55). ^{1}H-NMR (600 MHz, DMSO-d_6): δ 10.37 (br s, 1H), 9.04 (br s, 1H), 8.52 (br s, 2H), 8.10-7.34 (m, 4H), 3.30 (q, J = 6.7 Hz, 2H), 3.09 (q, J = 6.6 Hz, 2H), 2.86 (t, J = 7.5 Hz, 2H), 1.89 (quint, J = 7.4 Hz, 2H), 1.44 (quint, J = 7.1 Hz, 2H), 1.31-1.22 (m, 4H), 0.86 (t, J = 7.0 Hz, 3H). ^{13}C-NMR (151 MHz, DMSO-d_6): δ 168.77, 158.93 (q, J = 34.3 Hz, TFA), 157.42, 153.86, 153.68, 116.45 (q, J = 297.7 Hz, TFA), 40.05, 39.21, 28.60, 28.39, 27.34, 26.52, 21.75,

13.86. HRMS (ESI-MS): calcd. for $C_{12}H_{24}N_7OS^+$: 314.1758; found: 314.1761. MF: $C_{12}H_{23}N_7OS$ x $C_4H_2F_6O_4$. MW: (313.42 + 228.05).

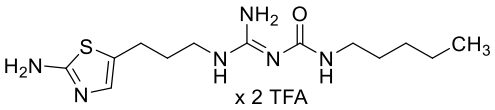

1-(Amino{[3-(2-aminothiazol-5-yl)propyl]amino}methylene)-3-(pentyl)urea dihydrotrifluoroacetate (5.32) was prepared from amine **5.12** (30 mg, 0.12 mmol, 1 equiv), **5.18** (39 mg, 0.13 mmol, 1.1 equiv), NEt_3 (41 µL, 0.29 mmol, 2.5 equiv) and $HgCl_2$ (64 mg, 0.23 mmol, 2 equiv) according to the general procedure yielding the product as a white, foamlike and hygroscopic solid (16.9 mg, 26%). R_f = 0.56 (CH_2Cl_2/MeOH 9:1). RP-HPLC: 99%, (t_R = 11.0 min, k = 2.43). ^{1}H-NMR (600 MHz, DMSO-d_6) δ 10.45 (br s, 1H), 9.41-8.85 (m, 3H), 8.50 (br s, 2H), 7.48 (br s, 1H), 7.07 (s, 1H), 3.26 (q, J = 6.6 Hz, 2H), 3.08 (q, J = 6.6 Hz, 2H), 2.63 (t, J = 7.5 Hz, 2H), 1.77 (quint, J = 7.3 Hz, 2H), 1.42 (quint, J = 7.2 Hz, 2H), 1.32-1.18 (m, 4H), 0.85 (t, J = 7.0 Hz, 3H). ^{13}C-NMR (151 MHz, DMSO-d_6) δ 169.37, 159.06 (q, J = 33.2 Hz, TFA), 153.82, 153.68, 123.95, 123.48, 116.62 (q, J = 296.7 Hz, TFA), 39.87, 39.10, 28.60, 28.46, 28.38, 23.29, 21.75, 13.86. HRMS (ESI-MS): calcd. for $C_{13}H_{25}N_6OS^+$: 313.1805; found: 313.1807. MF: $C_{13}H_{24}N_6OS$ x $C_4H_2F_6O_4$. MW: (312.44 + 228.05).

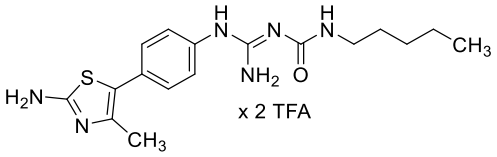

1-(Amino{[4-(2-amino-4-methylthiazol-5-yl)phenyl]amino}methylene)-3-(pentyl)urea dihydrotrifluoroacetate (5.33) was prepared from amine **5.15** (60 mg, 0.20 mmol, 1 equiv), **5.18** (66 mg, 0.22 mmol, 1.1 equiv), NEt_3 (68 µL, 0.49 mmol, 2.5 equiv) and $HgCl_2$ (107 mg, 0.39 mmol, 2 equiv) according to the general procedure yielding the product as a white, foamlike and hygroscopic solid (55 mg, 45%). R_f = 0.45 (CH_2Cl_2/MeOH 9:1). RP-HPLC: 100%, (t_R = 11.8 min, k = 2.68). ^{1}H-NMR (600 MHz, DMSO-d_6) δ 10.72 (br s, 1H), 10.13 (br s, 1H), 9.33-7.91 (m, 4H), 7.59 (t, J = 5.6 Hz, 1H), 7.51-7.45 (m, 2H), 7.41-7.35 (m, 2H), 3.11 (t, J = 7.0 Hz, 2H), 2.25 (s, 3H), 1.44 (quint, J = 7.1 Hz, 2H), 1.33-1.19 (m, 4H), 0.86 (t, J = 7.1 Hz, 3H). ^{13}C-NMR (151 MHz, DMSO-d_6): δ 166.94, 159.14 (q, J = 33.1 Hz, TFA), 153.48, 153.36,

138.18, 137.69, 132.72, 130.37, 129.35, 126.20, 116.55 (q, *J* = 298.0 Hz, TFA), 115.92, 39.20, 28.53, 28.39, 21.75, 14.43, 13.87. HRMS (ESI-MS): calcd. for $C_{17}H_{25}N_6OS^+$: 361.1805; found: 361.1806. MF: $C_{17}H_{24}N_6OS$ x $C_4H_2F_6O_4$. MW: (380.48 + 228.05).

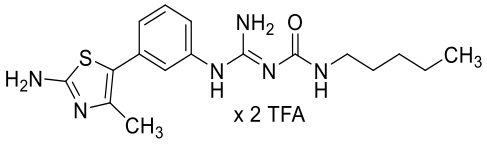

1-(Amino{[3-(2-amino-4-methylthiazol-5-yl)phenyl]amino}methylene)-3-(pentyl)urea dihydrotrifluoroacetate (5.34) was prepared from amine **5.16** (30 mg, 0.10 mmol, 1 equiv), **5.18** (33 mg, 0.11 mmol, 1.1 equiv), NEt_3 (33 µL, 0.25 mmol, 2.5 equiv) and $HgCl_2$ (53 mg, 0.20 mmol, 2 equiv) according to the general procedure yielding the product as a white, foamlike and hygroscopic solid (28 mg, 48%). R_f = 0.55 (CH_2Cl_2/MeOH 9:1). RP-HPLC: 100%, (t_R = 12.0 min, *k* = 2.74). ^{1}H-NMR (600 MHz, DMSO-d_6) δ 10.64 (br s, 1H), 10.00 (br s, 1H), 9.30-7.78 (m, 4H), 7.57 (t, *J*=5.6 Hz, 1H), 7.52 (t, *J* = 7.9 Hz, 1H), 7.39-7.35 (m, 1H), 7.34 (t, *J* = 2.0 Hz, 1H), 7.29-7.24 (m, 1H), 3.11 (t, *J* = 7.0 Hz, 2H), 2.25 (s, 3H), 1.44 (quint, *J* = 7.1 Hz, 2H), 1.34-1.19 (m, 4H), 0.86 (t, *J* = 7.1 Hz, 3H).^{13}C-NMR (151 MHz, DMSO-d_6) δ 166.86, 159.00 (q, *J* = 32.8 Hz, TFA), 153.52, 153.34, 134.31, 133.13, 130.40, 127.21, 125.21, 124.28, 116.66 (q, *J* = 296.3 Hz, TFA), 115.89, 39.17, 28.54, 28.38, 21.74, 14.82, 13.88. HRMS (ESI-MS): calcd. for $C_{17}H_{25}N_6OS^+$: 361.1805; found: 361.1811. MF: $C_{17}H_{24}N_6OS$ x $C_4H_2F_6O_4$. MW: (360.48 + 228.05).

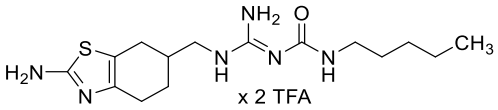

1-(Amino{[(2-amino-4,5,6,7-tetrahydrobenzo[*d*]thiazol-6-yl)methyl]amino}methylene)-3-(pentyl)urea dihydrotrifluoroacetate (5.35) was prepared from amine **5.17** (77 mg, 0.18 mmol, 1.1 equiv), **5.18** (50 mg, 0.17 mmol, 1 equiv), NEt_3 (57 µL, 0.41 mmol, 2.5 equiv) and $HgCl_2$ (90 mg, 0.33 mmol, 2 equiv) according to the general procedure yielding the product as a white, foamlike and hygroscopic solid (21 mg, 22%). R_f = 0.59 (CH_2Cl_2/MeOH 9:1). RP-HPLC: 100%, (t_R = 10.6 min, *k* = 2.30). ^{1}H-NMR (600 MHz, DMSO-d_6): δ 10.56 (br s, 1H), 9.28-8.81 (m, 3H), 8.56 (br s, 2H), 7.51 (br s, 1H), 3.36-3.22 (m, 2H), 3.08 (q, *J* = 6.6 Hz, 2H), 2.67-2.58 (m, 1H), 2.56-2.50 (m, 1H), 2.47-2.36 (m, 1H), 2.23-2.16 (m, 1H), 2.10-2.00 (m, 1H), 1.92-1.83 (m, 1H),

1.50-1.38 (m, 3H), 1.31-1.17 (m, 4H), 0.85 (t, J = 7.1 Hz, 3H). ^{13}C-NMR (151 MHz, DMSO-d_6): δ 168.63, 159.46 (q, J = 32.8 Hz, TFA), 154.08, 153.83, 134.60, 116.85 (q, J = 296.5 Hz, TFA), 113.20, 44.62, 40.05, 39.16, 33.22, 28.63, 28.42, 25.52, 24.53, 22.00, 21.78, 13.88. HRMS (ESI-MS): calcd. for $C_{15}H_{27}N_6OS^+$: 399.1962; found: 399.1964. MF: $C_{15}H_{26}N_6OS$ x $C_4H_2F_6O_4$. MW: (338.47 + 228.05).

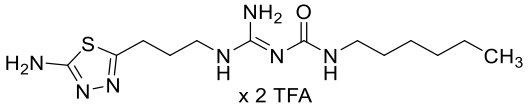

1-(Amino{[3-(5-amino-1,3,4-thiadiazol-2-yl)propyl]amino}methylene)-3-(hexyl)urea dihydrotrifluoroacetate (5.36) was prepared from amine **5.11** (22 mg, 0.086 mmol, 1 equiv), **5.19** (30 mg, 0.095 mmol, 1.1 equiv), NEt_3 (30 µL, 0.215 mmol, 2.5 equiv) and $HgCl_2$ (47 mg, 0.172 mmol, 2 equiv) according to the general procedure yielding the product as a white, foamlike and hygroscopic solid (8.44 mg, 18%). RP-HPLC: 96%, (t_R = 12.9 min, k = 3.02). ^{1}H-NMR (600 MHz, DMSO-d_6) δ 10.15 (br s, 1H), 9.01 (br s, 1H), 8.50 (br s, 2H), 8.03-7.24 (m, 3H), 3.30 (q, J = 6.7 Hz, 2H), 3.09 (q, J = 6.6 Hz, 2H), 2.86 (t, J = 7.5 Hz, 2H), 1.89 (quint, J = 7.4 Hz, 2H), 1.43 (quint, J = 6.9 Hz, 2H), 1.31-1.21 (m, 6H), 0.89-0.83 (m, 2H). ^{13}C-NMR (151 MHz, DMSO-d_6) δ 168.77, 157.42, 158.59 (q, J = 34.2 Hz, TFA), 153.79, 153.60, 116.18 (q, J = 293.6 Hz, TFA), 39.97, 39.14, 30.87, 28.87, 27.29, 26.52, 25.86, 22.01, 13.87. HRMS (ESI-MS): calcd. for $C_{13}H_{26}N_7OS^+$: 328.1914; found: 328.1917. MF: $C_{13}H_{25}N_7OS$ x $C_4H_2F_6O_4$. MW: (327.45 + 228.05).

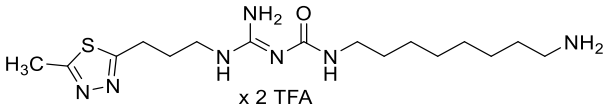

1-(Amino{[3-(5-methyl-1,3,4-thiadiazol-2-yl)propyl]amino}methylene)-3-(8-aminooctyl)urea dihydrotrifluoroacetate (5.38) was prepared from amine **5.10** (17 mg, 0.11 mmol, 1.1 equiv), **5.20** (46 mg, 0.1 mmol, 1 equiv), NEt_3 (35 µL, 0.25 mmol, 2.5 equiv) and $HgCl_2$ (54 mg, 0.2 mmol, 2 equiv) according to the general procedure yielding the product as a white, foamlike and hygroscopic solid (22 mg, 37%). R_f = 0.48 (CH_2Cl_2/MeOH 9:1). RP-HPLC: 97%, (t_R = 9.1 min, k = 1.83). ^{1}H-NMR (600 MHz, DMSO-d_6): δ 10.54 (br s, 1H), 9.05 (br s, 1H), 8.53 (br s, 2H), 7.77 (br s, 3H), 7.52 (br s, 1H), 3.40-3.29 (m, 4H), 3.11-3.05 (m, 4H), 2.76 (t,

J = 6.7 Hz, 2H), 2.67 (s, 3H), 1.96 (quint, *J* = 7.3 Hz, 2H), 1.51 (quint, *J* = 7.3 Hz, 2H), 1.46-1.39 (m, 2H), 1.32-1.21 (m, 8H). ^{13}C-NMR (151 MHz, DMSO-d_6): δ 169.62, 165.49, 159.38 (q, *J* = 31.3 Hz, TFA), 154.36, 154.18, 117.44 (q, *J* = 297.3 Hz, TFA), 40.48, 40.52, 39.26, 29.37, 28.91, 28.89, 28.40, 27.42, 26.77, 26.55, 26.19, 15.57. HRMS (ESI-MS): calcd. for $C_{16}H_{32}N_7OS^+$: 370.2384; found: 370.2388 MF: $C_{16}H_{31}N_7OS$ x $C_4H_2F_6O_4$. MW: (369.53 + 228.05).

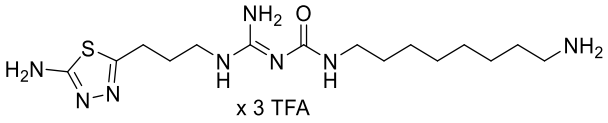

1-(Amino{[3-(5-amino-1,3,4-thiadiazol-2-yl)propyl]amino}methylene)-3-(8-aminooctyl)urea trihydrotrifluoroacetate (5.39) was prepared from amine **5.11** (15 mg, 0.054 mmol, 1 equiv), **5.20** (25 mg, 0.05 mmol, 1.1 equiv), NEt_3 (19 µL, 0.14 mmol, 2.5 equiv) and $HgCl_2$ (29 mg, 0.11 mmol, 2 equiv) according to the general procedure yielding the product as a white, foamlike and hygroscopic solid (10 mg, 26%). RP-HPLC: 96%, (t_R = 7.9 min, *k* = 1.46). ^{1}H-NMR (600 MHz, DMSO-d_6): δ 10.39 (br s, 1H), 9.05 (br s, 1H), 8.54 (br s, 2H), 7.88-7.29 (m, 6H), 3.32 (q, *J* = 6.7 Hz, 2H), 3.11 (q, *J* = 6.6 Hz, 2H), 2.87 (t, *J* = 7.5 Hz, 2H), 2.82-2.74 (m, 2H), 1.91 (quint, *J* = 7.4 Hz, 2H), 1.53 (quint, *J* = 7.4 Hz, 2H), 1.45 (q, *J* = 6.7 Hz, 2H), 1.28 (s, 8H). ^{13}C-NMR (151 MHz, DMSO-d_6): δ 168.65, 158.58 (q, *J* = 33.5 Hz, TFA), 157.35, 153.84, 153.67, 116.53 (q, *J* = 296.1 Hz, TFA), 39.94, 39.16, 38.80, 28.90, 28.44, 27.38, 26.96, 26.49, 26.10, 25.72. HRMS (ESI-MS): calcd. for $C_{15}H_{31}N_8OS^+$: 370.2384; found: 370.2388. MF: $C_{15}H_{30}N_8OS$ x $C_6H_3F_9O_6$. MW: (369.53 + 342.07).

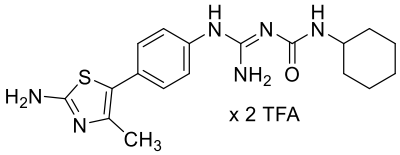

1-(Amino{[4-(2-amino-4-methylthiazol-5-yl)phenyl]amino}methylene)-3-(cyclohexyl)urea dihydrotrifluoroacetate (5.40) was prepared from amine **5.15** (50 mg, 0.16 mmol, 1 equiv), **5.21** (57 mg, 0.18 mmol, 1.1 equiv), NEt_3 (57 µL, 0.41 mmol, 2.5 equiv) and $HgCl_2$ (89 mg, 0.33 mmol, 2 equiv) according to the general procedure yielding the product as a white, foamlike and hygroscopic solid (51 mg, 53%). R_f = 0.54 (CH_2Cl_2/MeOH 9:1). RP-HPLC: 100%, (t_R = 11.6 min, *k* = 2.61). ^{1}H-NMR (600 MHz, DMSO-d_6): δ 10.87 (br s, 1H), 10.18 (br s, 1H),

9.39-8.20 (m, 4H), 7.64 (d, *J* = 7.6 Hz, 1H), 7.54-7.48 (m, 2H), 7.43-7.37 (m, 2H), 3.55-3.44 (m, 1H), 2.27 (s, 3H), 1.86-1.73 (m, 2H), 1.71-1.60 (m, 2H), 1.58-1.48 (m, 1H), 1.36-1.12 (m, 5H). ^{13}C-NMR (151 MHz, DMSO-d_6): δ 167.25, 159.13 (q, *J* = 33.7 Hz, TFA), 153.55, 152.60, 136.24, 133.04, 129.92, 129.45, 126.26, 116.57 (q, *J* = 297.3 Hz, TFA), 115.79, 48.40, 32.05, 24.96, 24.12, 13.95. HRMS (ESI-MS): calcd. for $C_{18}H_{25}N_6OS^+$: 373.1805; found: 373.1804. MF: $C_{18}H_{24}N_6OS$ x $C_4H_2F_6O_4$. MW: (372.49 + 228.05).

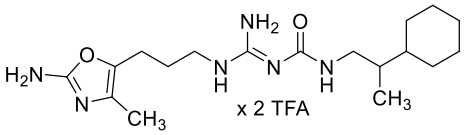

1-(Amino{[3-(2-amino4-methyloxazol-5-yl)propyl]amino}methylene)-3-(2-cyclohexylpropyl)urea dihydrotrifluoroacetate (5.41) was prepared from amine **5.9** (35 mg, 0.1 mmol, 1 equiv), **5.22** (36 mg, 0.1. mmol, 1 equiv), NEt_3 (35 µL, 0.25 mmol, 2.5 equiv) and $HgCl_2$ (54 mg, 0.2 mmol, 2 equiv) according to the general procedure yielding the product as a white, foamlike and hygroscopic solid (14.1 mg, 24%). R_f = 0.52 (CH_2Cl_2/MeOH 9:1). RP-HPLC: 97%, (t_R = 15.0 min, *k* = 3.67). ^{1}H-NMR (600 MHz, DMSO-d_6) δ 10.38 (br s, 1H), 9.00 (br s, 3H), 8.51 (br s, 2H), 7.48 (br s, 1H), 3.28 (q, *J* = 6.7 Hz, 2H), 3.19-3.12 (m, 1H), 2.99-2.92 (m, 1H), 2.59 (t, *J* = 7.3 Hz, 2H), 2.01 (s, 3H), 1.80-1.69 (m, 4H), 1.66-1.56 (m, 4H), 1.51-1.44 (m, 1H), 1.26-0.91 (m, 7H), 0.81 (d, *J* = 6.9 Hz, 3H). ^{13}C-NMR (151 MHz, DMSO-d_6) δ 158.83 (q, *J* = 32.5 Hz, TFA), 157.40, 153.84, 153.74, 139.03, 120.74, 116.81 (q, *J* = 295.7 Hz, TFA), 42.87, 40.06, 39.24, 37.79, 30.29, 27.92, 26.24, 26.17, 26.07, 25.93, 20.21, 14.04, 7.95. HRMS (ESI-MS): calcd. for $C_{18}H_{33}N_6O_2^+$: 365.2660; found: 365.2660. MF: $C_{18}H_{32}N_6O_2$ x $C_4H_2F_6O_4$. MW: (364.26 + 228.05).

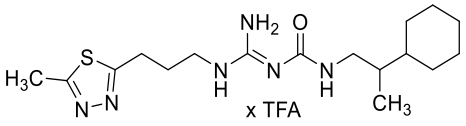

1-(Amino{[3-(5-methyl-1,3,4-thiadiazol-2-yl)propyl]amino}methylene)-3-(2-cyclohexylpropyl)urea hydrotrifluoroacetate (5.42) was prepared from amine **5.10** (22 mg, 0.14 mmol, 1.1 equiv), **5.22** (46 mg, 0.13 mmol, 1 equiv), NEt_3 (43 µL, 0.32 mmol, 2.5 equiv) and $HgCl_2$ (70 mg, 0.26 mmol, 2 equiv) according to the general procedure yielding the product as a white, foamlike and hygroscopic solid (12 mg, 19%). R_f = 0.54 (CH_2Cl_2/MeOH 9:1). RP-HPLC:

97%, (t_R = 17.9 min, k = 4.58). ^{1}H-NMR (600 MHz, DMSO-d_6): δ 10.19 (br s, 1H), 9.02 (br s, 1H), 8.51 (br s, 2H), 7.47 (br s, 1H), 3.35-3.31 (m, 2H), 3.17-3.04 (m, 3H), 2.97-2.89 (m, 1H), 2.68 (s, 3H), 1.97 (quint, J = 7.4 Hz, 2H), 1.75-1.66 (m, 2H), 1.64-1.53 (m, 3H), 1.51-1.42 (m, 1H), 1.25-0.90 (m, 6H), 0.80 (d, J = 6.9 Hz, 3H). ^{13}C-NMR (151 MHz, DMSO-d_6): δ 169.62, 165.49, 159.43 (q, J = 32.2 Hz, TFA), 154.23, 154.15, 117.50 (q, J = 296.6 Hz, TFA), 43.35, 40.51, 38.25, 30.76, 28.38, 26.78, 26.71, 26.64, 26.54, 15.58, 14.52. HRMS (ESI-MS): calcd. for $C_{17}H_{31}N_6OS^+$: 367.2275; found: 367.2301. MF: $C_{17}H_{30}N_6OS$ x $C_2HF_3O_2$. MW: (366.53 + 114.02).

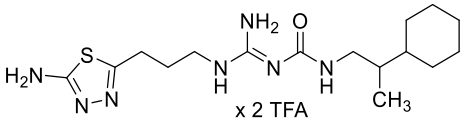

1-(Amino{[3-(5-amino-1,3,4-thiadiazol-2-yl)propyl]amino}methylene)-3-(2-cyclohexylpropyl)urea dihydrotrifluoroacetate (5.43) was prepared from amine **5.11** (20 mg, 0.08 mmol, 1 equiv), **5.22** (31 mg, 0.09 mmol, 1.1 equiv), NEt_3 (27 µL, 0.20 mmol, 2.5 equiv) and $HgCl_2$ (43 mg, 0.16 mmol, 2 equiv) according to the general procedure yielding the product as a white, foamlike and hygroscopic solid (8 mg, 17%). RP-HPLC: 99%, (t_R = 15.5 min, k = 3.83). ^{1}H-NMR (600 MHz, DMSO-d_6): δ 10.01 (br s, 1H), 8.98 (br s, 1H), 8.48 (br s, 2H), 7.46 (br s, 3H), 3.29 (q, J = 6.7 Hz, 2H), 3.16-3.09 (m, 1H), 2.96-2.89 (m, 1H), 2.84 (t, J = 7.5 Hz, 2H), 1.88 (quint, J = 7.3 Hz, 2H), 1.72-1.66 (m, 2H), 1.63-1.53 (m, 3H), 1.50-1.41 (m, 1H), 1.25-0.88 (m, 6H), 0.79 (d, J = 6.9 Hz, 3H). ^{13}C-NMR (151 MHz, DMSO-d_6): δ 168.60, 158.58 (q, J = 33.5 Hz, TFA), 157.33, 153.90, 153.68, 116.46 (q, J = 296.2 Hz, TFA), 42.88, 40.01, 39.45, 37.77, 30.28, 27.91, 27.37, 26.49, 26.24, 26.17, 26.07, 14.06. HRMS (ESI-MS): calcd. for $C_{16}H_{30}N_7OS^+$: 368.2227; found: 368.2230. MF: $C_{16}H_{29}N_7OS$ x $C_4H_2F_6O_4$. MW: (367.52 + 228.05).

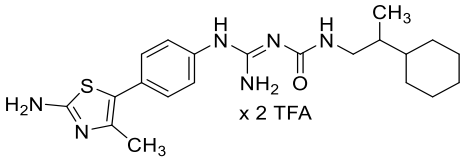

1-(Amino{[4-(2-amino-4-methylthiazol-5-yl)phenyl]amino}methylene)-3-(2-cyclohexylpropyl)urea dihydrotrifluoroacetate (5.44) was prepared from amine **5.15** (32 mg, 0.11 mmol, 1.1 equiv), **5.22** (34 mg, 0.10 mmol, 1 equiv), NEt_3 (33 µL, 0.24 mmol, 2.5 equiv) and $HgCl_2$ (52 mg, 0.19 mmol, 2 equiv) according to the general procedure yielding the product as a

white, foamlike and hygroscopic solid (41 mg, 64%). R_f = 0.50 (CH_2Cl_2/MeOH 9:1). RP-HPLC: 100%, (t_R = 15.6 min, k = 3.86). ^{1}H-NMR (600 MHz, DMSO-d_6): δ 10.86 (br s, 1H), 10.42 (br s, 1H), 9.48-8.14 (m, 4H), 7.61 (t, J = 5.8 Hz, 1H), 7.54-7.47 (m, 2H), 7.43-7.37 (m, 2H), 3.21-3.12 (m, 1H), 3.01-2.92 (m, 1H), 2.27 (s, 3H), 1.75-1.66 (m, 2H), 1.65-1.55 (m, 3H), 1.52-1.44 (m, 1H), 1.28-0.90 (m, 6H), 0.81 (d, J = 6.9 Hz, 3H). ^{13}C-NMR (151 MHz, DMSO-d_6): δ 167.22, 159.16 (q, J = 33.8 Hz, TFA), 153.50, 136.35, 133.09, 129.90, 129.43, 126.13, 116.56 (q, J = 297.3 Hz, TFA), 115.82, 42.99, 39.71, 37.75, 30.29, 27.92, 26.23, 26.17, 26.06, 14.07, 13.99. HRMS (ESI-MS): calcd. for $C_{21}H_{31}N_6OS^+$: 415.2275; found: 415.2275. MF: $C_{21}H_{30}N_6OS$ x $C_4H_2F_6O_4$. MW: (414.57 + 228.05).

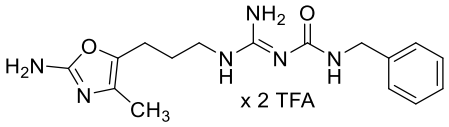

1-(Amino{[3-(2-amino-4-methyloxazol-5-yl)propyl]amino}methylene)-3-(benzyl)urea dihydrotrifluoroacetate (5.45) was prepared from amine **5.9** (35 mg, 0.1 mmol, 1 equiv), **5.23** (32 mg, 0.1 mmol, 1 equiv), NEt_3 (35 µL, 0.25 mmol, 2.5 equiv) and $HgCl_2$ (54 mg, 0.2 mmol, 2 equiv) according to the general procedure yielding the product as a white, foamlike and hygroscopic solid (14.9 mg, 27%). R_f = 0.52 (CH_2Cl_2/MeOH 9:1). RP-HPLC: 96%, (t_R = 10.4 min, k = 2.24). ^{1}H-NMR (600 MHz, DMSO-d_6) δ 10.51 (br s, 1H), 9.14-8.85 (m, 3H), 8.55 (br s, 2H), 8.00 (br s, 1H), 7.39-7.19 (m, 5H), 4.31 (d, J = 5.8 Hz, 2H), 3.27 (q, J = 6.7 Hz, 2H), 2.57 (t, J = 7.3 Hz, 2H), 1.99 (s, 3H), 1.75 (quint, J = 7.2 Hz, 2H). ^{13}C-NMR (151 MHz, DMSO-d_6) δ 158.79 (q, J = 32.4 Hz, TFA), 157.42, 153.82, 153.77, 139.01, 138.68, 128.40, 127.22, 127.11, 120.81, 116.87 (q, J = 298.7 Hz, TFA), 42.77, 40.06, 25.92, 20.22, 7.98. HRMS (ESI-MS): calcd. for $C_{16}H_{23}N_6O_2^+$: 331.1877; found: 331.1882. MF: $C_{16}H_{22}N_6O_2$ x $C_4H_2F_6O_4$. MW: (330.39 + 228.05).

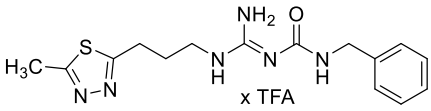

1-(Amino{[3-(5-methyl-1,3,4-thiadiazol-2-yl)propyl]amino}methylene)-3-(benzyl)urea hydrotrifluoroacetate (5.46) was prepared from amine **5.10** (25 mg, 0.16 mmol, 1.1 equiv), **5.23** (47 mg, 0.15 mmol, 1 equiv), NEt_3 (50 µL, 0.36 mmol, 2.5 equiv) and $HgCl_2$ (79 mg, 0.29 mmol,

2 equiv) according to the general procedure yielding the product as a white, foamlike and hygroscopic solid (13.5 mg, 20%). $R_f = 0.54$ (CH_2Cl_2/MeOH 9:1). RP-HPLC: 98%, (t_R = 12.6 min, k = 2.93). ^{1}H-NMR (600 MHz, DMSO-d_6): δ 10.40-10.08 (m, 1H), 9.03 (br s, 1H), 8.54 (br s, 2H), 8.05-7.95 (m, 1H), 7.38-7.22 (m, 5H), 4.31 (d, J = 5.8 Hz, 2H), 3.39-3.28 (m, 2H), 3.07 (t, J = 7.6 Hz, 2H), 2.67 (s, 3H), 1.96 (quint, J = 7.2 Hz, 2H). ^{13}C-NMR (151 MHz, DMSO-d_6): δ 169.62, 165.50, 159.42 (q, J = 30.9 Hz, TFA), 154.24, 139.13, 128.88, 127.70, 127.58, 117.47 (q, J = 296.9 Hz, TFA), 43.24, 40.55, 28.35, 26.79, 15.58. HRMS (ESI-MS): calcd. for $C_{15}H_{21}N_6OS^+$: 333.1492; found: 333.1501. MF: $C_{15}H_{20}N_6OS$ x $C_2HF_3O_2$. MW: (332.43 + 114.02).

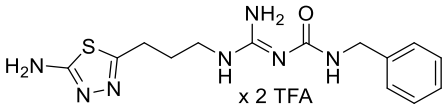

1-(Amino{[3-(5-amino-1,3,4-thiadiazol-2-yl)propyl]amino}methylene)-3-(benzyl)urea dihydrotrifluoroacetate (5.47) was prepared from amine **5.11** (48 mg, 0.19 mmol, 1.2 equiv), **5.23** (50 mg, 0.16 mmol, 1 equiv), NEt_3 (54 µL, 0.39 mmol, 2.5 equiv) and $HgCl_2$ (84 mg, 0.31 mmol, 2 equiv) according to the general procedure yielding the product as a white, foamlike and hygroscopic solid (20.8 mg, 23%). RP-HPLC: 98%, (t_R = 10.4 min, k = 2.24). ^{1}H-NMR (600 MHz, DMSO-d_6) δ 10.46 (br s, 1H), 9.06 (br s, 1H), 8.56 (br s, 2H), 8.35-7.51 (m, 2H), 7.36-7.22 (m, 5H), 4.31 (d, J = 5.8 Hz, 2H), 3.30 (q, J = 6.7 Hz, 2H), 2.86 (t, J = 7.6 Hz, 2H), 1.89 (quint, J = 7.3 Hz, 2H). ^{13}C-NMR (151 MHz, DMSO-d_6) δ 169.07, 158.95 (q, J = 34.7 Hz, TFA), 157.58, 153.84 (2C), 138.70, 128.41 (2C), 127.24 (2C), 127.10, 116.14 (q, J = 295.1 Hz, TFA) 42.78, 40.00, 27.16, 26.59. HRMS (ESI-MS): calcd. for $C_{14}H_{20}N_7OS^+$: 334.1445; found: 334.1447. MF: $C_{14}H_{19}N_7OS$ x $C_4H_2F_6O_4$. MW: (333.41 + 228.05).

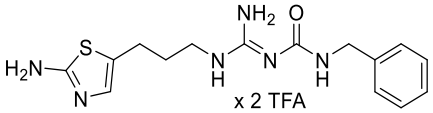

1-(Amino{[3-(2-aminothiazol-5-yl)propyl]amino}methylene)-3-(benzyl)urea dihydrotrifluoroacetate (5.48) was prepared from amine **5.12** (30 mg, 0.12 mmol, 1 equiv), **5.23** (41 mg, 0.13 mmol, 1.1 equiv), NEt_3 (41 µL, 0.29 mmol, 2.5 equiv) and $HgCl_2$ (64 mg, 0.23 mmol, 2 equiv) according to the general procedure yielding the product as a white, foamlike and hygroscopic solid (20.4 mg, 30%). $R_f = 0.56$ (CH_2Cl_2/MeOH 9:1). RP-HPLC: 100%,

(t_R = 10.2 min, k = 2.18). ^{1}H-NMR (600 MHz, DMSO-d_6) δ 10.68 (br s, 1H), 9.10 (br s, 3H), 8.57 (br s, 2H), 8.01 (br s, 1H), 7.43-7.20 (m, 5H), 7.06 (s, 1H), 4.32 (d, J = 5.9 Hz, 2H), 3.27 (q, J = 6.6 Hz, 2H), 2.64 (t, J = 7.5 Hz, 2H), 1.79 (quint, J = 7.3 Hz, 2H). ^{13}C-NMR (151 MHz, DMSO-d_6) δ 169.35, 159.24 (q, J = 32.7 Hz, TFA), 153.88, 153.83, 138.72, 128.40 (2C), 127.22 (2C), 127.09, 123.96, 123.88, 116.7 (q, J = 298.4 Hz, TFA), 42.76, 39.94, 28.49, 23.30. HRMS (ESI-MS): calcd. for $C_{15}H_{21}N_6OS^+$: 333.1492; found: 333.1495. MF: $C_{15}H_{20}N_6OS$ x $C_4H_2F_6O_4$. MW: (332.43 + 228.05).

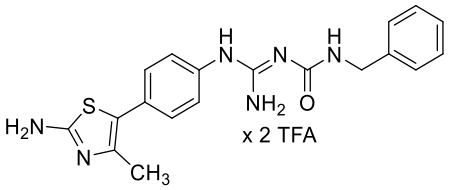

1-(Amino{[4-(2-amino-4-methylthiazol-5-yl)phenyl]amino}methylene)-3-(benzyl)urea dihydrotrifluoroacetate (5.49) was prepared from amine **5.15** (60 mg, 0.20 mmol, 1 equiv), **5.23** (70 mg, 0.22 mmol, 1.1 equiv), NEt_3 (68 µL, 0.49 mmol, 2.5 equiv) and $HgCl_2$ (107 mg, 0.39 mmol, 2 equiv) according to the general procedure yielding the product as a white, foamlike and hygroscopic solid (58 mg, 48%). R_f = 0.46 (CH_2Cl_2/MeOH 9:1). RP-HPLC: 99%, (t_R = 10.9 min, k = 2.40). ^{1}H-NMR (600 MHz, DMSO-d_6) δ 11.69-10.16 (m, 2H), 9.42-8.58 (m, 4H), 8.15 (t, J = 5.9 Hz, 1H), 7.54-7.49 (m, 2H), 7.45-7.39 (m, 2H), 7.38-7.25 (m, 5H), 4.35 (d, J = 5.8 Hz, 2H), 2.27 (s, 3H). ^{13}C-NMR (151 MHz, DMSO-d_6): δ 167.46, 159.52 (q, J = 33.6 Hz, TFA), 153.62, 138.52, 135.20, 133.36, 129.52, 128.43, 127.33, 127.17, 126.19, 116.55 (q, J = 295.9 Hz, TFA), 115.73, 42.88, 13.63. HRMS (ESI-MS): calcd. for $C_{19}H_{21}N_6OS^+$: 381.1492; found: 381.1491. MF: $C_{19}H_{20}N_6OS$ x $C_4H_2F_6O_4$. MW: (380.47 + 228.05).

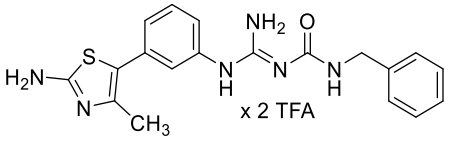

1-(Amino{[3-(2-amino-4-methylthiazol-5-yl)phenyl]amino}methylene)-3-(benzyl)urea dihydrotrifluoroacetate (5.50) was prepared from amine **5.16** (30 mg, 0.10 mmol, 1 equiv), **5.23** (35 mg, 0.22 mmol, 1.1 equiv), NEt_3 (33 µL, 0.25 mmol, 2.5 equiv) and $HgCl_2$ (53 mg, 0.20 mmol, 2 equiv) according to the general procedure yielding the product as a white, foamlike

and hygroscopic solid (27 mg, 44%). $R_f = 0.52$ (CH_2Cl_2/MeOH 9:1). RP-HPLC: 100%, ($t_R = 11.1$ min, $k = 2.46$). ^{1}H-NMR (600 MHz, DMSO-d_6): δ 10.90 (br s, 1H), 10.54 (br s, 1H), 8.42-9.20 (m, 4H), 8.11 (t, $J = 5.9$ Hz, 1H), 7.53 (t, $J = 8.0$ Hz, 1H), 7.42-7.23 (m, 8H), 4.34 (d, $J = 5.8$ Hz, 2H), 2.26 (s, 3H). ^{13}C-NMR (151 MHz, DMSO-d_6): δ 167.32, 159.14 (q, $J = 33.5$ Hz, TFA), 153.64, 153.60, 138.50, 136.81, 134.48, 132.36, 130.47, 128.42, 127.30, 127.16, 125.36, 124.75, 116.52 (q, $J = 295.6$ Hz, TFA), 115.65, 42.85, 14.04. HRMS (ESI-MS): calcd. for $C_{19}H_{21}N_6OS^+$: 381.1492; found: 381.1498. MF: $C_{19}H_{20}N_6OS$ x $C_4H_2F_6O_4$. MW: (380.47 + 228.05).

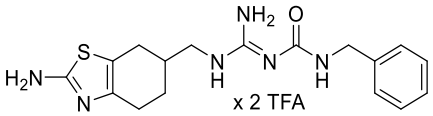

1-(Amino{[(2-amino-4,5,6,7-tetrahydrobenzo[*d*]thiazol-6-yl)methyl]amino}methylene)-3-(benzyl)urea dihydrotrifluoroacetate (5.51) was prepared from amine **5.17** (85 mg, 0.20 mmol, 1 equiv), **5.23** (71 mg, 0.22 mmol, 1.1 equiv), NEt_3 (76 µL, 0.55 mmol, 2.5 equiv) and $HgCl_2$ (119 mg, 0.44 mmol, 2 equiv) according to the general procedure yielding the product as a white, foamlike and hygroscopic solid (45 mg, 38%). $R_f = 0.48$ (CH_2Cl_2/MeOH 9:1). RP-HPLC: 100%, ($t_R = 9.8$ min, $k = 2.05$). ^{1}H-NMR (600 MHz, DMSO-d_6): δ 10.65 (br s, 1H), 9.27-8.84 (m, 3H), 8.61 (br s, 2H), 8.03 (br s, 1H), 7.35-7.30 (m, 2H), 7.30-7.23 (m, 3H), 4.31 (d, $J = 5.8$ Hz, 2H), 3.28 (q, $J = 6.8$ Hz, 2H), 2.63 (dd, $J = 16.2$, 5.0 Hz, 1H), 2.55-2.50 (m, 1H), 2.47-2.36 (m, 1H), 2.23-2.15 (m, 1H), 2.10-2.01 (m, 1H), 1.91-1.83 (m, 1H), 1.50-1.40 (m, 1H). ^{13}C-NMR (151 MHz, DMSO-d_6): δ 168.60, 159.33 (q, $J = 32.7$ Hz, TFA), 154.04, 153.98, 138.73, 134.64, 128.44, 127.26, 127.14, 116.82 (q, $J = 299.9$ Hz, TFA), 113.21, 44.67, 42.80, 33.20, 25.53, 24.54, 22.01. HRMS (ESI-MS): calcd. for $C_{17}H_{23}N_6OS^+$: 359.1649; found: 359.1645. MF: $C_{17}H_{22}N_6OS$ x $C_4H_2F_6O_4$. MW: (358.46 + 228.05).

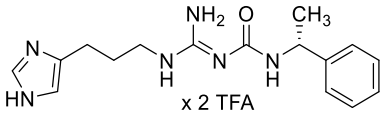

1-(Amino{[3-(1*H*-imidazol-4-yl)propyl]amino}methylene)-3-((*R*)-(1-phenylethyl))urea dihydrotrifluoroacetate (5.52) was prepared from **5.8** (327 mg, 0.89 mmol, 1 equiv), **5.24** (300 mg, 0.89 mmol, 1 equiv), $HgCl_2$ (265 mg, 0.98 mmol, 1.1 equiv) and NEt_3 (372 µL,

2.67 mmol, 3 equiv) according to the general procedure yielding 429.1 mg (73%) of Trt-/Boc-protected intermediate. 306 mg thereof were deprotected in the next step yielding **5.52** as a white, foamlike and hygroscopic solid after purification by preparative HPLC (129.7 mg, 51%). RP-HPLC: 100%, (t_R = 8.3 min, k = 2.11). ^{1}H-NMR (300 MHz, MeOD) δ 8.75 (d, J = 1.4 Hz, 1H), 7.35-7.18 (m, 6H), 4.94-4.85 (m, 1H), 3.38-3.29 (m, 2H), 2.81 (t, J = 7.3 Hz, 2H), 2.00 (quint, J = 7.4 Hz, 2H), 1.47 (d, J = 7.0 Hz, 3H). ^{13}C-NMR (75 MHz, MeOD) δ 161.87 (q, J = 34.4 Hz, TFA), 154.56, 153.29, 143.49, 133.46, 132.86, 128.72 (2C), 126.89, 125.56 (2C), 116.7 (q, J = 288.2 Hz, TFA), 114.97, 49.71, 39.99, 26.73, 21.29, 21.10. HRMS (ESI-MS): calcd. for $C_{16}H_{23}N_6O^+$: 315.1928, found: 315.1932. MF: $C_{16}H_{22}N_6O$ x $C_4H_2F_6O_4$. MW: (314.39 + 228.05).

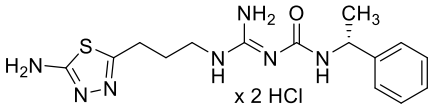

1-(Amino{[3-(5-amino-1,3,4-thiadiazol-2-yl)propyl]amino}methylene)-3-((*R*)-(1-phenylethyl))urea dihydrochloride (5.53) was prepared from **5.11** (407 mg, 1.47 mmol, 1 equiv), **5.24** (494 mg, 1.47 mmol, 1 equiv), $HgCl_2$ (438 mg, 1.61 mmol, 1.1 equiv) and NEt_3 (613 µL, 4.40 mmol, 3 equiv) according to the general procedure yielding the product as a white, foamlike and hygroscopic solid (50 mg, 8%). RP-HPLC: 100%, (t_R = 9.3 min, k = 2.48). ^{1}H-NMR (300 MHz, MeOD) δ 7.37-7.20 (m, 5H), 4.89-4.85 (m, 1H), 3.49-3.35 (m, 2H), 3.02 (t, J = 7.2 Hz, 2H), 2.09 (quint, J = 6.8 Hz, 2H), 1.47 (d, J = 6.9 Hz, 3H). ^{13}C-NMR (75 MHz, MeOD) δ 143.33, 128.26 (2C), 126.97, 125.65 (2C), 49.80, 40.08, 26.80, 26.63, 21.44, 4 C-signals are missing due to the low concentration of the sample. HRMS (ESI-MS): calcd. for $C_{15}H_{22}N_7OS^+$: 348.1601, found: 348.1605. MF: $C_{15}H_{21}N_7OS$ x H_2Cl_2. MW: (347.44 + 72.92).

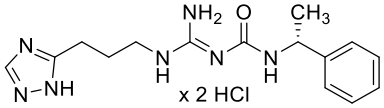

1-(Amino{[3-(1*H*-1,2,4-triazol-5-yl)propyl]amino}methylene)-3-((*R*)-(1-phenylethyl))urea dihydrochloride (5.54) was prepared from **5.13** (420 mg, 1.14 mmol, 1 equiv), **5.24** (423 mg, 1.25 mmol, 1.1 equiv), $HgCl_2$ (340 mg, 1.25 mmol, 1.1 equiv) and NEt_3 (474 µL, 3.42 mmol, 3 equiv) according to the general procedure yielding 560 mg (75%) of Trt-/Boc-protected intermediate. 540 mg thereof were deprotected in the next step yielding **5.54** as a white, foamlike

and hygroscopic solid after purification by preparative HPLC (200 mg, 63%). RP-HPLC: 100%, (t_R = 9.1 min, k = 2.41). ^{1}H NMR (300 MHz, MeOD) δ 9.27 (s, 1H), 7.41-7.19 (m, 5H), 4.88 (q, J = 6.8 Hz, 1H), 3.56-3.37 (m, 2H), 3.21-3.01 (m, 2H), 2.15 (quint, J = 7.3 Hz, 2H), 1.46 (d, J = 7.0 Hz, 3H). ^{13}C-NMR (75 MHz, MeOD) δ 155.98, 155.71, 154.19, 144.64, 143.46, 129.56 (2C), 128.27, 126.95 (2C), 51.11, 41.42, 26.36, 22.97, 22.84. HRMS (ESI-MS): calcd. for $C_{15}H_{22}N_7O^+$: 316,1880, found: 316.1883. MF: $C_{15}H_{21}N_7O$ x H_2Cl_2. MW: (315.38 + 72.92).

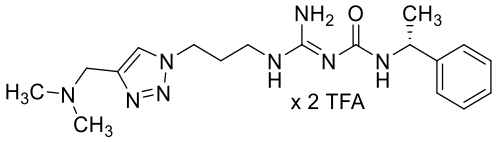

1-(Amino{[3-(4-((dimethylamino)methyl)-1*H*-1,2,3-triazol-1-yl)propyl]amino}methylene)-3-((*R*)-(1-phenylethyl))urea trihydrotrifluoroacetate (5.55) was prepared from **5.14** (298 mg, 1.63 mmol, 1 equiv), **5.24** (549 mg, 1.63 mmol, 1 equiv), $HgCl_2$ (486 mg, 1.79 mmol, 1.1 equiv) and NEt_3 (680 µL, 4.88 mmol, 3 equiv) according to the general procedure yielding the product as a white, foamlike and hygroscopic solid (50 mg, 5%). RP-HPLC: 98%, (t_R = 8.3 min, k = 2.11). ^{1}H-NMR (300 MHz, MeOD) δ 8.22 (s, 1H), 7.36-7.20 (m, 5H), 4.90-4.85 (m, 1H), 4.55 (t, J = 6.7 Hz, 2H), 4.42 (s, 2H), 3.34 (t, J = 6.7 Hz, 2H), 2.88 (s, 6H), 2.25 (p, J = 6.9 Hz, 2H), 1.47 (d, J = 7.0 Hz, 3H). ^{13}C-NMR (75 MHz, MeOD) δ 156.03, 144.86, 138.09, 129.63 (2C), 128.33, 128.05, 126.97 (2C), 52.42, 51.09, 48.65, 42.92 (2C), 39.51, 29.69, 22.70, 1 C signal is missing due to the low concentration of the sample. HRMS (ESI-MS): calcd. for $C_{18}H_{29}N_8O^+$: 373.2459, found: 373.2463. MF: $C_{18}H_{28}N_8O$ x $C_4H_2F_6O_4$. MW: (372.48 + 228.05).

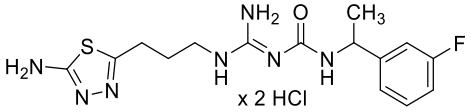

1-(Amino{[3-(5-amino-1,3,4-thiadiazol-2-yl)propyl]amino}methylene)-3-(1-(3-fluorophenyl)ethyl)urea dihydrochloride (5.56) was prepared from **5.11** (130 mg, 0.50 mmol, 1 equiv), **5.25** (179 mg, 0.50 mmol, 1 equiv), $HgCl_2$ (150 mg, 0.55 mmol, 1.1 equiv) and NEt_3 (211 µL, 1.51 mmol, 3 equiv) according to the general procedure yielding the product as a white, foamlike and hygroscopic solid (70 mg, 32%). RP-HPLC: 100%, (t_R = 9.8 min, k = 2.67). ^{1}H-NMR (300 MHz, MeOD) δ 7.40-7.29 (m, 1H), 7.20-7.06 (m, 2H), 7.02-6.92 (m, 1H), 4.91-4.86 (m, 1H), 3.46-3.38 (m, 2H), 3.03 (t, J = 7.4 Hz, 2H), 2.08 (p, J = 7.1 Hz, 2H), 1.47 (d, J = 7.0 Hz,

3H). ^{13}C-NMR (75 MHz, MeOD) δ 172.03, 164.29 (d, J = 244.2 Hz), 159.72, 155.61, 154.34, 147.72 (d, J = 7.0 Hz), 131.41 (d, J = 8.2 Hz), 122.88 (d, J = 2.7 Hz), 114.92 (d, J = 21.3 Hz), 113.81 (d, J = 22.2 Hz), 50.76, 41.44, 28.22, 27.50, 22.63. HRMS (ESI-MS): calcd. for $C_{15}H_{21}FN_7OS^+$: 366.1507, found: 366.1509. MF: $C_{15}H_{20}FN_7OS$ x H_2Cl_2. MW: (365.43 + 72.92).

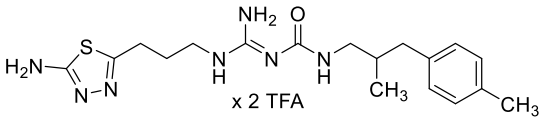

1-(Amino{[3-(5-amino-1,3,4-thiadiazol-2-yl)propyl]amino}methylene)-3-(2-methyl-3-(p-tolyl)propyl)urea dihydrotrifluoroacetate (5.57) was prepared from amine **5.11** (66 mg, 0.26 mmol, 1.1 equiv), **5.26** (85 mg, 0.22 mmol, 1 equiv), NEt_3 (78 µL, 0.56 mmol, 2.5 equiv) and $HgCl_2$ (121 mg, 0.45 mmol, 2 equiv) according to the general procedure yielding the product as a white, foamlike and hygroscopic solid (24 mg, 18%). RP-HPLC: 98%, (t_R = 15.0 min, k = 3.67). ^{1}H-NMR (600 MHz, DMSO-d_6): δ 10.28 (br s, 1H), 9.01 (br s, 1H), 8.50 (br s, 2H), 7.40-8.03 (s, 3H), 7.11-6.99 (m, 4H), 3.29 (q, J = 6.7 Hz, 2H), 3.12-3.02 (m, 1H), 2.96-2.89 (m, 1H), 2.85 (t, J = 7.5 Hz, 2H), 2.62-2.54 (m, 1H), 2.36-2.27 (m, 1H), 2.25 (s, 3H), 1.93-1.82 (m, 3H), 0.78 (d, J = 6.7 Hz, 3H). ^{13}C-NMR (151 MHz, DMSO-d_6) δ 168.81, 158.87 (q, J = 34.7 Hz, TFA), 157.45, 153.77, 136.97, 134.72, 128.81, 128.78, 116.33 (q, J = 294.0 Hz, TFA), 44.05, 40.06, 39.98, 34.86, 27.30, 26.53, 20.61, 17.08. HRMS (ESI-MS): calcd. for $C_{18}H_{28}N_7OS^+$: 390.2071; found: 390.2077. MF: $C_{18}H_{27}N_7OS$ x $C_4H_2F_6O_4$. MW: (389.52 + 228.05).

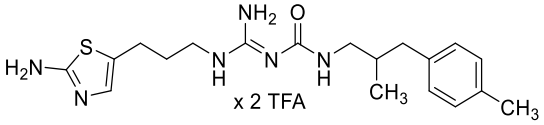

1-(Amino{[3-(2-aminothiazol-5-yl)propyl]amino}methylene)-3-(2-methyl-3-(p-tolyl)propyl)urea dihydrotrifluoroacetate (5.59) was prepared from amine **5.12** (37 mg, 0.15 mmol, 1.1 equiv), **5.26** (50 mg, 0.13 mmol, 1 equiv), NEt_3 (46 µL, 0.33 mmol, 2.5 equiv) and $HgCl_2$ (72 mg, 0.26 mmol, 2 equiv) according to the general procedure yielding the product as a white, foamlike and hygroscopic solid (18.2 mg, 23%). R_f = 0.55 (CH_2Cl_2/MeOH 9:1). RP-HPLC: 99%, (t_R = 14.5 min, k = 3.52). ^{1}H-NMR (600 MHz, DMSO-d_6) δ 10.51 (br s, 1H), 9.46-8.69 (m, 3H), 8.51 (br s, 2H), 7.56 (br s, 1H), 7.13-6.97 (m, 5H), 3.27 (q, J = 6.6 Hz, 2H), 3.13-3.03 (m, 1H), 2.98-2.87 (m, 1H), 2.64 (t, J = 7.5 Hz, 2H), 2.60-2.55 (m, 1H), 2.35-2.28 (m, 1H), 2.25 (s,

3H), 1.92-1.82 (m, 1H), 1.78 (quint, J = 7.3 Hz, 2H), 0.79 (d, J = 6.7 Hz, 3H). ^{13}C-NMR (151 MHz, DMSO-d_6) δ 169.30, 159.18 (q, J = 32.9 Hz, TFA) 153.81, 153.77, 136.97, 134.72, 128.81 (2C), 128.77 (2C), 123.96 (2C), 116.69 (q, J = 297.1 Hz, TFA), 44.64, 40.06, 39.90, 34.87, 28.52, 23.30, 20.61, 17.07. HRMS (ESI-MS): calcd. for $C_{19}H_{29}N_6OS^+$: 389.2118; found: 389.2122. MF: $C_{19}H_{28}N_6OS$ x $C_4H_2F_6O_4$. MW: (388.53 + 228.05).

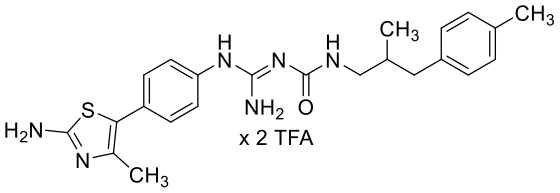

1-(Amino{[4-(2-amino-4-methylthiazol-5-yl)phenyl]amino}methylene)-3-(2-methyl-3-(p-tolyl)propyl)urea dihydrotrifluoroacetate (5.60) was prepared from amine **5.15** (50 mg, 0.16 mmol, 1 equiv), **5.26** (68 mg, 0.18 mmol, 1.1 equiv), NEt_3 (57 µL, 0.41 mmol, 2.5 equiv) and $HgCl_2$ (89 mg, 0.33 mmol, 2 equiv) according to the general procedure yielding the product as a white, foamlike and hygroscopic solid (58 mg, 55%). R_f = 0.64 (CH_2Cl_2/MeOH 9:1). RP-HPLC: 100%, (t_R = 15.2 min, k = 3.74). ^{1}H-NMR (600 MHz, DMSO-d_6): δ 10.88 (br s, 1H), 10.47 (br s, 1H), 9.29-8.29 (m, 4H), 7.70 (t, J = 5.8 Hz, 1H), 7.55-7.48 (m, 2H), 7.44-7.38 (m, 2H), 7.12-7.02 (m, 4H), 3.15-3.08 (m, 1H), 3.00-2.93 (m, 1H), 2.60 (dd, J = 13.5, 6.1 Hz, 1H), 2.32 (dd, J = 13.5, 8.2 Hz, 1H), 2.29-2.24 (m, 6H), 1.93-1.83 (m, 1H), 0.81 (d, J = 6.7 Hz, 3H). ^{13}C-NMR (151 MHz, DMSO-d_6) δ 167.31, 159.20 (q, J = 33.5 Hz, TFA), 153.55, 153.50, 136.94, 134.75, 133.23, 129.70, 129.47, 128.81, 128.79, 126.11, 116.59 (q, J = 295.9 Hz, TFA), 115.77, 44.74, 39.60, 34.83, 20.62, 17.09, 13.82. HRMS (ESI-MS): calcd. for $C_{23}H_{29}N_6OS^+$: 437.2118; found: 437.2118. MF: $C_{23}H_{28}N_6OS$ x $C_4H_2F_6O_4$. MW: (436.58 + 228.05).

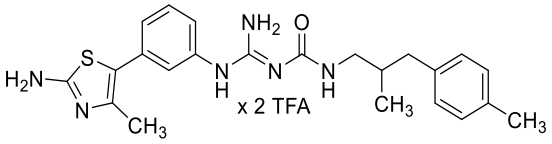

1-(Amino{[3-(2-amino-4-methylthiazol-5-yl)phenyl]amino}methylene)-3-(2-methyl-3-(p-tolyl)propyl)urea dihydrotrifluoroacetate (5.61) was prepared from amine **5.16** (20 mg, 0.07 mmol, 1 equiv), **5.26** (28 mg, 0.073 mmol, 1.1 equiv), NEt_3 (23 µL, 0.17 mmol, 2.5 equiv) and $HgCl_2$ (36 mg, 0.13 mmol, 2 equiv) according to the general procedure yielding the product

as a white, foamlike and hygroscopic solid (16 mg, 34%). R_f = 0.58 (CH_2Cl_2/MeOH 9:1). RP-HPLC: 100%, (t_R = 15.4 min, k = 3.80). ^{1}H-NMR (600 MHz, DMSO-d_6): δ 10.81 (br s, 1H), 10.37 (br s, 1H), 9.30-8.53 (m, 4H), 7.68 (t, J = 5.8 Hz, 1H), 7.59-7.53 (m, 1H), 7.43-7.38 (m, 2H), 7.35-7.30 (m, 1H), 3.15-3.06 (m, 1H), 3.00-2.91 (m, 1H), 2.63-2.55 (m, 1H), 2.35-2.20 (m, 7H), 1.93-1.82 (m, 1H), 0.80 (d, J = 6.7 Hz, 3H). ^{13}C-NMR (151 MHz, DMSO-d_6): δ 167.56, 158.84 (q, J = 34.5 Hz, TFA), 153.56, 136.92, 134.76, 134.56, 131.80, 130.57, 128.81, 128.79, 127.35, 125.47, 125.10, 116.83 (q, J = 295.7 Hz, TFA), 115.54, 44.71, 40.06, 34.85, 20.61, 17.07, 13.50. HRMS (ESI-MS): calcd. for $C_{23}H_{29}N_6OS^+$: 437.2118; found: 437.2116. MF: $C_{23}H_{28}N_6OS$ x $C_4H_2F_6O_4$. MW: (436.58 + 228.05).

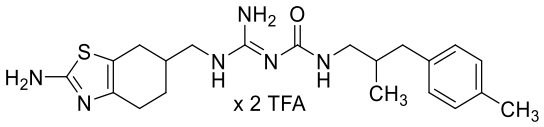

1-(Amino{[(2-amino-4,5,6,7-tetrahydrobenzo[*d*]thiazol-6-yl)methyl]amino}methylene)-3-(2-methyl-3-(p-tolyl)propyl)urea dihydrotrifluoroacetate (5.62) was prepared from amine **5.17** (82 mg, 0.19 mmol, 1.1 equiv), **5.26** (80 mg, 0.21 mmol, 1 equiv), NEt_3 (67 µL, 0.48 mmol, 2.5 equiv) and $HgCl_2$ (104 mg, 0.38 mmol, 2 equiv) according to the general procedure yielding the product as a white, foamlike and hygroscopic solid (22 mg, 16%). R_f = 0.49 (CH_2Cl_2/MeOH 9:1). RP-HPLC: 99%, (t_R = 14.1 min, k = 3.39). ^{1}H-NMR (600 MHz, DMSO-d_6): δ 10.36 (br s, 1H), 9.10 (br s, 1H), 8.90-8.32 (m, 4H), 7.58 (br s, 1H), 7.12-7.02 (m, 4H), 3.33-3.26 (m, 2H), 3.14-3.03 (m, 1H), 2.97-2.86 (m, 1H), 2.67-2.56 (m, 2H), 2.48-2.36 (m, 2H), 2.34-2.28 (m, 1H), 2.26 (s, 3H), 2.24-2.15 (m, 1H), 2.10-2.01 (m, 1H), 1.93-1.82 (m, 2H), 1.51-1.41 (m, 1H), 0.79 (d, J = 6.6 Hz, 3H). ^{13}C-NMR (151 MHz, DMSO-d_6) δ 168.13, 158.75 (q, J = 31.4 Hz, TFA), 153.94, 153.71, 136.95, 134.73, 128.81, 128.77, 117.06 (q, J = 297.8 Hz, TFA), 113.15, 44.66, 40.06, 34.86, 33.27, 25.59, 24.70, 22.44, 20.61, 17.08. HRMS (ESI-MS): calcd. for $C_{21}H_{31}N_6OS^+$: 415.2275; found: 415.2278. MF: $C_{21}H_{30}N_6OS$ x $C_4H_2F_6O_4$. MW: (414.57 + 228.05).

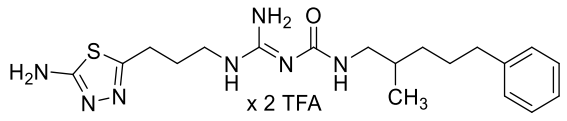

1-(Amino{[3-(5-amino-1,3,4-thiadiazol-2-yl)propyl]amino}methylene)-3-(2-methyl-5-phenylpentyl)urea dihydrotrifluoroacetate (5.63) was prepared from amine **5.11** (20 mg,

0.077 mmol, 1 equiv), **5.27** (33.5 mg, 0.085 mmol, 1.1 equiv), NEt_3 (27 µL, 0.19 mmol, 2.5 equiv) and $HgCl_2$ (42 mg, 0.15 mmol, 2 equiv) according to the general procedure yielding the product as a white, foamlike and hygroscopic solid (5.94 mg, 12%). RP-HPLC: 97%, (t_R = 16.4 min, k = 4.11). ^{1}H-NMR (600 MHz, DMSO-d_6) δ 9.92 (br s, 1H), 8.98 (br s, 1H), 8.49 (br s, 2H), 7.62-7.29 (m, 3H), 7.27-7.22 (m, 2H), 7.16 (d, J = 25.0 Hz, 3H), 3.29 (q, J = 6.7 Hz, 2H), 3.07-3.00 (m, 1H), 2.95-2.87 (m, 1H), 2.84 (t, J = 7.5 Hz, 2H), 2.58-2.52 (m, 2H), 1.88 (quint, J = 7.4 Hz, 2H), 1.66-1.48 (m, 3H), 1.36-1.27 (m, 1H), 1.13-1.05 (m, 1H), 0.83 (d, J = 6.7 Hz, 3H). ^{13}C-NMR (151 MHz, DMSO-d_6) δ 168.58, 158.46 (q, J = 33.9 Hz, TFA), 157.32, 153.69 (2C), 142.12, 128.23 (2C), 128.20 (2C), 125.62, 44.92, 40.00, 35.31, 33.21, 32.61, 28.31, 27.38, 26.48, 17.41, second TFA quartet at approx. 116 ppm was not visible. HRMS (ESI-MS): calcd. for $C_{19}H_{30}N_7OS^+$: 404.2227; found: 404.2232. MF: $C_{19}H_{29}N_7OS$ x $C_4H_2F_6O_4$. MW: (403.55 + 228.05).

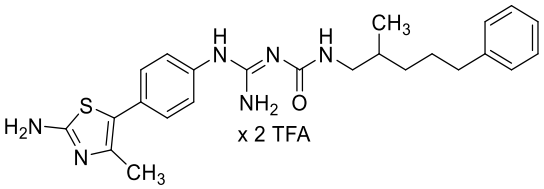

1-(Amino{[4-(2-amino-4-methylthiazol-5-yl)phenyl]amino}methylene)-3-(2-methyl-5-phenylpentyl)urea dihydrotrifluoroacetate (5.64) was prepared from amine **5.15** (50 mg, 0.16 mmol, 1 equiv), **5.27** (71 mg, 0.18 mmol, 1.1 equiv), NEt_3 (57 µL, 0.41 mmol, 2.5 equiv) and $HgCl_2$ (89 mg, 0.33 mmol, 2 equiv) according to the general procedure yielding the product as a white, foamlike and hygroscopic solid (45 mg, 41%). R_f = 0.64 (CH_2Cl_2/MeOH 9:1). RP-HPLC: 100%, (t_R = 16.2 min, k = 4.05). ^{1}H-NMR (600 MHz, DMSO-d_6): δ 10.84 (br s, 1H), 10.33 (br s, 1H), 9.15-8.40 (m, 2H), 7.64 (t, J = 5.8 Hz, 1H), 7.55-7.47 (m, 2H), 7.42-7.38 (m, 2H), 7.30-7.23 (m, 2H), 7.21-7.14 (m, 3H), 3.11-3.04 (m, 1H), 2.99-2.91 (m, 1H), 2.60-2.52 (m, 2H), 2.27 (s, 3H), 1.69-1.50 (m, 3H), 1.38-1.29 (m, 1H), 1.17-1.06 (m, 1H), 0.85 (d, J = 6.7 Hz, 3H). ^{13}C-NMR (151 MHz, DMSO-d_6): δ 167.14, 158.99 (q, J = 34.7 Hz, TFA), 153.54, 153.49, 142.13, 132.98, 130.03, 129.41, 128.23, 126.16, 125.63, 116.47 (q, J = 295.5 Hz, TFA), 115.83, 45.00, 35.32, 33.22, 32.58, 28.33, 17.41, 14.10. HRMS (ESI-MS): calcd. for $C_{24}H_{31}N_6OS^+$: 451.2275; found: 451.2274. MF: $C_{24}H_{30}N_6OS$ x $C_4H_2F_6O_4$. MW: (450.61 + 228.05).

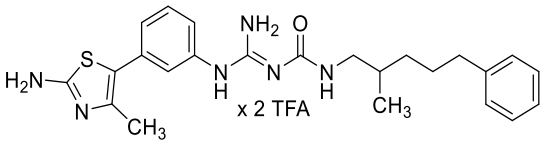

1-(Amino{[3-(2-amino-4-methylthiazol-5-yl)phenyl]amino}methylene)-3-(2-methyl-5-phenylpentyl)urea dihydrotrifluoroacetate (5.65) was prepared from amine **5.16** (20 mg, 0.07 mmol, 1 equiv), **5.27** (29 mg, 0.073 mmol, 1.1 equiv), NEt_3 (23 µL, 0.17 mmol, 2.5 equiv) and $HgCl_2$ (36 mg, 0.13 mmol, 2 equiv) according to the general procedure yielding the product as a white, foamlike and hygroscopic solid (18 mg, 38%). $R_f = 0.58$ (CH_2Cl_2/MeOH 9:1). RP-HPLC: 99%, ($t_R = 16.3$ min, $k = 4.08$). ^{1}H-NMR (600 MHz, DMSO-d_6): δ 10.80 (br s, 1H), 10.29 (br s, 1H), 9.17-8.26 (m, 2H), 7.63 (t, $J = 5.8$ Hz, 1H), 7.55 (t, $J = 7.9$ Hz, 1H), 7.42-7.36 (m, 2H), 7.32-7.24 (m, 3H), 7.21-7.14 (m, 3H), 3.12-3.04 (m, 1H), 2.99-2.92 (m, 1H), 2.62-2.51 (m, 2H), 2.27 (s, 3H), 1.68-1.50 (m, 3H), 1.37-1.29 (m, 1H), 1.16-1.08 (m, 1H), 0.85 (d, $J = 6.7$ Hz, 3H). ^{13}C-NMR (151 MHz, DMSO-d_6): δ 167.20, 158.53 (q, $J = 32.7$ Hz, TFA), 153.55, 142.13, 134.43, 132.54, 130.47, 128.23, 127.25, 125.63, 125.30, 124.61, 116.53 (q, $J = 297.6$ Hz, TFA), 115.73, 44.98, 35.33, 33.21, 32.59, 28.33, 17.40, 14.22. HRMS (ESI-MS): calcd. for $C_{24}H_{31}N_6OS^+$: 451.2275; found: 451.2283. MF: $C_{24}H_{30}N_6OS$ x $C_4H_2F_6O_4$. MW: (450.61 + 228.05).

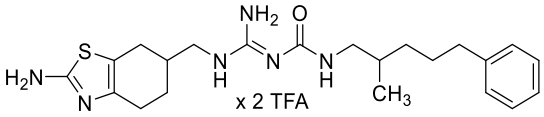

1-(Amino{[(2-amino-4,5,6,7-tetrahydrobenzo[*d*]thiazol-6-yl)methyl]amino}methylene)-3-(2-methyl-5-phenylpentyl)urea dihydrotrifluoroacetate (5.66) was prepared from amine **5.17** (81 mg, 0.19 mmol, 1 equiv), **5.27** (83 mg, 0.21 mmol, 1.1 equiv), NEt_3 (66 µL, 0.48 mmol, 2.5 equiv) and $HgCl_2$ (104 mg, 0.38 mmol, 2 equiv) according to the general procedure yielding the product as a white, foamlike and hygroscopic solid (18 mg, 14%). $R_f = 0.62$ (CH_2Cl_2/MeOH 9:1). RP-HPLC: 100%, ($t_R = 15.2$ min, $k = 3.74$). ^{1}H-NMR (600 MHz, DMSO-d_6): δ 10.39 (br s, 1H), 9.12 (br s, 1H), 8.88 (br s, 2H), 8.54 (br s, 2H), 7.52 (br s, 1H), 7.29-7.21 (m, 2H), 7.20-7.11 (m, 3H), 3.31-3.25 (m, 2H), 3.08-3.00 (m, 1H), 2.95-2.87 (m, 1H), 2.57-2.50 (m, 2H), 2.47-2.37 (m, 1H), 2.24-2.14 (m, 1H), 2.10-2.01 (m, 1H), 1.92-1.83 (m, 1H), 1.65-1.40 (m, 4H), 1.36-1.26 (m, 1H), 1.14-1.05 (m, 1H), 0.83 (d, $J = 6.7$ Hz, 3H). ^{13}C-NMR (151 MHz, DMSO-d_6): δ 168.85, 159.44 (q, $J = 30.5$ Hz, TFA), 154.38, 142.61, 135.59, 128.70, 128.66, 126.08, 117.35 (q,

J =297.5 Hz, TFA), 113.63, 45.39, 45.10, 40.50, 35.79, 33.67, 33.08, 28.79, 26.00, 25.04, 22.62, 17.87. HRMS (ESI-MS): calcd. for $C_{22}H_{33}N_6OS^+$: 429.2431; found: 429.2433. MF: $C_{22}H_{32}N_6OS$ x $C_4H_2F_6O_4$. MW: (428.60 + 228.05).

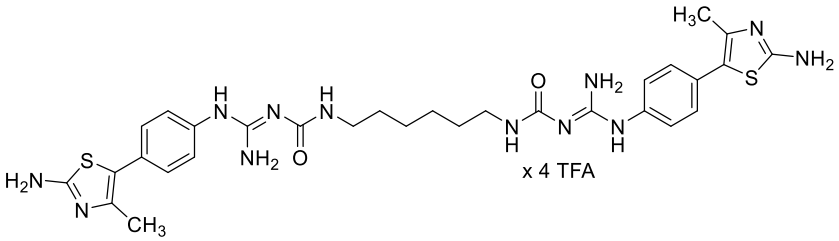

1-(Amino{[4-(2-amino-4-methylthiazol-5-yl)phenyl]amino}methylene)-3-{6-[3-(amino{[4-(2-amino-4-methylthiazol-5-yl)phenyl]amino}methylene)ureido]hexyl}urea tetrahydrotrifluoroacetate (5.67) was prepared from amine **5.15** (22 mg, 0.073 mmol, 2 equiv), **5.28** (20 mg, 0.036 mmol, 1 equiv), NEt_3 (25 µL, 0.18 mmol, 5 equiv) and $HgCl_2$ (40 mg, 0.144 mmol, 4 equiv) according to the general procedure yielding the product as a white, foamlike and hygroscopic solid (9.3 mg, 23%). R_f = 0.21 (CH_2Cl_2/MeOH 9:1). RP-HPLC: 98%, (t_R = 10.3 min, *k* = 2.21). ^{1}H-NMR (600 MHz, DMSO-d_6): δ 11.70-10.09 (m, 4H), 9.54-8.44 (m, 8H), 7.65 (t, *J* = 5.7 Hz, 2H), 7.53-7.45 (m, 4H), 7.42-7.33 (m, 4H), 3.12 (q, *J* = 6.6 Hz, 4H), 2.26 (s, 6H), 1.46 (t, *J* = 7.0 Hz, 4H), 1.34-1.25 (m, 4H). ^{13}C-NMR (151 MHz, DMSO-d_6): δ 167.93 (2C), 160.05 (q, *J* = 33.2 Hz, TFA), 154.07 (2C), 153.96 (2C), 135.55 (2C), 133.83 (2C), 129.97 (4C), 129.92 (2C), 126.56 (4C), 117.01 (q, *J* = 294.0 Hz, TFA), 116.17 (2C), 39.65 (2C), 29.26 (2C), 26.31 (2C), 14.03 (2C). HRMS (ESI-MS): calcd. for $C_{30}H_{39}N_{12}O_2S_2^+$: 663.2755; found: 663.2752. MF: $C_{30}H_{38}N_{12}O_2S_2$ x $C_8H_4F_{12}O_8$. MW: (662.84 + 456.09).

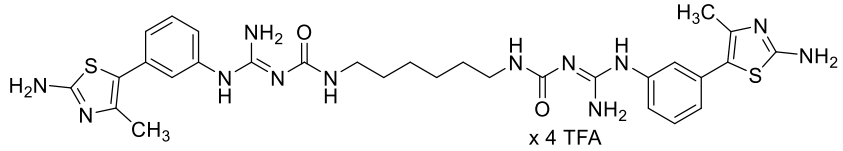

1-(Amino{[3-(2-amino-4-methylthiazol-5-yl)phenyl]amino}methylene)-3-{6-[3-(amino{[3-(2-amino-4-methylthiazol-5-yl)phenyl]amino}tmethylene)ureido]hexyl}urea tetrahydrotrifluoroacetate (5.68) was prepared from amine **5.16** (22 mg, 0.073 mmol, 2 equiv), **5.28** (20 mg, 0.036 mmol, 1 equiv), NEt_3 (25 µL, 0.18 mmol, 5 equiv) and $HgCl_2$ (40 mg, 0.144 mmol, 4 equiv) according to the general procedure yielding the product as a white, foamlike

and hygroscopic solid (5.8 mg, 14%). $R_f = 0.23$ (CH_2Cl_2/MeOH 9:1). RP-HPLC: 98%, ($t_R = 10.2$ min, $k = 2.18$). ^{1}H-NMR (600 MHz, DMSO-d_6): δ 10.72 (br s, 2H), 10.26 (br s, 2H), 9.08-8.53 (m, 1H), 8.10 (br s, 3H), 7.62 (t, $J = 5.7$ Hz, 2H), 7.52 (t, $J = 7.9$ Hz, 2H), 7.39-7.35 (m, 2H), 7.33 (t, $J = 2.0$ Hz, 2H), 7.28-7.23 (m, 2H), 3.11 (q, $J = 6.1$ Hz, 4H), 2.25 (s, 6H), 1.44 (quint, $J = 6.9$ Hz, 5H), 1.32-1.24 (m, 4H). HRMS (ESI-MS): calcd. for $C_{30}H_{39}N_{12}O_2S_2^+$: 663.2755; found: 663.2747. MF: $C_{30}H_{38}N_{12}O_2S_2$ x $C_8H_4F_{12}O_8$. MW: (662.84 + 456.09).

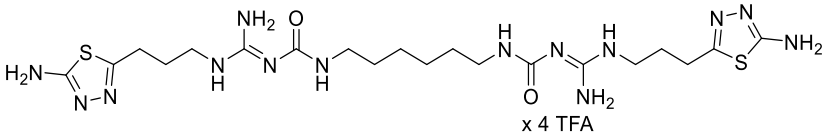

1-(Amino{[3-(5-amino-1,3,4-thiadiazol-2-yl)propyl]amino}methylene)-3-{6-[3-(amino{[3-(5-amino-1,3,4-thiadiazol-2-yl)propyl]amino}methylene)ureido]hexyl}urea tetrahydrotrifluoroacetate (5.69) was prepared from amine **5.11** (53.3 mg, 0.21 mmol, 2 equiv), **5.28** (57 mg, 0.10 mmol, 1 equiv), NEt_3 (71 µL, 0.52 mmol, 5 equiv) and $HgCl_2$ (112 mg, 0.41 mmol, 4 equiv) according to the general procedure yielding the product as a white, foamlike and hygroscopic solid (35 mg, 34%). RP-HPLC: 96%, ($t_R = 8.6$ min, $k = 1.68$). ^{1}H-NMR (600 MHz, DMSO-d_6) δ: 10.45 (br s, 2H), 9.05 (br s, 2H), 8.53 (br s, 4H), 8.06 (br s, 4H), 7.52 (br s, 2H), 3.30 (q, $J = 6.7$ Hz, 4H), 3.09 (q, $J = 6.6$ Hz, 4H), 2.87 (t, $J = 7.5$ Hz, 4H), 1.89 (quint, $J = 7.4$ Hz, 4H), 1.43 (quint, $J = 6.7$ Hz, 4H), 1.31-1.22 (m, 4H). ^{13}C-NMR (151 MHz, DMSO-d_6): δ 169.06, 159.16 (q, $J = 34.4$ Hz, TFA), 157.57, 153.90, 153.71, 39.60, 38.83, 28.88, 27.21, 26.58, 25.88. HRMS (ESI-MS): calcd. for $C_{20}H_{37}N_{14}O_2S_2^+$: 569.2660; found: 569.2660. MF: $C_{20}H_{36}N_{14}O_2S_2$ x $C_8H_4F_{12}O_8$. MW: (568.26 + 456.09).

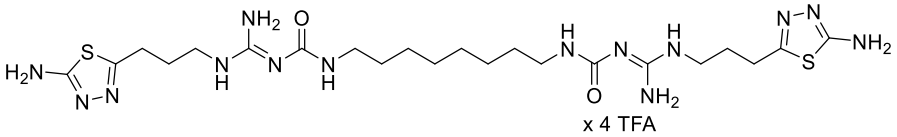

1-(Amino{[3-(5-amino-1,3,4-thiadiazol-2-yl)propyl]amino}methylene)-3-{8-[3-(amino{[3-(5-amino-1,3,4-thiadiazol-2-yl)propyl]amino}methylene)ureido]octyl}urea tetrahydrotrifluoroacetate (5.70) was prepared from amine **5.11** (99 mg, 0.38 mmol, 2.2 equiv), **5.29** (100 mg, 0.17 mmol, 1 equiv), NEt_3 (118 µL, 0.85 mmol, 5 equiv) and $HgCl_2$ (185 mg, 0.68 mmol, 4 equiv) according to the general procedure yielding the product as a white, foamlike

and hygroscopic solid (11.9 mg, 6.7%). RP-HPLC: 96%, (t_R = 10.3 min, k = 2.21). ^{1}H-NMR (600 MHz, DMSO-d_6) δ 10.26 (br s, 2H), 9.02 (br s, 2H), 8.50 (br s, 4H), 7.97 (br s, 3H), 7.49 (br s, 2H), 3.29 (q, J = 6.7 Hz, 4H), 3.07 (q, J = 6.6 Hz, 4H), 2.85 (t, J = 7.5 Hz, 4H), 1.88 (quint, J = 7.3 Hz, 4H), 1.46-1.37 (m, 4H), 1.28-1.22 (m, 8H). ^{13}C-NMR (151 MHz, DMSO-d_6) δ 168.97 (2C), 158.81 (q, J = 35.1 Hz, TFA), 157.53 (2C), 153.83 (2C), 153.64 (2C), 115.98 (q, J = 293.8 Hz, TFA), 40.06 (2C), 39.31 (2C), 28.92 (2C), 28.61 (2C), 27.20 (2C), 26.56 (2C), 26.18 (2C). HRMS (ESI-MS): calcd. for $C_{22}H_{41}N_{14}O_2S_2^+$: 597.2973; found: 597.2967. MF: $C_{22}H_{40}N_{14}O_2S_2$ x $C_8H_4F_{12}O_8$. MW: (596.78 + 456.09).

General procedure for the synthesis of oxadiazole derivatives 5.37 and 5.58. The oxadiazole heterocycle was formed according to a previously published procedure.[75] Cyanogen bromine (CNBr) is used as a reagent in this procedure, which is acutely toxic and potentially carcinogenic. It should be used only in a well-ventilated fume hood after reading the safety precautions and wearing proper lab safety equipment (gloves, safety googles and lab coat). Future synthetic work should consider replacements for CNBr. The respective acylhydrazine (**5.108** or **5.109**, 1 equiv, for details see Appendix 4, App4.2 Experimental Details for the Acylhydrazides **5.108** and **5.109**) was dissolved in a mixture of H_2O/ethanol (EtOH, 1:1 or 2:3 (v/v), 1-2 mL) and $KHCO_3$ (3.2 equiv) was added. After addition of BrCN (3 M in CH_2Cl_2, 1 equiv), the reaction mixture was heated at 60 °C for 2 h. The reaction mixture was cooled to rt and stirred for an additional hour. EtOH was removed in vacuum and the residue was purified by preparative HPLC.

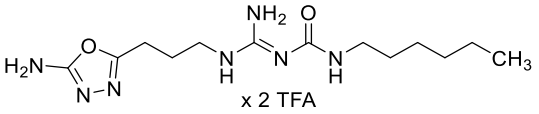

1-(Amino{[3-(5-amino-1,3,4-oxadiazol-2-yl)propyl]amino}methylene)-3-(hexyl)urea dihydrotrifluoroacetate (5.37) was prepared from **5.108** (82 mg, 0.16 mmol, 1 equiv), $KHCO_3$ (51 mg, 0.51 mmol, 3.2 equiv) and BrCN (3 M in CH_2Cl_2, 53 µL, 0.16 mmol, 1 equiv) in H_2O/EtOH (1 mL:1.5 mL) according to the general procedure yielding the product as a white, foamlike and hygroscopic solid (5.25 mg, 6.1%). RP-HPLC: 99%, (t_R = 13.5 min, k = 3.21). ^{1}H-NMR (600 MHz, DMSO-d_6) δ 10.03 (br s, 1H), 9.00 (br s, 1H), 8.50 (br s, 2H), 7.49 (t, J = 5.6 Hz, 1H), 6.93 (br s, 2H), 3.31 (q, J = 6.7 Hz, 2H), 3.09 (p, J = 6.4 Hz, 2H), 2.68 (t, J = 7.5 Hz, 2H),

1.87 (p, *J* = 7.4 Hz, 2H), 1.43 (p, *J* = 7.2 Hz, 2H), 1.29-1.24 (m, 6H), 0.91-0.82 (m, 3H). ^{13}C-NMR (151 MHz, DMSO-d_6) δ 163.52, 158.59 (q, *J* = 34.5 Hz, TFA), 158.48, 153.76, 153.55, 39.61, 38.85, 30.86, 28.86, 25.86, 24.71, 22.01, 21.73, 13.88. HRMS (ESI-MS): calcd. for $C_{13}H_{26}N_7O_2^+$: 312.2142; found: 312.2154. MF: $C_{13}H_{25}N_7O_2$ x $C_4H_2F_6O_4$. MW: (311.39 + 228.05).

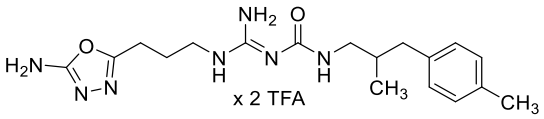

1-(Amino{[3-(5-amino-1,3,4-oxadiazol-2-yl)propyl]amino}methylene)-3-(2-methyl-3-(p-tolyl)propyl)urea dihydrotrifluoroacetate (5.58) was prepared from **5.109** (22 mg, 0.038 mmol, 1 equiv), $KHCO_3$ (12.2 mg, 0.122 mmol, 3.2 equiv) and BrCN (3 M in CH_2Cl_2, 15.3 µL, 0.046 mmol, 1.2 equiv) in H_2O/EtOH (0.5 mL:0.5 mL) according to the general procedure yielding the product as a white, foamlike and hygroscopic solid (13.97 mg, 61%). RP-HPLC: 100%, (t_R = 15.8 min, *k* = 3.92). ^{1}H-NMR (600 MHz, DMSO-d_6) δ 10.13 (br s, 1H), 9.02 (br s, 1H), 8.52 (br s, 2H), 7.57 (t, *J* = 5.8 Hz, 1H), 7.36-7.01 (m, 6H), 3.34 (q, *J* = 6.7 Hz, 2H), 3.14-2.90 (m, 2H), 2.71 (t, *J* = 7.4 Hz, 2H), 2.60 (dd, *J* = 13.5, 6.1 Hz, 1H), 2.36-2.30 (m, 1H), 2.28 (s, 3H), 1.95-1.83 (m, 3H), 0.81 (d, *J* = 6.7 Hz, 3H). ^{13}C-NMR (151 MHz, DMSO-d_6) δ 163.17, 158.59 (q, *J* = 34.7 Hz, TFA), 158.52, 153.72, 153.68, 136.95, 134.72, 128.80, 128.77, 116.05 (q, *J* = 293.9 Hz, TFA), 44.64, 39.59, 39.39, 34.85, 24.65, 21.73, 20.60, 17.08. HRMS (ESI-MS): calcd. for $C_{18}H_{28}N_7O_2^+$: 374.2299; found: 374.2300. MF: $C_{18}H_{27}N_7O_2$ x $C_4H_2F_6O_4$. MW: (373.22 + 228.05).

5.4.4 Control of the Chemical Stability of 5.30-5.35, 5.37, 5.41 and 5.57

The chemical stability of selected hH_2R ligands **5.30-5.35**, **5.37**, **5.41** and **5.57** was investigated at physiological pH in binding buffer[22] (12.5 mM $MgCl_2$, 1 mM EDTA and 75 mM Tris/HCl, pH 7.4). Incubation was started by addition of 50 µL of a 1 mM (**5.30**, **5.32-5.35**, **5.37** or **5.41**) or of a 2 mM (**5.31** or **5.57**) solution of the compounds in DMSO/H_2O 1:1, which were freshly prepared from a 10 mM stock solution in DMSO, to 950 µL of binding buffer to give a final concentration of 50 µM (**5.30**, **5.32-5.35**, **5.37** or **5.41**) or 100 µM (**5.31** or **5.57**). The samples were shaken for 2 weeks at 700 rpm. After 0 min, 60 min or 90 min, 2.5 h, 5 h, 10 h or 13 h 45 min, 24 h, 48 h, 1 week and 2 weeks a 50 µL aliquot was taken and diluted with 50 µL of a mixture of

MeCN, H_2O and 10% aq. TFA (60:90:1). Prior to HPLC analysis the samples were stored at -24 °C. 50 µL of the resulting solution were analyzed by HPLC as described before. The absorption was detected at 220 nm. The blank HPLC run was performed under identical conditions without any ligand.

5.4.5 Cell Culture

Cells were maintained in 25 or 75 cm² flasks (Sarstedt, Nümbrecht, Germany) in a humidified atmosphere (95% air, 5% CO_2) at 37 °C. HEK293T-CRE-Luc-hD_{2long}R cells[38], HEK293T-CRE-Luc-hD_3R cells[38], HEK293T NlucN-mGs/hH_2R-NlucC cells[40], HEK293T NlucN-mGs/gpH_2R-NlucC cells[25], HEK293T-ARRB2-H_2R cells[39], HEK293T ElucN-βarr2 hD_{2long}R-ElucC cells[38], and HEK293T ElucN-βarr2 hD_3R-ElucC cells[38] were cultured as described previously.

5.4.6 Radioligand Binding Experiments

Histamine H_{1-4} receptors[22, 35]: Competition binding experiments were performed with membrane preparations of Sf9 insect cells expressing the hH_1R + RGS4[76], hH_2R-$G_{s\alpha S}$ fusion protein[4], hH_3R + $G_{\alpha i2}$ + $G_{\beta 1\gamma 2}$[77] or the hH_4R + $G_{\alpha i2}$ + $G_{\beta 1\gamma 2}$[78]. General procedures for the generation of recombinant baculoviruses, culture of Sf9 cells and membrane preparations have been described elsewhere.[79] The competition binding experiments were performed as previously described in detail[22, 35] with one minor modification: PBS (8 g NaCl, 0.2 g KCl, 1.0 g Na_2HPO_4 x 2 H_2O, 0.15 g NaH_2PO_4 x H_2O, 0.1 g KH_2PO_4 in 1 L Millipore H_2O; pH 7.4; 4 °C) was used as washing buffer while harvesting instead of the previously used binding buffer[22, 35]. [^{3}H]mepyramine (specific activity: 20.0 or 87 Ci/mmol) was from Hartmann analytics (Braunschweig, Germany) or Novandi Chemistry AB (Södertälje, Sweden), [^{3}H]**1** (specific activity: 25.0 Ci/mmol) and [^{3}H]*N*$^\alpha$-methylhistamine (specific activity: 85.3 Ci/mmol) were from Hartmann analytics (Braunschweig, Germany). [^{3}H]UR-DE257[33] (specific activity: 63.0 Ci/mmol) and [^{3}H]UR-PI294[34] (specific activity: 41.8 Ci/mmol) were synthesized and characterized in our laboratories. Histamine dihydrochloride and diphenhydramine hydrochloride were from TCI Deutschland GmbH (Eschborn, Germany). Famotidine was from Alfa Aesar (Karlsruhe, Germany).

Dopamine $D_{2long/3}$ receptors: The competition binding experiments were performed on homogenates of HEK293T-CRE-Luc-hD_{2long}R or HEK293T-CRE-Luc-hD_3R cells using [^{3}H]*N*-methylspiperone (specific activity: 77 Ci/mmol, Novandi Chemistry AB, Södertälje, Sweden) as

published previously in detail.[38] (+)-Butaclamol was from Sigma (Taufkirchen, Germany). General procedure for the homogenate preparation has been described in the same publication.[38]

5.4.7 Functional Assays

The [^{35}S]GTPγS assay was performed on Sf9 membranes expressing the hH_2R-$G_{s\alpha S}$ fusion protein as described previously[22, 80] with one minor modification: PBS (8 g NaCl, 0.2 g KCl, 1.0 g Na_2HPO_4 x 2 H_2O, 0.15 g NaH_2PO_4 x H_2O, 0.1 g KH_2PO_4 in 1 L Millipore H_2O; pH 7.4; 4 °C) was used as washing buffer while harvesting instead of the previously used binding buffer.

Functional studies in the mini-G protein or β-arrestin2 recruitment assays using HEK293T NlucN-mGs/hH_2R-NlucC[40]-, HEK293T NlucN-mGs/gpH_2R-NlucC[25]-, HEK293T-ARRB2-H_2R[37, 39]-, HEK293T ElucN-βarr2 $hD_{2long}R$-ElucC[38]- or HEK293T ElucN-βarr2 hD_3R-ElucC[38] cells were performed as described previously.

5.4.8 Docking

Models of the active-state hH_2R and active-state hD_2R: For the receptor modelling, docking studies and presentation of the results, the software Sybyl 7.3 (Tripos Inc., St. Louis, MO, USA) was used. Since the compounds, for which the interaction with the hH_2R should be analyzed, were experimentally identified as partial agonists at the hH_2R, an active-state model of the hH_2R was generated by homology modelling, using the crystal structure of the β_2 adrenergic receptor-Gs protein complex (protein databank code: 3SN6) as template.[45] The Gαβγ-subunits (chain A, B, G), the endolysin and the camelid antibody VHH fragment (chain N) were deleted. According to an appropriate sequence alignment between $h\beta_2R$ and hH_2R, the homology model was generated by exchange of amino acids (tool: "Mutate Monomers" of Sybyl) into the corresponding amino acid of the hH_2R, where necessary. N-Terminus and loops (tool: "Loop Search" of Sybyl) were modelled, according to procedures, as described elsewhere.[81] The resulting active-state hH_2R was minimized with the Amber 7 FF99 force field.

Since the compounds, for which the interaction with the hD_2R should be analyzed, were also identified as partial agonists at the hD_2R by functional studies, an active-state model of the hD_2R was used. For this purpose, the crystal structure of the dopamine D_2 receptor-G protein complex (protein databank code: 6VMS) was used as template.[46] The Gαβγ-subunits (chain A, B, C) and

the scFv16 (chain E) were deleted. This model was refined by exchanging amino acids into the corresponding amino acid of the hD_2R (tool: "Mutate Monomers" of Sybyl), where necessary. The resulting active-state hD_2R was minimized with the Amber 7 FF99 force field. The model of the hD_2R was used to generate the receptor mutant hD_2R-$E^{ECL2.49}V$-$I^{ECL2.51}S$, using the same procedures, as described above.

The compounds **5.6**, **5.31** and **5.32**, provided with the Gasteiger-Hueckel charges, were docked manually into the orthosteric binding pocket of the respective receptor. The net charge for **5.6**, **5.31** and **5.32** was 1, with the positive charge being located on the carbamoylguanidine group. The resulting ligand-receptor complexes were minimized with the Amber7 FF99 force field.

5.4.9 Data Processing

Compound purities were calculated as the percentage peak area of the analyzed compound by UV detection at 220 nm. Retention (capacity) factors (k) were calculated from retention times (t_R) according to $k = (t_R - t_0)/t_0$, t_0 = dead time. Data from radioligand competition binding assays ($hH_{1\text{-}4}$[35] and $hD_{2long/3}$[38] receptors), from [^{35}S]GTPγS binding assay[35], from mini-G protein (hH_2R[40], gpH_2R[25]) or β-arrestin2 (hH_2[37, 39] and $hD_{2long/3}$[38] receptors) recruitment assays, and from H_2R assay on isolated guinea pig right atrium[35] were processed as reported previously. K_i values for the calculation of relative affinities (H_2R selectivity, Tables 5.1 and 5.2) were obtained by transforming the pK_i mean value to K_i ($K_i = 10^{-pKi}$).

5.5 References

1. Birnkammer, T.; Spickenreither, A.; Brunskole, I.; Lopuch, M.; Kagermeier, N.; Bernhardt, G.; Dove, S.; Seifert, R.; Elz, S.; Buschauer, A., The bivalent ligand approach leads to highly potent and selective acylguanidine-type histamine H_2 receptor agonists. *J. Med. Chem.* **2012,** *55*, 1147-1160.
2. Kraus, A.; Ghorai, P.; Birnkammer, T.; Schnell, D.; Elz, S.; Seifert, R.; Dove, S.; Bernhardt, G.; Buschauer, A., N^G-Acylated aminothiazolylpropylguanidines as potent and selective histamine H_2 receptor agonists. *ChemMedChem* **2009,** *4*, 232-240.
3. Xie, S.-X.; Ghorai, P.; Ye, Q.-Z.; Buschauer, A.; Seifert, R., Probing ligand-specific histamine H_1- and H_2-receptor conformations with N^G-acylated imidazolylpropylguanidines. *J. Pharmacol. Exp. Ther.* **2006,** *317*, 139-146.
4. Kelley, M. T.; Bürckstürmmer, T.; Wenzel-Seifert, K.; Dove, S.; Buschauer, A.; Seifert, R., Distinct interaction of human and guinea pig histamine H_2-receptor with guanidine-type agonists. *Mol. Pharmacol.* **2001,** *60*, 1210-1225.

5. Hill, S. J.; Ganellin, C. R.; Timmerman, H.; Schwartz, J. C.; Shankley, N. P.; Young, J. M.; Schunack, W.; Levi, R.; Haas, H. L., International union of pharmacology. XIII. Classification of histamine receptors. *Pharmacol. Rev.* **1997,** *49*, 253-278.
6. Panula, P.; Chazot, P. L.; Cowart, M.; Gutzmer, R.; Leurs, R.; Liu, W. L.; Stark, H.; Thurmond, R. L.; Haas, H. L., International union of basic and clinical pharmacology. XCVIII. Histamine receptors. *Pharmacol. Rev.* **2015,** *67*, 601-655.
7. Dove, S.; Elz, S.; Seifert, R.; Buschauer, A., Structure-activity relationships of histamine H_2 receptor ligands. *Mini-Re. Med. Chem.* **2004,** *4*, 941-954.
8. Traiffort, E.; Pollard, H.; Moreau, J.; Ruat, M.; Schwartz, J. C.; Martinez-Mir, M. I.; Palacios, J. M., Pharmacological characterization and autoradiographic localization of histamine H_2 receptors in human brain identified with [^{125}I]iodoaminopotentidine. *J. Neurochem.* **1992,** *59*, 290-299.
9. Black, J. W.; Duncan, W. A. M.; Durant, G. J.; Ganellin, C. R.; Parsons, M. E., Definition and antagonism of histamine H_2-receptors. *Nature* **1972,** *236*, 385-390.
10. Yanagisawa, I.; Hirata, Y.; Ishii, A., Studies on histamine H_2 receptor antagonists. 2. Synthesis and pharmacological activities of *N*-sulfamoyl and *N*-sulfonyl amidine derivatives. *J. Med. Chem.* **1987,** *30*, 1787-1793.
11. Schneider, E. H.; Neumann, D.; Seifert, R., Modulation of behavior by the histaminergic system: lessons from H_1R-and H_2R-deficient mice. *Neurosci. Biobeh. Rev.* **2014,** *42*, 252-266.
12. Deutsch, S. I.; Rosse, R. B.; Schwartz, B. L., Histamine H_2 receptor antagonists in schizophrenia. *CNS Drugs* **1997,** *8*, 276-284.
13. Farzin, D.; Hosseini, S. H.; Shafaat, A., A randomized double blind clinical trial in famotidine adjuvant therapy in schizophrenia. *Iran. J. Med. Sci.* **2005,** *30*, 59-62.
14. Johnston, T. H.; van der Meij, A.; Brotchie, J. M.; Fox, S. H., Effect of histamine H_2 receptor antagonism on levodopa–induced dyskinesia in the MPTP-macaque model of Parkinson's disease. *Mov. Disord.* **2010,** *25*, 1379-1390.
15. Meskanen, K.; Ekelund, H.; Laitinen, J.; Neuvonen, P. J.; Haukka, J.; Panula, P.; Ekelund, J., A randomized clinical trial of histamine 2 receptor antagonism in treatment-resistant schizophrenia. *J. Clin. Psychopharmacol.* **2013,** *33*, 472-478.
16. Shi, H.; Yang, X.; Zhao, H.; Zhang, S.; Zu, J.; Zhang, W.; Shen, X.; Cui, G.; Hua, F.; Yan, C., Ranitidine reduced levodopa-induced dyskinesia by remodeling neurochemical changes in hemiparkinsonian model of rats. *Neuropsychiatr. Dis. Treat.* **2015,** *11*, 1331-1337.
17. Ahmed, M. R.; Jayakumar, M.; Ahmed, M. S.; Zamaleeva, A. I.; Tao, J.; Li, E. H.; Job, J. K.; Pittenger, C.; Ohtsu, H.; Rajadas, J., Pharmacological antagonism of histamine H_2R ameliorated L-DOPA-induced dyskinesia via normalization of GRK3 and by suppressing FosB and ERK in PD. *Neurobiol Aging* **2019,** *81*, 177-189.
18. Oyewumi, L. K.; Vollick, D.; Merskey, H.; Plumb, C., Famotidine as an adjunct treatment of resistant schizophrenia. *J. Psychiatry Neurosci.* **1994,** *19*, 145-150.
19. White, J. M.; Rumbold, G. R., Behavioural effects of histamine and its antagonists: a review. *Psychopharmacology* **1988,** *95*, 1-14.
20. Ghorai, P.; Kraus, A.; Keller, M.; Götte, C.; Igel, P.; Schneider, E.; Schnell, D.; Bernhardt, G.; Dove, S.; Zabel, M.; Elz, S.; Seifert, R.; Buschauer, A., Acylguanidines as bioisosteres of guanidines: N^G-acylated imidazolylpropylguanidines, a new class of histamine H_2 receptor agonists. *J. Med. Chem.* **2008,** *51*, 7193-7204.

21. Ghorai, P.; Kraus, A.; Birnkammer, T.; Geyer, R.; Bernhardt, G.; Dove, S.; Seifert, R.; Elz, S.; Buschauer, A., Chiral N^G-acylated hetarylpropylguanidine-type histamine H_2 receptor agonists do not show significant stereoselectivity. *Bioorg. Med. Chem. Lett.* **2010,** *20*, 3173-3176.
22. Kagermeier, N.; Werner, K.; Keller, M.; Baumeister, P.; Bernhardt, G.; Seifert, R.; Buschauer, A., Dimeric carbamoylguanidine-type histamine H_2 receptor ligands: a new class of potent and selective agonists. *Bioorg. Med. Chem.* **2015,** *23*, 3957-3969.
23. Biselli, S.; Bresinsky, M.; Tropmann, K.; Forster, L.; Honisch, C.; Buschauer, A.; Bernhardt, G.; Pockes, S., Pharmacological characterization of a new series of carbamoylguanidines reveals potent agonism at the H_2R and D_3R. *Eur. J. Med. Chem.* **2021,** *214*, 113190.
24. Biselli, S. Synthesis and Pharmacological Characterization of Subtype-Selective Ligands, Including Radio- and Fluorescence Labeled Ligands, for the Histamine H_2 Receptor. Ph.D. Thesis. University of Regensburg, 2020.
25. Tropmann, K.; Höring, C.; Plank, N.; Pockes, S., Discovery of a G protein biased radioligand for the histamine H_2 receptor with reversible binding properties. *J. Med. Chem.* **2020,** *63*, 13090-13102.
26. Mierau, J., Pramipexole: a dopamine-receptor agonist for treatment of Parkinson's disease. *Clin. Neuropharmacol.* **1995,** *18*, 195-206.
27. Bennett, J. P., Jr.; Piercey, M. F., Pramipexole-a new dopamine agonist for the treatment of Parkinson's disease. *J. Neurol. Sci.* **1999,** *163*, 25-31.
28. Ganellin, C. R., *Chemistry and Structure Activity Relationships of Drugs Acting at Histamine Receptors*. Ganellin, C. R., Parson, M. E., Eds. Wright PSG: Bristil, London, Boston: 1982, 10-102.
29. Bastos, C., M.; Munoz, B.; Tait, B. Compounds, Compositions, and Methods for Increasing CFTR Activity. WO 2015/138909, Mar 13, 2015; *Chem. Abstr.* **2015**, *163*, 438650.
30. Geyer, R.; Kaske, M.; Baumeister, P.; Buschauer, A., Synthesis and functional characterization of imbutamine analogs as histamine H_3 and H_4 receptor ligands. *Arch. Pharm.* **2014,** *347*, 77-88.
31. Geyer, R.; Igel, P.; Kaske, M.; Elz, S.; Buschauer, A., Synthesis, SAR and selectivity of 2-acyl- and 2-cyano-1-hetarylalkyl-guanidines at the four histamine receptor subtypes: a bioisosteric approach. *MedChemComm* **2014,** *5*, 72-81.
32. Kim, K. S.; Qian, L., Improved method for the preparation of guanidines. *Tetrahedron Lett.* **1993,** *34*, 7677-7680.
33. Baumeister, P.; Erdmann, D.; Biselli, S.; Kagermeier, N.; Elz, S.; Bernhardt, G.; Buschauer, A., [^{3}H]UR-DE257: development of a tritium-labeled squaramide-type selective histamine H_2 receptor antagonist. *ChemMedChem* **2015,** *10*, 83-93.
34. Igel, P.; Schnell, D.; Bernhardt, G.; Seifert, R.; Buschauer, A., Tritium-labeled N^1-[3-(1H-imidazol-4-yl)propyl]-N^2-propionylguanidine ([^{3}H]UR-PI294), a high-affinity histamine H_3 and H_4 receptor radioligand. *ChemMedChem* **2009,** *4*, 225-231.
35. Pockes, S.; Wifling, D.; Keller, M.; Buschauer, A.; Elz, S., Highly potent, stable, and selective dimeric hetarylpropylguanidine-type histamine H_2 receptor agonists. *ACS Omega* **2018,** *3*, 2865-2882.
36. Pertz, H. H.; Görnemann, T.; Schurad, B.; Seifert, R.; Straßer, A., Striking differences of action of lisuride stereoisomers at histamine H_1 receptors. *Naunyn-Schmiedeberg's Arch. Pharmacol.* **2006,** *374*, 215-222.

37. Grätz, L.; Tropmann, K.; Bresinsky, M.; Müller, C.; Bernhardt, G.; Pockes, S., NanoBRET binding assay for histamine H_2 receptor ligands using live recombinant HEK293T cells. *Sci. Rep.* **2020,** *10, e13288*.
38. Forster, L.; Grätz, L.; Mönnich, D.; Bernhardt, G.; Pockes, S., A split luciferase complementation assay for the quantification of β-arrestin2 recruitment to dopamine D_2-like receptors. *Int. J. Mol. Sci.* **2020,** *21, 6103*.
39. Felixberger, J. Luciferase Complementation for the Determination of Arrestin Recruitment: Investigation of Histamine and NPY receptors. Ph.D. Thesis. University of Regensburg, 2014.
40. Höring, C.; Seibel, U.; Tropmann, K.; Grätz, L.; Mönnich, D.; Pitzl, S.; Bernhardt, G.; Pockes, S.; Strasser, A., A dynamic, split-luciferase-based mini-G protein sensor to functionally characterize ligands at all four histamine receptor subtypes. *Int. J. Mol. Sci.* **2020,** *21, 8440*.
41. Carpenter, B.; Tate, C. G., Engineering a minimal G protein to facilitate crystallisation of G protein-coupled receptors in their active conformation. *Protein Eng. Des. Sel.* **2016,** *29*, 583-594.
42. Nehmé, R.; Carpenter, B.; Singhal, A.; Strege, A.; Edwards, P. C.; White, C. F.; Du, H.; Grisshammer, R.; Tate, C. G., Mini-G proteins: novel tools for studying GPCRs in their active conformation. *PLOS ONE* **2017,** *12*, e0175642.
43. Wan, Q.; Okashah, N.; Inoue, A.; Nehmé, R.; Carpenter, B.; Tate, C. G.; Lambert, N. A., Mini G protein probes for active G protein–coupled receptors (GPCRs) in live cells. *J. Biol. Chem.* **2018,** *293*, 7466-7473.
44. Yung-Chi, C.; Prusoff, W. H., Relationship between the inhibition constant (K_i) and the concentration of inhibitor which causes 50 per cent inhibition (I_{50}) of an enzymatic reaction. *Biochem. Pharmacol.* **1973,** *22*, 3099-3108.
45. Rasmussen, S. G. F.; DeVree, B. T.; Zou, Y.; Kruse, A. C.; Chung, K. Y.; Kobilka, T. S.; Thian, F. S.; Chae, P. S.; Pardon, E.; Calinski, D.; Mathiesen, J. M.; Shah, S. T. A.; Lyons, J. A.; Caffrey, M.; Gellman, S. H.; Steyaert, J.; Skiniotis, G.; Weis, W. I.; Sunahara, R. K.; Kobilka, B. K., Crystal structure of the β_2 adrenergic receptor–Gs protein complex. *Nature* **2011,** *477*, 549-555.
46. Yin, J.; Chen, K.-Y. M.; Clark, M. J.; Hijazi, M.; Kumari, P.; Bai, X.-c.; Sunahara, R. K.; Barth, P.; Rosenbaum, D. M., Structure of a D_2 dopamine receptor–G-protein complex in a lipid membrane. *Nature* **2020,** *584*, 125-129.
47. Simpson, M. M.; Ballesteros, J. A.; Chiappa, V.; Chen, J.; Suehiro, M.; Hartman, D. S.; Godel, T.; Snyder, L. A.; Sakmar, T. P.; Javitch, J. A., Dopamine D_4/D_2 receptor selectivity is determined by a divergent aromatic microdomain contained within the second, third, and seventh membrane-spanning segments. *Mol. Pharmacol.* **1999,** *56*, 1116-1126.
48. Bruysters, M.; Jongejan, A.; Gillard, M.; van de Manakker, F.; Bakker, R. A.; Chatelain, P.; Leurs, R., Pharmacological differences between human and guinea pig histamine H_1 receptors: Asn^{84} (2.61) as key residue within an additional binding pocket in the H_1 receptor. *Mol. Pharmacol.* **2005,** *67*, 1045-1052.
49. Strasser, A.; Striegl, B.; Wittmann, H. J.; Seifert, R., Pharmacological profile of histaprodifens at four recombinant histamine H_1 receptor species isoforms. *J. Pharmacol. Exp. Ther.* **2008,** *324*, 60-71.
50. Michino, M.; Donthamsetti, P.; Beuming, T.; Banala, A.; Duan, L.; Roux, T.; Han, Y.; Trinquet, E.; Newman, A. H.; Javitch, J. A.; Shi, L., A single glycine in extracellular loop 1 is the

critical determinant for pharmacological specificity of dopamine D_2 and D_3 receptors. *Mol. Pharmacol.* **2013,** *84*, 854-864.
51. Vass, M.; Podlewska, S.; de Esch, I. J. P.; Bojarski, A. J.; Leurs, R.; Kooistra, A. J.; de Graaf, C., Aminergic GPCR-ligand interactions: a chemical and structural map of receptor mutation data. *J. Med. Chem.* **2019,** *62*, 3784-3839.
52. Ferruz, N.; Doerr, S.; Vanase-Frawley, M. A.; Zou, Y.; Chen, X.; Marr, E. S.; Nelson, R. T.; Kormos, B. L.; Wager, T. T.; Hou, X.; Villalobos, A.; Sciabola, S.; De Fabritiis, G., Dopamine D_3 receptor antagonist reveals a cryptic pocket in aminergic GPCRs. *Sci. Rep.* **2018,** *8*, 897.
53. Wang, S.; Che, T.; Levit, A.; Shoichet, B. K.; Wacker, D.; Roth, B. L., Structure of the D_2 dopamine receptor bound to the atypical antipsychotic drug risperidone. *Nature* **2018,** *555*, 269-273.
54. Chemel, B. R.; Bonner, L. A.; Watts, V. J.; Nichols, D. E., Ligand-specific roles for transmembrane 5 serine residues in the binding and efficacy of dopamine D_1 receptor catechol agonists. *Mol. Pharmacol.* **2012,** *81*, 729-738.
55. Fowler, J. C.; Bhattacharya, S.; Urban, J. D.; Vaidehi, N.; Mailman, R. B., Receptor conformations involved in dopamine D_{2L} receptor functional selectivity induced by selected transmembrane-5 serine mutations. *Mol. Pharmacol.* **2012,** *81*, 820-831.
56. Woodward, R.; Coley, C.; Daniell, S.; Naylor, L. H.; Strange, P. G., Investigation of the role of conserved serine residues in the long form of the rat D_2 dopamine receptor using site-directed mutagenesis. *J. Neurochem.* **1996,** *66*, 394-402.
57. Sartania, N.; Strange, P. G., Role of conserved serine residues in the interaction of agonists with D_3 dopamine receptors. *J. Neurochem.* **1999,** *72*, 2621-2624.
58. Braden, M. R.; Nichols, D. E., Assessment of the roles of serines 5.43(239) and 5.46(242) for binding and potency of agonist ligands at the human serotonin 5-HT_{2A} receptor. *Mol. Pharmacol.* **2007,** *72*, 1200-1209.
59. Pollock, N. J.; Manelli, A. M.; Hutchins, C. W.; Steffey, M. E.; MacKenzie, R. G.; Frail, D. E., Serine mutations in transmembrane V of the dopamine D_1 receptor affect ligand interactions and receptor activation. *J. Biol. Chem.* **1992,** *267*, 17780-17786.
60. Almaula, N.; Ebersole, B. J.; Ballesteros, J. A.; Weinstein, H.; Sealfon, S. C., Contribution of a helix 5 locus to selectivity of hallucinogenic and nonhallucinogenic ligands for the human 5-hydroxytryptamine2A and 5-hydroxytryptamine2C receptors: direct and indirect effects on ligand affinity mediated by the same locus. *Mol. Pharmacol.* **1996,** *50*, 34-42.
61. Leurs, R.; Smit, M. J.; Tensen, C. P.; Terlaak, A. M.; Timmerman, H., Site-directed mutagenesis of the histamine H_1-receptor reveals a selective interaction of asparagine^{207} with subclasses of H_1-receptor agonists. *Biochem. Bioph. Res. Co.* **1994,** *201*, 295-301.
62. Ohta, K.; Hayashi, H.; Mizuguchi, H.; Kagamiyama, H.; Fujimoto, K.; Fukui, H., Site-directed mutagenesis of the histamine H_1 receptor: roles of aspartic acid^{107}, asparagine^{198} and threonine^{194}. *Biochem. Bioph. Res. Co.* **1994,** *203*, 1096-1101.
63. Jongejan, A.; Lim, H. D.; Smits, R. A.; de Esch, I. J. P.; Haaksma, E.; Leurs, R., Delineation of agonist binding to the human histamine H_4 Receptor using mutational analysis, homology modeling, and ab initio aalculations. *J. Chem. Inf. Model.* **2008,** *48*, 1455-1463.
64. Shin, N.; Coates, E.; Murgolo, N. J.; Morse, K. L.; Bayne, M.; Strader, C. D.; Monsma, F. J., Jr., Molecular modeling and site-specific mutagenesis of the histamine-binding site of the histamine H_4 receptor. *Mol. Pharmacol.* **2002,** *62*, 38-47.
65. Hwa, J.; Perez, D. M., The unique nature of the serine interactions for α_1-adrenergic receptor agonist binding and activation. *J. Biol. Chem.* **1996,** *271*, 6322-6327.

66. Cho, W.; Taylor, L. P.; Mansour, A.; Akil, H., Hydrophobic residues of the D_2 dopamine receptor are important for binding and signal transduction. *J. Neurochem.* **1995,** *65*, 2105-2115.
67. Seifert, R.; Wenzel-Seifert, K.; Burckstummer, T.; Pertz, H. H.; Schunack, W.; Dove, S.; Buschauer, A.; Elz, S., Multiple differences in agonist and antagonist pharmacology between human and guinea pig histamine H_1-receptor. *J. Pharmacol. Exp. Ther.* **2003,** *305*, 1104-1115.
68. Wieland, K.; Laak, A. M.; Smit, M. J.; Kühne, R.; Timmerman, H.; Leurs, R., Mutational analysis of the antagonist-binding site of the histamine H_1 receptor. *J. Biol. Chem.* **1999,** *274*, 29994-30000.
69. Lan, H.; DuRand, C. J.; Teeter, M. M.; Neve, K. A., Structural determinants of pharmacological specificity between D_1 and D_2 dopamine receptors. *Mol. Pharmacol.* **2006,** *69*, 185-194.
70. Lundstrom, K.; Turpin, M. P.; Large, C.; Robertson, G.; Thomas, P.; Lewell, X. Q., Mapping of dopamine D_3 receptor binding site by pharmacological characterization of mutants expressed in CHO cells with the Semliki Forest virus system. *J. Recept. Signal Transduct.* **1998,** *18*, 133-150.
71. Woodward, R.; Daniell, S. J.; Strange, P. G.; Naylor, L. H., Structural studies on D_2 dopamine receptors: mutation of a histidine residue specifically affects the binding of a subgroup of substituted benzamide drugs. *J. Neurochem.* **1994,** *62* (5), 1664-1669.
72. Matsui, H.; Lazareno, S.; Birdsall, N. J., Probing of the location of the allosteric site on m1 muscarinic receptors by site-directed mutagenesis. *Mol. Pharmacol.* **1995,** *47*, 88-98.
73. Fulmer, G. R.; Miller, A. J. M.; Sherden, N. H.; Gottlieb, H. E.; Nudelman, A.; Stoltz, B. M.; Bercaw, J. E.; Goldberg, K. I., NMR chemical shifts of trace impurities: common laboratory solvents, organics, and gases in deuterated solvents relevant to the organometallic chemist. *Organometallics* **2010,** *29*, 2176-2179.
74. Gottlieb, H. E.; Kotlyar, V.; Nudelman, A., NMR chemical shifts of common laboratory solvents as trace impurities. *J. Org. Chem.* **1997,** *62*, 7512-7515.
75. Bleicher, K.; Mutel, V.; Vieira, E.; Wichmann, J.; Woltering, T. J. Preparation of carbamic acid derivatives and evaluation of their use as metabotropic glutamate receptor ligands. WO 2000/063166, Oct 26, 2000; *Chem. Abstr.* **2000**, *133*, 321633, 2000.
76. Houston, C.; Wenzel-Seifert, K.; Bürckstümmer, T.; Seifert, R., The human histamine H_2-receptor couples more efficiently to Sf9 insect cell G_s-proteins than to insect cell G_q-proteins: limitations of Sf9 cells for the analysis of receptor/G_q-protein coupling. *J. Neurochem.* **2002,** *80*, 678-696.
77. Schnell, D.; Strasser, A.; Seifert, R., Comparison of the pharmacological properties of human and rat histamine H_3-receptors. *Biochem. Pharmacol.* **2010,** *80*, 1437-1449.
78. Schneider, E. H.; Schnell, D.; Papa, D.; Seifert, R., High constitutive activity and a G-protein-independent high-affinity state of the human histamine H_4-receptor. *Biochemistry* **2009,** *48*, 1424-1438.
79. Pop, N.; Igel, P.; Brennauer, A.; Cabrele, C.; Bernhardt, G.; Seifert, R.; Buschauer, A., Functional reconstitution of human neuropeptide Y (NPY) Y_2 and Y_4 receptors in Sf9 insect cells. *J. Recept. Signal Transduct.* **2011,** *31*, 271-285.
80. Biselli, S.; Alencastre, I.; Tropmann, K.; Erdmann, D.; Chen, M.; Littmann, T.; Maia, A. F.; Gomez-Lazaro, M.; Tanaka, M.; Ozawa, T.; Keller, M.; Lamghari, M.; Buschauer, A.; Bernhardt, G., Fluorescent H_2 receptor squaramide-type antagonists: synthesis, characterization and applications. *ACS Med. Chem. Lett.* **2020,** *11*, 1521-1528.

81. Wifling, D.; Löffel, K.; Nordemann, U.; Strasser, A.; Bernhardt, G.; Dove, S.; Seifert, R.; Buschauer, A., Molecular determinants for the high constitutive activity of the human histamine H_4 receptor: functional studies on orthologues and mutants. *Br. J. Pharmacol.* **2015,** *172*, 785-798.

Appendix 4 Abolishing Dopamine D_{2long}/D_3 Receptor Affinity of Subtype-Selective Carbamoylguanidine-Type Histamine H_2 Receptor Agonists

App4.1 Experimental Details for the Amines 5.8-5.17 and the Guanidinylating Reagents 5.18-5.29

The amines **5.8**[1], **5.10**[2], **5.12**[3] and **5.13**[4-5] and the guanidinylating reagents **5.18-5.19**[6], **5.20**[7], **5.21-5.27**[6] and **5.28-5.29**[8] were synthesized as published previously.

App4.1.1 Synthesis of the Amine 5.9

The oxazole building block **5.9** was synthesized from urea and *N*-protected α-bromo-ω-amino ketone (**5.71**, Scheme App4.1). The *N*-protected α-bromo-ω-amino ketone **5.71** was synthesised as published priviosly.[3] The ring-closure reaction was carried out with urea in DMF (c0mpd. **5.72**). After replacement of the formyl group by a Boc-group (**5.73**), the phtahlimide residue was cleaved by hydrazinolysis to give *tert*-butyl (5-(3-aminopropyl)-4-methyloxazol-2-yl)carbamate (**5.9**).

Scheme App4.1. Synthesis of *tert*-Butyl (5-(3-aminopropyl)-4-methyloxazol-2-yl)carbamate (5.9)[a]

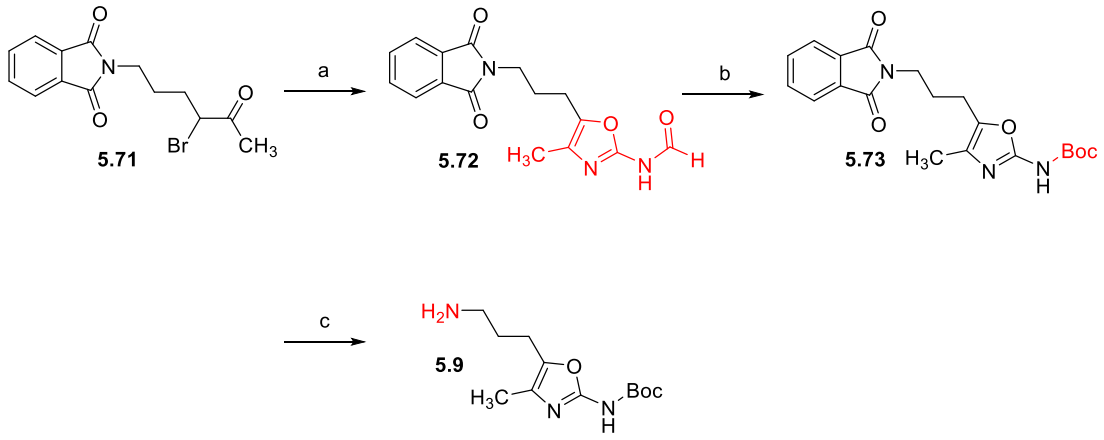

[a]Reagents and conditions: (a) urea, DMF, 100 °C, 3 h, 6%; (b) Boc_2O, NEt_3, DMAP (cat.), chloroform, rt, 48 h, 43%; (c) N_2H_4 x H_2O, EtOH, rt, 48 h, 80%.

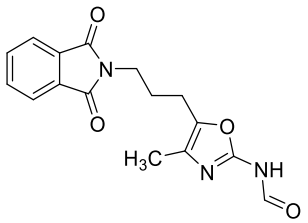

***N*-(5-(3-(1,3-Dioxoisoindolin-2-yl)propyl)-4-methyloxazol-2-yl)formamide (5.72)**. To a solution of **5.71** (2.59 g, 8.01 mmol, 1 equiv) in DMF (10 mL) a solution of urea (481 mg, 8.01 mmol, 1 equiv) in DMF (10 mL) was added and the mixture was heated at 100 °C for 3 h. After cooling and evaporation under reduced pressure, the crude product was purified by flash chromatography on silica gel (gradient: 0-20 min: PE/EtOAc 100:0-50:50, 35 min: 30:70, SF 12 g) to obtain the product as a yellow solid (150 mg, 6%). R_f = 0.41 (PE/EtOAc 1:4). ^{1}H-NMR (400 MHz, $CDCl_3$) δ 8.79 (br s, 1H), 7.88-7.55 (m, 4H), 3.78-3.63 (m, 2H), 2.61 (t, *J* = 7.4 Hz, 2H), 2.08-1.91 (m, 5H). ^{13}C-NMR (101 MHz, $CDCl_3$) δ 168.28 (2C), 162.80, 151.46, 142.07, 134.07 (2C), 131.90 (2C), 130.04, 123.24 (2C), 37.33, 26.56, 22.01, 10.96. HRMS (ESI-MS): calcd. for $C_{16}H_{16}N_3O_4^+$: 314.1135, found: 314.1136. MF: $C_{16}H_{15}N_3O_4$. MW: 313.31.

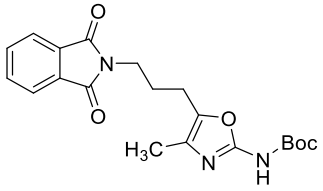

***tert*-Butyl (5-(3-(1,3-dioxoisoindolin-2-yl)propyl)-4-methyloxazol-2-yl)carbamate (5.73). 5.72** (150 mg, 0.48 mmol, 1 equiv) was dissolved in chloroform (10 mL) and di-*tert*-butyl dicarbonate (Boc_2O, 124 mg, 0.57 mmol, 1.2 equiv), NEt_3 (85 µL, 0.61 mmol, 1.3 equiv) and 4-dimethylaminopyridine (DMAP, 50 mg, cat.) were added. The mixture was stirred at rt for 48 h. The solvent was removed in vacuum and the crude product was purified by flash chromatography on silica gel (gradient: 0-20 min: PE/EtOAc 100:0-50:50, 40 min: 50:50, SF 8 g) to obtain the product as a white solid (80 mg, 43%). R_f = 0.25 (PE/EtOAc 1:1). ^{1}H-NMR (300 MHz, $CDCl_3$) δ 10.01 (s, 1H), 7.84-7.74 (m, 2H), 7.71-7.61 (m, 2H), 3.70 (t, *J* = 7.0 Hz, 2H), 2.60 (t, *J* = 7.6 Hz, 2H), 2.04-1.91 (m, 5H), 1.47 (s, 9H). ^{13}C-NMR (75 MHz, $CDCl_3$) δ 168.32 (2C), 152.35, 151.18, 141.52, 134.00 (2C), 132.05 (2C), 129.12, 123.24 (2C), 81.72, 37.48, 28.26 (3C), 27.15, 22.28, 11.17. HRMS (ESI-MS): calcd. for $C_{20}H_{24}N_3O_5^+$: 386.1710; found: 386.1728. MF: $C_{20}H_{23}N_3O_5$. MW: 385.42.

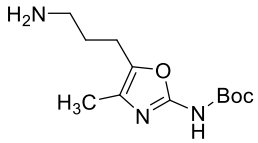

***tert*-Butyl (5-(3-aminopropyl)-4-methyloxazol-2-yl)carbamate (5.9). 5.73** (80 mg, 0.21 mmol, 1 equiv) was dissolved in EtOH (3 mL) and hydrazine hydrate (N_2H_4 x H_2O, 68 µL, 1.40 mmol, 6.7 equiv) was added. The mixture was stirred at rt for 48 h. The resulting white solid was removed by filtration. The solvent was removed in vacuum to obtain the crude product as a colorless oil (43 mg, 80%). The crude product was used in the next step without further purification. R_f = 0.01 (CH_2Cl_2/MeOH 9:1). ^{1}H-NMR (300 MHz, MeOD) δ 2.95-2.82 (m, 2H), 2.64 (t, *J* = 7.1 Hz, 2H), 2.00 (s, 3H), 1.95-1.75 (m, 2H), 1.49 (d, *J* = 3.2 Hz, 9H). ^{13}C-NMR (75 MHz, MeOD) δ 153.4, 153.06, 142.59, 130.87, 82.46, 40.49, 28.83, 28.40 (3C), 22.21, 10.92. HRMS (ESI-MS): calcd. for $C_{12}H_{22}N_3O_3^+$: 256.1656; found: 256.1661. MF: $C_{12}H_{21}N_3O_3$. MW: 255.32.

App4.1.2 Synthesis of the Amine 5.11

Procedure A: The preparation of amine **5.11** was accomplished by a slightly modified procedure of the original synthesis (Scheme App4.2).[9] γ-Aminobutyric acid (GABA, **5.74**) was converted to the corresponding phthalimide derivative **5.75** with phthalic anhydride in DMF under reflux.[10] The corresponding acyl chloride **5.76** was subsequently obtained by reaction of **75** with $SOCl_2$ in CH_2Cl_2.[11] Acylation of thiosemicarbazide with the acyl chloride **5.76** in the presence of pyridine afforded compound **5.77**, which was cyclized in concentrated H_2SO_4 and gave the thiadiazole **5.78**.[9] In the next step, thiadiazole **5.78** was Boc-protected and after hydrazinolysis of intermediate **5.79** the amine **5.11** was obtained.

Scheme App4.2. Synthesis of *tert*-Butyl (5-(3-Aminopropyl)-1,3,4-thiadiazol-2-yl)carbamate (5.11)[a]

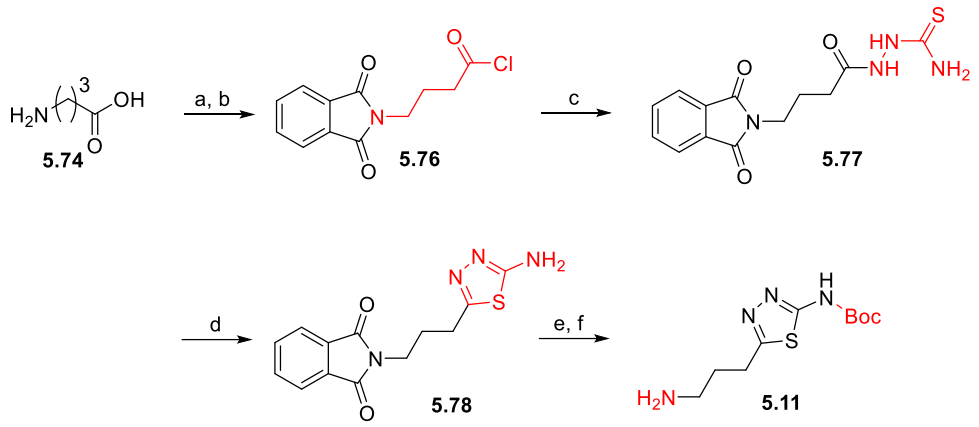

[a]Reagents and conditions: (a) phthalic anhydride, 170 °C, 5 h, 88%; (b) $SOCl_2$, CH_2Cl_2, reflux, 5 h, 100%; (c) thiosemicarbazide, pyridine, 0 °C, 3 h, 37%; (d) H_2SO_4, 100 °C, 15 min, 78%; (e) Boc_2O, NEt_3, DMAP (cat.), chloroform, rt, 16 h, 12%; (f) N_2H_4 x H_2O, EtOH, reflux, 2 h, 100%.

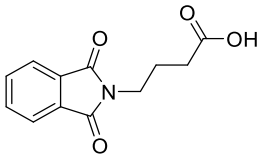

4-(1,3-Dioxoisoindolin-2-yl)butanoic acid (5.75).[10] A mixture of GABA (**5.74**, 2.0 g, 19.4 mmol, 1 equiv) and phthalic anhydride (2.9 g, 19.4 mmol, 1 equiv) was stirred at 170 °C for 5 h. After cooling to rt, the resulting solid was dissolved in CH_2Cl_2 (100 mL) and washed with 0.1 M HCl (3 x 50 mL). The organic layer was dried over Na_2SO_4, filtered, and concentrated in vacuum to yield the product as a white solid (4.0 g, 88%). R_f = 0.45 (PE/EtOAc 1:1). ^{1}H-NMR (300 MHz, $CDCl_3$): δ 10.63 (s, 1H), 7.88-7.78 (m, 2H), 7.75-7.65 (m, 2H), 3.74 (t, *J* = 6.8 Hz, 2H), 2.40 (t, *J* = 7.4 Hz, 2H), 1.99 (quint, *J* = 7.1 Hz, 2H). ^{13}C-NMR (75 MHz, $CDCl_3$): δ 178.58, 168.40 (2C), 134.03 (2C), 131.96 (2C), 123.32 (2C), 37.07, 31.27, 23.61. NMR data matches literature reference.[10] HRMS (ESI-MS): calcd. for $C_{12}H_{11}NNaO_4^+$: 256.0580; found: 256.0583. MF: $C_{12}H_{11}NO_4$. MW: 233.22.

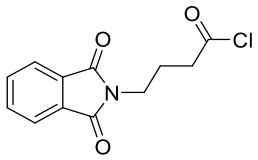

4-(1,3-Dioxoisoindolin-2-yl)butanoyl chloride (5.76).[11] **5.75** (1.0 g, 4.3 mmol, 1 equiv) was dissolved in CH_2Cl_2 (10 mL) and $SOCl_2$ (2.6 mL, 35.2 mmol, 8.2 equiv) was added. The mixture was refluxed for 5 h. After cooling to rt, the solvent and the excess of $SOCl_2$ were removed in vacuum. The residue was dissolved in *n*-hexane and evaporated in vacuum for two times to give the crude product as a yellow oil (1.08 g, 100%). The crude product was used in the next step without further purification. ^{1}H-NMR (300 MHz, $CDCl_3$): δ 7.88-7.79 (m, 2H), 7.77-7.67 (m, 2H), 3.75 (t, J = 6.7 Hz, 2H), 2.98 (t, J = 7.3 Hz, 2H), 2.08 (quint, J = 6.9 Hz, 2H). ^{13}C-NMR (75 MHz, $CDCl_3$): δ 173.30, 168.41 (2C), 134.31 (2C), 132.01 (2C), 123.55 (2C), 44.53, 36.50, 24.34. NMR data matches literature reference.[11] MF: $C_{12}H_{10}ClNO_3$. MW: 251.67.

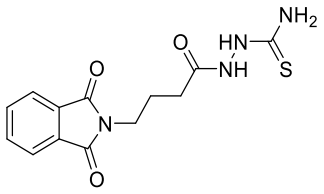

2-(4-(1,3-Dioxoisoindolin-2-yl)butanoyl)hydrazine-1-carbothioamide (5.77).[9] **5.76** (1.05 g, 4.17 mmol, 1 equiv) was treated with thiosemicarbazide (0.40 g, 4.38 mmol, 1.05 equiv) in pyridine (20 mL) at 0 °C for 3 h. After standing overnight, the mixture was poured into ice-water (160 mL). The aqueous phase was extracted three times with EtOAc (150 mL). The combined organic layers were washed with H_2O (50 mL) and subsequently with brine (50 mL), dried over Na_2SO_4, filtered, and evaporated in vacuum. The crude product was purified by flash chromatography (gradient: CH_2Cl_2/MeOH 100:0-95:5, 40 min: 95:5, SF 12 g) yielding the product as a white solid (0.47 g, 37%). R_f = 0.47 (PE/EtOAc 1:1). ^{1}H-NMR (300 MHz, DMSO-d_6): δ 9.70 (s, 1H), 9.16 (s, 2H), 7.94-7.78 (m, 4H), 7.40 (s, 1H), 3.58 (t, J = 6.7 Hz, 2H), 2.15 (t, J = 7.7 Hz, 2H), 1.84 (quint, J = 7.6 Hz, 2H). ^{13}C-NMR (75 MHz, DMSO-d_6): δ 181.84, 170.90, 168.02 (2C), 134.40 (2C), 131.61 (2C), 123.03 (2C), 37.05, 30.46, 23.47. HRMS (ESI-MS): calcd. for $C_{13}H_{15}N_4O_3S^+$: 307.0859; found: 307.0864. MF: $C_{13}H_{14}N_4O_3S$. MW: 306.34.

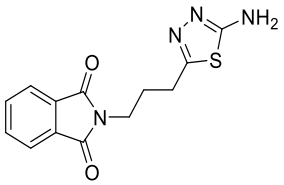

2-(3-(5-Amino-1,3,4-thiadiazol-2-yl)propyl)isoindoline-1,3-dione (5.78).[9] **5.77** (1.6 g, 5.1 mmol) was dissolved under stirring in 98% H_2SO_4 (50 mL). The solution was heated to 100 °C for 15 min. After cooling, the solution was poured oved ice and neutralized with 30% NaOH solution to pH = 7.5. The obtained precipitate was filtered and washed with H_2O in order to remove the coprecipitated Na_2SO_4 and recrystallized from 1,4-dioxane/H_2O (1:1 (v/v)) to give the product as a white solid (1.14 g, 78%). R_f = 0.10 (PE/EtOAc 1:1).^{1}H-NMR (300 MHz, DMSO-d_6) δ 7.93-7.77 (m, 4H), 7.00 (s, 2H), 3.64 (t, *J* = 7.0 Hz, 2H), 2.84 (t, *J* = 7.6 Hz, 2H), 1.96 (quint, *J* = 7.4 Hz, 2H). ^{13}C-NMR (75 MHz, DMSO-d_6) δ 168.23 (2C), 167.95, 157.32, 134.29 (2C), 131.70 (2C), 122.96 (2C), 36.88, 27.58, 27.04. HRMS (ESI-MS): calcd. for $C_{13}H_{13}N_4O_2S^+$: 289.0754; found: 289.0757. MF: $C_{13}H_{12}N_4O_2S$. MW: 288.33.

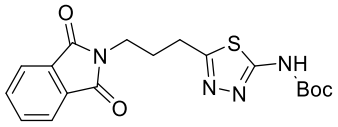

***tert*-Butyl (5-(3-(1,3-dioxoisoindolin-2-yl)propyl)-1,3,4-thiadiazol-2-yl)carbamate (5.79). 5.78** (1.14 g, 3.95 mmol, 1 equiv) was dissolved in chloroform and Boc_2O (0.95 g, 4.35 mmol, 1.1 equiv), NEt_3 (0.66 mL, 4.74 mmol, 1.2 equiv) and DMAP (50 mg, cat.) were added. The mixture was stirred for 16 h at rt. The solvent was removed in vacuum and the crude product was purified by flash chromatography on silica gel (gradient: 0-20 min: PE/EtOAc 100:0-50:50, SF 8 g) to obtain the product as a white solid (190 mg, 12%). R_f = 0.28 (PE/EtOAc 1:1). ^{1}H-NMR (300 MHz, $CDCl_3$): δ 7.89-7.81 (m, 2H), 7.75-7.69 (m, 2H), 3.83 (t, *J* = 6.9 Hz, 2H), 3.05 (t, *J* = 7.6 Hz, 2H), 2.20 (quint, *J* = 8.0 Hz, 2H), 1.56-1.51 (m, 9H). ^{13}C-NMR (101 MHz, $CDCl_3$): δ 168.26 (2C), 162.86, 161.89, 152.40, 134.01 (2C), 132.01 (2C), 123.28 (2C), 82.95, 37.22, 28.11 (3C), 28.00, 27.46. HRMS (ESI-MS): calcd. for $C_{18}H_{21}N_4O_4S^+$: 389.1278; found: 389.1284. MF: $C_{18}H_{20}N_4O_4S$. MW: 388.44.

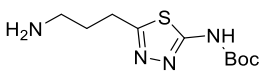

***tert*-Butyl (5-(3-aminopropyl)-1,3,4-thiadiazol-2-yl)carbamate (5.11).** A mixture of **5.79** (0.19 g, 0.49 mmol, 1 equiv) and N_2H_4 x H_2O (48 µL, 0.98 mmol, 2 equiv) in EtOH (6 mL) was

refluxed for 2 h. After cooling down to rt, the resulting white solid was removed by filtration and the filtrate was evaporated in vacuum to obtain the crude product as a colorless oil (0.13 g, 100%). The crude product was used in the next step without further purification. $R_f = 0.01$ (CH_2Cl_2/MeOH 9:1). ^{1}H-NMR (300 MHz, MeOD): δ 3.16-2.96 (m, 4H), 2.13 (quint, $J = 7.5$ Hz, 2H), 1.54 (s, 9H); slightly different chemical shifts than in the product of method B, since some EtOAc was left in the product. ^{13}C-NMR (101 MHz, MeOD): δ 163.27, 160.94, 154.52, 83.60, 40.23, 28.95, 28.46 (3C), 27.54. HRMS (ESI-MS): calcd. for $C_{10}H_{19}N_4O_2S^+$: 259.1223; found: 259.1226. MF: $C_{10}H_{18}N_4O_2S$. MW: 258.34.

Procedure B: An alternative synthetic route B for amine **5.11** was developed (Scheme App4.3) because the synthetic route A consists of 6 steps and provides a very low overall yield (3% over 6 steps). The synthesis route B consists of 4 steps and provides an overall yield of 6%. The synthesis of the amine **5.11** started with the cyclocondensation of the 2-bromobutanoic acid **5.80** with thiosemicarbazide in fuming hydrochloric acid. This reaction occurs according to the mechanism published elsewhere.[12] In the same step, the bromide in 2-bromobutanoic acid was exchanged by chloride. After Boc-protection of the aromatic amine group (compd. **5.82**), the alkyl chloride was converted to the corresponding azide in an S_N2 reaction in DMF (compd. **5.83**). In the last step, the azide was reduced to the corresponding amine **5.11** by a Staudinger reaction.[13]

Scheme App4.3. Synthesis of *tert*-Butyl (5-(3-Aminopropyl)-1,3,4-thiadiazol-2-yl)carbamate (5.11)[a]

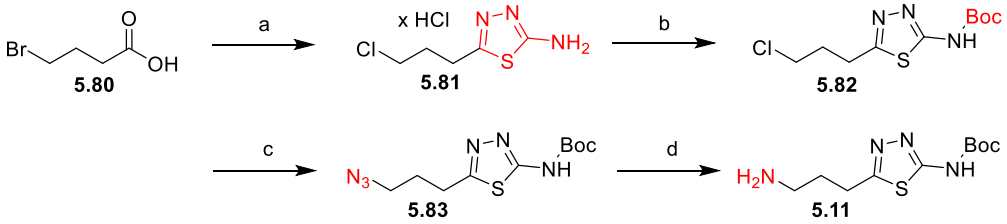

[a]Reagents and conditions: (a) thiosemicarbazide, HCl (37% in H_2O), reflux, 5 h, 83%; (b) Boc_2O, NEt_3, DMAP (cat.), CH_2Cl_2, rt, 24 h, 23%; (c) NaN_3, DMF, 75 °C, overnight; (d) PPh_3, THF, 45 °C, 5 h; H_2O, 45 °C, overnight, 34% over 2 steps.

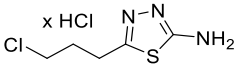

5-(3-Chloropropyl)-1,3,4-thiadiazole-2-amine hydrochloride (5.81). To a solution of 4-bromobutanoic acid (**5.80**, 1.73 g, 10.36 mmol, 1.18 equiv) in 5 mL HCl (37% in H_2O)

thiosemicarbazide (0.80 g, 8.78 mmol, 1 equiv) was added. The mixture was heated under reflux for 5 h. After cooling, the solvent was removed in vacuum. The white residue was washed with diethyl ether (3 x 20 mL) yielding 1.56 g (83%) of a white solid. The product was used without any further purification. HRMS (ESI-MS): calcd. for $C_5H_9ClN_3S^+$: 178.0200, found: 178.0199. MF: $C_5H_8ClN_3S$ x HCl. MW: (177.65 + 36.46).

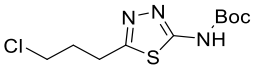

***tert*-Butyl (5-(3-chloropropyl)-1,3,4-thiadiazol-2-yl)carbamate (5.82). 5.81** (1.56 g, 7.29 mmol, 1 equiv), NEt_3 (2.23 mL, 16.03 mmol, 2.2 equiv) and DMAP (40 mg, cat.) were dissolved in 150 mL CH_2Cl_2. Boc_2O (1.59 g, 7.29 mmol, 1 equiv) was slowly added to this solution over a period of 1 h. After the addition was complete, the reaction mixture was stirred at rt for 24 h. The organic phase was washed with 0.1 N HCl, brine and water. The organic layer was dried over Na_2SO_4 and the solvent was removed in vacuum. The residue was purified by column chromatography (PE/EtOAc 1:1) to give 467 mg (23%) of a white solid. $R_f = 0.45$ (PE/EtOAc 1:1). ^{1}H-NMR (400 MHz, $CDCl_3$) δ 3.64 (t, $J = 6.4$ Hz, 2H), 3.14 (t, $J = 7.2$ Hz, 2H), 2.29-2.22 (m, 2H), 1.54 (s, 9H). ^{13}C-NMR (101 MHz, $CDCl_3$) δ 162.33, 162.21, 152.58, 82.98, 43.59, 31.40, 28.11 (3C), 26.81. HRMS (ESI-MS): calcd. for $C_{10}H_{17}ClN_3O_2S^+$: 278.0725, found: 278.0727. MF: $C_{10}H_{16}ClN_3O_2S$. MW: 277.77.

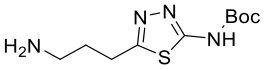

***tert*-Butyl (5-(3-aminopropyl)-1,3,4-thiadiazol-2-yl)carbamate (5.11). 5.82** (407 mg, 1.47 mmol, 1 equiv) was dissolved in DMF (20 mL). NaN_3 (95.3 mg, 1.47 mmol, 1 equiv, caution - NaN_3 is toxic and may explode when shocked, heated, or treated with acid) was added. The reaction mixture was heated to 75 °C and stirred overnight. The mixture was concentrated in vacuum and taken up in CH_2Cl_2 (20 mL). The organic layer was washed with water, dried over Na_2SO_4, and then concentrated in vacuum resulting in *tert*-butyl (5-(3-azidopropyl)-1,3,4-thiadiazol-2-yl) carbamate (**83**). HRMS (ESI-MS): calcd. for $C_{10}H_{17}N_6O_2S^+$: 285.1128, found: 285.1131. MF: $C_{10}H_{16}N_6O_2S$. MW: 284.34. The residue was dissolved in THF (20 mL). Triphenylphosphine (PPh_3, 577 mg, 2.20 mmol, 1.5 equiv) was added to the solution. The mixture was heated to 45 °C. After 5 hours of continuously stirring, water (20 mL) was added to the solution and the mixture was further stirred at 45 °C overnight. The mixture was

concentrated in vacuum and the residue was purified by column chromatography (CH_2Cl_2/MeOH 90:10 → CH_2Cl_2/MeOH/25% NH_3 in H_2O 50:50:1) yielding 130 mg (34%) of a colorless oil. R_f = 0.21 (CH_2Cl_2/MeOH/25% NH_3 in H_2O 50:50:1). ^{1}H-NMR (300 MHz, MeOD) δ 2.95 (t, *J* = 7.6 Hz, 2H), 2.69 (t, *J* = 7.6 Hz, 2H), 1.95-1.78 (m, 2H), 1.44 (s, 9H). ^{13}C-NMR (101 MHz, MeOD): δ 164.18, 163.25, 154.49, 81.32, 39.99, 31.37, 27.11 (3C), 26.56. HRMS (ESI-MS): calcd. for $C_{10}H_{19}N_4O_2S^+$: 259.1223, found: 259.1225. MF: $C_{10}H_{18}N_4O_2S$. MW: 258.34.

App4.1.3 Synthesis of the Amine 5.14

The preparation of the amine **5.14** (Scheme App4.4) started with 3-chloropropan-1-ol (**5.84**). In the first step, the chloride in **5.84** was replaced by azide in an S_N2 reaction. The so formed azide **5.85** was converted in the next step with *N*,*N*-dimethylpropargylamine in a copper-catalyzed click-reaction to the 1,2,3-triazole **5.86**. To transform the primary alcohol into an amine, a Mitsunobu reaction using phthalimide, PPh_3 and diisopropyl azodicarboxylate (DIAD) was performed to obtain the *N*-substituted phthalimide **5.87**.[14] In the last step, the amine was liberated from the phthalimide by hydrazinolysis yielding compound **5.14**.

Scheme App4.4. Synthesis of 3-(4-((Dimethylamino)methyl)-1*H*-1,2,3-triazol-1-yl)propan-1-amine (5.14)[a]

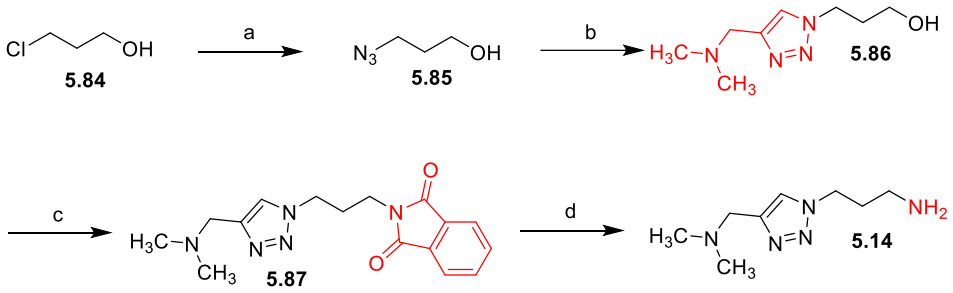

[a]Reagents and conditions: (a) NaN_3, DMF, 70 °C 16 h, 98%; (b) *N*,*N*-dimethylpropargylamine, sodium ascorbate, $CuSO_4$ x H_2O, H_2O/*tert*-butanol (1:1), rt, 16 h, 68%; (c) phthalimide, PPh_3, DIAD, THF, 0 °C to rt, overnight, 32%; (d) N_2H_4 x H_2O, *n*-butanol, rt, overnight, 100%.

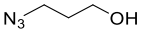

3-Azidopropan-1-ol (5.85).[15] 3-Chloropropan-1-ol (**5.84**, 1.0 g, 10.58 mmol, 1 equiv) and NaN_3 (1.03 g, 15.86 mmol, 1.5 equiv, caution - NaN_3 is toxic and may explode when shocked,

heated, or treated with acid) were dissolved in DMF (30 mL). The mixture was stirred at 70 °C for 16 h. After cooling to room temperature, water (100 mL) was added to the reaction mixture. The product was extracted with CH_2Cl_2. The organic layers were combined, washed 3-times with 0.1 M HCl, dried over Na_2SO_4 and evaporated to dryness under reduced pressure to afford the product as a yellowish liquid (1.05 g, 98%). Note for this molecule, (C+O)/N = 1.3, thus this compound should be handled with caution and stored in solution below rt and in the dark. R_f = 0.69 (PE/EtOAc 1:1). ^{1}H-NMR (300 MHz, $CDCl_3$) δ 3.72 (t, *J* = 6.0 Hz, 2H), 3.43 (t, *J* = 6.6 Hz, 2H), 2.23 (s, 1H), 1.81 (t, *J* = 6.1 Hz, 2H). ^{13}C-NMR (75 MHz, $CDCl_3$) δ 59.79, 48.46, 31.44. NMR data matches literature reference.[16-18] Due to its structure, low weight and volatility, no HRMS could be performed on this compound. MF: $C_3H_7N_3O$. MW: 101.11.

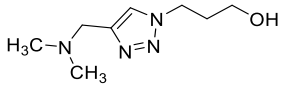

3-(4-((Dimethylamino)methyl)-1*H*-1,2,3-triazol-1-yl)propan-1-ol (5.86). 5.85 (810 mg, 8.01 mmol, 1 equiv), sodium ascorbate (159 mg, 0.80 mmol, 0.1 equiv) and *N*,*N*-dimethylpropargylamine (666 mg, 8.01 mmol, 1 equiv) were dissolved in H_2O/*tert*-butanol (1:1 (v/v), 60 mL). The flask was set under argon atmosphere and $CuSO_4$ x H_2O (40 mg, 0.16 mmol, 0.02 equiv) was added. After stirring the mixture at rt for 16 h, the solvent was evaporated under reduced pressure. The obtained residue was purified by column chromatography (CH_2Cl_2/MeOH/25% NH_3 in H_2O 50:50:1), which resulted in 1 g (68%) of an orange oil. R_f = 0.4 (CH_2Cl_2/MeOH/25% NH_3 in H_2O 50:50:1). ^{1}H-NMR (300 MHz, MeOD) δ 7.97 (s, 1H), 4.53 (t, *J* = 7.0 Hz, 2H), 3.71 (s, 2H), 3.56 (t, *J* = 6.1 Hz, 2H), 2.32 (s, 6H), 2.19-2.03 (m, 2H). ^{13}C-NMR (75 MHz, MeOD) δ 142.46, 124.43, 57.87, 52.76, 46.93, 43.36 (2C), 32.67. HRMS (ESI-MS): calcd. for $C_8H_{17}N_4O^+$: 185.1397, found: 185.1394. MF: $C_8H_{16}N_4O$. MW: 184.24.

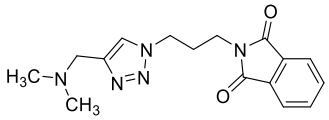

2-(3-(4-((Dimethylamino)methyl)-1*H*-1,2,3-triazol-1-yl)propyl)isoindoline-1,3-dion (5.87). 5.86 (950 mg, 5.16 mmol, 1 equiv) was dissolved in THF (70 mL). The flask was set under argon atmosphere and cooled to 0 °C by using an ice-bath. Phthalimide (1.14 g,

7.73 mmol, 1.5 equiv) and triphenylphosphine (2.03 g, 7.73 mmol, 1.5 equiv) were added to the mixture. Diisopropyl azodicarboxylate (DIAD, 2.23 mL, 11.34 mmol, 2.2 equiv) dissolved in THF (30 mL) was added dropwise over the period of 1.5 h to the solution. The ice-bath was removed, and the mixture was stirred overnight. The solvent was removed under reduced pressure and the residue was purified by column chromatography (CH_2Cl_2/MeOH/25% NH_3 in H_2O 50:50:1), which resulted in 510 mg (32%) of a colorless oil. $R_f = 0.75$ (CH_2Cl_2/MeOH/25% NH_3 in H_2O 50:50:1). ^{1}H-NMR (300 MHz, $CDCl_3$) δ 7.69-7.62 (m, 2H), 7.61-7.53 (m, 2H), 4.27 (t, $J = 7.0$ Hz, 2H), 3.57 (t, $J = 6.6$ Hz, 2H), 3.49 (d, $J = 7.1$ Hz, 2H), 2.27-2.14 (m, 2H), 2.13 (s, 6H). ^{13}C-NMR (75 MHz, $CDCl_3$) δ 168.18 (2C), 144.11, 134.16 (2C), 131.71 (2C), 123.37 (2C), 123.24, 53.85, 47.67, 44.67 (2C), 34.91, 29.26. HRMS (ESI-MS): calcd. for $C_{16}H_{20}N_5O_2^+$: 314.1612, found: 314.1617. MF: $C_{16}H_{19}N_5O_2$. MW: 313.36.

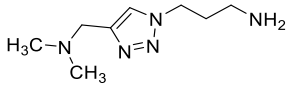

3-(4-((Dimethylamino)methyl)-1*H*-1,2,3-triazol-1-yl)propan-1-amine (5.14). 5.87 (510 mg, 1.63 mmol, 1 equiv) was dissolved in *n*-butanol (30 mL), N_2H_4 x H_2O (395 µL, 8.14 mmol, 5 equiv) was added and the solution was stirred at rt overnight. The mixture was cooled to 0 °C, the produced white precipitate was removed by filtration and the solvent was evaporated under reduced pressure. The residue was purified by column chromatography (CH_2Cl_2/MeOH 100:10 → CH_2Cl_2/MeOH/25% NH_3 in H_2O 50:50:1), which resulted in 298 mg (100%) of a white solid. $R_f = 0.45$ (CH_2Cl_2/MeOH 100:10). ^{1}H-NMR (300 MHz, MeOD) δ 8.24 (s, 1H), 4.58 (t, $J = 6.8$ Hz, 2H), 3.95 (s, 2H), 2.98-2.91 (m, 2H), 2.51 (s, 6H), 2.33 (d, $J = 7.7$ Hz, 2H). ^{13}C-NMR (75 MHz, MeOD) δ 140.89, 125.65, 52.20, 47.05, 42.73 (2C), 36.55, 27.82. HRMS (ESI-MS): calcd. for $C_8H_{18}N_5^+$: 184.1557, found: 184.1557. MF: $C_8H_{17}N_5$. MW: 183.26.

App4.1.4 Synthesis of the Amine 5.15

The rigidized thiazole building block **5.15** was synthesized as shown in Scheme App4.5. **5.89** could be directly obtained by refluxing *N*-anilinothiourea (**5.88**) and α-chloroacetone in MeOH under neutral conditions according to Lee et al.[19] The HCl generated in the first step, acts as an acid catalyst for a [5,5]-shift of *N*-phenyl-*N'*-[2-(4-methyl)thiazolyl]hydrazine.[19] The subsequent selective protection of the 2-aminothiazole in **5.89** with di-*tert*-butyl dicarbonate gave amine **5.15**.

Scheme App4.5. Synthesis of *tert*-Butyl (5-(4-Aminophenyl)-4-methylthiazol-2-yl)carbamate (5.15)[a]

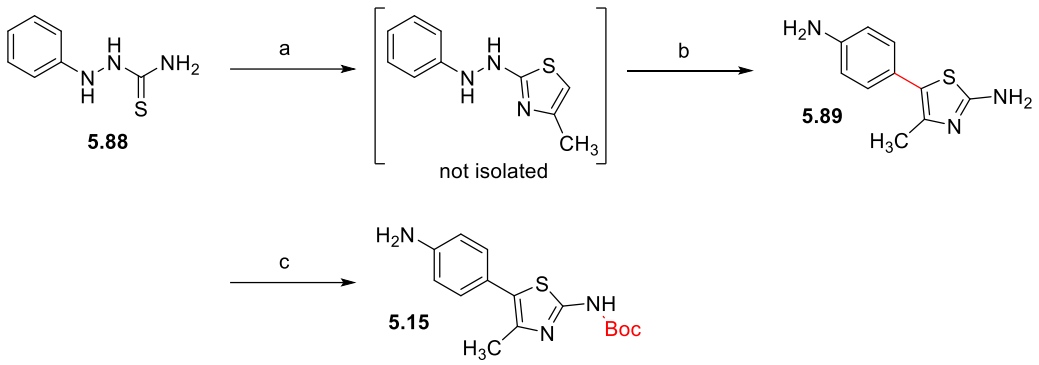

[a]Reagents and conditions: (a/b) chloroacetone, MeOH, reflux, 32 h, 49%; (c) Boc_2O, NEt_3, DMAP (cat.), chloroform, 0 °C to rt, 16 h, 30%.

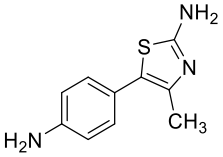

5-(4-Aminophenyl)-4-methylthiazol-2-amine (5.89).[19] 1-Phenylhydrazine-1-carbothioamide (**5.88**, 2.0 g, 11.96 mmol, 1 equiv) and chloroacetone (1.2 g, 13.2 mmol, 1.1 equiv) were dissolved in MeOH (50 mL) and refluxed for 32 h. After 32 h, additional MeOH (250 mL) was added. The solid was filtered off and the solvent was removed in vacuum. The residue (red-brown solid) was purified by flash chromatography (gradient: 0-20 min: PE/EtOAc 100:0-50:50, 40 min: 0:100, 50-60 min: isocratic CH_2Cl_2/MeOH 90:10, SF 24 g) yielding the product as a red-brown solid (1.2 g, 49%). R_f = 0.66 (EtOAc). ^{1}H-NMR (300 MHz, DMSO-d_6): δ 7.03-6.95 (m, 2H), 6.75 (s, 2H), 6.63-6.52 (m, 2H), 5.26 (br s, 2H), 2.09 (s, 3H). ^{13}C-NMR (101 MHz, DMSO-d_6) δ 165.69, 147.57, 134.51, 129.13 (2C), 118.36, 118.16, 114.32 (2C), 14.24. NMR data matches literature reference.[19] HRMS (ESI-MS): calcd. for $C_{10}H_{12}N_3S^+$: 206.0746; found: 206.0752. MF: $C_{10}H_{11}N_3S$. MW: 205.28.

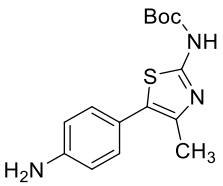

***tert*-Butyl (5-(4-aminophenyl)-4-methylthiazol-2-yl)carbamate (5.15). 5.89** (1.0 g, 4.87 mmol, 1 equiv), NEt_3 (783 µL, 5.65 mmol, 1.16 equiv) and DMAP (50 mg, cat.) were dissolved in chloroform (25 mL). The solution was cooled to 0 °C (ice-bath) and a solution of

Boc_2O (1.06 g, 4.87 mmol, 4.87 mmol) in chloroform (25 mL) was added dropwise. The reaction mixture was stirred at rt for 16 h and the solvent was removed in vacuum. The residue was purified by flash chromatography (gradient: 0-20 min: PE/EtOAc 1:0-67:33, 20-40 min: isocratic 30:70, SF 4 g) yielding an orange solid (0.45 g, 30%). R_f = 0.19 (PE/EtOAc 2:1). ^{1}H-NMR (300 MHz, DMSO-d_6): δ 11.26 (s, 1H), 7.16-6.99 (m, 2H), 6.67-6.54 (m, 2H), 5.34 (br s, 2H), 2.23 (s, 3H), 1.47 (s, 9H). ^{13}C-NMR (101 MHz, $CDCl_3$) δ 157.95, 152.57, 145.94, 140.16, 130.21 (2C), 125.36, 122.35, 115.29 (2C), 82.65, 28.44 (3C), 15.79. HRMS (ESI-MS): calcd. for $C_{15}H_{20}N_3O_2S^+$: 306.1271; found: 306.1273. MF: $C_{15}H_{19}N_3O_2S$. MW: 305.40.

App4.1.5 Synthesis of the Amine 5.16

5.16 was synthesized in a multistep sequence (Scheme App4.6). In the first step 1-iodo-3-nitrobenzene (**5.90**) was used as starting material in a palladium catalyzed cross-coupling to yield **5.91**. After bromination of the benzylic position (compd. **5.92**) cyclisation with thiourea in DMF yielded **5.93**. Reduction of the nitro group and the subsequent deformylation and Boc protection yielded the target amine **5.16**.

Scheme App4.6. Synthesis of *tert*-Butyl (5-(3-Aminophenyl)-4-methylthiazol-2-yl)carbamate (5.16)[a]

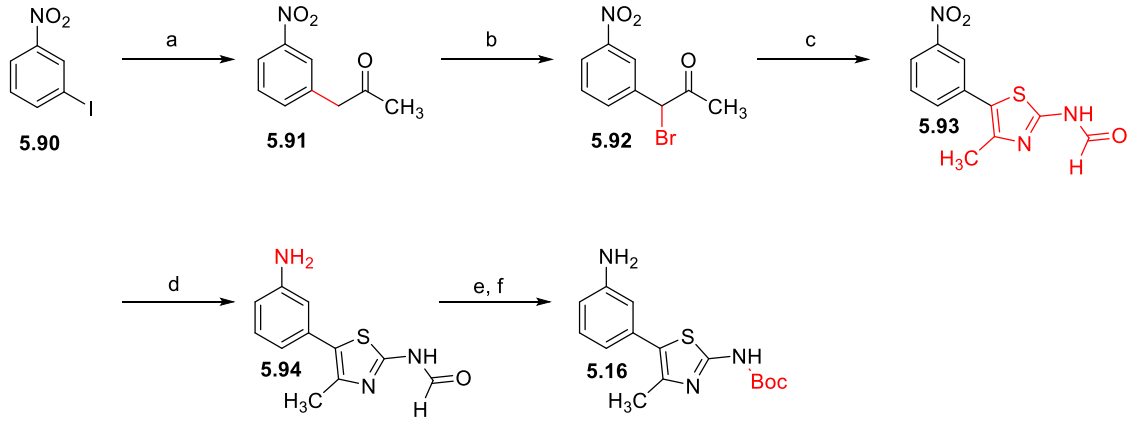

[a]Reagents and conditions: (a) $Pd(OAc)_2$, PPh_3, Cs_2CO_3, 4-hydroxy-4-methylpentan-2-one, toluene, 120 °C, 5 h, 40%; (b) Br_2, diethyl ether, rt, overnight, 68%; (c) thiourea, DMF, 100 °C, 4 h, 79%; (d) Fe, NH_4Cl, EtOH/H_2O, 90 °C, 4 h, 70%; (e) 1 N HCl in MeOH, MeOH, rt, 48 h, 100%; (f) Boc_2O, NEt_3, DMAP (cat.), chloroform, rt, overnight, 17%.

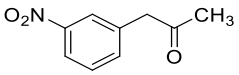

1-(3-Nitrophenyl)propan-2-one (5.91).[20] $Pd(OAc)_2$ (230 mg, 1.01 mmol, 0.05 equiv), PPh_3 (1.05 g, 4.02 mmol, 0.2 equiv), 1-iodo-3-nitrobenzene (**5.90**, 5.0 g, 20.1 mmol, 1 equiv) and Cs_2CO_3 (9.82 g, 30.2 mmol, 1.5 equiv) were added to an oven-dried Schlenk tube equipped with a stir bar. The tube was then sealed, evacuated, and backfilled with nitrogen three times using standard Schlenk techniques. Toluene (150 mL) and 4-hydroxy-4-methyl-pentan-2-one (14.9 mL, 120.5 mmol, 6 equiv) were sequentially added by syringe at rt. The resulting mixture was vigorously stirred and heated at 120 °C for 5 h. After the mixture was cooled to rt, H_2O (300 mL) was added. The resulting mixture was extracted three times with 200 mL EtOAc. The combined organic layers were then washed with 150 mL brine, dried over Na_2SO_4, and concentrated in vacuum. The residue was purified by flash chromatography on silica gel (gradient: 0-20 min: PE/EtOAc 100:0-67:33, SF 40 g) to provide the product as a yellow oil (1.45 g, 40%). $R_f = 0.40$ (PE/EtOAc 2:1). ^{1}H-NMR (300 MHz, $CDCl_3$): δ 8.11-7.97 (m, 2H), 7.56-7.37 (m, 3H), 3.83 (s, 2H), 2.21 (s, 3H). ^{13}C-NMR (75 MHz, $CDCl_3$): δ 204.53, 148.20, 136.01, 135.96, 129.44, 124.49, 122.03, 49.55, 29.83. NMR data matches literature reference.[20] HRMS (ESI-MS): calcd. for $C_9H_{13}N_2O_3^+$: 197.0921; found: 197.0923. MF: $C_9H_9NO_3$. MW: 179.18.

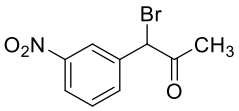

1-Bromo-1-(3-nitrophenyl)propan-2-one (5.92). To a stirred solution of **5.91** (1.45 g, 8.1 mmol, 1 equiv) in diethyl ether (50 mL) at rt a solution of Br_2 (0.42 mL, 8.1 mmol, 1 equiv) in diethyl ether (5 mL) was added dropwise in the dark. After addition, the reaction mixture was stirred overnight and then diluted with CH_2Cl_2 (100 mL) and extracted subsequently with H_2O (2 x 150 mL), brine (100 mL), dried over Na_2SO_4, filtered, and concentrated in vacuum. The residue was purified by flash chromatography on silica gel (gradient: 0-20 min: PE/EtOAc 100:0-80:20, SF 12 g) to provide the product as a yellow oil (1.43 g, 68%). $R_f = 0.70$ (PE/EtOAc 2:1). ^{1}H-NMR (300 MHz, $CDCl_3$): δ 8.28-8.21 (m, 1H), 8.17-8.08 (m, 1H), 7.80-7.69 (m, 1H), 7.60-7.47 (m, 1H), 5.53 (s, 1H), 2.38 (s, 3H). ^{13}C-NMR (75 MHz, $CDCl_3$): δ 198.33, 148.03, 137.12, 135.22, 129.87, 124.02, 123.82, 52.59, 27.01. HRMS (ESI-MS): calcd. for $C_9H_{12}BrN_2O_3^+$: 275.0026; found: 275.0011. MF: $C_9H_8BrNO_3$. MW: 258.07.

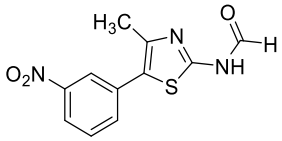

***N*-(4-Methyl-5-(3-nitrophenyl)thiazol-2-yl)formamide (5.93).** To a stirred solution of **5.92** (1.43 g, 5.54 mmol, 1 equiv) in DMF (10 mL), a solution of thiourea (423 mg, 5.54 mmol, 1 equiv) in DMF (10 mL) was added and the mixture was heated at 100 °C for 4 h. After cooling and removing of the solvent in vacuum, a mixture of EtOAc/MeOH (1:1 (v/v)) was added and stirred for 30 min. Subsequently, the precipitate was filtered off, washed with EtOAc and diethyl ether and the solid was dried in vacuum yielding the product as a yellow solid (1.16 g, 79%). R_f = 0.74 (CH_2Cl_2/MeOH 9:1). ^{1}H-NMR (300 MHz, DMSO-d_6): δ 12.40 (s, 1H), 8.53 (s, 1H), 8.24-8.15 (m, 2H), 7.96-7.90 (m, 1H), 7.78-7.70 (m, 1H), 2.40 (s, 3H). ^{13}C-NMR (101 MHz, DMSO-d_6): δ 159.78, 154.20, 148.09, 144.10, 134.85, 133.56, 130.53, 122.57, 122.22, 121.92, 15.96. HRMS (ESI-MS): calcd. for $C_{11}H_{10}N_3O_3S^+$: 264.0437; found: 264.0441. MF: $C_{11}H_9N_3OS$. MW: 263.27.

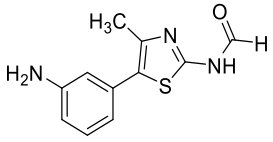

***N*-(5-(3-Aminophenyl)-4-methylthiazol-2-yl)formamide (5.94).**[21] To a solution of **5.93** (230 g, 0.87 mmol, 1 equiv) in EtOH/H_2O (2:1 (v/v), 13 mL) iron (273 mg, 4.89 mmol, 5.6 equiv) and NH_4Cl (26 mg, 0.49 mmol, 0.56 equiv) were added. The reaction mixture was stirred at 90 °C for 4 h. After cooling, the reaction mixture was diluted with EtOAc (50 mL). The mixture was filtered through Celite 545 and the solvent was removed in vacuum. The crude product was purified by flash chromatography on silica gel (gradient: 0-20 min: CH_2Cl_2/MeOH 100:0-98:2, SF 4 g) to provide the product as a white solid (140 mg, 70%). R_f = 0.61 (CH_2Cl_2/MeOH 9:1). ^{1}H-NMR (300 MHz, DMSO-d_6): δ 12.18 (s, 1H), 8.46 (s, 1H), 7.11-7.03 (m, 1H), 6.68-6.64 (m, 1H), 6.60-6.49 (m, 2H), 5.23 (s, 2H), 2.33 (s, 3H). ^{13}C-NMR (75 MHz, DMSO-d_6): δ 159.41, 152.87, 149.10, 141.39, 132.24, 129.38, 125.52, 115.91, 113.73, 112.99, 16.14. HRMS (ESI-MS): calcd. for $C_{11}H_{12}N_3OS^+$: 234.0696; found: 234.0709. MF: $C_{11}H_{11}N_3OS$. MW: 233.29.

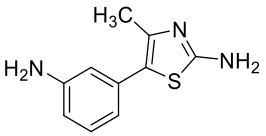

5-(3-Aminophenyl)-4-methylthiazol-2-amine (5.95).[22] A solution of **5.94** (130 mg, 0.56 mmol) in MeOH:1 N HCl in MeOH (1:1.1 (v/v), 2.1 mL) was stirred at rt for 48 h. The mixture was neutralized with an equivalent amount of 1 N NaOH in MeOH, filtered and concentrated in vacuum yielding the crude product as a light green oil (115 mg, 100%). The crude product was used in the next step without further purification. R_f = 0.01 (CH_2Cl_2/MeOH 9:1). ^{1}H-NMR (300 MHz, DMSO-d_6): δ 7.02-6.94 (m, 1H), 6.90-6.82 (m, 2H), 6.56-6.51 (m, 1H), 6.48-6.38 (m, 2H), 5.18-5.08 (m, 2H), 2.15 (s, 3H). ^{13}C-NMR (75 MHz, MeOD): δ 168.83, 149.06, 142.88, 134.78, 130.37, 121.10, 119.62, 116.60, 115.19, 16.11. HRMS (ESI-MS): calcd. for $C_{10}H_{12}N_3S^+$: 206.0746; found: 206.0745. MF: $C_{10}H_{11}N_3S$. MW: 205.28.

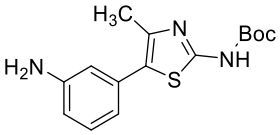

***tert*-Butyl (5-(3-aminophenyl)-4-methylthiazol-2-yl)carbamate (5.16).**[23] **5.95** (520 mg, 2.53 mmol, 1 equiv) was dissolved in chloroform (25 mL) and Boc_2O (541 µL, 1.53 mmol, 1 equiv), NEt_3 (407 µL, 2.93 mmol, 1.16 equiv) and DMAP (25 mg, cat.) were added. The mixture was stirred overnight at rt. The solvent was removed in vacuum and the crude product was purified by flash chromatography on silica gel (gradient: 0-20 min: PE/EtOAc 100:0-67:33, SF 12 g) to give the product as a yellow foam (130 mg, 17%). R_f = 0.39 (CH_2Cl_2/MeOH 95:5). ^{1}H-NMR (300 MHz, $CDCl_3$): δ 7.22-7.15 (m, 1H), 6.88-6.78 (m, 1H), 6.77-6.71 (m, 1H), 6.69-6.55 (m, 1H), 2.41 (s, 3H), 1.55 (s, 9H). ^{13}C-NMR (75 MHz, $CDCl_3$) δ 158.75, 152.91, 146.75, 142.05, 133.60, 129.72, 125.03, 119.37, 115.51, 114.12, 82.59, 28.45 (3C), 16.23. HRMS (ESI-MS): calcd. for $C_{15}H_{20}N_3O_2S^+$: 306.1271; found: 306.1273. MF: $C_{15}H_{19}N_3O_2S$. MW: 305.40.

App4.1.6 Synthesis of the Amine 5.17

The synthesis of bromo ketone **5.100** (Scheme App4.7) started with the preparation of **5.98** by reductive cyanation of 1,4-cyclohexanedione monoethylene acetal (**5.96**) with tosylmethylisocyanide (TosMIC) and subsequent reduction of the nitrile **5.97** with lithium aluminum hydride. After protection of the amino group of **5.98** as phthalimide, cleavage of the 1,3-dioxolane ring with hydrochloric acid gave **5.99**. The ketone **5.99** was α-brominated (compd. **5.100**). The condensation of the bromo ketone **5.100** with thiourea lead to compound

5.101. Finally, 2-aminothiazole **5.101** was trityl protected and after hydrazinolysis of the intermediate **5.102** the rigid amine **5.17** was obtained.

Scheme App4.7: Synthesis of 6-(Aminomethyl)-*N*-trityl-4,5,6,7-tetrahydrobenzo[*d*]thiazol-2-amine (5.17)[a]

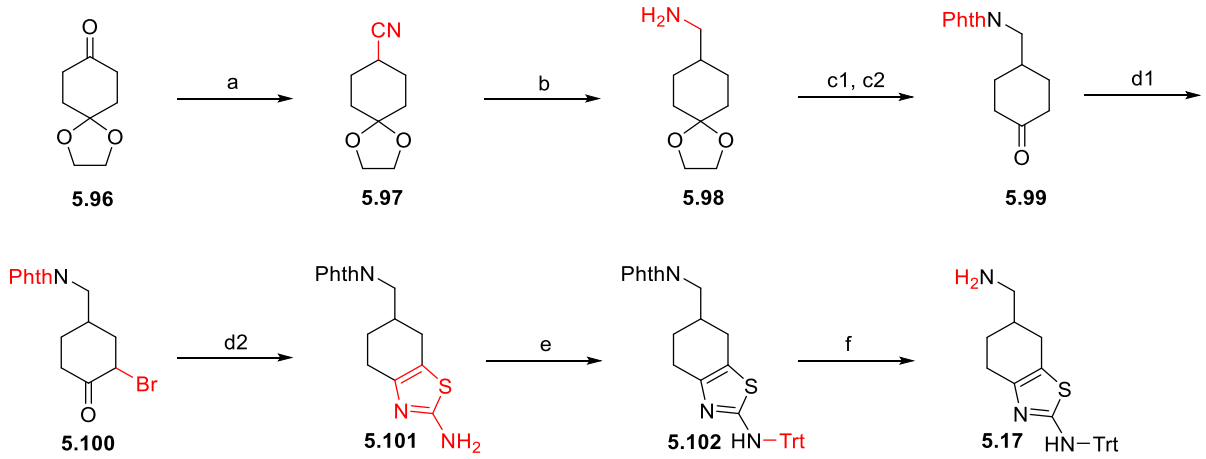

[a]Reagents and conditions: (a) TosMIC, *t*-BuOK, DME/EtOH, 0 °C, 1 h, then rt, 2 h, 75%; (b) $LiAlH_4$, THF, reflux, 2 h, then rt, 12 h, 99%; (c) 1) phthalanhydride, 135 °C, 30 min, 2) 1 M aq HCl, 135 °C, 2 h, 32% over two steps; (d) 1) Br_2, CH_2Cl_2, reflux, 1 h, 99%, 2) thiourea, EtOH, reflux, 2 h, 37%; (e) Trt-Cl, NEt_3, MeCN, rt, 16 h, 50%; (f) N_2H_4 x H_2O, EtOH, rt, 16 h, 100%.

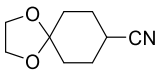

1,4-Dioxaspiro[4,5]decane-8-carbonitrile (5.97).[24] To a cooled (-10 °C) suspension of 1,4-cyclohexanedione monoethylene acetal (**5.96**, 5.26 g, 33.7 mmol, 1 equiv) and tosylmethylisocyanide (TosMIC, 8.55 g, 43.8 mmol, 1.3 equiv) in DME (105 mL) containing abs. EtOH (3.5 mL) was added *t*-BuOK (8.69 g, 77.5 mmol, 2.3 equiv) portionwise over the period of 30 min so that the temperature was maintained at <5 °C. After the addition was completed, the reaction mixture was stirred for 1 h at 0 °C and then for 2 h at rt. The mixture was concentrated to an orange-brown solid. H_2O (100 mL) was added to the residue and the aqueous phase was extracted with Et_2O (5 x 70 mL). The combined extracts were washed with brine (3 x 50 mL) and dried over Na_2SO_4. Concentration in vacuum gave a yellow oil which was purified by column chromatography (isocratic: PE/EtOAc 2:1) to give the product as a colorless oil (4.24 g, 75%). R_f = 0.70 (PE/EtOAc 2:1). ^{1}H-NMR (300 MHz, $CDCl_3$): δ 3.97-3.80 (m, 4H), 2.70-2.57 (m, 1H), 2.01-1.87 (m, 4H), 1.87-1.75 (m, 2H), 1.66-1.54 (m, 2H). ^{13}C-NMR (75 MHz, $CDCl_3$) δ 121.91, 107.13, 64.53 (2C), 32.79 (2C), 27.05 (2C), 26.73. NMR

data matches literature reference.[24] HRMS (EI-MS): calcd. for $C_9H_{12}NO_2^{+\cdot}$: 166.0863; found: 166.0850. MF: $C_9H_{13}NO_2$. MW: 167.21.

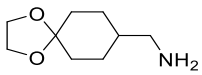

1,4-Dioxaspiro[4,5]dec-8-ylmethanamine (5.98).[24] To an ice-bath-cooled 1 M solution of $LiAlH_4$ in THF (44 mL, 44.2 mmol, 1.5 equiv), **5.97** (4.92 g, 29.4 mmol, 1 equiv) was added dropwise over 1 h. After the addition was complete, the solution was heated to reflux for 2 h and then stirred at rt for 12 h. The reaction mixture was quenched by careful sequential addition of distilled H_2O (5.6 mL), 15% NaOH (5.6 mL), and H_2O (15.7 mL). The initial H_2O portion was diluted with THF to aid addition and to reduce the exothermicity of the quench. The resulting precipitate was removed by filtration. Concentration in vacuum and purification by column chromatography (isocratic: CH_2Cl_2/MeOH 9:1) of the resulting oil gave the product as a colorless oil (5.0 g, 99%). R_f = 0.43 (CH_2Cl_2/MeOH 9:1). ^{1}H-NMR (400 MHz, MeOD): δ 4.00-3.89 (m, 4H), 2.50 (d, *J* = 6.5 Hz, 1H), 1.90-1.68 (m, 4H), 1.68-1.58 (m, 1H), 1.58-1.46 (m, 2H), 1.46-1.27 (m, 1H), 1.27-1.19 (m, 1H). ^{13}C-NMR (101 MHz, MeOD) δ 110.28, 65.26 (2C), 48.41, 40.60, 35.37 (2C), 28.97 (2C). NMR data matches literature reference.[24] HRMS (ESI-MS): calcd. for $C_9H_{18}NO_2^+$: 172.1259; found: 172.1332. MF: $C_9H_{17}NO_2$. MW: 171.24.

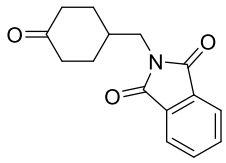

2-((4-Oxocyclohexyl)methyl)isoindoline-1,3-dione (5.99)[25] was prepared from **5.98** (4.00 g, 23.4 mmol, 1 equiv) and phthalanhydride (3.46 g, 23.4 mmol, 1 equiv). Both components were placed in a 20 mL microwave vial. The vial was sealed and heated (behind a safety shield) in an oil bath at 135 °C for 30 min while stirring. The vial was then allowed to cool to rt and cautiously opened, and 1 M HCl (aq, 9 mL) was added. The flask was resealed and heated (behind the safety shield) in an oil bath at 135 °C for 2 h with vigorous stirring. After this period, it was allowed to cool to rt and cautiously opened, and CH_2Cl_2 (100 mL) was added in portions. The organic layer was collected, washed with 100 mL 1 M HCl, dried over Na_2SO_4, and then concentrated in vacuum to afford the ketone as an off-white solid (1.91 g, 32%), which was used for the next reaction without further purification. R_f = 0.37 (PE/EtOAc 2:1). ^{1}H-NMR (300 MHz, $CDCl_3$): δ 7.85-7.63 (m, 4H), 3.61 (d, *J* = 7.2 Hz, 2H), 2.41-2.08 (m,

5H), 2.05-1.90 (m, 2H), 1.56-1.36 (m, 2H). ^{13}C-NMR (75 MHz, $CDCl_3$): δ 210.98, 168.52 (2C), 134.16 (2C), 131.89 (2C), 123.37 (2C), 42.42, 40.11 (2C), 35.44, 30.22 (2C). NMR data matches literature reference.[25] HRMS (ESI-MS): calcd. for $C_{15}H_{16}NO_3^+$: 258.1052; found: 258.1131. MF: $C_{15}H_{15}NO_3$. MW: 257.29.

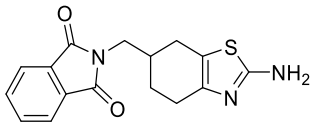

(±)-2-((2-Amino-4,5,6,7-tetrahydrobenzo[*d*]thiazol-6-yl)methyl)isoindoline-1,3-dione (5.101). A freshly prepared solution of Br_2 (1.24 g, 7.74 mmol, 1 equiv) in CH_2Cl_2 (20 mL) was added dropwise over a period of 1 h, to a stirred solution of **5.99** (1.99 g, 7.74 mmol, 1 equiv) in CH_2Cl_2 (38 mL). After the addition was complete, the reaction mixture was refluxed for 1 h. The solvent was removed in vacuum to obtain the bromo ketone **5.100** (2.58 g, 99%) as a brown foam, which was used without further purification. HRMS (ESI-MS): calcd. for $C_{15}H_{14}BrNNaO_3^+$: 358.0049; found: 358.0048. MF: $C_{15}H_{14}BrNO_3$. MW: 336.19. The crude bromo ketone **100** (2.58 g, 7.67 mmol) was dissolved in abs. EtOH (40 mL). To this solution, thiourea (759 mg, 10.0 mmol, 1.3 equiv) was added and the mixture was heated under reflux for 2 h. The solvent was removed in vacuum. H_2O (40 mL) was added to the residue, the solution was alkalized with 1 M NaOH to pH 10 and the mixture was extracted with EtOAc (3 x 20 mL), dried over Na_2SO_4, and evaporated in vacuum. The product was purified by column chromatography (isocratic: PE/EtOAc 1:3) to obtain the product as a yellow solid (0.9 g, 37%). R_f = 0.34 (PE/EtOAc 1:4). ^{1}H-NMR (300 MHz, DMSO-d_6): δ 7.92-7.79 (m, 4H), 6.72-6.54 (m, 2H), 3.68-3.49 (m, 2H), 2.64-2.08 (m, 5H, overlapped with DMSO), 1.95-1.76 (m, 1H), 1.43-1.29 (m, 1H). ^{13}C-NMR (75 MHz, DMSO-d_6): δ 168.07 (2C), 165.65, 144.39, 134.36 (2C), 131.56 (2C), 122.94 (2C), 113.08, 42.11, 34.08, 26.50, 26.39, 25.17. HRMS (ESI-MS): calcd. for $C_{16}H_{16}N_3O_2S^+$: 314.0885; found: 314.0976. MF: $C_{16}H_{15}N_3O_2S$. MW: 313.38.

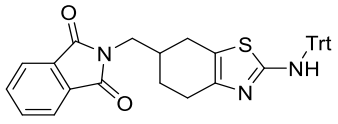

(±)-2-((2-(Tritylamino)-4,5,6,7-tetrahydrobenzo[*d*]thiazol-6-yl)methyl)isoindoline-1,3-dione (5.102). To a solution of **5.101** (0.9 mg, 2.87 mmol, 1 equiv) and NEt_3 (717 µL, 5.17 mmol, 1.8 equiv) in MeCN (16 mL) a solution of Trt-Cl (0.96 g, 3.45 mmol, 1.2 equiv) in MeCN (10 mL) was added dropwise. After stirring the mixture at rt for 16 h, the solvent was

removed in vacuum. The crude product was purified by column chromatography (isocratic: PE/EtOAc 2:1) yielding a yellow and foamlike solid (0.79 mg, 50%). $R_f = 0.72$ (PE/EtOAc 1:4). ^{1}H-NMR (300 MHz, $CDCl_3$) δ 7.90-7.62 (m, 4H), 7.39-7.16 (m, 15H), 6.54 (s, 1H), 3.76-3.55 (m, 2H), 2.71-2.09 (m, 5H), 1.95-1.83 (m, 1H), 1.39-1.63 (m, 1H). ^{13}C-NMR (75 MHz, $CDCl_3$): δ 168.61 (2C), 166.12, 143.88 (3C), 143.84, 134.11 (2C), 132.02 (2C), 129.35 (6C), 128.19 (6C), 127.46 (3C), 123.39 (2C), 116.78, 71.59, 43.04, 34.87, 27.26, 27.18, 25.58. HRMS (ESI-MS): calcd. for $C_{35}H_{30}N_3O_2S^+$: 556.1980; found: 556.2067. MF: $C_{35}H_{29}N_3O_2S$. MW: 555.70.

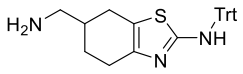

(±)-6-(Aminomethyl)-*N*-trityl-4,5,6,7-tetrahydrobenzo[*d*]thiazol-2-amine (5.17). A mixture of **5.102** (1.14 mg, 2.05 mmol, 1 equiv) and N_2H_4 x H_2O (470 µL, 10.3 mmol, 5 equiv) in EtOH (15 mL) was stirred at rt for 16 h. After removal of insoluble material by filtration, the filtrate was evaporated in vacuum yielding a colorless and sticky oil (870 mg, 100%), which was used in the next step without further purification. $R_f = 0.01$ (PE/EtOAc 2:1). ^{1}H-NMR (300 MHz, MeOD): δ 7.35-7.04 (m, 15H), 2.75-2.34 (m, 6H), 2.11-1.68 (m, 2H), 1.42-1.17 (m, 1H). ^{13}C-NMR (75 MHz, MeOD): δ 152.97, 145.31 (3C), 144.55, 130.47 (6C), 129.12 (6C), 128.47 (3C), 118.05, 73.01, 46.85, 37.69, 27.87, 27.62, 26.37. HRMS (ESI-MS): calcd. for $C_{27}H_{28}N_3S^+$: 426.1926; found: 426.2006. MF: $C_{27}H_{27}N_3S$. MW: 425.59.

App4.2 Experimental Details for the Acylhydrazides 5.108 and 5.109

The 1,3,4-oxadiazole derivatives **5.37** and **5.58** were synthesized from carboxybenzyl (Cbz)-protected GABA **5.103** (Scheme App4.8 or Scheme 5.2 in the chapter 5). The carboxyl group of **5.103** was activated using 1-ethyl-3-(3-dimethylaminopropyl)carbodiimide hydrochloride (EDC x HCl) and subsequently coupled with *tert*-butyl carbazate (compd. **5.104**). The Cbz group was removed using hydrogen and Pd/C. The exposed primary amine **5.105** was reacted with the guanidinylating reagents **5.19** or **5.26** in the presence of $HgCl_2$ and NEt_3 giving the N^G-carbamoylguanidines **5.106** or **5.107**. These were treated with TFA to remove the Boc-protecting group (compd. **5.108** and **5.109**). The formation of the heterocycle (compd. **5.37** and **5.58**) was performed using cyanogen bromide and $KHCO_3$ in a H_2O/EtOH mixture (for details see the Experimental Section in the chapter 5).

Scheme App4.8: Synthesis of 1,3,4-Oxadiazole Derivatives 5.37 and 5.58[a]

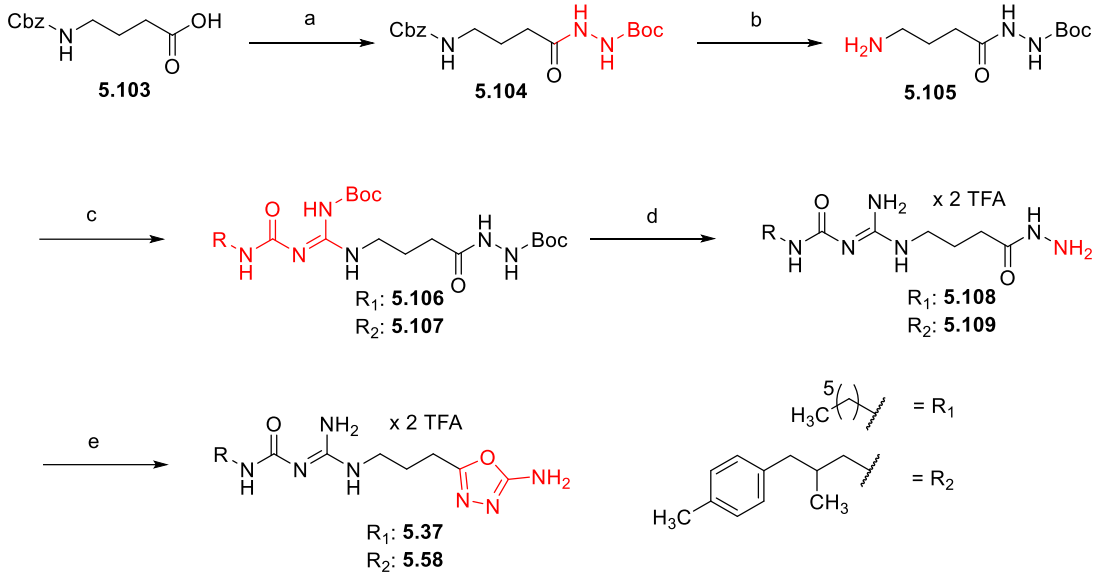

[a]Reagents and conditions: (a) *tert*-butyl carbazate, EDC x HCl, DIPEA, CH_2Cl_2, rt, 24 h, 20%; (b) Pd/C, H_2 (10 bar), THF/MeOH, rt, 4 h, 100%; (c) **5.19** or **5.26**, $HgCl_2$, NEt_3, CH_2Cl_2, rt, overnight, **5.106**: 46% and **5.107**: 89%; (d) TFA, CH_2Cl_2, rt, 4-6 h, **5.108**: 94% and **5.109**: 17%; (e) BrCN, $KHCO_3$, H_2O/EtOH, 60 °C, 2 h, **5.37**: 6.1% and **5.58**: 61%. Experimental details for **5.37** and **5.58** are shown in the chapter 5.

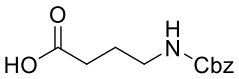

4-(((Benzyloxy)carbonyl)amino)butanoic acid (5.103).[26,27,28] GABA (**5.74**, 0.77 g, 7.5 mmol, 1 equiv) was dissolved in H_2O (6 mL), and $NaHCO_3$ (0.69 g, 8.2 mmol, 1.1 equiv) was added. A solution of benzyl chloroformate (1.0 mL, 7.1 mmol, 0.95 equiv) in 1,4-dioxane (6 mL) was added dropwise at 0 °C. The stirring was continued for 18 h at rt. 1,4-Dioxane was removed in vacuum. The residue was extracted with diethyl ether (3 x 50 mL). The combined organic layers were washed with 1 M NaOH (3 x 50 mL). The aqueous layer was acidified with 37% HCl (pH = 2) and extracted with diethyl ether (3 x 50 mL). The organic phase was dried over Na_2SO_4, filtered, and the solvent was evaporated in vacuum to obtain 0.95 g (53%) of the product as a colorless oil, which solidified upon storage. R_f = 0.33 (PE/EtOAc 1:1). ^{1}H-NMR (400 MHz, $CDCl_3$) δ 10.18 (s, 1H), 7.40-7.27 (m, 5H), 5.09 (s, 2H), 5.05-4.93 (m, 1H), 3.31-3.12 (m, 2H), 2.39 (t, J = 7.3 Hz, 2H), 1.83 (quint, J = 7.1 Hz, 2H). ^{13}C-NMR (101 MHz, $CDCl_3$) δ 178.48, 156.62, 136.43, 128.54 (2C), 128.16 (2C), 128.13, 66.82, 40.27, 31.15, 24.95. NMR data matches literature reference.[28] HRMS (ESI-MS): calcd. for $C_{12}H_{16}NO_4^+$: 238.1074; found: 238.1080. MF: $C_{12}H_{15}NO_4$. MW: 237.26.

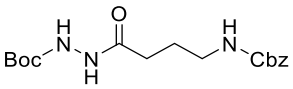

***tert*-Butyl 2-(4-(((benzyloxy)carbonyl)amino)butanoyl)hydrazine-1-carboxylate (5.104).**[29] To a stirred solution of **5.103** (0.64 g, 4.94 mmol, 1 equiv) in dry CH_2Cl_2 (15 mL) DIPEA (3.65 mL, 20.9 mmol, 3.6 equiv) and EDC x HCl (1.11 g, 5.82 mmol, 1.2 equiv) were added, and the mixture was stirred for 30 min at rt. *tert*-Butyl carbazate (1.12 g, 8.47 mmol, 1.75 equiv) was added, and the reaction mixture was stirred for 24 h at rt. The solution was diluted with CH_2Cl_2 (100 mL) and washed with 5% aqueous HCl (2 x 50 mL), saturated $NaHCO_3$ (50 mL), and brine (50 mL). The organic phase was dried over Na_2SO_4, filtered, and concentrated in vacuum. The crude product was purified by flash chromatography on silica gel (gradient: 0-30 min: CH_2Cl_2/MeOH 100:0-90:10, 40 min: 80:20, 50 min: 80:20, SF 8 g) to obtain the product as a colorless oil (340 mg, 20%). $R_f = 0.57$ (CH_2Cl_2/MeOH 9:1). ^{1}H-NMR (400 MHz, $CDCl_3$) δ 7.38-7.26 (m, 5H), 5.06 (s, 2H), 3.30-3.11 (m, 2H), 2.28-2.19 (m, 2H), 1.82 (quint, $J = 6.6$ Hz, 2H), 1.42 (s, 9H), 3 NH signals are missing. ^{13}C-NMR (101 MHz, $CDCl_3$) δ 176.15, 172.76 (2C), 157.13, 136.64, 128.61 (2C), 128.20 (2C), 81.68, 66.80, 40.11, 31.12, 28.26 (3C), 26.01. NMR data matches literature reference.[29] HRMS (ESI-MS): calcd. for $C_{17}H_{26}N_3O_5^+$: 352.1867; found: 352.1869. MF: $C_{17}H_{25}N_3O_5$. MW: 351.40.

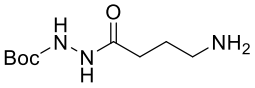

***tert*-Butyl 2-(4-aminobutanoyl)hydrazine-1-carboxylate (5.105)**. The Cbz-protected amine **5.104** (130 mg, 0.34 mmol) was dissolved in a mixture of THF/MeOH (1:1 (v/v), 10 mL) and Pd/C (10 wt%, 50 mg) was added. The mixture was placed in a Parr bomb. The Parr bomb was filled with H_2 gas (10 bar) and the mixture was stirred at rt for 4 h. The reaction mixture was transferred in a Falkon tube (50 mL) and centrifuged (4000 x *g*, 5 min). The supernatant was decanted. The pellet was resuspended in fresh THF/MeOH 1:1 mixture and centrifuged a second time (4000 x *g*, 5 min). The supernatant was decanted. The combined supernatants were concentrated in vacuum yielding the crude product as a yellow foam (74 mg, 100%). The crude product was used in the next step without further purification. $R_f = 0.01$ (CH_2Cl_2/MeOH 9:1). ^{1}H-NMR (300 MHz, $CDCl_3$) δ 5.53 (s, 4H), 2.75-2.64 (m, 2H), 2.24 (t, $J = 7.2$ Hz, 2H), 1.83-1.65 (m, 2H), 1.46-1.28 (m, 9H). ^{13}C-NMR (75 MHz, $CDCl_3$) δ 172.81, 155.79, 80.94, 40.61, 31.15, 28.26, 28.04 (3C). HRMS (ESI-MS): calcd. for $C_9H_{20}N_3O_3^+$: 218.1499; found: 218.1499. MF: $C_9H_{19}N_3O_5$. MW: 217.27.

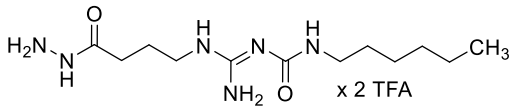

1-(Amino{[4-(hydrazineyl-4-oxo)butyl]amino}methylene)-3-(hexyl)urea dihydrotrifluoroacetate (5.108). The guanidinylating reagent **5.19** (117 mg, 0.37 mmol, 1 equiv) and the amine **5.105** (80 mg, 0.37 mmol, 1 equiv) were dissolved in CH_2Cl_2 (10 mL). NEt_3 (128 µL, 0.92 mmol, 2.5 equiv) and $HgCl_2$ (200 mg, 0.74 mmol, 2 equiv) were added to the mixture. The mixture was stirred at rt overnight. The reaction mixture was diluted with CH_2Cl_2 (10 mL). The precipitate was removed by filtration through Celite 545 and washed with CH_2Cl_2 (20 mL) and EtOAc (20 mL). The filtrate was concentrated in vacuum and the crude product was purified by column chromatography on silica gel (gradient: 0-20 min: CH_2Cl_2/MeOH 100:0-90:10, 30 min: 90:10, SF 8 g) to obtain **5.106** as a yellow oil (82 mg, 46%). R_f = 0.64 (CH_2Cl_2/MeOH 9:1). ^{1}H-NMR (300 MHz, $CDCl_3$) δ 12.26 (s, 1H), 8.56 (s, 1H), 6.19 (s, 1H), 3.52 (q, *J* = 6.4 Hz, 2H), 3.24-3.08 (m, 2H), 2.45-2.25 (m, 2H), 2.01-1.78 (m, 2H), 1.57-1.38 (m, 20H), 1.35-1.19 (m, 6H), 0.93-0.78 (m, 3H), 2 NH signals are missing. HRMS (ESI-MS): calcd. for $C_{22}H_{43}N_6O_6^+$: 487.3239; found: 487.3296. MF: $C_{22}H_{42}N_6O_6$. MW: 486.61. To a stirred solution of Boc-protected hydrazine derivative **5.106** (82 mg, 0.17 mmol) in CH_2Cl_2 (4 mL) TFA (1 mL) was added. The solution was stirred for 4 h at rt. The solvent was removed in vacuum to obtain the crude product (**5.108**) as a yellowish oil (82 mg, 94%). The crude product was used in the next step without further purification. R_f = 0.56 (CH_2Cl_2/MeOH 9:1). ^{1}H-NMR (400 MHz, MeOD) δ 3.43-3.32 (m, 1H), 3.19 (t, *J* = 7.1 Hz, 2H), 2.47-2.35 (m, 2H), 1.97 (quint, *J* = 7.2 Hz, 2H), 1.58-1.45 (m, 3H), 1.41-1.22 (m, 6H), 0.97-0.84 (m, 3H). ^{13}C-NMR (101 MHz, MeOD) δ 173.57, 156.00, 155.45, 41.45, 40.79, 32.59, 30.40, 29.57, 27.50, 24.53, 23.59, 14.32. HRMS (ESI-MS): calcd. for $C_{12}H_{27}N_6O_2^+$: 287.2190; found: 287.2189. MF: $C_{12}H_{26}N_6O_2$ x $C_4H_2F_6O_4$. MW: (286.38+228.05).

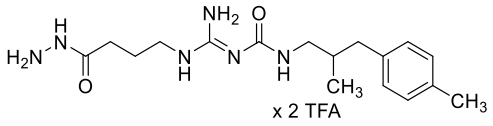

1-(Amino{[4-(hydrazineyl-4-oxo)butyl]amino}methylene)-3-(2-methyl-3-(p-tolyl)propyl)urea dihydrotrifluoroacetate (5.109) The guanidinylating reagent **5.26** (100 mg, 0.26 mmol, 1 equiv) and the amine **5.105** (58 mg, 0.27 mmol, 1.01 equiv) were dissolved in CH_2Cl_2 (5 mL). NEt_3 (84 µL, 0.66 mmol, 2.5 equiv) and $HgCl_2$ (143 mg, 0.53 mmol, 2 equiv) were added to the mixture. The mixture was stirred at rt overnight. The reaction mixture was diluted with CH_2Cl_2 (10 mL). The precipitate was removed by filtration through Celite 545 and

washed with CH_2Cl_2 (20 mL) and EtOAc (20 mL). The filtrate was concentrated in vacuum and the crude product was purified by column chromatography on silica gel (gradient: 0-40 min: CH_2Cl_2/MeOH 100:0-80:20; SF 8 g) to obtain **5.107** as a yellow oil (127 mg, 89%). R_f = 0.68 (CH_2Cl_2/MeOH 9:1). ^{1}H-NMR (400 MHz, $CDCl_3$) δ 7.10-6.94 (m 4H), 3.46-3.38 (m, 2H), 3.15-2.93 (m, 2H), 2.70-2.58 (m, 1H), 2.33-2.20 (m, 6H), 1.89-1.81 (m, 3H), 1.40 (s, 18H), 0.80 (d, *J* = 6.7 Hz, 3H). MF: $C_{27}H_{44}N_6O_6$. MW: 548.69. To a stirred solution of Boc-protected hydrazine derivative **5.107** (127 mg, 0.23 mmol) in CH_2Cl_2 (3.5 mL) TFA (1.5 mL) was added. The solution was stirred for 6 h at rt. The solvent was removed in vacuum to obtain the crude product as a yellow oil. The crude product was purified using preparative HPLC yielding **5.109** as a white solid (22 mg, 17%). R_f = 0.54 (CH_2Cl_2/MeOH 9:1). ^{1}H-NMR (400 MHz, MeOD) δ 7.11-7.00 (m, 4H), 3.35 (t, *J* = 7.0 Hz, 2H), 3.22-2.98 (m, 2H), 2.68-2.59 (m, 1H), 2.44-2.33 (m, 3H), 2.29 (s, 3H), 1.96 (quint, *J* = 7.1 Hz, 3H), 0.87 (d, *J* = 6.7 Hz, 3H). ^{13}C-NMR (101 MHz, MeOD) δ 173.48, 155.56, 155.43, 138.44, 136.52, 130.00 (2C), 129.92 (2C), 46.48, 41.59, 41.37, 36.64, 30.83, 24.77, 21.08, 17.71. HRMS (ESI-MS): calcd. for $C_{17}H_{29}N_6O_2^+$: 349.2347; found: 349.2354. MF: $C_{17}H_{28}N_6O_2$ x $C_4H_2F_6O_4$. MW: (348.45+228.05).

App4.3 Determination of the pK_a Value

The determination of the negative logarithm of the acid dissociation constant (pK_a) value was performed as described by Biselli et al.[6] 2-Amino-5-methyl-1,3,4-thiadiazole hydrochloride (9.6 mg, 10.0 mg, or 10.1 mg) was dissolved in Millipore water (20 mL) and titrated with 0.01 M NaOH solution. The titration was performed using a freshly calibrated glass electrode (BlueLine, Schott Instruments, Mainz, Germany; calibration solutions: pH 4,0, 7,0, 9,0 ± 0.02, Roth, Fisher), a potentiometer (Lab 850, Schott Instruments) and a burette (10 mL). The pH-value was recorded after each addition (0.05-0.10 mL) at room temperature. The pK_a value was determined using the half-equivalence point method (Figure App4.1) and was 3.49 ± 0.01 (mean ± SE, N = 3; reference: 3.56[30]).

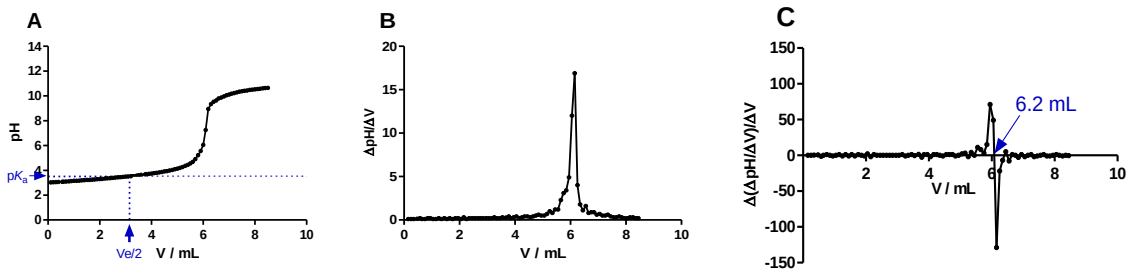

Figure App4.1. **A**: Representative titration curve of 2-amino-5-methyl-1,3,4-thiadiazole hydrochloride with 0.01 M NaOH. **B**: The first derivative, ΔpH/ΔV, of the titration curve. **C**: The second derivative, Δ(ΔpH/ΔV)/ΔV, which is the derivative of the first derivative. End point is taken as *zero crossing* of the second derivative. Ve: volume of titrant at equivalence point.

App4.4 Bias Analysis

To test for biased agonism, we calculated the bias factors (BF). To calculate the BF's we either used efficacy BF (eBF) or potency BF (pBF).[31] Using this method, a biased agonist is defined as an agonist that has a statistically-significant different BF compared to the BF of the endogenous agonist histamine (**5.1**). The eBF for an agonist is calculated as the ratio between maximal responses (E_{max}) of two different signaling pathways ($pathway_1$:$pathway_2$).[31] The pBF of an agonist is calculated as the ratio between EC_{50} of two different signaling pathways ($pathway_1$:$pathway_2$).[31] However, for analysis of statistic difference between pBF of histamine and pBF of the agonist of interest we used the negative logarithm of the pBF or: $ppBF(pathway_1:pathway_2) = pEC_{50}(pathway_1) - pEC_{50}(pathway_2)$.[31] This is necessary since statistic information of SEM is only available for pEC_{50} and not for EC_{50}.

Most compounds (eBFs: 1.29-7.30) possessed significantly higher efficacy bias factors than histamine (**5.1**, eBF: 1.00), which was used as an unbiased reference compound. Only in case of UR-SB291[6, 32] this efficacy bias was not significant (cf. Table App4.1 and Figure App4.2A). Among the propyl spacer containing 2-aminothiazoles, the efficacy bias was most striking for UR-SB527[6, 32] (eBF: 7.30 ± 0.76; 2-methyl-3-(p-tolyl)propyl side residue, Table App4.1), which was a strong partial agonist in the mini-G protein recruitment assay (E_{max} = 0.73, cf. Table 5.3, Chapter 5), but showed only a very weak partial agonistic activity (E_{max} = 0.10, cf. Table 5.3, Chapter 5) in the β-arrestin2 recruitment assay. We also observed that the efficacy bias for 2-amino-4-methylthiazoles (UR-KAT523 (**5.6**)[6], UR-CH22[6, 32] and UR-SB257[6, 32]) was more pronounced than for the corresponding 2-aminothiazoles (**5.32**, **5.48** and **5.39**, cf. Table App4.1).

By contrast, all 2-aminothiadiazoles exhibited no (**5.31**, **5.39**, **5.43**, **5.47**, **5.53** & **5.56**) or a less pronounced (**5.57** & **5.63**, eBF: 1.72-2.21) efficacy bias for G-protein activation. Among the 2-aminothiadiazoles, the efficacy bias was most striking for **5.63** (eBF: 2.21 ± 0.24; 2-methyl-5-phenylpentyl side residue). We observed that the efficacy bias was greatest within a series of compounds with the same heterocycle if bulky side residues (e.g. 2-methyl-3-(p-tolyl)propyl- or 2-methyl-5-phenylpentyl-side residues) were used (cf. Table App4.1 and Figure App4.2A).

Table App4.1. Efficacy Bias Factors (eBF) and Negative Logarithm of the Potency Bias Factors (ppBF)

compd.	eBF (mGs:β-arrestin2) ± SEM	ppBF (mGs:β-arrestin2) ± SEM
5.1	1.00 ± 0.00	1.52 ± 0.06
5.5[8]	2.97 ± 040	0.82 ± 0.14
5.6[6]	5.50 ± 0.69	1.59 ± 0.13
UR-CH20[6, 32]	3.11 ± 0.33	0.97 ± 0.04
UR-SB291[6, 32]	2.10 ± 0.32	0.87 ± 0.14
UR-CH22[6, 32]	2.70 ± 0.25	1.14 ± 0.09
UR-Po563[6]	2.59 ± 0.09	0.70 ± 0.11
UR-MB-69[6]	2.97 ± 0.10	0.88 ± 0.11
UR-SB257[6, 32]	7.30 ± 0.76	0.53 ± 0.12
UR-KAT527[6]	5.85 ± 0.95	1.68 ± 0.14
5.31	0.99 ± 0.06	1.61 ± 0.23
5.32	1.39 ± 0.09	0.97 ± 0.06
5.36	0.82 ± 0.04	2.25 ± 0.07
5.37	1.52 ± 0.06	1.22 ± 0.06
5.39	1.07 ± 0.06	1.73 ± 0.15
5.43	0.98 ± 0.05	1.10 ± 0.09
5.47	0.98 ± 0.06	1.62 ± 0.15
5.48	1.29 ± 0.07	1.00 ± 0.15
5.52	1.29 ± 0.11	1.00 ± 0.04
5.53	1.05 ± 0.03	1.15 ± 0.10
5.54	2.43 ± 0.14	1.10 ± 0.11
5.56	0.91 ± 0.03	0.97 ± 0.06
5.57	1.72 ± 0.13	0.32 ± 0.19
5.59	5.19 ± 0.33	0.48 ± 0.09
5.63	2.21 ± 0.24	1.08 ± 0.19
5.69	1.15 ± 0.08	1.31 ± 0.14
5.70	1.16 ± 0.10	1.40 ± 0.00

eBF's comparing efficacy and ppBF's comparing potency in Gs and β-arrestin2 signaling pathways. The eBF for an agonist is calculated as the ratio between maximal responses (E_{max}) of Gs pathway and β-arrestin2 pathway [eBF = E_{max} (mGs) - pEC_{50} (β-arrestin2)]. The ppBF of an agonist is calculated as the difference between pEC_{50} values between Gs pathway and β-arrestin2 pathway [ppBF = pEC_{50} (mGs) - pEC_{50} (β-arrestin2)]. The E_{max} and pEC_{50} values used for these calculations are depicted in the Table 5.3 in the chapter 5.

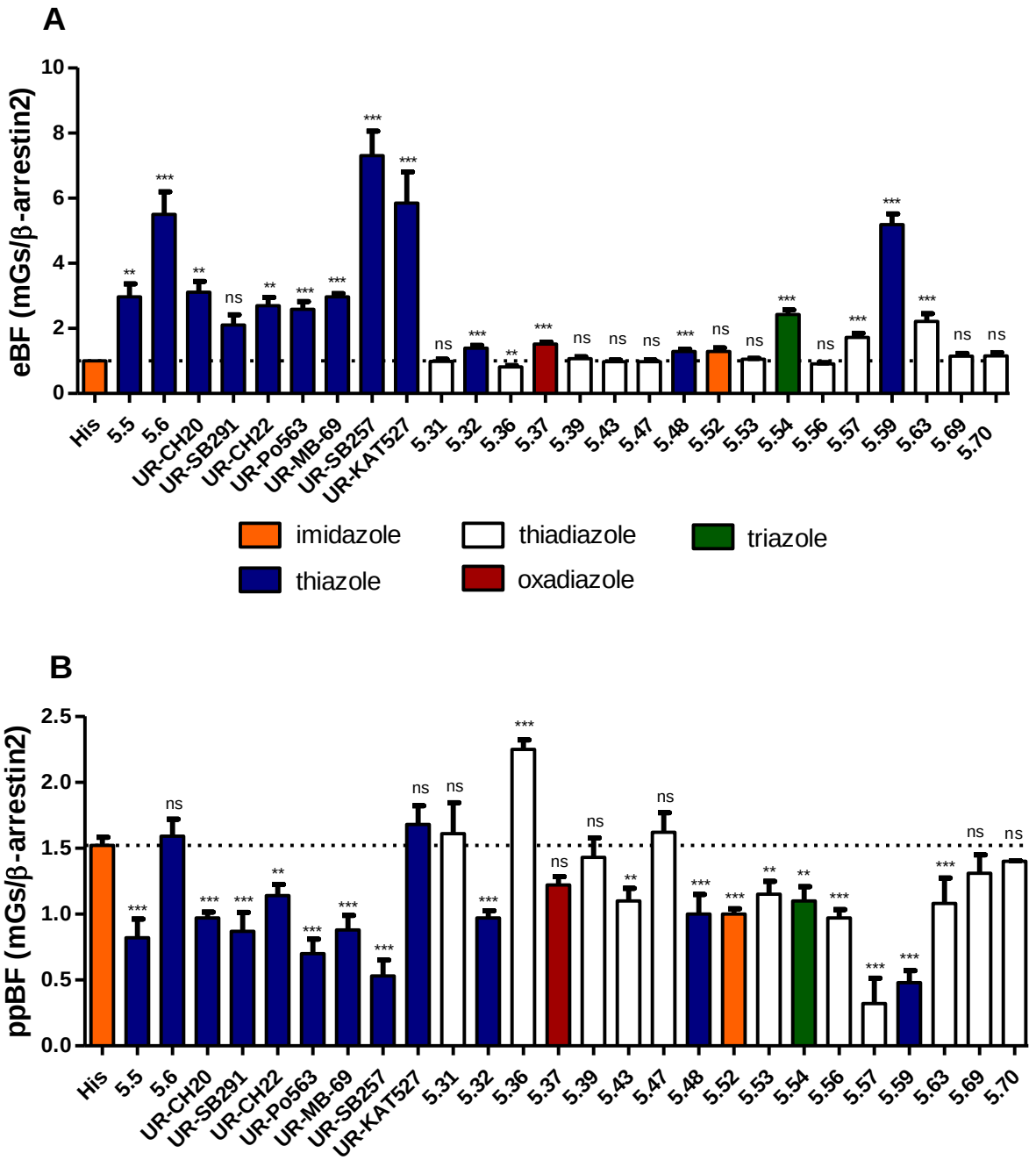

Figure App4.2. Histograms comparing the efficacy bias factors (eBF, **A**) and the negative logarithm of the potency bias factors (ppBF, **B**). Statistical comparison of values was performed by using a one-way ANOVA of BF for each agonist and Dunnett's post-tests were used to compare BF for histamine (His) to BF's for all other agonists (ns: not significant, ***p <0.001, **p<0.01, *p <0.05, as described by Thomsen et al.[31]).

The functional data of the H_2R agonists from either the mini-G protein or β-arrestin2 recruitment assay were also fitted to the operational model as described by van der Westhuizen et al.[33] As a result, we obtained transduction coefficients ($\log(\tau/K_A)$, Table App4.2), a parameter sufficient to describe agonism for a given pathway. The transduction coefficients for the tested compounds were normalized to $\log(\tau/K_A)$ of the endogenous ligand, thereby cancelling out potential systematic bias generated by the difference in the cellular background and/or signal amplification of the chosen readout systems.[33-34] The comparison of the normalized transduction coefficients of a ligand for different signaling pathways then allow for quantification of the ligand bias.[33] An unbiased response of given ligand for the two investigated pathways would result in a bias factor $\Delta\Delta\log(\tau/K_A)$ around 0, while positive or negative values indicate a bias either for the G-protein (mGs) or β-arrestin2 pathway. Data were analyzed in a pairwise manner using a two-tailed unpaired student's t-test (on the $\Delta\Delta\log(\tau/K_A)$ ratios) to determine the significance of the ligand biases.[33]

According to the present bias analysis some of the tested ligands possess a significant preference for the G protein (mGs) and some others a preference for the β-arrestin2 pathway (Figure App4.3). Unfortunately, we did not find a clear trend which could be unambiguously assigned to a specific structure-pathway bias.

Table App4.2. Transduction Coefficients (log(τ/K_A)), Ratios Towards the mGs and β-Arrestin2 Pathways in HEK293T Cells and Bias Factors ΔΔlog(τ/K_A)

compd.	log(τ/K_A)[a] β-arr.2	Δlog(τ/K_A)[b] β-arr.2	log(τ/K_A)[a] mGs	Δlog(τ/K_A)[b] mGs	ΔΔlog(τ/K_A)[c]
5.1	5.52 ± 0.04	0.00 ± 0.06	6.95 ± 0.05	0.00 ± 0.07	0.00 ± 0.09
5.5[8]	6.10 ± 0.22	0.59 ± 0.22	7.55 ± 0.01	0.60 ± 0.04	0.01 ± 0.22
5.6[6]	6.00 ± 0.04	0.49 ± 0.06	8.25 ± 0.04	1.31 ± 0.06	0.82 ± 0.08
UR-CH22[6, 32]	6.35 ± 0.17	0.83 ± 0.17	8.07 ± 0.02	1.13 ± 0.05	0.30 ± 0.18
UR-CH20[6, 32]	6.57 ± 0.11	1.05 ± 0.12	7.99 ± 0.04	1.04 ± 0.06	-0.01 ± 0.14
UR-SB257[6, 32]	5.86 ± 0.06	0.34 ± 0.07	7.32 ± 0.03	0.37 ± 0.05	0.04 ± 0.09
UR-KAT527[6]	4.41 ± 0.12	-1.11 ± 0.13	7.18 ± 0.08	0.24 ± 0.09	1.34 ± 0.16
UR-SB291[6, 32]	6.10 ± 0.14	0.58 ± 0.15	7.47 ± 0.07	0.52 ± 0.08	-0.06 ± 0.17
UR-MB-69[6]	6.66 ± 0.09	1.14 ± 0.10	8.01 ± 0.01	1.07 ± 0.04	-0.07 ± 0.11
UR-Po563[6]	6.83 ± 0.07	1.31 ± 0.08	7.98 ± 0.02	1.03 ± 0.05	-0.29 ± 0.09
5.31	6.73 ± 0.07	1.21 ± 0.08	7.96 ± 0.14	1.01 ± 0.14	-0.20 ± 0.16
5.32	7.01 ± 0.04	1.57 ± 0.06	8.15 ± 0.04	1.21 ± 0.06	-0.36 ± 0.08
5.36	6.15 ± 0.03	0.63 ± 0.05	8.20 ± 0.06	1.25 ± 0.07	0.62 ± 0.09
5.37	5.51 ± 0.04	-0.01 ± 0.06	6.90 ± 0.06	-0.05 ± 0.08	-0.04 ± 0.10
5.39	6.44 ± 0.12	0.92 ± 0.13	8.10 ± 0.04	1.16 ± 0.06	0.23 ± 0.14
5.43	6.78 ± 0.07	1.26 ± 0.08	7.91 ± 0.05	0.96 ± 0.06	-0.30 ± 0.10
5.47	6.86 ± 0.10	1.34 ± 0.11	8.44 ± 0.07	1.49 ± 0.08	0.15 ± 0.14
5.48	7.17 ± 0.05	1.65 ± 0.06	8.12 ± 0.03	1.17 ± 0.05	-0.48 ± 0.04
5.52	7.06 ± 0.04	1.54 ± 0.06	8.12 ± 0.01	1.18 ± 0.04	-0.36 ± 0.07
5.53	6.59 ± 0.03	1.08 ± 0.05	7.63 ± 0.05	0.69 ± 0.07	-0.39 ± 0.08
5.54	6.10 ± 0.11	0.58 ± 0.11	7.55 ± 0.03	0.60 ± 0.05	0.02 ± 0.12
5.56	7.17 ± 0.05	1.65 ± 0.06	8.06 ± 0.04	1.12 ± 0.06	-0.53 ± 0.09
5.57	6.59 ± 0.17	1.07 ± 0.17	7.15 ± 0.08	0.20 ± 0.09	-0.87 ± 0.20
5.59	5.87 ± 0.11	0.35 ± 0.12	7.11 ± 0.07	0.17 ± 0.08	-0.19 ± 014
5.63	5.74 ± 0.20	0.22 ± 0.21	7.50 ± 0.08	0.56 ± 0.09	0.34 ± 0.23
5.69	6.16 ± 0.03	0.64 ± 0.05	7.65 ± 0.12	0.70 ± 0.13	0.06 ± 0.14
5.70	6.27 ± 0.12	0.75 ± 0.13	8.05 ± 0.04	1.11 ± 0.06	0.35 ± 0.14

[a]The transduction coefficients (log(τ/K_A)) were derived from functional data of 3-6 independent experiments fitted to the operational model of agonism as described by van der Westhuizen et al.[33] [b]Δlog(τ/K_A) (mGs or β-arrestin2) = log(τ/K_A) (ligand) - log(τ/K_A) (histamine). [c]ΔΔlog(τ/K_A) = Δlog(τ/K_A) (mGs) - Δlog(τ/K_A) (β-arrestin2). Data are given as means ± SEM[a,b] or SE[c] (calculated as described by van der Westhuizen et al.[33]).

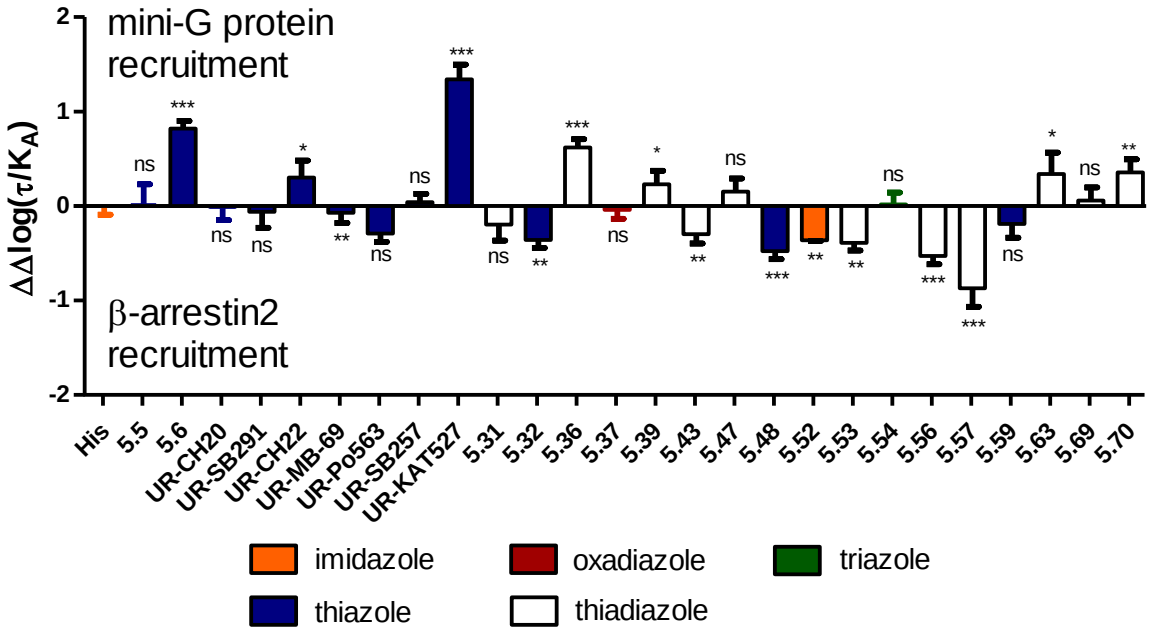

Figure App4.3. Bias analysis for histamine (His), **5.5**[8], **5.6**[6], UR-CH20[6, 32], UR-SB291[6, 32], UR-CH22[6, 32], UR-MB-69[6], UR-Po563[6], UR-SB257[6, 32], UR-KAT527[6], **5.31**-**5.32**, **5.36**-**5.37**, **5.39**, **5.43**, **5.47**-**5.48**, **5.52**-**5.54**, **5.56**-**5.57**, **5.59**, **5.63** and **5.69**-**5.79** performed as described by van der Westhuizen at al.[33], using histamine as reference agonist. A $\Delta\Delta\log(\tau/K_A)$ ratio = 0 indicate an equal activation of the G protein- and β-arrestin2 pathways, while a $\Delta\Delta\log(\tau/K_A)$ ratio ≠ 0 indicates a preference for one signal pathway over the other. Data represent mean ± SEM of 3-6 independent experiments performed in duplicates or triplicates. Data were analyzed in a pairwise manner using a two-tailed unpaired student's t-test to determine the significance of the ligand biases (ns: not significant, ***p <0.001; **p <0.01,*p <0.05, as described by van der Westhuizen et al.[33]).

App4.5 References

1. Ghorai, P.; Kraus, A.; Keller, M.; Götte, C.; Igel, P.; Schneider, E.; Schnell, D.; Bernhardt, G.; Dove, S.; Zabel, M.; Elz, S.; Seifert, R.; Buschauer, A., Acylguanidines as bioisosteres of guanidines: N^G-acylated imidazolylpropylguanidines, a new class of histamine H_2 receptor agonists. *J. Med. Chem.* **2008,** *51*, 7193-7204.
2. Bastos, C., M.; Munoz, B.; Tait, B. Compounds, Compositions, and Methods for Increasing CFTR Activity. WO 2015/138909, Mar 13, 2015; *Chem. Abstr*. **2015**, *163*, 438650.
3. Kraus, A.; Ghorai, P.; Birnkammer, T.; Schnell, D.; Elz, S.; Seifert, R.; Dove, S.; Bernhardt, G.; Buschauer, A., N^G-Acylated aminothiazolylpropylguanidines as potent and selective histamine H_2 receptor agonists. *ChemMedChem* **2009,** *4*, 232-240.
4. Geyer, R.; Kaske, M.; Baumeister, P.; Buschauer, A., Synthesis and functional characterization of imbutamine analogs as histamine H_3 and H_4 receptor ligands. *Arch. Pharm.* **2014,** *347*, 77-88.

5. Geyer, R.; Igel, P.; Kaske, M.; Elz, S.; Buschauer, A., Synthesis, SAR and selectivity of 2-acyl- and 2-cyano-1-hetarylalkyl-guanidines at the four histamine receptor subtypes: a bioisosteric approach. *MedChemComm* **2014,** *5*, 72-81.
6. Biselli, S.; Bresinsky, M.; Tropmann, K.; Forster, L.; Honisch, C.; Buschauer, A.; Bernhardt, G.; Pockes, S., Pharmacological characterization of a new series of carbamoylguanidines reveals potent agonism at the H_2R and D_3R. *Eur. J. Med. Chem.* **2021,** *214*, 113190.
7. Tropmann, K.; Höring, C.; Plank, N.; Pockes, S., Discovery of a G protein biased radioligand for the histamine H_2 receptor with reversible binding properties. *J. Med. Chem.* **2020,** *63*, 13090-13102.
8. Kagermeier, N.; Werner, K.; Keller, M.; Baumeister, P.; Bernhardt, G.; Seifert, R.; Buschauer, A., Dimeric carbamoylguanidine-type histamine H_2 receptor ligands: a new class of potent and selective agonists. *Bioorg. Med. Chem.* **2015,** *23*, 3957-3969.
9. Supuran, C. T.; Barboiu, M.; Luca, C.; Pop, E.; Brewster, M. E.; Dinculescu, A., Carbonic anhydrase activators. Part 14. Syntheses of mono and bis pyridinium salt derivatives of 2-amino-5-(2-aminoethyl)- and 2-amino-5-(3-aminopropyl)-1,3,4-thiadiazole and their interaction with isozyme II. *Eur. J. Med. Chem.* **1996,** *31*, 597-606.
10. Guénin, E.; Monteil, M.; Bouchemal, N.; Prangé, T.; Lecouvey, M., Syntheses of phosphonic esters of alendronate, pamidronate and neridronate. *Eur. J. Org. Chem.* **2007,** *2007*, 3380-3391.
11. Mizrahi, D. M.; Waner, T.; Segall, Y., α-Amino acid derived bisphosphonates. Synthesis and anti-resorftive activity. *Phosphorus, Sulfur, Silicon Relat. Elem.* **2001,** *173*, 1-25.
12. Barbosa, G. A. D.; de Aguiar, A. P., Synthesis of 1,3,4-thiadiazole derivatives and microbiological cctivities: a review. *Rev. Virtual Quim.* **2019,** *11*, 806-848.
13. Staudinger, H.; Meyer, J., Über neue organische Phosphorverbindungen III. Phosphinmethylenderivate und Phosphinimine. *Helv. Chim. Acta* **1919,** *2*, 635-646.
14. Mitsunobu, O.; Yamada, M., Preparation of esters of carboxylic and phosphoric acid via quaternary phosphonium salts. *J. Org. Chem.* **1967,** *40*, 2380-2382.
15. Pak, J. K.; Hesse, M., Synthesis of penta-*N*-protected homocaldopentamine and its selective acylation. *J. Org. Chem.* **1998,** *63*, 8200-8204.
16. Puodziukynaite, E.; Wang, H.-W.; Lawrence, J.; Wise, A. J.; Russell, T. P.; Barnes, M. D.; Emrick, T., Azulene methacrylate polymers: synthesis, electronic properties, and solar cell fabrication. *J. Am. Chem. Soc.* **2014,** *136*, 11043-11049.
17. Macerata, E.; Mossini, E.; Scaravaggi, S.; Mariani, M.; Mele, A.; Panzeri, W.; Boubals, N.; Berthon, L.; Charbonnel, M.-C.; Sansone, F.; Arduini, A.; Casnati, A., Hydrophilic clicked 2,6-bis-triazolyl-pyridines endowed with high cctinide selectivity and radiochemical stability: toward a closed nuclear fuel cycle. *J. Am. Chem. Soc.* **2016,** *138*, 7232-7235.
18. van Dongen, S. F. M.; Clerx, J.; Nørgaard, K.; Bloemberg, T. G.; Cornelissen, J. J. L. M.; Trakselis, M. A.; Nelson, S. W.; Benkovic, S. J.; Rowan, A. E.; Nolte, R. J. M., A clamp-like biohybrid catalyst for DNA oxidation. *Nat. Chem.* **2013,** *5*, 945-951.
19. Lee, B. W.; Lee, S. D., [5,5] Sigmatropic shift of *N*-phenyl-*N*′-(2-thiazolyl)hydrazines and *N*,*N*′-bis(2-thiazolyl)hydrazines into 2-amino-5-(p-aminophenyl)thiazoles and 5,5′-bis(2-aminothiazole) derivatives. *Tetrahedron Lett.* **2000,** *41*, 3883-3886.
20. Zhang, S.-L.; Yu, Z.-L., C-C activation by retro-aldol reaction of two β-hydroxy carbonyl compounds: synergy with Pd-catalyzed cross-coupling to access mono-α-arylated ketones and esters. *J. Org. Chem.* **2016,** *81*, 57-65.
21. Altman, M. D.; Andresen, B. M.; Arrington, K. L.; Burch, J.; Childers, K. K.; Cote, B.; Di Francesco, M. E.; Donofrio, A.; Dupont-Gaudet, K.; Ellis, J. M.; Fischer, C.; Guay, D.; Guerin, D. J.; Haidle, A. M.; Kattar, S.; Knowles, S. L.; Li, C.; Lim, J.; Machacek, M. R.; Northrup, A. B.; O'Boyle, B. M.; Otte, R. D.; Reutershan, M. H.; Romeo, E.; Schell, A. J.; Siu,

T.; Spencer, K. B.; Taoka, B. M.; Trotter, B. W.; Zhou, H. Aminopyrimidines as Syk Inhibitors WO 2011/075515, Dec 15, 2010; *Chem. Abstr.* **2011**, *155*, 123427, 2010.
22. Sheehan, J. C.; Yang, D.-D. H., The use of *N*-formylamino acids in peptide synthesis. *J. Am. Chem. Soc.* **1958,** *80*, 1154-1158.
23. Kraus, A. Highly Potent, Selective Acylguanidine-Type Histamine H_2 Receptor Agonists: Synthesis and Structure-Activity Relationships. PhD Thesis. University of Regensburg, 2007.
24. Peterlin-Mašič, L.; Jurca, A.; Marinko, P.; Jančar, A.; Kikelj, D., A general synthetic approach to novel conformationally resticted arginine side chain mimetics. *Tetrahedron* **2002,** *58*, 1557-1563.
25. Kelly, T. R.; Lebedev, R. L., Synthesis of some unsymmetrical bridged terpyridines. *J. Org. Chem.* **2002,** *67*, 2197-2205.
26. Hoggard, L. R.; Zhang, Y.; Zhang, M.; Panic, V.; Wisniewski, J. A.; Ji, H., Rational design of selective small-molecule inhibitors for β-catenin/B-cell lymphoma 9 protein-protein interactions. *J. Am. Chem. Soc.* **2015,** *137*, 12249-12260.
27. Cardenal, C.; Vollrath, S. B. L.; Schepers, U.; Bräse, S., Synthesis of functionalized glutamine- and asparagine-type peptoids - scope and limitations. *Helv. Chim. Acta* **2012,** *95*, 2237-2248.
28. Škalamera, Đ.; Blažek Bregović, V.; Antol, I.; Bohne, C.; Basarić, N., Hydroxymethylaniline photocages for carboxylic acids and alcohols. *J. Org. Chem.* **2017,** *82*, 12554-12568.
29. Damalanka, V. C.; Kim, Y.; Alliston, K. R.; Weerawarna, P. M.; Galasiti Kankanamalage, A. C.; Lushington, G. H.; Mehzabeen, N.; Battaile, K. P.; Lovell, S.; Chang, K.-O.; Groutas, W. C., Oxadiazole-based cell permeable macrocyclic transition state inhibitors of norovirus 3CL protease. *J. Med. Chem.* **2016,** *59*, 1899-1913.
30. Al-Attas, A. S.; Habeeb, M. M.; Al-Raimi, D. S., Spectrophotometric determination of some amino heterocyclic donors through charge transfer complex formation with chloranilic acid in acetonitrile. *J. Mol. Liq.* **2009,** *148*, 58-66.
31. Thomsen, A. R. B.; Hvidtfeldt, M.; Bräuner-Osborne, H., Biased agonism of the calcium-sensing receptor. This model is only valid for ligands which are agonists in both pathways. The model can not be applied to ligands which are e.g. agonists in G protein and antagonists in arrestin pathway. *Cell Calcium* **2012,** *51*, 107-116.
32. Biselli, S. Synthesis and Pharmacological Characterization of Subtype-Selective Ligands, Including Radio- and Fluorescence Labeled Ligands, for the Histamine H_2 Receptor. Ph.D. Thesis. University of Regensburg, 2020.
33. van der Westhuizen, E. T.; Breton, B.; Christopoulos, A.; Bouvier, M., Quantification of ligand bias for clinically relevant β_2-adrenergic receptor ligands: implications for drug taxonomy. *Mol. Pharmacol.* **2014,** *85*, 492-509.
34. Felixberger, J. Luciferase Complementation for the Determination of Arrestin Recruitment: Investigation of Histamine and NPY receptors. Ph.D. Thesis. University of Regensburg, 2014.

6 Summary

The discovery of the histamine H_2 receptor (H_2R) happened more than 50 years ago. Although it has since been intensively studied by both the pharmaceutical industry and universities, its function in the central nervous system (CNS) is still largely unknown. One of the main reasons for this is the lack of selective ligands which ideally also have access to the CNS. Before this work started, 2-amino-4-methylthiazole-containing carbamoylguanidines were published as highly potent and subtype-selective H_2R agonists which might be able to access the CNS (shown on acylguanidines). However, their applicability to elucidate the function of the central H_2R is impaired by their high affinity for D_2-like ($D_{2/3/4}$) receptors. This affinity originates most likely from the 2-amino-4-methylthiazole motif, which is a vital element of the D_2-like receptor agonist pramipexole. In addition, the recently published pharmacological tools for the H_2R (e.g. radio and fluorescent ligands) still possess significant structure-inherent drawbacks (e.g. pseudo-irreversible binding), which hamper the correct investigation of the receptor.

Consequently, the aim of this work was the synthesis of H_2R ligands which possess a selectivity over D_2-like receptors, and which can be used as new molecular tools with e.g. improved kinetic properties.

In the course of this doctoral thesis a new, high affinity, subtype-selective and G-protein-biased H_2R radioligand ([^{3}H]UR-KAT479) was synthesized and characterized. The binding of this radioligand to h/gp/mH_2R (co) expressing HEK293(T) cells was satiating and highly specific. The affinity for h- and gpH_2R was high (K_d = 24/28 nM; h/gp) and moderate for mH_2R (K_d = 98 nM). The most important property of [^{3}H]UR-KAT479 is the complete dissociation (60-180 min) from the h/gp/mH_2 receptors in kinetic experiments after a rapid association (60 min), which is good evidence for the reversible binding of this and structurally related ligands of the carbamoylguanidine class. The reversible binding enabled the determination of pK_i values of unlabeled standard ligands on e.g. the h/gp/mH_2R in the equilibrium according to the Cheng-Prusoff equation. In addition, [^{3}H]UR-KAT479 can be used as a model compound to investigate the pharmacokinetic properties (e.g. erythrocyte binding and protein binding) of the ligands of the carbamoylguanidine class.

In another project, fluorescence ligands with varying degrees of efficacy (E_{max}) in the β-arrestin1/2 assays were synthesized and their ability to trigger receptor internalization in hH_2R (co)expressing HEK293T cells was investigated using confocal microscopy. Indeed, no visible internalization of the H_2R could be observed for a ligand with E_{max} = 0.09 in the β-arrestin1 and

E_{max} = 0.12 in the β-arrestin2 assays. However, three other fluorescent ligands showed moderate to good efficacies in the β-arrestin1/2 assays (E_{max}: 0.22-0.61) and the internalization of the H_2R could be observed. These results are a good visual indication that an adequate level of β-arrestin recruitment is crucial for the internalization process of H_2R. Similarly to the structurally related radioligand, the fluorescence ligands showed improved kinetic properties and could also be used to determine the pK_i values of unlabeled ligands. In addition, these ligands can be used in the future to elucidate the co-localization of the H_2R-ligand complex with other proteins involved in the internalization process to get a better understanding of the exact internalization of the H_2R.

Two additional projects dealt with the selectivity problem of H_2R ligands with respect to D_2-like receptors. Two different strategies were applied in the investigations. In the first project, the ligand PB513 (H_2R: pK_i = 7.84), a 2-arylbenzimidazole derived from H_4R ligands, should be structurally optimized towards a higher subtype selectivity over the H_3R. This was because PB513 showed selectivity towards dopamine receptors in a preliminary study. In the second project, ligands of the carbamoylguanidine class were structurally modified (linker, heterocycle, and side chain variations) to generate a selectivity over the D_2-like receptors.

During the 2-arylbenzimidazole project the following elements of PB513 were identified as important for H_2R affinity: the 2-arylbenzimidazole, the secondary amine, the double bond, and the imidazole. On the other hand, the amide did not seem to be of great importance for the H_2R affinity, but mainly influenced the subtype selectivity. Although 27 analogues of PB513 were synthesized it was not possible to achieve a sufficient subtype selectivity (factor 100). In addition, PB513's previously reported selectivity for the H_4R (K_i (H_4) / K_i (H_2): reported: 148, obtained: 14) and preference for the H_3R (K_i (H_3) / K_i (H_2): reported: 47, obtained: 6) could not be reproduced. For this reason, the synthesized molecules were not examined at the dopamine receptors.

To improve the selectivity of the carbamoylguanidine class ligands, 40 analogues with different heterocycles, spacers and side residues were synthesized. Replacing the problematic 2-amino-(4-methyl)thiazole ring with a 2-aminothiadiazole led to an increase in the H_2R affinity (pK_i: 8.09-8.52) while maintaining the subtype selectivity (K_i ($H_{1/3/4}$) / K_i (H_2) > 100). In addition, these ligands showed selectivity towards the D_2-like receptors. The compounds were agonists at the h/gpH_2R (h: mini-G, [^{35}S]GTP$_\gamma$S, β-arrestin; gp: mini-G, atrium) and showed no or a less pronounced G-protein bias compared with their corresponding 2-amino-(4-methyl)thiazoles. To identify the molecular interactions leading to this selectivity over D_2-like

receptors, molecular docking studies were carried out with selected thiazole and thiadiazole-containing compounds. It was found that the amino acids in positions 3.28, 3.34, ELC2.49, ELC2.49, ELC2.51, 5.42 and 7.35 are most likely responsible for the selectivity.

In summary, in this work new, labeled (radioactive or fluorescent) molecular tools for the H_2R with improved kinetic properties were discovered. In addition, an exchange of thiazole with thiadiazole in ligands of the carbamoylguanidine class was found to lead to high-affinity, subtype-, and D_2-like receptor-selective H_2R agonists. The results of this work represent a very important step for future studies of H_2R agonists of the carbamoylguanidine type in order to get a better understanding the cellular mechanisms of the H_2R in general and specifically its function in the CNS (in vivo).

7 Zusammenfassung

Obwohl die Entdeckung des Histamin H_2 Rezeptors (H_2R) bereits mehr als 50 Jahre zurückliegt und er seitdem auf intensivste Weise sowohl von der pharmazeutischen Industrie als auch an Hochschulen erforscht wurde, ist seine Funktion im zentralen Nervensystem (ZNS) noch immer weitgehend unbekannt. Eine der wesentlichen Ursachen dafür ist der Mangel an geeigneten selektiven Liganden, die idealerweise gleichzeitig ZNS-gängig sind. Die vor Beginn dieser Arbeit publizierten 2-Amino-4-methylthiazol-haltigen Carbamoylguanidine sind hoch potente, subtypselektive und vermutlich sogar ZNS-gängige (gezeigt an Acylguanidinen) H_2R Agonisten. Allerdings ist ihre Anwendbarkeit zur Aufklärung der Funktion des zentralen H_2R durch ihre hohe Affinität zu D_2-artigen ($D_{2/3/4}$) Rezeptoren beeinträchtigt. Diese Affinität entsteht sehr wahrscheinlich durch das 2-Amino-4-methylthiazol-Motiv, welches auch ein Bestandteil des D_2-artigen Rezeptor Agonisten Pramipexol ist. Zudem weisen die kürzlich für den H_2R publizierten pharmakologischen Werkzeuge (z.B. Radio- and Fluoreszenzliganden) immer noch strukturbedingte Nachteile auf (z.B. pseudo-irreversible Bindung), welche eine korrekte Untersuchung dieses Rezeptors behindern.

Das Ziel dieser Arbeit war deshalb die Synthese von H_2R-Liganden, welche eine Selektivität gegenüber D_2-artigen Rezeptoren aufweisen und von neuen molekularen Werkzeugen mit z.B. verbesserten kinetischen Eigenschaften.

Im Laufe dieser Doktorarbeit wurde ein neuer, hoch affiner, subtypselektiver und G-protein-biased H_2R Radioligand ([^{3}H]UR-KAT479) synthetisiert und charakterisiert. Die Bindung dieses Radioliganden an h/gp/mH_2R (co)exprimierende HEK293(T) Zellen war sättigend und sehr spezifisch. Die Affinität am h- und gpH_2R war hoch (K_d = 24/28 nM; h/gp) und moderat am mH_2R (K_d = 98 nM). Die wichtigste Eigenschaft von [^{3}H]UR-KAT479 ist die vollständige Dissoziation (60-180 min) von den h/gp/mH_2 Rezeptoren in kinetischen Experimenten nach einer schnellen Assoziation (60 min), was ein Beweis für das reversible Bindungsverhalten von diesem und strukturell verwandten Liganden der Carbamoylguanidin-Klasse ist. Das reversible Bindungsverhalten ermöglichte die Bestimmung der pK_i Werte unmarkierter Standardliganden am z.B. h/gp/mH_2R im Gleichgewicht gemäß der Cheng-Prusoff Gleichung. Zudem kann [^{3}H]UR-KAT479 als Modelverbindung zur Untersuchung der pharmakokinetischen Eigenschaften (z.B. Erythrozyten-Bindung und Protein-Bindung) der Liganden der Carbamoylguanidine-Klasse benutzt werden.

In einem weiteren Projekt wurden Fluoreszenzliganden mit unterschiedlich stark ausgeprägten Wirkungsmaxima (E_{max}) in den β-arrestin1/2 Assays synthetisiert und deren Fähigkeit die Internalisierung in hH_2R (co)exprimierenden HEK293T Zellen auszulösen konfokal-mikroskopisch überprüft. Tatsächlich konnte für einen Liganden mit E_{max} = 0.09 im β-arrestin1 und E_{max} = 0.12 im β-arrestin2 Assay keine sichtbare Internalisierung des H_2R beobachtet werden. Drei weitere Fluoreszenzliganden zeigten jedoch moderate bis gute Wirkungsmaxima in den β-arrestin1/2 Assays (E_{max}: 0.22-0.61) und für diese konnte eine Internalisierung des H_2 Rezeptors beobachtet werden. Diese Ergebnisse sind ein guter visueller Hinweis, dass eine ausreichende Rekrutierung von β-arrestin für den Internalisierungsprozess des H_2R entscheidend ist. Genau wie der strukturverwandte Radioligand, zeigten die Fluoreszenzliganden verbesserte kinetische Eigenschaften und konnten zur Bestimmung von pK_i Werten unmarkierter Liganden benutzt werden. Darüber hinaus können diese Liganden in Zukunft für die Aufklärung der Co-Lokalisierung des H_2R-Ligand-Komplexes mit an der Internalisierung beteiligten Proteinen benutzt werden, um den genauen Internalisierungsprozess des H_2R besser zu verstehen.

In zwei weiteren Projekten wurde versucht das Selektivitätsproblem gegenüber D_2-artigen Rezeptoren zu beheben. Hierfür wurden zwei unterschiedliche Strategien angewendet. Im ersten Projekt wurde versucht, den Liganden PB513 (H_2R: pK_i = 7.84), ein von den H_4R Liganden abstammendes 2-Arylbenzimidazol, strukturell so zu optimieren, sodass es eine höhere Subtypselektivität gegenüber H_3R aufweist. Der Grund dafür war, dass PB513 in einer vorläufigen Studie eine Selektivität gegenüber Dopaminrezeptoren gezeigt hat. Im zweiten Projekt wurden an Liganden der Carbamoylguanidine-Klasse strukturelle Modifikationen vorgenommen (Linker-, Heterozyklus- und Seitenketten-Variationen), um eine Selektivität gegenüber des D_3Rs zu erzeugen.

Beim 2-Arylbenzimidazol-Projekt wurden die folgenden Elemente von PB513 als wichtig für die H_2R Affinität identifiziert: das 2-Arylbenzimidazol, das sekundäre Amin, die Doppelbindung und das Imidazol. Das Amid scheint keine große Bedeutung für die Affinität am H_2R zu haben, sondern hauptsächlich die Subtypselektivität zu beeinflussen. Trotz zahlreicher Variationen von PB513 (27 Analoga wurden synthetisiert) ist es nicht gelungen eine ausreichende Subtypselektivität (Faktor 100) zu erzielen. Zudem konnte die zuvor berichtete Selektivität zum H_4R (K_i (H_4) / K_i (H_2): berichtet: 148, erhalten: 14) und Präferenz für den H_3R (K_i (H_3) / K_i (H_2): berichtet: 47, erhalten: 6) von PB513 nicht reproduziert werden. Aus diesem

Grund wurden die synthetisierten Substanzen nicht weiter an den Dopamin Rezeptoren untersucht.

Um die Selektivität der Liganden der Carbamoylguanidin-Klasse zu verbessern, wurden 40 Analoga synthetisiert. Dabei wurden der Heterozyklus, der Spacer und die Seitenkette variiert. Der Austausch des problematischen 2-Amino-(4-methyl)thiazol-Rings durch ein 2-Aminothiadiazol führte zu einer Erhöhung der H_2R Affinität (pK_i: 8.09-8.52), bei gleichzeitiger Erhaltung der Subtypselektivität (K_i ($H_{1/3/4}$) / K_i (H_2) > 100). Zudem zeigten diese Liganden eine Selektivität gegenüber den D_2-artigen Rezeptoren. Am h/gpH_2R wirkten diese Substanzen agonistisch (h: mini-G, [^{35}S]GTPγS, β-arrestin2; gp: mini-G, Atrium) und zeigten keinen oder einen weniger ausgeprägten G-protein Bias verglichen mit den entsprechenden 2-Amino-(4-methyl)thiazolen. Um die molekularen Wechselwirkungen zu identifizieren, die zu dieser Selektivität gegenüber D_2-like Rezeptoren führen, wurden molekulare Docking-Studien mit ausgewählten Thiazol- und Thiadiazol-haltigen Verbindungen durchgeführt. Es wurde herausgefunden, dass wahrscheinlich die Aminosäuren in Positionen 3.28, 3.34, ECL2.49, ECL2.49, ECL2.51, 5.42 und 7.35 für die Selektivität verantwortlich sind.

Zusammenfassend wurden in dieser Arbeit neue, markierte (radioaktiv oder fluoreszierend) molekulare Werkzeuge für den H_2R mit verbesserten kinetischen Eigenschaften beschrieben. Außerdem wurde gezeigt, dass der Thiazol/Thiadiazol-Austausch in Liganden der Carbamoyguanidin-Klasse zu hochaffinen, subtyp- und D_2-like Rezeptor-selektiven H_2R Agonisten führt. Die Ergebnisse dieser Arbeit stellen einen sehr wichtigen Schritt für zukünftige Untersuchungen von H_2R Agonisten vom Carbamoyguanidin-Typ dar, um die zellulären Mechanismen des H_2R im Allgemeinen und spezifisch seine Rolle im ZNS (in-vivo) besser zu verstehen.

8 List of Abbreviations and Acronyms

	δ	chemical shift in ppm
	βarr(.)2	β-arrestin2 protein
	µ	micro
	°C	degree Celsius
	2D	two-demensional
A	aa	amino acid
	abs.	absolute, purity of 100%
	AC	adenylyl cyclase
	aq	aqueous
	approx.	approximately
	ARRBx	β-arrestin protein, x = 1,2
	atm	standard atmosphere
	AU	absorption units
B	bar	metric unit of pressure
	BB	building block
	BMY	Bristol-Myers Squibb
	Bq	becquerel
	B_{max}	maximum specific binding in the same unit as Y
	Bq	becquerel
	br	broad
	Br_2	bromine
	Boc	*tert*-butyloxycarbonyl
	Boc_2O	di-*tert*-butyl dicarbonate
	BODIPY	dipyrromethene boron difluoride
	BRET	bioluminescence resonance energy transfer
	BSA	bovine serum albumin
	Btk	Bruton's tyrosine kinase
	Bu	butyl
C	c	canine, molar concentration
	calcd.	calculated
	cAMP	3`,5`-cyclic adenosine monophosphate
	cat.	catalyst
	C_b	drug concentration in whole blood
	Cbz	benzyloxycarbonyl
	$CDCl_3$	deuterated chloroform
	C_e	drug concentration in RBCs
	cf.	confer/conferatur
	CH_2Cl_2	dichloromethane
	CHO	Chinese hamster ovary cell line
	Ci	curie
	CI	confidence interval
	CNBr	cyanogen bromide
	c(om)pd.	compound
	COSY	correlation spectroscopy
	cpm	counts per minute
	C_p	drug concentration in plasma

	CRE-Luc	cAMP-response element-driven transcriptional luciferase reporter
	CREB	cAMP response element binding protein
	CNS	central nervous system
	$CuSO_4$	copper(II) sulfate
D	d	day(s), doublet (spectral)
	Da	Dalton
	DAD	diode array detector
	db	double bond
	DEPT	distortionless enhancement by polarization transfer
	DIAD	diisopropyl azodicarboxylate
	DIPEA	*N*,*N*-diisopropylethylamine
	DMAP	4-dimethylaminopyridine
	DME	dimethyl ether
	DMEM	Dulbecco's modified Eagle's medium
	DMF	dimethylformamide
	DMSO	dimethyl sulfoxide
	DMSO-d_6	deuterated DMSO
	dpm	disintegrations per minute
	D_xR	dopamine D receptor subtype x
E	e.g.	exampli gratia
	eBF	efficacy bias factor
	EC_{50}	half maximal effective concentration
	ECL	extracellular loop
	EDC	1-ethyl-3-(3-dimethylaminopropyl)carbodiimide
	EDTA	ethylenediaminetetraacetic acid
	EGFR	epidermal growth factor receptor
	EI	electron ionization
	ELuc	Emerald luciferase
	ELucC	C-terminal Eluc fragment
	ELucN	N-terminal Eluc fragment
	EMA	European Medicines Agency
	E_{max}	maximal inducible receptor response referenced to a standard compound
	equiv	equivalent(s)
	ESI	electrospray ionization
	Et_2O	diethyl ether
	EtOAc	ethyl acetate
	EtOH	ethanol
F	FCS	fetal calf serum
	FDA	Food and Drug Administration
	FLAG	polypeptide protein tag with sequence motif DYKDDDDK
G	g	gram(s) or number of times the gravitational force
	G418	geneticin
	$G_{\alpha i2}$	α- subunit of the G_{i2} protein that mediates the inhibition of adenyl cyclase
	$G_{\beta 1\gamma 2}$	G protein β_1- and γ_2-subunits
	GABA	γ-aminobutyric acid
	gp	guinea pig
	GPCR(s)	G protein coupled receptor(s)
	GRK	G protein-coupled kinase

	Gs	adenylyl cyclase stimulatory G protein
	$G_{s\alpha S}$	α-subunit (short splice variant) of the G_s protein that mediates the stimulation of adenylyl cyclase
	GSK	GlaxoSmithKline
	$G_{s\alpha S}$	α-subunit (short splice variant) of the Gs protein that mediates the stimulation of adenylyl cyclase
	GTPγS	guanosine 5`-O-[gamma-thio]triphosphate
H	h	human or hour(s)
	H_2	hydrogen gas
	H_2O	water
	H_2SO_4	sulfuric acid
	HBr	hydrogen bromide, hydrobromic acid
	Hc	hematocrit
	HCl	hydrogen chloride, hydrochloric acid
	HCN2	potassium/sodium hyperpolarization-activated cyclic nucleotide-gated channel 2
	HD-PE	high density polyethylene
	HEK293	human embryonic kidney 293 cell line
	HEK293T	human embryonic kidney 293T cell line, derived from the HEK293 cell line, that expresses a mutant version of the Simian Vacuolating Virus 40 large T antigene
	HEPES	2-[4-(2-hydroxyethyl)piperazin-1-yl]-ethanesulfonic acid
	Het	heterocycle
	HGT-1	human gastric adenocarcinoma cell line
	$HgCl_2$	mercury(II) chloride
	His	histamine
	HMBC	heteronuclear multiple bond correlation
	HOBt	hydroxybenzotriazole
	HPLC	high-performance liquid chromatography
	HR	histamine receptor, high-resolution
	HRMS	high resolution mass spectrometry
	HSQC	heteronuclear single quantum correlation
	H_xR	histamine H receptor subtype x
	Hz	hertz
I	IC_{50}	half-maximum inhibitory concentration
	IP3	inositol triphosphate
K	*k*	retention (or capacity) factor (HPLC)
	K	clone
	K_2CO_3	potassium carbonate
	K_b	dissociation constant obtained from functional assays
	KCl	potassium chloride
	K_d	dissociation constant obtained from a saturation binding Experiment
	KH_2PO_4	monopotassium phosphate
	K_i	dissociation constant obtained from a competition binding experiment
	KI	potassium iodide
	kin	kinetic
	k_{obs}	observed association rate constant
	k_{off}	dissociation constant
	KOH	potassium hydroxide

	k_{on}	association rate constant
	$KRAS^{G12C}$	Kirsten rat sarcoma protein p.G12C mutant
	Kv3.2	voltage-gated potassium channel
L	L	liter(s)
	L-DOPA	levodopa
	LC	liquid chromatography
	$LiAlH_4$	lithium aluminium hydride
	$\log(\tau/K_A)$	transduction coefficient
M	m	mouse, multiplet (spectral), milli, meter(s)
	M	molar (moles per liter), mega
	MeCN	acetonitrile
	MF	molecular formula
	MeCN	acetonitrile
	MeOD	deuterated methanol
	MeOH	methanol
	mG /mini-G	engineered minimal G protein
	$MgCl_2$	magnesium chloride
	mGs	engineered guanosine triphosphate hydrolase domain of $G_{\alpha s}$ subunit (long splice variant)
	min	minute
	mol	mole(s), molecular (as in mol wt)
	MS	mass spectrometry
	MW	molecular weight
N	n	length of the linker given as the number of carbon atoms, nano
	N	sodium hydride, number of biological replicates
	n.a.	not applicable
	n.d.	not determined
	Na_2HPO_4	disodium phosphate
	NaCl	sodium chloride
	NaH	sodium hydride
	NaH_2PO_4	monosodium phosphate
	NaOH	sodium hydroxide
	n-BuOH	*n*-butanol
	NanoBRET	NanoLuc luciferase-based bioluminescence resonance energy transfer
	NEt_3	triethylamine
	N_2H_4	hydrazine
	NHS	*N*-hydroxysuccinimid
	Nluc	NanoLuc luciferase
	NlucC	C-terminal NanoLuc fragment
	NlucN	N-terminal NanoLuc fragment
	NMR	nuclear magnetic resonance
	non-sp.	non-specific
P	p	p-value (level of marginal significance within a statistical hypothesis test, representing the probability of the occurrence of a given event)
	PAINS	pan-assay interference compounds
	pBF	potency bias factor
	PBS	phosphate buffered saline
	Pd/C	palladium on carbon

	PDB	protein data base
	PE	petroleum ether
	pEC_{50}	negative logarithm of the half-maximum activity concentration in M
	pH	potential or power of hydrogen
	Phth	phthalimide
	pK_a	acid dissociation constant
	pK_b	negative logarithm of K_b in M
	pK_i	negative logarithm of K_i in M
	PKA	protein kinase A
	PLC	phospholipase C
	PPh_3	triphenylphosphine
	ppBF	negative logarithm of pBF
	ppm	parts per million
	Py-5	4-((1*E*,3*E*)-4-(4-(dimethylamino)phenyl)buta-1,3-dien-1-yl)-2,6-dimethylpyrylium tetrafluoroborate
R	r	rat
	R	residue
	RBC	red blood cell
	RGS4	regulator of G protein signaling 4
	R_f	retention factor (in chromatography)
	[RL]	radioligand concentration
	RP-HPLC	reversed-phase HPLC
	rt	room temperature
Q	q	quartet (spectral)
	Q-TOF	quadrupole time of flight
	qs5-HA	chimeric Gαq protein incorporating a hemagglutinin epitope
	quint	quintet
S	s	singlet (spectral), seconds
	S0223	2-[5-[1-(5-carboxypentyl)-1,3-dihydro-3,3-dimethyl-2*H*-indol-2-ylidene]-penta-1,3-dienyl]-1,3,3-trimethyl-3*H*-indolium bromide
	S0436	2-[5-[1-carboxypentyl-1,3-dihydro-3,3-dimethyl-2*H*-indol-2-ylidene]-penta-1,3-dienyl]-3,3-dimethyl-1-(4-sulfobutyl)-3*H*-indolium hydroxide, inner salt
	S0387	2-[5-[1-(5-carboxypencyl)-1,3-dihydro-3,3-dimethyl-5-sulfo-2*H*-indol-2-ylidene]-penta-1,3-dienyl]-3,3-dimethyl-1-(4- sulfobutyl)-3*H*-indolium hydroxide, inner salt, sodium salt
	S/N	signal to noise ratio
	SAR	structure-activity relationship
	sb	single bound
	scFv16	single-chain variable fragment derived from mAb16 antibody
	SE	standard error
	SEM	standard error of the mean
	SF	SuperFlash
	Sf9	*Spodoptera frugiperda* insect cell line
	SK	small-conductance calcium-activated potassium channel
	SK-N-MC	human Askin’s tumor cell line

	SK&F	Smith, Kline & French
	$SOCl_2$	thionyl chloride
	SP	signal peptide: subunit A of the murine type 3 receptor for 5-hydroxytryptamine
T	t	time, triplet (spectral)
	t-BuOK	potassium *tert*-butoxide
	t_0	dead time
	TFA	trifluoroacetic acid
	THF	tetrahydrofuran
	TLC	thin-layer chromatography
	TM	transmembrane
	TosMIC	toluenesulfonylmethyl isocyanide
	t_R	retention time
	Tris	tris(hydroxymethyl)aminomethane
	Trt	trityl
	Trt-Cl	triphenylmethyl chloride
U	U937	human lymphoblast cell line
	UHD	ultrahigh definition
	UV	ultraviolet
V	VHH	variable domain of heavy chain of heavy-chain antibody
	vs.	versus
W	wt%	mass fraction (percentage by weight)

9 List of Posters and Publications

Poster presentations:

Tropmann, K., Biselli, S., Plank, N., Forster, L., Felixberger, J., Hübner, H., Gmeiner, G., Bernhard, G., Buschauer, A., Strasser, A., Restoring histamine H_2R specificity versus dopamine D3/D2 receptors of carbamoylguanidine-type H_2R agonists, GRK1910 Evaluation, **2017**.

Tropmann, K., Littmann, T., Buschauer, A., Bernhardt, G., Strasser, A., G protein-biased fluorescent histamine H_2 receptor agonists failing to induce β-arrestin2 recruitment and receptor internalization, 9th Summer School "Medicinal Chemistry", University of Regensburg, September 19-21, **2018**.

Publications:

Biselli, S., Alencastre, I., **Tropmann, K.**, Erdmann, D., Mengya, C., Littmann, T., Maia, A. F., Gomez-Lazaro, M., Tanaka, M., Ozawa, T., Keller, M., Lamghari, M., Buschauer, A., Bernhardt, G., Fluorescent H_2 receptor squaramide-type antagonists: synthesis, characterization and applications, ACS Med. Chem. Lett., **2020**, 11, 1521-1528.

Grätz, L., **Tropmann, K.**, Bresinsky, M., Müller, C., Bernhardt, G., Pockes, S., NanoBRET binding assay for histamine H_2 receptor ligands using live recombinant HEK293T cells, *Sci. Rep.*, **2020**, 10, e13288.

Tropmann, K., Höring, C., Plank, N., Pockes, S., Discovery of a G protein-biased radioligand for the histamine H_2 receptor with reversible binding properties, *J. Med. Chem.*, **2020**, 63, 13090-13102.

Höring, C., Seibel, U., **Tropmann, K.**, Grätz, L., Mönnich, D., Pitzl, S., Bernhardt, G., Pockes, S., Strasser, A., A dynamic, split-luciferase-based mini-G protein sensor to functionally characterize ligands at all four histamine receptor subtypes, *Int. J. Mol. Sci.*, **2020**, 21, 8440; Cover: *Int. J. Mol. Sci.*, (November-2 **2020**), 21, 22, - 466 articles.

Biselli, S.*, Bresinsky, M.*, **Tropmann, K.***, Forster, L., Honisch, C., Buschauer, A., Bernhardt, G., Pockes, S., Pharmacological characterization of a new series of carbamoylguanidines reveals potent agonism at the H_2R and D_3R, *Eur. J. Med. Chem.*, **2021**, *214*, 113190.

Pockes, S. & **Tropmann, K.**, Histamine H_2 receptor radioligands: triumphs and challenges. *Future Med. Chem.*, **2021**, *13*, 1073-1081.

Tropmann, K., Bresinsky, M., Forster, L., Mönnich, D., Buschauer, A., Wittmann, H.-J., Pockes, S., Strasser, A., Abolishing dopamine D_{2long}/D_3 receptor affinity of subtype-selective carbamoylguanidine-type histamine H_2 receptor agonists, *J. Med. Chem.*, **2021**, submitted for publication.

Tropmann, K., Seibel, U., Littmann, T., Strasser, A., Synthesis and pharmacological characterization of fluorescent histamine H_2 receptor carbamoylguanidine-type agonists, *Bioorg. Med. Chem. Lett.*, **2021**, manuscript in preparation.

*contributed equally

10 Danksagungen

Zuallererst gilt mein Dank PD Dr. Andrea Strasser für die Vergabe des interessanten und herausfordernden Promotionsthemas. Ich bedanke mich für ihre Unterstützung während der gesamten Zeit, das Vertrauen in mich, meine Projekte selbst zu entwickeln und die Erstellung des Erstgutachtens.

Ich danke auch sehr dem leider zu früh von uns gegangenen Prof. Dr. Buschauer für die Aufnahme an seinem Lehrstuhl und das Wecken meines Interesses für die Familie der Histamin Rezeptoren im Rahmen meiner Masterarbeit.

Prof. Dr. Joachim Wegener danke ich für die Erstellung des Zweitgutachtens und Prof. Dr. Frank-Michael Matysik für die Übernahme der Rolle als Drittprüfer. Außerdem danke ich Prof. Dr. Achim Göpferich für den Vorsitz in meinem Promotionskolloquium.

Für die Finanzierung meiner Promotion und wissenschaftliche Förderung danke ich dem Graduiertenkolleg (GRK) 1910 „Medizinische Chemie selektiver GPCR-Liganden“.

Ich danke all meinen Kooperationspartnern: PD Dr. Andrea Strasser, Dr. Steffen Pockes, Prof. Dr. Armin Buschauer, Dr. Hans-Joachim Wittmann, Prof. Dr. Günther Bernhardt, Lisa Forster, Merlin Bresinsky, Dr. Sabrina Biselli, Lukas Grätz, Carina Höring, Dr. Nicole Plank, Claudia Honisch, Ulla Seibel und Dr. Timo Littmann für eine gute Zusammenarbeit.

Ein besonderer Dank gebührt Dr. Steffen Pockes für die hervorragende Zusammenarbeit, seine Unterstützung bei der Radiosynthese und analytischen Charakterisierung des Radioliganden, seine hilfreichen Ratschläge, seine fachliche Leitung und Betreuung und sein Fachwissen insbesondere auf dem Fachgebiet der Histamin Rezeptoren.

Ich danke Prof. Dr. Detlef Neumann (Medizinische Hochschule, Hannover, Germany) für die Bereitstellung von HEK293-mH_2R Zellen.

Ich danke Prof. Dr. Achim Göpferich für die Bereitstellung des Zeiss Axiovert 200M Mikroskops.

Ich danke Prof. Dr. Robert Schupfner für die Bestimmung der Aktivität von [^{3}H]UR-KAT479.

Ich danke Dr. Harald Hübner (Department Chemie und Pharmazie, Lehrstuhl für Pharmazeutische Chemie (Prof. Dr. Gmeiner)) für seine aufschlussreichen Ratschläge zu Bindungstests an Dopamin D_{2long}/D_3 Rezeptoren und die Testung von einigen H_2R Liganden an $D_{1\text{-}5}$ Rezeptoren.

Des Weiteren möchte ich mich bei Christine Braun und Kerstin Röhrl (Durchführung der organpharmakologischen Testungen), Astrid Seefeld und Franz Wiesenmayer (Blutentnahme), Elvira Schreiber (Schulung in der Durchführung der Versuche am Durchflusszytometer), Maria Beer-Krön (Bereitstellung von Sf9 Zellen, Schulung in Zellkulturtechniken und der Membranpräparation) und Denise Mönnich (Durchführung zahlreicher Radioligand- und GTPγS-Bindungstests) für die hervorragende technische Unterstützung bedanken.

Dr. Max Keller danke ich für seine aufschlussreichen Ratschläge zur Radiosynthese, für die Organisation der Mäuse für den Erythrozyten Bindungsversuch und seine Hilfe bei Problemen an der HPLC-Anlage.

Den Mitarbeitern der Abteilungen für Massenspektrometrie (Josef Kiermaier und Wolfgang Söllner) und NMR-Spektroskopie (insbesondere Fritz Kastner) gilt ein großes Dankeschön für ihre hervorragende Arbeit.

Meinen Forschungs- und Wahlpflichtpraktikanten Diana Braun, Valerie Grossegger, Stefanie Peulter, Daniela Bethge und Luisa Friebe Vasconcellos danke ich für ihre fleißige und tatkräftige Unterstützung in Labor und Mithilfe bei meinen Forschungsprojekten.

Mein Dank gilt auch allen ehemaligen (insbesondere Dr. Sabrina Biselli) und aktuellen Kollegen des AK Buschauer für die unverzichtbare Vorarbeit, die Unterstützung, die Zusammenarbeit und die Gespräche, ob nun fachlicher oder fachfremder Natur.

Meinen Eltern und meinem Bruder für ihre Geduld, Unterstützung und Hilfe in jeglicher Art und Weise in all den Jahren und vor allem meinem Lebenspartner Daniel Petzold, ohne dessen Liebe, unermessliche Geduld, Unterstützung und Rückhalt ich es wohl nicht so weit geschafft hätte.

Ich erkläre hiermit an Eides statt, dass ich die vorliegende Arbeit ohne unzulässige Hilfe Dritter und ohne Benutzung anderer als der angegebenen Hilfsmittel angefertigt habe; die aus anderen Quellen direkt oder indirekt übernommenen Daten und Konzepte sind unter Angabe des Literaturzitats gekennzeichnet.

Einige der experimentellen Arbeiten wurden in Zusammenarbeit mit anderen Personen durchgeführt. Vermerke zu den Beiträgen der betreffenden Personen finden sich in den jeweiligen Kapiteln.

Weitere Personen waren an der inhaltlich-materiellen Erstellung der vorliegenden Arbeit nicht beteiligt. Insbesondere habe ich hierfür nicht die entgeltliche Hilfe eines Promotionsberaters oder anderer Personen in Anspruch genommen. Niemand hat von mir, weder unmittelbar noch mittelbar, geldwerte Leistungen für Arbeiten erhalten, die im Zusammenhang mit dem Inhalt der vorgelegten Dissertation stehen.

Diese Arbeit wurde bisher weder im In- noch im Ausland in gleicher oder ähnlicher Form einer andren Prüfungsbehörde vorgelegt.

_____

Katharina Tropmann